UNIVERSIDAD COMPLUTENSE DE MADRID

FACULTAD DE CIENCIAS QUÍMICAS

TESIS DOCTORAL

Desarrollo y aplicación de metodologías alternativas in vivo e in vitro para la evaluación de la toxicidad, bioacumulación y biotransformación de contaminantes orgánicos persistentes

Development and application of alternative in vivo and in vitro methodologies for the assessment of toxicity, bioaccumulation and biotransformation of persistent organic pollutants

MEMORIA PARA OPTAR AL GRADO DE DOCTORA

PRESENTADA POR

Paloma de Oro Carretero

DIRIGIDA POR

Jon Sanz Landaluze

Universidad Complutense de Madrid
Facultad de Ciencias Químicas

Desarrollo y aplicación de metodologías alternativas *in vivo* e *in vitro* para la evaluación de la toxicidad, bioacumulación y biotransformación de contaminantes orgánicos persistentes

Development and application of alternative *in vivo* and *in vitro* methodologies for the assessment of toxicity, bioaccumulation and biotransformation of persistent organic pollutants

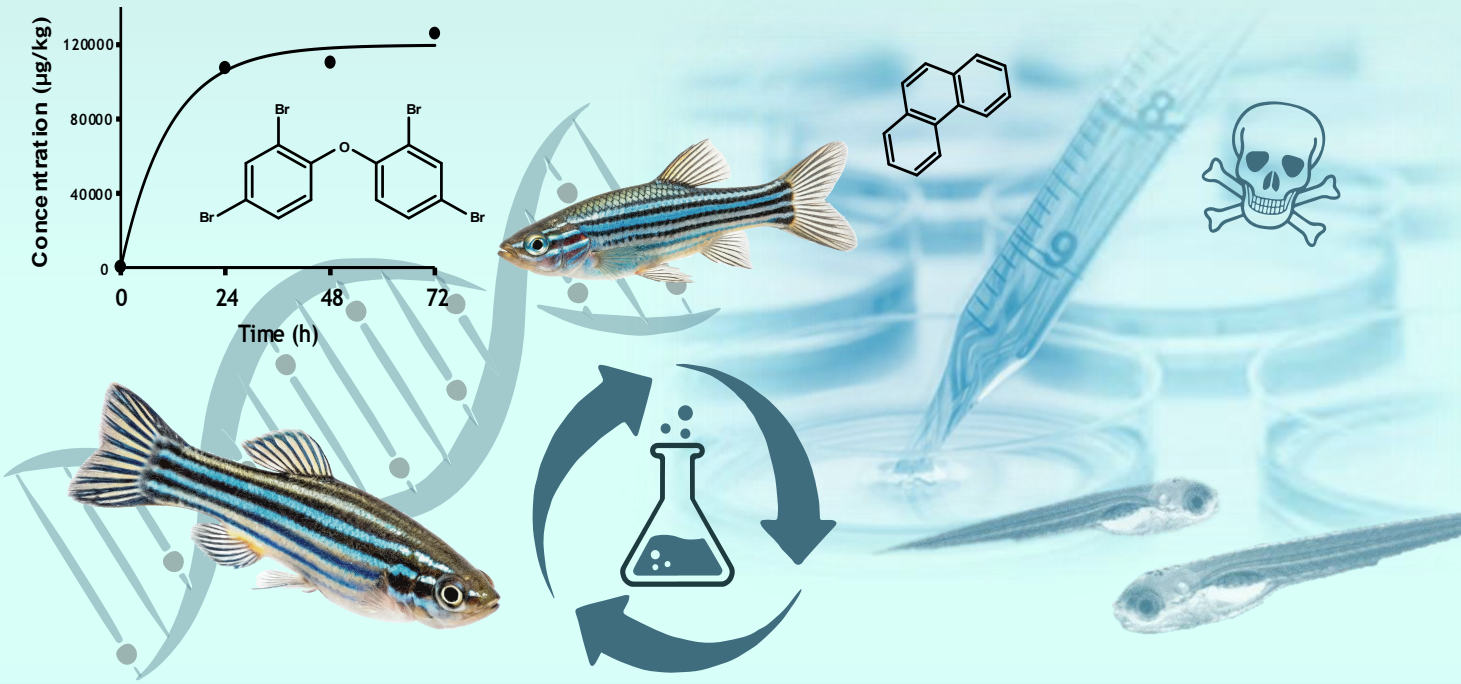

Paloma de Oro Carretero

Director:

Jon Sanz Landaluze

Tesis Doctoral

Madrid, 2025

UNIVERSIDAD COMPLUTENSE DE MADRID

FACULTAD DE CIENCIAS QUÍMICAS

DOCTORADO EN QUÍMICA AVANZADA

Tesis Doctoral

Desarrollo y aplicación de metodologías alternativas *in vivo* e *in vitro* para la evaluación de la toxicidad, bioacumulación y biotransformación de contaminantes orgánicos persistentes

Development and application of alternative *in vivo* and *in vitro* methodologies for the assessment of toxicity, bioaccumulation and biotransformation of persistent organic pollutants

PALOMA DE ORO CARRETERO

DIRECTOR

Jon Sanz Landaluze

Mención Internacional

Madrid, 2025

Esta Tesis Doctoral ha sido realizada en el marco de los Proyectos de Investigación financiados por el Ministerio de Ciencia e Innovación: PID2020-114714RBI00 y PID2023-600 148425NB-I00.

Se agradece la financiación recibida a través del contrato predoctoral para la formación de doctores/as del Programa Estatal para Desarrollar, Atraer y Retener Talento del Ministerio de Ciencia, Innovación y Universidades (PRE2021/097956) para desarrollar el trabajo de investigación presentado.

A mis abuelos y abuelas

Ponerlo todo patas arriba,
cuestionar los axiomas,
cambiar las teclas
y revolver las hormonas.

Mr. Kilombo

AGRADECIMIENTOS

Hacer un doctorado es un camino que comienza con la "simple" decisión de embarcarte en una aventura llena de esfuerzo, incertidumbres, aprendizajes, desafíos y, sobre todo, crecimiento. Ese cóctel culmina en esta Tesis Doctoral, y puedo decir que me siento orgullosa de aquella decisión y de la persona en la que me he convertido. Pero todo este recorrido, no hubiera sido posible, ni tendría sentido, sin el apoyo y la compañía de personas que han hecho que merezca la pena, y a ellas quiero dedicar estas líneas de agradecimiento.

En primer lugar, a mi director de Tesis, Jon Sanz Landaluze, por apostar y confiar siempre en mí, por la paciencia, por estar siempre disponible y por compartir conmigo tu forma de ver las cosas. Pero, sobre todo, con nuestros más y nuestros menos, gracias por ser mucho más que un jefe. Todos estos años, desde que nos conocemos, incluyendo mi primer año de carrera, TFG y TFM, has sabido darme la seguridad y el apoyo que necesitaba para seguir en este camino, tanto en la investigación como en lo personal. Creo que hemos formado un buen equipo y espero que podamos seguir cerca en el resto de los caminos que vengan.

Es evidente que esta Tesis no tendría sentido sin nombrar a las personas que también me han acompañado en el día a día en el laboratorio, en la cafetería, en el despacho o en los pasillos de la Facultad. Quiero empezar por todos los componentes que están o han estado en el grupo de investigación de *Determinación de Trazas, Especiación y Proteómica*: Yolanda, Milagros, Ángela, Bea, Elena, Emma, Esther, Estefanía, Eugenia, Gus, Juanjo, Lucía, Miguel, Mónica, Natalia, Noelia, Rian, Sandra, Teresa, David… muchas gracias por las comidas, "cafés", aventuras en la montaña… y, sobre todo, por vuestra ayuda y acogimiento. Quiero extender estos últimos agradecimientos a todo el personal del Departamento de Química Analítica: a María Pedrero como su directora, por estar disponible y tener paciencia con el pitidito de mi incubador; a los técnicos de laboratorio (Miriam, Marcos y David) como piezas clave en los turnos de prácticas; al personal de limpieza y, en especial a Isabel y Erika, por darnos el bienestar de la Facultad por su trabajo y por alguna que otra merienda…, al resto de personal docente y secretarias del departamento. Y, por último, a los doctorandos e investigadores contratados por apoyarme para ser

representante en el Consejo de Departamento, los saludos y nimos por el pasillo y vuestra ayuda; en especial a Andrés con los comienzos con las células y Pilar por ser mi compa era de preparación de las prácticas. Extendiéndolo a otros departamentos y facultades también tengo que agradecer a Sara y Bego por acompañar, apoyar y ayudar a desconectar en los ratillos de fotosíntesis (o *homeless*), a Enrique por las charlas, a Rubén, Emma, Laura y Cristián por contar conmigo en vuestros proyectos, del mismo modo que Irene y Elena, además de por los ratillos a remojo en la pisci…

Me gustaría hacer una mención especial a Elena y a Natalia, las dos personas fundamentales para que pudiera llegar hasta aquí sin perderme (demasiado) en la locura. Elena, tú has estado desde el principio, en todas las etapas, estados de ánimo, problemas y alegrías, tanto dentro como fuera de las paredes universitarias e incluso estoy segura de que ambas seríamos capaces de explicar la tesis de la otra. Natalia, llegaste hace poco, siendo huevito, pero, incluso con todas mis estancias, has sido fundamental en esta recta final. Espero que sigamos con más descansitos (sanos) en las siguientes etapas dentro y fuera de la Facultad.

Como los comienzos nunca son fáciles, ahí estuvieron Alberto, Julia y Gema del Laboratorio de Salud Pública. Gracias por enseñarme de cromatografía, de vestimenta o de la vida; por ponérmelo fácil para compaginar trabajo y doctorado al mismo tiempo hasta que conseguí el contrato predoctoral. Me dio mucha pena el día que os dije que me iba, pero tanto por el cariño, como en lo profesional, sabemos que nuestros caminos se van a seguir cruzando.

Del mismo modo, agradecer a TFGs, TFMs e invitadas, que han aportado en gran medida a esta investigación: Marta, Victoria, Laura, Lucía, Sumaiya y Bianca. Sin vosotras, y sobre todo al principio, hubiera sido todo más complicado. Me alegro de haber trabajado y aprendido junto a vosotras.

Una de mis mayores preocupaciones eran las estancias. Y sin el apoyo de muchas personas a las que menciono en todo este apartado no me hubiera lanzado a una de las experiencias más enriquecedoras de este camino. Por lo personal, por lo profesional pero, sobre todo, por la gente que me he encontrado.

Gracias a la Dra. Nerea Roher del Institut de Biotecnologia i de Biomedicina de la Universitat Autònoma de Barcelona (IBB-UAB) por darme la oportunidad de forma altruista de aprender, de realizar los últimos experimentos de esta Tesis y de conocer al resto del equipo con la misma filosofía y cercanía: Marlid, Paty, Mauri y Borja. También mencionar a Gala y su sonrisa contagiosa pese a las inundaciones que formábamos. Espero que podamos seguir en contacto. Pero lo que realmente me llevo de esta estancia, son 3 amigos (Marlid, Manu y Albert) que me acogieron en su casa como una más y que, pese a las mil horas cuidando de células y peces, lo que me quedo son los karaokes, la noche de San Juan, el camping y rutas en la montaña… Marlid, si tuviera que destacar el mayor descubrimiento de esta Tesis, serías tú. Moltes gràcies!

Thanks to Dr. Luise Henneberger and Dr. Beate Escher from Helmholtz Centre for Environmental Research - UFZ (Leipzig, Germany) for kindly welcoming me, integrating me as one of your team, letting me do my work and teaching me all your knowledge. Thanks also to the rest of the *Cell Toxicology* department, especially Julia for being my partner in the lab and teaching me your work. Dankeschön! A Naroa, por tu cercanía y por ser apoyo e integración en el grupo de amigos fuera del laboratorio. También hay otras personas que no puedo olvidar como Wiebke por las excursiones en bici, Dani por nuestras cenas viendo *Aquí no hay quien viva* y Luigi por los bailes, momentos y tu préstamo de la bici.

Y ahora sí, es el momento de agradecer, más fuerte si cabe, a aquellas personas que han estado dándome su apoyo tanto antes como durante la Tesis.

En primer lugar, mis *Químicas Everywhere* (Andrea, Marina, Lucía, Nerea, Sara, Marta, María, Lúa y Yaiza) y mi *Grupito* (Elena, Lucía y Teresa). Quién mejor que vosotras para saber cómo es el caminito de la ciencia y la universidad…. Menos mal que celebraciones, amigos invisibles, actualizaciones de vida, casas rurales, viajes… nos siguen y seguirán juntando, desde primero y segundo de carrera.

A Alberto, siguiendo las líneas de tu Tesis, mi más antiguo compañero de viaje científico. Y es que es verdad, hemos vivido todas las etapas juntos desde el instituto… y lo vamos a conseguir, vamos a ser doctores!!! Gracias por estar y seguir estando, que nos queda mucho por recorrer.

A Lidia, mi más fiel compañera de vida, mi amiga desde primaria y uno de mis mayores apoyos, incluso viviendo a 1500 km. Aunque ya lo sabes todo, te mereces que te diga que soy mejor por tenerte cerca y que te admiro. Gracias por cada momento, por seguir creciendo juntas, por escuchar, por disfrutar y por estar siempre.

Y como dentro de esta locura, se necesita más de una terapia… Dentro del baile, gracias a Kiko, Sara y Luis por estar siempre siguiendo y apoyando mis pasos. Dentro del taekwondo, gracias a todo el equipo y familia de *TKD Maldonado Team* por mostrarme los valores y la disciplina del esfuerzo, respeto, confianza y humildad, unido al disfrute, risas y amistad: Pedro, Laura y Nuria Maldonado, Laura L., Dani, Miguel, Pedro (Batman), Nerea, Guille, Héctor, Bernard, Javi, David, Son, Sonia, familia Rivier... y a mis *Old School*: Álvaro, Iván Navas, María, Diego M., Pablo, Iván (pitbull), Diego Z., Javi, Sara, Edgar, Yesenia…En especial, quiero agradecer a Nuria y Laura, por hacerme mejor cada día, por formar conmigo el mejor trío, no sé si en medallas, aunque alguna ha caído, pero sí en compañerismo y, sobre todo, amistad fuera y dentro del tapiz. Y a Álvaro, gracias por estar a diario, por darme apoyo y confianza, por tus tonterías, piques y debates de ideas, por abrirte y por todos los momentos, como los juegos de mesa.

Por último, mi agradecimiento más profundo es para los pilares que, pase lo que pase, siempre están. Papá y mamá, gracias por vuestro esfuerzo en darme la mejor educación y todo lo mejor que podéis. Tías Inma y Carmen, gracias por pararos a escuchar y apoyar en todo momento. Abuelos y abuelas (Jose, Pepi, Carmen y Lorenzo) gracias por cuidarme y por darme vuestro cariño incondicional siempre. Y llegamos a mis mayores acompañantes: Jaime, mi primo, hermano y amigo, gracias por seguirme a todas mis locuras, conciertos y charlas; Natalia, mi hermana, amiga, compañera de batallas… muchas gracias por tu confianza, nuestras risas, nuestras peleas y tu apoyo. Solo deseo que sigamos mano a mano en todo, cuidándonos, como siempre. Gracias a tod@s por apoyarme en aquella “simple” decisión inicial, pese al desconocimiento, y acompañarme en este camino.

Muchas gracias a cada una de las personas que aquí menciono, nada de lo que pueda escribir expresaría todo lo afortunada que me siento de teneros a mi lado.

TABLA DE CONTENIDO

TABLA DE CONTENIDO

I. RESUMEN

I. RESUMEN

La toxicología moderna del siglo XXI ha evolucionado más allá de la observación exclusiva de los efectos adversos que una sustancia química puede provocar. Actualmente, y conforme a las normativas vigentes, se requiere una descripción integral del comportamiento de estas sustancias en los organismos y el medio ambiente durante todo su ciclo de vida, con especial atención a la exposición combinada a múltiples compuestos. A su vez, las agencias internacionales están promoviendo enfoques alternativos y metodologías innovadoras que transformen la experimentación animal, basándose en el principio de las 3Rs (Reducción, Refinamiento y Reemplazo), con el fin de evaluar el riesgo toxicológico de manera más ética, eficiente y económicamente viable.

El aumento significativo de contaminantes orgánicos persistentes (POPs) y nanoplásticos en el medio ambiente ha suscitado una creciente preocupación social debido a su capacidad de penetrar en los organismos y generar efectos adversos, tanto por su exposición individual como simultánea. Diversos estudios han demostrado que los nanoplásticos pueden adsorber sustancias químicas tóxicas del entorno, como los POPs, facilitando así su transferencia hacia los organismos.

En este contexto, la presente Tesis Doctoral tiene el objetivo de ***Desarrollar y aplicar metodologías alternativas in vivo e in vitro para estudiar la toxicidad, bioacumulación y biotransformación de contaminantes orgánicos persistentes***. Para ello, se proponen dos enfoques alternativos basados en ensayos *in vivo* utilizando larvas de pez cebra y ensayos *in vitro* con líneas celulares que, una vez desarrollados, se aplican para el estudio de la exposición combinada de POPs con la presencia de nanoplásticos de poliestireno. Durante la investigación, se seleccionaron el fenantreno y el BDE-47 como modelos representativos de POPs.

La primera metodología propuesta se basa en un método previamente diseñado en el grupo de investigación para determinar el factor de bioconcentración (BCF), siguiendo la guía oficial OECD 305, que evalúa la bioacumulación mediante el uso de larvas de pez cebra. Este enfoque se adaptó para estudiar simultáneamente los procesos de bioacumulación y biotransformación, obteniendo resultados

favorables y comparables con los obtenidos mediante organismos acuáticos vivos. Se demuestra que las larvas de pez cebra tienen la capacidad de biotransformar los compuestos a partir de las 72 horas post fecundación.

En el ámbito *in vitro*, se siguió la guía OECD 280, que utiliza cultivos primarios de hepatocitos de trucha arcoíris y modelos matemáticos *in silico* para su posterior extrapolación *in vivo* (IVIVE). No obstante, esta metodología aún está en desarrollo y presenta limitaciones prácticas, descritas por la propia guía. En respuesta a esto, se propone el uso de líneas celulares como una alternativa para determinar el BCF, evaluando líneas celulares derivadas de tejidos de embriones de pez cebra (ZF4), hepatoma humano (HepG2) e hígado de pez cebra (ZFL). Estas últimas líneas celulares resultaron ser las más adecuadas para estudiar simultáneamente los procesos de bioacumulación y biotransformación. Además, se introdujo una mejora en el modelo existente mediante el desarrollo e incorporación de metodologías analíticas miniaturizadas y diseños experimentales que permiten determinar la concentración interna y biodisponible tanto del compuesto parental como de sus metabolitos mayoritarios. Estos avances proporcionan datos experimentales más precisos, los cuales pueden integrarse en los modelos matemáticos existentes, mejorando la predicción del BCF al incluir cinéticas de absorción y biotransformación, y así obtener resultados más cercanos a los obtenidos a través de métodos *in vivo*.

Finalmente, se aplicaron estas metodologías alternativas en el estudio de la toxicidad, la bioacumulación, la biotransformación del fenantreno y la internalización de nanoplásticos de poliestireno (60 nm) en situaciones de exposición combinada e individual. Los resultados mostraron interacciones sinérgicas y/o antagónicas, dependiendo de la funcionalidad celular y la complejidad biológica. Estos hallazgos subrayan la importancia de considerar los efectos combinados en las evaluaciones ecotoxicológicas, proporcionando información valiosa y complementaria para los estudios de cribado y evaluación de riesgos.

En conclusión, la presente Tesis Doctoral ha desarrollado metodologías alternativas que permiten sustituir las evaluaciones actuales que implican experimentación animal. Además, se han aportado datos significativos y se han discutido aspectos clave para el refinamiento de las guías oficiales en toxicología. Este trabajo destaca el papel fundamental de la química analítica en la evaluación toxicológica, especialmente en el estudio del comportamiento de los compuestos dentro de los organismos y en el medio ambiente. Las metodologías propuestas son eficaces para evaluar simultáneamente la bioacumulación y biotransformación de contaminantes y nanoplásticos, y establecen una base sólida para futuras investigaciones sobre la exposición combinada de estos contaminantes.

II. ABSTRACT

II. ABSTRACT

Modern toxicology in the 21st century has evolved beyond the sole observation of the adverse effects that a chemical substance may cause. Currently, and in accordance with existing regulations, a comprehensive description of the behaviour of these substances within organisms and the environment throughout their entire life cycle is required, with particular emphasis on combined exposure to multiple compounds. At the same time, international agencies are promoting alternative approaches and innovative methodologies that aim to transform animal experimentation, based on the 3Rs principle (Reduction, Refinement, and Replacement), in order to assess toxicological risk in a more ethical, efficient, and economically viable manner.

The significant increase in persistent organic pollutants (POPs) and nanoplastics in the environment has raised growing social concern due to their ability to penetrate organisms and generate adverse effects, both from individual and simultaneous exposure. Various studies have shown that nanoplastics can adsorb toxic chemicals from the environment, such as POPs, thereby facilitating their transfer into organisms.

In this context, the present Doctoral Thesis aims to ***Develop and apply alternative in vivo and in vitro methodologies to study the toxicity, bioaccumulation, and biotransformation of persistent organic pollutants*****.** To achieve this, two alternative approaches are proposed based on in vivo assays using zebrafish larvae and in vitro assays with cell lines, which, once developed, will be applied to the study of combined exposure to POPs in the presence of polystyrene nanoplastics. During the research, phenanthrene and BDE-47 were selected as representative models of POPs.

The first proposed methodology is based on a previously designed method by the research group to determine the bioconcentration factor (BCF), following the official OECD 305 guideline, which evaluates bioaccumulation using zebrafish larvae. This approach was adapted to simultaneously study bioaccumulation and biotransformation processes, yielding favourable results comparable to those

obtained through live aquatic organisms. It was demonstrated that zebrafish larvae are capable of biotransforming compounds from 72 hours post-fertilization.

In the *in vitro* domain, the OECD 280 guideline, which uses primary trout hepatocyte cultures and *in silico* mathematical models for subsequent *in vivo* extrapolation (IVIVE), was followed. However, this methodology is still under development and presents practical limitations, as described by the guideline itself. In response, the use of cell lines was proposed as an alternative to determine the BCF, evaluating cell lines derived from zebrafish embryo tissues (ZF4), human hepatoma (HepG2), and zebrafish liver (ZFL). The latter cell lines proved to be the most suitable for simultaneously studying bioaccumulation and biotransformation processes. Furthermore, an improvement to the existing model was introduced through the development and incorporation of miniaturized analytical methodologies and experimental designs that allow for the determination of both parent compound and major metabolite concentrations, both internal and bioavailable. These advancements provide more precise experimental data, which can be integrated into existing mathematical models, improving BCF prediction by including absorption and biotransformation kinetics, thus yielding results closer to those obtained through *in vivo* methods.

Finally, these alternative methodologies were applied to the study of general toxicity, bioaccumulation, biotransformation of phenanthrene, and polystyrene nanoplastics (60 nm) internalization under both combined and individual exposure scenarios. The results showed synergistic and/or antagonistic interactions depending on cellular functionality and biological complexity. These findings underline the importance of considering combined effects in ecotoxicological assessments, providing valuable and complementary information for screening studies and risk assessment.

In conclusion, this Doctoral Thesis has developed alternative methodologies that allow for the replacement of current assessments involving animal experimentation. Additionally, significant data have been provided, and key aspects have been discussed for the refinement of official toxicology guidelines. This work highlights the essential role of analytical chemistry in toxicological assessment, especially in the study of the behaviour of compounds within organisms and the environment. The proposed methodologies are effective in simultaneously evaluating bioaccumulation and biotransformation of contaminants and nanoplastics and establish a solid foundation for future research on the combined exposure of these pollutants.

III. INTRODUCCIÓN

III. INTRODUCCIÓN

1. Evolución del concepto de toxicidad.

Hubo una época en que la comprensión de la **toxicidad** se limitaba a observar las consecuencias inmediatas de la exposición a determinadas sustancias[1]. La toxicología se construía sobre una base de la experiencia directa, frecuentemente marcada por eventos trágicos. Sin embargo, a lo largo de la historia, el ser humano ha convivido con el veneno y el remedio, a menudo sin distinguir con claridad uno del otro. Lo que ayer parecía inofensivo, hoy se evalúa con cautela; lo que cura hoy, puede presentar riesgos mañana. Como toda disciplina científica, **la toxicología ha ido transformándose**, dejando atrás su carácter estrictamente empírico para adentrarse en una comprensión más profunda y sistemática de los complejos mecanismos mediante los cuales las sustancias químicas interactúan con los sistemas biológicos y medioambientales (**Figura 1**). Esta evolución, detallada a continuación, impulsada por el progreso tecnológico, analítico y científico, ha dado lugar a nuevas metodologías, más integradoras y predictivas, permitiendo una evaluación y regulación de la toxicidad más eficaz[2].

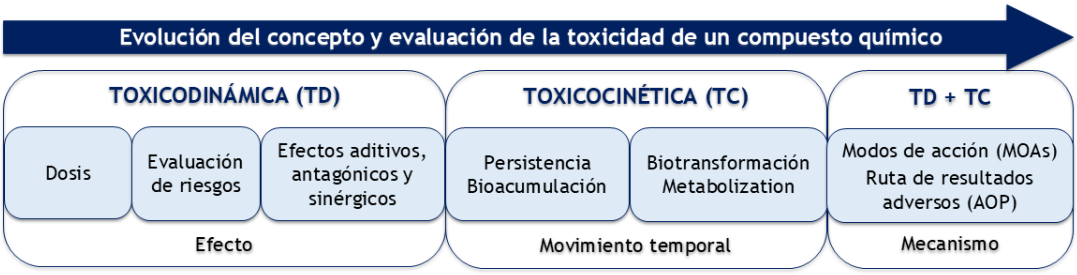

***Figura 1**. Evolución temporal del concepto de toxicidad.*

Uno de los primeros referentes en la historia de la toxicología fue Paracelso (Theophrastus Phillippus Aureolus Bombastus von Hohenheim), médico y alquimista del siglo XVI, considerado el padre de esta ciencia[3]. Fue él quien formuló una de las frases más recordadas en este campo: *"**La dosis hace el veneno**"*. Con

[1] **Silbergeld**. Cap. 33. *Toxicología*. **1998**.
[2] **Choudhuri *et al***. From classical toxicology to Tox21: Some critical conceptual and technological advances in the molecular understanding of the toxic response beginning from the last Quarter of the 20th century. *Toxicol. Sci*. **2018**.
[3] **Gantenbein**. Poison and Its Dose: Paracelsus on Toxicology. *Toxicology in the Middle Ages and Renaissance.* **2017**.

esa afirmación, Paracelso sentó una base crucial: cualquier sustancia puede provocar un efecto perjudicial dependiendo de la cantidad administrada. Incluso el agua, fuente de vida por excelencia, puede provocar una intoxicación si se ingiere en cantidades desmesuradas en poco tiempo, al disminuir la concentración de sodio en la sangre (conocido como hiponatremia).

Con el transcurso de los siglos, la toxicología fue refinando su enfoque. Se comprendió que, aunque la dosis sigue siendo un factor fundamental, no era el único factor determinante en la aparición de efectos tóxicos. También resultaba necesario considerar la vía de exposición, las propiedades fisicoquímicas de la sustancia, y las características fisiológicas del organismo receptor[4]. Este cambio de paradigma dio lugar a una evaluación del **riesgo químico** más completa. En este marco surgieron conceptos como ***toxicidad aguda***, (asociada a exposiciones breves e intensas) y ***toxicidad crónica*** (ligada a exposiciones prolongadas a bajas dosis). Ambos enfoques resultan clave para estimar el verdadero riesgo de una sustancia y para fijar límites seguros de exposición. Uno de los indicadores más utilizados para este propósito es la **concentración letal media ($\mathbf{LC_{50}}$)**, que representa la cantidad necesaria para provocar la muerte del 50 % de una población expuesta.

Hasta este punto, la toxicología se había centrado exclusivamente en los efectos que una sustancia produce sobre el organismo, lo que se conoce como **toxicodinámica** (TD). Pero con el tiempo, se hizo evidente que, para comprender esos efectos en toda su complejidad, era necesario también entender el recorrido de la sustancia. La herramienta para ello ya existía, la **toxicocinética** (TC), una rama nacida en el ámbito de la farmacología, utilizada desde hacía tiempo para estudiar el destino de los medicamentos en el cuerpo: cómo se absorben, se distribuyen, se metabolizan y se eliminan[5]. Esta perspectiva se incorporó también al estudio de sustancias químicas no terapéuticas, ampliando así su alcance y relevancia dentro de la toxicología. Gracias a esta mirada, se empezaron a considerar factores clave como la ***persistencia*** (capacidad de una sustancia de

[4] **McCarty** *et al.* Evaluation of the Inherent Toxicity Concept in Environmental Toxicology and Risk Assessment. *Environ. Toxicol. Chem*. **2020**.

[5] **Ashauer and Escher**. Advantages of toxicokinetic and toxicodynamic modelling in aquatic ecotoxicology and risk assessment. *J. Environ. Monitoring.* **2010**.

permanecer en el organismo o en el medioambiente durante largos períodos), la ***bioacumulación*** (acumulación progresiva en los tejidos a lo largo del tiempo) o la ***biotransformación*** (conversión en el organismo de una sustancia en compuestos potencialmente más reactivos). Todos ellos influyen en la manifestación de efectos adversos, incluso mucho después de que haya cesado la exposición inicial o se realice en dosis bajas.

Estos avances científicos, resultado de un arduo esfuerzo investigativo, no solo enriquecieron el pensamiento toxicológico, sino que evidenciaron la necesidad de adaptar el **marco normativo** vigente. En Europa, esta transformación quedó reflejada en el Reglamento nº 1907/2006[6], conocido como REACH (Registro, Evaluación, Autorización y Restricción de Sustancias Químicas), una normativa que propuso un enfoque más exhaustivo y preventivo para la gestión de sustancias químicas. Por su parte, en Estados Unidos, la Agencia de Protección Ambiental (EPA) solicitó al Consejo Nacional de Investigación una **revisión profunda de las metodologías toxicológicas tradicionales**, resultando en un informe pionero bajo el nombre de "*Toxicity Testing in the 21st Century: A Vision and a Strategy*" [7].

Estas normativas marcaron un punto de inflexión en la manera de abordar la evaluación toxicológica. La **toxicología moderna** ha dejado de ser una disciplina enfocada exclusivamente en la identificación puntual de efectos adversos. Hoy, contempla el ciclo completo de vida de las sustancias químicas mediante la **integración del análisis toxicodinámico y toxicocinético** (TD+TC). Desde esta base metodológica y conceptual, han surgido nuevos marcos que han transformado la forma de comprender y anticipar la toxicidad, como los ***Modos de Acción*** (MOAs) y las ***Vías de Resultados Adversos*** (AOPs). El estudio de los MOAs se centra en clasificar las sustancias según el tipo de acción biológica que desencadenan, lo que permite prever, de forma general, las respuestas que podrían generar en los organismos. El análisis de los AOPs, por su parte, profundiza en esa información al describir una secuencia estructurada de eventos biológicos que se inicia a nivel molecular y culmina en un efecto adverso observable. En conjunto,

[6] **REACH No 1907**. Regulation (EC) No1907/2006 of the European Parliament and of the Council. **2006**.

[7] **National Research Council**, Toxicity testing in the 21st century: A vision and a strategy. National Academies Press. **2007**.

estos dos enfoques no solo complementan la evaluación toxicológica, sino que la enriquecen, proporcionando un **marco mecanicista más detallado y predictivo**, capaz de anticipar con mayor precisión los riesgos que las sustancias químicas pueden representar[8,9].

Siguiendo el cambio normativo y la evolución en los enfoques metodológicos, la **toxicología del siglo XXI** también se enfrenta a una realidad aún más compleja, inevitable y cada vez más urgente: la **exposición combinada a múltiples sustancias**. En el medio ambiente, los organismos no están expuestos a una sola sustancia a la vez, sino a un cóctel de compuestos que pueden interactuar entre sí, alterando significativamente los resultados de la toxicidad. Estas interacciones pueden sumar sus efectos (aditivas, 1+1=2), contrarrestarse (antagónicas, 1+1<2) o incluso amplificarse (sinérgicas 1+1>2)[1,10]. La comprensión de estas combinaciones es esencial para evaluar escenarios de exposición más realistas.

Este viaje, que abarca desde la observación empírica hasta los modelos cinéticos y predictivos, y que evoluciona del estudio de la dosis de un veneno solitario a un cóctel complejo de sustancias, ha revolucionado por completo la forma de entender la toxicidad. La toxicología del presente no puede concebirse sin reconocer la complejidad inherente a los múltiples factores que la configuran. En este contexto, esta **Tesis Doctoral** nace en ese cruce de caminos con el propósito de ofrecer enfoques innovadores y metodologías avanzadas que permitan evaluar, predecir y comprender, con precisión y fiabilidad, los riesgos asociados a la exposición combinada de contaminantes orgánicos persistentes y sus efectos toxicocinéticos. Además, no se limita a un avance técnico, si no que pretende dar un paso decisivo hacia una toxicología más modera, al integrar una **dimensión ética hacia metodologías responsables**, que lejos de ser una limitación, se convierta en un motor para garantizar un impacto positivo tanto en la evaluación del riesgo toxicológico como en la sociedad.

---

[1] **Silbergeld**. Cap. 33. *Toxicología*. **1998**.

[8] **Escher** *et al.* Crucial role of mechanisms and modes of toxic action for understanding tissue residue toxicity and internal effect concentrations of organic chemicals. *Integrated Environmental Assessment and Management.* **2010**.

[9] **Ankley** *et al*. Adverse outcome pathways: A conceptual framework to support ecotoxicology research and risk assessment. *Environ. Tox. Chem.* **2010**.

[10] **Bureš** *et al*. Modelling the toxicity of pollutants mixtures for risk assessment: a review. *Environ. Chem. Letters.* **2021**.

2. Bioacumulación.

Como se ha descrito, de acuerdo con el enfoque y reglamento REACH[6] actuales, la **bioacumulación** es un parámetro fundamental para evaluar el riesgo de los compuestos químicos. Este proceso se define como el incremento de la concentración de una sustancia química en un organismo, a lo largo del tiempo, en comparación con el medio ambiente que lo rodea, debido a la exposición continua a través de distintas vías, como el agua, el aire, el suelo o la dieta[11]. Dentro del concepto de bioacumulación, la **biomagnificación** también sirve para caracterizar el comportamiento de acumulación de un compuesto, pero se trata de un fenómeno distinto (**Figura 2**). Este proceso se refiere al aumento progresivo de la concentración de una sustancia a medida que se avanza en la cadena trófica, pudiendo afectar en mayor medida a los organismos de mayor nivel[12].

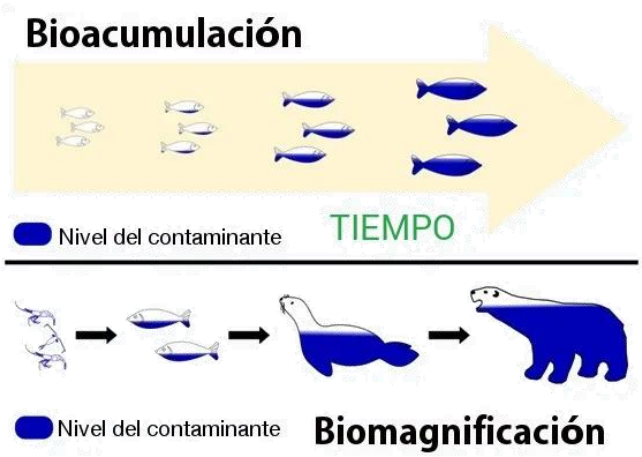

Figura 2. *Diferencia entre bioacumulación y biomagnificación.*

La bioacumulación se cuantifica, de la manera más representativa del comportamiento de una sustancia en condiciones naturales, mediante el **factor de bioacumulación** (BAF)[13]. Este factor se cuantifica mediante la relación entre la concentración de un contaminante en un organismo y la concentración de dicho

[6] **REACH No 1907**. Regulation (EC) No1907/2006 of the European Parliament and of the Council. **2006**.

[11] **Arnot and Gobas**, A review of bioconcentration factor (BCF) and bioaccumulation factor (BAF) assessments for organic chemicals in aquatic organisms. *Environ. Rev.* **2006**.

[12] **Mackay**. Bioconcentration, bioaccumulation, biomagnification and trophic magnification: A modelling perspective. *Environ Sci*. **2018**.

[13] **Costanza** *et al*. Use of the bioaccumulation factor to screen chemicals for bioaccumulation potential. *Environ. Toxicol. Chem*. **2012**.

contaminante en el medio ambiente, generalmente el agua o el suelo. Sin embargo, el BAF suele ser complejo de medir, ya que depende de múltiples factores, como las condiciones ambientales, características biológicas del organismo, dietas y modos de exposición, lo que limita su uso en estudios de laboratorio y de regulación. De forma rutinaria, se suele utilizar el **factor de bioconcentración** (BCF). La diferencia radica en que se tiene en cuenta únicamente la exposición controlada a través de las superficies respiratorias y dérmicas, es decir, la exposición química en la dieta no está incluida, proporcionando una medida estandarizada y reproducible. Por tanto, el BCF es el resultado neto de tasas competitivas (**Figura 3**) de absorción (dérmica, respiratoria) y eliminación (respiratoria, dilución debida al crecimiento del organismo, biotransformación metabólica y excreción).

Las sustancias químicas que tienden a ser bioacumulativas comparten ciertas características:

- **Persistencia**: Compuestos que no se degradan fácilmente en el ambiente ni en los organismos, como los compuestos orgánicos persistentes (POPs).
- **Lipofilicidad**: Sustancias con alta afinidad a almacenarse en tejidos adiposos. Ejemplos comunes incluyen pesticidas, dioxinas, compuestos aromáticos, halogenados y organometálicos.
- **Baja excreción**: Sustancias que no pueden ser metabolizadas o eliminadas eficientemente por los organismos, como ciertos compuestos fluorados.

Sin embargo, hay ciertas sustancias que, si son muy bioacumulables, se puede adherir a partículas del medio y no presentar **biodisponibilidad** para su absorción.

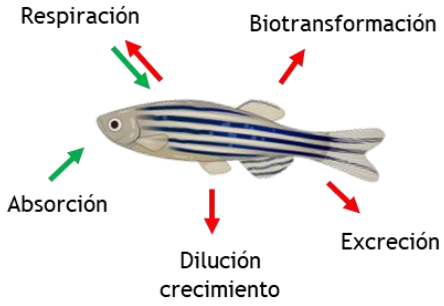

Figura 3. *Procesos implicados en la medida del factor de bioconcentración.*

Los **criterios** utilizados por las agencias regulatorias internacionales como la OECD (Organización para la Cooperación y el Desarrollo Económicos), la EPA y la ECHA (Agencia Europea de Sustancias y Mezclas Químicas) para determinar si una sustancia es bioacumulable son el BCF y el coeficiente de partición octanol-agua (K_{ow}). Los valores fijados se muestran en la **Tabla 1**.

Tabla 1. *Criterios para la clasificación de sustancias bioacumulables.*

Evaluación	Criterio según K_{ow}[14]	Criterio según BCF (log BCF)[15]
No bioacumulativa	log K_{ow} < 2.5	BCF < 1000 (3.0)
Bioacumulativa	2.5 < log K_{ow} < 5.0	1000 < BCF < 5000
Muy bioacumulativa	log K_{ow} > 5.0	BCF > 5000 (3.7)

2.1. Determinación del BCF

Aunque existen varias guías estandarizadas para la determinación del BCF, descritas por la Oficina de Prevención, Plaguicidas y Sustancias Tóxicas (OPPTS 850.1730[16]) y la EPA (ASTM E1022-94[17]), la guía de **Ensayo 305** de la **OECD**[18] es el método mayormente aceptado y utilizado para determinar el BCF de sustancias químicas en organismos acuáticos, específicamente en peces, bajo unas **condiciones definidas**:

- Las condiciones del agua tienen que mantenerse a 26 ± 2 °C, oxígeno disuelto ≥ 60% y pH 7.8 ± 0.2. Debe contener 294.0 mg·L^{-1} $CaCl_2 \cdot 2\ H_2O$, 123.3 mg·L^{-1} $MgSO_4 \cdot 7\ H_2O$, 63.0 mg·L^{-1} $NaHCO_3$ y 5.5 mg·L^{-1} KCl.
- La concentración nominal de la sustancia a estudiar tiene que mantenerse en un rango de ± 20 % durante todo el ensayo.
- Se propone evaluar la bioacumulación a dos niveles de concentración para cada sustancia. Las concentraciones son seleccionadas de acuerdo con el

[14] **Gimeno** *et al*. Are current regulatory log K_{ow} cut-off values fit-for-purpose as a screening tool for bioaccumulation potential in aquatic organisms? *Reg. Toxicol. Pharm*. **2024**.
[15] **CE No 1272/2008**. Clasificación, etiquetado y envasado de sustancias y mezclas. Diario Oficial de la Unión Europea. **2008**.
[16] **EPA**. Ecological Effects Test Guidelines. Fish BCF. OPPTS 850.1730. **1996**.
[17] Guide for Conducting Bioconcentration Tests with Fishes and Saltwater Bivalve Mollusks. **ASTM** International. **2013**.
[18] **OECD No 305**. Bioaccumulation in Fish: Aqueous and Dietary Exposure. **2012**.

valor LC_{50} de la sustancia, esto es, un 1% y 0.1% del valor del LC_{50}, siempre que los métodos analíticos permitan su determinación.

- El proceso consta de dos fases: una fase de exposición al contaminante, denominada "fase de absorción" y una fase de post-exposición, denominada "fase de depuración", donde los peces se transfieren a un medio exento del compuesto. La fase de absorción debe durar 28 días, a menos que pueda demostrarse que se ha alcanzado antes el estado estacionario (concentración en el organismo constante en el tiempo). La fase de depuración, un periodo de la mitad de la fase de absorción suele ser suficiente para que se produzca una reducción adecuada (95%). Si el tiempo se alarga significativamente para conseguir la reducción y se considera poco práctico, puede tolerarse una reducción del 10%.
- El muestreo se lleva a cabo a distintos tiempos durante las dos fases de ensayo, siendo obligatorio a mitad y al final de cada una de ellas.
- Se debe realizar un experimento en paralelo de control, sin exposición al contaminante.
- Se deben tomar 4 o 5 peces por punto de muestreo, lo que hace un total de 80-120 peces necesarios para el ensayo de exposición y control.

Según la guía, el **BCF** se calcula como la relación entre la concentración del compuesto en el pez (C_f) con respecto a la media calculada en el medio circundante (C_W) en estado estacionario (SS) (**Ecuación 1**):

$$BCF_{ss} = \frac{C_f\ (ng \cdot kg^{-1})}{C_W\ (ng \cdot L^{-1})} \qquad \text{Ec. (1)}$$

No obstante, cuando no se alcanza el estado estacionario, el BCF puede calcularse mediante un modelo cinético de primer orden (**Ecuación 2**)[19,20].

$$\frac{dC_f}{dt} = k_1 \cdot C_W - k_2 \cdot C_f\ (\text{absorción})\ ;\quad \frac{dC_f}{dt} = -k_2 \cdot C_f\ (\text{depuración}) \qquad \text{Ec. (2)}$$

[19] **Gobas and Zhang**. Measuring bioconcentration factors and rate constants of chemicals in aquatic organism under conditions of variable water concentrations and short exposure time. *Chemosphere.* **1992**.

[20] **Mackay and Fraser.** Bioaccumulation of persistent organic chemicals: mechanisms and models. *Environ. Poll*. **2000**.

Donde, t es el tiempo de exposición (h), k_1 es la constante de absorción de primer orden ($L \cdot kg^{-1} \cdot h^{-1}$) y k_2 es la constante de eliminación de primer orden (h^{-1}).

Suponiendo que en t = 0h, la concentración del analito en los peces es cero y que la concentración en el medio de exposición es constante, se obtiene la **Ecuación 3**.

$$C_f = \frac{k_1}{k_2} \cdot C_W \left(1 - e^{-k_2 t}\right) \text{ (absorción) ; } C_f = C_{f,0} \cdot e^{-k_2 t} \text{ (depuración)} \quad \text{Ec. (3)}$$

Donde $C_{f,0}$ es la concentración del analito en el pez al inicio del proceso de depuración. Ajustando las ecuaciones a los datos experimentales, pueden obtenerse k_1 y k_2. En condiciones de SS, la Ec. (1) se simplifica a la **Ecuación 4**.

$$BCF_K = \frac{C_f}{C_W} = \frac{k_1}{k_2} \quad \text{Ec. (4)}$$

3. Biotransformación.

La **biotransformación** es el proceso de metabolización por el cual un organismo convierte una sustancia química, normalmente exógena (**xenobiótico**), en compuestos diferentes para facilitar su eliminación, mediante reacciones bioquímicas (enzimáticas)[21]. Por regla general, se transforman los xenobióticos liposolubles en metabolitos hidrosolubles que se puedan excretar con facilidad. La biotransformación se lleva a cabo principalmente en el hígado[22] y consta de 3 fases (**Figura 4**):

- **Fase I** (activación): Reacciones como oxidación, reducción o hidrólisis, que introducen o exponen grupos funcionales en la molécula. Suele estar mediada por enzimas del citocromo P450 (CYP450)[23].
- **Fase II** (conjugación): Reacciones en las que el compuesto modificado en la Fase I se une a una molécula endógenas para formar un producto más soluble en agua. Las enzimas más comunes en esta fase son glucuroniltransferasas (UGTs), sulfotransferasas (SULTs), Glutatión-S-transferasas (GSTs) y N-acetiltransferasas (NATs).

[21] **Almazroo**, *et al*, Drug Metabolism in the Liver. *Clinics in Liver Disease*. **2017**.
[22] **Ewa and Danuta**. Polycyclic aromatic hydrocarbons and PAH-related DNA adducts. *J Appl Gen*. **2017**.
[23] **Benedetti** *et al*. Drug metabolism and pharmacokinetics. *Drug Met Rev*. **2009**.

- **Fase III** (excreción): Detoxificación y eliminación del xenobiótico mediante proteínas transportadoras como MRP (proteína asociada a la resistencia a múltiples fármacos o P-gp (glicoproteínas).

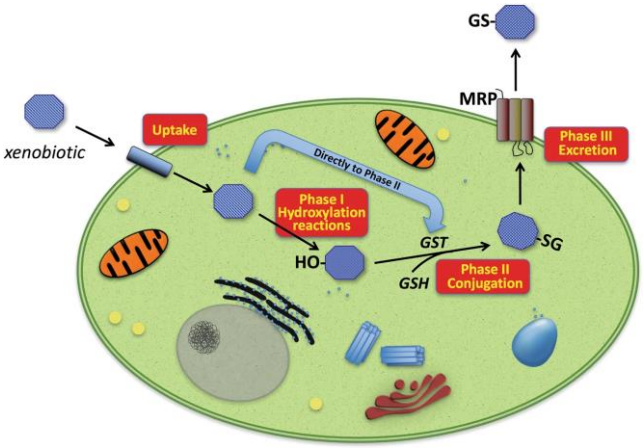

Figura 4. *Fases en la biotransformación de un xenobiótico*[24].

En términos generales, la biotransformación contribuye a la **detoxificación** de sustancias, sin embargo, algunas veces puede generar **metabolitos más tóxicos** o activos que la sustancia inicial[25]. Además, es un factor clave en la **modificación de la bioacumulación**[26]. Sin embargo, como se ha descrito anteriormente, en el modelo estandarizado OECD 305 para determinar el BCF de las sustancias, no se hace diferencia entre la eliminación debida a la excreción, la eliminación debida a la respiración y a la biotransformación. Además, aunque se está empezando a estudiar y redactar las primeras guías[27,28], todavía no existe un método estandarizado para la evaluación de la biotransformación. Por todo ello, es importante profundizar en el estudio de la biotransformación de forma específica para conocer cómo afecta a la toxicidad, a la bioacumulación y dilucidad las rutas metabólicas de los xenobióticos.

[24] **Allocati** *et al.* Glutathione transferases: Substrates, inihibitors and pro-drugs in cancer and neurodegenerative diseases. *Oncogenesis*. **2018**.
[25] **McCormick** *et al.* Microbially mediated O-methylation of bisphenol a result in metabolites with increased toxicity to the developing Zebrafish (Danio rerio) embryo. *Environ Sci Technol*. **2011**.
[26] **Fu** *et al*. Biotransformation Changes Bioaccumulation and Toxicity of Diclofenac in Aquatic Organisms. *Environ Sci Technol*. **2020**.
[27] **OECD No 319A**. Determination of in vitro intrinsic clearance using cryopreserved rainbow trout hepatocytes (RT-HEP). **2018**.
[28] **OECD No 319B**. Determination of in vitro intrinsic clearance using rainbow trout liver S9 sub-cellular fraction (RT-S9). **2018**.

4. Organismos modelo.

Los **organismos modelo** son especies no humanas estudiadas de manera exhaustiva para analizar y comprender diversos fenómenos biológicos, con el objetivo de que la información, los datos y el conocimiento generados sean aplicados en la investigación científica[29]. En la elección de un determinado organismo modelo, debe tenerse en cuenta su abundancia, facilidad de obtener y manejar en condiciones de laboratorio, ser representativo del ecosistema estudiado y obtener mediciones reproducibles. Dentro de estas características, como ya se ha mencionado, los **organismos acuáticos** son los modelos más comunes utilizados para determinar el BCF. En la **Tabla 2**, se muestran algunos de los organismos modelo mayormente empleados y las ventajas para su elección en la evaluación de la bioacumulación y biotransformación.

Tabla 2. *Modelos acuáticos modelo en la evaluación de la bioacumulación.*

Organismo acuático	Nombre científico	Nombre común	Ventajas
Vertebrados (Peces)	*Danio rerio*	Pez cebra	▪ Representan diferentes hábitats acuáticos (agua dulce o salada). ▪ Poseen rutas metabólicas relevantes para evaluar la transformación de compuestos. ▪ Acumulación en tejidos grasos, músculos y órganos específicos.
	Oncorhynchus mykiss	Trucha arcoiris	
	Cyprinus carpio	Carpa común	
Invertebrados (crustáceos y moluscos)	*Daphnia magna*	Pulga de agua	▪ Menor tamaño y facil manejo. ▪ Representan rutas tróficas relevantes en ambientes acuáticos. ▪ Acumulan contaminantes disueltos y partículas en suspensión, lo que amplía el análisis de diferentes rutas de exposición.
	Mytilus edulis	Mejillón común	
	Gammarus spp.		
Algas y plantas	*Pseudo kirchneriella subcapitata*	Microalga verde	▪ Transferencia inicial de contaminantes en la red trófica. ▪ Evaluación preliminar de la solubilidad y adsorción de sustancias químicas.
	Lemna minor	Lenteja de agua	

[29] **Leonelli and Ankeny**. What makes a model organism? *Endeavour.* **2013**.

4.1. Pez cebra: modelo para la bioacumulación y biotransformación

El **pez cebra** (*Danio rerio*) es un pequeño pez de agua dulce originario del sudeste asiático. Su cuerpo es alargado, alcanzando entre 2.5 y 4 cm de longitud en la adultez, y presenta un patrón distintivo de franjas horizontales azules y plateadas que recorren su cuerpo desde la cabeza hasta la cola (**Figura 5**)[30].

Es un organismo modelo ampliamente utilizado en la investigación científica debido a su facilidad de cuidado, reproducción rápida, bajo coste y **ventajas** beneficiosas para estudios biológicos, biomédicos y ecotoxicológicos. Entre ellas, la más característica (**Figura 5**) es que, su genoma ha sido completamente secuenciado y comparte más de un **70% de homología genética** con los humanos[31]. Además, presenta facilidad para realizar modificaciones genéticas y regenerar tejidos como el corazón, las aletas, medula espinal y retiniano[32,33]. Estas características lo convierten en un modelo esencial para investigar mecanismos aplicables a terapias humanas y obtener resultados comparables.

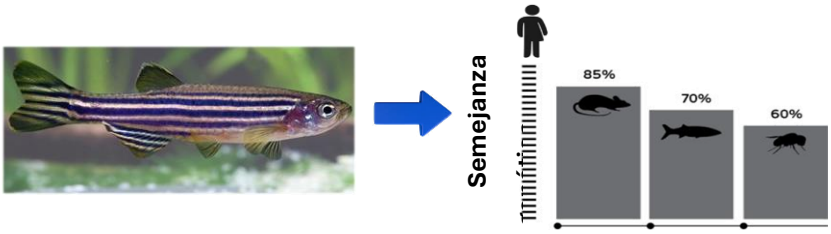

Figura 5. *Imagen pez cebra y su mayor ventaja como organismo modelo.*

Por otro lado, el proceso de maduración embrionaria se produce *Ex vivo*, es decir, fuera del organismo, y en las primeras fases del desarrollo es transparente, lo que facilita la visualización de las respuestas[34]. Por ello, el uso del pez cebra como modelo puede ser interesante en todas sus etapas de crecimiento: embrión, larva, juvenil y adulto.

[30] **Lima** *et al*. Zebrafish: A Versatile Model Organism for Toxicological Research and Applications. *Adv Res.* **2024**.
[31] **Howe** *et al*. The zebrafish reference genome sequence and its relationship to the human genome. *Nature*. **2013**.
[32] **Gemberling** *et al*. The zebrafish as a model for complex tissue regeneration, *Trends in Genetics*. **2013**.
[33] **Mitra** *et al*. Cardiac Regeneration in Adult Zebrafish: A Review of Signaling and Metabolic Coordination. *Current cardiology reports.* **2025**.
[34] **Garcia** *et al*. Advancements in zebrafish applications for 21st century toxicology. *Pharmacology and Therapeutics*. **2016**.

El pez cebra se destaca como un **modelo idóneo para los estudios de bioacumulación y biotransformación**, debido a la presencia de sistemas enzimáticos de detoxificación altamente desarrollados, entre los que sobresalen las enzimas del citocromo P450, responsables de la metabolización de una amplia gama de compuestos xenobióticos. Asimismo, comparte rutas metabólicas clave con otros vertebrados, lo que facilita la extrapolación de los resultados obtenidos. Su eficiente sistema hepático, junto con la capacidad de absorber contaminantes tanto por vía branquial como dérmica, permite una evaluación precisa de la acumulación, distribución y transformación de sustancias químicas en su organismo.

5. Modelos alternativos: Principio de las 3R en experimentación animal.

La **producción masiva de nuevos productos** de origen antropogénico con el objetivo de mejorar la actividad industrial, tecnológica, económica, social y humana ha provocado una enorme expansión en la aparición de contaminantes químicos en el medio ambiente. Un estudio con un inventario de 19 países involucrados reveló que en los últimos 30 a 40 años se han registrado unas 350.000 sustancias químicas para su producción y uso a gran escala[35]. Del mismo modo, cada año, en el marco de REACH, se registran oficialmente unas 1700 sustancias nuevas y existentes[36]. Considerando estos valores, se proyecta que la producción global de sustancias químicas podría multiplicarse por seis para el año 2050 (**Figura 6**).

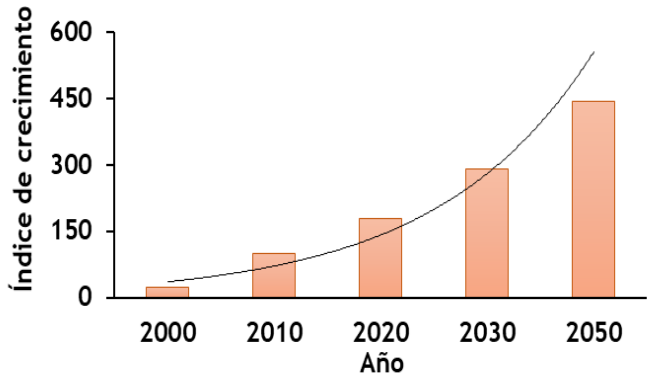

Figura 6. *Producción global de compuestos químicos*

[35] **Wang** *et al.* Toward a Global Understanding of Chemical Pollution: A First Comprehensive Analysis of National and Regional Chemical Inventories. *Environ Sci Technol.* **2020**.

[36] **Muir** *et al*. How Many Chemicals in Commerce Have Been Analyzed in Environmental Media? A 50 Year Bibliometric Analysis. *Environ Sci Technol.* **2023**.

En este contexto actual de constante crecimiento, **las agencias internacionales están demandando nuevos enfoques y metodologías** que permitan la evaluación del riesgo toxicológico de los compuestos químicos de manera eficaz, rápida y económicamente viable, facilitando además la toma de decisiones en el ámbito normativo. En este sentido, el informe "*Toxicity Testing in the 21st Century: A Vision and a Strategy*"[7], redactado por la NCR y publicado por la EPA en 2007, subraya, además, la urgencia de transformar los largos métodos tradicionales, particularmente en lo que respecta al uso de animales, en el empleo de ensayos más éticos y sostenibles.

Esto se logra a través de la implementación de **metodologías de nuevo enfoque** (NAMs), que se caracterizan por enmarcarse en el **principio de las "3Rs"**, es decir, en la **"Reducción, Refinamiento y Reemplazo"** de los animales en la investigación[37]. La **reducción** implica optimizar los diseños experimentales para obtener la mayor cantidad de información posible con el menor número de animales. El **refinamiento** se refiere a mejorar los procedimientos experimentales para minimizar el sufrimiento de los animales empleando técnicas menos invasivas. Finalmente, el **reemplazo** promueve el uso de métodos alternativos que no impliquen el uso de animales. Las NAMs integran herramientas como el **cribado de alto rendimiento**, que permite evaluar miles de compuestos de forma automatizada, así como enfoques **ómicos** (genómica, proteómica, metabolómica), que aportan información a nivel molecular sobre los mecanismos de toxicidad. A su vez, el desarrollo **AOPs** proporciona marcos para vincular eventos moleculares iniciales con efectos tóxicos finales, fortaleciendo la capacidad predictiva de estos métodos[9].

En el campo de la **ecotoxicología**, también se están aplicando estas metodologías avanzadas, enfocándose en ensayos alternativos ***in vivo*** **con embriones de peces** y sistemas ***in vitro*** **con células**, que representan alternativas éticas a los modelos tradicionales en vertebrados. Los **modelos matemáticos *in***

[7] **National Research Council**, Toxicity testing in the 21st century: A vision and a strategy. National Academies Press. **2007**.

[37] **Burden** *et al*. Pioneering Better Science through the 3Rs: An Introduction to the National Centre for the Replacement, Refinement, and Reduction of Animals in Research (NC3Rs). *J Am Assoc Lab Anim Sci.* **2015**.

silico y los **modelos de extrapolación *in vitro-in vivo*** (IVIVE) son cada vez más comunes, permitiendo hacer predicciones sobre la toxicidad y el comportamiento de las sustancias. La combinación del poder predictivo con los datos experimentales, están permitiendo avances significativos en la evaluación del riesgo ecotoxicológico.

5.1. Modelos alternativos *in vivo.*

Dentro del ámbito de la ecotoxicología, los organismos internacionales han validado un **protocolo estandarizado** para el ensayo de **toxicidad** embrión-larval (FET, *Fish Embryo Test, OECD 236*[38]). Este ensayo marcó un hito en la adopción de métodos alternativos, y actualmente, los embriones y larvas de peces se utilizan de manera extensiva para la evaluación de una amplia gama de contaminantes. En particular, los embriones y larvas del pez cebra son los modelos más empleados en estos estudios, debido tanto a las características ventajosas de la especie, descritas previamente, como a los beneficios inherentes al uso de las etapas tempranas de desarrollo.

Por un lado, la **transparencia y rapidez de desarrollo de las larvas** hacen posible la evaluación eficaz del comportamiento y toxicidad. Las larvas emergen del corion aproximadamente entre los 2 y 3 días posteriores a la fertilización (dpf) y presentan todos los órganos principales prácticamente desarrollados a los 5 dpf[39]. Por otro lado, en la Unión Europea, el uso de los embriones de pez cebra **no requieren permiso ético** para la experimentación animal hasta las 120 horas posteriores a la fertilización (hpf), momento en el que comienza la autoalimentación[40], debido a que no se consideran sistemas *in vivo* según el reglamento actual[41]. Sin embargo, fuera de lo legislativo, desde el punto de vista funcional, se puede considerar un sistema prácticamente *in vivo*, debido a que

[9] **Ankley** *et al*. Adverse outcome pathways: A conceptual framework to support ecotoxicology research and risk assessment. *Environ. Tox. Chem.* **2010**.

[38] **OECD No 236**. Fish embryo acute toxicity (FET) Test. **2013**.

[39] **Kimmel** *et al.* Stages of embryonic development of the zebrafish. *Dev Dyn.***1995**.

[40] **Strähle** *et al*. Zebrafish embryos as an alternative to animal experiments-A commentary on the definition of the onset of protected life stages in animal welfare regulations. *Reprod Toxicol.* **2012**.

[41] DIRECTIVE **2010/63/EU.** Protection of animals used for scientific purposes. **2010**.

permite estudiar procesos biológicos, donde interactúan tejidos, órganos y sistemas ya formados[42].

Sin embargo, el método validado OECD 236 con larvas de pez cebra, se basa únicamente en la evaluación de ensayos de toxicidad basados en el efecto que provoca el compuesto químico objeto de estudio. Actualmente, **no hay un método** estandarizado y validado para evaluar los procesos de **bioacumulación y biotransformación** con larvas. En este sentido, el grupo e investigación al que pertenezco (Determinación de Trazas, Especiación y Proteómica, **TrEP**), siguiendo las recomendaciones de un panel de expertos, ha desarrollado y ha estado testando con gran variedad de compuestos, un **método alternativo** basado en eleuteroembriones (etapa intermedia entre el corión y la larva formada completamente) de pez cebra para el **cálculo de BCF**[43].

El método se ha diseñado siguiendo las mismas condiciones de obtención y exposición de larvas que el modelo estandarizado de toxicidad OECD 236[38] y las mismas restricciones que la guía OECD 305[18], mencionadas en la *Sección "Bioacumulación: Determinación del BCF",* para la determinación del BCF. En el modelo desarrollado, resumido en la **Figura 7**, se sustituye el periodo de absorción y depuración por 48 y 24 horas en vez los 28 y 14 días indicados en el ensayo original estandarizado. Esta modificación, mejora significativamente la rapidez del método, reduciendo también la etapa analítica, obteniendo resultados comparables y eliminando además la experimentación animal.

[18] **OECD No 305**. Bioaccumulation in Fish: Aqueous and Dietary Exposure. **2012**.
[38] **OECD No 236.** Fish embryo acute toxicity (FET) Test. **2013**.
[42] **Lungu-Mitea** *et al.* Modeling Bioavailable Concentrations in Zebrafish Cell Lines and Embryos Increases the Correlation of Toxicity Potencies across Test Systems. *Environ Sci Technol.* **2021**.
[43] **Sanz-Landaluze** *et al.* Zebrafish (danio rerio) eleutheroembryo-based procedure for assessing bioaccumulation. *Environ Sci Technol*. **2015**.

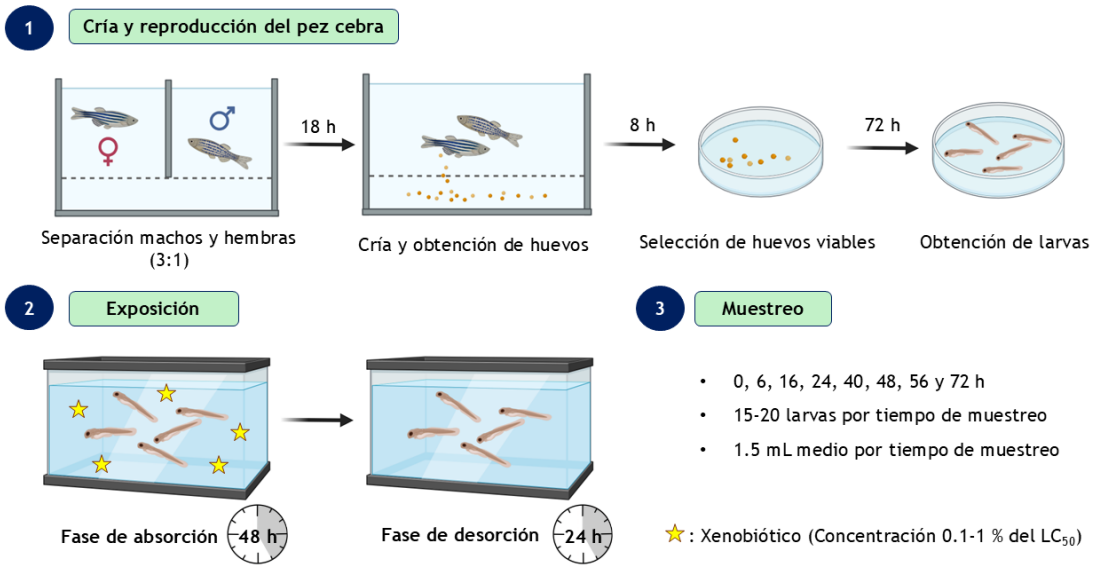

***Figura 7**. Ensayo de bioconcentración desarrollado como alternativa al modelo OECD 305 para la determinación del BCF.*

5.2. Modelos alternativos *in silico*.

Ante las dificultades de los métodos experimentales, la necesidad de evaluaciones rápidas de la toxicidad y en el marco del principio de las 3Rs, los modelos alternativos *in silico* han emergido como herramientas innovadoras y eficientes para la predicción de propiedades químicas y biológicas de sustancias[44,45].

Dentro del campo de la bioacumulación, se puede estimar utilizando modelos matemáticos cuantitativos de relaciones estructura-actividad (QSAR) y modelos de balance de masas (MBM)[46,47]. Los **modelos QSAR**, por su definición, predicen el factor de BCF basándose, únicamente, en la estructura química del compuesto. Para ello, como principal factor, se utiliza el coeficiente de partición octanol-agua (K_{ow}) de las sustancias, crucial para predecir la capacidad de acumulación en los tejidos

[44] **Cronin** *et al*. The predictivity of QSARs for toxicity: Recommendations for improving model performance. *Computational Toxicology.* **2025**.
[45] **Li**. Novel Quantitative Structure–Activity Relationship Tox21 Techniques for Combined Toxicity Prediction. *Toxicol Assessment Combined Chem in Environ*. **2025**.
[46] **Bittner** *et al*. Combined Ion-Trapping and Mass Balance Models to Describe the pH-Dependent Uptake and Toxicity of Acidic and Basic Pharmaceuticals in Zebrafish Embryos (Danio rerio). *Environ Sci Technol.* **2019**.
[47] **Veltman** *et al*. Bioaccumulation potential of air contaminants: Combining biological allometry, chemical equilibrium and mass-balances to predict accumulation of air pollutants in various mammals. *Toxicol Appl Pharmacol*. **2009**.

lipídicos de un organismo (**Tabla 1**). Por su parte, los **MBM** utilizan principios de conservación de masa para describir cómo un compuesto químico se distribuye en función de las entradas, salidas, acumulación y transformación de este dentro de un organismo. Para ello, se necesitan conocer características como el K_{ow}, la solubilidad en agua, la volatilidad, tasas cinéticas y rutas metabólicas, entre otras.

Existen diferentes programas reconocidos por las agencias internacionales como puede ser *OECD QSAR Toolbox*[48] o *EPI Suite™-Estimation Program Interface*, desarrollada por la EPA[49] o desarrolladas por expertos como la plataforma *Exposure And Safety Estimation (EAS-E) Suite*[50] y *The Bioaccumulation Assessment Tool (BAT)*[51] de *ARC Arnot Research and Consulting* (ARC). Sin embargo, aunque muchas de ellas predicen valores de BCF bastante fiables, actualmente, la incorporación de procesos de biotransformación, que mitigan la acumulación de los compuestos, aún presenta un desafío[52]. Esto es debido a que implica la integración de información sobre rutas metabólicas, enzimas involucradas y variabilidad entre especies y tipos de compuestos. Esto hace que se tengan que simplificar los procesos biológicos complejos. Por ello, los modelos *in silico* aún tienen la **dependencia** de obtener **más** cantidad de **datos experimentales** de alta calidad para mejorar los modelos existentes.

5.3. Modelos alternativos *in vitro*.

Los ensayos de toxicidad en el siglo XXI pretenden aprovechar los avances de las tecnologías celulares y moleculares para desarrollar un enfoque ético y eficaz que permita caracterizar y predecir los peligros de la exposición química en los seres humanos y al medio ambiente[7,53].

---

[7] **National Research Council**, Toxicity testing in the 21st century: A vision and a strategy. National Academies Press. **2007**.
[48] **ECHA-OECD**. OECD QSAR Toolbox (version 4.7). **2012**.
[49] **EPA.** Estimation Programs Interface SuiteTM for Microsoft® Windows, v4.11. **2012**.
[50] **ARC Arnot Research and Consulting Inc**, EAS-E Suite. Ver.0.972. **2024**.
[51] **Arnot** *et al*. A weight of evidence approach for bioaccumulation assessment. *Integr Environ Assess Manag*. **2023**.
[52] **Grasse** *et al.* Impact of Biotransformation on Internal Concentrations and Specificity Classification of Organic Chemicals in the Zebrafish Embryo (Danio rerio). *Environ Sci Techn*. **2024**.
[53] **Proença** *et al*. Effective exposure of chemicals in in vitro cell systems: A review of chemical distribution models. *Toxicol In Vitro.* **2021**.

El objetivo principal de cualquier modelo *in vitro* es simplificar las variables experimentales en condiciones bien controladas y fáciles de evaluar. Con este enfoque, el **cultivo celular** permite el mantenimiento de células conservando sus propiedades fisiológicas, bioquímicas y genéticas. Además, debido a que permiten el aislamiento de distintos componentes de órganos, pueden reflejar diferentes niveles de organización celular y comportamiento, y proporcionar diferentes grados de información relevante[54]. Se distinguen tres tipos de cultivo celular:

- **Cultivo primario:** Formado por células que se cultivan directamente a partir de un tejido u órgano de un organismo vivo, normalmente disgregándolas de forma mecánica o enzimática. Son las células más representativas de las funcionalidades y complejidades originales del tejido del que se aislaron. Sin embargo, la mayoría de los cultivos primarios suelen ser heterogéneos, tienen fracción de crecimiento baja y una vida útil corta[55].
- **Líneas celulares establecidas:** Cuando las células de un cultivo primario proliferan (fase exponencial) y alcanzan la confluencia (ocupan toda la superficie disponible de cultivo), es necesario dividirlas (subcultivo) debido a que el contacto entre ellas mismas inhibe su crecimiento (fase de Plateu) (**Figura 8a**). Los sucesivos cultivos, así formados, se convierten en una línea celular. Este nuevo cultivo tiene una población homogénea y puede mantener sus características hasta 20-100 generaciones (**línea celular finita**)[54]. Después de ese límite, las células entran en una fase denominada senescencia en la que pierden su capacidad de proliferar y mueren. Algunas células evitan esta fase y dan lugar a **líneas celulares continuas o inmortalizadas** (**Figura 8b**). Dentro de la inmortalización, pueden encontrarse células cancerosas o no cancerosas. Las **células cancerosas** crecen con un ritmo de proliferación más rápido, incluso descontrolado. El inconveniente de estas células es que se transforman perdiendo parte de su función especializada (desdiferenciación), a diferencia de las **células inmortalizadas no cancerosas**, que mantienen propiedades fisiológicas más cercanas a las de tejidos normales. El uso de células inmortalizadas se ha generalizado enormemente en la mayoría de los estudios debido a que presentan resultados reproducibles, son económicas,

[54] **Astashkina** *et al.* A critical evaluation of in vitro cell culture models for high-throughput drug screening and toxicity. *Pharmacol Ther.* **2012**.
[55] **Philippeos** *et al*. Introduction to cell culture. *Methods Mol Biol.* **2012**.

pueden almacenarse en criopreservación y son fáciles de mantener y cuidar, sin tener que fabricar nuevas células primarias desde un organismo vivo[56].

- **Cultivos celulares tridimensionales (3D)**: A diferencia de los cultivos convencionales en 2D, donde las células crecen en una superficie plana (en monocapa/adherentes o en suspensión), los cultivos 3D recrean las interacciones célula-células y célula-matriz extracelular en todas las direcciones. Estos cultivos representan un enfoque más avanzado debido a que simulan mejor la estructura y función de los tejidos *in vivo*, por lo que se utilizan para estudiar procesos más complejos. Sin embargo, presentan mayores desafíos técnicos, reproducibles y económicos[57].

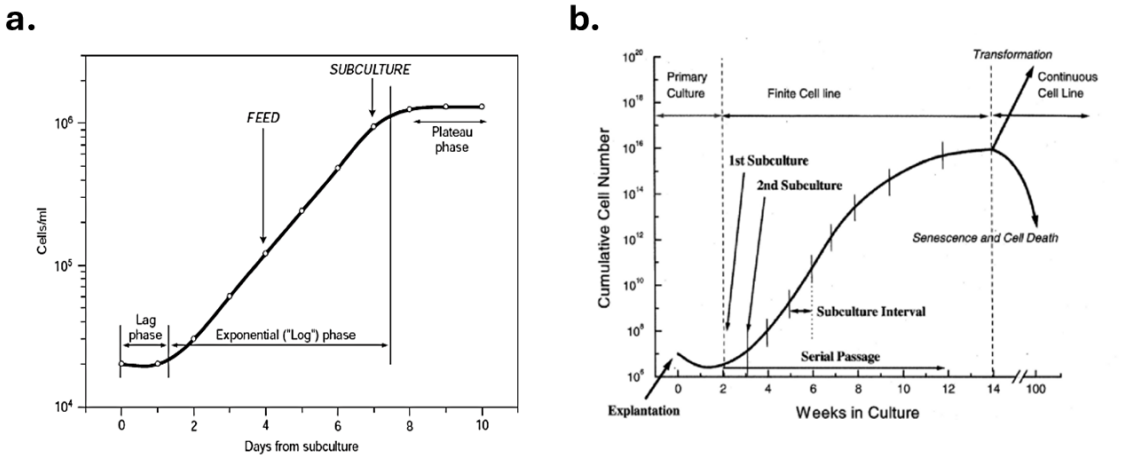

***Figura 8**. Fases de crecimiento de un cultivo celular (a) y formación de líneas celulares a partir de un cultivo primario (b).*

Para evaluar la toxicidad de compuestos químicos, es crucial seleccionar el modelo celular y tipo de ensayo adecuados según el objetivo del estudio para obtener resultados más representativos y relevantes. La **elección del modelo celular** depende de factores como el organismo de referencia (mamíferos o peces), el tipo de toxicidad a investigar (aguda, crónica o dirigida) y las capacidades funcionales de las células en cuestión. Por ejemplo, los ensayos con líneas celulares derivadas de peces pueden ser ideales para estudios relacionados con toxicidad ambiental en ecosistemas acuáticos, mientras que los modelos de células de

[56] **Bols** *et al.* Use of fish cell lines in the toxicology and ecotoxicology of fish. Piscine cell lines in environmental toxicology. *Biochemistry and Molecular Biology of Fishes.* **2005**.
[57] **Haycock**. 3D Cell Culture: A Review of Current Approaches and Techniques. *Methods Mol Biol.* **2011**.

mamíferos son más adecuados para evaluar efectos en la salud humana. Además, si se decide un tipo celular de tejido específico como las neuronales, se puede centrar la investigación en toxicidad dirigida, en este caso la neurotoxicidad. Por otro lado, células con alta actividad metabólica, como hepatocitos (células de hígado), son cruciales para ensayos que exploren la detoxificación de compuestos; mientras que las células intestinales sirven para estudios de permeabilidad y transporte a través de la membrana celular. Algunos de los modelos celulares mayormente utilizados en la evaluación de la toxicidad de contaminantes ambientales se muestran en la **Tabla 3**.

***Tabla 3**. Modelos celulares mayormente utilizados en toxicología ambiental.*

Clasificación	Línea celular	Especie	Tejido de origen
Inmortalizada Cancerosa	HeLa	*Homo sapiens* (humano)	Útero
	HepG2		Hígado
	Caco-2		Intestino, Colon
	SH-SY5Y		Neuroblastoma
	Neuro-2a	*Mus musculus* (ratón)	Neuroblastoma
Inmortalizada No cancerosa	RTgill-W1	*Oncorhynchus mykiss* (trucha arcoíris)	Branquia
	RTL-W1		Hígado
	RTgutGC		Intestino
	ZF4	*Danio rerio* (pez cebra)	Embrión
	ZFL		Hígado

Varios estudios[58,59] propusieron en la primera década de este siglo el uso de líneas celulares de peces como alternativa no animal en ecotoxicología. Después de años de investigación, finalmente se culminó en la publicación de la **directriz 249** de la OECD[60] basada en el uso de la línea celular RTgill-W1 para los **ensayos de toxicidad**.

[58] **Castaño** *et al.* The Use of Fish Cells in Ecotoxicology. *ATLA*. **2003**.
[59] **Schirmer**. Proposal to improve vertebrate cell cultures to establish them as substitutes for the regulatory testing of chemicals and effluents using fish. *Toxicology.* **2006**.
[60] **OECD 249**. Fish Cell Line Acute Toxicity: The RTgill-W1 cell line assay. **2021**.

En el caso de la **bioacumulación**, actualmente no hay un método *in vitro* validado, completamente experimental, para la determinación del BCF. Una de las principales razones es la discrepancia entre la concentración nominal de efecto (C_{nom}) y la **concentración biodisponible** (C_{free}) en los sistemas basados en células. La dificultad encontrada hasta ahora es la complejidad experimental para la cuantificación de las concentraciones en el interior celular y biodisponible en el medio. Esta discrepancia entre C_{nom} y C_{free} provoca que los estudios *in vitro* sean menos sensibles y comparables con los estudios *in vivo* (se profundiza más adelante, en la *Sección 5.3.1. "Concentración biodisponible"*). Esto se debe esencialmente a que los ensayos con peces o embriones se exponen en agua en recipientes de vidrio, mientras que las células se exponen en placas de plástico con medios complejos que contienen suero, proteínas y lípidos que pueden retener los compuestos[61].

En los últimos años, se está centrando el esfuerzo en el desarrollo de técnicas de **extrapolación *in vitro-in vivo*** (IVIVE) para solventar esta problemática, a partir de células derivadas de peces[62]. La OECD ha elaborado una guía OECD No. 280[63] basada en un modelo IVIVE para la determinación del BCF. Este modelo se considera un método alternativo mixto, debido a que consta de una parte experimental *in vitro* y una parte de extrapolación matemática *in silico* (se profundiza más adelante en la *Sección 5.4. "Modelo alternativo IVIVE"*). La ventaja que presenta, con respecto a otros modelos, es que tiene en cuenta la tasa de biotransformación del compuesto en el organismo para no sobreestimar la acumulación, determinada únicamente mediante el coeficiente K_{ow}[64]. Para ello, se evalúa el aclaramiento hepático *in vitro* a través del enfoque de agotamiento del sustrato en hepatocitos recién aislados y criopreservados (RT-HEP) o fracciones

[61] **Segner**. Cytotoxicity Assays with Fish Cells as an Alternative to the Acute Lethality Test with Fish. *ATLA.* **2004**.
[62] **Stadnicka-Michalak** *et al.* Measured and modeled toxicokinetics in cultured fish cells and application to in vitro - In vivo toxicity extrapolation. *PLoS ONE.* **2014**.
[63] **OECD No. 280**. Guidance document on the determination of in vitro intrinsic clearance using cryopreserved hepatocytes (RT-HEP) or liver S9 sub-cellular fractions (RT-S9) from rainbow trout and extrapolation to in vivo intrinsic clearance series on testing and assessment. **2018**.
[64] **Laue** *et al.* Examining Uncertainty in in Vitro-In Vivo Extrapolation Applied in Fish Bioconcentration Models. *Environ Sci Technol*. **2020**.

hepáticas subcelulares S9 (RT-S9) del pez trucha arcoíris, desarrollado por Nichols *et. al*[65] y descrito en las guías OECD 319 A/B[27,28].

5.3.1. Concentración biodisponible.

La **concentración libre biodisponible** (C_{free}) es aquella que es totalmente accesible para ser internalizada por la célula. En los sistemas *in vitro*, la **concentración nominal** (C_{nom}), es decir, aquella que se añade al medio de exposición para realizar el ensayo, se reparte en los diferentes compartimentos del sistema[53]:

- **Sorción al plástico:** Los ensayos *in vitro* actuales se realizan mayormente en materiales de poliestireno. Aunque la superficie se trata para hacer su superficie más hidrofílica y con carga negativa para facilitar la adhesión celular, los compuestos con propiedades hidrofóbicas (log K_{ow} > 3) van a quedarse en parte, retenidos en ella. El equilibrio se describe por el coeficiente de partición aparente ($K_{PS/medio}$) para determinar la fracción asociada al plástico de la superficie de cultivo.
- **Unión al suero del medio de cultivo:** Los medios de cultivo de las células, normalmente, se suelen complementar con un 2-20% de suero fetal bovino (FBS) para favorecer su crecimiento. Esta adición, incrementa las concentraciones de proteínas y lípidos en el medio, provocando la unión de los compuestos a su superficie. La proteína globular albúmina de suero bovino (BSA) representa el 60% (51-84%, según el lote) de la proteína total del FBS. Tiene tres dominios con dos subdominios cada uno, cuyas cavidades de unión median interacciones hidrofóbicas y contienen un pequeño grupo de aminoácidos cargados positivamente que pueden

[27] **OECD No 319A**. Determination of in vitro intrinsic clearance using cryopreserved rainbow trout hepatocytes (RT-HEP). **2018**.
[28] **OECD No 319B**. Determination of in vitro intrinsic clearance using rainbow trout liver S9 sub-cellular fraction (RT-S9). **2018**.
[53] **Proença** *et al*. Effective exposure of chemicals in in vitro cell systems: A review of chemical distribution models. *Toxicol In Vitro.* **2021**
[65] **Nichols** *et al.* Toward improved models for predicting bioconcentration of well-metabolized compounds by rainbow trout using measured rates of in vitro intrinsic clearance. *Environ Toxicol Chem*. **2013**.

interactuar con grupo electronegativos[66]. El equilibrio se describe por el coeficiente de partición aparente ($K_{albúmina/medio}$) para determinar la fracción asociada a la unión con el suero del medio de cultivo.

- **Pérdida en la fase gaseosa:** La mayoría de los ensayos *in vitro* son sistemas semiabiertos para permitir el flujo de aire. Debido a esto, se hace difícil alcanzar el equilibrio y, por tanto, la disminución de la concentración nominal se debe a pérdidas por evaporación. Esta pérdida suele suceder en sustancias químicas con una constante de la ley de Henry (K_H) de 1-10 $Pa \cdot m^3 \cdot mol^{-1}$[67].
- **Absorción en la célula:** La concentración en el interior celular (C_{cell}) es el resultado de la absorción de la sustancia química por la célula. Este valor está basado en coeficientes de partición, permeabilidad y tasas de metabolismo. Por tanto, el proceso de equilibrio se produce con los lípidos que forman la membrana ($K_{lípidos/medio}$).

Esta distribución de C_{nom}, rebaja la concentración accesible y, por tanto, la concentración internalizada en las células (C_{cell}). Por tanto, la relación C_{nom}, C_{free} y C_{cell} depende de los procesos de distribución química en los diferentes equilibrios entre los compartimentos del sistema (**Figura 9**)[68].

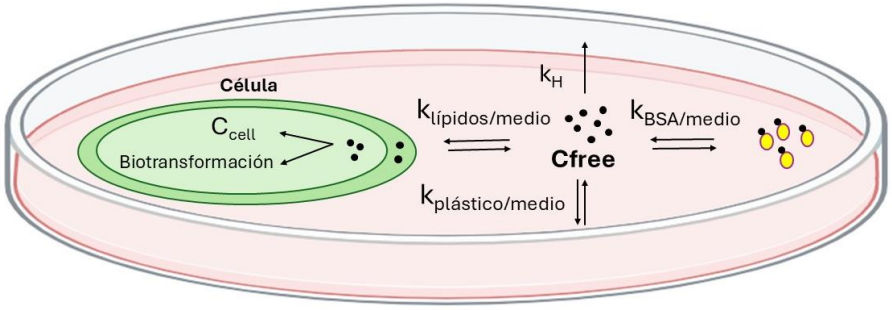

Figura 9. *Equilibrios de distribución química entre los compartimentos del sistema in vitro.*

[66] **Rostamnezhad and Fatemi**. Comprehensive investigation of binding of some polycyclic aromatic hydrocarbons with bovine serum albumin: Spectroscopic and molecular docking studies. *Bioorg Chem.* **2022**.

[67] **OECD No. 23**. Guidance Document on aqueous-phase aquatic toxicity testing of difficult test chemicals. **2019**.

[68] **Kramer** et al. Quantifying processes determining the free concentration of phenanthrene in basal cytotoxicity assays. *Chem Res Toxicol*. **2012**.

En la mayoría de los ensayos de toxicidad, es muy común utilizar la concentración nominal para evaluar el efecto de un compuesto. Sin embargo, para cuantificar la bioacumulación se tiene que relacionar la concentración dentro del organismo o la célula (C_{cell}) con la concentración en el medio. En **compuestos orgánicos con propiedades hidrofóbicas**, la discrepancia entre los valores C_{free} y C_{nom} se incrementa significativamente[53,69] y, por tanto, la consideración única de C_{nom} puede ocasionar subestimaciones del BCF y, con ello, una evaluación errónea del comportamiento de la sustancia[42,70]. Por ello, actualmente, se está haciendo un esfuerzo en la comprensión de los diferentes equilibrios, la determinación de las constantes de partición y la estimación de C_{free}. Sin embargo, su aplicación en estudios de toxicidad y bioacumulación aún no está tan avanzado.

Actualmente, se están desarrollando diferentes aproximaciones para la **determinación de C_{free}**:

- **Modelos de balance de masa** (MBM): La estrategia es determinar las fracciones de unión del compuesto en cada compartimiento del sistema *in vitro* del ensayo para predecir C_{free} a partir de C_{nom}. Para ello, se utilizan un conjunto de ecuaciones que describen los procesos de distribución química en los diferentes equilibrios. Estas ecuaciones dependen de las condiciones de ensayo (tamaño de la placa de cultivo, porcentaje de FBS en el medio de cultivo, número y tipo de células, tipo y componentes del medio celular, etc.), las propiedades químicas del compuesto a estudiar y las constantes de partición que describen los equilibrios.

  Sin embargo, aunque se está demostrando que obtienen buenas aproximaciones, todavía presentan algunas **limitaciones**:

  - Actualmente, un solo modelo no es capaz de tener en cuenta todos los equilibrios y procesos que ocurren el sistema *in vitro*. Esto es debido a que las variables son muy diversas dependiendo del

[42] **Lungu-Mitea** *et al.* Modeling Bioavailable Concentrations in Zebrafish Cell Lines and Embryos Increases the Correlation of Toxicity Potencies across Test Systems. *Environ SciTechnol.* **2021**.
[53] **Proença** *et al*. Effective exposure of chemicals in in vitro cell systems: A review of chemical distribution models. *Toxicol In Vitro.* **2021**
[69] **Huchthausen** *et al*. Experimental Exposure Assessment of Ionizable Organic Chemicals in in Vitro Cell-Based Bioassays. *Chem Res Toxicol*. **2020**.
[70] **Henneberger** *et al*. Quantitative in Vitro-to- In Vivo Extrapolation: Nominal versus Freely Dissolved Concentration. *Chem Res Toxicol*. **2021**.

experimento que se quiera realizar en cada investigación. Además, como aún están en investigación y desarrollo, los autores se centran en el estudio independiente de los equilibrios más representativos para la comprensión del comportamiento de cada tipo de compuesto y determinación de las contantes de partición.

- Hay tipos de líneas celulares y compuestos nuevos en los que aún se desconoce su composición lipídica y constantes de partición, respectivamente.
- Aquellos modelos que, además de C_{free}, estiman C_{cell}, no suelen tener en cuenta los procesos de biotransformación y mecanismos específicos de absorción.

- **Determinación analítica:** La estrategia analítica para la determinación de la concentración libre, experimentalmente, es utilizar herramientas que emplean matrices que extraen sustancias químicas no unidas, como recubrimientos poliméricos en **microextracción en fase sólida** (SPME) o membranas de diálisis. Actualmente, SPME (se profundiza en la *Sección 7.2.2. "Cuantificación de la concentración biodisponible".*) es el método más prometedor para determinar C_{free} de sustancias químicas hidrófobas[71]. Aunque se ha demostrado su integración en flujos de trabajo de bioensayos, con volúmenes de muestra pequeños y matrices biológicas ricas en proteínas y lípidos, una de las limitaciones que presenta es la dificultad experimental.

5.4. Modelo alternativo IVIVE.

Los modelos alternativos de extrapolación *in vitro-in vivo* (IVIVE) son **herramientas computacionales y experimentales** que permiten predecir la toxicidad y bioacumulación de sustancias químicas sin la necesidad de realizar ensayos extensivos en animales. Estos modelos combinan datos obtenidos de estudios *in vitro* con enfoques de modelado matemático y toxicocinético para estimar la absorción, distribución, metabolismo y excreción de compuestos en

[71] **Birch** *et al.* Time-Resolved Freely Dissolved Concentrations of Semivolatile and Hydrophobic Test Chemicals in In Vitro Assays - Measuring High Losses and Crossover by Headspace Solid-Phase Microextraction. *Chem Res Toxicol*. **2019**.

organismos vivos. Su uso es fundamental en la toxicología moderna, ya que mejora la eficiencia de las evaluaciones, reduce costos y minimiza el uso de animales en la experimentación.

Como se ha mencionado, la OECD ha elaborado una guía (OECD No. 280)[63] basada en un **modelo BCF-IVIVE** desarrollado por Nichols *et al.*[65] para la determinación del BCF ($L \cdot kg^{-1}$), según la **Ecuación 5**.

$$BCF_K = \frac{C_{fiss,ss}}{C_{W/TOT}} = \frac{k_1}{k_2 + k_E + k_G + k_{MET}} \qquad Ec.(5)$$

Donde, la **concentración del compuesto** total en los peces en estado estacionario ($C_{fish,ss}$; $mg \cdot kg^{-1}$) se predice utilizando el modelo matemático de 1 compartimento desarrollado por Arnot y Gobas[72]. Es importante destacar que estos modelos predicen el BCF para un **pez estandarizado** (10 g de trucha arcoíris con un 5% de lípidos en todo el cuerpo), que es el típico de los peces que suelen someterse a pruebas *in vivo* con arreglo a la guía OECD 305[18]. El cálculo incluye constantes de velocidad que describen la absorció n química (k_1, $L \cdot d^{-1} \cdot kg^{-1}$), pérdida a través de las branquias (k_2, d^{-1}), la tasa de egestión fecal (k_E, d^{-1}) y la tasa de crecimiento (k_G, d^{-1}), aunque esta última no se tiene en cuenta en el modelo y se fija en 0. Estas constantes se determinan mediante ecuaciones, basadas, principalmente, en el coeficiente de partición octanol-agua (K_{ow}) del compuesto. La **concentración total en el medio** ($C_{W/TOT}$, $mg \cdot L^{-1}$) se corresponde con la concentración nominal de ensayo. A diferencia de todos los parámetros mencionados, determinados *in silico*, la **constante de metabolización** (k_{MET}, d^{-1}), se estima experimentalmente mediante un ensayo *in vitro*, cuyo valor luego se extrapola matemáticamente a un valor *in vivo*. Para la determinación de k_{MET}, se realizan los cálculos secuenciales que se resumen a continuación (debido a la

[18] **OECD No 305**. Bioaccumulation in Fish: Aqueous and Dietary Exposure. **2012**.
[63] **OECD No. 280**. Guidance document on the determination of in vitro intrinsic clearance using cryopreserved hepatocytes (RT-HEP) or liver S9 sub-cellular fractions (RT-S9) from rainbow trout and extrapolation to in vivo intrinsic clearance series on testing and assessment. **2018**.
[65] **Nichols** *et al.* Toward improved models for predicting bioconcentration of well-metabolized compounds by rainbow trout using measured rates of in vitro intrinsic clearance. *Environ Toxicol Chem*. **2013**.
[72] **Arnot and Gobas**. A Generic QSAR for Assessing the Bioaccumulation Potential of Organic Chemicals in Aquatic Food Webs. *QSAR Comb. Sci.* **2003**.

complejidad y extensión de las ecuaciones, únicamente se muestran los aspectos más representativos):

1) Se determina la **tasa de eliminación** (k_e, h^{-1}) mediante el **enfoque de agotamiento de sustrato**, según la guía OECD No. 319A[27] (utilizando hepatocitos de trucha arcoíris, RT-HEP) o OECD No. 319B[28] (utilizando fracciones subcelulares S9 de hígado de trucha arcoíris, RT-S9). De aquí en adelante, se van a mostrar, únicamente, los cálculos para el uso de hepatocitos, debido a la semejanza con los experimentos y cálculos realizados en esta Tesis Doctoral y que se explicarán más en profundidad en sucesivos capítulos. Para ello, se realiza un ensayo en el que se miden las **concentraciones experimentales** de sustrato en el medio de exposición a lo largo del tiempo. Estas concentraciones, transformadas en $\log_{10}$, se representan frente al tiempo y, k_e se determina según la **Ecuación 6**.

$$k_e = -2.3 \times pendiente\ del\ descenso\ log.lineal \qquad Ec.(6)$$

Aunque en la guía oficial no se contempla, según el estudio posterior de Black *et al.*[73] se debe aplicar una corrección al valor de k_e en experimentos con compuestos orgánicos con tendencia a **pérdidas** abióticas debidas a la **volatilización**. Para la aplicación del **factor de corrección** se tienen que cumplir los siguientes requisitos: i) las pérdidas abióticas debidas a la volatilización no están dentro de un margen aceptable del 80-120%, ii) el proceso de pérdida muestra una cinética de primer orden y iii) la relación entre k_e y la constante de velocidad de volatilizació n (k_{volat}) es inferior a 10 ($k_e/k_{volat} < 10$). Esta constante se determina representando concentraciones medidas experimentalmente en el medio de exposición de un experimento paralelo sin células en el sistema *in vitro*, a las mismas condiciones de ensayo, frente al tiempo. La corrección se basa en restar la pendiente de k_{volat} y la pendiente de k_e. La constante corregida por las pérdidas abióticas

[27] **OECD No 319A**. Determination of in vitro intrinsic clearance using cryopreserved rainbow trout hepatocytes (RT-HEP). **2018**.
[28] **OECD No 319B**. Determination of in vitro intrinsic clearance using rainbow trout liver S9 sub-cellular fraction (RT-S9). **2018**.
[73] **Black** *et al*. Evaluation and comparison of in vitro intrinsic clearance rates measured using cryopreserved hepatocytes from humans, rats, and rainbow trout. *Toxicology*. **2021**.

($k_{e,loss}$) se determina del mismo modo, utilizando la **Ecuación 6** y es el valor que se debe utilizar en los posteriores cálculos del modelo.

2) Siguiendo de nuevo la guía OECD 2018, se calcula la tasa de **aclaramiento intrínseco *in vitro*** ($CL_{IN\ VITRO,INT}$, $ml \cdot h^{-1} \cdot 10^{-6}$ células). El cálculo utiliza la normalización de la tasa de eliminación con respecto a la concentración de células (C_{HEP}, 10^6 células$\cdot mL^{-1}$) utilizadas en el experimento (**Ecuación 7**).

$$CL_{IN\ VITRO,INT} = \frac{k_e}{C_{HEP}} \qquad Ec.(7)$$

3) Se multiplica por el contenido de células en el hígado ($510 \cdot 10^6$ células/g hígado) y el peso fraccional del hígado (0.015 g hígado/ g pez), basado en estudios previos realizados por los autores y descritos anteriormente, para un pez estandarizado (**Ecuación 8**). De esta forma, se extrapola el valor *in vitro* para obtener el **aclaramiento intrínseco *in vivo*** ($CL_{IN\ VIVO,INT}$, $L \cdot d^{-1} \cdot kg^{-1}$ pez).

$$CL_{IN\ VIVO,INT} = CL_{IN\ VITRO,INT} \times \frac{células}{g\ hígado} \times \frac{g\ hígado}{g\ pez} \qquad Ec.(8)$$

4) El aclaramiento intrínseco se convierte en una estimación del **aclaramiento hepático *in vivo*** (CL_H; $L \cdot d^{-1} \cdot kg^{-1}$ pez) utilizando el **modelo de hígado bien agitado**[74]. Este cálculo aplica factores de corrección que tienen en cuenta las posibles limitaciones de velocidad impuestas por el flujo sanguíneo hepático (Q_H) y los posibles efectos de unión química (f_u), basados en el coeficiente de partición sangre-agua (P_{BW}), K_{ow}, entre otros.

$$CL_{IN\ VIVO,INT} \xrightarrow{Q_H,\ f_u,\ P_{BW},\ K_{ow}} CL_H$$

5) Finalmente, **k_{MET}**, referido a todo el cuerpo, se calcula dividiendo CL_H por el volumen aparente de distribución de la sustancia química ($V_{D,BL}$, $L \cdot kg^{-1}$) (**Ecuación 9**). Este volumen, está referido a la concentración química en sangre, estimada como la relación de los coeficientes de partición pez-agua y sangre-agua, cada uno de los cuales se calcula utilizando algoritmos basados en log K_{ow}.

[74] **Nichols** *et al.* Hepatic clearance of 6 polycyclic aromatic hydrocarbons by isolated perfused trout livers: Prediction from In vitro clearance by liver S9 fractions. *Toxicol Sci*. **2013**.

$$k_{MET} = \frac{CL_H}{V_{D,BL}} \qquad Ec.(9)$$

En la guía oficial, además de proporcionar la orientación para predecir el BCF, los propios autores muestran las incertidumbres y **limitaciones del modelo**. Algunas de las limitaciones más importantes recogidas en la guía, junto con limitaciones adiciones observadas en estudios posteriores de otros autores[75] y durante el desarrollo de esta Tesis Doctoral son:

- Los sistemas de ensayo RT-HEP y RT-S9 tienen una vida útil corta, limitada a 2-4 h de exposición[76,77]. Por tanto, el modelo no es válido para el estudio de compuestos con cinética de biotransformación lenta.
- El modelo se ha desarrollado para sustancias químicas orgánicas neutras bien metabolizadas con log K_{ow} entre 3-8.
- En el caso de algunas sustancias químicas hidrófobas, hay una escasa correlación entre los BCF empíricos y los BCF predichos utilizando el supuesto de unión modelizado completo f_u.
- Se utiliza la concentración nominal (C_{nom}) para los cálculos del BCF ($C_{fiss}/C_{w,TOT}$) y no se tiene en cuenta la C_{free}. Henneberger *et al.*[70] informan de que, aunque $IVIVE_{nom}$ puede ser útil y es un modelo que se puede considerar conservador, se debe dar preferencia a $IVIVE_{free}$ debido a las diferencias de biodisponibilidad entre *in vitro* e *in vivo*.
- Los sistemas *in vitro* RT-HEP y RT-S9 son cultivos primarios recién obtenidos del organismo vivo. Por tanto, aunque en menor medida, siguen requiriendo el sacrificio de peces. Además, la actividad de estos puede variar en función del estado y cepa del pez, la temporada y el procedimiento de aislamiento[78].

---

[70] **Henneberger** *et al.* Quantitative in Vitro-to- In Vivo Extrapolation: Nominal versus Freely Dissolved Concentration. *Chem Res Toxicol*. **2021**.

[75] **Kosfeld** *et al.* Comparison of Alternative Methods for Bioaccumulation Assessment: Scope and Limitations of In Vitro Depletion Assays with Rainbow Trout and Bioconcentration Tests in the Freshwater Amphipod Hyalella Azteca. *Environ Toxicol Chem*. **2020**.

[76] **Fay** *et al.* Determination of metabolic stability using cryopreserved hepatocytes from rainbow trout (Oncorhynchus mykiss). *Curr Protoc Toxicol.* **2015**.

[77] **Johanning** *et al.* Assessment of metabolic stability using the rainbow trout (Oncorhynchus mykiss) liver S9 fraction. *Curr Protoc Toxicol.* **2012**.

[78] **Balk** *et al*. Investigating the bioaccumulation potential of anionic organic compounds using a permanent rainbow trout liver cell line. *Environ Int.* **2023**.

- Sobrepredicción de la cinética de biotransformación con el enfoque de agotamiento del sustrato debido a que solo se basa en la medición de la concentración en el medio de exposición. Dicho enfoque supone que toda la bajada de concentración en el medio es debida a la biotransformación. Sin embargo, las células utilizadas pueden a su vez bioacumular compuesto, que no es biotransformado y, por tanto, no se contempla en la estimación.
- No se determina, de forma experimental, la concentración en el interior celular. La estimación se realiza mediante modelos empíricos basados, únicamente, en las propiedades químicas del compuesto, como K_{ow}. Por tanto, no se tiene en cuenta, los mecanismos de absorción y transporte dependientes del organismo de estudio.

Teniendo en cuenta estas limitaciones, los **propios autores** de la guía OECD, **solicitan más estudios** sobre otras sustancias químicas, para ampliar el dominio de aplicabilidad del método. Además, requieren de más investigación para proporcionar más datos y mejorar el rendimiento para solventar las limitaciones mostradas.

6. Contaminantes Orgánicos Persistentes (POPs).

Los **Contaminantes Orgánicos Persistentes** (POPs, por sus siglas en inglés) son una serie de moléculas orgánicas que poseen propiedades fisicoquímicas tales que son capaces de persistir **intactas en el medio ambiente** durante mucho tiempo al resistir la degradación fotolítica, química y biológica que se dan en el ambiente[79,80].

Los POPs están en **continuo movimiento** migrando entre aire, agua, suelos y sedimentos, encontrándose a altas y bajas concentraciones. Debido a su carácter **semivolátil**, se transportan a grandes distancias en la atmósfera. Los POPs son poco solubles en agua, sin embargo, se adsorben en las partículas en suspensión tanto del aire, de aguas dulces y aguas marinas. Debido a su **carácter hidrofóbico**, se acumulan fácilmente en sedimentos y tejidos grados de los seres vivos. Esta

[79] **Aktar** *et al*. Persistent Organic Pollutants (POPs): Sources, types, impacts and their remediation. *Environ Poll Remediation*. **2021**.
[80] **El-Shahawi** *et al.* An overview on the accumulation, distribution, transformations, toxicity and analytical methods for the monitoring of persistent organic pollutants. *Talanta*. **2010**.

propiedad ocasiona que se introduzcan fácilmente en la cadena alimentaria, incrementando su concentración provocando efectos de **bioacumulación y biomagnificación**[81]. Los diferentes estudios sobre la **toxicidad** de los POPs han demostrado que pueden provocar algunos tipos de cáncer, defectos congénitos y disfunciones de los sistemas inmunitario, endocrino y reproductor. Por tanto, los POPs pueden causar un importante impacto en el medioambiente y en la salud de los seres vivos en el presente y en el futuro.

La **clasificación de POPs** puede ser según sus fuentes o sus usos (**Figura 10**). Tras la Segunda Guerra Mundial, se crearon gran variedad de sustancias químicas con **origen antropogénico** para erradicar plagas, enfermedades o mejorar la agricultura, la industria y la calidad de vida. Entre estos compuestos, se encuentran los pesticidas o retardantes de llama, como los éteres difenílicos polibromados (PBDEs), entre otros. Sin embargo, hay POPs como los hidrocarburos aromáticos policíclicos (PAHs) que también pueden tener **origen natural**, formados principalmente por combustión, en actividades volcánicas, incendios forestales o algunos procesos químicos en las industrias[82,83].

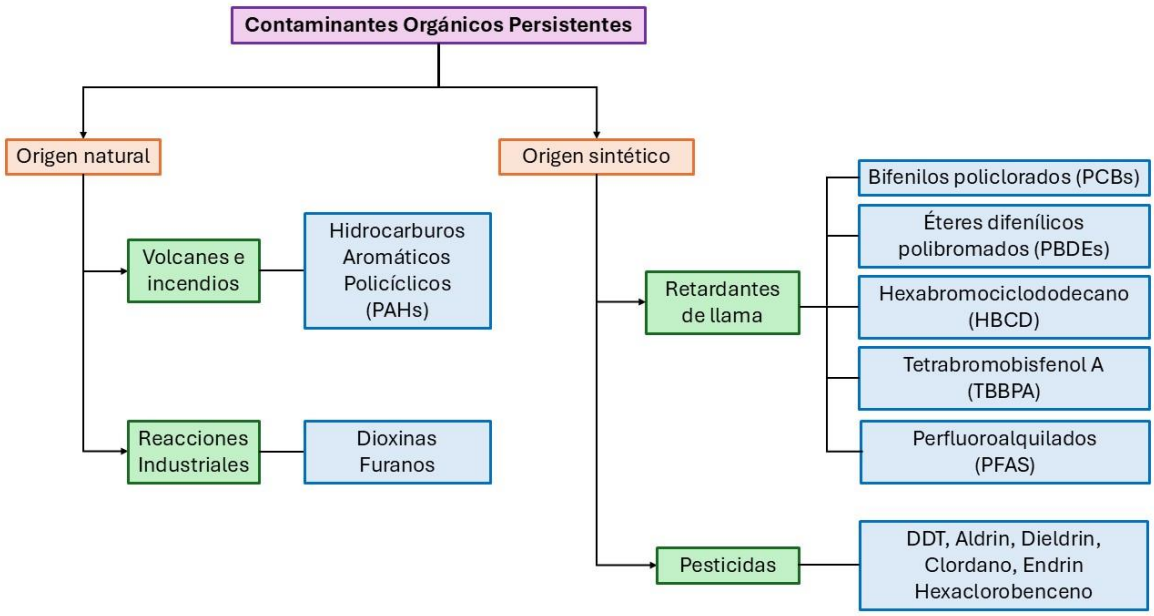

Figura 10. *Origen y tipos de Contaminantes Orgánicos Persistentes (POPs).*

[81] **Han and Currell**. Persistent organic pollutants in China's surface water systems. *Sci Total Environ.* **2017**.
[82] **Gong** *et al.* Persistent organic pollutant cycling in forests. *Nat Rev Earth Environ.* **2021**.
[83] **Najam and Alam**. Occurrence, Distribution, and Fate of Emerging Persistent Organic Pollutants (POPs) in the Environment. *Emerging Contaminants and Plants*. **2023**.

Con el objetivo de reducir o eliminar las emisiones de los POPs en el medio ambiente, en 1998 se creó el **Protocolo Aarhus**, firmado por la Comisión Económica de las Naciones Unidas para Europa[84]. Sus bases se centraron en la transparencia de uso y producción de algunos compuestos químicos de origen antropogénico, así como, la responsabilidad de reducir emisiones de compuestos de origen natural. Al principio, enumeraba 21 sustancias diferentes: 16 plaguicidas/pesticidas, 2 productos químicos industriales (PCBs y hexaclorobenceno) y 3 subproductos (PAHs, dioxinas y furanos).

Con las bases sentadas en el Protocolo Aarhus, el Programa de las Naciones Unidas para el Medio Ambiente creó el **Convenio de Estocolmo** en 2001[85]. El objetivo del Convenio era el mismo que el Protocolo Aarhus, proteger a los seres humanos y el medioambiente, eliminando los productos químicos peligroso y persistentes. La mejora llevada a cabo fue la inclusión de mecanismos más estrictos para eliminar y regular los POPs, además de expandir su alcance a nivel global. Inicialmente, en 2004, se prohibieron 12 compuestos conocidos como "la docena sucia" (**Figura 11**). La eliminación de algunos POP en su lista fue debido a diferencias en sus enfoques y criterios de selección. El Protocolo Aarhus tenía un enfoque más focalizado en la contaminación ambiental del aire y el Convenio de Estocolmo se centró en fuentes industriales y agrícolas, más controlables a nivel mundial. Por tanto, compuestos como PAHs y hexaclorobenceno, quedaron fuera del Convenio, aunque este último se incluyó años más tarde. Sin embargo, los PAHs siempre se han reconocido como potenciales POPs[84] y, más tarde, entrarían en regulación alimentaria[86]. A lo largo de los años se han ido realizando reuniones donde se han añadido nuevos compuestos en la lista del Convenio de Estocolmo, sumando un total de 29 compuestos actualmente[87] (**Figura 11**).

---

84 **Kumar** *et al.* Persistent organic pollutants in water resources: Fate, occurrence, characterization and risk analysis. *Sci Total Environ*. **2022**.

85 **Xu** *et al*. Analytical chemistry of the persistent organic pollutants identified in the Stockholm Convention: A review. *Anal Chem Acta.* **2013**.

86 **CE No 1881/2006**. REGLAMENTO (CE) No 1881/2006 por el que se fija el contenido máximo de determinados contaminantes en los productos alimenticios. EUR-Lex.

87 **UNEP**. UNITED NATIONS SC Stockholm Convention on Persistent Organic Pollutants Preliminary report for the effectiveness evaluation of the Stockholm Convention pursuant to Article 16. **2022**.

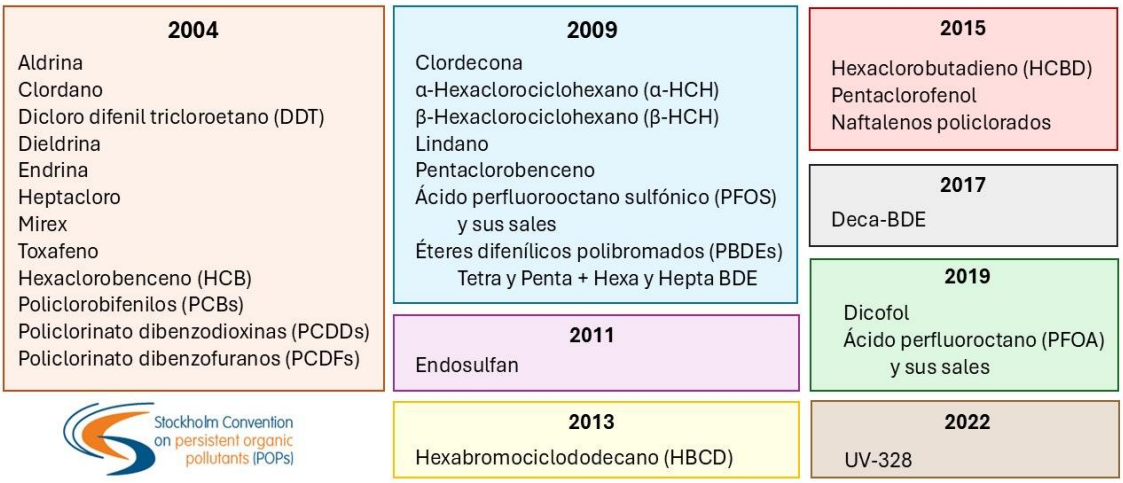

Figura 11. *POPs incluidos en el Convenio de Estocolmo.*

A pesar de la prohibición de producción y uso a algunos POPs del Convenio de Estocolmo, **su estudio sigue siendo fundamental** debido a que por su persistencia, bioacumulación y biomagnificación siguen muy presentes en el medioambiente, pudiendo concentrarse a lo largo de la cadena alimentaria y generar impactos en la salud humana. Sin embargo, aún no se han esclarecido completamente todos sus mecanismos de acción. Además, se está observando que los subproductos de estos contaminantes o la presencia en forma de mezclas puede tener un mayor impacto, aún desconocido. Finalmente, el estudio de estos compuestos es crucial para desarrollar **nuevas estrategias** de remediación ambiental y evaluar el impacto de sus sustitutos, garantizando que las alternativas utilizadas no presenten riesgos similares.

6.1. Hidrocarburos Aromáticos Policíclicos (PAHs).

6.1.1. Composición y propiedades químicas.

Los **hidrocarburos aromáticos policíclicos** (PAHs) están conformados, únicamente de hidrógeno y carbono, formando múltiples anillos bencénicos fusionados, en orientación angular, en racimo o lineal. Se forman principalmente a partir de hidrocarburos saturados en condiciones de falta de oxígeno, siendo la pirosíntesis y pirólisis los principales mecanismos de formación de PAHs[88].

[88] **Reizer, Viskolcz, and Fiser**. Formation and growth mechanisms of polycyclic aromatic hydrocarbons: A mini-review. *Chemosphere.* **2022**.

La Agencia de Protección del Medio Ambiente (EPA) especificó 16 PAH como compuestos prioritarios, debido principalmente a su abundancia y potencial carcinogénico (**Figura 12**). Esta estructura química es altamente apolar, cuyos enlaces conjugados aportan gran resistencia a la degradación química y térmica. Por lo general, los PAHs tienen, una baja solubilidad en agua[89], una baja presión de vapor[90]. Sin embargo, dependiendo del número y disposición de los anillos, las **propiedades fisicoquímicas** pueden variar (**Tabla 4**), provocando diferentes niveles de toxicidad (TEF: factor de equivalencia tóxica utilizado para evaluar la toxicidad de compuestos químicos con mecanismos de acción similares. Para los PAHs se utiliza como referencia el BaP, TEF=1), hidrofobicidad y persistencia en el medio ambiente[89,91].

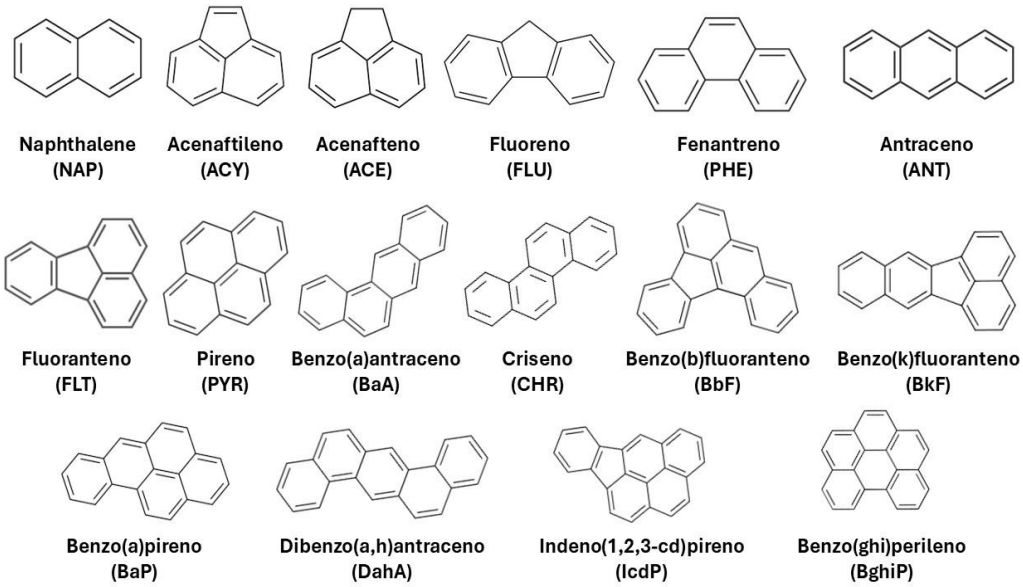

***Figura 12**. Estructura química 2D de los 16 principales PAHs.*

[89] **Sverdrup, Nielsen, and Krogh**. Soil ecotoxicity of polycyclic aromatic hydrocarbons in relation to soil sorption, lipophilicity, and water solubility. *Environ Sci Technol.* **2002**.

[90] **Dat and Chang**. Review on characteristics of PAHs in atmosphere, anthropogenic sources and control technologies. *Sci Total Environ.* **2017**.

[91] **Sahu and Pandit**. Estimation of octanol-water partition coefficients for polycylic aromatic hydrocarbons using reverse-phase HPLC. *J. Liq. Chromat. & Related Tech*. **2003**.

***Tabla 4**. Propiedades fisicoquímicas de los 16 PAHs prioritarios.*

PAH	Peso molecular ($g \cdot mol^{-1}$)	Nº anillos	Solubilidad en agua (25°C, $mg \cdot L^{-1}$)	Presión de vapor (25°C, Pa)	Log K_{ow}	TEF
NAP	128.2	2	31	11.1	3.3	0.001
ACY	152.2	3	3.9	3.9	3.6	0.001
ACE	154.2	3	16	3.1	3.8	0.001
FLU	166.2	3	2.0	1.7	4.0	0.001
PHE	178.2	3	1.3	0.1	4.1	0.001
ANT	178.2	3	0.7	$8.6 \cdot 10^{-4}$	4.2	0.01
FLT	202.2	4	0.3	$8.6 \cdot 10^{-4}$	4.5	0.001
PYR	202.2	4	0.1	$5.0 \cdot 10^{--5}$	4.7	0.001
BaA	228.3	4	0.01	$5.4 \cdot 10^{-4}$	5.1	0.1
CHR	228.3	4	0.002	$4.0 \cdot 10^{-6}$	5.1	0.01
BbF	252.3	5	0.001	$5.0 \cdot 10^{-7}$	5.6	0.1
BkF	252.3	5	0.0008	$5.2 \cdot 10^{-8}$	5.4	0.1
BaP	252.3	5	0.004	$6.0 \cdot 10^{-8}$	5.8	1
DahA	278.4	5	0.0006	$1.3 \cdot 10^{-8}$	6.0	1
IcdP	276.3	6	0.0002	$1.3 \cdot 10^{-7}$	6.1	0.01
BghiP	252.3	6	0.0004	$1.4 \cdot 10^{-8}$	6.3	0.1

6.1.2. Fuentes de los PAHs en el medioambiente.

La presencia generalizada de PAHs en el medio ambiente se debe a su formación y liberación en los procesos de combustión incompleta de compuestos orgánicos. Las **fuentes** pueden ser tanto en procesos naturales (erupciones volcánicas e incendios forestales) como en actividades antropogénicas (combustión de carbón o madera, automoción, residuos municipales o humos industriales, humo del tabaco, alimentos tostados en exceso, entre otros). Además, biológicamente, los PAHs se pueden producir en la síntesis bacteriana y algal o la descomposición del aceite vegetal[92]. Por tanto, los PAHs pueden encontrarse en distintas **matrices ambientales.**

[92] **Yebra-Pimentel** *et al.* A critical review about the health risk assessment of PAHs and their metabolites in foods. *Critical Reviews in Food Science and Nutrition.* **2015**.

La principal vía de transporte a largas distancias es el aire, donde se adhieren a partículas finas en suspensión (PM2.5 y PM10), encontrándose concentraciones que van de menos de 50 $pg \cdot m^{-3}$ a más de 1.7 $\mu g \cdot m^{-3}$, dependiendo de la actividad social e industrial o las condiciones climatológicas de la zona medida[89]. En el agua y el suelo pueden disolverse parcialmente o adsorberse a sedimentos, respectivamente, incorporándose en la cadena alimentaria, especialmente en peces y mariscos. Por tanto, la **exposición en humanos** ocurre, principalmente, por inhalación o por consumo de agua y alimentos contaminados.

6.1.3. Toxicidad, bioacumulación y biotransformación.

Los PAHs pueden atravesar las membranas celulares de los organismos fácilmente por difusión pasiva[93] donde se **bioacumulan** en los tejidos debido a su naturaleza lipofílica e hidrofóbica. En la literatura, se han encontrado diversos valores de BCF para un mismo compuesto, dependiendo de la vía de exposición y el organismo estudiado. Sin embargo, la tendencia observada siempre es la misma; los PAHs con mayor número de anillos y, por tanto, mayor log K_{ow}, muestran una mayor bioacumulación. Y, por consiguiente, suele provocar una mayor toxicidad[94].

La mayoría de los PAHs se consideran compuestos mutagénicos, carcinogénicos e inmunotóxicos[95] y, aunque existen límites legales para los PAHs en alimentos[96], gran parte de la **toxicidad** es debida a los productos de metabolización activados que se generan en los organismos durante los procesos de detoxificación[97,98].

---

89 **Sverdrup, Nielsen, and Krogh**. Soil ecotoxicity of polycyclic aromatic hydrocarbons in relation to soil sorption, lipophilicity, and water solubility. *Environ Sci Technol.* **2002**.

93 **Moorthy** *et al*. Polycyclic aromatic hydrocarbons: From metabolism to lung cancer. *Toxicol Sci.* **2015**.

94 **Bleeker and Verbruggen**. Bioaccumulation of polycyclic aromatic hydrocarbons in aquatic organisms. *RIVM report.* **2009**.

95 **Patel** *et al*. Polycyclic Aromatic Hydrocarbons: Sources, Toxicity, and Remediation Approaches. *Front. Microbiol.* **2020**.

96 **EU 835/2011**. Commission Regulation (EC) No 835/2011 amending Regulation No 1881/2006 as regards maximum levels for polycyclic aromatic hydrocarbons in foodstuffs.

97 **Honda and Suzuki**. Toxicities of polycyclic aromatic hydrocarbons for aquatic animals. *Int J Environ Res Public Health.* **2020**.

98 **Luo** *et al.* Cigarette smoking enhances the metabolic activation of the polycyclic aromatic hydrocarbon phenanthrene in humans. *Carcinogenesis.* **2021**.

El objetivo de la **metabolización** de los xenobióticos es aumentar la polaridad de los compuestos con el fin de acelerar su eliminación. Los PAHs son biotransformados en los organismos por la familia de enzimas del citocromo P450 (CYP1A1, CYP1A2 y CYP1B1), formando **PAHs hidroxilados** (OH-PAHs), fácilmente excretables. Por ello, los biomarcadores destacados de la exposición de PAHs en los seres humanos son hidroxipirenos, hidroxinaftalenos e hidroxifenantrenos porque se excretan en gran medida en la orina[92]. Sin embargo, dentro del proceso de **detoxificación**, los PAHs pueden continuar por otras vías metabólicas, donde están implicadas enzimas como la epóxido hidrolasa (vía CYP/EH), CYP peroxidasa y las aldo-ceto reductasas (vía AKR). En estas vías, se forman **compuestos intermedios activos**, como diol-epóxidos, cationes radicales u oquinonas reactivas y redox-activas, que pueden reaccionar con el ADN y producir aductos, dando lugar a mutaciones cancerígenas[93]. Un ejemplo característico es el Benzo(a)pireno (BaP), que se convierte en benzo(a)pireno-7,8-diol-9,10-epóxido (BPDE), un metabolito altamente mutagénico y carcinogénico. Una característica estrechamente asociada a la carcionogenicidad es la región de bahía en la molécula entre los ciclos aromáticos. Sin embargo, el fenantreno (PHE), aunque también presenta la bahía en su estructura química pero no es potencialmente cancerígeno, debido a que sólo tiene tres anillos aromáticos. Los mecanismos de biotransformación del BaP y PHE se muestran en la **Figura 13**.

Por otro lado, además se ha demostrado que los PAHs pueden transformarse en el medio ambiente, dando lugar a la producción de derivados tóxicos que contienen oxígeno (O-PAHs), nitrógeno (N-PAHs y aazarenos, AZA) o azufre (PASHs)[99].

[92] **Yebra-Pimentel** *et al.* A critical review about the health risk assessment of PAHs and their metabolites in foods. *Critical Reviews in Food Science and Nutrition.* **2015**.
[93] **Moorthy** *et al*. Polycyclic aromatic hydrocarbons: From metabolism to lung cancer. *Toxicol Sci.* **2015**.
[99] **Krzyszczak and Czech**. Occurrence and toxicity of polycyclic aromatic hydrocarbons derivatives in environmental matrices. *Sci Total Environ.* **2021**.

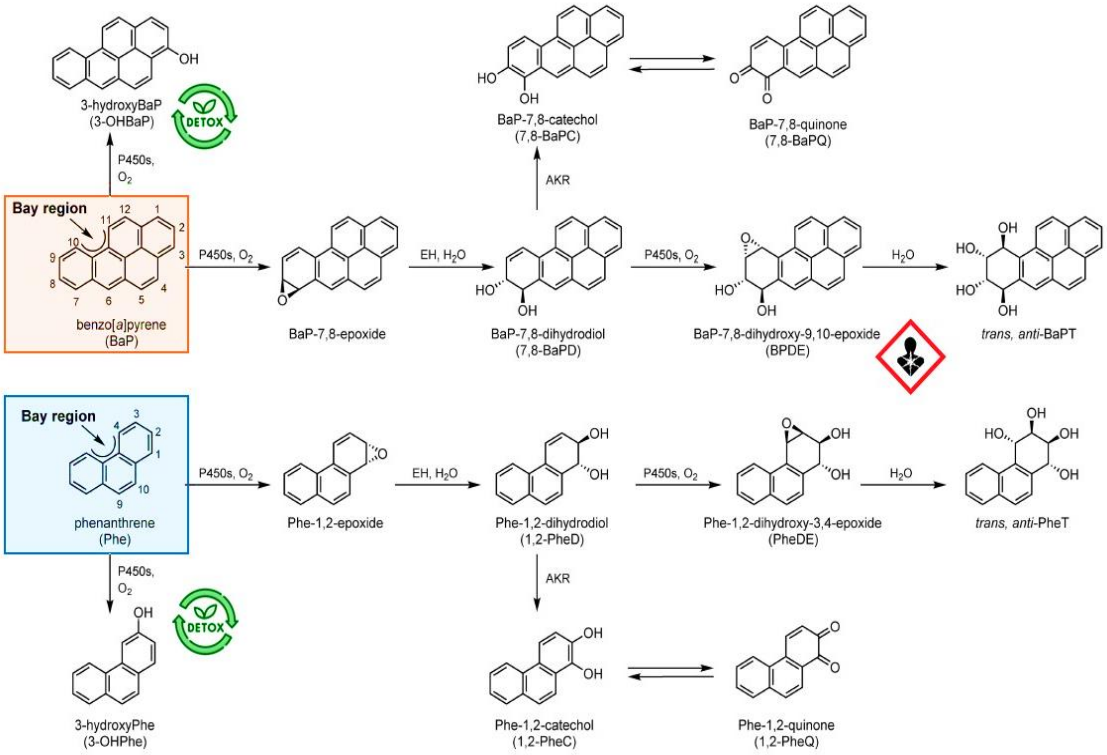

***Figura 13**. Mecanismo de biotransformación del BaP y PHE*[97].

6.2. Polibromo difenil éteres (PBDEs).

6.2.1. Composición y propiedades químicas

Los polibromo difenil éteres (PBDEs) tienen una **estructura química** compuesta por dos anillos de benceno conectados por un átomo de oxígeno, en cuyas posiciones de hidrógeno pueden sustituirse entre uno y diez átomos de bromo ($C_{12}H_{10-x}Br_xO$; x=m+n =1-10, **Figura 14**)[100].

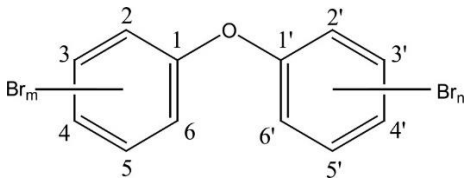

***Figura 14.** Estructura general de los PBDEs.*

[97] **Honda and Suzuki**. Toxicities of polycyclic aromatic hydrocarbons for aquatic animals. *Int J Environ Res Public Health.* **2020**.

[100] **Pietroń and Małagocki**. Quantification of polybrominated diphenyl ethers (PBDEs) in food. A review. *Talanta.* **2017**.

La cantidad y posición de los átomos de bromo en su estructura química genera 209 compuestos diferentes (congéneres). La Unión Internacional de Química Pura y Aplicada (IUPAC) enumera y clasifica los PBDEs de tres formas diferentes:

- **Nombre homólogo:** Esta clasificación indica el número de átomos de bromo en la molécula utilizando el prefijo indicador del número de bromos (mono-, di-, tri-, tetra-, penta-, etc.), seguido de "éter de bromodifenilo, BDE". Se utiliza para relacionar las propiedades más importantes a nivel medioambiental y de toxicidad.
- **Congéneres**: Sus nombres indican la posición del bromo en la molécula. Las posiciones se denominan "orto" (2 y 2', 6 y 6'), "meta" (3 y 3', 5 y 5') y "para" (4 y 4').
- **Denominación numérica BZ**: Ballschmiter y Zell establecieron una clasificación para identificar cada uno de los diferentes congéneres que componen los PBDE en función del número y posición de los bromos, asignándoles un número del 1 al 209.

De acuerdo con las **propiedades fisicoquímicas** (**Tabla 5**), los PBDEs son resistentes a la degradación química y biológica. Tienen baja presión de vapor, la cual disminuye a medida que aumenta el número de átomos de bromo en la molécula. Esta propiedad está relacionada con la capacidad de evaporación (punto de ebullición), de forma que los congéneres con menor número de bromo tienen mayor capacidad de transferencia a la atmósfera[101]. Además, tienen muy baja solubilidad en agua y altos coeficientes de partición octanol-agua[102]. Estas propiedades, le dan un carácter bastante bioacumulativo en los tejidos de los organismos vivos.

[101] **Wong** *et al*. Vapor pressures of the polybrominated diphenyl ethers. *Environ Toxicol Chem.* **2001**.

[102] **Harner and Shoeib**. Measurements of octanol-air partition coefficients (KOA) for polybrominated diphenyl ethers (PBDEs): Predicting partitioning in the environment. *J Chem Eng Data.* **2002**.

Tabla 5. *Propiedades físicoquímicas de los PBDEs.*

Grupo Homólogo	Congéneres BZ	Peso molecular ($g \cdot mol^{-1}$)	Solubilidad en agua (25˚C, $\mu g \cdot L^{-1}$)	Presión de vapor (25˚C, Pa)	Log K_{ow}
monoBDE	1-3	283.9	-	-	-
diBDE	4-15	328.0	21	$1.3 \cdot 10^{-3}$	5.03
triBDE	16-39	406.9	-	$2.7 \cdot 10^{-3}$	5.5-5.6
tetraBDE	40-81	485.8	11	$2.5 \cdot 10^{-4}$	5.9-6.9
pentaBDE	82-127	564.7	9	$4.0 \cdot 10^{-5}$	6.7-7.1
hexaBDE	128-169	643.6	4	$1.6 \cdot 10^{-6}$	6.9-7.9
heptaBDE	170-193	722.3	-	$1.8 \cdot 10^{-7}$	7.5-8.3
octaBDE	194-205	801.4	0.5	$2.3 \cdot 10^{-7}$	8.4-8.9
nonaBDE	206-208	880.4	-	$2.4 \cdot 10^{-8}$	9.5
decaBDE	209	959.2	< 0.1	$2.9 \cdot 10^{-9}$	10

6.2.2. Fuentes en el medioambiente

Los PBDEs son aditivos utilizados como **retardantes de llama** en la **industria** eléctrica, automotriz y textil, así como, para equipos electrónicos, muebles y materiales de construcción[103]. El enlace carbono-bromo, relativamente débil, es térmicamente lábil. La energía térmica libera radicales de bromo que interceptan los radicales de carbono para disminuir la llama, reduciendo simultáneamente el calor y la producción de monóxido de carbono[104]. Por tanto, las **fuentes en el medio ambiente** se deben a residuos industriales, productos de consumo, vertederos o aguas residuales. Además, aunque al principio se creía que los PBDEs no podían tener un origen natural, varios estudios han demostrado que ciertas esponjas marinas son capaces de sintetizarlos en pequeñas cantidades[105].

Los **seres humanos** están expuestos a los PBDE a través de la dieta (alimentos con mayor contenido en grasa debido a la acumulación en los tejidos de los

[103] **Yang** *et al.* Translocation of polybrominated diphenyl ethers from field-contaminated soils to an edible plant. *J Hazard Mater.* **2018**.
[104] **Siddiqi** *et al.* Polybrominated Diphenyl Ethers (PBDEs): New Pollutants-Old Diseases. *Clin Med Res.* **2003**.
[105] **Teuten** *et al.* Two abundant bioaccumulated halogenated compounds are natural products. *Science*. **2005**.

organismos), la inhalación, la ingestión accidental de polvo y el contacto dérmico[106]. Y, aunque están prohibidos por el Convenio de Estocolmo desde 2009, actualmente, se siguen encontrando concentraciones significativas en matrices medioambientales, biológicas y humanas[107]. Sin embargo, en las mezclas comerciales de PBDEs que se han utilizado sólo incluyen un número limitado de congéneres y así sólo se han identificado unos 40 PBDEs en muestras reales, la mayoría de los cuales son PBDE-28, 47, 99, 100, 153, 154, 183, 209, todos ellos incluidos en la lista de aquellos cuya producción ya está regulada[108]. Que estos congéneres sean los mayormente encontrados es debido a 3 factores: i) dependiendo de las condiciones de síntesis, se favorecen ciertos niveles de bromación, ii) el oxígeno del éter de bifenilo favorece la incorporación de bromuros en las posiciones para- y otro- (la última en menor grado) y iii) a medida que aumenta el nivel de bromuros en los anillos, el efecto desactivador de los átomos de halógeno y el impedimento estérico favorecen la formación preferente de unos congéneres sobre otros.

6.2.3. Toxicidad, bioacumulación y biotransformación

Los PBDEs se definen como **disruptores endocrinos** debido a su similitud estructural con las hormonas endocrinas, como las hormonas tiroideas, la tiroxina T4 en particular, causando tumores hepáticos y disfunciones del neurodesarrollo[109,110].

La **biotransformación** de los PBDEs, al igual que la mayoría de los xenobióticos, y como se ha descrito en el caso de los PAHs, se lleva a cabo por las enzimas hepáticas del citocromo P450. Además, de la usual enzima CYP1A de la fase I, se ha demostrado que la enzima CYP2B6 es la predominante en el citocromo P450

[106] **De la Torre** *et al.* Organophosphate compounds, polybrominated diphenyl ethers and novel brominated flame retardants in European indoor house dust: Use, evidence for replacements and assessment of human exposure. *J Hazard Mater.* **2020**.
[107] **Ohoro** *et al.* Polybrominated diphenyl ethers in the environmental systems: a review. J *Environ Health Sci Eng.* **2021**.
[108] **Pietron** *et al*. Feed as a source of polybrominated diphenyl ethers (PBDEs). *Environ Res*. **2023**.
[109] **Li** *et al*. Hormone activity of hydroxylated polybrominated diphenyl ethers on human thyroid receptor-β: In vitro and in silico investigations. *Environ Health Perspect*. **2010**.
[110] **Klinčić** *et al.* Levels and distribution of polybrominated diphenyl ethers in humans and environmental compartments: a comprehensive review of the last five years of research. *Environ Sci Pollut Res.* **2020**.

implicada en el metabolismo de los PBDE a sus correspondientes metabolitos hidroxilados (OH-BDEs)[111]. Posteriormente, estos compuestos pueden seguir otras vías alternativas a la detoxificación, transformándose en metabolitos metoxilados (MeO-BDEs), más difíciles de excretar debido a que presenta propiedades físico-quimicas apolares[112]. Por otro lado, puede ocurrir la pérdida de un bromo (debromación), convirtiéndose en otro congénere de PBDE inferior que, a su vez, puede biotransformarse en sus respectivos metabolitos OH-BDEs y MeO-BDEs[113]. Además, también puede suceder procesos de isomerización entre metabolitos de estructura similar o incluso el desplazamiento de un Br a la vez que ocurre una hidroxilación, metabolización o debromación[114]. En la **Figura 15**, se muestra un ejemplo de las vías de biotransformación para la formación de los algunos metabolitos del congénere BDE-47 (2,2′,4,4′-tetrabromodifeniléter).

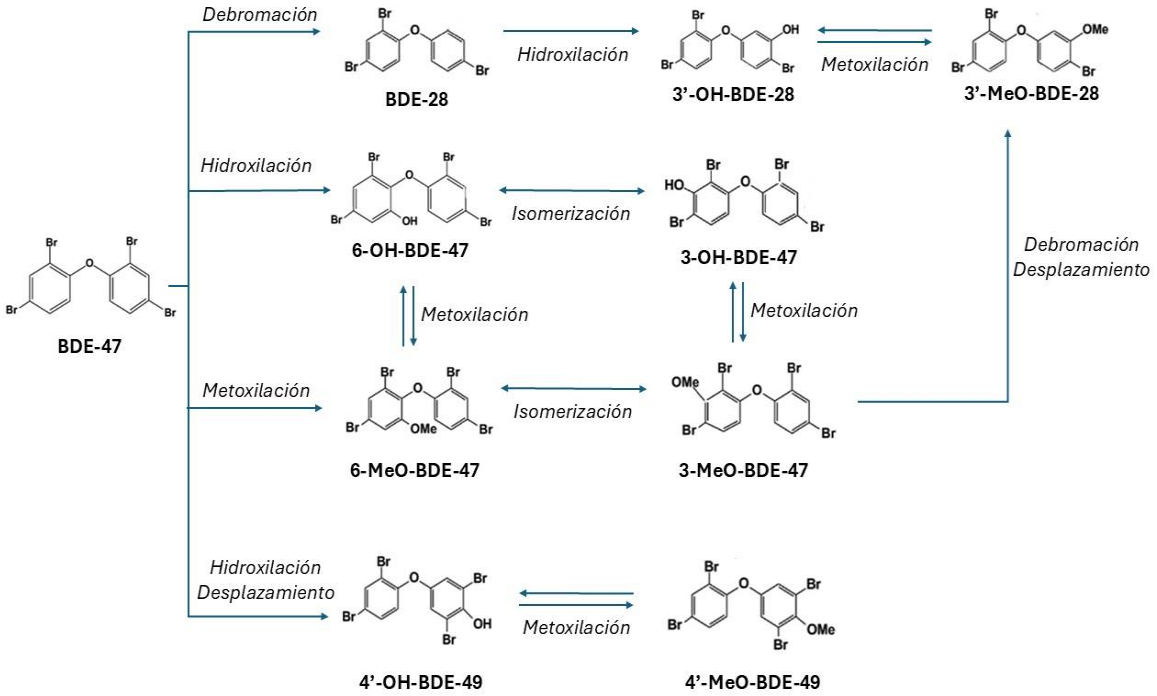

***Figura 15**. Mecanismos de biotransformación del BDE-47.*

[111] **Butryn** *et al.* Retention of polybrominated diphenyl ethers and hydroxylated metabolites in paired human serum and milk in relation to CYP2B6 genotype. *J Hazard Mater*. **2020**.

[112] **Zheng** *et al.* Accumulation and biotransformation of BDE-47 by zebrafish larvae and teratogenicity and expression of genes along the hypothalamus-pituitary-thyroid axis *Environ Sci Technol.* **2012**.

[113] **Sun** *et al*. In vivo metabolism of 2,2′,4,4′-tetrabromodiphenyl ether (BDE-47) in young whole pumpkin plant," *Environ Sci Technol*. **2013**.

[114] **Xu** *et al.* Biotransformation kinetics and pathways of 2,2′,4,4′-tetrabromodiphenyl ether (BDE-47) and its hydroxylated and methoxylated derivatives (6-OH-BDE-47 and 6-MeO-BDE-47) in earthworms (Eisenia fetida). *Sci Total Environ.* **2023**.

Por tanto, la preocupación de la exposición a PBDEs, no solo viene dada por los propios compuestos originales, sino porque se ha puesto de manifiesto que los metabolitos OH-BDES y MeO-BDEs mantienen grupos bioactivos, mostrando una toxicidad y poder de **bioacumulación** similar o incluso mayor que los PBDE nativos[115,116]. Además, los metabolitos OH-BDEs y MeO-BDEs se han detectado en gran variedad de matrices medioambientales, biológicas y humanas[117,118].

6.3. Interacción de POPs con Micro(nano)plásticos (MNPLs).

6.3.1. Propiedades y clasificación de los plásticos

Los **plásticos** son polímeros orgánicos sintéticos formados a partir de hidrocarburos, ya sean sustituidos o no, mediante procesos de adición o condensación. Se caracterizan por su estabilidad, resistencia al agua y afinidad por las grasas[119]. Por tanto, aunque actualmente, no están catalogados como tal, presentan similares características a los POPs, ya que permanecen largo tiempo en el medio ambiente. Además de las características de durabilidad y flexibilidad, su bajo coste los ha convertido en materiales ampliamente utilizados en productos comerciales e industriales, impulsando su producción de manera exponencial.

Los plásticos pueden **clasificarse** según los materiales poliméricos que los componen, su tamaño o su fuente de producción.

- Según el **material** de composición, los tipos más comunes son poliestireno (PS), el polietileno (PE), el polipropileno (PP), cloruro de polivinilo (PVC) y poliamida (PA, comúnmente denominada nailon)[120].

[115] **Usenko** *et al*. Hydroxylated PBDEs induce developmental arrest in zebrafish. *Toxicol Appl Pharmacol.* **2012**.
[116] **Choo** *et al*. Species and habitat-dependent accumulation and biomagnification of brominated flame retardants and PBDE metabolites. *J Hazard Mater*. **2019**.
[117] **Sun** *et al.* Bioaccumulation and Trophic Transfer of Polybrominated Diphenyl Ethers and Their Hydroxylated and Methoxylated Analogues in Polar Marine Food Webs. *Environ Sci Technol.* **2020**.
[118] **Cruz** *et al.* Polybrominated diphenyl ethers and metabolites – An analytical review on seafood occurrence. *TrAC*. **2017**.
[119] **Benson** *et al.* Micro(nano)plastics Prevalence, Food Web Interactions, and Toxicity Assessment in Aquatic Organisms: A Review. *Front Mar Sci.* **2022**.
[120] **Yu** *et al*. Adsorption behaviour and interaction of organic micropollutants with nano and microplastics – A review. *Sci Total Environ.* **2021**.

- Según el **tamaño**, se catalogan como macroplásticos, mesoplásticos, microplásticos (MPLs) y nanoplásticos (NPLs). Sin embargo, todavía no hay un consenso para establecer los límites de tamaño para cada uno de ellos. En los últimos años, se ha hecho un gran esfuerzo para establecer una definición común que permita gestionar y controlar la contaminación de plásticos[121]. Por tanto, generalmente, se habla de "macroplásticos" si presentan un tamaño menor a 2.5 cm, "MPLs" si tienen un diámetro menos a 5 mm, "NPLs" si este es menor a 100 nm y "mesoplásticos" si se encuentran entre el tamaño de macro y microplásticos.
- Según su **fuente de producción**, se encuentran los "plásticos primarios", aquellos originalmente facturados, y los "plásticos secundarios", plásticos más pequeños formados por el proceso de degradación química, física o biológica de trozos más grandes[122].

6.3.2. Interacción de POPs y MNPLs

Los micro(nano)plásticos, como se ha descrito, están compuestos mayoritariamente por polímeros inertes. Sin embargo, debido a sus propiedades fisicoquímicas, se pueden **adherir moléculas** en su superficie, creando una capa que puede aumentar, considerablemente, su **reactividad biológica**. Esta capa suele consistir en iones metálicos, polisacáridos, proteínas, microorganismos y contaminantes orgánicos como POPs o productos farmacéuticos (antibióticos y antidepresivos)[123,124].

Los **POPs**, debido a su carácter hidrofóbico, tienen una alta tendencia a combinarse con partículas con propiedades análogas, como es el caso de los MNPLs. Entre los POP mayormente encontrados en la superficie de MNPLs se encuentran los PAHs, PCBs y PBDEs[124]. La interacción entre ellos puede ocurrir mediante **mecanismos de adsorción** tales como, interacciones hidrofóbicas, π-π,

[121] **Hartmann** *et al.* Are We Speaking the Same Language? Recommendations for a Definition and Categorization Framework for Plastic Debris. *Environ Sci Technol*. **2019**.
[122] **Okoye** *et al.* Toxic Chemicals and Persistent Organic Pollutants Associated with Micro-and Nanoplastics Pollution. *Chemical engineering journal advances.* **2022**.
[123] **Trevisan** *et al.* PAH Sorption to Nanoplastics and the Trojan Horse Effect as Drivers of Mitochondrial Toxicity and PAH Localization in Zebrafish. *Front Environ Sci*. **2020**.
[124] **Fred-Ahmadu** *et al.* Interaction of chemical contaminants with microplastics: Principles and perspectives. *Sci Total Environ.* **2020**.

electroestáticas, iónicas, fuerzas de Van der Waals o enlaces de hidrógeno[125], dependiendo del tipo de material del MNPLs o la molécula de POP (**Figura 16a**). Sin embargo, lo más habitual es que el proceso de adsorción suela verse facilitado sinérgicamente por múltiples fuerzas. Además del tipo de polímero y la estructura química de los contaminantes, el comportamiento de adsorción depende de otros **factores** como los recogidos en la **Figura 16b**.

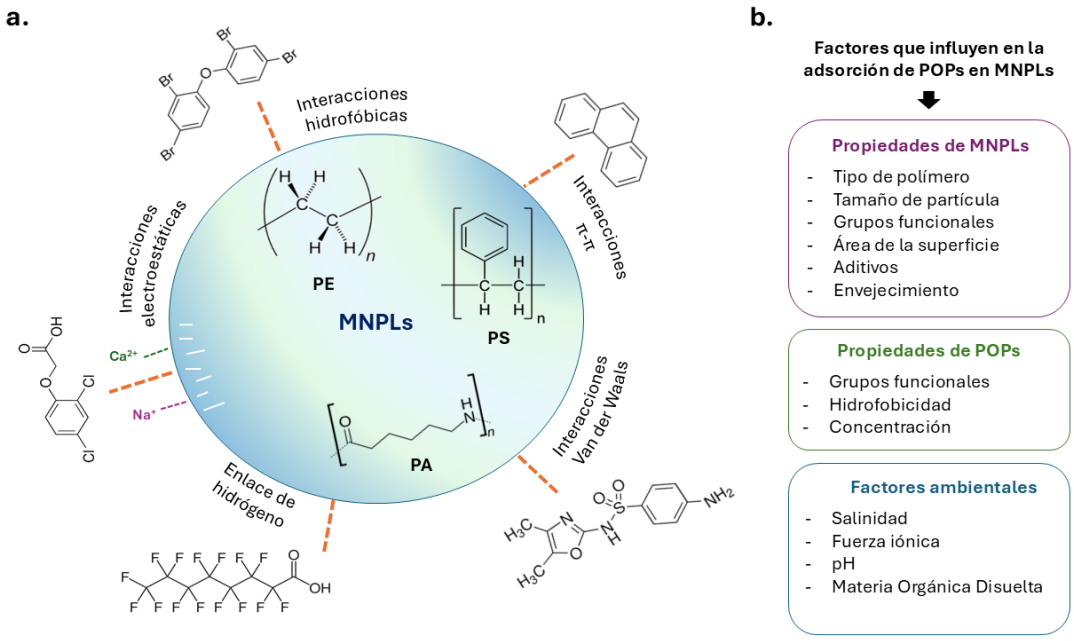

Figura 16. *Interacciones (a) y factores (b) que influyen en la adsorción de POPs en los MNPLs.*

Actualmente, los estudios se centran en investigar la capacidad de adsorción de determinados POPs dependiendo del tipo de polímero y el tamaño de las partículas. Aunque algunos autores difieren, afirmando que el material PE es el que presentaba mayor adsorción en su estudio[126], la mayoría observaron que el material **PS** es el que tenía **mayor poder de adsorción** de POPs, debido a su estructura diversa[127,128,129]. Además, muchos de ellos, también coinciden en que

[125] **Atugoda** *et al.* Interactions between microplastics, pharmaceuticals and personal care products: Implications for vector transport. *Environ Int.* **2021**.
[126] **Zuo** *et al.* Sorption and desorption of phenanthrene on biodegradable poly(butylene adipate co-terephtalate) microplastics. *Chemosphere*. **2019**.
[127] **Hüffer and Hofmann**. Sorption of non-polar organic compounds by micro-sized plastic particles in aqueous solution. *Environ Poll*. **2016**.
[128] **Lee** *et al.* Sorption capacity of plastic debris for hydrophobic organic chemicals. *Sci Total Environ.* **2014**.
[129] **Rochman** *et al.* Polystyrene plastic: A source and sink for polycyclic aromatic hydrocarbons in the marine environment. *Environ Sci Technol*. **2013**.

los **NPLs** tienen una **superficie específica** mucho **mayor** para la adsorción de POPs que los MPLs[130,131]. Sin embargo, el coeficiente de partición resultante entre el agua y el plástico depende mayormente del coeficiente de partición octanol-agua del compuesto estudiado.

6.3.3. Impacto medioambiental por la co-exposición de POPs y MNPLs

Según las estimaciones, se prevé unos 270 millones de toneladas métricas de plásticos en los ecosistemas acuáticos anuales en 2060[132]. Las **concentraciones de MNPLs** que se encuentran en determinadas áreas están directamente correlacionadas con la densidad y la actividad humana en esas áreas[133]. La mayor contribución de plásticos en el ambiente procede de países asiáticos (8.82 millones de toneladas métricas/año), muy por encima de los 84 países europeos (0.31 millones de toneladas métricas/año)[134,135]. Se han encontrado en **lugares remotos** como la Antártida[136], aguas rurales y paisajes forestales[137], alimentos y bebidas[138], así como en el interior de organismos y ecosistemas acuáticos[139]. Entre todos los tipos de plásticos, el **PS** es el que presenta **mayor biodisponibilidad** para los organismos debido a su abundancia en productos manufacturados[140] y a su densidad intermedia (0.96-1.05 g/cm^3), cercana a la del agua, distribuyéndose tanto en aguas superficiales como de fondo[141,142].

---

130 **Zhang and Goss**. Potentiation of polycyclic aromatic hydrocarbon uptake in zebrafish embryos by nanoplastics. *Environ Sci Nano*. **2020**.

131 **Mattsson** *et al.* Nano-plastics in the aquatic environment. *Environ. Sci.: Processes Impacts.* **2015**.

132 **Lebreton and Andrady**. Future scenarios of global plastic waste generation and disposal. *Palgrave Commun.* **2019**.

133 **Kushwaha** *et al.* Microplastics pollution in the marine environment: A review of sources, impacts and mitigation. *Mar Pollut Bull.* **2024**.

134 **Jambeck** *et al.* Plastic waste inputs from land into the ocean. *Science*. **2015**.

135 **Patidar** *et al.* Assessing the microplastic pandemic: Prevalence, detection, and human health impacts in Asian aquatic environments. *Physics and Chemistry of the Earth.* **2025**.

136 **Waller** *et al*. Microplastics in the Antarctic marine system: An emerging area of research. *Sci Total Environ.* **2017.**

137 **Materić** *et al*. Presence of nanoplastics in rural and remote surface waters. *Environ Research Letters.* **2022**.

138 **Vitali** *et al*. Microplastics and nanoplastics in food, water, and beverages. *TrAC.* **2023**.

139 **Al-Thawadi.** Microplastics and Nanoplastics in Aquatic Environments: Challenges and Threats to Aquatic Organisms. *Arab J Sci Eng.* **2020**.

140 **Kik** *et al.* Polystyrene nanoparticles: Sources, occurrence in the environment, distribution in tissues, accumulation and toxicity to various organisms. *Environ Poll.* **2020**.

141 **Erni-Cassola** *et al.* Distribution of plastic polymer types in the marine environment; A meta-analysis. *J Hazard Mater*. **2019**.

142 **Martínez-Álvarez** *et al.* Effects of polystyrene nano- and microplastics and of microplastics with sorbed polycyclic aromatic hydrocarbons in adult zebrafish. *Sci Total Environ.* **2024**.

Las **principales vías de entrada** de MNPLs en los organismos acuáticos incluyen los vertidos municipales e industriales, la deposición atmosférica y las plantas de tratamiento de aguas y aguas residuales. Los MNPLs pueden causar **efectos adversos** en los organismos y salud humana[143,144,] ya que penetran fácilmente a través de las membranas biológicas[145] y se acumulan en el interior de los organismos[146]. Sin embargo, los MNPLs no están aislados en el medio ambiente y, como se ha comentado en los apartados anteriores, pueden adsorber fácilmente otros contaminantes, facilitando su transporte e internalización en diferentes organismos vivos (**efecto caballo de Troya, Figura 17**)[147,148].

Muchos estudios han demostrado la **toxicidad sinérgica** de los MNPLs y POPs en diferentes organismos[149,150,151]. Sin embargo, otros observan un **efecto antagónico**, mitigando los efectos tóxicos[152,153,154]. Por ello, aún se **necesitan más estudios** para, por un lado, conocer el impacto real de la co-exposición de los MNPLs y POPs en el medio ambiente y los organismos y, por otro lado, conocer el mecanismo de acción de estos dos contaminantes.

---

143 **Shi** *et al*. Emergence of nanoplastics in the aquatic environment and possible impacts on aquatic organisms. *Sci Total Environ.* **2024**.
144 **Yee** *et al.* Impact of microplastics and nanoplastics on human health. *Nanomaterials.* **2021**.
145 **Stapleton**. Toxicological considerations of nano-sized plastics. *AIMS Environ Sci.* **2019**.
146 **Brandts** *et al.* Polystyrene nanoplastics accumulate in ZFL cell lysosomes and in zebrafish larvae after acute exposure, inducing a synergistic immune response: In vitro without affecting larval survival in vivo. *Environ Sci Nano.* **2020**.
147 **Trevisan** *et al.* Nanoplastics decrease the toxicity of a complex PAH mixture but impair mitochondrial energy production in developing Zebrafish. *Environ Sci Technol.* **2019**.
148 **Hu** *et al.* Developmental toxicity and mechanism of polychlorinated biphenyls 126 and nano-polystyrene combined exposure to zebrafish larvae. *Ecotoxicol Environ Saf*. **2024**.
149 **Narayanan** *et al.* Toxic effects of polystyrene nanoplastics and polycyclic aromatic hydrocarbons (chrysene and fluoranthene) on the growth and physiological characteristics of Chlamydomonas reinhardtii. *Aquatic Toxicol*. **2024**.
150 **Sun** *et al*. Combined toxicity of micro/nanoplastics loaded with environmental pollutants to organisms and cells: Role, effects, and mechanism. *Environ Int.* **2023**.
151 **Wang** *et al.* The combined effects of phenanthrene and micro-/nanoplastics mixtures on the cellular stress responses of the thick-shell mussel Mytilus coruscus. *Environ Poll.* **2024**.
152 **Li** *et al.* Metabolic profile changes of zebrafish larvae in the single- and co-exposures of microplastics and phenanthrene. *Sci Total Environ*. **2024**.
153 **Koelmans** *et al.* Plastic as a carrier of POPs to aquatic organisms: A model analysis. *Environ Sci Technol.* **2013**.
154 **Wang** *et al.* Effects of individual and combined polystyrene nanoplastics and phenanthrene on the enzymology, physiology, and transcriptome parameters of rice (Oryza sativa L.). *Chemosphere*. **2022**.

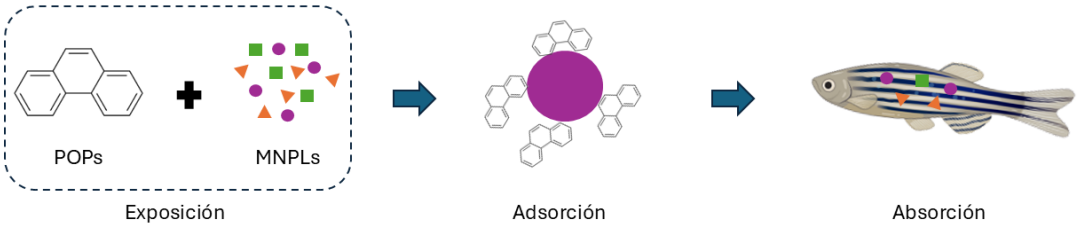

Figura 17. *Internalización de POPs mediante MNPLs como vectores*[155].

7. Técnicas y metodologías (bio)analíticas.

Los métodos (bio)analíticos desempeñan un papel fundamental en el campo de la toxicología experimental, permitiendo la detección, identificación, cuantificación y caracterización de las sustancias en diversos tipos de muestras biológicas y ambientales. De esta forma, son una herramienta para la comprensión del comportamiento, las concentraciones, la distribución, el metabolismo y la excreción de un tóxico en el organismo tras la exposición, contribuyendo significativamente a la evaluación del riesgo toxicológico.

7.1. Evaluación de la toxicidad.

Actualmente, existen múltiples formas de evaluar la toxicidad de una sustancia. Sin embargo, los ensayos que permiten determinar conclusiones esenciales sobre la toxicidad, de una forma rápida, suelen reducirse a **ensayos de viabilidad celular,** en el caso de sistemas *in vitro,* o **curvas dosis-respuesta** en sistemas *in vivo*, permitiendo determinar parámetros como el LC_{50}.

Los métodos más comunes de evaluación de la **viabilidad celular** se basan en ensayos de conteo, colorimétricos o de citometría de flujo. En la **Tabla 6**, se enumeran los ensayos de viabilidad celular mayormente utilizados, así como, un resumen del fundamento, ventajas y limitaciones para cada uno de ellos. La **elección** de un ensayo específico depende de factores como el modelo de cultivo celular, las propiedades fisicoquímicas de la sustancia, el mecanismo de citotoxicidad, los métodos de detección y los criterios de valoración. Por tanto, la

[155] **Yu** *et al.* Distribution, abundance and risks of microplastics in the environment. *Chemosphere*. **2020**.

selección del más adecuado vendrá dada por las necesidades, según el objetivo del estudio y la configuración del diseño experimental[156].

La guía OECD 249[60] describe un protocolo que combina los ensayos de resazurina, CFDA-AM (Carboxifluoresceína Diacetato Acetoximetil Éster) y Neutral Red para la evaluación de la toxicidad aguda con la línea celular RTgill-W1. Aunque el ensayo MTT (metil tiazol tetrazolio) es el más ampliamente utilizado, Segner, en el capítulo destinado a líneas celulares de peces en el libro basado en ecotoxicología de peces de Braunbeck *et al*[157]., mostró que el MTT no funciona bien con algunas líneas celulares de peces debido a la baja actividad del succinato deshidrogenasa en las mitocondrias[56]. Por ello, en la guía OECD 249[60] no se contempla, reemplazándolo por el ensayo de resazurina (Alamar Blue, según su nombre comercial), que también se basa en la actividad metabólica, pero mediante la reducción de enzimas mitocondriales y citoplasmáticas.

[156] **Jain** *et al*. Models and Methods for In Vitro Toxicity. *In Vitro Toxicol*. **2018**.
[56] **Bols** *et al.* Use of fish cell lines in the toxicology and ecotoxicology of fish. Piscine cell lines in environmental toxicology," *Biochemistry and Molecular Biology of Fishes.* **2005**.
[60] **OECD 249**. Fish Cell Line Acute Toxicity: The RTgill-W1 cell line assay. **2021**.
[157] **Braunbeck** *et al.* Fish cell lines as a tool in aquatic toxicology. *Fish Ecotoxicology.* **1998**.

Tabla 6. *Ensayos de viabilidad celular: fundamento, ventajas y limitaciones*

Ensayo / Técnica	Principio	Indicador Viabilidad	Ventajas	Limitaciones
MTT	Reducción de MTT a formazán en células viables	Actividad metabólica	Amplio uso y alta reproducibilidad	Pérdida de cultivo celular. No funciona en algunas líneas células
Resazurina (Alamar Blue)	Conversión de resazurina en resorufina en células viables	Actividad metabólica	No tóxico. Mediciones en tiempo real	Puede verse afectado por reductores en el medio
Yoduro de Propidio	Unión a ADN de células con membrana dañada	Integridad de la membrana celular	Sensible, distingue células necróticas	Requiere citometría de flujo o microscopía de fluorescencia
LDH (Lactato Deshidrogenasa)	Liberación de LDH de células dañadas al medio	Integridad de la membrana celular	No lisado celular. Fácil de cuantificar	No distingue apoptosis de necrosis
CFDA-AM (Carboxifluoresceína Diacetato Acetoximetil Éster)	Conversión de CFDA-AM en carboxifluoresceína en células viables	Membrana celular y actividad enzimática	Alta sensibilidad, compatible con microscopía y citometría de flujo	Puede requerir calibración
Neutral Red	Acumulación del colorante en lisosomas activos	Funcionalidad lisosomal	Fácil de usar	Puede verse afectado por cambios en el pH celular
Trypan Blue	Exclusión del colorante en células viables	Membrana celular y Proliferación	Rápido, barato	Subjetivo, requiere microscopia
Citometría de Flujo	Uso de fluorocromos para evaluar apoptosis, necrosis y viabilidad celular	Diferenciación entre células vivas, apoptóticas y necróticas	Alta sensibilidad, análisis en tiempo real	Costoso y requiere equipo especializado

En esta Tesis Doctoral, debido al objetivo de evaluar la biotransformación, se utilizan los ensayos basados en la actividad metabólica, esto es, los ensayo MTT y resazurina; además de citometría de flujo, como medida genérica de viabilidad.

Tanto el **ensayo MTT** como el **Alamar Blue**, se basan en una medición colorimétrica daba por la transformación de 3-(4, 5-dimethylthiazol-2-yl)-2,5-diphenyltetrazolium bromide (MTT, color amarillo) o resazurina (color azul) en formazán (color morado) o resofurina (color rosa), respectivamente, mediante enzimas reductoras de células viables. De esta forma, midiendo la absorbancia (ensayo MTT) o fluorescencia (ensayo Alamar Blue) del producto formado, se puede cuantificar, de formar relativa frente a un control, la viabilidad celular (**Figura 18a**).

La **citometría de flujo** es una técnica basada en la medida (metría) continua e individual de células (cito) en movimiento (flujo), mediante el equipo denominado citómetro de flujo. El fundamento básico se representa en la **Figura 18b**. La muestra compuesta de células en suspensión es dirigida por un sistema hidrodinámico, que permite la interacción individual de cada partícula con un haz de luz láser en un lugar denominado punto de interrogación[158]. Cuando la luz impacta con la célula, esta dispersa la luz en todas direcciones. Esta luz dispersada es detectada por dos detectores diferentes:

- **Forward scatter** (FSC, dispersión frontal): detecta la luz dispersada por las células hacia delante y da información sobre el tamaño de la partícula.

- **Side scatter** (SSC, dispersión lateral): detecta la luz dispersada perpendicularmente y da información sobre la complejidad interna y la granularidad de la partícula.

Con la información de estos detectores se genera, mediante un software, un **histograma bidimensional**, que relaciona el tamaño (FSC, eje X) con la complejidad (SSC, eje Y). Esta representación hace posible discriminar entre subpoblaciones que presenten estas características concretas dentro de una muestra o dentro de una misma subpoblación, aquellas que presenten estructura

[158] **Jaroszeski and Radcfiff**. Fundamentals of Flow Cytometry. *Mol Biotechnol.* **1999**.

amorfa o no viable. Además, en dirección frontal, los citómetros presentan **detectores de fluorescencia** (FLD, **Figura 18b**), adaptados con diferentes longitudes de onda. La luz fluorescente emitida por las células viene dada, bien por la autofluorescencia de la célula o por la presencia de un fluoróforo internalizado en esta, bien sea un colorante para la evaluación de la viabilidad o compuestos marcados con el objetivo de detectarlos.

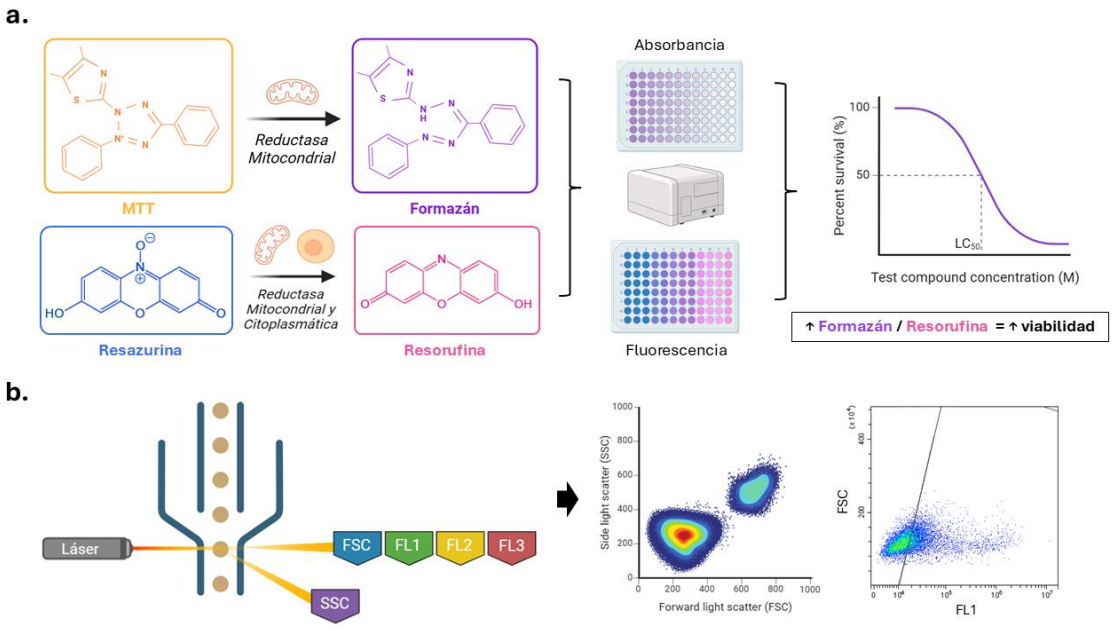

Figura 18. *Fundamento de los ensayos MTT y Alamar Blue (a) y la técnica de citometría de flujo (b).*

7.2. Evaluación de la bioacumulación y biotransformación.

7.2.1. Cuantificación de POPs (PAHs y PBDEs) y sus metabolitos en muestras biológicas.

Las técnicas analíticas utilizadas para la determinación de POPs en muestras biológicas han avanzado significativamente en los últimos años. Estos progresos permiten el desarrollo de métodos altamente sensibles, capaces de detectar concentraciones extremadamente bajas, propias del nivel de trazas, y aún más reducidas en el caso de sus productos de metabolización. Asimismo, conseguir optimizar el tiempo de preparación y análisis de las muestras, además de implementar métodos de extracción y detección simultánea para compuestos con propiedades fisicoquímicas similares. En muestras de pequeño tamaño, desarrollar

técnicas miniaturizadas, y, finalmente, se han diseñado metodologías más sostenibles y respetuosas con el medio ambiente, que requieren menores cantidades de disolventes orgánicos.

Considerando la amplia variedad de protocolos de **extracción** y **limpieza** disponibles, la **Tabla 7** destaca el rendimiento general de los comúnmente utilizados para PAHs, PBDEs y sus metabolitos, según la eficacia, cantidad de disolvente utilizado, coste, y facilidad de uso[118,159,160]. Técnicas tradicionales como el Soxhlet ofrecen buena eficacia, pero presentan limitaciones en cuanto a consumo de tiempo y uso de solventes. Métodos más modernos como la extracción asistida con ultrasonidos, microondas o fluidos supercríticos mejoran el rendimiento y reducen el uso de disolventes, aunque requieren equipamiento más especializado y suponen un mayor coste. En cuanto a la limpieza, la cromatografía de permeación en gel es eficaz, pero poco eficiente en términos de tiempo y coste. La fase sólida, por su parte, presenta un buen equilibrio entre eficacia y practicidad. Destacan especialmente los métodos integrados como QuEChERS ("*Quick, Easy, Cheap, Effective, Rugged and Safe*"; rápido, fácil, barato, efectivo, robusto y seguro), especialmente en su variante de fase sólida dispersiva (d-SPE), que combinan alta eficacia con bajo coste, rapidez y facilidad de uso, posicionándose como una de las opciones más versátiles para análisis de gran variedad de POPs.

En esta Tesis Doctoral, se realiza una metodología miniaturizada basada en una extracción sólido-líquido (células o larvas) o líquido-líquido (medios de exposición), en el que los compuestos se transfieren por contacto directo con un disolvente orgánico con propiedades afines. En el caso de las muestras sólidas, se asiste con una sonda de ultrasonidos para la lisis del tejido biológico, con el fin de liberar los compuestos interiorizados al disolvente orgánico. En cuanto a la etapa de limpieza, se realiza una d-SPE, que consiste en la adición de adsorbentes como

[118] **Cruz** *et al.* Polybrominated diphenyl ethers and metabolites – An analytical review on seafood occurrence. *TrAC*. **2017.**

[159] **Adeniji** *et al.* Analytical Methods for Polycyclic Aromatic Hydrocarbons and their Global Trend of Distribution in Water and Sediment: A Review. *Recent Insights in Petroleum Science and Engineering*. **2018**.

[160] **Wang** *et al*. Determination of hydroxylated metabolites of polycyclic aromatic hydrocarbons in sediment samples by combining subcritical water extraction and dispersive liquid-liquid microextraction with derivatization. *Anal Chim Acta.* **2012**.

amina primaria/secundaria (PSA), C18, Florisil etc. en función del tipo de compuestos y muestra, para retener los interferentes de la matriz.

Tabla 7. *Rendimiento global de los métodos de extracción y limpieza utilizados habitualmente en PAHs, PBDEs y sus metabolitos.*

Método	Eficacia	Solvente	Tiempo	Coste	Facilidad
Extracción					
Soxhlet	+	-	-	+	++
Líquida presurizada	+	+	+	-	-
Ultrasonidos	+	+	+	+	-
Microondas	+	+	+	-	-
Fluido supercrítico	+	++	+	-	-
Limpieza					
Cromatografía de permeación en gel	+	-	-	-	+
Fase sólida	++	-	-	+	+
Extracción + Limpieza					
QuEChERS Fase sólida dispersiva	++	++	++	++	++
Dispersión de matriz en fase sólida	+	+	+	++	+

*(-), menos favorable; (+), favorable; (++), muy favorable

Debido a las propiedades volátiles de los PAHs y PBDEs, la cromatografía de gases (GC) suele ser la técnica mayormente utilizada para la **separación** de estos compuestos[161]. Sin embargo, también es habitual la utilización de la cromatografía de líquidos (LC) en la determinación de PAHs y, sobre todo, para los metabolitos hidroxilados, que presentan gran polaridad[162]. Algunos métodos, también determinan los metabolitos hidroxilados mediante GC con un previo proceso de derivatización, donde se introduce un elemento a la molécula para que adquieran propiedades apolares y volátiles. En compuestos como OH-PAHs y OH-BDEs, la sililación es el método de derivatización[163,164].

[161] **Shelepchikov** *et al.* A New Method for Purifying Fat-Containing Extracts in the Determination of Polybrominated Diphenyl Ethers. *J Anal Chem*. **2019**.

[162] **Song** *et al.* Simultaneous determination of polybrominated diphenyl ethers and hydroxylated analogues in human serum using high-performance liquid chromatography-inductively coupled plasma mass spectrometry. *J Chromatogr B Analyt Technol Biomed Life Sci.* **2020**.

[163] **Motorykin** *et al.* Determination of parent and hydroxy PAHs in personal PM2.5 and urine samples collected during Native American fish smoking activities. *Science Total Environ*, **2015**.

En cuanto a la **detección**, los PAHs tienen propiedades físicoquímicas de fluorescencia, por lo que suele ser muy habitual la determinación mediante cromatografía líquida con **detector de fluorescencia** (FLD), ya que es bastante selectiva (cada PAH tiene su $\lambda_{excitación}$ y $\lambda_{emisión}$) y sensible. Por otro lado, los PBDEs, presentan gran sensibilidad con **detectores de captura electrónica** (ECD). Este detector suele ir acoplado a cromatografía de gases y es capaz de detectar compuestos que contienen átomos electronegativos, como halógenos. Funciona emitiendo una corriente de electrones continua en presencia de un gas portador, donde los analitos con alta afinidad electrónica capturan estos electrones, reduciendo la corriente medida, la cual es convertida en señal. A pesar de la gran sensibilidad que presentan estos detectores para los compuestos específicos, carecen de selectividad, es decir, la identificación es complicada cuando se trata de una muestra muy compleja o se van a determinar compuestos similares, como pueden ser congéneres o metabolitos isoméricos. En estos casos, se suele optar por detectores como la **espectrometría de masas** (MS), bien sea acoplada a cromatografía líquida o gaseosa. Esto es debido a que la espectrometría de masas permite identificar y cuantificar compuestos en una muestra mediante la medición de la relación masa-carga (m/z) de sus iones. Funciona ionizando y fragmentando las moléculas, separándolas según su m/z en un analizador previamente a ser detectadas. De esta forma, se genera un gráfico denominado espectro de masas, que representa los picos (señal que relaciona la m/z con la intensidad detectada) correspondientes a los fragmentos iónicos del compuesto analizado. Estos espectros de masas actúan como "huellas dactilares" únicas, facilitando información precisa sobre el peso molecular, estructura química y composición isotópica de los compuestos, permitiendo la identificación precisa de sustancias, incluso en mezclas complejas, gracias a su alta sensibilidad y especificidad.

El estudio de la **metabolómica** es crucial para evaluar la biotransformación. Sin embargo, dependiendo del objetivo del trabajo, el enfoque puede estar en una metabolómica dirigida (metabolitos preseleccionados) o metabolómica no dirigida (análisis global de metabolitos), y con ello, la elección de la técnica analítica. En los

[164] **Butryn** *et al*. One-shot' analysis of polybrominated diphenyl ethers and their hydroxylated and methoxylated analogs in human breast milk and serum using gas chromatography-tandem mass spectrometry. *Anal Chim Acta*. **2015**.

últimos años, la cromatografía líquida-espectrometría de masas en tándem (LC-MS/MS) se ha convertido en un método potente para la metabolómica no dirigida, debido a que permite un rango más amplio de metabolitos con diferentes polaridades y pesos moleculares[165]. Sin embargo, como en esta Tesis Doctoral, si el objetivo es la determinación dirigida de metabolitos (volátiles o fácilmente derivatizables) con estructuras isoméricas, lo ideal es la utilización de la cromatografía de gases[166]. Esto es debido a que la cromatografía de gases suele utilizar la fuente de impacto electrónico para ionizar las moléculas, con un haz de electrones que siempre trabaja a la misma alta energía (70 eV). De esta forma, las moléculas siempre se fragmentan del mismo modo, pudiéndolas identificar fácilmente, gracias a las librerías generadas en las bases de datos con espectros característicos de cada compuesto.

7.2.2. Cuantificación de la concentración biodisponible

Como se ha comentado anteriormente, la estrategia analítica para la determinación de la concentración libre es utilizar herramientas que emplean matrices que extraen sustancias químicas no unidas, como recubrimientos poliméricos en microextracción en fase sólida (SPME) o membranas de diálisis. Sin embargo, compuesto lipofílicos como POPs, tienen tendencia a unirse al plástico o a las membranas de diálisis y, por ello, la técnica SPME es la más apropiada, actualmente[53,167.]

La técnica **SPME** consiste en la exposición directa de una fibra de vidrio, recubierta con un recubrimiento polimérico selectivo afín al compuesto objeto de estudio, sobre la muestra. Para diferentes compuesto hidrofóbicos y neutros, se han utilizado fibras SPME de materiales basados en poliacrilato (PA)[168],

[53] **Proença** *et al*. Effective exposure of chemicals in in vitro cell systems: A review of chemical distribution models. *Toxicol In Vitro.* **2021**.

[165] **Yue** *et al.* Biotransformation-based metabolomics profiling method for determining and quantitating cancer-related metabolites. *J Chromatogr A*. **2018**.

[166] **Johnson-Restrepo** *et al.* Polycyclic aromatic hydrocarbons and their hydroxylated metabolites in fish bile and sediments from coastal waters of Colombia. *Environ Poll*. **2008**.

[167] **Henneberger** *et al.* Quantification of freely dissolved effect concentrations in in vitro cell-based bioassays. *Arch Toxicol*. **2019**.

[168] **Endo** *et al.* Polyparameter linear free energy models for polyacrylate fiber-water partition coefficients to evaluate the efficiency of solid-phase microextraction. *Anal Chem*. **2011**.

poli(dimetilsiloxano) (PDMS)[169] y C18[170]. El recubrimiento sirve como fase sólida que extrae moléculas libremente disueltas. Este proceso se suele realizar en 2 modalidades diferentes (**Figura 19**):

- **Extracción directa** (Headspace, HS-SPME): La fibra se coloca en el espacio de cabeza sobre la muestra para capturar compuestos volátiles.
- **Extracción en inmersión** (DI-SPME): La fibra se sumerge directamente en la muestra líquida.

Durante la exposición, los analitos se adsorben a la fibra llegando a alcanzar una distribución equilibrada entre la matriz de la muestra y el revestimiento de la fibra. En este punto, la concentración de analito permanece constante, independientemente del aumento del tiempo de extracción. Una vez alcanzado el equilibrio, se realiza una desorción térmica con análisis directo por cromatografía de gases o en solvente para su posterior análisis (**Figura 19**). La cantidad de moléculas extraídas es proporcional a su concentración en la muestra y depende del valor de la constante de equilibrio (coeficiente de partición o relación de distribución) del analito entre la muestra y el material que recubre la fibra[171,172,173].

[169] **Endo** *et al.* Liposome and protein-water partitioning of polybrominated diphenyl ethers (PBDEs). *Chemosphere*. **2013**.
[170] **Henneberger** *et al.* C18-Coated Solid-Phase Microextraction Fibers for the Quantification of Partitioning of Organic Acids to Proteins, Lipids, and Cells. *Chem Res Toxicol*. **2019**.
[171] **Flores-Ramírez** *et al.* Rapid analysis of persistent organic pollutants by solid phase microextraction in serum samples. *Talanta*. **2014**.
[172] **Schmidt and Podmore**. Solid Phase Microextraction (SPME) Method Development in Analysis of Volatile Organic Compounds (VOCS) as Potential Biomarkers of Cancer. *Journal of Molecular Biomarkers & Diagnosis.* **2015**.
[173] **Sereshti** *et al.* Nanosorbent-based solid phase microextraction techniques for the monitoring of emerging organic contaminants in water and wastewater samples. *Microchimica Acta*. **2020**.

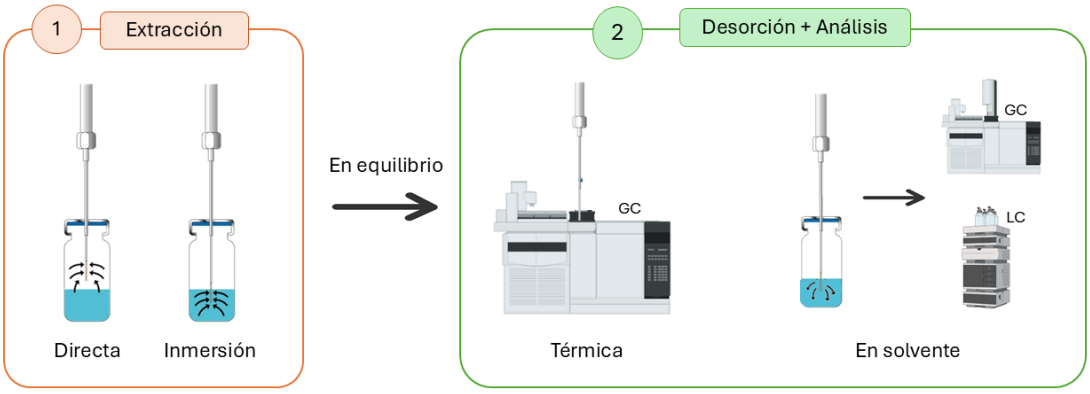

Figura 19. *Procedimiento de la técnica microextracción en fase sólida (SPME).*

Sin embargo, la **dificultad analítica** en la determinación de la concentración libre en un sistema *in vitro* mediante SPME radica en que **no existe un único equilibrio entre la fibra y el compuesto disuelto**. En este tipo de sistema se establecen múltiples equilibrios, ya descritos en la *Sección 5.3.1 "Concentración biodisponible"* y representados en la **Figura 9**, los cuales se ven modificados ($D_{unido/medio}$) al introducir un nuevo equilibrio, correspondiente a la interacción fibra/medio ($D_{fibra/medio}$), como se muestra en la **Figura 20**. Esta alteración afecta a la constante de equilibrio global, lo que complica notablemente la reproducción experimental del sistema completo de equilibrios y la determinación precisa de las constantes asociadas a cada uno de ellos, tanto antes como después de la incorporación de la fibra. En este contexto, **la estrategia más viable actualmente** consiste en estimar el potencial de unión de un compuesto con la fibra, ajustando el diseño experimental de manera que se asemeje lo máximo posible a un sistema sin la presencia de la fibra. En el marco de esta Tesis Doctoral, y de acuerdo con el diseño experimental desarrollado en esta, el equilibrio de unión más relevante en el sistema es el correspondiente a la interacción con la proteína BSA del suero añadido al medio de cultivo. Por tanto, se ha empleado una única constante de partición, $D_{fibra/medio+BSA}$, para el compuesto en estudio. Esta constante se ha determinado en un medio que contiene BSA, considerando insignificantes las contribuciones al equilibrio por parte de las células y del material de la placa, dado que se han utilizado placas de vidrio, como se describe en la metodología experimental.

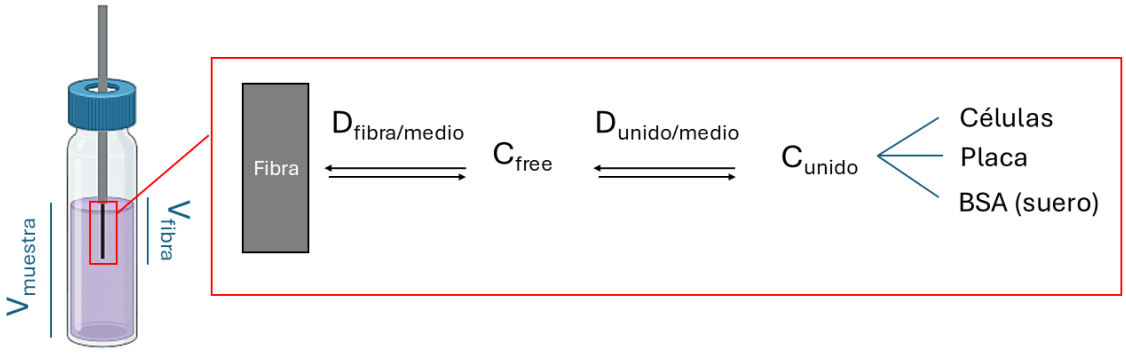

Figura 20. *Equilibrios presentes en el sistema in vitro después de añadir la fibra SPME.*

Teniendo en cuenta lo anterior, la **concentración libre estimada** antes de la introducción de la fibra se determina mediante la **Ecuación 10**. Este cálculo depende del volumen total de la muestra ($V_{muestra}$), del volumen de la fibra (V_{fibra}), el cual se define en función del material y la longitud de esta, de la concentración inicial total en el medio antes de la introducción de la fibra ($C_{medio,0h}$), de la constante de partición del sistema fibra-medio-BSA, así como de la concentración en la fibra una vez alcanzado el equilibrio. Esta última se determina a partir de la **Ecuación 11**, que depende de la concentración analizada ($C_{desorción}$) y del volumen empleado ($V_{desorción}$) en el proceso de desorción en disolvente tras alcanzar el equilibrio.

$$C_{free} = \frac{C_{medio,0h} \cdot V_{muestra}}{D_{fibra/medio+BSA} \cdot \left(\frac{C_{medio,0h} \cdot V_{muestra}}{C_{fibra}} - V_{fibra}\right)} \qquad \text{Ec. (10)}$$

$$C_{fibra} = \frac{C_{desorción} \cdot V_{desorción}}{V_{fibra}} \qquad \text{Ec. (11)}$$

7.2.3. Caracterización y detección de MNPLs.

La caracterización, detección y cuantificación de MNPLs en estudios de ecotoxicidad es fundamental para evaluar su presencia en los ecosistemas y en los organismos, así como para comprender sus efectos. Sin embargo, esta tarea representa un desafío analítico debido a su compleja composición, la variedad de tamaños y sus propiedades físicoquímicas heterogéneas y, en muchos casos,

desconocidas[174]. Actualmente, no existe una técnica analítica "universal", siendo necesario la combinación de diferentes técnicas complejas.

Tal como se resume en la **Tabla 8**, las técnicas de **microscopía** electrónica de barrido (SEM), electrónica de transmisión (TEM), de fluorescencia, microscopía o confocal permiten analizar la **morfología y tamaño**, aunque presentan limitaciones como la falta de identificación química o la necesidad de marcadores específicos. Las **técnicas espectroscópicas** de infrarrojo con transformada de Fourirer (FTIR) o Raman permiten la **identificación química**, pero su sensibilidad disminuye con partículas muy pequeñas. Por otro lado, las técnicas destructivas como pirolisis cromatografía de gases espectrometría de masas (py-GC-MS) ofrecen buena resolución química, aunque requieren equipos especializados. Para la **cuantificación y distribución de tamaños**, técnicas como espectrometría de masas con plasma acoplado inductivamente en su modalidad de partícula única (sp-ICP-MS)**,** dispersión dinámica de la luz (DLS), citometría de flujo y análisis de seguimiento de nanopartículas (NTA) son útiles, aunque no distinguen composición y están limitadas por el rango de detección. Finalmente, los métodos de **separación** como cromatografía por exclusión de tamaño (SEC), fraccionamiento de campo-flujo de flujo asimétrico (AF4) son eficaces en el fraccionamiento de partículas, pero necesitan acoplarse a técnicas analíticas adicionales para la caracterización completa[175,176].

[174] **Huber** *et al.* Physicochemical characterization and quantification of nanoplastics: applicability, limitations and complementarity of batch and fractionation methods. *Anal Bioanal Chem*. **2023**.

[175] **Mahapatra** *et al.* Microplastics and nanoplastics in environment: Sampling, characterization and analytical methods. *Groundwater for Sustainable Development.* **2024**.

[176] **Fu** *et al.* Separation, characterization and identification of microplastics and nanoplastics in the environment. *Sci Total Environ*. **2020**.

Tabla 8. *Aplicaciones y limitaciones de las diferentes técnicas analíticas para caracterizar, detectar y/o cuantificar MNPLs.*

Categoría	Técnica	Aplicación	Limitaciones
Microscopia	SEM	Morfología, tamaño y estructura superficial	No proporciona identificación química
	TEM + RDX	Análisis elemental	No diferencia entre tipo de polímero
	Fluorescencia Confocal	Detección de MNPLs marcados	Depende de colorante específico
Espectroscopia	FTIR	Identificación	Baja resolución para NPLs
	Raman	Detección partículas	Sensible a la fluorescencia de muestras
Espectrometria	Py-GC-MS	Identificación polímeros	Destructiva. Requiere equipo especializado
	GC-MS	Detección aditivos o compuestos adheridos	No identifica morfología
	ICP-MS	Identificación trazas metálicas adheridas	No caracteriza
	sp-ICP-MS	Cuantificación y distribución de tamaño	Equipo especializado, baja sensibilidad, limitado por tamaño
Dispersión	DLS	Medida del tamaño	No distingue entre plásticos y otras partículas
	NTA	Tamaño, concentración y movilidad	No distingue composición química. Limitada por tamaño
	Citometría de flujo	Cuantificación. Detección individual de partícula por luz dispersada y fluorescencia por partícula marcada	Limitación de tamaño para la cuantificación.
Separación	Filtración y Centrifugación	Separación por tamaño de partícula	Difícil en NPLs. Retención en los materiales usados
	SEC		Requiere pretatamiento de la muestra
	AF4		Requiere acoplamiento a técnicas de detección como DLS o ICP-MS

IV. OBJETIVOS

IV. OBJETIVOS

El incremento masivo de contaminantes orgánicos persistentes en el medio ambiente, la necesidad de evaluar su toxicidad y la demanda de las agencias internacionales por transformar la experimentación animal hacia ensayos más éticos, desemboca en el impulso por desarrollar **metodologías alternativas**, enmarcadas dentro del principio de las "3R", eficaces, rápidas y económicamente viables. Este enfoque, sumado al **concepto de toxicidad actual**, basado en la evaluación tanto de los efectos como en la comprensión de los mecanismos, movimientos y vías de toxicidad durante todo el ciclo de vida de los compuestos, conducen a la formulación de un **doble objetivo general** de la presente Tesis Doctoral:

i) **Desarrollo y evaluación** de metodologías alternativas *in vivo* (larvas de pez cebra) e *in vitro* (líneas celulares) para el estudio de la toxicidad, bioacumulación y biotransformación de contaminantes orgánicos persistentes.
ii) **Aplicación** de las metodologías alternativas para la evaluación de la toxicidad, bioacumulación y biotransformación de contaminantes orgánicos persistentes con la presencia de nanoplásticos.

Para alcanzar el doble objetivo general, se plantearon los **objetivos específicos** que se describen a continuación:

<u>Objetivo general 1:</u>

1.1. Desarrollar **metodologías analíticas** miniaturizadas, selectivas y sensibles que permitan la cuantificación simultánea de dos POPs (fenantreno y BDE-47) y sus metabolitos mayoritarios preseleccionados en muestras biológicas (larvas, células y medios de exposición) para su implementación como herramienta fundamental en la evaluación de la bioacumulación y biotransformación.
1.2. **Evaluar** la metodología analítica desarrollada previamente, para el estudio de la **bioacumulación** (determinación del BCF) y su enfoque en el estudio de **biotransformación** de POPs mediante **larvas de pez cebra**.

1.3. Desarrollar un **diseño experimental** que permita el estudio de las cinéticas de bioacumulación y biotransformación de los dos POPs seleccionados en un sistema *in vitro*.

1.4. Evaluar la capacidad de diferentes líneas celulares para bioacumular y biotransformar POPs, para su implementación como un **modelo alternativo *in vitro***.

1.5. Evaluar diferentes metodologías de **estimación del BCF** *in vitro*.

1.6. **Aportar datos** y mayor **conocimiento** sobre el comportamiento de los POPs en sistemas *in vitro*, así como discusión de las limitaciones, para refinar los modelos existentes.

Objetivo general 2:

2.1. Selección de **técnicas (bio)analíticas** para la evaluación de la citotoxicidad y detección de NPLs en muestras biológicas.

2.2. **Aplicación de las metodologías** elegidas, así como las técnicas (bio)analíticas, para la evaluación de la toxicidad, bioacumulación y biotransformación de POPs seleccionados en **presencia de NPLs** mediante larvas de pez cebra y líneas celulares de peces.

V. OBJECTIVES

V. OBJECTIVES

The massive increase of persistent organic pollutants in the environment, the need to assess their toxicity, and the demand from international agencies to shift animal experimentation toward more ethical testing methods have driven the development of **alternative methodologies**, framed within the "3Rs" principle, that are effective, rapid, and economically viable. This approach, combined with the **current concept of toxicity**, which is based not only on the evaluation of effects but also on the understanding of mechanisms, movements, and toxicity pathways throughout the entire life cycle of compounds, leads to the formulation of the **dual general objective** of this Doctoral Thesis:

i) **Development and evaluation** of alternative *in vivo* (zebrafish larvae) and *in vitro* (cell lines) methodologies for the study of toxicity, bioaccumulation, and biotransformation of persistent organic pollutants.

ii) **Application** of alternative methodologies for the evaluation of the toxicity, bioaccumulation, and biotransformation of persistent organic pollutants in the presence of nanoplastics.

To achieve the dual general objective, the **specific objectives** outlined below were established

<u>General objective 1:</u>

1.1. To develop miniaturized, selective, and sensitive **analytical methodologies** that enable the simultaneous quantification of two POPs (phenanthrene and BDE-47) and their major preselected metabolites in biological samples (larvae, cells, and exposure media) for their implementation as a fundamental tool in the evaluation of bioaccumulation and biotransformation.

1.2. To **evaluate** the previously developed analytical methodology for the study of **bioaccumulation** (determination of BCF) and its application in the study of POPs **biotransformation** using **zebrafish larvae**.

1.3. To develop an **experimental design** that enables the study of the bioaccumulation and biotransformation kinetics of the two selected POPs in an *in vitro* system.

1.4. To evaluate the capacity of different cell lines to bioaccumulate and biotransform POPs, for their implementation as an **alternative *in vitro* model**.

1.5. To evaluate different methodologies for the **estimation of *in vitro* BCF.**

1.6. To **provide data** and **further knowledge** on the behaviour of POPs in *in vitro* systems, as well as a discussion of the limitations, to refine existing models.

General objective 2:

2.1. Selection of **(bio)analytical techniques** for the evaluation of cytotoxicity and detection of NPLs in biological samples.

2.2. **Application of the selected methodologies,** as well as the (bio)analytical techniques, for the evaluation of toxicity, bioaccumulation, and biotransformation of selected POPs in the **presence of NPLs** using zebrafish larvae and fish cell lines.

VI. PLAN DE TRABAJO

VI. PLAN DE TRABAJO

Para alcanzar el doble objetivo general planteado en esta Tesis Doctoral, se ha diseñado y seguido un Plan de Trabajo, representado en la **Figura 21**. Cada uno de los objetivos generales se desarrolla en una sección diferenciada dentro de la metodología experimental. En particular, el primer objetivo se subdivide en dos subsecciones, en las cuales se describe el desarrollo y la evaluación de una metodología alternativa mediante enfoques *in vivo* e *in vitro*, respectivamente. Cada sección y/o subsección se vincula con uno o más artículos científicos, ya sea publicados o en proceso de publicación, derivados de los resultados obtenidos en esta investigación. A continuación, se detalla el Plan de Trabajo empleado.

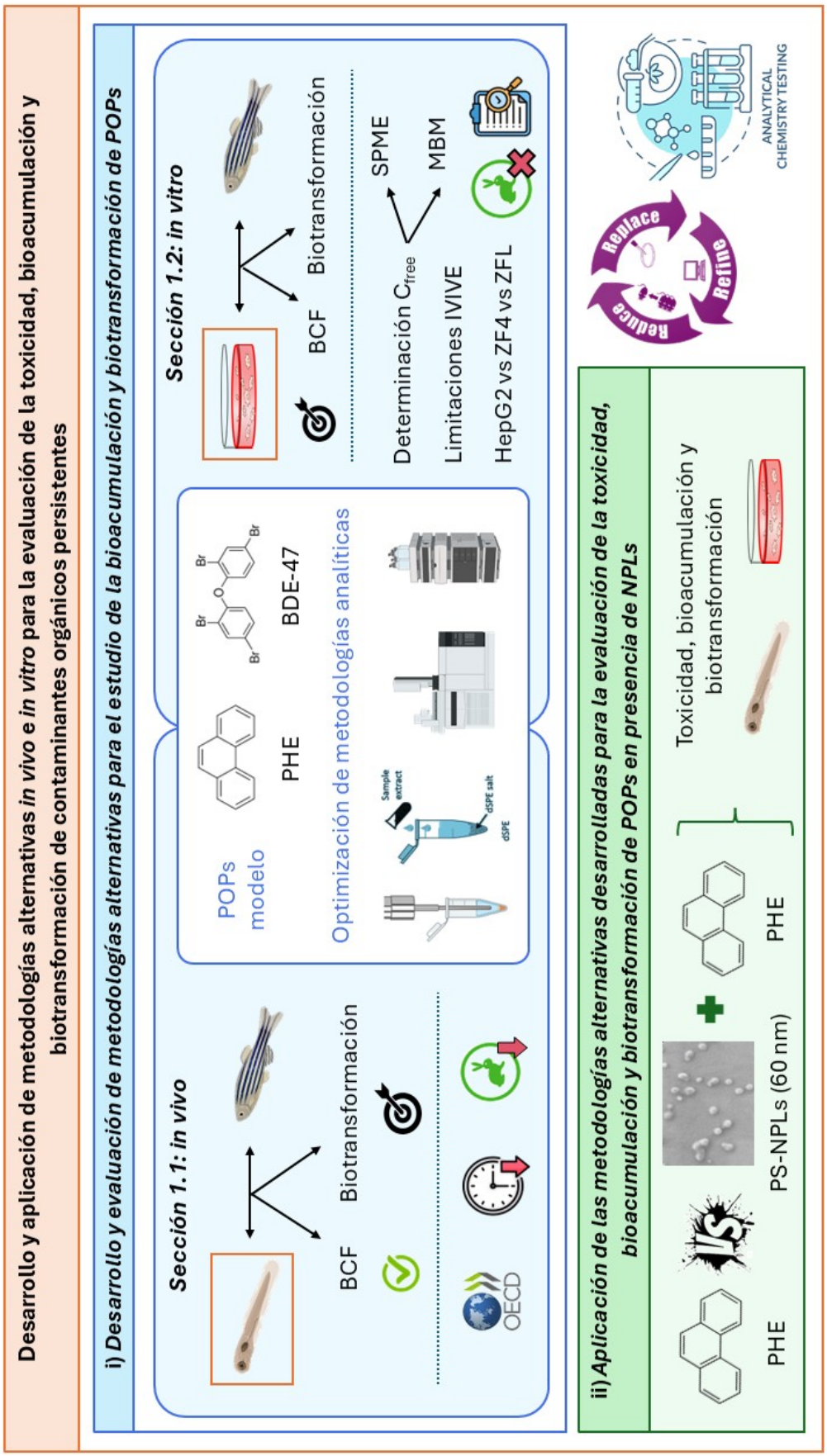

Figura 21. *Plan de Trabajo*

Capítulo 1. *Desarrollo y evaluación de metodologías alternativas para el estudio de la toxicidad, bioacumulación y biotransformación de POPs*.

- Seleccionar compuestos orgánicos persistentes "modelo" y, actualmente, interesantes, de acuerdo con la literatura, para el desarrollo, evaluación y aplicación de las metodologías alternativas: Fenantreno (PHE) y BDE-47.
- Seleccionar los metabolitos mayoritarios de los compuestos seleccionados para el estudio biotransformativo dirigido: OH-PHE, OH-BDEs y MeO-BDEs.
- Optimización de técnicas cromatográficas LC y GC para la separación de los diferentes metabolitos y compuestos parentales para su detección mediante MS, fluorescencia y/o microECD, que permita su identificación y cuantificación: Evaluación de diferentes rampas de temperatura, fase móvil, condiciones de derivatización y patrones internos.
- Desarrollo de un método de preparación de muestra eficaz, rápido, de bajo coste y miniaturizado, capaz de extraer de forma cuantitativa y simultánea los compuestos de las matrices biológicas (larvas y células) y medios de exposición: Evaluación de diferentes técnicas, extractantes y sales limpiadoras.

Sección 1.1. *Metodología in vivo mediante larvas de pez cebra.*

- Diseño experimental para la evaluación de la biotransformación mediante larvas de pez cebra (72 hpf) con la colaboración del Centro Tecnológico y de Investigación Marina y Alimentaria - AZTI, donde se lleva a cabo la exposición, basado en las condiciones establecidas de cuidado y experimentación de la guía oficial OECD 305 y el diseño experimental, desarrollado previamente por el grupo de investigación donde se realiza esta Tesis Doctoral, para ensayos de bioacumulación.
- Utilizando como compuesto modelo de interés el BDE-47, exponer las larvas y muestrearlas de acuerdo con el diseño experimental y determinar la concentración del compuesto y sus metabolitos en el interior de las larvas y medios de exposición con la metodología analítica desarrollada.

- Tratamiento de datos mediante ecuaciones toxicocinéticas de acuerdo con la guía OECD 305 para la estimación del BCF y ratios de metabolización de los metabolitos detectados.
- Discusión de los resultados obtenidos mediante la comparación con estudios *in silico* y con organismos vivos recogidos en la literatura para evaluar la validez de la metodología alternativa con larvas de pez cebra, así como la metodología analítica desarrollada, para estudios de bioacumulación y biotransformación.

Sección 1.2. *Metodología in vitro mediante líneas celulares.*

- Diseño experimental para la evaluación de la bioacumulación y biotransformación de los POPs seleccionados (PHE y BDE-47) mediante líneas celulares: tipo de placa de cultivo (material y tamaño), tiempos de muestreo, cantidad de células, controles y cálculos adicionales necesarios y preparación de muestras.
- Evaluación de la viabilidad celular (Ensayo MTT o Resazurina) de cada línea celular utilizada (HepG2, ZF4 y ZFL) con cada compuesto en estudio para determinar el límite de concentración de exposición (>70% viabilidad) adecuado para el experimento.
- Estudio de las cinéticas de bioacumulación y el poder biotransformativo de las líneas celulares seleccionadas mediante el diseño experimental y metodología analítica desarrollada, determinando la concentración del compuesto y sus metabolitos en el interior de las células y medios de cultivo a los diferentes tiempos de exposición.
- Determinación de la concentración biodisponible mediante la estimación través de modelos de balance de masa (MBM) y experimentalmente con la técnica SPME.
- Evaluación de la importancia de la determinación experimental de la concentración biodisponible en un sistema *in vitro* y concentraciones internas de las células para la determinación del BCF más cercano a la realidad, en comparación con las estimadas a partir de MBM.

- Tratamiento de datos para la estimación del BCF mediante diferentes metodologías: relación directa de concentraciones en los diferentes tiempos de muestreo, modelo toxicocinético y modelo IVIVE.
- Estudio de las limitaciones del modelo IVIVE y aportación de datos y observaciones para el refinamiento del modelo.
- Discusión de los resultados obtenidos mediante la comparación con estudios *in vivo* e *in silico* recogidos en la literatura y/o con los resultados obtenidos mediante larvas de pez cebra en el transcurso de esta Tesis Doctoral para evaluar la validez de la metodología alternativa con líneas celulares, así como la metodología analítica desarrollada, para estudios de bioacumulación y biotransformación.

Capítulo 2. *Aplicación de las metodologías desarrolladas para la evaluación de la toxicidad, bioacumulación y biotransformación de PHE en presencia de NPLs.*

- Diseño experimental para la evaluación de la toxicidad, bioacumulación y biotransformación de PHE mediante larvas de pez cebra (72 hpf) y líneas celulares de peces con la colaboración del Instituto de Biotecnología y Biomedicina de la Universidad Autónoma de Barcelona (IBB-UAB).
- Evaluación de la toxicidad de diferentes concentraciones de PHE en combinación con dos concentraciones (no tóxicas) de nanoplásticos de poliestireno de 44 nm mediante ensayos de citotoxicidad (MTT y citometría de flujo) con las líneas celulares ZFL y RTgutGC y ensayos efecto-respuesta con larvas de pez cebra.
- Evaluación de la absorción de los PS-NPLs (marcados con Dragon Green) en las células, mediante citometría de flujo y microscopía confocal y en larvas de pez cebra mediante microscopía de fluorescencia, en presencia de PHE.
- Evaluación de la bioacumulación y biotransformación de PHE en células y larvas de pez cebra, mediante la aplicación de la metodología experimental desarrollada, en presencia de PS-NPLs.
- Discusión de los efectos observados de acuerdo con los resultados obtenidos para los diferentes sistemas estudiados según su complejidad, tejido y organismo.

VII. METODOLOGÍA EXPERIMENTAL

VII. METODOLOGÍA EXPERIMENTAL

1. Desarrollo y evaluación de metodologías alternativas para el estudio de la toxicidad, bioacumulación y biotransformación de POPs.

De acuerdo con el **Reglamento Europeo** en vigor[6] relativo al Registro, la Evaluación, la Autorización y la Restricción de las sustancias y preparados químicos (REACH), para **evaluar la toxicidad** de los compuestos químicos, además de valorar el efecto y riesgo de estos, se debe describir su movimiento y comportamiento en los organismos y en el medio ambiente. En este sentido, la **bioacumulación** de las sustancias químicas en los organismos se ha convertido en un parámetro fundamental en la evaluación del riesgo tóxico. Además, se ha demostrado que la **biotransformación** puede ser también un factor clave debido a que, por un lado, los metabolitos formados pueden ser más o menos tóxicos y/o activos que la sustancia inicial y, por otro lado, puede reducir la bioacumulación de esta. Por tanto, el estudio de los procesos de bioacumulación y biotransformación es importante para conocer el comportamiento y la toxicidad real de las sustancias a una dosis determinada. Sin embargo, y al contrario que la bioacumulación para cuya evaluación existen métodos oficiales como la guía OECD 305[18], no existe todavía una metodología oficial validada para el estudio de la biotransformación. Es cierto que hay muchos trabajos centrados en el estudio de la biotransformación, sin embargo, son muy pocos los que dan valores conjuntos o se encargan de **estudiar** los dos procesos **de forma simultánea**.

Al mismo tiempo, las agendas internacionales están demandando una revisión integral y la transformación de las metodologías para evaluar la toxicidad hacia ensayos que Reduzcan, Reemplacen y Refinen la experimentación animal (**Principio de las 3Rs**). Para el estudio de los efectos que una sustancia provoca a un organismo, desde hace bastantes años, se vienen utilizando **ensayos alternativos** con embriones de peces, con células o modelos matemáticos. Sin embargo, en el campo de la bioacumulación y biotransformación, como se describe en las siguientes secciones, todavía queda mucho por investigar y desarrollar para

[6] **REACH**. Regulation (EC) **No1907/2006** of the european parliament and of the council. **2006**.
[18] **OECD No 305**. Bioaccumulation in Fish: Aqueous and Dietary Exposure. **2012**.

obtener resultados más realistas que permitan aplicar oficialmente estas metodologías alternativas.

Los **POPs** representan una preocupación ambiental y de salud pública debido a su alta estabilidad química, su capacidad de bioacumulación en los organismos y su potencial para sufrir biotransformaciones que pueden alterar su toxicidad. A pesar de las regulaciones que han prohibido o restringido su uso, muchos de estos compuestos siguen presentes en el ambiente, lo que hace necesario continuar su estudio para comprender sus mecanismos de acción y su impacto en los ecosistemas. En este contexto se encuentran los **PAHs** y los **PBDEs**, los cuales, además, ya han sido evaluados mediante metodologías validadas y oficiales, lo que los convierte en **modelos** clave para desarrollar enfoques alternativos de monitoreo y análisis. Además, no solo permiten profundizar en el conocimiento de los procesos de bioacumulación y biotransformación, sino que también sirven como referencia para el estudio de nuevos POPs emergentes con propiedades similares, facilitando la optimización de estrategias para su detección, evaluación de riesgos y control ambiental.

De la mano con el desarrollo de metodologías alternativas en toxicología, el desarrollo de **metodologías analíticas** es fundamental para la detección, identificación y cuantificación de sustancias en matrices biológicas, permitiendo una mejor comprensión de su comportamiento y una evaluación más precisa de su toxicidad. Una de las principales limitaciones de los modelos alternativos actuales es la ausencia de determinaciones experimentales de las concentraciones en los organismos, debido a la dificultad que representa el pequeño tamaño de las muestras. Esto obliga a recurrir a estimaciones basadas en modelos de distribución química y en las propiedades fisicoquímicas de los compuestos o, en su defecto, a realizar mediciones exclusivamente en los medios de exposición. Por ello, en esta tesis doctoral, se desarrollan metodologías analíticas como herramienta para evaluar simultáneamente la bioacumulación y biotransformación de manera rápida, eficaz y de bajo coste en muestras de pequeño tamaño, como larvas o células, y para proporcionar información acerca del comportamiento de los compuestos en sistemas alternativos, contribuyendo a mejorar los modelos existentes.

1.1. Metodología *in vivo* mediante larvas de pez cebra.

De acuerdo con el enfoque expuesto, en esta sección se presentan las evaluaciones de una metodología alternativa *in vivo*, basada en larvas de pez cebra, para el estudio de la bioacumulación y la biotransformación, contribuyendo a la **reducción** de la experimentación animal según el principio de las 3R.

Actualmente, los ensayos alternativos con embriones/larvas están estandarizados para la evaluación de la toxicidad (OECD 236[38]). Sin embargo, no existe un método validado que sirva como alternativa a la guía oficial con peces adultos para la evaluación de la bioacumulación (OECD 305[18]). En estudios anteriores dentro del grupo de investigación, se desarrolló un método (**Figura 7**) con eleuteroembriones (72 hpf) con el que se obtienen resultados comparables de BCF a los obtenidos con el ensayo estandarizado para gran variedad de sustancias químicas[43]. Para investigar si el método puede ser viable para el estudio de la biotransformación y, sobre todo, de forma simultánea a la bioacumulación, se llevó a cabo el primer trabajo (**Artículo 1**) titulado ***Bioaccumulation and biotransformation of BDE-47 using zebrafish eleutheroembryos (Danio rerio). (Environmental Toxicology and Chemistry, 42 (4), 835–845, 2023).***

Para ello, se decidió evaluar la metodología con el compuesto **BDE-47** (2,2',4,4'-tetrabromodifeniléter) ya que, a pesar de haber sido ampliamente estudiado, el conocimiento sobre las ratios de metabolización y su impacto en la bioacumulación no ha sido apenas investigado. Del mismo modo, y de acuerdo con la revisión de la bibliografía, se eligieron los **metabolitos mayoritarios** del BDE-47 encontrados en otros organismos (BDE-28, 2'-OH-BDE-28, 6-MeO-BDE-47, 5-MeO-BDE-47, 3-MeO-BDE47, 5-OH-BDE-47 y 3-OH-BDE-47) con el objetivo de realizar una determinación dirigida para evaluar si las larvas de 72 hpf son capaces de biotransformar durante el transcurso del ensayo (hasta las 144 hpf).

Para alcanzar el objetivo, la mayor parte del trabajo y la principal dificultad se centró en el **desarrollo de un método analítico** que permitiera la determinación

[18] **OECD No 305**. Bioaccumulation in Fish: Aqueous and Dietary Exposure. **2012**.
[38] **OECD No 236**. Fish embryo acute toxicity (FET) Test. **2013**.
[43] **Sanz-Landaluze** *et al.* Zebrafish (danio rerio) eleutheroembryo-based procedure for assessing bioaccumulation. *Environ Sci Technol*. **2015**.

simultánea del BDE-47 y sus metabolitos en una misma muestra, facilitando así una comparación directa entre ellos. En primer lugar, se optimizó la separación y detección cromatográfica mediante **GC-MS-µECD**, examinando diferentes columnas y condiciones hasta garantizar la resolución de los compuestos con la misma estructura isomérica. Gracias a la **detección simultánea** debida al acoplamiento de los dos detectores al final de la columna cromatográfica, se consiguió la selectividad y sensibilidad adecuadas a las concentraciones de trazas esperadas de los metabolitos para la identificación y cuantificación de los compuestos. En particular, para la determinación de los metabolitos OH-BDEs fue necesaria una **derivatización** previa, basada en una reacción de sililación, mediante la incubación térmica con MTBSTFA (N-metil-N-terc-butildimetilsililtrifluoroacetamida) como reactivo en una proporción de 20% a 70˚C durante 30 minutos. Este calentamiento de los extractos provocaba la pérdida de los compuestos que no requerían derivatización, como son los PBDEs y los metabolitos MeO-BDEs, por lo que se decidió no incubar la totalidad del extracto y realizar una doble determinación mediante la toma de una alícuota de este, destinada a la derivatización y análisis de los metabolitos OH-BDEs y la determinación directa del resto de compuestos.

Por otro lado, dado el reducido tamaño de las larvas, se desarrolló un procedimiento miniaturizado para la **preparación de muestras**, con el objetivo añadido de minimizar el uso de disolventes y reducir el tiempo de preparación de muestra. Se implementó una etapa de **extracción** asistida por sonda de ultrasonidos para liberar los compuestos del interior de las larvas al disolvente, seguida de una fase de limpieza de los extractos, necesaria debido a la alta presencia de lípidos e interferentes de la matriz. Esta **limpieza** se llevó a cabo mediante una extracción en fase sólida dispersiva (**d-SPE**). Para optimizar el proceso, se evaluaron diversas mezclas de disolventes de extracción con afinidad por los compuestos (hexano, metil-terc-butiléter (MTBE), diclorometano (DCM)), así como diferentes sales de limpieza (C18, PSA, Z-Sep y Florisil). La selección final (hexano:MTBE, 1:1 como disolvente de extracción y Florisil como sal de limpieza) se basó en un consenso entre las diferentes propiedades fisicoquímicas de los compuestos, como son la apolaridad del BDE-47 y los metabolitos MeO-BDEs en

comparación con los metabolitos OH-BDEs (polares). Por último, paso previo a la derivatización y análisis por GC-MS-μECD, se evaporaron los extractos hasta sequedad con el objetivo de reconstituir en isooctano, más adecuado para el análisis, y para realizar una concentración los compuestos, que asegurara su detección. Para controlar la recuperación del procedimiento experimental, al inicio de este se añadieron BDE-99 como **patrón interno** para los compuestos PBDEs y MeO-BDEs, y triclosán (TCS) como patrón interno para los OH-BDEs.

Los **eleuteroembriones** fueron expuestos, en el centro tecnológico AZTI, de acuerdo con el **diseño experimental** desarrollado previamente[43] para la evaluación de la bioacumulación (**Figura 7**). Siguiendo las restricciones del modelo oficial OECD 305[18], se expusieron a 1 y 10 $\mu g \cdot L^{-1}$ BDE-47, concentraciones inferiores al 1 y 0.1% del LC_{50} (4.2 $mg \cdot L^{-1}$[177]), respectivamente, hasta las 48h (fase de absorción) y, a continuación, se dejaron sin contaminante hasta las 72h (fase de desorción). Debido a la solubilidad limitada del BDE-47 en agua (11 $\mu g \cdot L^{-1}$[178]; 21.2 $\mu g \cdot L^{-1}$[179]), se disolvió en dimetilsulfóxido (DMSO) de modo que el medio contenga finalmente un 0.5% de DMSO[180]. Se fueron muestrearon 15 larvas y 1.5 mL de medio a los diferentes tiempos de exposición: 0, 17, 24, 41, 48, 65 y 72h. Adicionalmente, para asegurar la observación de metabolitos, se realizó un experimento a 100 y 250 $\mu g \cdot L^{-1}$ BDE-47, muestreándose únicamente a 0 y 48h. Además, de forma paralela se preparó un experimento control sin la adición del BDE-47.

Con el método analítico desarrollado, se determinaron las concentraciones del BDE-47 y los metabolitos seleccionados tanto en el interior de las larvas como en el medio a los diferentes tiempos de exposición. Por un lado, mediante la representación gráfica de dichas concentraciones se pudo observar la cinética de

[18] **OECD No 305**. Bioaccumulation in Fish: Aqueous and Dietary Exposure. **2012**.
[43] **Sanz-Landaluze** *et al.* Zebrafish (danio rerio) eleutheroembryo-based procedure for assessing bioaccumulation. *Environ Sci Technol*. **2015**.
[177] **Usenko** *et al*. PBDE developmental effects on embryonic zebrafish. *Environ Toxicol Chem*. **2011**.
[178] **Pereira** *et al.* Comparative study of genotoxicity induced by six different PBDEs. *Pharm Toxicol.* **2016**.
[179] **CompTox Chemicals Dashboard** v2.5.3. EPA. **2024**.
[180] **Hallare** *et al.* Comparative embryotoxicity and proteotoxicity of three carrier solvents to zebrafish (Danio rerio) embryos. *Ecotox Environ Safety*. **2006**.

absorción del BDE-47, así como, obtener el **BCF_k**, mediante el modelo toxicocinético descrito en la guía OECD 305. Los resultados obtenidos fueron comparables con los reportados en otros estudios con organismos acuáticos vivos.

Por otro lado, se identificaron y cuantificaron los metabolitos BDE-28, 2'-OH-BDE-28 y 5-MeO-BDE-47 en ambos experimentos, pudiendo obtener de forma directa la **ratio de metabolización** en relación con la concentración de BDE-47; confirmar la capacidad de biotransformación de las larvas de 72 hpf y aportar datos de las cinéticas de bioacumulación y biotransformación de forma **simultánea**. De este modo, se ha evaluado y demostrado la viabilidad de la metodología alternativa *in vivo* mediante larvas de pez cebra para el estudio de la bioacumulación y biotransformación, **reduciendo** de esta forma la experimentación animal.

ARTÍCULO 1:

Bioacumulación y biotransformación del BDE-47 utilizando eleuteroembriones de pez cebra (*Danio rerio*).

Bioaccumulation and biotransformation of BDE-47 using zebrafish eleutheroembryos (*Danio rerio*).

*Paloma De Oro-Carretero, Jon Sanz-Landaluze**

Environmental Toxicology and Chemistry 42, (4), 835–845, 2023 (IF: 3.6, Q2)

*Autor de correspondencia.

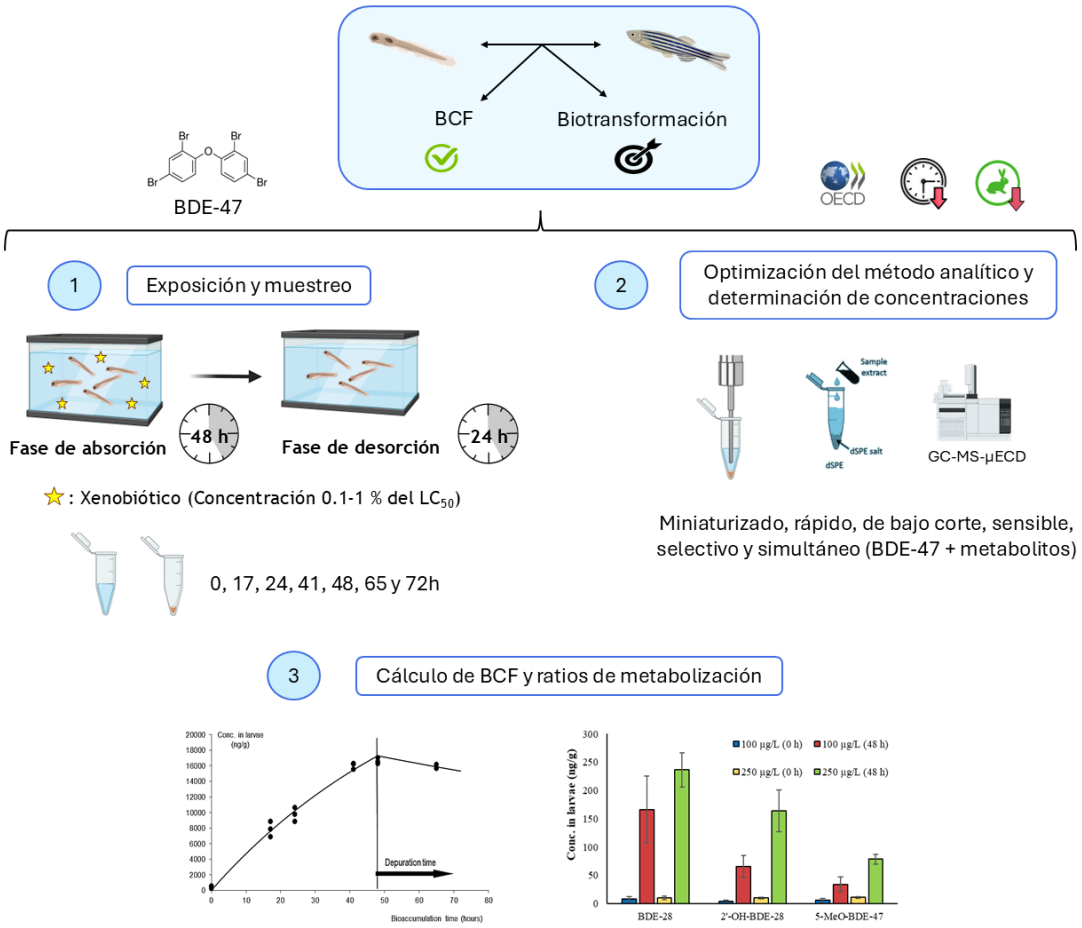

BCF similar a la guía oficial *in vivo*
Larvas 72 hpf pueden biotransformar
Estudio simultáneo bioacumulación y biotransformación

Environmental Toxicology and Chemistry—Volume 42, Number 4—pp. 835–845, 2023
Received: 22 September 2022 | Revised: 2 November 2022 | Accepted: 15 January 2023

Environmental Toxicology

Bioaccumulation and Biotransformation of BDE-47 Using Zebrafish Eleutheroembryos (*Danio rerio*)

Paloma De Oro-Carretero and Jon Sanz-Landaluze*

Department of Analytical Chemistry, Faculty of Chemical Science, Complutense University of Madrid, Madrid, Spain

Abstract: Polybrominated diphenyl ethers (PBDEs) are well-known endocrine disrupting chemicals identified as organic persistent pollutants. Their metabolites OH-BDE and MeO-BDE have been reported to be potentially more toxic than the postulated precursor PBDEs. One of the most predominant congeners of PBDEs in the environment is BDE-47, due to its high presence in industrially used mixtures. In the present study, the bioaccumulation and biotransformation of BDE-47 into its major metabolites is evaluated using zebrafish (*Danio rerio*) eleutheroembryos adapting a previously developed alternative method to bioconcentration official guideline Organisation for Economic Co-ordination and Development 305, which reduces the animal suffering, time, and cost. For the simultaneous determination of BDE-47 and its metabolites in larvae and exposure medium, and considering the polarity difference of the analytes and the small sample size, the development of a validated analytical method is a step to ensure quality results. In the present study, an ultrasound-assisted extraction followed by a solid phase extraction dispersive clean-up step and gas chromatography-mass spectrometry-microelectron capture detector (GC-MS-μECD) with a previous derivatization process was optimized and validated. Bioconcentration factors (BCFs) were calculated using a first-order one-compartment toxicokinetic model. The profiles found show rapid absorption in the first hours of larval development and great bioaccumulative capacity, finding BCFs of 7294 ± 899 and $36\,363 \pm 5702$ at nominal concentrations of 10 and 1 $\mu g\,L^{-1}$, respectively. Metabolization studies show increasing concentrations of the metabolites BDE-28, 2′-OH-BDE-28, and 5-MeO-BDE-47 throughout the exposure time. The results obtained show the feasibility of the method for bioaccumulation and open up the possibility of metabolic studies with zebrafish eleutheroembryos, which is a very underdeveloped field without official testing or regulation. *Environ Toxicol Chem* 2023;42:835–845. © 2023 The Authors. *Environmental Toxicology and Chemistry* published by Wiley Periodicals LLC on behalf of SETAC.

Keywords: Bioconcentration; Biotransformation; BDE-47; GC-MS-μECD; Metabolites; Zebrafish eleutheroembryos

INTRODUCTION

Polybrominated diphenyl ethers (PBDEs) are industrial substances that have been widely used as flame retardants for decades in commercial products due to their good thermal stability and low cost (Wen et al., 2015). Their proven toxicity (Zhang, Zhao, et al., 2020; Zhang, Zhou, et al., 2020) and structural similarity to thyroid hormones and thyroxine in particular, which induce neurodevelopmental and endocrine disrupting effects in humans (Butryn et al., 2020), have meant that nowadays some commercial PBDEs mixtures are banned, and they have been identified as Persistent Organic Pollutants by the Stockholm Convention since 2009 (United Nations Environmental Program, 2019). However, as a consequence of this persistence in the environment through long-term use and recycling processes, these chemicals are still detected at potentially dangerous levels in humans and in a wide range of biological and environmental samples (De la Torre et al., 2020; Klinčić et al., 2020; Liu et al., 2020).

In addition, hydroxylated (OH-BDE) and methoxylated (MeO-BDE) and, recently, dihydroxylated (diOH-BDE) products (Zhang, Zhou, et al., 2020) have been found in a wide diversity of environmental samples (Liu et al., 2014; Sun et al., 2020). Several studies have evidenced that metabolites maintain bioactive groups, exhibiting similar or even greater toxicity than the native PBDEs (Usenko et al., 2012), increasing the concern about these compounds. Although the mechanism of biotransformation of PBDEs, oxidated by hepatic cytochrome P450 (CYP) enzymes, has been proven (Li et al., 2010), there are contradictory reports

This article includes online-only Supporting Information.

* Address correspondence to jsanzlan@ucm.es
Published online 27 January 2023 in Wiley Online Library (wileyonlinelibrary.com).
DOI: 10.1002/etc.5569

of PBDE biotransformation depending on the organism studied (Erratico et al., 2013; Liu et al., 2015; Sun et al., 2013) and therefore they need to be further studied. In the present study, the bioaccumulation and biotransformation of 2,2′,4,4′-tetrabromodiphenyl ether (BDE-47) has been evaluated due to its abundance, toxicity (median lethal concentration [LC50] 4.2 mg L^{-1}; Usenko et al., 2011), persistence, and bioavailability (log K_{ow} 6.81; Pereira et al., 2016) in the environment.

The degree of bioaccumulation of a compound is expressed by the bioaccumulation factor, defined experimentally as the ratio between the concentration of the analyte in the organism and its surrounding medium. The bioconcentration factor (BCF) is also used for aquatic species (El-Amrani et al., 2012) and estimated under controlled laboratory conditions (Arnot & Gobas, 2006). The official method for assessing the BCF, proposed by the European Regulation for the Registration, Evaluation, and Authorisation of Chemicals (REACH), is guideline 305 of the Organisation for Economic Co-operation and Development (OECD, 2012). This test requires many adult fish (up to 104) and a long exposure time (up to 60 days), which creates a high cost for the experiments. On the other hand, in recent years, these same international organizations have called for a transformation in toxicity testing, seeking greater efficiency and a reduction in animal experimentation. Zebrafish is gaining interest as an ecotoxicology model organism (Lillicrap et al., 2016) because of its fast production, low cost, transparency, and close genomic homology with humans (more than 80%). Furthermore, because thyroid hormone regulators are highly conserved among vertebrate species, zebrafish is a useful model to investigate thyroid hormone-related compounds (Vancamp et al., 2019). In addition, European legislation considers eleutheroembryos as in vitro systems up to the self-feeding stage (2010/63/EU, 2010). In this sense, an alternative method based on the OECD 305 assay, developed in a research group using zebrafish eleutheroembryos (*Danio rerio*; Sanz-Landaluze et al., 2015) for bioaccumulation studies, is used in the present study, drastically reducing the time, cost, and animal suffering. In addition, in our recent studies (Molina-Fernández et al., 2021) it has been observed that eleutheroembryos are able to biotransform the parental compounds into some of their metabolites during the exposure time with this alternative method. This has opened up the possibility for us to continue using it for metabolic studies because this is an underdeveloped field with no official testing or regulation.

BDE-47 in zebrafish has been investigated in some studies (Liu et al., 2015; Wen et al., 2015; Zheng et al., 2012), but information on the full spectrum of potential metabolites and the metabolic pathways involved is still unclear. Therefore, the aim of the present study was the evaluation of bioaccumulation and the biotransformation of BDE-47 in the most abundant metabolites founded in the literature, 6-MeO-BDE-47, 5-MeO-BDE-47, 3-MeO-BDE-47, 6-OH-BDE-47, 5-OH-BDE-47, 3-OH-BDE-47, and 2′-OH-BDE-28 (Lacorte et al., 2010; Liu et al., 2015; Wen et al., 2015; Zhai et al., 2014) using zebrafish eleutheroembryos. For this purpose, it was necessary to develop a determination method for BDE-47 and its metabolites, both in the larvae and in the exposure medium. It is important to bear in mind that zebrafish eleutheroembryos samples are very small (0.44 mg/larvae dry wt), have a high lipid content (~15%), and their exposure concentrations are always below toxicological values (<1% of LC50). These sample characteristics make it necessary to implement extremely sensitive determination methodologies, capable of dealing with very small samples. For this reason, conventional Soxhlet, which has traditionally been the most widely used extraction method for PBDE from solid samples in a variety of matrices (Cruz et al., 2017), is not appropriate. To minimize the use of solvents and sample treatment time, the analytical protocol proposed in the present study is based on simultaneous miniaturized ultrasonic probe-assisted extraction with dispersive solid phase extraction (SPE) clean-up. Gas chromatography-mass spectrometry (GC-MS) is the most commonly used technique for the determination of PBDEs and MeO-PBDEs (Shelepchikov et al., 2019) and liquid chromatography for OH-BDEs (Song et al., 2020). However, the official method of the US Environmental Protection Agency (USEPA) for the detection of PBDEs is based on electron captured detection (ECD) because this is the most sensitive detection method. For this reason, simultaneous gas chromatography-mass spectrometry-microelectron capture detector (GC-MS-μECD) analysis by previous derivatization of OH-BDEs was carried out to determine the BDE-47 and its metabolites (MeO-BDEs and OH-BDEs) concentration under the same instrumental conditions.

MATERIAL AND METHODS

Reagent and samples

Individual commercial standards of 1 ml of PBDEs 28 (150 mg L^{-1}), 47 (350 mg L^{-1}), and 99 (116 mg L^{-1}) in methanol were purchased from Dr. Ehrenstorfer; individual 1-ml standards of the metabolites 6-MeO-BDE-47 (10 mg L^{-1}), 5-MeO-BDE-47 (50 mg L^{-1}), 3-MeO-BDE-47 (50 mg L^{-1}) in methanol, and 5-OH-BDE-47 (50 mg L^{-1}), 3-OH-BDE-47 (50 mg L^{-1}), and 2′-OH-BDE-28 (50 mg L^{-1}) in acetonitrile were supplied by AccuStandard 1,2,3,4-Tetrachloronaphthalene (TCN; 10 mg L^{-1} in isooctane; Dr. Ehrenstorfer) was used as internal standard for the PBDE congeners and the methoxylated metabolites (MeO-BDE) and triclosan (TCS; 10 mg L^{-1} in acetone; Dr. Ehrenstorfer) for the hydroxylated metabolites (OH-BDE). From these commercial solutions, individual working solutions of 1 mg L^{-1} in the same solvents and a mix of 100 μg L^{-1} of all the analytes to be determined (PBDEs, MeO-BDEs, and OH-BDEs) in isooctane were prepared by dilution. The derivatization reagent used for the analysis of the OH-BDE metabolites was N-tert-butyldimethylsilyl-N-methyltrifluoroacetamide (MTBSTFA) + 1% tert-butyl-methylchlorosilane supplied by Sigma Aldrich. The adsorbents of the "clean-up" stage were C_{18} ODS SPE Buk Sorbent (Agilent Technologies), PSA SPE Bulk Sorbent (Agilent Technologies), SupelTM QuE Z-Sep (Sigma Aldrich), and Florisil (E. Merck). The analytical-grade solvents used (isooctane, n-hexane, dichloromethane, methyl tert-butyl ether [MTBE], and dimethyl sulfoxide [DMSO]) were purchased from Sigma Aldrich. The exposed zebrafish (*Danio rerio*) media and eleutheroembryos were provided by AZTI Tecnalia (Bizkaia, Spain).

Instrument and apparatus

A Genie-2 vortex mixer from Scientific Industries and a Vibra cell VCx130 ultrasound probe from Sonics & Materials. with a 2-mm diameter titanium microtip and a 130-W high-frequency generator at 20 KHz were used for extraction procedures. An X50S Metal Carbide technical nitrogen stream and an Eppendorf 5415 R microcentrifuge were used for evaporation and centrifugation, respectively.

A gas chromatograph Agilent Mod. 7890 A Series equipped with an HP 7683B Series autoinjector, μECD and HP 5975 C VL MSD MS detector with ChemStation software (Agilent Technologies) was used for final separation and quantification of the PBDEs and their metabolites. The detectors worked simultaneously thanks to the use of a flow splitter, placed at the end of the chromatographic column. The GC system was equipped with two polydimethylsiloxane (95%) capillary cross-linked columns: DB-5 (20 m × 0.1 mm × 0.1 μm) and ZB-5 (30 m × 0.25 mm internal diameter, 0.25-μm film thickness) from Phenomenex, using Helium Premier (99.999% purity) X50S Metal Carbide as the carrier gas.

Analytical procedure

Instrumental determination. Chromatographic separation and detection were carried out using a GC-MS-μECD system. The MS was used for the identification of the analytes and the μECD for the quantification. A double determination of the analytes was carried out, one before derivatization for the analysis of PBDEs and MeO-BDEs with TCN as internal standard and another after, for the analysis of OH-BDEs using TCS as internal standard because PBDEs are not stable to derivatization. The determination of OH-BDEs was carried out by derivatizing with MTBSTFA for 30 min to 70 °C to determine them as tert-butyldimethylsilylated derivatives (TBDMS): OH-TBDMS-BDE.

Finally, samples (1 μl) were injected in the splitless mode at 280 °C. Helium was used as the carrier gas at a constant pressure of 28 psi (~1.5 ml min^{-1}). The temperature of the column (ZB-5MS) was programmed to increase from 130 °C (2 min) to 230 °C (2 min) at a rate of 25 °C/min and then to 280 °C (2 min) at 2 °C/min. The total time for each chromatogram was 35 min. The temperature of the ion source and the transfer line of the mass spectrometer were set at 250 and 270 °C, respectively, and the electron beam was set at 70 eV. SCAN mode was used to establish the *m/z* values (Table 1) with standards for each analyte, as well as the mass spectra displayed in the libraries of the National Institute of Standards and Technology databases and by bibliography (Butryn et al., 2015). The μECD temperature was set at 320 °C and nitrogen was used as the makeup gas (30 ml min^{-1}). The flow ratio of the splitter was 1:1 thanks to the additional helium input at a constant pressure of 15 psi and the restrictors length of each detector calculating with a manual supplied by Agilent (Agilent Technologies, 2011).

Sample preparation. To avoid contamination of the sample, plastic materials were not used due to the possible transfer of pollutants to or from the material. Hamilton syringes were always used for the addition of solutions. All reused glass material was washed with acetone, rinsed with deionized water and left overnight in the oven at 250 °C.

Zebrafish eleutheroembryos in groups of 15 were extracted with 500 μl of the n-hexane:MTBE mixture (1:1) and sonicated with an ultrasound probe for 4 min at 40% of power and a pulse every second (on/off, 1 s/1 s). The internal standards TCN and TCS were previously added so that the extract to be injected contained 20 μg L^{-1} of each. The mixture was centrifuged for 10 min at 10 000 rpm, the organic phase was separated, and the extraction was repeated. The organic phases were purified with 50 mg of florisil through dispersive SPE and mixed for 30 s in the vortex. The extract was then centrifuged and evaporated to dryness under a gentle stream of nitrogen and reconstituted in 500, 1000, or 2000 μl of isooctane depending on the time at which the sample was collected from experiments.

Extracts from embryo water were prepared as follows: 500 μl of the exposed solution was extracted by 500 μl of n-hexane:MTBE (1:1) and mixed for 30 s in the vortex. The second step of extract clean-up was not applied in the exposure media because they did not show any interference or matrix effect due to the lipidic fat. The internal standards TCN and TCS were previously added. The mixture was centrifuged for 10 min at 10 000 rpm, the organic phase was separated, and the extraction was repeated. The organic phases were mixed,

TABLE 1: Mass spectrometer conditions in SIM mode for electron impact ionization

Analyte	Retention time (min)	*m/z*	Initial scanning time (min)
TCN	9.31	266, 264, 268, 194	8 (solvent delay)
BDE-28	12.48	248, 246, 406, 408	11
TBDMS-TCS	13.71	290, 288, 218	12.8
BDE-47	16.98	326, 486, 484, 488	15
2′-OH-TBDMS-BDE-28	19.69	423, 421, 425, 81	18.5[a]
6-MeO-BDE-47	20.13	516, 514, 518, 420	
3-MeO-BDE-47	21.23	356, 516, 341, 514	
5-MeO-BDE-47	21.62	516, 356, 358, 326	
BDE-99	22.98	404, 406, 564, 566	22
5-OH-TBDMS-BDE-47	27.07	502, 504, 500, 81	25
3-OH-TBDMS-BDE-47	31.72	502, 474, 266, 419	29

[a]A joint window is established because they elude close retention times, so that the majority *m/z* of each is monitored (marked in the table).
TCN = 1,2,3,4-Tetrachloronaphthalene; TBDMS-TCS = tert-butyldimethylsilylated derivative of triclosan.

concentrated in a gentle stream of nitrogen and reconstituted in 50 µl of isooctane.

Finally, 80 and 50 µl of the volume obtained for eleutheroembryos and embryo water, respectively, were derivatised with 20 µl of MTBSTFA to 70 °C for 30 min in the oven and injected into the GC-µECD-MS to determine the OH-BDE in the form of OH-TBDMS-BDE. Polybrominated diphenyl ethers and MeO-BDEs were determined by direct injection of the remaining volume of isooctane extracts into the GC-µECD-MS.

Exposure of zebrafish eleutheroembryos: Bioconcentration and biotransformation experiments

Zebrafish eleutheroembryos were obtained from adult zebrafish bred, maintained, and exposed in the AZTI Tecnalia (Bizkaia, Spain) under standard conditions (Westerfield, 2007). The OECD Technical Guidance OECD 305 (OECD, 2012) was used to establish the growing conditions (dissolved oxygen ≥60%, 26 ± 2 °C and pH 7.8 ± 0.2) and nominal exposure concentrations.

Exposure solutions were prepared with a composition of fresh river water (International Organization for Standardization 7346-3, 1996): 220.5 mg of $CaCl_2$, 63 mg of $NaHCO_3$, 5.5 mg of KCl, and 60.1 mg of $MgSO_4$ per litre of distilled water. The OECD Test 305 states that the exposure concentrations should be 1% and 0.1% of the LC50 (if detection limits enable it to be determined). Usenko et al. (2011) show a BDE-47 zebrafish embryos LC50 value of 4.2 mg L^{-1}. Thus, the nominal concentrations chosen to carry out the bioconcentration experiment were 1 and 10 µg L^{-1} for BDE-47, and 100 and 250 µg L^{-1} for the metabolization experiment. Due to the limited solubility of BDE-47 in water (11 µg L^{-1} [Pereira et al., 2016]; 21.24 µg L^{-1} [USEPA Comptox data base]), it is dissolved in DMSO so that the medium finally contains 0.5% DMSO (Hallare et al., 2006).

Bioconcentration and metabolization experiments were carried out according to an alternative method developed previously (Sanz-Landaluze et al., 2015). Zebrafish eleutheroembryos were exposed to contaminated solution of BDE-47 at 72 h post fertilization (hpf) during 48 h (uptake phase). Afterwards, they were exposed for 24 h to the medium without contaminant (depuration phase). Thus, they are not considered laboratory animals because until 144 hpf they do not feed on their own (Sanz-Landaluze et al., 2015). Three groups of zebrafish eleutheroembryos were used (a total of 1050 individuals, 350 in each tank), each in 1-L glass tank, ensuring a density of 2 ml/individual: two tanks included zebrafish contaminated with the studied analyte at mentioned concentrations and the third tank had the nonexposed individuals (control), with only the addition of solvent. The exposure medium was refreshed every 24 h to keep a constant nominal concentration. During exposure, 15 eleutheroembryos and 1.5 ml of medium were pulled out from the tanks at different moments for analysis: 0 (start of the experiment), 17, 24, 41, 48, 65, and 72 h to determine the bioaccumulated concentration of each compound, and 0 and 48 h for the metabolization experiment. Three replicates of exposure and blank or control samples were collected for each time evaluated.

Toxicokinetic model equations for BCF

In the present study, the quantitative estimation of the degree of bioconcentration is going to be estimated according to the OECD 305 guideline (OECD, 2012). According to this test guideline, the BCF is estimated as the ratio of the concentration of the compound in the fish (C_f) to that of the mean calculated in the surrounding medium (C_W) at a steady state (Equation 1):

$$BCF_{ss} = \frac{C_f\,(\text{ng kg}^{-1})}{C_W\,(\text{ng L}^{-1})} \quad (1)$$

Nevertheless, when the steady state is not reached, BCF can be calculated using a bioconcentration first-order kinetic model (BCF_k) that describes the chemical uptake and depuration process (Gobas & Zhang, 1992; Mackay & Fraser, 2000; Equation 2):

$$\frac{dC_f}{dt} = k_1 \times C_W - k_2 \times C_f\,(\text{uptake}),$$
$$\frac{dC_f}{dt} = -k_2 \times C_f\,(\text{depuration}) \quad (2)$$

where C_f is expressed in ng kg^{-1}, t is the exposure time (h), k_1 is the first-order uptake constant (L kg^{-1} h^{-1}), C_w is expressed in ng L^{-1}, and k_2 is the first-order elimination rate constant (h^{-1}). Assuming that at $t = 0$ the concentration of the analyte in the fish is zero and that the concentration in the exposure medium is constant, Equation (3) is obtained:

$$C_f = \frac{k_1}{k_2} \times C_W(1 - e^{-k_2 t})(\text{uptake}),$$
$$C_f = C_{f,0} \times e^{-k_2 t}(\text{depuration}) \quad (3)$$

where $C_{f,0}$ is the concentration of the analyte in the fish at the beginning of the purification process. By fitting the equations to the experimental data, k_1 and k_2 can be obtained. Under steady state conditions, Equation (1) is simplified to Equation 4:

$$BCF_k = \frac{C_f}{C_W} = \frac{k_1}{k_2} \quad (4)$$

The BCF is usually expressed in L kg^{-1} units. The software OriginPro Ver. 8.5 (OriginLab) and NONLIN 5.1., which is specific for no-linear fits were used for kinetic calculations (BCF_k). In the present study, because no steady state is reached, a BCF at maximum uptake time BCF_{48h} was also calculated for comparison purposes.

RESULTS AND DISCUSSION

Setting the analytical procedure

Several parameters for the chromatographic separation and determination (chromatographic column, derivatization reagent and solvent) and sample preparation (extraction

solvents and sorbents for the clean-up step) were optimized (Supporting Information). As a conclusion of the instrumental setting, a double determination was necessary (Supporting Information, Figure S1), injecting extracted isooctane directly to the GC for determination of PBDEs and MeO-BDEs, and with a derivatization step for OH-PBDEs. The results obtained for the sample preparation setting (Supporting Information, Figure S2) were observed with two purposes: to clean the extract and to obtain high recoveries, being the n-hexane:MTBE (1:1,v/v) and Florisil combination meeting both requirements for the majority of analytes (Supporting Information, Figure S3).

In this way, a method for the simultaneous extraction and cleaning of PBDEs, MeO-BDEs and OH-BDEs was optimized, reaching a consensus among the analytes of different polarity that resulted in good recoveries, greatly reducing the cost and time of sample treatment. In addition, the combination of both detection systems allows the identification (MS) and quantification (μECD) of trace compounds in complex mixtures with a high degree of selectivity and sensitivity.

Method validation: QA/QC

The developed method was evaluated in accordance with selectivity, linearity, recovery, and detection limits (Supporting Information, Table S1). Selectivity was tested using several blanks for each sample type. The interference peaks were evaluated for each selected *m/z* of the analytes. Interferences observed in the zebrafish samples were eliminated by the clean-up step. The medium samples did not show any interference peaks. Reagent and sample blanks were always measured to subtract the background signal from that obtained for the samples. Exposure solutions were prepared by dilution from stock solutions with culture water containing 0.5% DMSO. No adverse effects were observed in control samples using 0.5% DMSO. Great linearity was obtained in all analytes ($R^2 > 0.994$) and the limits of detection (LODs) and limits of quantification (LOQ) were evaluated on the basis of external calibration curves and calculating the result of adding three (LOD) or 10 (LOQ) times the standard deviation to the target signal. Method LODs and LOQ values were between 0.10–0.22 and 0.25–0.68 μg L^{-1}, respectively, and relative standard deviation was <12%. To assess recoveries and because no Certified Reference Material with these compounds and similar matrix is readily available, sample fortification was used.

Bioconcentration and toxicokinetics in zebrafish eleutheroembryos

The results of the bioconcentration showed that no BDE-47 was detected in unexposed zebrafish samples (control experiment). In contrast, as illustrated in Figure 1, the profiles obtained show a rapid absorption in the first hours of larval development and a high capacity of bioconcentration because the concentrations of BDE-47 found in larvae increased greatly

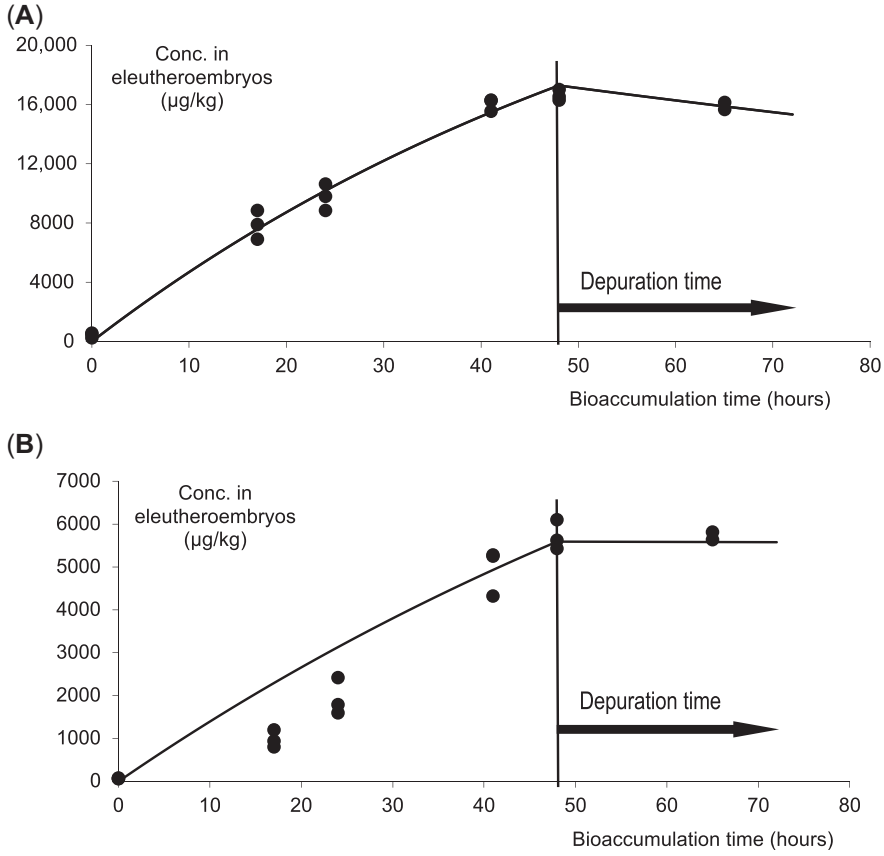

FIGURE 1: BDE-47 bioconcentration in zebrafish eleutheroembryos samples exposed to (**A**) 10 μg L^{-1} and (**B**) 1 μg L^{-1}.

with time at both exposure levels. As explained in the Toxicokinetic model equations for BCF section, BCFs were calculated according to OECD 305 in two different ways: (i) BCF_{48h} (Equation 1) using average BDE-47 concentrations determined experimentally in the exposure media (Table 2 and Supporting Information, Figure S4) and larvae concentration at the maximum time of uptake phase, and (ii) BCF_k by applying Equation (4), representing the variation of BDE-47 concentration in eleutheroembryos versus time of uptake (Figure 1) and by fitting data to Equation (3) using nonlinear regression fits. The toxicokinetic and BCF values obtained by both calculation procedures are shown in Table 2. The values obtained by both calculation procedures resulted in not matching values of BCF_k and BCF_{48h} because the value does not completely reach the stable state in the absorption phase. According to the OECD 305 consideration, the BCF_k values were preferred for further discussion. In a general view, the European Chemicals Bureau sets a value of BCF > 5000 in substances with log K_{ow} between 5 and 8 (Mhadhbi et al., 2014), according to the result obtained in the present study (BDE-47 log K_{ow} 6.81; Pereira et al., 2016).

Similar bioaccumulation studies of these compounds in different species can be found in the literature. Gustafsson et al. (1999) and Vidal-Liñán et al. (2015) calculated BCFs in *Mytilus galloprovincialis* (mussel), obtaining values of 26 000 L kg^{-1} (exposed to 0.31 ng L^{-1}) and 10 900 L kg^{-1} (exposed to 8 μg L^{-1}), respectively. Gu et al. (2017) gives values with a higher degree of magnitude, obtaining 6.44×10^5 L kg^{-1} in the same species and 2.76×10^6 L kg^{-1} in oyster exposed to the concentration found in a marine environment (0.26 ng L^{-1}). On the other hand, Lebrun et al. (2014) estimated a lower kinetic BCF in amphipod crustacean *Gammarus pulex* of close to 5000 when exposed to a nominal BDE-47 concentration of 1 μg L^{-1}. The variability in the results is mainly due to the natural dispersion due to the different species used in the experiments.

Related to fish, Mhadhbi et al. (2014) reported BCF values of BDE-47 in a young *Psetta maxima* of 24 125, 15 531, and 33 103 L kg^{-1} at exposure to BDE-47 concentrations of 1, 0.1, and 0.001 μg L^{-1}, respectively. The order of magnitude of Mhadhbi et al. (2014) BCFs with those obtained in the present study match closely. Liu et al. (2015) presented data on the bioconcentration of BDE-47 on zebrafish (*Danio rerio*) embryos. The BCF values estimated were 26, 68, 489, 750, 2489, and 2430 at 12, 24, 48, 72, 96, and 120 hpf, respectively, at a nominal exposure concentration of 300 μg L^{-1}. These BCFs were calculated directly using Equation (1) at each sample time and show certain variability in the real concentrations found in the exposure water (decreasing from 300 to 40 μg L^{-1}). Even though exposure time is higher in the present study (from 4 to 120 hpf) than in ours (72 to 120 hpf) and considering that between 96 and 120 hpf a steady state is reached, the obtained BCF values are lower than found in the present study. This lower value at higher concentrations is found in this and multiple studies (Gustafsson et al., 1999; McGeer et al., 2003; Sanz-Landaluze et al., 2015; Vidal-Liñán et al., 2015). Theoretically, the accumulation of a compound depends only on diffusion and storage in lipids (Beek et al., 2000) and should not depend on concentration, but BCFs have a relationship with concentration, probably because other physiological mechanisms when interiorising compounds, showing saturable kinetics (McGeer et al., 2003). Therefore, the importance of determining the actual concentration of the compounds in the water during the experiment should be emphasized because most bioconcentration studies calculate BCFs with nominal concentrations (Molina-Fernandez et al., 2017; Zheng et al., 2012).

For prediction of the bioaccumulation potential of lipophilic compounds, the water–octanol partition coefficient K_{ow} is the parameter used most often, with the general trend that higher hydrophobicity means higher accumulation (Arnot & Gobas, 2006). Based on quantitative models of structure–activity relationships (QSAR), equations (Table 3) have been developed that can predict the value of BCF in relation to the octanol–water partition coefficient, log K_{ow} (BDE-47 log K_{ow} 6.81; Pereira et al., 2016). In European Chemicals Agency (2003), parabolic relationships are given for substances with a log $K_{ow} > 6$ and linear equations were proposed by Arnot and Gobas (2006) and Petersen and Kristensen (1998) to determine the BCFs in fish and zebrafish larvae, respectively. This estimation of BCF is based on the substance's ability to be distributed in the lipid fraction. However, an experimentally obtained BCF is preferable to these QSAR methods because the bioconcentration also depends on the physiological responses of each organism, and the exposure and duration of the study, among other factors, and although the estimation models are improving, there are still many of these processes that are not perfectly modelled.

Biotransformation in zebrafish eleutheroembryos

The Toxicity Estimation Software Tool (TEST; USEPA) software, Ver. 4.1, predicts ecotoxicity values using quantitative structure–activity relationships. These values (Supporting Information, Table S2) seem to confirm previously reported results describing similar toxicological effects of biotransformation

TABLE 2: Bioconcentration factor values (BCF_{48h}, BCF_k) and toxicokinetic parameters obtained for BDE-47

Nominal conc. (μg L^{-1})	Measured conc., C_w (μg L^{-1})	k_1 (L μg h^{-1})	$k_{2(uptake)}$ (μg L^{-1})	BCF_k (log BCF_k) (L kg^{-1})	BCF_{48h} (log BCF_{48h}) (L kg^{-1})
10	4.2	124 ± 8	0.017 ± 0.001	7294 ± 899 (3.86)	4106 (3.61)
1	0.34	430 ± 30	0.0101 ± 0.0009	36363 ± 5702 (4.56)	16392 (4.21)

TABLE 3: BDE-47 Bioconcentration factor values estimated from different QSAR models

Reference	QSAR equation	Life stage	Estimated BCF (log BCF)
European Chemicals Agency (2003)	$\log BCF = -0.20 \times \log K_{ow}^2 + 2{,}74 \times \log K_{ow} - 4{,}72$	Aquatic organism	46200 (4.66)
Arnot and Gobas (2006)	$\log BCF = 0.60 \times \log K_{ow} - 0{,}23$	Fish	7180 (3.86)
Petersen and Kristensen (1998)	$\log BCF = 0.86 \times \log K_{ow} - 0{,}4634$	Zebrafish larvae	247000 (5.39)
EPI Suite v4.1 (US EPA, 2012)		Fish	13600 (4.13)

BCF = bioconcentration factor; QSAR = quantitative model of structure–activity relationship.

products to their parental compounds in certain biological systems.

Zebrafish eleutheroembryos exposed to BDE-47 at 100 and 250 μg L^{-1} was trasnformated to their metabolites BDE-28, 2′-OH-BDE-28, and 5-MeO-BDE-47 after 48 h of exposure (Figure 2). No quantifiable amounts of the other metabolites tested (3- and 6-MeO-BDE-47, 3- and 5-OH-BDE-47) were detected. In addition, increasing concentrations of BDE-28, 2′-OH-BDE-28, and 5-MeO-BDE-47 over time were found in the BDE-47 bioconcentration experiment (10 μg L^{-1}; Figure 3). No metabolite was detected in the bioconcentration study of 1 μg L^{-1}. The ratios between metabolites and BDE-47 concentration found in larvae at different exposure times in both metabolization and bioaccumulation experiment were also determined (Supporting Information, Tables S2 and S4), showing that the biotransformation contributed less than 1% of the parental BDE 47 bioaccumulated in all experiments (maximum value of 0.75% for BDE-28, 0.25% for 2′-OH-BDE-28, and 0.13% for 5-MeO-BDE-47). Wiseman et al. (2011) suggested the contamination of BDE standards with a small amount of MeO/OH-BDEs and also that MeO-BDEs can be biotransformed to OH-BDEs. The metabolism of MeO-BDEs is said to contribute greater amounts of OH-BDEs than the parent PBDE. However, none of the metabolites they studied were detected in quantifiable amounts in the surrounding media at initial exposure ($t = 0$ h; Supporting Information, Table S5 and Figure S5) and the concentration of 5-MeO-BDE-47 found in eleutheroembryos is much smaller than that of OH metabolites.

The main metabolite formed is BDE-28, through the elimination of a bromine atom. Previous studies have also shown that halogen removal from PBDEs during metabolic degradation can form lower brominated BDE congeners within fish tissues (Stapleton & Baker, 2003) and this is most likely to occur at the ortho position of the biphenyl (Sun et al., 2013). The formation of 2′-OH-BDE-28 could be caused by hydroxylation of BDE-28 or by OH radicals attacking the bromine atom in the ortho position of BDE-47 under oxygenase catalysis (Yamazoe et al., 2004). Formation of OH-BDE-47 from BDE-47 is carried out in the same way as the formation of 2′-OH-BDE-28. However, 2′-OH-BDE-28 may be predominant because it has fewer bromine atoms, suffers reduction and oxidation reactions more readily, and is therefore more likely to be attacked by reducing H and OH radicals (Erratico et al., 2013; Tang et al., 2021).

Exploring the literature, Tang et al. (2021) have shown aerobic degradation of BDE-47 to debrominated (BDE-28 and BDE-7) and hydroxylated (6-OH-BDE-47, 5-OH-BDE-47, 2′-OH-BDE-28, and 4′-OH-BDE-17) metabolites by *Pseudomonas aeruginosa* YH through the biological action of P450 enzyme and dioxygenase. In another study, four species of microalgae (*Isochrysis galbana*, *Prorocentrum minimum*, *Skeletonema grethae*, and *Thalassiosira pseudonana*) were exposed to 20 μg L^{-1} of BDE-47 and debromination to BDE-28 occurred in all species with concentration ratios of 0.36%, 0.45%, 0.87%, and 0.04%, respectively, on the sixth day of exposure. However, biotransformation to OH-BDEs was only found in *I. galbana* on exposure to high concentration (2000 μg L^{-1}; Po et al., 2017). On the other hand, Deng & Tam (2016) found ratios of less than 0.3% of BDE-28 biodegradation in the freshwater microalgae *Chlorella isolate* and the metabolites 6-OH- (0.4%–3%), 5-OH- (3%–15%), and 6-MeO-BDE-47 (<3%), from the hydroxylation and methoxylation of BDE-47 (10 μg L^{-1}). The congeners BDE-28, 6-OH-BDE-47, 5-OH-BDE-47 and a methoxylation product (4-MeO-BDE-42) were observed in young whole pumpkin plants with concentration ratios of 0.7%, 0.013%, 0.023%, and 0.24%, respectively (Sun et al., 2013). Methoxylation products were also detected in rainbow trout after exposure to deca-BDEs (Feng et al., 2010). Erratico et al. (2013) reported the biotransformation of BDE-47 to 6-OH-BDE-47, 5-OH-BDE-47, 3-OH-BDE-47, 2,4-dibromophenol (2,4-DBP), and 2′-OH-BDE-28 metabolites by human liver microsomes through P450 2B6 enzymes. Zebrafish have enzymes that are highly conserved in mammals and have

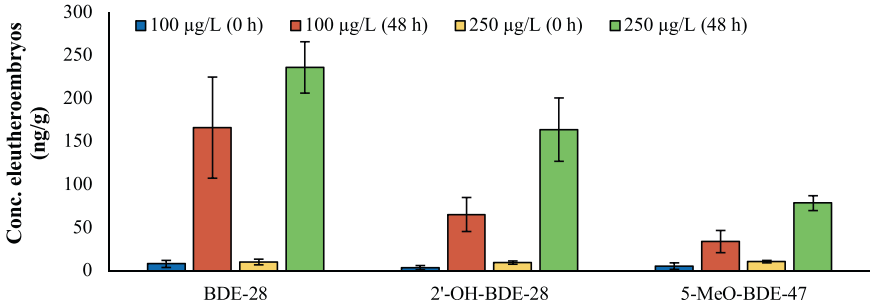

FIGURE 2: Transformation of BDE-47 (100 and 250 μg L^{-1}) by zebrafish eleutheroembryos after 48 h of exposure.

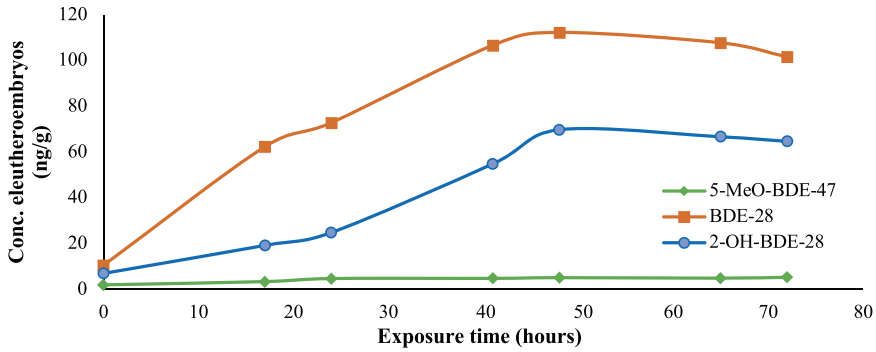

FIGURE 3: Metabolites of BDE-47 (10 µg L^{-1}) observed by transformation in zebrafish eleutheroembryos over time.

orthologues with humans, including enzymes of the CYP family, glucuronosyltransferases (UGTs), and sulfotransferases (SULTs), therefore zebrafish can perform phase I metabolism reactions, such as oxidation, N-demethylation, O-demethylation, and N-dealkylation, and phase II metabolism reactions, such as sulphation and glucuronidation (De Souza Anselmo et al., 2018). Yang et al. (2017) observed a CYP1A induction in vivo at BDE-47 exposure belonging to the phase I liver enzymes metabolizing in zebrafish larvae at 120 hpf. Yang and Chan (2015) observed a slight increase in transthyretin at 96 h and an effect on transcription of the enzymes UGT2A1 and SULT1 in the zebrafish liver cell line. This suggests that the chemical BDE-47 could be hydroxylated because it has binding affinity for transthyretin.

In contrast, Liu et al. (2015), Wen et al. (2015), and Zheng et al. (2012) studied the biotransformation in vivo of BDE-47 in zebrafish embryos and did not find hydroxylated and methoxylated metabolites. They found a small amount of 2′-OH-BDE-28, BDE-28, BDE-85, and BDE- 99 but did not take these quantities as transformation of the BDE-47. However, they used zebrafish from 4 (embryos) to 120 hpf (larvae) and the biotransformation capacity has been shown to vary dynamically throughout the embryonic development of zebrafish and proved immature in early life stages (Zindler et al., 2020). Our eleutheroembryos began exposure with a higher metabolic capacity (72 hpf) when the zebrafish CYP1A expression increased dramatically (Saad et al., 2016), which may have been a key factor in finding significant concentrations of BDE-28 and 2′-OH-BDE-28. Therefore, the age of the zebrafish should be considered during the experimental design and when contrasting the results.

The results obtained demonstrate the ability of zebrafish eleutheroembryos to metabolize compounds after 72 hpf, which can open the way to the use of these experiments to replace experimentation with adult fish. At present there are no official guidelines to carry out metabolization studies in higher organisms. Hence, in line with the recent approval of two new OECD test guidelines (319A and 319B) to determine biotransformation rates but using in vitro assays by primary hepatocytes (RT-HEP) or liver S9 subcellular fractions (RT-S9) from rainbow trout, metabolization by zebrafish eleutheroembryos could be considered as the leap to higher organisms, as request by other authors asking for further research involving continued "step-wise comparisons" of in vitro rates and increased levels of biological organization (Laue et al., 2020).

CONCLUSIONS

A scaled-down analytical method has been developed to determine simultaneously the BDE-47 and their metabolites (MeO-BDEs and OH-BDEs) with different polarities in aqueous and larvae samples by GC-MS-µECD. Moreover, the use of both detectors at the same time, thanks to the splitter, achieves unambiguous identification and a high-sensitivity quantification suitable for trace and metabolites determination is achieved thanks to the advantages of each detector.

The experimental BCF values estimated in our study showed that BDE-47 fulfils the bioaccumulative criterion (vB-) according to European regulations (REACH; BCF > 5000; REACH, 2006) with satisfactory agreement with the results of the literature for other aquatic organisms and those predicted by QSAR models. Therefore, the results obtained show the feasibility of the method for bioconcentration and opens up the possibility of metabolic studies with zebrafish eleutheroembryos, which is a very underdeveloped field without official testing or regulation. Although these results are promising, more studies are needed to generate a large amount of data that will allow us to compare the benefits offered by this methodology with the other methods that are being proposed as alternatives for the study of the bioaccumulation and biotransformation of substances.

Supporting Information—The Supporting Information are available on the Wiley Online Library at https://doi.org/10.1002/etc.5569.

Acknowledgments—Authors are grateful to AZTI Tecnalia (Bizkaia, Spain) for providing the eleutheroembryo samples. The present study was supported by the Spanish Ministry of Science and Innovation (grant numbers PID2020-114714RB-100) and Comunidad Autónoma of Madrid (grant numbers 2018/BAA4393-AVANSECAL-II-CM). Paloma de Oro thanks the Spanish Ministry of Science and Innovation for her FPI predoctoral contract (PRE2021/097956).

Disclaimer—The authors declare that they have no known competing financial interests or personal relationships that

could have appeared to influence the work reported in the present study.

Author Contributions Statement—**Paloma De Oro-Carretero**: Data curation; Formal analysis; Investigation; Methodology; Software; Supervision; Validation; Visualization; Roles/Writing—original draft. **Jon Sanz-Landaluze**: Conceptualization; Data curation; Funding acquisition; Methodology; Project administration; Resources; Software; Supervision; Validation; Visualization; Writing—review & editing.

Data Availability Statement—Authors confirm that the data supporting the findings of the present study are available within the article and/or its supplementary information materials.

REFERENCES

Agilent Technologies. (2011). Two-way splitter kit with makeup gas installation and operation guide. Agilent G3180B, 5th Edition. http://pdfstream.manualsonline.com/0/0f9a330b-71c6-4850-8640-5645215a1326.pdf

Arnot, J. A., & Gobas, F. A.P. C. (2006). A review of bioconcentration factor (BCF) and bioaccumulation factor (BAF) assessments for organic chemicals in aquatic organisms. *Environmental Reviews*, *14*, 257–297. https://doi.org/10.1139/A06-005

Beek, B., Böhling, S., Bruckmann, U., Franke, C., Jöhncke, U., & Studinger, G. (2000). The assessment of bioaccumulation. In Bioaccumulation—New aspects and developments. The Handbook of Environmental Chemistry (Vol. 2 Series: Reactions and Processes), vol 2J. Springer, Berlin, Heidelberg. Beek B. (e). https://doi.org/10.1016/0045-6535(94)90281-X

Butryn, D. M., Chi, L. H., Gross, M. S., McGarrigle, B., Schecter, A., Olson, J. R., & Aga, D. S. (2020). Retention of polybrominated diphenyl ethers and hydroxylated metabolites in paired human serum and milk in relation to CYP2B6 genotype. *Journal of Hazardous Materials*, *386*, 121904. https://doi.org/10.1016/j.jhazmat.2019.121904

Butryn, D. M., Gross, M. S., Chi, L. H., Schecter, A., Olson, J. R., & Aga, D. S. (2015). "One-shot" analysis of polybrominated diphenyl ethers and their hydroxylated and methoxylated analogs in human breast milk and serum using gas chromatography-tandem mass spectrometry. *Analytica Chimica Acta*, *892*, 140–147. https://doi.org/10.1016/j.aca.2015.08.026

Cruz, R., Cunha, S. C., Marques, A., & Casal, S. (2017). Polybrominated diphenyl ethers and metabolites—An analytical review on seafood occurrence. *TrAC*, *87*, 129–144. https://doi.org/10.1016/j.trac.2016.12.005

De la Torre, A., Navarro, I., Sanz, P., & de los Ángeles Martínez, M. (2020). Organophosphate compounds, polybrominated diphenyl ethers and novel brominated flame retardants in European indoor house dust: Use, evidence for replacements and assessment of human exposure. *Journal of Hazardous Materials*, *382*, 121009. https://doi.org/10.1016/j.jhazmat.2019.121009

De Souza Anselmo, C., Sardela, V. F., de Sousa, V. P., & Pereira, H. M. G. (2018). Zebrafish (*Danio rerio*): A valuable tool for predicting the metabolism of xenobiotics in humans? *CBPC*, *212*, 34–46. https://doi.org/10.1016/j.cbpc.2018.06.005

Deng, D., & Tam, N. F. Y. (2016). Adsorption-uptake-metabolism kinetic model on the removal of BDE-47 by a Chlorella isolate. *Environmental Pollution*, *212*, 290–298. https://doi.org/10.1016/j.envpol.2016.01.063

El-Amrani, S., Pena-Abaurrea, M., Sanz-Landaluze, J., Ramos, L., Guinea, J., & Cámara, C. (2012). Bioconcentration of pesticides in Zebrafish eleutheroembryos (*Danio rerio*). *Science of the Total Environment*, *425*, 184–190. https://doi.org/10.1016/j.scitotenv.2012.02.065

Erratico, C. A., Szeitz, A., & Bandiera, S. M. (2013). Biotransformation of 2,2′,4,4′-tetrabromodiphenyl ether (BDE-47) by human liver microsomes: Identification of cytochrome P450 2B6 as the major enzyme involved. *Chemical Research in Toxicology*, *26*, 721–731. https://doi.org/10.1021/tx300522u

European Chemicals Agency. (2003). Technical guidance document on risk assessment. Part II. Protection institute for health and consumer. *European Chemical Bureau*, *337*. https://echa.europa.eu/documents/10162/16960216/tgdpart1_2ed_en.pdf

European Commission. (2006). European Commission (2006) Regulation (EC) No. 1907/2006 of the European Parliament and of the Council of 18 December 2006 concerning the Registration, Evaluation, Authorisation and Restriction of Chemicals (REACH), establishing a European Chemicals Agency. *Official Journal of the European Union*. https://doi.org/10.1039/9781782622222-00468

European Parliament, Council of the European Union. (2010). Directive 2010/63/EU of the European parliament and of the council of 22 September 2010 on the protection of animals usedfor scientific purposes. *Official Journal of the European Union 276*, 33–79.

Feng, C., Xu, Y., He, Y., Luo, Q., Zha, J., & Wang, Z. (2010). Debrominated and methoxylated polybrominated diphenyl ether metabolites in rainbow trout (*Oncorhynchus mykiss*) after exposure to decabromodiphenyl ether. *Journal of Environmental Sciences*, *22*, 1425–1434. https://doi.org/10.1016/S1001-0742(09)60271-0

Gobas, F. A. P. C. & Zhang, X. (1992). Measuring bioconcentration factors and rate constants of chemicals in aquatic organism under conditions of variable water concentrations and short exposure time. *Chemosphere*, *25*, 1961–1971.

Gu, S. Y., Ekpeghere, K. I., Kim, H. Y., Lee, I. S., Kim, D. H., Choo, G., & Oh, J. E. (2017). Brominated flame retardants in marine environment focused on aquaculture area: Occurrence, source and bioaccumulation. *Science of the Total Environment*, *601–602*, 1182–1191. https://doi.org/10.1016/j.scitotenv.2017.05.209

Gustafsson, K., Björk, M., Burreau, S., & Gilek, M. (1999). Bioaccumulation kinetics of brominated flame retardants (polybrominated diphenyl ethers) in blue mussels (*Mytilus edulis*). *Environmental Toxicology and Chemistry*, *186*, 1218–1224. https://doi.org/10.1897/1551-5028(1999)018<1218:BKOBFR>2.3.CO;2

Hallare, A., Nagel, K., Kohler, H. R., & Triebskorn, R. (2006). Comparative embryotoxicity and proteotoxicity of three carrier solvents to zebrafish (*Danio rerio*) embryos. *Ecotoxicology and Environmental Safety*, *63*(3), 378–388. https://doi.org/10.1016/j.ecoenv.2005.07.006

International Organization for Standardization. (1996). Water quality—Determination of the acute lethal toxicity of substances to a freshwater fish (*Brachydanio rerio* Hamilton-Buchanan (Teleostei, Cyprinidae)). Flow-through method, 7346-3.

Klinčić, D., Dvoršćak, M., Jagić, K., Mendaš, G., & Herceg Romanić, S. (2020). Levels and distribution of polybrominated diphenyl ethers in humans and environmental compartments: A comprehensive review of the last five years of research. *Environmental Science and Pollution Research*, *27*, 5744–5758. https://doi.org/10.1007/s11356-020-07598-7

Lacorte, S., Ikonomou, M. G., & Fischer, M. (2010). A comprehensive gas chromatography coupled to high resolution mass spectrometry based method for the determination of polybrominated diphenyl ethers and their hydroxylated and methoxylated metabolites in environmental samples. *Journal of Chromatography, A*, *1217*, 337–347. https://doi.org/10.1016/j.chroma.2009.11.024

Laue, H., Hostettler, L., Badertscher, R. P., Jenner, K. J., Sanders, G., Arnot, J. A., & Natsch, A. (2020). Examining uncertainty in in vitro-in vivo extrapolation applied in fish bioconcentration models. *Environmental Science & Technology*, *54*, 9483–9494. https://doi.org/10.1021/acs.est.0c01492

Lebrun, J. D., Leroy, D., Giusti, A., Gourlay-Francé, C., & Thomé, J. P. (2014). Bioaccumulation of polybrominated diphenyl ethers (PBDEs) in *Gammarus pulex*: Relative importance of different exposure routes and multipathway modeling. *Aquatic Toxicology*, *154*, 107–113. https://doi.org/10.1016/j.aquatox.2014.05.015

Li, F., Xie, Q., Li, X., Li, N., Chi, P., Chen, J., Wang, Z., & Hao, C. (2010). Hormone activity of hydroxylated polybrominated diphenyl ethers on human thyroid receptor-β: In vitro and in silico investigations. *Environmental Health Perspectives*, *118*, 602–606. https://doi.org/10.1289/ehp.0901457

Lillicrap, A., Belanger, S., Burden, N., Pasquier, D. D., Embry, M. R., Halder, M., Lampi, M. A., Lee, L., Norberg-King, T., Rattner, B. A., Schirmer, K., & Thomas, P. (2016). Alternative approaches to vertebrate ecotoxicity tests in the 21st century: A review of developments over the last 2 decades and current status. *Environmental Toxicology and Chemistry*, *35*, 2637–2646. https://doi.org/10.1002/etc.3603

Liu, H., Tang, S., Zheng, X., Zhu, Y., Ma, Z., Liu, C., Hecker, M., Saunders, D. M. V., Giesy, J. P., Zhang, X., & Yu, H. (2015). Bioaccumulation, biotransformation, and toxicity of BDE-47, 6-OH-BDE-47, and

6-MeO-BDE-47 in early life-stages of zebrafish (*danio rerio*). *Environmental Science & Technology*, *49*, 1823–1833. https://doi.org/10.1021/es503833q

Liu, X., Jiao, Y., Lin, C., Sun, K., & Zhao, Y. (2014). PBDEs, hydroxylated PBDEs and methoxylated PBDEs in bivalves from Beijing markets. *Chemosphere*, *110*, 97–103. https://doi.org/10.1016/j.chemosphere.2014.02.019

Liu, Y., Feng, Y., Li, J., Zhou, D., Guo, R., Ji, R., & Chen, J. (2020). The bioaccumulation, elimination, and trophic transfer of BDE-47 in the aquatic food chain of Chlorella pyrenoidosa-*Daphnia magna*. *Environmental Pollution*, *258*, 113720. https://doi.org/10.1016/j.envpol.2019.113720

Mackay, D., & Fraser, A. (2000). Bioaccumulation of persistent organic chemicals: Mechanisms and models. *Environmental Pollution*, *110*, 375–391.

McGeer, J. C., Brix, K. V., Skeaff, J. M., DeForest, D. K., Brigham, S. I., Adams, W. J., & Green, A. (2003). Inverse relationship between bioconcentration factor and exposure concentration for metals: Implications for hazard assessment of metals in the aquatic environment. *Environmental Toxicology and Chemistry*, *22*(5), 1017–1037. https://doi.org/10.1002/etc.5620220509

Mhadhbi, L., Fumega, J., & Beiras, R. (2014). Uptake kinetics, bioconcentration and debromination of BDE-47 in juvenile marine fish Psetta maxima. *Water, Air, & Soil Pollution*, *225*, 2072. https://doi.org/10.1007/s11270-014-2072-0

Molina-Fernandez, N., Perez-Conde, C., Rainieri, S., & Sanz-Landaluze, J. (2017). Method for quantifying NSAIDs and clofibric acid in aqueous samples, lumpfish (*Cyclopterus lumpus*) roe, and zebrafish (*Danio rerio*) eleutheroembryos and evaluation of their bioconcentration in zebrafish eleutheroembryos. *Environmental Science and Pollution Research*, *24*, 10907–10918. https://doi.org/10.1007/s11356-016-6671-8

Molina-Fernández, N., Rainieri, S., Muñoz-Olivas, R., De Oro-Carretero, P., & Sanz-Landaluze, J. (2021). Development of a method for assessing the accumulation and metabolization of antidepressant drugs in zebrafish (*Danio rerio*) eleutheroembryos. *Analytical and Bioanalytical Chemistry*, *413*(20), 5169–5179. https://doi.org/10.1007/s00216-021-03486-2

Organisation for Economic Co-operation and Development. (2012). Test No. 305 Bioaccumulation in Fish: Aqueous and Dietary Exposure. Guidelines For Testing Of Chemicals.

Pereira, L. C., de Souza, A. O., Meireles, G., Franco-Bernardes, M. F., Tasso, M. J., Bruno, V., Dorta, D. J., & de Oliveira, D. P. (2016). Comparative study of genotoxicity induced by six different PBDEs. *Basic & Clinical Pharmacology & Toxicology*, *119*, 396–404. https://doi.org/10.1111/bcpt.12595

Petersen, G. I., & Kristensen, P. (1998). Bioaccumulation of lipophilic substances in fish early life stages. *Environmental Toxicology and Chemistry*, *17*, 1385–1395. https://doi.org/10.1897/1551-5028(1998)017<1385:BOLSIF>2.3.CO;2

Po, B. H., Ho, K. L., Lam, M. H., Giesy, J. P., & Chiu, J. M. (2017). Uptake and biotransformation of 2,2′,4,4′-tetrabromodiphenyl ether (BDE-47) in four marine microalgae species. *Scientific Reports*, *7*, 44263. https://doi.org/10.1038/srep44263

Saad, M., Cavanaugh, K., Verbueken, E., Pype, C., Casteleyn, C., Ginneken, C. V., & Cruchten, S. V. (2016). Xenobiotic metabolism in the zebrafish: A review of the spatiotemporal distribution, modulation and activity of cytochrome p450 families 1 to 3. *Journal of Toxicological Sciences*, *41*, 1–11. https://doi.org/10.2131/jts.41.1

Sanz-Landaluze, J., Pena-Abaurrea, M., Muñoz-Olivas, R., Cámara, C., & Ramos, L. (2015). Zebrafish (*Danio rerio*) eleutheroembryo-based procedure for assessing bioaccumulation. *Environmental Science & Technology*, *49*, 1860–1869. https://doi.org/10.1021/es504685c

Shelepchikov, A. A., Ovcharenko, V. V., Kozhushkevich, A. I., Brodskii, E. S., Komarov, A. A., Turbabina, K. A., & Kalantaenko, A. M. (2019). A new method for purifying fat-containing extracts in the determination of polybrominated diphenyl ethers. *Journal of Analytical Chemistry*, *74*, 574–583. https://doi.org/10.1134/S1061934819040130

Song, S., Yang, C., Shao, M., Chao, J., Zheng, N., Wang, W., He, Y., & Li, P. (2020). Simultaneous determination of polybrominated diphenyl ethers and hydroxylated analogues in human serum using high-performance liquid chromatography-inductively coupled plasma mass spectrometry. *Journal of Chromatography B*, *1147*, 122130. https://doi.org/10.1016/j.jchromb.2020.122130

Stapleton, H. M., & Baker, J. E. (2003). Comparing polybrominated diphenyl ether and polychlorinated biphenyl bioaccumulation in a food web in Grand Traverse Bay, Lake Michigan. *Archives of Environmental Contamination and Toxicology*, *45*, 227–234. https://doi.org/10.1007/s00244-003-0165-7

Sun, H., Li, Y., Hao, Y., Zhu, Y., Yang, R., Wang, P., Zhang, Q., & Jiang, G. (2020). Bioaccumulation and trophic transfer of polybrominated diphenyl ethers and their hydroxylated and methoxylated analogues in polar marine food webs. *Environmental Science & Technology*, *53(24)*, 15086–15096. https://doi.org/10.1021/acs.est.0c05427

Sun, J., Liu, J., Yu, M., Wang, C., Sun, Y., Zhang, A., Wang, T., Lei, Z., & Jiang, G. (2013). In vivo metabolism of 2,2′,4,4′-tetrabromodiphenyl ether (BDE-47) in young whole pumpkin plant. *Environmental Science and Technology*, *47*, 3701–3707. https://doi.org/10.1021/es4003263

Tang, S., Yin, H., Yu, X., Chen, S., Lu, G., & Dang, Z. (2021). Transcriptome profiling of *Pseudomonas aeruginosa* YH reveals mechanisms of 2,2′,4,4′-tetrabrominated diphenyl ether tolerance and biotransformation. *Journal of Hazardous Materials*, *403*, 124038. https://doi.org/10.1016/j.jhazmat.2020.124038

United Nations Environmental Program. (2019). Stockholm Convention on Persistent Organic Pollutants (POPs), Text and Annexes. http://chm.pops.int/TheConvention/Overview/TextoftheConvention/tabid/2232/Default.aspx

US Environmental Protection Agency. (2012). Estimation Programs Interface Suite™ for Microsoft® Windows, v 4.1. Washington, DC, USA. https://www.epa.gov/tsca-screening-tools/epi-suitetm-estimation-program-interface.

Usenko, C. Y., Hopkins, D. C., Trumble, S. J., & Bruce, E. D. (2012). Hydroxylated PBDEs induce developmental arrest in zebrafish. *Toxicology and Applied Pharmacology*, *262*, 43–51. https://doi.org/10.1016/j.taap.2012.04.017

Usenko, C., Robinson, E. M., Usenko, S., Brooks, B. W., & Bruce, E. D. (2011). PBDE developmental effects on embryonic zebrafish. *Environmental Toxicology and Chemistry*, *30*, 1865–1872. https://doi.org/10.1002/etc.570

Vancamp, P., Houbrechts, A. M., & Darras, V. M. (2019). Insights from zebrafish deficiency models to understand the impact of local thyroid hormone regulator action on early development. *General and Comparative Endocrinology*, *279*, 45–52. https://doi.org/10.1016/j.ygcen.2018.09.011

Vidal-Liñán, L., Bellas, J., Fumega, J., & Beiras, R. (2015). Bioaccumulation of BDE-47 and effects on molecular biomarkers acetylcholinesterase, glutathione-S-transferase and glutathione peroxidase in *Mytilus galloprovincialis* mussels. *Ecotoxicology*, *24*, 292–300. https://doi.org/10.1007/s10646-014-1377-5

Wen, Q., Liu, H. L., Zhu, Y. T., Zheng, X. M., Su, G. Y., Zhang, X. W., Yu, H. X., Giesy, J. P., & Lam, M. H. W. (2015). Maternal transfer, distribution, and metabolism of BDE-47 and its related hydroxylated, methoxylated analogs in zebrafish (*Danio rerio*). *Chemosphere*, *120*, 31–36. https://doi.org/10.1016/j.chemosphere.2014.05.050

Westerfield, M. (2007). Guide for the Laboratory Use of Zebrafish (*Danio rerio*) (5th Edition). University of Oregon Press.

Wiseman, S. B., Wan, Y., Chang, H., Zhang, X., Hecker, M., Jones, P. D., & Giesy, J. P. (2011). Polybrominated diphenyl ethers and their hydroxylated/methoxylated analogs: Environmental sources, metabolic relationships, and relative toxicities. *Marine Pollution Bulletin*, *63*, 179–188. https://doi.org/10.1016/j.marpolbul.2011.02.008

Yamazoe, A., Yagi, O., & Oyaizu, H. (2004). Biotransformation of fluorene, diphenyl ether, dibenzo-p-dioxin and carbazole by *Janibacter* sp. *Biotechnology Letters*, *26*, 479–486. https://doi.org/10.1023/B:BILE.0000019554.49484.40

Yang, J., & Chan, K. M. (2015). Evaluation of the toxic effects of brominated compounds (BDE-47, 99, 209, TBBPA) and bisphenol a (BPA) using a zebrafish liver cell line, ZFL. *Aquatic Toxicology*, *159*, 138–147. https://doi.org/10.1016/j.aquatox.2014.12.011

Yang, J., Zhao, H., & Chan, K. M. (2017). Toxic effects of polybrominated diphenyl ethers (BDE 47 and 99) and localization of BDE-99–induced cyp1a mRNA in zebrafish larvae. *Toxicology Reports*, *4*, 614–624. https://doi.org/10.1016/j.toxrep.2017.11.003

Zhai, C., Peng, S., Yang, L., & Wang, Q. (2014). Evaluation of BDE-47 hydroxylation metabolic pathways based on a strong electron-withdrawing pentafluorobenzoyl derivatization gas chromatography/electron capture negative ionization quadrupole mass spectrometry. *Environmental Science & Technology*, *48*, 8117–8126. https://doi.org/10.1021/es405446y

Zhang, M., Zhao, F., Zhang, J., Shi, J., Tao, H., Ge, H., Guo, W., Liu, D., & Cai, Z. (2020). Toxicity and accumulation of 6-OH-BDE-47 and newly synthesized 6,6′-diOH-BDE-47 in early life-stages of Zebrafish (*Danio*

rerio). *Science of the Total Environment*, *763*, 143036. https://doi.org/10.1016/j.scitotenv.2020.143036

Zhang, T., Zhou, X., Xu, A., Tian, Y., Wang, Y., Zhang, Y., Gu, Q., Wang, S., & Wang, Z. (2020). Toxicity of polybrominated diphenyl ethers (PBDEs) on rodent male reproductive system: A systematic review and meta-analysis of randomized control studies. *Science of the Total Environment*, *720*, 137419. https://doi.org/10.1016/j.scitotenv.2020.137419

Zheng, X., Zhu, Y., Liu, C., Liu, H., Giesy, J. P., Hecker, M., Lam, M. H. W., & Yu, H. (2012). Accumulation and biotransformation of BDE-47 by zebrafish larvae and teratogenicity and expression of genes along the hypothalamus-pituitary-thyroid axis. *Environmental Science & Technology*, *46*, 12943–12951. https://doi.org/10.1021/es303289n

Zindler, F., Tisler, S., Loerracher, A. K., Zwiener, C., & Braunbeck, T. (2020). Norfluoxetine is the only metabolite of fluoxetine in zebrafish (*Danio rerio*) embryos that accumulates at environmentally relevant exposure scenarios. *Environmental Science and Technology*, *54*, 4200–4209. https://doi.org/10.1021/acs.est.9b07618

Bioaccumulation and biotransformation of BDE-47 using zebrafish eleutheroembryos (*Danio rerio*)

Paloma De Oro-Carretero, Jon Sanz-Landaluze*

Department of Analytical Chemistry, Faculty of Chemical Science, Complutense University of Madrid, Avenida Complutense s/n, 28040 Madrid, Spain

E-mail addresses: pdeoro@ucm.es, jsanzlan@ucm.es* ***Phone:*** +034-91 394 4322; Fax: +034-91 394 4329

Supplementary Information

Setting the gas chromatographic separation and determination

Two low-polarity capillary columns: DB-5 and ZB-5MS and different chromatographic parameters were evaluated. The remaining parameters had been optimized previously (El-Amrani et al., 2012). Based on sensitivity, ZB-5MS was selected for separation despite the increase in retention time with respect to the DB-5 column. MTBSTFA was chosen as a derivatization reagent because it is the most common in phenolic compounds (Schummer et al., 2009). Thus, it avoids the commonly used reagents for methylation of OH-BDEs, diazomethane (DM) and trimethylsilyl diazomethane (TMSDM) (Zhai et al., 2014) which forms MeO-PBDEs derivatized and can be confused with MeO-BDEs metabolites. Although theoretically, PBDEs and MeO-BDEs remain structurally unchanged by the derivatization process with MTBSTFA, a significant loss of these compounds is observed, reducing greatly sensitivity (Fig. S1). Because of this, a double determination was carried out, injecting extracted isooctane directly to GC for determination of PBDEs and MeO-BDEs and with derivatization step for MeO-PBDEs. In addition, three different solvents are tested for derivatization, isooctane, hexane and acetone, with no significant differences (Fig. S1). Therefore, as isooctane is usually used for PBDEs and MeO-BDE, it is the one chosen in the derivatisation process.

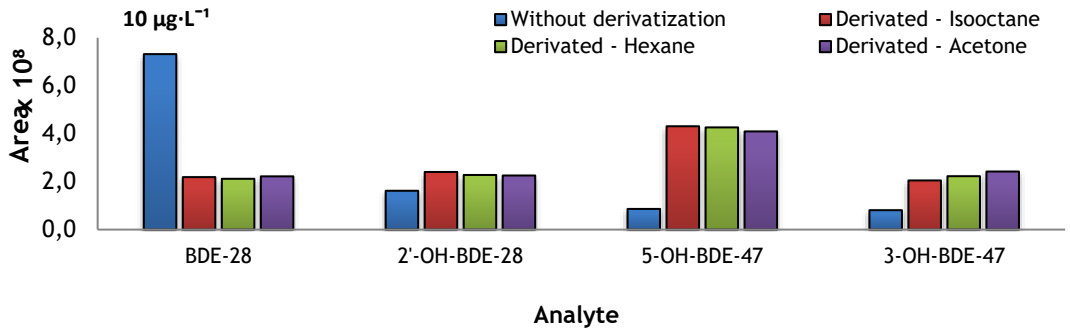

Fig. S1. Analytical signal obtained by derivatising a mixture of OH-BDEs and a BDE in different solvents

Setting the gas chromatographic separation and determination

Mixture of extraction solvents n-hexane:DCM (1:1, v/v) and n-hexane: MTBE (1:1, v/v) and several common commercial sorbents (C_{18}, PSA, Z-Sep, Florisil) were evaluated (Fig. S2) (Cruz et al., 2017). Good recoveries for PBDEs and MeO-BDEs were obtained using PSA. Nonetheless, the OH-BDEs were completely lost because PSA is usually used to remove polar compounds from a non-polar matrix (Barci et al., 2020). C18 ensures that OH-BDE is not lost in the cleaning stage because eliminate non-polar lipid interferences (Lacorte et al., 2010). However, the recoveries obtained show interferences due to the sample matrix. Supel™ QuE Z-Sep consists of a mixture with ratio 2/5 of ZrO2/C18 (Lozano et al., 2014), where ZrO2 attracts substances with polar hydroxyl groups (electron-donor group) and C18 interacts with non-polar compounds in the lipids. Therefore, favourable recoveries of PBDEs and MeO-BDEs were obtained but the action of ZrO2 on polar compounds results in the loss of a very important quantity of OH-BDEs. Despite florisil also removed polar compounds (Zhao et al., 2016), it does not affect OH-BDEs as is the case with PSA and Z-Sep. So, the recoveries of PBDEs, MeO-BDEs and OH-BDEs are compensated. On the other hand, with n-hexane:MTBE mixture (1:1), the compounds are extracted from the matrix better than with the n-hexane:DCM mixture (1:1), as better recovery results are obtained for most analytes. The same behaviour in the exposure media is observed.

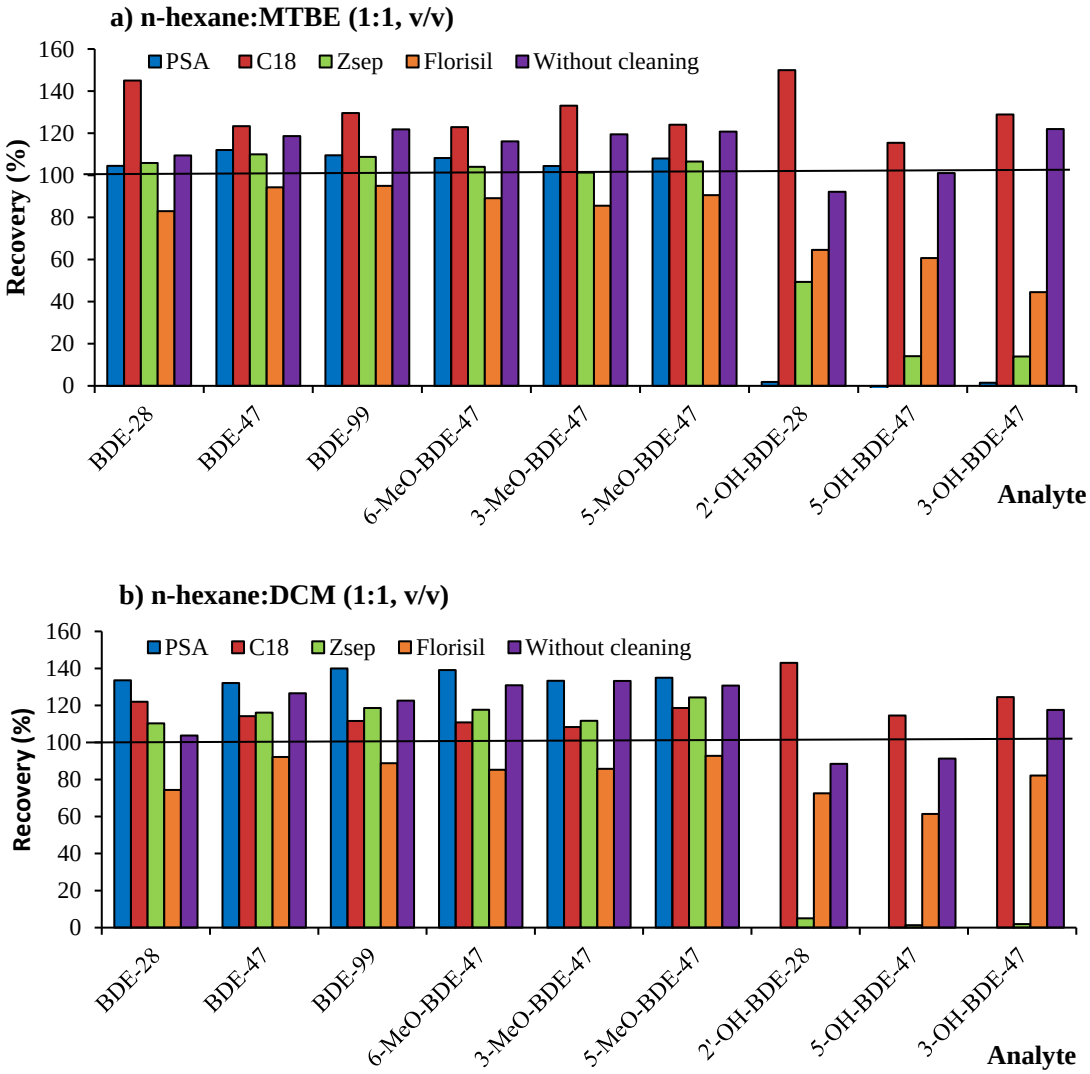

Fig. S2. Recoveries obtained with the different adsorbents by extraction with a) n-hexane:MTBE (1:1, v/v) and b) n-hexane:DCM (1:1, v/v) in zebrafish eleutheroembryos of known concentration (10 $\mu g \cdot L^{-1}$).

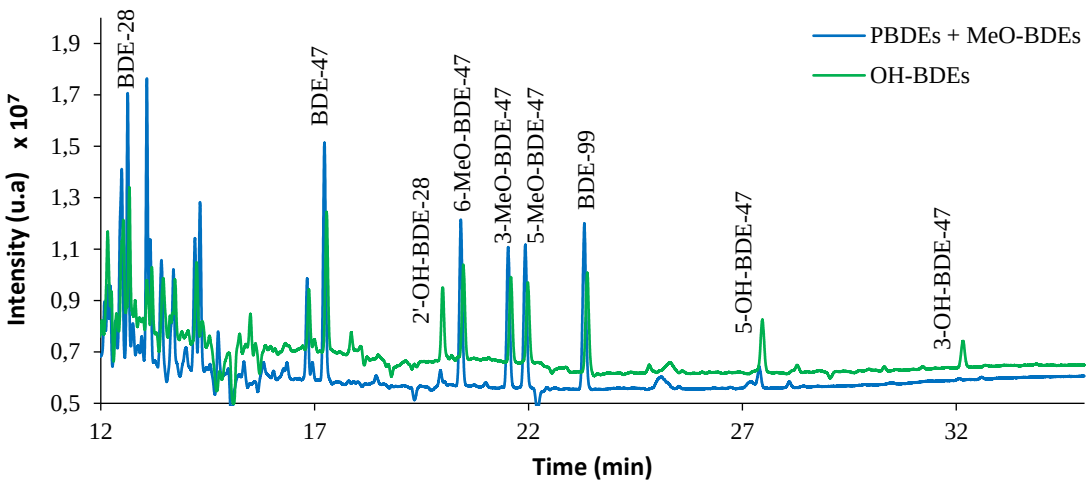

Fig. S3. Chromatogram obtained with n-hexane:MTBE (1:1, v/v) and Florisil as an adsorbent.

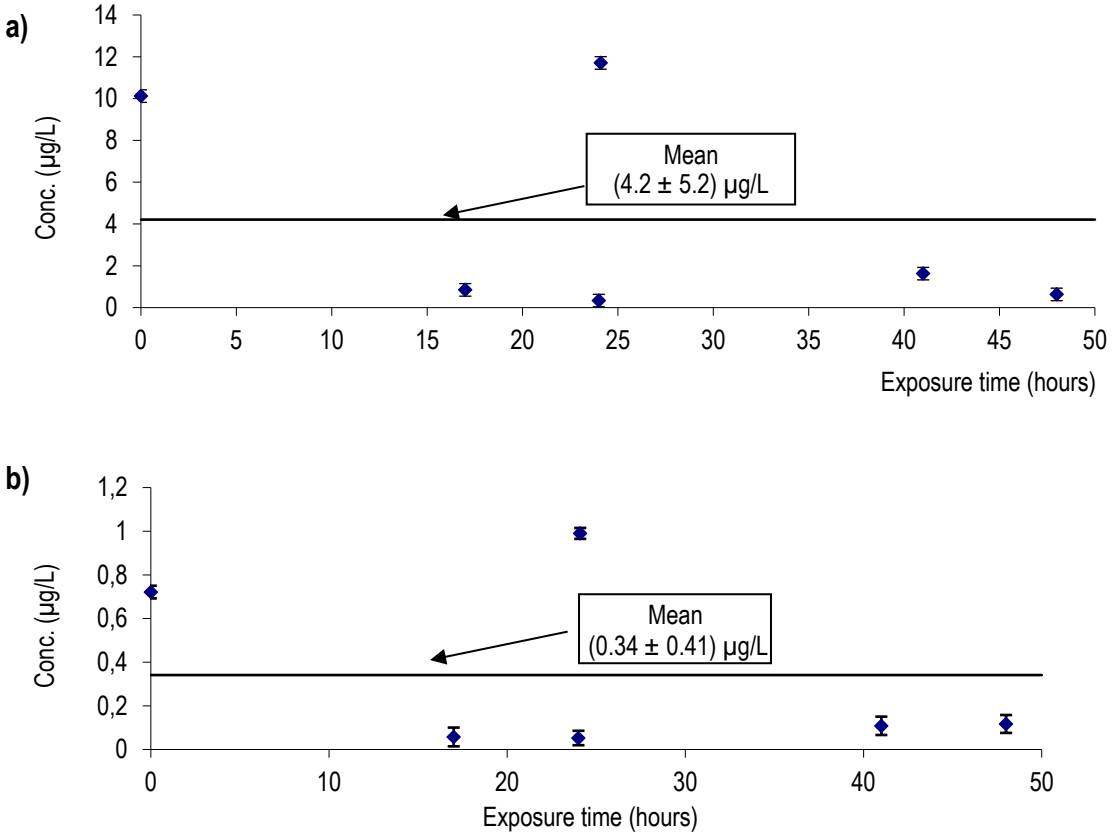

Fig. S4. BDE-47 concentration determined experimentally in the exposure media ($\mu g \cdot L^{-1}$), a) nominal exposure concentration: 10 $\mu g \cdot L^{-1}$ and b) nominal exposure concentration: 1 $\mu g \cdot L^{-1}$

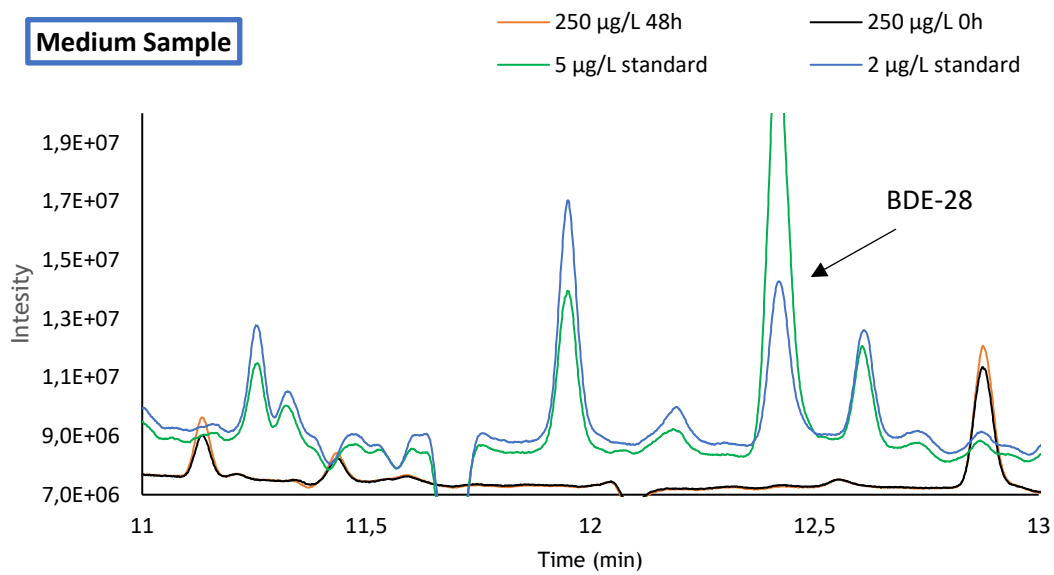

Fig. S5. GC-µECDchromatogram of the exposure media at 0 and 48 h (nominal exposure concentration BDE-47 at 250 µg·L^{-1}) compared with 2 and 5 µg·L^{-1} BDE-28 analytical standards.

Table S1 LODs, LOQs RSD, R^2 and method recoveries

Analyte	R^2	LOD (µg·L^{-1})	LOQ (µg·L^{-1})	Recovery of zebrafish eleutheroembryos (%)	Recovery of exposure medium (%)	RSD (%)
BDE-28	0.9993	0.21	0.44	98 ± 5	85 ± 7	7
BDE-47	0.9992	0.10	0.25	102 ± 3	98 ± 5	5
BDE-99	0.9991	0.11	0.25	99 ± 5	89 ± 5	7
6-MeO-BDE-47	0.9989	0.13	0.41	98 ± 5	83 ± 5	6
3-MeO-BDE-47	0.9986	0.16	0.54	102 ± 5	92 ± 6	8
5-MeO-BDE-47	0.9985	0.17	0.31	96 ± 4	87 ± 5	6
2'-OH-BDE-28	0.9946	0.19	0.58	87 ± 5	79 ± 6	8
5-OH-BDE-47	0.9945	0.19	0.51	67 ± 4	65 ± 6	8
3-OH-BDE-47	0.9962	0.22	0.68	42 ± 6	52 ± 7	11

Table S2 Predicted 50 % lethal concentrations (LC_{50}, mol·L^{-1}) and 50 % growth inhibition concentrations (IGC_{50}, mol·L^{-1}) of BDE-47 and metabolites for different tests with TEST software 4.1 (consensus method) (EPA, 2008)

Toxicological parameter	**log LC_{50} (48h) (mol/L)**	**log IGC_{50} (mol/L)**	**Log LC_{50} (96h) (mol/L)**	**BCF (log BCF)**
Analyte / Organism	*Daphnia magna*	*Tetrahymena pyriformis*	*Fathead minnow*	
BDE-28	6.45	5.70	6.28	443.14 (2.65)
BDE-47	7.3	6.12	6.65	280.24 (2.45)
BDE-99	7.77	6.58	6.95	322.09 (2.51)
6-MeO-BDE-47	7.02	6.10	6.63	304.84 (2.48)
5-MeO-BDE-47	7.15	6.16	6.75	450.68 (2.65)
3-MeO-BDE-47	7.54	6.03	6.69	559.04 (2.75)
2'-OH-BDE-28	6.30	5.54	6.35	109.48 (2.04)
5-OH-BDE-47	6.78	6.18	6.76	271.56 (2.43)
3-OH-BDE-47	6.99	6.17	6.83	149.36 (2.17)

Table S3 Ratio between metabolites and BDE-47 concentration (in %) in the experiment of metabolization (t = 48h)

	BDE-28/BDE-47	**2'OH-BDE-28 / BDE-47**	**5-MeO-BDE-47/ BDE-47**
100 µg·L^{-1}	0,753	0,247	0,129
250 µg·L^{-1}	0,249	0,173	0,083

Table S4 Ratio between their metabolites and BDE-47 in the 10 µg·L^{-1} bioaccumulation experiment

	BDE-28/BDE-47	**2'OH-BDE-28 / BDE-47**	**5-MeO-BDE-47/ BDE-47**
t = 17h	0,790	0,243	0,043
t = 24h	0,745	0,254	0,059
t = 41h	0,665	0,197	0,018
t = 48h	0,676	0,420	0,027
t = 65h	0,684	0,423	0,025
t = 72h	0,662	0,422	0,038

Table S5 Areas obtained in GC-μECD determination of exposure media and larvae at 0 and 48 h (nominal exposure concentration BDE-47 at 250 μg·L^{-1}) compared with 2 and 5 μg·L^{-1} BDE analytical standards.

Areas·10^{-7}	BDE-28	BDE-47	2'-OH-BDE-28	6-MeO-BDE-47	5-MeO-BDE-47	3-MeO-BDE-47	5-OH-BDE-47	3-OH-BDE-47
Medium Sample								
250 μg·L^{-1} – 0h	0,492	133	n.d.	0,307	0,170	2,31	n.d.	n.d.
250 μg·L^{-1} – 48h	0,467	14,8	n.d.	0,450	0,470	1,76	n.d.	n.d.
Larvae Sample								
250 μg·L^{-1} – 0h	0,767	475	0,254	0,093	0,206	1,45	2,05	0.700
250 μg·L^{-1} – 48h	26,5	10100	6,76	0,609	8,14	1,80	0,958	1,01
2 μg·L^{-1} standard	24,0	31,3	19,5	26,3	24,4	23,2	16,7	12,9
5 μg·L^{-1} standard	52,6	66,9	49,5	62,1	49,9	49,4	44,6	33,3

References

Barci, P.E.P., Alves, L.S, Avellar, Á.A.S., Cendon, L.R, dos Santos, P.J, Stringhini, F.M, Prestes, O.D, Zanella, R., 2020. Modified QuEChERS Method for Multiresidue Determination of Pesticides in Pecan Nuts by Liquid Chromatography Tandem Mass Spectrometry. *Food*. Anal. Methods. 13, 793–801. https://doi.org/10.1007/s12161-019-01696-0.

Cruz, R., Cunha, S.C., Marques, A., Casal, S., 2017. Polybrominated diphenyl ethers and metabolites – An analytical review on seafood occurrence. *TrAC* 87, 129–144 https://doi.org/10.1016/j.trac.2016.12.005.

El-Amrani, S., Pena-Abaurrea, M., Sanz-Landaluze, J., Ramos, L., Guinea, J., Cámara, C., 2012. Bioconcentration of pesticides in Zebrafish eleutheroembryos (*Danio rerio*). *Sci. Total. Environ.* 425, 184–190. https://doi.org/10.1016/j.scitotenv.2012.02.065.

EPA, 2008. Toxicity Estimation Software Tool - T.E.S.T. (version 4.1): A Program to Estimate Toxicity from Molecular Structure. Environmental Protection Agency. https://www.epa.gov/chemical-research/toxicity-estimation-software-tool-test.

Lacorte, S., Ikonomou, M.G., Fischer, M., 2010. A comprehensive gas chromatography coupled to high resolution mass spectrometry based method for the determination of polybrominated diphenyl ethers and their hydroxylated and methoxylated metabolites in environmental samples. *J. Chromatogr. A.* 1217, 337–347. https://doi.org/10.1016/j.chroma.2009.11.024

Lozano, A., Rajski, Ł., Uclés, S., Belmonte-Valles, N., Mezcua, M, Fernández-Alba, A.R., 2014. Evaluation of zirconium dioxide-based sorbents to decrease the matrix

effect in avocado and almond multiresidue pesticide analysis followed by gas chromatography tandem mass spectrometry. *Talanta* 118, 68–83. https://doi.org/10.1016/j.talanta.2013.09.053

Schummer, C., Delhomme, O., Appenzeller, B.M.R., Wennig, R., Millet, M., 2009. Comparison of MTBSTFA and BSTFA in derivatization reactions of polar compounds prior to GC/MS analysis. *Talanta*. 77, 1473–1482. https://doi.org/10.1016/j.talanta.2008.09.043.

Zhai, C., Peng, S., Yang, L., Wang, Q., 2014. Evaluation of BDE-47 hydroxylation metabolic pathways based on a strong electron-withdrawing pentafluorobenzoyl derivatization gas chromatography/ electron capture negative ionization quadrupole mass spectrometry. *Environ Sci Technol.* 48, 8117–8126. https://doi.org/10.1021/es405446y.

Zhao, X., Zhou, Y., Kong, W., Gong, B., Chen, D., Wei, J., Yang, M., 2016. Multi-residue analysis of 26 organochlorine pesticides in Alpinia oxyphylla by GC-ECD after solid phase extraction and acid cleanup. *J Chromatogr B.* 1017–1018, 211–220. https://doi.org/10.1016/j.jchromb.2016.03.009

1.2. Metodología *in vitro* mediante líneas celulares.

De acuerdo con el enfoque descrito y los objetivos establecidos en esta Tesis Doctoral, en esta sección se continúa con el desarrollo de metodologías alternativas enmarcadas en el principio de las 3R. Mientras que en la *Sección 1.1 "Metodología in vivo mediante larvas de pez cebra",* se abordó la Reducción de la experimentación animal, esta sección se enfoca en su **Reemplazo** y en el **Refinamiento** de los modelos existentes. En este sentido, la propuesta a evaluar es la utilización de líneas celulares como metodología alternativa *in vitro* para el estudio de la bioacumulación y biotransformación.

Dado que una de las principales limitaciones de los modelos actuales es la falta de determinaciones experimentales de las concentraciones internas en las células, en primer lugar, se desarrolla un **método analítico** para la cuantificación simultánea de los compuestos y sus metabolitos. Las optimizaciones realizadas se presentan en el primer trabajo de esta sección (**Artículo 2**), titulado ***Miniaturized method for the quantification of persistent organic pollutants and their metabolites in HepG2 cells: assessment of their biotransformation* (*Analytical and Bioanalytical Chemistry*, 415, 4813-4825, 2023)**. Además, para evaluar la viabilidad del método analítico, se aplica este en un estudio de biotransformación con células HepG2, seleccionadas por su uso previo en la literatura para este tipo de investigaciones. Con ello, también se establece un diseño experimental válido para los estudios posteriores de bioacumulación y biotransformación de contaminantes orgánicos persistentes (POPs).

Para el desarrollo de esta metodología, en esta ocasión se emplean como modelos el **BDE-47**, menos estudiado en sistemas *in vitro,* pero evaluado mediante metodología oficial in vivo, y el **PHE** (fenantreno), seleccionado por ser uno de los compuestos más estudiados en ensayos *in vitro* debido a sus propiedades hidrófobas y volátiles[71,181]. Del mismo modo, de acuerdo con la revisión de la

[71] **Birch** *et al.* Time-resolved freely dissolved concentrations of semivolatile and hydrophobic test chemicals in in vitro assays - measuring high losses and crossover by headspace solid-phase microextraction. *Chem Res Toxicol.* **2019**.

[181] **Fischer** *et al.* Application of experimental polystyrene partition constants and diffusion coefficients to predict the sorption of neutral organic chemicals to multiwell plates in in vivo and in vitro bioassays. *Environ Sci Technol*. **2018**.

bibliografía, se eligieron los **metabolitos mayoritarios** de ambos compuestos: MeO-BDEs y OH-BDEs para el BDE-47, especificados en la sección anterior, y OH-PHEs (1-OH-PHE, 2-OH-PHE, 3-OH-PHE, 4-OH-PHE y 9-OH-PHE) para el PHE, utilizados habitualmente como biomarcadores de su exposición.

Se decidió aplicar el mismo concepto de extracción miniaturizada mediante sonda de ultrasonidos para la liberación de los compuestos del interior celular, previamente desarrollada para la metodología con larvas, descrita en la sección anterior. La única diferencia fue que no se requirió una etapa adicional de limpieza de los extractos. La separación y detección para la identificación y cuantificación del BDE-47 y sus metabolitos fue la misma (**GC-MS-µECD**), descrita en la anterior sección. En el caso del PHE, se seleccionó el análisis mediante cromatografía de líquidos con detección por fluorescencia (**LC-FLD**), empleando una rampa de fase móvil de acetonitrilo (ACN) y agua. En cambio, para los OH-PHEs, se optó por el análisis mediante **GC-MS**, previa derivatización. Para la optimización de este proceso, se probaron diferentes **reactivos de derivatización**, todos basados en la sililación de los compuestos, como N, O-Bis(trimethylsilyl)acetamide (BSA-deriv.), N,O-bis(trimethylsilyl)trifluoroacetamide (BSTFA) y MTBSTFA, siendo este último el que mejores resultados mostró. Además, se probaron diferentes proporciones, temperaturas y tiempos de incubación; donde se determinó en un 20% a 60˚C durante 30 minutos, respectivamente.

En cuanto al **proceso de extracción**, se optimizó la mezcla de disolventes tanto para las muestras de células HepG2 como para los medios de exposición. Al igual que en la extracción de larvas, la mezcla de hexano:MTBE (1:1) resultó ser la más adecuada para la extracción simultánea de BDE-47 y sus metabolitos (MeO-BDEs y OH-BDEs) en ambos tipos de muestras.Para la extracción de compuestos OH-PHEs, la mezcla óptima fue hexano:DCM (1:1), tanto en células HepG2 como en los medios de exposición. La diferencia principal entre ambas determinaciones, realizadas mediante GC-MS-(µECD), radicó en el disolvente utilizado para la reconstitución posterior a la evaporación: se empleó isooctano para los PBDEs y hexano para los OH-PHEs. Además, en el caso de los OH-PHEs, no se utilizó **patrón interno** debido a que los dos compuestos disponibles para este propósito (9-OH-fluoreno y triclosán) presentaron limitaciones: 9-OH-fluoreno mostró baja

sensibilidad y escasa estabilidad con el reactivo derivatizante MTBSTFA, mientras que el triclosán no presentó recuperaciones consistentes con el disolvente de extracción seleccionado. Ante la ausencia de patrón interno, se realizaron extracciones y análisis paralelos de muestras fortificadas con concentraciones conocidas (altas y bajas) de los analitos, con el fin de evaluar posibles pérdidas durante la determinación y, en caso necesario, aplicar las correcciones correspondientes. Finalmente, para la extracción de PHE se seleccionó acetonitrilo como disolvente, utilizando fluoreno como patrón interno, en muestras de células y medios de exposición. En estos últimos, fue necesario añadir NaCl para facilitar la separación de fases entre acetonitrilo y la fracción acuosa del medio de exposición (la adición de NaCl disminuye la solubilidad del acetonitrilo en agua al aumentar la fuerza iónica de la disolución, lo que reduce la disponibilidad de moléculas de agua para interactuar con el acetonitrilo, favoreciendo así la separación de fases por efecto *salting out* o efecto salino).

El **diseño experimental** se elaboró teniendo en cuenta los diferentes equilibrios presentes en el sistema *in vitro* (**Figura 9**) y las necesidades experimentales para la evaluación de la bioacumulación y metabolización. En primer lugar, se evaluó la **absorción de PHE en la placa de cultivo** de plástico, resultando en una pérdida del 84% a las 48h de exposición. Por ello, se decidió realizar los experimentos en placas de vidrio donde se reduzco las pérdidas a un 26% y 14% de PHE y BDE-47, respectivamente. Estas pérdidas fueron consecuencia de la evaporación de los compuestos debido a sus propiedades volátiles y al uso de un sistema abierto para permitir la entrada de CO_2. Con el fin de controlar y cuantificar dichas pérdidas por volatilización, además de las muestras de exposición con células en los diferentes tiempos de exposición, se decidió llevar a cabo un experimento paralelo sin células. Además, se cuantificó la concentración de la disolución inicial (tiempo 0 h) para realizar una comparación real. La **concentración del experimento** se decidió de acuerdo con un **ensayo de viabilidad** previo (ensayo MTT) donde se dictaminó la concentración a la cual las células presentaban una capacidad de metabolización adecuada y el aseguramiento de la entrada del compuesto, esto es, que presentaran una viabilidad entre 70-80%. Este ensayo de viabilidad se llevó a cabo bajo las mismas condiciones establecidas

para el experimento de biotransformación, es decir, con un 10% de FBS para simular la concentración biodisponible según el equilibrio esperado. Por último, ante la necesidad de obtener una **muestra representativa de pellet celular** para la extracción de los compuestos de su interior, el experimento se llevó a cabo en **placas de vidrio P100** (10 mm), donde aproximadamente se siembran $2 \cdot 10^6$ células, con el fin de maximizar la cantidad de células obtenidas. Además, para normalizar la concentración en función del número de células en cada experimento, se optó por secar el pellet celular mediante una corriente de nitrógeno y posteriormente determinar su peso. De este modo, la concentración se establece en relación con el peso de cada muestra.

Una vez desarrollado el método analítico, se **expusieron** las células HepG2 según el diseño experimental, a 15 y 20 $mg \cdot L^{-1}$ de PHE y BDE-47, respectivamente, y se **cuantificaron** tanto los compuestos parentales como sus metabolitos en el interior celular y medios de exposición a las 48h, mediante los métodos analíticos desarrollados. Los balances de masa mostraron una recuperación cercana al 100 %, con valores del 78 % para PHE y del 87 % para BDE-47. Estos resultados indican que los **metabolitos** determinados son mayoritarios y **representan** adecuadamente el proceso de **biotransformación**, además de confirmar la **idoneidad** del **método** analítico y del diseño experimental para estudios de bioacumulación y biotransformación.

Como parte del desarrollo metodológico, se llevó a cabo el siguiente estudio (**Artículo 3**), titulado ***In vitro approach to refine bioconcentration and biotransformation predictions of organic persistent pollutants using cell lines (Chemosphere 364, 143020, 2024)***. Este trabajo recopila las investigaciones realizadas en el estudio de la bioacumulación mediante la determinación del BCF y la obtención de datos cinéticos de biotransformación, empleando líneas celulares. Para ello, se seleccionaron líneas celulares hepáticas, dado que el hígado es el principal órgano implicado en la biotransformación, incluyendo las células **HepG2** y **ZFL**, así como líneas celulares derivadas del pez cebra, utilizado como organismo modelo en estudios de bioacumulación, como ZFL y **ZF4**. Además, se optó por iniciar el estudio con el compuesto **PHE**, debido a su amplio respaldo en la literatura.

En primer lugar, se plantea la **obtención del BCF** mediante el enfoque habitual de determinación, según el protocolo estandarizado **OECD 305**. Esto es, mediante la relación de las concentraciones dentro del organismo (células, C_{cell}) y el medio de exposición si se alcanza el estado estacionario (BCF_{ss}) o mediante el modelo toxicocinético (BCF_K) (*Sección 2.1 de la Introducción*). Para ello, según el diseño experimental desarrollado, se expusieron las células HepG2 y ZF4 a 15 $mg \cdot L^{-1}$ PHE y las células ZFL a 10 y 50 $mg \cdot L^{-1}$ PHE, previo ensayo de viabilidad (MTT para ZFL y HepG2; Alamar Blue para ZF4) a diferentes tiempos (0, 24, 48 y 72 h) en placas P100 de vidrio. Una vez muestreados los medios y pellet celulares, se cuantificaron las concentraciones mediante el método analítico desarrollado y se determinó el BCF. Debido a la diferencia entre las concentraciones nominal y biodisponible (C_{free}) en los sistemas *in vitro* para POPs con tendencia hidrofóbica, se subestimó el BCF en comparación con valores *in vivo*.

Por tanto, seguidamente, se planteó la necesidad de la **determinación de C_{free}**. Debido al diseño experimental realizado, en el que la principal disminución de la concentración nominal radica en el equilibrio con el suero FBS del medio, se empleó el **modelo de distribución química (MBM)** desarrollado por Fischer *et al*[182]. Para ello, se introdujeron las concentraciones determinadas experimentalmente en el medio de exposición, las condiciones de ensayo (tamaño de placa, porcentaje FBS, número de células, tipo de medio celular etc.) y los valores de constantes de partición PHE-BSA y PHE-lípidos, obtenidas mediante la herramienta UFZ-LSER[183]. La hoja de cálculo del modelo estima las fracciones de cada compartimiento celular y la concentración correspondiente, incluida C_{cell} y C_{free}. Mediante el uso de C_{free}, los valores de BCF_{ss} (72 h) y BCF_k obtenidos para ZFL y ZF4 no presentaron diferencias significativas con un nivel de confianza del 95% en comparación con valores *in vivo* reportados en la literatura. En cuanto a las cinéticas de bioacumulación, las células ZFL y ZF4 lograron alcanzar el estado estacionario durante el ensayo, sin embargo, las HepG2 no lo hicieron. Por otro lado, se observó un incremento en las concentraciones de metabolitos en la exposición con células HepG2 y ZFL, pero no se detectaron concentraciones de

[182] **Fischer** *et al.* Modeling exposure in the Tox21 in vitro bioassays. *Chem. Res. Toxicol.* **2017**.
[183] **Ulrich** *et al.* **UFZ-LSER Database** v3.2.1 [Internet]. Helmholtz Centre for Environmental. Research-UFZ, Leipzig, Germany. (Accedido el 5 de abril de 2024).

metabolitos en las células ZF4, probablemente debido a que no son células hepáticas con capacidad biotransformadora.

Por otro lado, se evaluó la aplicabilidad de las líneas celulares propuestas en el **método IVIVE** (OECD No. 280[63]). Esta evaluación se llevó a cabo como alternativa a las limitaciones que presenta el método, descritas en la *Sección 5.4 de la Introducción*, así como debido a la solicitud de los autores de su validación en otros enfoques y con distintos compuestos, con el fin de ampliar su dominio de aplicabilidad y proporcionar más datos que contribuyan a subsanar dichas limitaciones. El PHE y BDE-47 son compuestos bastante hidrofóbicos, aunque dentro del rango de aplicabilidad del modelo (log K_{ow} entre 3-8), volátiles y con diferente cinética de bioacumulación y biotransformación, lo que los hace adecuados para utilizarse como modelo en este trabajo. En este contexto, las líneas celulares representan una alternativa viable, ya que permiten la realización de ensayos de 72 h para el estudio de compuestos con cinéticas de biotransformación más lentas, sin la necesidad de utilizar un organismo vivo para su obtención. Debido al uso de líneas celulares, **se incorpora la utilización de C_{free}** en vez de la concentración nominal o del medio y la corrección por pérdidas debidas a la volatilización. Adicionalmente, gracias a la capacidad del método analítico desarrollado para determinar las concentraciones de los metabolitos en el interior celular, se contrapone el enfoque de agotamiento del sustrato, propuesto en el modelo, donde solo se determina la concentración en el medio de exposición suponiendo que toda la bajada observada es debida a biotransformación, con un **enfoque basado en la formación de productos**, permitiendo así un estudio más preciso de las cinéticas de biotransformación. Los resultados mostraron que los valores de BCF obtenidos mediante el modelo IVIVE fueron altamente comparables con los reportados en estudios *in vivo* disponibles en la literatura. En este caso, con la utilización de todas las líneas celulares testadas se obtuvieron resultados satisfactorios. En base a lo observado en el ensayo anterior, donde las células HepG2 no fueron adecuadas para la determinación del BCF, y considerando que las células hepáticas poseen capacidad de metabolización, se concluyó que la línea

[63] **OECD No. 280**. Guidance document on the determination of in vitro intrinsic clearance using cryopreserved hepatocytes (RT-HEP) or liver S9 sub-cellular fractions (RT-S9) from rainbow trout and extrapolation to in vivo intrinsic clearance series on testing and assessment. **2018.**

celular ZFL era la más adecuada para estudios simultáneos de bioacumulación y biotransformación.

Con el objetivo de seguir evaluando la metodología, se llevó a cabo el último trabajo de esta sección (**Artículo 4**) titulado ***Assessing bioconcentration and biotransformation of BDE-47 in vitro: The relevance of bioavailable and intracellular concentrations (Journal of Xenobiotics, 15, 93, 2025)***. En este trabajo se optó por estudiar el compuesto **BDE-47**, además de lo ya expuesto previamente en esta Tesis Doctoral, debido a sus mayores propiedades hidrofó bicas y una cinética de metabolizació n más lenta en comparació n con el PHE, pero aú n dentro del rango de trabajo del modelo IVIVE. Considerando los resultados previos, en este estudio se evaluó exclusivamente la línea celular **ZFL**. De igual manera a lo ya descrito, se expusieron las células ZFL a 1 y 2 $mg \cdot L^{-1}$ en placas P100 de vidrio con 10% de FBS; se muestrearon tanto los pellets celulares y los medios de exposició n a 0, 24, 48 y 72h; se cuantificaron las concentraciones mediante el método analítico desarrollado y **se determinó el BCF mediante tres enfoques**: la relació n de concentraciones, el modelo toxicocinético y el modelo IVIVE. En esta ocasió n, el modelo IVIVE se estimó adicionalmente utilizando los **parámetros de extrapolación provenientes del pez cebra**, en lugar de únicamente los establecidos por el modelo, basados en el pez trucha arcoíris. Los resultados mostraron que los valores de $\mathbf{BCF_k}$ e **IVIVE** (ambas extrapolaciones) fueron comparables con los resultados *in silico* de modelos matemáticos validados, los valores *in vivo* de la literatura obtenidos en organismos adultos y, en este caso, debido a la utilización del BDE-47, también con los resultados *in vivo* de esta Tesis Doctoral en larvas de pez cebra.

Adicionalmente a la evaluación y aplicación directa del modelo IVIVE validado, en este trabajó **se estudió más en profundidad y se aportó otro enfoque de estimación**, aprovechando los métodos analíticos y el diseño experimental desarrollado, con el objetivo de obtener **valores más cercanos a la realidad para diferentes compuestos**. El modelo IVIVE determina el BCF mediante la relación de la concentración interna del organismo y la concentración total en el medio. La determinación de la concentración interna se basa en un modelo toxicocinético que combina la determinación experimental *in vitro* para estimar la constante de

metabolización, que luego se extrapola a un valor *in vivo,* y una determinación *in silico* para estimar las constantes de absorción y desorción, entre otras. Estas últimas se basan, a su vez, únicamente, en la constante de partición octanol-agua del compuesto. Por tanto, ante esta estimación carente de estimación experimental, se realizó una **comparación** entre las **concentraciones internas de las células y biodisponibles** obtenidas mediante **MBM o experimentalmente**. La concentración libre experimental (C_{free}) se determinó utilizando un ensayo basado en la técnica de microextracción en fase sólida (**SPME**), replicando las condiciones del ensayo de bioacumulación y biotransformación (1 y 2 mg·L^{-1}de BDE-47, 28 ˚C y 10% FBS), siguiendo el protocolo propuesto por Henneberger *et al.*[167], cuyas ecuaciones se detallan en la *Sección 7.2.1 "Cuantificación de la concentración biodisponible*" de la Introducción. Los parámetros del ensayo, como el tipo de fibra, tiempos de equilibrio y desorción, disolvente de desorción y la constante global de equilibrio del sistema fibra-compuesto-BSA, fueron seleccionados a partir de una revisión bibliográfica. Para el caso del BDE-47 se emplearon fibras de polidimetilsiloxano (PDMS)[169]. Asimismo, se realizó una comparación con el compuesto fenantreno (PHE), utilizando fibras de poliacrilato (PA)[168].

De este modo, se evaluó y se demostró que la línea celular ZFL podría ser una alternativa adecuada para la estimación rápida del BCF, permitiendo el **reemplazo** completo de la experimentación animal. También se ha desarrollado un método analítico de determinación de las concentraciones internas de POP y metabolitos para implementar en los estudios simultáneos de bioacumulación y biotransformación, así como de la concentración biodisponible, remarcando la importancia de las determinaciones experimentales. Y, por último, se han aportado más datos y discusiones que pueden servir para **refinar** los modelos existentes.

[167] **Henneberger** *et al.* Quantification of freely dissolved effect concentrations in in vitro cell-based bioassays. *Arch Toxicol*. **2019**.
[168] **Endo** *et al.* Polyparameter linear free energy models for polyacrylate fiber-water partition coefficients to evaluate the efficiency of solid-phase microextraction. *Anal Chem*. **2011**.
[169] **Endo** *et al.* Liposome and protein-water partitioning of polybrominated diphenyl ethers (PBDEs). *Chemosphere*. **2013**.

ARTÍCULO 2:

Método miniaturizado para la cuantificación de contaminantes orgánicos persistentes y sus metabolitos en células HepG2: evaluación de su biotransformación.

Miniaturized method for the quantification of persistent organic pollutants and their metabolites in HepG2 cells: assessment of their biotransformation.

Paloma De Oro-Carretero, Jon Sanz-Landaluze*

Analytical and Bioanalytical Chemistry 415, 4813–4825, 2023 (IF: 3.8, Q1)

**Autora de correspondencia*

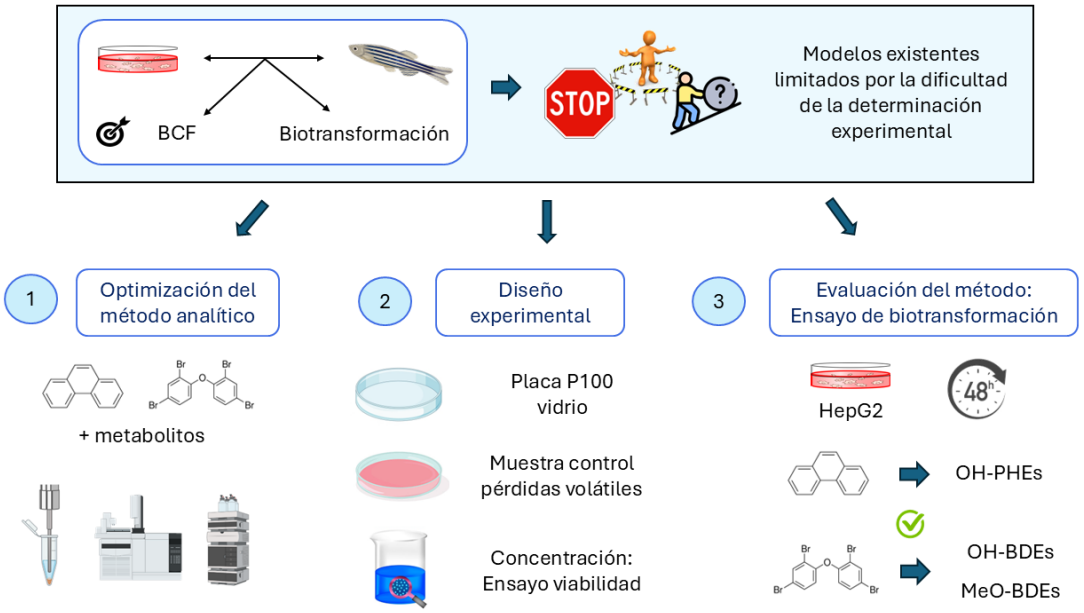

Analytical and Bioanalytical Chemistry (2023) 415:4813–4825
https://doi.org/10.1007/s00216-023-04781-w

RESEARCH PAPER

Miniaturized method for the quantification of persistent organic pollutants and their metabolites in HepG2 cells: assessment of their biotransformation

Paloma De Oro-Carretero[1] · **Jon Sanz-Landaluze**[1]

Received: 8 March 2023 / Revised: 22 May 2023 / Accepted: 30 May 2023 / Published online: 8 June 2023

Abstract
Biotransformation can greatly influence the accumulation and, subsequently, toxicity of substances in living beings. Although traditionally these studies to quantify metabolization of a compound have been carried out with in vivo species, currently, in vitro test methods with very different cell lines are being developed for their evaluation. However, this is still a very limited field due to multiple variables of a very diverse nature. So, an increasing number of analytical chemists are working with cells or other similar biological samples of very small size. This makes it necessary to address the development of analytical methods that allow determining their concentration both inside the cells and in their exposure medium. The aim of this study is to develop a set of analytical methodologies for the quantification of polycyclic aromatic hydrocarbons, PAHs (phenanthrene, PHE), and polybrominated diphenyl ethers, PBDEs (2,2′,4,4′-tetrabromodiphenyl ether, BDE-47), and their major metabolites in cells and their exposure medium. Analytical methodologies, based on miniaturized ultrasound probe-assisted extraction, gas chromatography–mass spectrometry–microelectron capture detector (GC–MS-μECD), and liquid chromatography–fluorescence detector (LC-FL) determination techniques, have been optimized and then applied to a biotransformation study in HepG2 at 48 h of exposure. Significant concentrations of the major metabolites of PHE (1-OH, 2-OH, 3-OH, 4-OH-, and 9-OH-PHE) and BDE-47 (5-MeO-, 5-OH-, and 3-OH-BDE-47) were detected and quantified inside the cells and in the exposure medium. These results provide a new method for determination and improve information on the metabolization ratios for a better knowledge of the metabolic pathways and their toxicity.

Keywords PAHs · PBDEs · GC–MS-μECD · Metabolites · HepG2 · Metabolization

Introduction

Persistent organic pollutants (POPs) are highly lipophilic, degradation-resistant, and bioaccumulative in the environment, organisms, and food chain compounds [1, 2]. To assess the risk to human health and the environment, the European Registration of Chemicals Regulation (REACH) classifies chemicals according to persistence, bioaccumulation, and toxicity studies during their entire life cycle, including transformation processes in the environment and metabolization. There is evidence that the bioactive metabolites [3, 4] can change the bioaccumulation and overall toxicity of the parent pollutants they come from [5–7]. In this context, analytical chemistry has become an essential part of the strategy to understand the ecotoxicity of POPs [8], through the determination of metabolites to elucidate metabolic pathways and their concentration to assess real exposure levels [7].

Most metabolization studies have been focused on analyzing tissues from in vivo experiments [1, 9, 10]. However, due to the increasing need for rapid assessment and the high cost and use of animal experimentation of official in vivo methods [3, 11], in recent years, there has been considerable

These results were presented at the XXII meeting of the Spanish Society of Analytical Chemistry (SEQA 2022) in Oviedo (Spain) on July 12–14, 2022, by Paloma de Oro-Carretero, and have been awarded with an ABC Best Poster Award.

✉ Paloma De Oro-Carretero
pdeoro@ucm.es

Jon Sanz-Landaluze
jsanzlan@ucm.es

[1] Department of Analytical Chemistry, Faculty of Chemical Science, Complutense University of Madrid, Avenida Complutense S/N, 28040 Madrid, Spain

interest in developing and refining alternative (in vitro) cell line tests [12–15]. In addition, other lines of research have been implemented to transfer experimental results obtained in vitro to in vivo data (in vitro to in vivo extrapolation-IVIVE) [16]. To improve in silico predictions of chemical bioaccumulation in fish, a greater understanding of all biotransformation pathways is needed to help understand all the mechanisms involved in these processes. Currently, two official guidelines have been developed to estimate the biotransformation rate using rainbow trout hepatocytes (RT-HEP) (OECD TG 319A) [17] and rainbow trout liver S9 subcellular fraction (RT S9) (OECD TG 319B) [18] to assess the bioconcentration factor (BCF). These test guidelines (TG) describe a chemical assay using a substrate depletion approach where only the determination of the starting test compound in the exposure medium is necessary, assuming that the decrease in the concentration of the parent compound is the result of biotransformation and considering that no bioaccumulation processes take place. The development of accurate and reliable analytical methods could help to overcome these approaches and determine not only the depletion on the medium of the parent compounds, but also their concentration and metabolization products in cells [19] and other similar biological samples [20, 21]. The difficulties of these determinations lie in the different physico-chemical characteristics of the compounds, the large and sometimes unknown number of metabolites, their low concentration, and the small size of the samples. Furthermore, chemicals can be differentially distributed between compartments of the in vitro assay, including the exposure medium with the globular protein bovine serum albumin [22], the plastic of the plate [23], and the headspace for some volatile substances [24]. Several publications, such as those mentioned above, determine models which estimate the real concentrations available in the cell with respect to the nominal exposure, considering the physico-chemical properties [25]. This is important to correctly assess the toxicity and kinetics metabolization of persistent organic pollutants as most of them are hydrophobic and semi-volatile. Therefore, more methods are still needed to determine the concentration of compounds and their metabolites both in the exposure medium and inside the cell.

The aim of this study is to develop analytical methodologies for the quantification of polycyclic aromatic hydrocarbons (PAHs) and polybrominated diphenyl ethers (PBDEs) as models of well-known POPs and metabolization process, with carcinogenic and endocrine-disrupting properties, respectively, and their major metabolites (OH-PAHs, OH-BDEs, and MeO-BDEs) in cells and their culture medium. Phenanthrene (PHE) was chosen because it is one of the most studied compounds in in vitro assays due to its hydrophobic and volatile properties [23–25]; and 2,2′,4,4′-tetrabromodiphenyl ether BDE-47 because of its abundance and toxicity in the environment [26]. The analytical methodologies must be extremely sensitive and selective. For selective identification and characterization of metabolic profiles, nuclear magnetic resonance (NMR) and mass spectrometry (MS) are often used [27]. To achieve sensitivity for the quantification of PBDEs and PAHs, electronic capture detection (ECD) and fluorescence detection (FL), respectively, or MS detectors in both cases, coupled with chromatographic techniques are widely used [28, 29]. Related to sample preparation, different extraction methods, such as Soxhlet, microwave, and ultrasound, have been used to extract PAHs, PBDEs, and their metabolites from environmental samples [30, 31]. Nowadays, there is a tendency to use more environmentally friendly methods, minimizing solvent volumes and sample treatment time. Taking steps in this direction and due to the small size of the samples, the analytical protocol here devised is based on miniaturized ultrasonic probe-assisted extraction. The methodology was applied to the PHE and BDE-47 biotransformation assay in human hepatoma cells (HepG2) at 48 h of exposure. HepG2 cell line was selected as a model for biotransformation studies, as metabolism of much of xenobiotics usually takes place in the liver [32].

Material and methods

Reagents

Individual solid standards of BDE-47, PHE, fluorene (FLU), 1-OH-PHE, 2-OH-PHE, 3-OH-PHE, and 4-OH-PHE were purchased from Sigma-Aldrich (Madrid, Spain). Individual commercial standards of BDE-28, BDE-99 in methanol, and triclosan (TCS) in acetone were purchased from Dr. Ehrenstorfer GmbH (Augsburg, Germany); individual standards of 5-MeO-BDE-47, 3-MeO-BDE-47 in methanol, 5-OH-BDE-47, 3-OH-BDE-47, and 2′-OH-BDE-28 in acetonitrile were supplied by AccuStandard Inc. (New Haven, CT, USA). The derivatization reagents N-tert-butyldimethylsilyl-N-methyltrifluoroacetamide (MTBSTFA) + 1% tert-butyl-methylchlorosilane, N,O-bis(trimethylsilyl)trifluoroacetamide (BSTFA), and N, O-Bis(trimethylsilyl)acetamide (BSA) were supplied by Sigma-Aldrich (Madrid, Spain). Analytical-grade solvents acetonitrile (ACN), chloroform, isooctane, n-hexane, dichloromethane (DCM), methyl tert-butyl ether (MTBE), dimethyl sulfoxide (DMSO), and acetone were purchased from Scharlab (Barcelona, Spain). NaCl was supplied by Sigma-Aldrich (Madrid, Spain).

Dulbecco's Modified Eagle Medium (DMEM), penicillin (10,000 U/ml)/streptomycin (10,000 µg/mL) mixture, trypsin–EDTA (0.05%), phosphate-buffered saline (PBS), fetal bovine serum (FBS), and trypan blue 0.4% were purchased from Thermo Fisher Scientific (Spain). 3-(4,5-dimethylthiazol-2-yl)-2,5-diphenyltetrazolium

bromide (MTT) was supplied by Sigma-Aldrich (Madrid, Spain).

Instrument and apparatus

Sample preparation was carried out using a vortex mixer from Scientific Industries (NY, USA), a Vibra cell VCx130 ultrasound probe from Sonics & Materials Inc. (CT, USA) with a 2 mm diameter titanium microtip and a 130 W high-frequency generator at 20 kHz, X50S metal carbide technical nitrogen stream (Barcelona, Spain), and the Eppendorf 5415R microcentrifuge (Hamburg, Germany). Plastic and glass P100 culture plates, 96-well plates, and a CO_2 incubator (MIDI 40) were purchased from Thermo Fisher Scientific (Spain).

Instrumental determination was performed by Agilent Gas Chromatographic Mod. 7890A Series (Agilent Technologies, Madrid, Spain) equipped with a HP 7683B autoinjector, a microelectron capture detector (μECD), a HP 5975C VL MSD mass spectrometry detector, and a polydimethylsiloxane (95%) ZB-5 capillary column (30 m × 0.25 mm I.D., 0.25-μm film thickness); and HPLC Spectra System P 4000 (Thermo Electron Corporation, San Jose, USA) equipped with a programmable fluorescence detector FL 3000 and Hypersil Green PAH columns (150 mm × 3 mm; particle size 3 μm) attached to a Phenomenex C18 pre-column.

Cell culture

Human hepatoma cells (HepG2), provided by American Type Culture Collection, ATCC (VA, USA), were cultured in plastic P100 plates with a complete cell culture medium consisting of DMEM supplemented with 10% heat-inactivated FBS and 1% penicillin (10,000 $U \cdot mL^{-1}$)/streptomycin (10,000 $\mu g \cdot mL^{-1}$) mixture and maintained in a humidified incubator at 37 °C and 5% CO_2. The medium was changed every 2 or 3 days and cells passed at 70% confluence.

Cell viability

Cell viability was determined by MTT assay. First, 10,000 cells/well were cultured in 96-well plates for 24 h at 37 °C and 5% CO_2. After that time, the culture medium was replaced with a culture medium containing different concentrations (0–70 $mg \cdot L^{-1}$) of PHE and BDE-47 for 48 h of exposure under the same incubated conditions. After that, 20 μL MTT solution (5 $mg \cdot mL^{-1}$ diluted in PBS) was added and incubated for the following 4 h. Viable cellular metabolic reduction of MTT produced formazan crystals, which were dissolved in 100 μL sterile DMSO and quantified with absorbance measurement at 595 nm in a Multiskan Sky High (Tecan Thermo Fisher). The cell viability was estimated by using Eq. (1).

$$\%\ Viability = \frac{A_{exp} - A_{blank}}{A_{control} - A_{blank}} \bullet 100 \quad (1)$$

where $A_{control}$, A_{exp}, and A_{blank} are the mean absorbance value (6 replicates) of the control group (cells without pollutant), experimental group, and blank group (only cell culture medium), respectively. Five independent assays were carried out with the same conditions. The results have been subsequently used for the design of the biotransformation experiment.

Biotransformation experiment

Exposure of HepG2 cells (3 replicates) was performed by initially seeding approximately $2 \cdot 10^6$ cells in glass P100 plates and being incubated for 24 h at 37 °C (5% CO_2) with 10 mL of DMEM supplemented with 10% FBS. The culture medium was replaced with contaminated medium (15 $mg \cdot L^{-1}$ for PHE and 20 $mg \cdot L^{-1}$ for BDE-47) and incubated for 48 h under the same conditions. The nominal exposure concentration was estimated by the previous MTT viability study, in which, more than 70% of the cells were alive at the end of the test (lethal concentration 30, LC_{30}) to ensure good metabolizing capacity. Part of the contaminated medium was stored to determine the concentration at time 0 of exposure ("$t = 0$ h"). In addition, to consider possible analyte loss, a plate of control cells without pollutant ("blank") and a plate with contaminated medium without cells ("no cells") were incubated under the same conditions. After 48 h of incubation, the exposure medium of each sample was stored in glass vials at − 4 °C until analysis. Since the determination of PHE is carried out by LC-FL and its metabolites by GC–MS, the cell pellet was divided in half for each analysis. For this purpose, the adherent cells were lifted in suspension by trypsinization, and the total volume of the homogenous cell suspension was divided in half. Then, the resulting cell pellet from each fraction was collected by centrifuging at 1500 rpm for 5 min and removing the medium. However, for the determination of BDE-47 and its metabolites, the complete pellet obtained is analyzed because a simultaneous extraction is performed for both analyses. The obtained pellet was dried under a gentle stream of nitrogen, weighed on a precision analytical balance (± 0.00001 g), and stored at − 4 °C until analysis. Three independent assays were carried out with the same conditions, each with 3 replicates (plates) of the same concentration.

Analytical procedure

Instrumental determination

HPLC-FL and GC–MS were used for the determination of PHE and its OH-PHE metabolites (1-OH-PHE, 2-OH-PHE,

3-OH-PHE, and 4-OH-PHE) respectively. For PHE and FLU (used as internal standard, IS) separation, the mobile phase was made up of ACN and water, increasing from 70:30 ratio to 100:0 over 7 min and recovering to initial conditions at 15 min, with 0.3 mL·min^{-1} constant flow rate. Twenty microliters of the sample was injected into the column at 30 °C and fluorescence wavelengths used were 276 nm for excitation and 346 nm for emission. For the separation and determination of OH-PHE metabolites in the GC–MS, samples (1 µL) were injected in splitless mode at 280 °C. Helium was used as carrier gas at a constant pressure of 25 psi. The temperature of the column was programmed to increase from 80 °C (2 min) to 150 °C (2 min) at a rate of 30 °C·min^{-1}, then to 250 °C (2 min) at 20 °C·min^{-1} and finally to 270 °C (2 min) at 10 °C·min^{-1}. The temperature of the ion source and the transfer line of the mass spectrometer was set at 250 and 270 °C, respectively, and 70 eV for the electron beam.

The GC–MS-µECD system was used for the determination of BDE-47, its metabolites (BDE-28, 6-MeO-BDE-47, 5-MeO-BDE-47, 3-MeO-BDE-47, 5-OH-BDE-47, 3-OH-BDE-47, and 2′-OH-BDE-28), BDE-99 (used as IS for BDEs and MeO-BDEs), and TCS (IS for OH-BDEs). The MS was used for the identification and the µECD for their quantification. Both detectors work simultaneously thanks to the use of a flow splitter, placed at the end of the chromatographic column. Injection and MS conditions were the same as previously used for OH-PHE determination. Column temperature was programmed to increase from 130 °C (2 min) to 230 °C (2 min) at a rate of 25 °C·min^{-1} and then to 280 °C (2 min) at 2 °C·min^{-1}. The µECD temperature was set at 320 °C and nitrogen was used as makeup gas (30 mL·min^{-1}). The flow ratio of the splitter was 1:1 thanks to the additional helium input and the restrictors length of each detector according to the manual supplied by Agilent [33]. SCAN mode with standards for each analyte and mass spectra displayed in the libraries of the NIST databases and by bibliography [34, 35] were used to establish the *m/z* values for the SIM program of both GC–MS methods (Tables S1 and S2). A double determination was carried out for BDE-47 and its metabolites, directly injected into the GC–MS-µECD for determination of PBDEs and MeO-BDEs. Under the same chromatographic method, a derivatization step was needed for OH-PBDEs.

Sample preparation

To obtain the concentration of the analytes from the cell pellet and the exposure medium, an optimization of the sample preparation was carried out (see "Setting the analytical procedure"), testing various extraction solvents, derivatizing agents, and conditions for the different compounds in fortified samples of known concentration. Finally, the most optimal variables used for the experiment are shown below.

In the PHE experiments, for PHE quantification in cells, half of the pellet obtained (~5 mg) was extracted with 400 µL of ACN and sonicated with an ultrasound probe for 1 min at 30% of amplitude and a pulse on/off:2 s/5 s. On the other hand, 50 µL of exposure medium was extracted with 400 µL of ACN (+50 mg NaCl) with vortex for 30 s. Internal standard FLU was previously added to the extraction step to both cells and exposure medium. The mixture was centrifuged for 10 min at 10,000 rpm and the organic extract was directly injected into the LC-FL. The other half of the pellet was obtained (~5 mg) and 500 µL of the medium was used for OH-PHE quantification. In this case, the same extraction method was performed but using 500 µL of the hexane:DCM (1:1) mixture as a solvent. No IS was used for OH-PHE quantification as explained in the "Results and discussion" section, but recuperation studies were carried out to check losses. After the centrifugation step, the remaining extracts were evaporated to dryness under a gentle stream of nitrogen and reconstituted in 100 µL of hexane. Finally, 80 µL of the volume obtained was derivatized with 20 µL of MTBSTFA at 60 °C for 30 min in the oven and injected into GC–MS.

In the BDE-47 assay, extraction for BDE-47 and its metabolites was simultaneously performed. The entire pellet obtained (~10 mg) and 500 µL of exposure medium were extracted with 500 µL of hexane:MTBE mixture (1:1) under the same conditions (sonication and centrifugation) as the PHE assay. The IS BDE-99 and TCS were previously added. The organic phase was separated, and the extraction step was repeated. The remaining extracts were evaporated to dryness under a gentle stream of nitrogen and reconstituted in 100 µL isooctane. Finally, 80 µL of the volume obtained was derivatized with 20 µL of MTBSTFA at 70 °C for 30 min in the oven and injected into GC-µECD-MS for the OH-BDE quantification. PBDEs and MeO-BDEs were determined by direct injection of the remaining volume of isooctane extracts into the GC-µECD-MS because PBDEs are not stable after the derivatization process.

Results and discussion

Setting the analytical procedure

Phenanthrene and metabolites

For the PHE determination, HPLC-FL was used instead of GC–MS as it has higher sensitivity [29] and due to the different concentrations of PHE and its metabolites in the experiment that make it difficult to perform a simultaneous determination by GC–MS. Sensitive co-determination wavelengths for PHE and FLU, used as an internal standard

(IS), were selected based on the literature [36, 37]. For OH-PHE metabolite determination, two different IS were proven (9-OH-FLU and triclosan) but 9-OH-PHE did not show good sensitivity and was not stable with the derivatizing reagent MTBSTFA and triclosan did not show the same recoveries with the extraction solvent which was better for OH-PHE. Because no IS was used in each analysis run, a parallel extraction and detection of fortified samples with known concentrations (high and low) of the study analytes was performed to check if there is a loss in the determination.

Several solvents were evaluated over fortified cells and medium samples for an optimal PHE extraction: hexane, DCM, ACN, chloroform, hexane:DCM (50:50), and hexane:chloroform (50:50). Figure 1a shows the highest extraction recoveries for both PHE and FLU when chloroform and hexane:DCM (50:50) were used as extractant; however, values well above 100% were obtained due to sample interferences being extracted. So, the best recovery results were obtained with ACN and hexane as extractants. Finally, based on recovery values and the cleaning of the extracts, ACN was chosen as an extractant agent, as they can be injected directly into HPLC. ACN is miscible with aqueous samples, so this was overcome by adding a small amount of NaCl to facilitate the separation of the aqueous and organic phases. It was proved that the volume of the medium sample was a variable in improving recovery. Higher recovery was obtained with 500 µL (Fig. S1); however, 50 µL was chosen for better interpolation on the calibration line without prior dilution of the extract.

GC–MS was used for unambiguous identification and quantification of the OH-PHEs with a prior derivatization step. The optimization process was performed by only using two metabolites (2-OH-PHE and 3-OH-PHE); however, the rest of the OH-PHEs showed the same behavior. Silylation is the most used derivatization method for OH-PAHs with derivatization reagents such as N-methyl-N-(trimethylsilyl) trifluoroacetamide (MSTFA), BSTFA, MTBSTFA, and BSA [34]. So, MTBSTFA, BSTFA, and BSA were tested at different temperatures and derivatization times looking for better derivatization conditions (Figs. S2 and S3). MTBSTFA was selected because it gave a higher analytical response and more stability, as Schummer et al. [38] also concluded. As the derivatization temperature rises, the analytical response considerably decreases and increases slightly over time. The best area/time ratio was found at 60 °C and 30 min. All injected solutions were prepared in hexane because, as shown in Fig. S4, it provided a better analytical response compared to other solvents tested. Once chromatographic conditions were optimized, several solvents were evaluated over fortified cells and medium samples: hexane, DCM, MTBE, and a mixture of them. Figure 1b shows the highest extraction recoveries for medium and cell samples when hexane:DCM (1:1) was used as the extractant solvent.

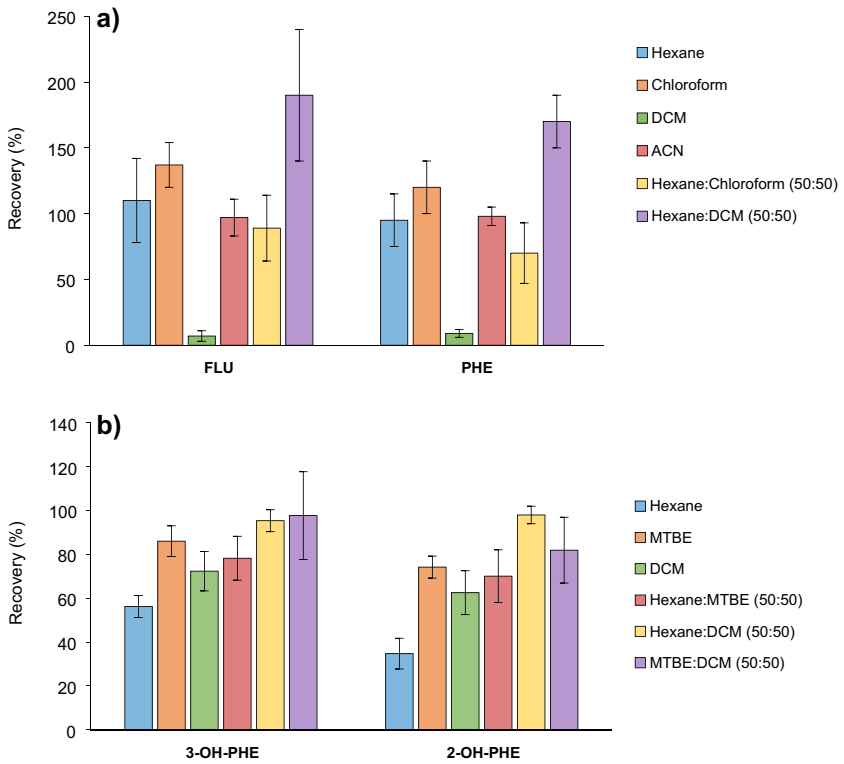

Fig. 1 Recoveries obtained with the different extractants in cell samples of known concentration (20 µg·L^{-1}) for **a** PHE and **b** OH-PAH determination. Similar behavior in the exposure media was observed

BDE-47 and metabolites

GC–MS-μECD system was used for PBDE, MeO-BDE, and OH-BDE determination. MTBSTFA was chosen as a derivatization reagent because it has been shown to be better for the determination of phenolic compounds [38]. When different solvents were tested, no differences were found; however, a significant loss of PBDEs and MeO-BDEs was observed in the derivatization process (Fig. S5). So, a double determination was carried out (see "Sample preparation"), one for PBDEs and MeO-BDEs without the derivatization step and the other for OH-BDEs by derivatization resulting in two chromatograms with the same separation conditions where the compounds do not overlap (Fig. S6). For the extraction setting, several solvents were evaluated over fortified samples for an optimal simultaneous extraction of BDE-47 and their metabolites: MTBE, hexane, and a mixture of them and hexane:DCM (Fig. 2). Finally, hexane:MTBE (1:1) was chosen as the extractant for a simultaneous extraction of PBDEs, MeO-BDEs, and OH-BDEs with a consensus among the analytes of different polarity based on good recoveries and clean chromatogram and to reduce the cost and time of sample treatment.

Method validation: QA/QC

Plastic materials were not used to avoid contaminants bonding to this material. Therefore, Hamilton syringes were always used for volume addition. All reused glass material was washed with acetone, rinsed with deionized water, and left overnight in the oven at 250 °C. The culture materials, such as glass plates, were previously sterilized with wet heat. The developed method was assessed in terms of linearity, detection and quantification limits, recoveries, and selectivity (Table S3). Selectivity was tested using several blanks for each sample type. A high degree of linearity was obtained in all analytes ($R^2 > 0.997$). The limits of detection (LODs) and quantification (LOQ) were evaluated by integrating the result of the sum of three (LOD) or ten (LOQ) times the standard deviation of the target signal into the calibration curve. LOD values were 1.7 $\mu g \cdot L^{-1}$ and 1.0 $\mu g \cdot L^{-1}$ for PHE and BDE-47 respectively and between 1.9–2.6 $\mu g \cdot L^{-1}$ and 0.5–1.7 $\mu g \cdot L^{-1}$ for its metabolites. LOQ values were 3.1 $\mu g \cdot L^{-1}$ and 2.1 $\mu g \cdot L^{-1}$ for PHE and BDE-47 respectively and between 4.8–5.8 $\mu g \cdot L^{-1}$ and 0.9–2.0 $\mu g \cdot L^{-1}$ for its metabolites. To assess recoveries and as no certified reference material was available, sample fortification was used. Thus, higher recoveries of 83 and 87% were obtained in the determination of PHE and its metabolites for cell and medium samples, respectively. Eighty-four percent and 72% percentage recoveries were obtained in BDE-47 and its metabolites determination.

Optimization of the cell exposure process

A major problem in in vitro cell assays is the loss of compound during the exposure process to estimate the effective concentration available to the cell and to correctly

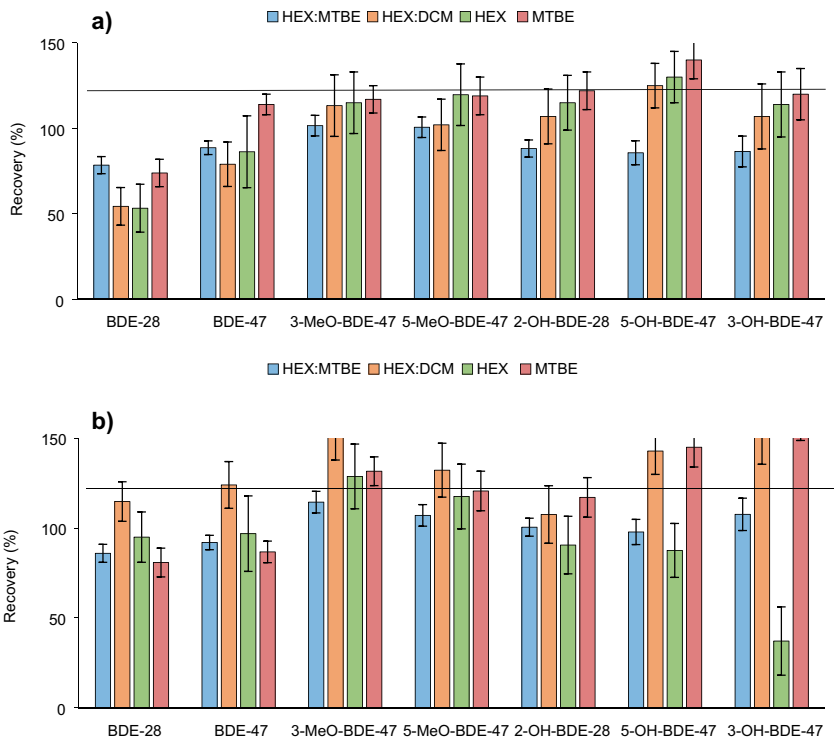

Fig. 2 Recoveries obtained with the different extractants in **a** cells and **b** medium samples of known concentration (20 $\mu g \cdot L.^{-1}$)

Table 1 PHE concentration in plastic and glass plate exposure test. M1, M2, and M3 are three independent experiments with cells and contaminated medium

Sample of contaminated culture medium	Conc. PHE Plastic plate exposure ($mg{\cdot}L^{-1}$)	Conc. PHE Glass plate exposure ($mg{\cdot}L^{-1}$)
$t=0$ h	5.57	4.37
M1 – 24 h	-	2.74
M2 – 24 h	-	2.97
M3 – 24 h	-	2.89
No cells – 24 h	-	3.69
M1 – 48 h	0.57	2.21
M2 – 48 h	0.73	2.47
M3 – 48 h	0.62	2.37
No cells – 48 h	0.88	3.16

assess the toxicity and metabolization kinetics of POPs, as most of them are hydrophobic and semi-volatile [22–25]. Firstly, when concentration was determined in the exposure and *no cells* medium samples at the end of the test (48 h) using plastic Petri dishes, a loss of 89% and 84% compared to the $t=0$ h sample was found in the cells and *no cells* sample respectively (Table 1). This loss, similar to that found in previous studies [23, 24], is mainly explained by absorption into polystyrene, the main component of in vitro culture plates [39] or evaporation processes because these compounds have a Henry law constant (K_H) between 1 and 10 $Pa{\cdot}m^3{\cdot}mol^{-1}$ [11] (7.90 $Pa{\cdot}m^3{\cdot}mol^{-1}$ for PHE at 35 °C [13] and 3.78 $Pa{\cdot}m^3{\cdot}mol^{-1}$ for BDE-47 at 40 °C [40]). The remaining concentration in the medium that had not been lost by evaporation or absorbed into the cells was retained in the protein serum [22]. The difference in concentration loss between samples with and without cells indicates that is practically the same loss and that only 4 ± 1% of PHE has been taken up by the cells, which makes it difficult to appreciate differences in behavior between the experiments set out. A fraction dissolved in the medium accessible to the cells of 3.5% for anthracene (log K_{ow} 4.5) was obtained introducing the conditions of this work into the chemical partitioning model developed by Fischer et al. [41]. Schreiber et al. [39] compared the binding of phenanthrene on different polymers and showed that, while 94% of the initial concentration was absorbed on polystyrene, the main component of in vitro culture plates, when glass is used this absorption decreases to only 2%. Therefore, it should be considered to avoid the use of plastic in tests that requires P100 plates with a very high surface area/volume ratio of the medium when studying neutral chemicals with a log $K_{ow}>3$, as is the case of PHE (log K_{ow} 4.46 [39]) and BDE-47 (log K_{ow} 6.81 [26]).

Using glass plates, a loss of 47% and 26% for cells and *no cells* samples, respectively, was found at the end of the assay (48 h) (Table 1), and the concentration absorbed by the cells increased from 4 ± 1 to 18 ± 3%. For BDE-47, a loss of only 14% because of volatilization and an absorbed concentration of 24 ± 2% resulted using a glass plate, as BDE-47 is less volatile and more hydrophobic than PHE, favoring cell uptake [42]. Birch et al. [24] calculated a cell-free fraction of 13% for PHE in HepG2 cells with 10% of FBS in the medium considering the evaporation losses using glass vials. Between 8.0 and 14.6% of the polychlorinated biphenyl (PCB) concentration with log K_{ow} 6.2–7.3 were recovered from HepG2 cell pellets at 48 h of exposure using plastic plates and culture medium with 10% of FBS by Zhang et al. [43]. So, considering all this, losses and assay conditions using glass plates can be considered acceptable for the metabolization experiment.

Cell viability

Cell viability of each concentration was estimated by using Eq. (1) according to the absorbance values obtained in the MTT assay. The dose–response values were fitted by Origin Pro 2021 with a polynomial equation (shown in Fig. 3) from which the LC value was estimated. The cytotoxicity of different PHE and BDE-47 concentrations in HepG2 cells at 48 h of exposure is shown in Fig. 3. LC_{50} (50% viability) and LC_{30} (70% viability) were estimated by the polynomial fitting of the mean cell viability data obtained from three independent experiments. Cell viability in HepG2 decreased by 30% at 22 $mg{\cdot}L^{-1}$ PHE and 38 $mg{\cdot}L^{-1}$ BDE-47 and up to 50% at 38 $mg{\cdot}L^{-1}$ PHE and 46 $mg{\cdot}L^{-1}$ BDE-47. Branco

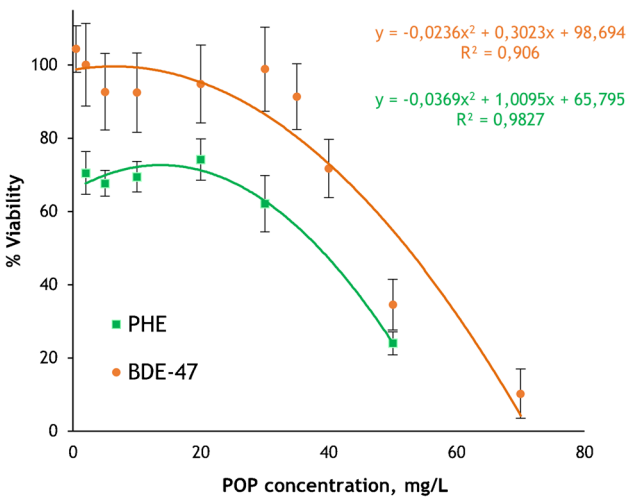

Fig. 3 Cell viability of different PHE and BDE-47 concentration in HepG2 cells at 48 h of exposure

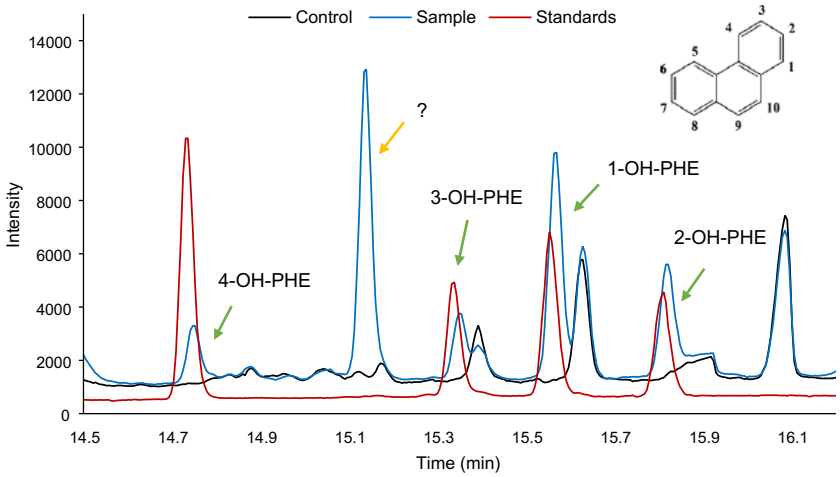

Fig. 4 Chromatogram of medium sample obtained after 48 h of exposure to 15 mg·L.$^{-1}$ PHE in HepG2

et al. [44] obtained a LC_{50} value of 114 µM (20.3 mg·L^{-1}) in HepG2 at 48 h of PHE exposure and Liu et al. [45] and Hu et al. [46] of 100 µM (48.6 mg·L^{-1}) in the case of BDE-47. The calculated LC_{30} values have been subsequently used for the design of the biotransformation experiments.

Biotransformation in HepG2

Phenanthrene

After 48 h of HepG2 exposure to 15 mg·L^{-1} of PHE, significant concentrations of 1-OH, 2-OH, 3-OH, 4-OH-PHE, and an unidentified compound were observed both inside and outside (exposure medium) the cell (Fig. 4 and Table 2). In control samples (*blank*, *no cells*, and $t = 0$ h), no concentrations ("n.d.") above the limits of detection and quantification of any metabolite were detected. The ratio between metabolites and PHE was also determined (Table 2).

Metabolism of xenobiotics usually takes place mainly in the liver [32]. HepG2 cells have a large amount of cytochrome P450 (CYP) enzymes that enable phase I (activation) and phase II (conjugation) reactions involved in the metabolism of PAHs [47]. The first step is oxidation to form reactive epoxide intermediates, followed by hydrolysis (epoxide hydrolase) to produce hydroxylated metabolites (OH-PAHs) [48], being more soluble in water, so more easily excreted (detoxification process) [49]. These processes could explain why the metabolization ratios found in the exposure medium were higher than the ratios obtained in cells. To the best of the authors' knowledge, no other articles in the literature evaluate either the metabolization ratio or the identification of metabolites of PHE in the HepG2 cell line are found. Metabolization studies have been performed with liver microsomes, rat cell lines, or in vivo [50]. According to these results found in the literature, major PHE metabolites transformed by the CYP 450 are 1-, 2-, 3-, 4-, and 9-OH-PHE [20], so the unidentified compound shown in Fig. 4, with an elution time of 15.1 min, is proposed to be metabolite 9-OH-PHE. The commercial standard was not available for its quantification or confirmation by retention time; however, Gaudreau et al. [48] obtains the same elution order. In addition, the *m/z* and mass spectra match this compound. Very intense 9-OH and 1-OH-PHE peaks were achieved, confirming previous results that use these metabolites as PAHs and phenanthrene inhalation biomarkers [49].

Table 2 Concentration found in culture medium and cells at 48 h. Biotransformation ratio between metabolites and PHE of three individual experiments (*n.d.* no detected)

	PHE	4-OH-PHE	3-OH-PHE	1-OH-PHE	2-OH-PHE
Concentration					
Medium	(mg·L^{-1})	(µg·L^{-1})			
Samples	5.7 ± 0.7	5 ± 1	4.0 ± 0.7	7.7 ± 0.9	5.2 ± 0.9
No cells	8 ± 2	n.d	n.d	n.d	n.d
$t = 0$ h	12 ± 1	n.d	n.d	n.d	n.d
Cells	(µg·g^{-1})	(ng·g^{-1})			
Samples ($n = 3$)	521 ± 144	260 ± 85	195 ± 33	72 ± 27	284 ± 92
Biotransformation ratio					
Medium	-	0.16	0.13	0.22	0.15
Cells	-	0.05	0.04	0.01	0.06

Considering the masses obtained for the parent compound and the metabolites in the medium and in the cells, a mass balance has been performed according to Eqs. (2) and (3), where a recovery of 78 ± 4% was shown at 48 h compared to 0 h. This confirms that the monohydroxy compounds formed are the major metabolites as the balance closes almost completely. It must be considered that a large part of the remaining percentage may be represented by the mass of the metabolite 9-OH-PHE, not quantified in this work, being one of the majority congeners formed. Therefore, analytical methodologies developed in this work are suitable for the quantification of metabolites in cells and their exposure media. On the other hand, although the major function of the liver is detoxification in the form of OH-PHEs, a part of them can still be reacted and hydrolyzed with the same enzymatic sequence, so that diols are formed. For this, they first activate in the form of epoxide diols, which can be coupled to endogenous compounds such as sulfuric acid, glucuronic acid, and glutathione in phase II [49]. All these intermediates, although formed in smaller proportions, also represent the unquantified percentage in the mass balance. These PAH metabolic intermediates show genotoxic and carcinogenic properties, so it would be important for future studies to develop a method of identification and quantification of each of them like this work.

$$m_{Total} = mPOP_{0h} = (mPOP_{medium})_{48h} + (mPOP_{cells})_{48h} + (mPOP_{loss})_{48h} + \sum mMetabolites_{medium})_{48h} + \sum mMetabolites_{cells})_{48h} \quad (2)$$

$$(mPOP_{loss})_{48h} = (mPOP_{medium\ without\ cells})_{48h} - (mPOP_{medium\ with\ cells})_{48h} \quad (3)$$

BDE-47

After 48 h of exposure of HepG2 cells to 20 mg·L^{-1} BDE-47, 5-MeO-BDE-47 and two unidentified compounds at retention times of 25.6 (a) and 28.5 min (b) (Fig. 5) were observed inside the cells. 3-OH-BDE-47 and 5-OH-BDE-47 were found also in the exposure medium. The ratio between metabolites and BDE-47 concentration found in cells and medium was determined (Table 3). Biotransformation of PBDEs, as with PAHs, is carried out by liver cytochrome P450 enzymes, in which phase I enzymes introduce a polar group (OH-BDEs). In addition, several studies revealed that conversion between OH-BDEs and MeO-BDEs is possible [51]. Therefore, higher amounts of OH-BDEs are found in the culture medium when they are excreted after metabolization, while higher concentrations of MeO-BDEs were found inside the cells as their excretion is more difficult due to their lower polarity. For the same reason, the unidentified compounds are more hydrophobic metabolites and therefore they could not be removed from the environment during the experiment. A significant concentration of BDE-28 was detected in cell samples such as what we also observed in a previous zebrafish eleutheroembryo biotransformation study with these same compounds [52]. One of the major biotransformation metabolites of BDE-47 is BDE-28 by loss of bromine in the ortho position [53]. In addition, both BDE-47 and BDE-28 can be biotransformed into 2′-OH-BDE-28 [54]. However, in this case, certain amounts were also found in the control samples (*no cells* and $t = 0$ h) due to impurity of the commercial standard BDE-47 as also reported in other studies [55]. Because of that, results for BDE-28 and 2-OH-BDE-28 are not considered in this study. No quantifiable amounts of 3-MeO-BDE-47 were detected. Hu et al. [46] and Song et al. [28] showed increased expression of cytochrome P450 enzymes, involved in the metabolism of PBDEs, upon

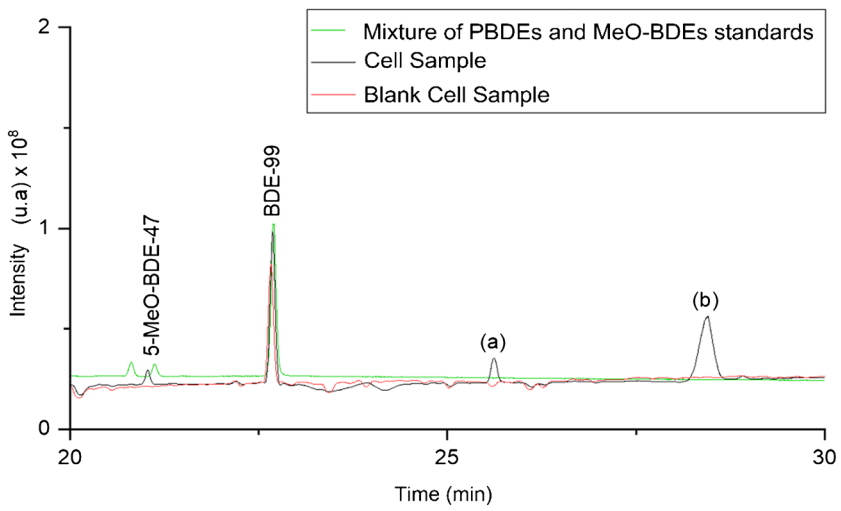

Fig. 5 Chromatogram of cell sample obtained after 48 h of exposure to 20 mg·L.$^{-1}$ BDE-47 in HepG2

Table 3 Concentration found in culture medium and cells. Biotransformation ratio between metabolites and BDE-47 of three individual experiments (*n.d.* no detected)

	BDE-47	BDE-28	3-MeO-BDE-47	5-MeO-BDE-47	2'-OH-BDE-28	5-OH-BDE-47	3-OH-BDE-47
Concentration							
Medium	($mg{\cdot}L^{-1}$)	($\mu g{\cdot}L^{-1}$)					
Samples	13 ± 2	577 ± 92	0.51 ± 0.09	1.2 ± 0.9	3.2 ± 0.2	6.2 ± 0.5	4.3 ± 0.2
No cells	14 ± 3	651 ± 36	n.d	n.d	n.d	n.d	n.d
$t = 0$ h	16 ± 1	662 ± 18	n.d	n.d	n.d	n.d	n.d
Cells	($\mu g{\cdot}g^{-1}$)	($ng{\cdot}g^{-1}$)					
Samples	737 ± 120	18 ± 5	n.d	0.12 ± 0.02	0.11 ± 0.09	0.27 ± 0.08	0.21 ± 0.10
Biotransformation ratio							
Medium	-	-	-	0.01	-	0.06	0.04
Cells	-	-	-	0.03	-	0.01	0.01

exposure to BDE-47 in HepG2 cells. To our knowledge, there are no previous studies in the literature evaluating either the metabolization ratio or the identification of metabolites in HepG2 or other cell lines.

Considering the masses obtained for the parent compound and the metabolites in the medium and in the cells, a mass balance has been performed according to Eqs. (2) and (3), where a recovery of 87 ± 5% was shown at 48 h compared to 0 h. This confirms that the metabolites studied were the predominant biotransformed compounds. Other studies have confirmed the formation of all the metabolites studied in this work by the biotransformation of BDE-47 in bacteria [56], microalgae [57], or more developed organisms [53]. Erratico et al. [21] studied the biotransformation of BDE-47 to 6-OH-BDE-47, 5-OH-BDE-47, 3-OH-BDE-47, 2,4-DBP, and 2'-OH-BDE-28 metabolites by human liver microsomes through P450 2B6 enzymes. In addition, as with PAHs, diols can be formed [58] and can be conjugated in phase II with endogenous compounds [59]. Therefore, it would be interesting to identify and quantify other metabolites represented in the small remaining percentage of the mass balance. These could include the unquantified compounds BDE-28 and 2′OH-BDE-28, the unidentified compounds appearing in the chromatogram, and other unstudied compounds such as 6-OH-BDE-47, 6-MeO-BDE, diols, or metabolites conjugated with endogenous compounds. However, the proposed method has been shown to be suitable for the quantification of metabolites in cells and in exposure media.

Conclusions

Two miniaturized analytical methods have been developed to determine PHE and its metabolites (OH-PHEs) and BDE-47 and its metabolites (MeO-BDEs and OH-BDEs) simultaneously. Both methods have been optimized considering different aspects: the small amount of sample, the large difference in physico-chemical properties of the analytes and their metabolites, their low concentration, and the minimum consumption of organic solvent to produce less harmful residues. The analytical techniques used give unambiguous identification and highly sensitive quantification, suitable for trace and metabolite determination due to the advantages of each detector. Therefore, the methods developed could be applied to extremely small biological samples, showing low detection limits and high reproducibility. In addition, this method has been shown to be suitable for application in metabolization studies. HepG2 cells can biotransform POPs metabolized by CYP 450 enzymes where the major metabolites of PHE and BDE-47 have been detected at 48 h of exposure inside the cells and in their exposure medium. These results indicate that compounds can be removed back to the culture medium or follow other metabolic pathways. Therefore, it would be interesting to evaluate the overall metabolization rate of the compound to know its real toxicity. Although in vitro metabolomics has already been successfully applied in a few studies using primary human hepatocytes or HepG2 [19], it would be interesting to extend this study and this method to other types of pollutants and cells to explore whether they show the same behavior.

These results may provide information on the effective concentration available to the cell relative to the nominal one and metabolization ratios for developing new methods. Also, this shown knowledge may contribute and be useful to the authors who are currently working with cells, as well as for the extrapolation data obtained in in vivo and in vitro models [60–62] to reduce animal suffering during trials. These aspects will be examined and discussed in future ecotoxicology studies through the application of the analytical method developed in this work.

Supplementary information The online version contains supplementary material available at https://doi.org/10.1007/s00216-023-04781-w.

Author contribution P. De Oro-Carretero: data curation; formal analysis; investigation; methodology; software; supervision; validation; visualization; roles/writing—original draft.

J. Sanz-Landaluze: conceptualization; data curation; funding acquisition; methodology; project administration; resources; software; supervision; validation; visualization; writing—review and editing.

Funding Open Access funding provided thanks to the CRUE-CSIC agreement with Springer Nature. The authors received financial support for this work from the Ministry of Science and Innovation [PID 2020 114714 RB 100], Autonomous Community of Madrid [AVANSECAL II CM, 2018 /BAA 4393], and Complutense University of Madrid supporting the research group "Trace Determination, Speciation and Proteomics." Paloma de Oro thanks the Spanish Ministry of Science and Innovation for her predoctoral contract [PRE2021/097956].

Declarations

Competing interests The authors declare no competing interests.

References

1. Acosta-Tlapalamatl M, Romo-Gómez C, Anaya-Hernández A, Juárez-Santacruz L, Gaytán-Oyarzún JC, Acebedo-Sandoval OA, García-Nieto E. Metabolomics: a new approach in the evaluation of effects in human beings and wildlife associated with environmental exposition to POPs. Toxics. 2022;10(7):380. https://doi.org/10.3390/toxics10070380.
2. Chen H, Wang C, Li HH, Ma R, Yu Z, Li L, Xiang M, Chen X, Hua X, Yu Y. A review of toxicity induced by persistent organic pollutants (POPs) and endocrine-disrupting chemicals (EDCs) in the nematode Caenorhabditis elegans. J Environ Manag. 2019;237:519–25. https://doi.org/10.1016/j.jenvman.2019.02.102.
3. Almazroo OA, Miah MK, Venkataramanan R. Drug metabolism in the liver. Clin Liver Dis. 2021;21:1–20. https://doi.org/10.1016/j.cld.2016.08.001.
4. Cervantes FJ, Martínez CM, Gonzalez-Estrella J, Márquez A, Arriaga S. Kinetics during the redox biotransformation of pollutants mediated by immobilized and soluble humic acids. Appl Microbiol Biotechnol. 2013;97(6):2671–9. https://doi.org/10.1007/s00253-012-4081-5.
5. Molina-Fernández N, Rainieri S, Muñoz-Olivas R, de Oro-Carretero P, Sanz-Landaluze J. Development of a method for assessing the accumulation and metabolization of antidepressant drugs in zebrafish (Danio rerio) eleutheroembryos. Anal Bioanal Chem. 2021;413(20):5169–79. https://doi.org/10.1007/s00216-021-03486-2.
6. McCormick JM, van Es T, Cooper KR, White LA, Häggblom MM. Microbially mediated O-methylation of bisphenol a result in metabolites with increased toxicity to the developing zebrafish (Danio rerio) embryo. Environ Sci Technol. 2011;45(15):6567–74. https://doi.org/10.1021/es200588w.
7. Fu Q, Fedrizzi D, Kosfeld V, Schlechtriem C, Ganz V, Derrer S, Rentsch D, Hollende J. Biotransformation changes bioaccumulation and toxicity of diclofenac in aquatic organisms. Environ Sci Technol. 2020;54(7):4400–8. https://doi.org/10.1021/acs.est.9b07127.
8. Wei S, Wei Y, Gong Y, Chen Y, Cui J, Li L, Yan H, Yu Y, Lin X, Li G, Yi L. Metabolomics as a valid analytical technique in environmental exposure research: application and progress. Metabolomics. 2022;18(6):35. https://doi.org/10.1007/s11306-022-01895-7.
9. Kim HM, Kang JS. Metabolomic studies for the evaluation of toxicity induced by environmental toxicants on model organisms. Metabolites. 2021;11(8):485. https://doi.org/10.3390/metabo11080485.
10. Eriksson ANM, Rigaud C, Rokka A, Skaugen M, Lihavainen JH, Vehniäinen ER. Changes in cardiac proteome and metabolome following exposure to the PAHs retene and fluoranthene and their mixture in developing rainbow trout alevins. Sci Total Environ. 2022;830:154846. https://doi.org/10.1016/j.scitotenv.2022.154846.
11. OECD. Guidance document on aquatic toxicity testing of difficult substances and mixtures. In: Organisation for Economic Co-operation and Development. Series on testing and assessment. Paris: OECD Publishing; 2019. https://doi.org/10.1787/0ed2f88e-en.
12. Silva RJ, Tamburic SA. A State-of-the-art review on the alternatives to animal testing for the safety assessment of cosmetics. Cosmetics. 2022;9(5):90. https://doi.org/10.3390/cosmetics9050090.
13. Kramer NI, Krismartina M, Rico-Rico A, Blaauboer BJ, Hermens JLM. Quantifying processes determining the free concentration of phenanthrene in basal cytotoxicity assays. Chem Res Toxicol. 2012;25(2):436–45. https://doi.org/10.1021/tx200479k.
14. U.S. National Research Council. Toxicity Testing in the 21st century: a vision and a strategy. In: Committee on Toxicity Testing and Assessment of Environmental Agents. Washington, DC: The National Academies Press; 2007. https://doi.org/10.17226/11970.
15. Nichols JW, Huggett DB, Arnot JA, Fitzsimmons PN, Cowan-Ellsberry CE. Toward improved models for predicting bioconcentration of well-metabolized compounds by rainbow trout using measured rates of in vitro intrinsic clearance. Environ Toxicol Chem. 2013;32(7):1611–22. https://doi.org/10.1002/etc.2219.
16. Bell SM, Chang X, Wambaugh JF, Allen DG, Bartels M, Brouwer KLR, Casey WM, Choksi N, Ferguson SS, Fraczkiewicz G, Jarabek AM, Ke A, Lumen A, Lynn SG, Paini A, Price PS, Ring C, Simon TW, Sipes NS, Sprankle CS, Strickland J, Troutman J, Wetmore BA, Kleinstreuer NC. In vitro to in vivo extrapolation for high throughput prioritization and decision making. Toxicol In Vitro. 2018;47:213–27. https://doi.org/10.1016/j.tiv.2017.11.016.
17. OECD 319A. In: Determination of in vitro intrinsic clearance using cryopreserved rainbow trout hepatocytes (RT HEP). OECD Guideline for testing of chemicals. Paris: OECD Publishing; 2018. https://doi.org/10.1787/9789264303218-en.
18. OECD 319B. In: Determination of in vitro intrinsic clearance using rainbow trout liver S9 sub cellular fraction (RT S9). OECD guideline for testing of chemicals. Paris: OECD Publishing; 2018. https://doi.org/10.1787/9789264303232-en.
19. Ruiz-Aracama A, Peijnenburg A, Kleinjans J, Jennen D, van Delft J, Hellfrisch C, Lommen A. An untargeted multi-technique metabolomics approach to studying intracellular metabolites

of HepG2 cells exposed to 2,3,7,8-tetrachlorodibenzo-p-dioxin. BMC Genomics. 2011;12:251. https://doi.org/10.1186/1471-2164-12-251.
20. Wang D, Schramm V, Pool J, Pardali E, Brandenburg A, Rietjens IMCM, Boogaard PJ. The effect of alkyl substitution on the oxidative metabolism and mutagenicity of phenanthrene. Arch Toxicol. 2022;96(4):1109–31. https://doi.org/10.1007/s00204-022-03239-9.
21. Erratico CA, Szeitz A, Bandiera SM. Biotransformation of 2,2′,4,4′-tetrabromodiphenyl ether (BDE-47) by human liver microsomes: identification of cytochrome P450 2B6 as the major enzyme involved. Chem Res Toxicol. 2013;26(5):721–31. https://doi.org/10.1021/tx300522u.
22. Kwon JH, Lee HJ, Escher BI. Bioavailability of hydrophobic organic chemicals on an in vitro metabolic transformation using rat liver S9 fraction. Toxicol In Vitro. 2020;66:104835. https://doi.org/10.1016/j.tiv.2020.104835.
23. Fischer FC, Cirpka OA, Goss KU, Henneberger L, Escher BI. Application of experimental polystyrene partition constants and diffusion coefficients to predict the sorption of neutral organic chemicals to multiwell plates in in vivo and in vitro bioassays. Environ Sci Technol. 2018;52(22):13511–22. https://doi.org/10.1021/acs.est.8b04246.
24. Birch H, Kramer NI, Mayer P. Time-resolved freely dissolved concentrations of semivolatile and hydrophobic test chemicals in in vitro assays - measuring high losses and crossover by headspace solid-phase microextraction. Chem Res Toxicol. 2019;32(9):1780–90. https://doi.org/10.1021/acs.chemrestox.9b00133.
25. Proença S, Escher BI, Fischer FC, Fisher C, Grégoire S, Hewitt NJ, Nicol B, Paini A, Kramer NI. Effective exposure of chemicals in in vitro cell systems: a review of chemical distribution models. Toxicol In Vitro. 2021;73:105133. https://doi.org/10.1016/j.tiv.2021.105133.
26. Pereira LC, de Souza AO, Meireles G, Franco-Bernardes MF, Tasso MJ, Bruno V, Dorta DJ, de Oliveira DP. Comparative study of genotoxicity induced by six different PBDEs. Basic Clin Pharmacol Toxicol. 2016;119:396–404. https://doi.org/10.1111/bcpt.12595.
27. Kumar B, Prakash A, Ruhela RK, Medhi B. Potential of metabolomics in preclinical and clinical drug development. Pharmacol Rep. 2014;66(6):956–63. https://doi.org/10.1016/j.pharep.2014.06.010.
28. Song S, Yang C, Shao M, Chao J, Zheng N, Wang W, He Y, Li P. Simultaneous determination of polybrominated diphenyl ethers and hydroxylated analogues in human serum using high-performance liquid chromatography-inductively coupled plasma mass spectrometry. J Chromatogr B Analyt Technol Biomed Life Sci. 2020;1147:122130. https://doi.org/10.1016/j.jchromb.2020.122130.
29. Adeniji AO, Okoh OO, Okoh AI. Analytical methods for polycyclic aromatic hydrocarbons and their global trend of distribution in water and sediment: a review in Recent Insights in Petroleum Science And Engineering. INTECH. 2018. https://doi.org/10.5772/intechopen.71163.
30. Wang X, Lin L, Luan T, Yang L, Tam NFY. Determination of hydroxylated metabolites of polycyclic aromatic hydrocarbons in sediment samples by combining subcritical water extraction and dispersive liquid-liquid microextraction with derivatization. Anal Chim Acta. 2012;753:57–63. https://doi.org/10.1016/j.aca.2012.09.028.
31. Cruz R, Cunha SC, Marques A, Casal S. Polybrominated diphenyl ethers and metabolites – an analytical review on seafood occurrence. TrAC. 2017;87:129–44. https://doi.org/10.1016/j.trac.2016.12.005.
32. Ewa B, Danuta MŠ. Polycyclic aromatic hydrocarbons and PAH-related DNA adducts. J Appl Genet. 2017;58(3):321–30. https://doi.org/10.1007/s13353-016-0380-3.
33. Agilent Technologies. Two-way splitter kit with makeup gas installation and operation guide. Agilent G3180B, 1st edn. Wilmington, DE: Agilent Technologies, Inc; 2011. Available in: https://www.agilent.com/cs/library/usermanuals/Public/G3181-90120_045611.pdf.
34. Motorykin O, Schrlau J, Jia Y, Harper B, Harris S, Harding A, Stone D, Kile M, Sudakin D, Staci L, Simonich M. Determination of parent and hydroxy PAHs in personal PM2.5 and urine samples collected during Native American fish smoking activities. Sci Total Environ. 2015;505:694–703. https://doi.org/10.1016/j.scitotenv.2014.10.051.
35. Butryn DM, Gross MS, Chi LH, Schecter A, Olson JR, Aga DS. One-shot' analysis of polybrominated diphenyl ethers and their hydroxylated and methoxylated analogs in human breast milk and serum using gas chromatography-tandem mass spectrometry. Anal Chim Acta. 2015;892:140–7. https://doi.org/10.1016/j.aca.2015.08.026.
36. Sanz-Landaluze J, Bocanegra-Salazar M, Ortiz-Pérez D, Cámara C. Miniaturisated method for the analysis of polycyclic aromatic hydrocarbons in leaf samples. J Chrom A. 2010;1217(22):3567–74. https://doi.org/10.1016/j.chroma.2010.03.049.
37. Joseph M. HPLC detector options for the determination of polynuclear aromatic hydrocarbons varian application note number 7. 2012. www.agilent.com/chem. Accessed 6 May 2022.
38. Schummer C, Delhomme O, Appenzeller BMR, Wennig R, Millet M. Comparison of MTBSTFA and BSTFA in derivatization reactions of polar compounds prior to GC/MS analysis. Talanta. 2009;77(4):1473–82. https://doi.org/10.1016/j.talanta.2008.09.043.
39. Schreiber R, Altenburger R, Paschke A, Küster E. How to deal with lipophilic and volatile organic substances in microtiter plate assays. Environ Toxicol Chem. 2008;27(8):1676–82. https://doi.org/10.1897/07-504.1.
40. Cetin B. Odabasi Measurement of Henry's law constants of seven polybrominated diphenyl ether (PBDE) congeners as a function of temperature. Atmos Environ. 2005;39(29):5273–80. https://doi.org/10.1016/j.atmosenv.2005.05.029.
41. Fischer FC, Henneberger L, König M, Bittermann K, Linden L, Goss KU, Escher BI. Modeling exposure in the Tox21 in vitro bioassays. Chem Res Toxicol. 2017;30(5):1197–208. https://doi.org/10.1021/acs.chemrestox.7b00023.
42. Quinn CL, van der Heijden SA, Wania F, Jonker MTO. Partitioning of polychlorinated biphenyls into human cells and adipose tissues: evaluation of octanol, triolein, and liposomes as surrogates. Environ Sci Technol. 2014;48(10):5920–8. https://doi.org/10.1021/es500090x.
43. Zhang CY, Flor S, Ludewig G, Lehmler HJ. Atropselective partitioning of polychlorinated biphenyls in a HepG2 cell culture system: experimental and modeling results. Environ Sci Technol. 2020;54(21):13817–27. https://doi.org/10.1021/acs.est.0c02508.
44. Branco V, Matos B, Mourato C, Diniz M, Carvalho C, Martins M. Synthesis of glutathione as a central aspect of PAH toxicity in liver cells: a comparison between phenanthrene, Benzo[b] Fluoranthene and their mixtures. Ecotoxicol Environ Saf. 2021. https://doi.org/10.1016/j.ecoenv.2020.111637.
45. Liu X, Wang J, Lu C, Zhu C, Qian B, Li Z, Liu C, Shao J, Yan J. The role of lysosomes in BDE 47-mediated activation of mitochondrial apoptotic pathway in HepG2 cells. Chemosphere. 2015;124(1):10–21. https://doi.org/10.1016/j.chemosphere.2014.10.054.
46. Hu X, Zhang J, Jiang Y, Lei Y, Lu L, Zhou J, Huang H, Fang D, Tao G. Effect on metabolic enzymes and thyroid receptors induced by BDE-47 by activation the pregnane X receptor in HepG2, a

human hepatoma cell line. Toxicol In Vitro. 2014;28(8):1377–85. https://doi.org/10.1016/j.tiv.2014.07.004.
47. Kang Y, Cheung KC, Wong MH. Polycyclic aromatic hydrocarbons (PAHs) in different indoor dusts and their potential cytotoxicity based on two human cell lines. Environ Int. 2010;36(6):542–7. https://doi.org/10.1016/j.envint.2010.04.006.
48. Gaudreau É, Bérubé R, Bienvenu JF, Fleury N. Stability issues in the determination of 19 urinary (free and conjugated) monohydroxy polycyclic aromatic hydrocarbons. Anal Bioanal Chem. 2016;408(15):4021–33. https://doi.org/10.1007/s00216-016-9491-2.
49. Gao P, da Silva E, Hou L, Denslow ND, Xiang P, Ma LQ. Human exposure to polycyclic aromatic hydrocarbons: metabolomics perspective. Environ Int. 2018;119:466–77. https://doi.org/10.1016/j.envint.2018.07.017.
50. Schober W, Pusch G, Oeder S, Reindl H, Behrendt H, Buters JTM. Metabolic activation of phenanthrene by human and mouse cytochromes P450 and pharmacokinetics in CYP1A2 knockout mice. Chem Biol Interact. 2010;183(1):57–66. https://doi.org/10.1016/j.cbi.2009.09.008.
51. Zheng X, Zhu Y, Liu C, Liu H, Giesy JP, Hecker M, Lam MHW, Yu H. Accumulation and biotransformation of BDE-47 by zebrafish larvae and teratogenicity and expression of genes along the hypothalamus-pituitary-thyroid axis. Environ Sci Technol. 2012;46(33):12943–51. https://doi.org/10.1021/es303289n.
52. De Oro-Carretero P, Sanz-Landaluze J. Bioaccumulation and biotransformation of BDE-47 using zebrafish eleutheroembryos (Danio rerio). Environ Toxicol Chem. 2023;42:835–45. https://doi.org/10.1002/etc.5569.
53. Sun J, Liu J, Yu M, Wang C, Sun Y, Zhang A, Wang T, Lei Z, Jiang G. In vivo metabolism of 2,2′,4,4′-tetrabromodiphenyl ether (BDE-47) in young whole pumpkin plant. Environ Sci Technol. 2013;47(8):3701–7. https://doi.org/10.1021/es4003263.
54. Yamazoe A, Yagi O, Oyaizu H. Biotransformation of fluorene, diphenyl ether, dibenzo-p-dioxin and carbazole by Janibacter sp. Biotech Lett. 2004;26:479–86. https://doi.org/10.1023/B:BILE.0000019554.49484.40.
55. Wiseman SB, Wan Y, Chang H, Zhang X, Hecker M, Jones PD, Giesy JP. Polybrominated diphenyl ethers and their hydroxylated/methoxylated analogs: environmental sources, metabolic relationships, and relative toxicities. Mar Pollut Bullet. 2011;63:179–88. https://doi.org/10.1016/j.marpolbul.2011.02.008.
56. Tang J, Hu B, Zheng H, Qian X, Zhang Y, Zhu J, Xu G, Chen D, Jin X, Li W, Xu L. 2,2′,4,4′-Tetrabromodiphenyl ether (BDE-47) activates aryl hydrocarbon receptor (AhR) mediated ROS and NLRP3 inflammasome/p38 MAPK pathway inducing necrosis in cochlear hair cells. Ecotoxicol Environ Saf. 2021;221:112423. https://doi.org/10.1016/j.ecoenv.2021.112423.
57. Deng D, Tam NFY. Adsorption-uptake-metabolism kinetic model on the removal of BDE-47 by a Chlorella isolate. Environ Poll. 2016;212:290–8. https://doi.org/10.1016/j.envpol.2016.01.063.
58. Zhang M, Zhao F, Zhang J, Shi J, Tao H, Ge H, Guo W, Liu D, Cai Z. Toxicity and accumulation of 6-OH-BDE-47 and newly synthesized 6,6′-diOH-BDE-47 in early life-stages of zebrafish (Danio rerio). Sci Total Environ. 2020;763:143036. https://doi.org/10.1016/j.scitotenv.2020.143036.
59. De Souza AC, Sardela VF, De Sousa VP, Pereira HMG. Zebrafish (Danio rerio): a valuable tool for predicting the metabolism of xenobiotics in humans? CBPC. 2018;212:34–46. https://doi.org/10.1016/j.cbpc.2018.06.005.
60. Laue H, Hostettler L, Badertscher RP, Badertscher RP, Jenner KJ, Sanders G, Arnot JA, Natsch A. Examining uncertainty in in vitro-in vivo extrapolation applied in fish bioconcentration models. Environ Sci Technol. 2020;54(15):9483–94. https://doi.org/10.1021/acs.est.0c01492.
61. Yamazaki S, Evers R, de Zwart L. Physiologically-based pharmacokinetic modelling to evaluate in vitro-to-in vivo extrapolation for intestinal P-glycoprotein inhibition. CPT Pharmacometrics Syst Pharmacol. 2022;11(1):55–67. https://doi.org/10.1002/psp4.12733.
62. Grimard C, Mangold-Döring A, Schmitz M, Alharbi H, Jones PD, Giesy JP, Hecker M, Brinkmann M. In vitro-in vivo and cross-life stage extrapolation of uptake and biotransformation of benzo[a]pyrene in the fathead minnow (Pimephales promelas). Aquat Toxicol. 2020;228:105616. https://doi.org/10.1016/j.aquatox.2020.105616.

Miniaturized method for the quantification of Persistent Organic Pollutants and their metabolites in HepG2 cells: assessment of their biotransformation

Paloma De Oro-Carretero* and Jon Sanz-Landaluze

Department of Analytical Chemistry, Faculty of Chemical Science, Complutense University of Madrid, Avenida Complutense s/n, 28040 Madrid, Spain

Contact emails: pdeoro@ucm.es* (P. De Oro-Carretero), jsanzlan@ucm.es (J. Sanz-Landaluze)
Phone: +034-91 394 4322; Fax: +034-91 394 4329

*****Corresponding author

Supporting information

Table S1. Mass spectrometer conditions in SIM mode for OH-PHEs

Analyte	Retention time (min)	m/z	Initial scanning time (min)
4-OH-PHE	14.73	308, 251, 235	8 (solvent delay)
3-OH-PHE	15.34		18
1-OH-PHE	15.55		
2-OH-PHE	15.80		

Table S2. Mass spectrometer conditions in SIM mode for BDE-47 and their metabolites

Analyte	Retention time (min)	m/z	Initial scanning time (min)
BDE-28	12.01	248, 246, 406, 408	8 (solvent delay)
TMDS-TCS	13.36	290, 288, 218	12.5
BDE-47	16.55	326, 486, 484, 488	15.50
2'-OH-TMDS-BDE-28	19.59	423, 421, 425, 81	
3-MeO-BDE-47	20.83	356, 516, 341, 514	19.0*
5-MeO-BDE-47	21.15	516, 356, 358, 326	
BDE-99	22.73	404, 406, 564, 566	22.00
5-OH-TMDS-BDE-47	27.20	502, 504, 500, 81	25.50
3-OH-TMDS-BDE-47	31.94	502, 474, 266, 419	29.50

* A joint window is established as they elude close retention times, so that the majority m/z of each is monitored (marked in the table)

Table S3. LODs, LOQs RSD, R^2 and method recoveries.

Analyte	R^2	LOD (µg·L^{-1})	LOQ (µg·L^{-1})	Recovery of cell samples (%)	Recovery of medium samples (%)
PHE	0.9990	1.71	3.11	96 ± 7	105 ± 11
4-OH-PHE	0.9980	2.65	5.89	85 ± 9	87 ± 9
3-OH-PHE	0.9984	2.30	5.30	86 ± 9	91 ± 8
1-OH-PHE	0.9989	1.98	4.87	90 ± 5	91 ± 7
2-OH-PHE	0.9985	2.52	5.36	83 ± 10	87 ± 10
BDE-28	0.9997	0.60	1.25	91 ± 7	85 ± 7
BDE-47	0.9990	1.01	2.06	97 ± 6	98 ± 5
3-MeO-BDE-47	0.9984	0.70	1.02	112 ± 3	92 ± 6
5-MeO-BDE-47	0.9991	0.39	0.68	105 ± 9	87 ± 5
2'-OH-BDE-28	0.9992	1.52	2.03	87 ± 11	89 ± 6
5-OH-BDE-47	0.9984	0.55	0.96	95 ± 10	75 ± 6
3-OH-BDE-47	0.9972	1.70	2.13	84 ± 6	72 ± 7

Fig. S1. Recoveries obtained with the different sample volume of medium (20 µg·L^{-1}).

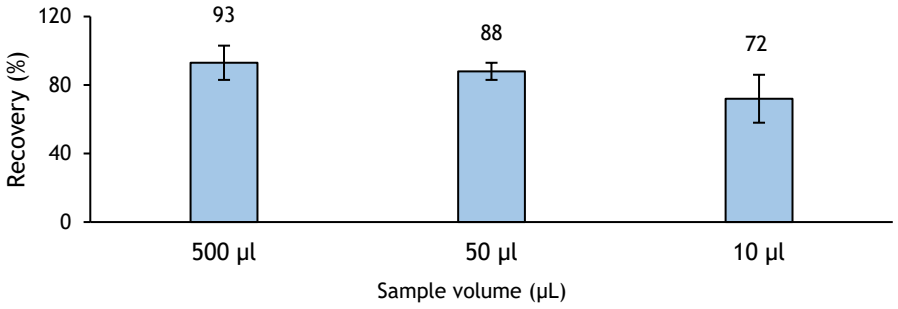

Fig. S2. Derivatized metabolites areas (20 µg·L^{-1}) with different reagents for 30 min at 60 °C.

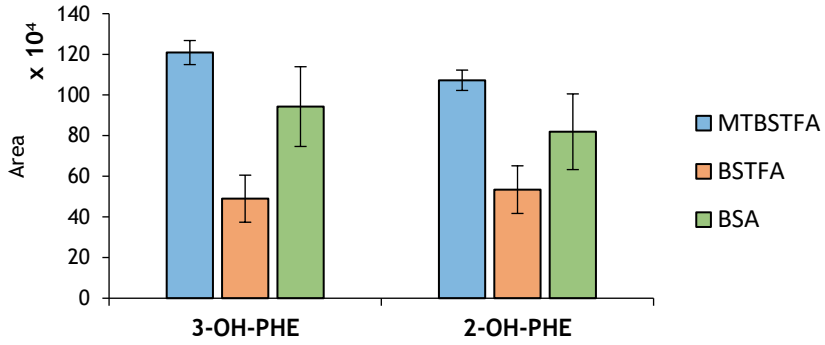

Fig. S3. Areas of the metabolites (20 µg·L^{-1}) with different conditions of derivatization with MTBSTFA reagent.

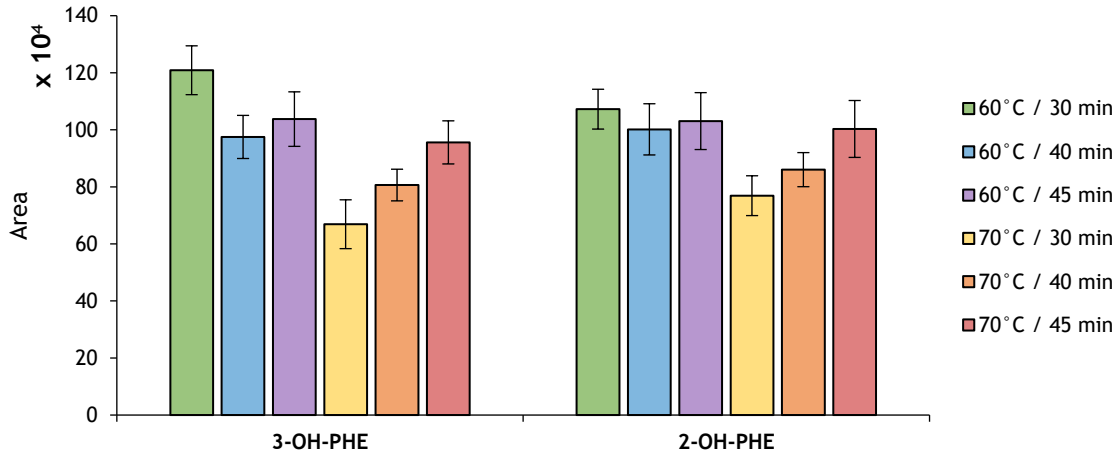

Fig. S4. Areas of the derivatized metabolites (MTBSTFA - 20 µg·L^{-1}) with different solvents.

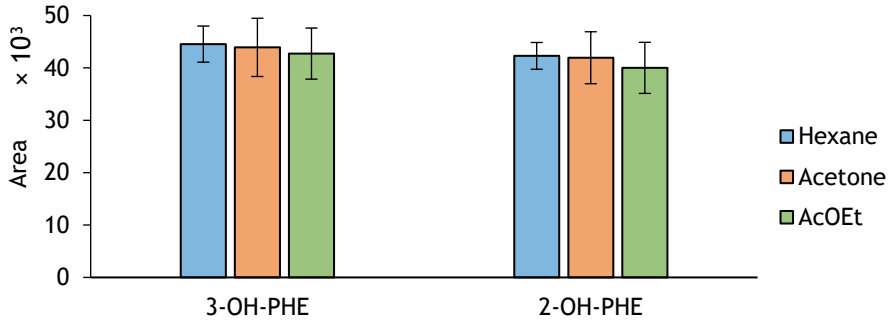

Fig. S5. Analytical signal obtained by derivatising a mixture of OH-BDEs and a BDE in different solvents (10 µg·L^{-1}).

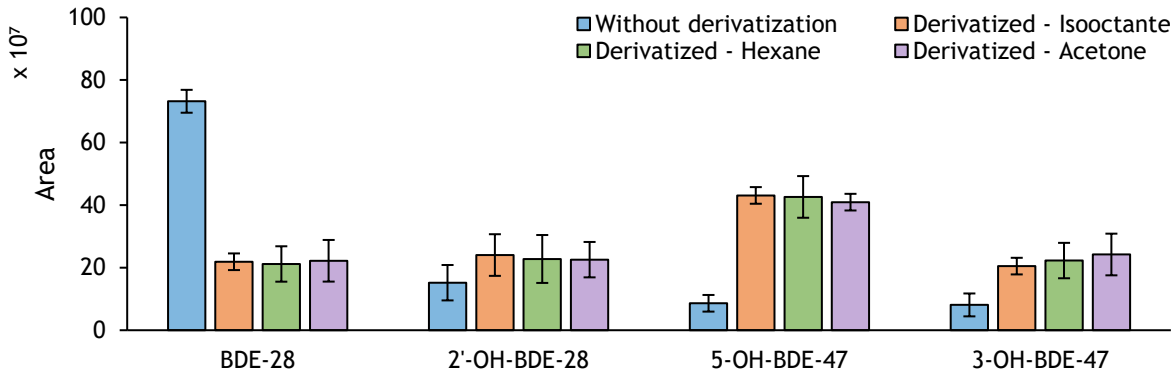

Fig. S6. Chromatogram of a mixture of the analytes (10 µg·L^{-1}) obtained with µECD detector (is like MS detector).

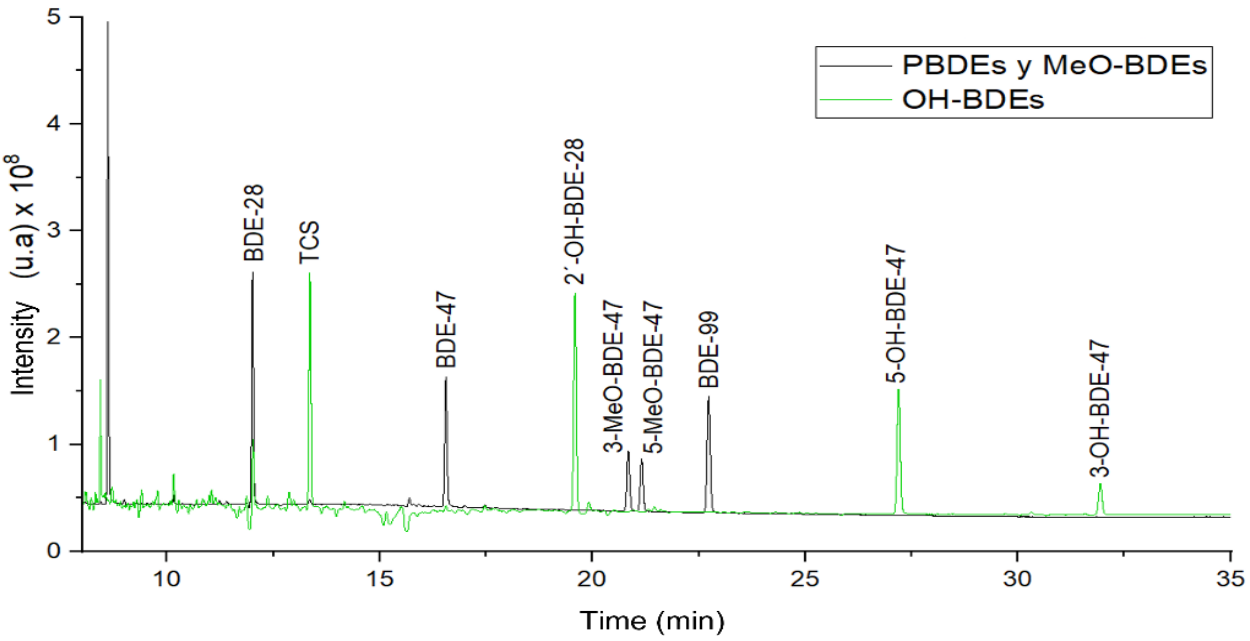

ARTÍCULO 3:

Enfoque *in vitro* para refinar las predicciones de bioconcentración y biotransformación de contaminantes orgánicos persistentes utilizando líneas celulares.

In vitro approach to refine bioconcentration and biotransformation predictions of organic persistent pollutants using cell lines.

Paloma De Oro-Carretero, Jon Sanz-Landaluze*

Chemosphere 364, 143020, 2024 (IF: 8.1, Q1)

**Autora de correspondencia.*

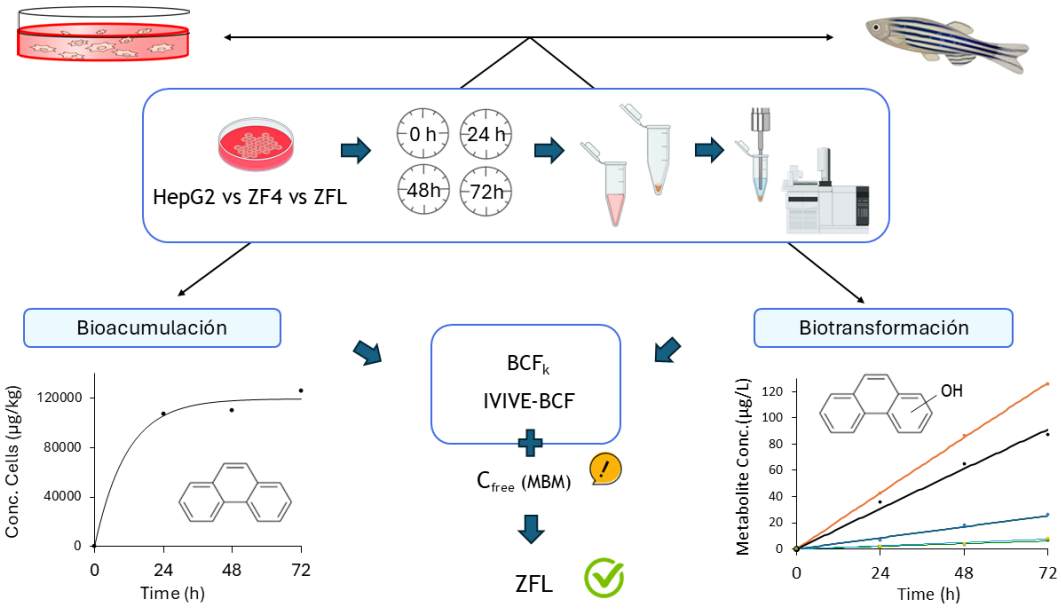

Chemosphere 364 (2024) 143020

Contents lists available at ScienceDirect

Chemosphere

journal homepage: www.elsevier.com/locate/chemosphere

In vitro approach to refine bioconcentration and biotransformation predictions of organic persistent pollutants using cell lines

Paloma De Oro-Carretero *, Jon Sanz-Landaluze

Department of Analytical Chemistry, Faculty of Chemical Science, Complutense University of Madrid, Avenida Complutense s/n, 28040, Madrid, Spain

HIGHLIGHTS

- Study of the limitations of IVIVE-BCF models.
- Cell lines provide information on compounds with slow biotransformation kinetics.
- Cell lines are suitable for BCF and biotransformation kinetics estimation.
- The free bioavailable concentration is essential for BCF calculation.

GRAPHICAL ABSTRACT

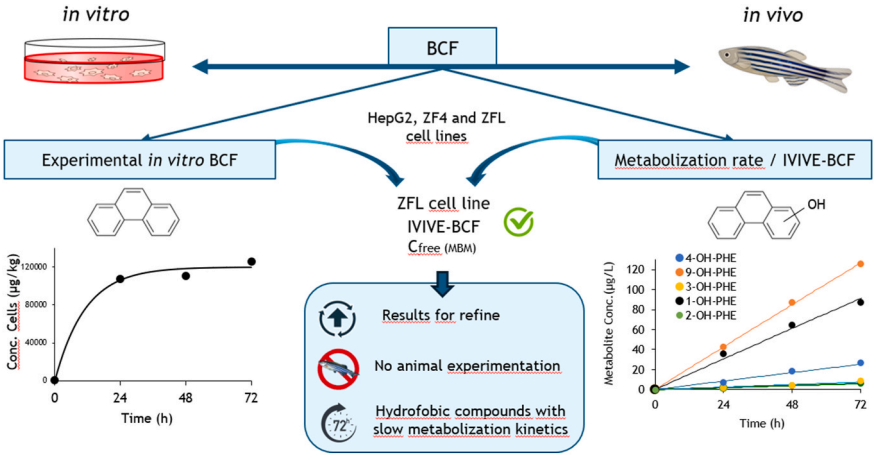

ARTICLE INFO

Handling editor: A. Gies

Keywords:
Bioconcentration
C_{free}
IVIVE
Cell lines
Biotransformation
In vitro

ABSTRACT

The application of the 3Rs (Replacement, Reduction, and Refinement) in animal experimentation has recently concentrated its efforts on utilizing cellular systems to predict toxicity in organisms. In this context, while refining the data obtained from cell lines, this study assesses their bioaccumulation potential and various methods for extrapolating the *in vitro* metabolization rate constant to support modelled bioaccumulation assessments for fish and their limitations. For this purpose, the concentrations of the parent compound, phenanthrene, and its major metabolites within the cells and in the medium at various exposure times were quantified. A chemical distribution model (mass balance) was applied to calculate the concentrations of the cell-bioaccessible compounds (C_{free}) based on the experimentally determined concentrations. An elevated matching was observed between the *in vitro* bioconcentration factor (BCF) and the *in vivo* BCFs reported in the literature for zebrafish liver cells (ZFL). This study demonstrates the importance of further investigating *in vitro* biotransformation kinetics. The results obtained with the approach developed here provide valuable information to enhance current models. Additionally, it underscores the potential of cell lines as a strategy for rapid, simple, and cost-effective predictions without the need for animal experimentation.

* Corresponding author.
E-mail addresses: pdeoro@ucm.es (P. De Oro-Carretero), jsanzlan@ucm.es (J. Sanz-Landaluze).

https://doi.org/10.1016/j.chemosphere.2024.143020
Received 22 April 2024; Received in revised form 12 June 2024; Accepted 2 August 2024
Available online 3 August 2024

1. Introduction

The bioaccumulation factor (BCF) is commonly used to measure the degree of accumulation of a substance from surrounding media in aquatic organisms. It is considered as a pivotal parameter in assessing the ecotoxicological characteristics of a substance (El-Amrani et al., 2012). In recent years, environmental protection agencies across different countries have been using these parameters to identify and regulate the risks associated with manufactured and marketed substances, in order to enhance the safeguarding of both human health and the environment. European Regulation for the Registration, Evaluation, Authorization, and Restriction of Chemicals (REACH) propose Guideline 305 from the Organisation for Economic Co-operation and Development as official method for assessing the BCF (OECD, 2012). Environmental protection agencies and scientists have promoted many efforts to implement the "3Rs" (reduce, replace, and refine) in these animal experiments (Halder et al., 2014), and so the development of OECD Guideline 236 (OECD, 2013) based on Fish Embryo Toxicity (FET) tests encouraged the progress of alternative methods using the zebrafish model.

Numerous studies in the literature (Knöbel et al., 2012; Belanger et al., 2013), including our prior research on bioaccumulation and metabolism assays (Sanz-Landaluze et al., 2015; De Oro-Carretero and Sanz-Landaluze, 2023), have illustrated the connection between embryos and adult fish. Another ethically and economically feasible approach to assess the effects of chemical compounds on living organisms and the environment can be achieved through *in vitro* (Castaño et al., 2003) or *in silico* (Arnot and Gobas, 2006) models, although it has been shown that cell-based studies are less sensitive than *in vivo* studies. Among other factors, one of the main reasons that explains this lower sensitivity is the discrepancy between the nominal effect concentration and the bioavailable concentration (C_{free}). This is essentially because fish or embryo assays are exposed in water, while cells are exposed in complex media containing serum, proteins, and lipids that can retain compounds (Segner, 2004). Lungu et al., 2021 (Lungu-Mitea et al., 2021) have successfully studied the correlation between cells and larvae for the same objective, considering the bioavailable concentration within the systems (Proença et al., 2021).

In aims on replacing animal testing with alternative methods, cell-based techniques as *in vitro-in vivo* extrapolation (IVIVE) (Bell et al., 2018) are being explored as they are optimal in High-Throughput Screening (HTS) and the Adverse Outcome Pathways (AOP) concepts (Ankley et al., 2010). This is another strategy being pursued to decrease the use of animals in experiments, *in silico* models integrating hepatic biotransformation to predict bioconcentration factors (BCFs) (Cowan-Ellsberry et al., 2009; Laue et al., 2014), reflecting evidence that metabolism could impact bioaccumulation (Fu et al., 2020). One promising approach involves assessing clearance through the utilization *in-vitro* metabolising systems derived from liver tissue (Nichols et al., 2006). In line with this methodology, OECD 319 guideline (OECD, 2018a; OECD, 2018b) has been developed based on predictive empirical regression models by determining *in-vitro* intrinsic clearance through the substrate depletion approach in cryopreserved hepatocytes (RT-HEP) or subcellular liver fractions S9 (RT-S9) from rainbow trout and extrapolating to *in-vivo* intrinsic clearance (OECD, 2018c). This approach has been shown to have great potential for BCF assessment (Bourgeois et al., 2022), but it has many limitations that requires further research to provide more data and improve performance (Kosfeld et al., 2020). Some of these limitations considered in this study are: i) RT-HEP and RT-S9 test systems have time-limited exposures that restrict their use for chemicals with a very low biotransformation rates (OECD, 2018c), ii) overprediction of biotransformation kinetics with the substrate depletion approach and a well-stirred liver because not all of the substrate is biotransformed as some is bioaccumulating at that instant and iii) nominal concentration is only used for calculations and C_{free} is not considered if cell lines are used (Bell et al., 2018; Henneberger et al., 2021).

In order to explore alternatives to these limitations, cell lines that allow kinetic studies for longer experimental periods were evaluated for their suitability for assessing BCF; as well as for biotransformation kinetics to provide data to improve IVIVE estimation. The OECD 249 guideline (OECD, 2021) uses the RTgill-W1 cell line for toxicity assays. However, the selection of liver tissues for *in vitro* bioassays better represents the organism since the liver is the main site of biotransformation (Ewa and Danuta, 2017). In this study, the well previously studied metabolic (De Oro-Carretero et al., 2023) and bioaccumulative potential (Niu et al., 2020), of human hepatoma HepG2 cells, which have been shown in previous studies to have high metabolism capacity was evaluated alongside zebrafish embryo ZF4 cells to assess their correlation with the *in vivo* FET model. The correlation of zebrafish liver ZFL cells with the *in vivo* system was examined, drawing upon its previous application in IVIVE toxicity studies (Pree and Bruce, 2017).

On the other hand, two recent strategies exist for estimating C_{free}. The first involves advanced analytical methods of experimental quantification based on solid-phase microextraction (SPME) (Henneberger et al., 2019a, 2019b). The second involves well-studied models of chemical distribution (mass balance model, MBM) in the different compartments of an *in vitro* system (Proença et al., 2021) abased on the physic-chemical properties of the compounds (Fischer et al., 2017; Birch et al., 2019; Kramer et al., 2012). The IVIVE model offers the advantage of a quick and easy analytical method for determining the compound in the exposure medium (OECD, 2018c). In this line of work, the total compound concentration in the exposure medium was determined, and the C_{free} was estimated using MBM. Additionally, the compound and metabolite concentrations inside and outside the cell were estimated using the quick and simple method developed in our previous work (De Oro-Carretero et al., 2023). Phenanthrene (PHE) was chosen as it is one of the most commonly studied compounds in *in vitro* assays due to its hydrophobic and volatile properties (Birch et al., 2019; Kwon et al., 2020; Fischer et al., 2018; Fay et al., 2015).

2. Material and methods

2.1. Reagents

Individual solid standard of phenanthrene (PHE), fluorene (FLU), 1-OH-PHE, 2-OH-PHE, 3-OH-PHE, 4-OH-PHE and 9-OH-PHE; the derivatization reagent N-*tert*-butyldimethylsilyl-N-methyltrifluoroacetamide (MTBSTFA) + 1% tert-butyl-methylchlorosilane and NaCl were supplied by Sigma Aldrich (Madrid, Spain). Analytical-grade solvents acetonitrile (ACN), n-hexane, dichloromethane (DCM) and dimethyl sulfoxide (DMSO) were purchased from Scharlab (Barcelona, Spain).

Dulbecco's Modified Eagle Medium (DMEM), DMEM/F12 (1:1), streptomycin (10,000 μg/ml)/penicillin (10,000 U/ml) mixture (s/p), Antibiotic/Antimycotic (A/A), Trypsin-EDTA (0.05%) for HepG2 and ZF4, TrypLE™ Express for ZFL, Phosphate Buffered Saline (PBS), Fetal Bovine Serum (FBS), Trypan Blue 0.4% and Resazurin sodium salt were purchased from Thermo Fisher Scientific (Spain). 3-(4,5-dimethylthiazol-2-yl)-2,5-diphenyltetrazolium bromide (MTT), mouse epidermal growth factor (EGF) and insulin bovine were supplied by Sigma-Aldrich (Madrid, Spain).

2.2. Instrument and apparatus

For sample preparation, Vibra cell VCx130 ultrasound probe with a 2 mm diameter titanium microtip and a 130 W high frequency generator at 20 KHz from Sonics & Materials Inc. (Connecticut, USA), X50S Metal Carbide technical nitrogen stream (Barcelona, Spain), vortex mixer from Scientific Industries (NY, USA) and the Eppendorf 5415R microcentrifuge (Hamburg, Germany) were used.

Instrumental determination was performed by Agilent Gas Chromatographic Mod. 7890A Series equipped with a HP 7683B

autoinjector, a micro-Electron Capture Detector (μECD), a HP 5975C VL MSD mass spectrometry detector (Agilent Technologies, Madrid, Spain) and a ZB-5 capillary column (30 m × 0.25 mm I.D., 0.25-μm film thickness); and HPLC Spectra System P 4000 (Thermo Electron Corporation, San Jose, USA) equipped with a fluorescence detector FL 3000 and Hypersil Green PAH columns (150 mm × 3 mm; particle size 3 μm) attached to a Phenomenex C18 pre-column.

2.3. Cell culture

Human hepatoma cells (HepG2), zebrafish embryo fibroblast cells (ZF4) and zebrafish liver cells (ZFL) were supplied by American Type Culture Collection, ATCC (Virginia, USA). HepG2 cells were routinely cultured at 37 °C, 5% CO_2 in DMEM supplemented with 10% heat inactivated FBS and 1% s/p. ZF4 were cultured with DMEM/F12 (1:1) supplemented with 10% FBS and 1% s/p at 28 °C and 5% CO_2. ZFL cells were cultured with DMEM supplemented with 10% FBS, 5% A/A, 50 ng/mL EGF, 0.01 mg/mL insulin and 0.5% heat inactivated Trout Serum (Brandts et al., 2020) at 28 °C and 5% CO_2. All cell lines were cultured in humidified air atmosphere.

2.4. Cell viability

Cell viability was determined by MTT assay for HepG2 and ZFL and the resazurin salt assay for ZF4. First, 10,000 cells/well were seeded in 96-wells plates for 24 h under culture conditions. After that time, the culture medium was replaced by medium contaminated with different concentrations of PHE. After 72h, MTT solution or resazurin salt were added to provide a final concentration of 0.5 and 0.01 mg/mL, respectively, and incubated for the following 4h. For MTT assay, formazan crystals were dissolved in 100 μL sterile DMSO and quantified with absorbance measurement at 595 nm in a Multiskan Sky High (Tecan Thermo Fisher). For resazurin salt assay, fluorescence was measured with a CLARIOstar microplate reader (BMG LABTECH) with an excitation wavelength of 550 nm and an emission wavelength of 590 nm. Three independent assays were carried out with the same conditions. The results have been subsequently used for the design of the biotransformation experiment.

2.5. Cell exposure. Bioconcentration and biotransformation experiment

The cell optimization and exposure procedure were developed in the previous study (De Oro-Carretero et al., 2023). HepG2, ZF4 and ZFL were exposed in the same way. Briefly, $2{\cdot}10^6$ cells were seeded in P100 glass plates and incubated for 24h under the culture conditions. The culture medium was then replaced by a contaminated medium that resulted in viability of more than 70% at the end of the test based on the cell viability study above. HepG2 and ZF4 cells were exposed to 15 mg L^{-1} and ZFL cells to 10 (Experiment A) and 50 mg L^{-1} (Experiment B) for 24, 48 and 72h. In addition, parallel experiments are performed to estimate losses: one with cells without contaminated medium ("blank") and one with contaminated medium without cells ("no cells"). Finally, cell pellets and medium obtained from all exposure times, including the initial medium ("t = 0h"), were collected. The cell pellets were divided into 2 fractions for the determination of phenanthrene and its metabolites, dried under nitrogen stream and accurately weighed. All samples are stored at −20 °C until analysis.

2.6. Analytical procedure. Extraction and determination

For PHE quantification in cells, half of the pellet obtained (~5 mg) was extracted with 400 μL of ACN and sonicated with an ultrasound probe for 1 min at 30% of amplitude and an on/off:2s/5s pulse. On the other hand, 50 μL of exposure medium was extracted with 400 μL of ACN (+50 mg NaCl) with vortex for 30s. Internal standard FLU was previously added to the extraction step to both cells and exposure medium. The mixture was centrifuged for 10 min at 10,000 rpm and the organic extract was directly injected into the LC-FL. The chromatographic method consisted of a 0.3 mL min^{-1} constant flow of ACN and H_2O mobile phase. The ratio started at 70:30 and increases to 100:0 over 7 min and the initial conditions were recovered after 15 min. 20 μL of the sample was injected into the column at 30 °C and fluorescence wavelengths used were 276 nm for excitation and 346 nm for emission.

The other half of the pellet obtained (~5 mg) and 500 μL of medium was used for OH-PHEs quantification. In this case, same extraction method was performed but using 500 μL of the hexane:DCM (1:1) mixture as solvent for the exposure of the cell pellets and the HepG2 and ZF4 exposure media and the hexane:MTBE(1:1) mixture for the exposure of the ZFL medium. No IS was used for OH-PHEs quantification as explained in De Oro and Sanz (2023) (De Oro-Carretero et al., 2023), but recuperation studies were carried out to check losses. After centrifugation step, the remaining extracts were evaporated to dryness under a gentle stream of nitrogen and reconstituted in 100 μL of hexane. Finally, 80 μL of the volume obtained was derivatised with 20 μL of MTBSTFA at 60 °C for 30 min in the oven and injected into GC-MS. Samples (1 μL) were injected in splitless mode at 280 °C with Helium as carrier gas at a constant pressure of 25 psi. The temperature of the column was programmed to increase from 80 °C (2 min) to 150 °C (2 min) at a rate of 30 °C·min^{-1}, then to 250 °C (2 min) at 20 °C·min^{-1} and finally to 270 °C (2 min) at 10 °C·min^{-1}. The temperature of the ion source and the transfer line of the mass spectrometer was set at 250 and 270 °C, respectively, and 70 eV for the electron beam.

2.7. Data analysis for BCF prediction

The BCF is estimated for the 3 cell lines with different models, either using only the experimental data obtained or supplemented with computational models. A first calculation is carried out by using the experimental data obtained, according to the definition of BCF (Equation (1)). That is, the ratio between the chemical concentration in the organisms, in this case in the cells (C_{cell}), and the chemical concentration of the surrounding medium at steady state (C_w) (OECD, 2012; Niu et al., 2020). Both concentrations are experimentally determined.

$$BCF_{exp} = \frac{C_{cell}\ (\mu g{\cdot}kg^{-1})}{C_w\,(\mu g{\cdot}L^{-1})} \quad (1)$$

In a second estimation, the free dissolved concentration (C_{free}) is considered for BCF calculation. In this study, due to the use of glass plates, the level of serum in the exposure medium has the greatest impact on the decrease in C_{free} because of the high affinity of phenanthrene for proteins and/or lipids (Kramer et al., 2012). Therefore, the mass balance model (MBM) developed by Fischer et al., (2017) (Fischer et al., 2017) was applied to estimate the protein/lipid bound fractions, depending on the percentage of FBS supplemented and bioavailable concentrations. This model has default parameters set for the HepG2 cell line, however, for ZF4 and ZFL the input data for cell line type and culture medium were left blank and generic parameters were set (Lungu-Mitea et al., 2021) (See SI, Table S1). The binding values for the MBM input of phenanthrene distribution in the relevant BSA and lipid phases were obtained using the UFZ-LSER tool (Ulrich et al., 2017) (See SI, Table S2). Then, the MBM spreadsheet by Fischer et al., (2017) estimates the fractions of cell (f_{cell}), total medium (f_{medium}), cell membrane (f_{mem}) and the water phase of the medium ($f_{w,medium}$) compartment (Table S3) and applies them to each experimentally determined PHE concentration in the medium (Table 1) to estimate the C_{free} at each exposure time (Table S4). Therefore, BCF_{Cfree} (Equation (2)) was estimated as the ratio of the concentration obtained in the cells experimentally (C_{cell}) (Table 1) and the C_{free} estimated with the MBM model (Table S4).

$$BCF_{Cfree} = \frac{C_{cell}\ (\mu g{\cdot}kg^{-1})}{C_{free}\,(\mu g{\cdot}L^{-1})} \quad (2)$$

The third estimate was carried out using the first-order toxicokinetic model (Equations (3) and (4)), which describes the uptake and desorption processes (Gobas and Zhang, 1992; Mackay and Fraser, 2000):

$$C_{cell} = \frac{k_1}{k_2} \cdot C_W\left(1 - e^{-k_2 t}\right) \text{ (uptake)} \; ; \; C_{cell} = C_{cell,0} \cdot e^{-k_2 t} \text{ (depuration)} \quad (3)$$

$$BCF_K = \frac{C_{cell}}{C_W} = \frac{k_1}{k_2} \quad (4)$$

where, $C_{cell,0}$ is the concentration in the cells at the start of the purification process, t is the exposure time (h), k_1 is the first-order uptake constant ($L \cdot kg^{-1} \cdot h^{-1}$) and k_2 is the first order elimination rate constant (h^{-1}). In this model, for the chemical concentration of the surrounding medium, C_w, the one experimentally calculated or free dissolved concentration (C_{free}) can be used, and so, two different estimations of BCF_k can be calculated.

$$C_{X-OH-PHE} = \frac{k_X}{k_1 + k_2 + k_3 + k_4 + k_5} \cdot C_{PHE}\left(1 - e^{-(k_1+k_2+k_3+k_4+k_5)\cdot t}\right) \quad (5)$$

$$k_f\left(h^{-1}\right) = \sum k_x \quad (6)$$

Where x = 1, 2, 3, 4 and 5, with k_1, k_2, k_3, k_4 and k_5 representing the formation constants of the metabolites 1-OH-PHE, 2-OH-PHE, 3-OH-PHE, 4-OH-PHE and 9-OH-PHE, respectively, and C_{PHE} being the concentration of PHE in the medium or free.

Finally, the mass balance of the *in vitro* system was performed (Equations (7) and (8)), considering the experimentally determined concentrations of PHE and their metabolites in the cells and exposure media at each exposure time (xh) and the losses due to compound volatility (Equation (9)), and the recovery at the end of the test was estimated (Equation (10)).

$$m_{Total} = mPHE_{0h} = m_{xh} \quad (7)$$

$$m_{xh} = (mPHE_{medium})_{xh} + (mPHE_{cells})_{xh} + (mPHE_{loss})_{xh} + \left(\sum mMetabolites_{medium}\right)_{xh} + \sum mMetabolites_{cells}\Big)_{xh} \quad (8)$$

The latest estimate of BCF is based on intrinsic clearance *in vitro* and biotransformation rates with further IVIVE as published by Nichols et al., (2013) (Nichols et al., 2021) and approved in the guidelines OECD 319 (OECD, 2018a; OECD, 2018b). For this, on one hand, the substrate depletion approach was used to estimate the reaction rate (k_e) and the Spreadsheet of the HEP-BCF model according to OECD 2018a (OECD, 2018c). According to the Black et al., 2021 (Black et al., 2013) study, a correction to the k_e value should be applied if the following requirements occur: i) the abiotic losses due to volatilisation observed by calculating the recovery of the negative control samples 'no cells' at each exposure time relative to the initial time are not within an acceptable 80–120%, ii) the loss process shows first order kinetics and iii) the ratio of k_e and the volatilisation rate constant (k_{volat}) is less than 10 ($k_e/k_{volat} < 10$). Correction proposed is based on subtracting the volatilisation rate constant (k_{volat}) from the depletion rate constant (k_e). In these cases the corrected constant ($k_{e,loss}$) is used for the calculation of the BCF in the IVIVE-BCF model. On the other hand, the same model is applied but using a product (metabolite) formation approach to estimate the reaction rate constant (k_f) (Equations (5) and (6)) and the same BCF-IVIVE model. A summary of the model and further details of the calculations are given in the supplementary material.

$$mPHE_{loss,xh} = \left(mPHE_{medium\ sample}\right)_{xh} - \left(mPHE_{medium\ no\ cells}\right)_{xh} \quad (9)$$

$$\text{Recovery } (\%) = \frac{m_{xh}}{mPHE_{0h}} \cdot 100 \quad (10)$$

Table 1
Concentration found experimentally in the culture medium and in the cells when exposed to 15 mg L^{-1} with HepG2 and ZF4 and 10 mg L^{-1} (A) and 50 mg L^{-1} (B) with ZFL at different exposure times.

Cell lines	Time exposure	Cells Sample (PHE, $\mu g \cdot g^{-1}$)		Medium Sample (PHE, $mg \cdot L^{-1}$)		Medium no cells (PHE, $mg \cdot L^{-1}$)	
HepG2	0h	0.80 ± 0,05		13.2 ± 0.3		13.2 ± 0.3	
	24h	326 ± 68		9 ± 1		11.9 ± 0.8	
	48h	475 ± 115		7 ± 1		10.0 ± 0.2	
	72h	915 ± 134		6.0 ± 0.9		8 ± 1	
ZF4	0h	0.25 ± 0,09		12 ± 3		12 ± 3	
	24h	84 ± 38		9 ± 3		10 ± 2	
	48h	97 ± 21		8 ± 2		9 ± 2	
	72h	89 ± 35		8 ± 2		8 ± 2	
		(A)	(B)	(A)	(B)	(A)	(B)
ZFL	0h	0.7	0.5	6	42	6	42
	24h	19	107	4	19	6	21
	48h	20	110	4	18	5	20
	72h	29	126	4	18	6	20

3. Results and discussion

3.1. Optimization of the analytical procedure

The miniaturised analytical method to quantify PHE and its hydroxylated metabolites was optimized for the HepG2 cell line in the previous study (De Oro-Carretero et al., 2023). The same method was used for the extraction of PHE and metabolites in the ZF4 cell line resulting in good recoveries. The same was observed for PHE extractions in the medium and ZFL cells, as well as for the metabolites in ZFL cells. However, due to the complex exposure medium used for the ZFL cell culture, hexane:MTBE (1:1) worked best for the extraction of the metabolites as shown in Fig. S1. In the previous study, the metabolite 9-OH-PHE was identified as a major metabolite, but its extraction was not optimized and was not quantified. In this study it has been shown to behave in the same way as its isomers, so the same methods were used. All limits of detection and quantification are shown in Tables S5 and S6, respectively.

3.2. Cell viability

The viability test was carried out with the aim of estimating the exposure concentration that results in viability greater than 70% at the end of the test. The dose-response values and their polynomial fit using Origin Pro2021 are shown in Fig. S2. MTT assay for HepG2 cells showed that cell viability decreased by 30% at 22 mg L^{-1} PHE. MTT experiments on the ZFL cell line resulted in a constant viability up to 50 mg L^{-1} PHE that declined to 80% viability. For the ZF4 cell line, the MTT assay was first performed and cell viability was found to decrease by 30% at 40 mg L^{-1}. However, Dong et al., 2020 (Di et al., 2020) observed more than 80% viability up to 100 μg mL^{-1} in HepG2 exposed to PAHs and 70% viability at 10 μg mL^{-1} exposure in ZF4 using a supplemented medium with 1% FBS. So, ZF4 and ZFL are more sensitive than HepG2 to PAH exposure. However, it is important to keep in mind that this study used

10% FBS, which affects the bioavailable concentration for the cells and, therefore, their viability. Consequently, the values shown in this study are not considered to estimate the real toxicity of phenanthrene but are instead intended to determine the appropriate concentration for bioaccumulation and metabolization experiments that maintain at least 70% viability. Since these experiments were conducted with 10% FBS, the viability test was performed under the same conditions. Hamid et al., 2004 (Hamid et al., 2004) compared the MTT assay with the Alamar Blue (resazurin salt) assay in drugs with HepG2 cells, concluding that the latter was more sensitive and that MTT could give false positives or negatives due to inducers and/or inhibitors of metabolic enzymes. Segner H. 1998 (Segner, 1998) found that MTT does not work well with some fish cell lines because of low succinate dehydrogenase activity in mitochondria (Bols et al., 2005). Therefore, it was decided to perform the resazurin salt assay for ZF4 cells obtaining a 30% reduction in viability with 11 mg L^{-1} PHE, which was considered suitable for estimating the exposure concentration in the experiments. Considering these results, it was decided to expose HepG2 and ZF4 to 15 mg L^{-1} and ZFL cells to 10 (Experiment A) and 50 mg L^{-1} (Experiment B). It should be clarified that the solubility of phenanthrene in aqueous media is 0.82 mg L^{-1} (4.6 μM (Kramer et al., 2012)), however, the free dissolved and cell-accessible concentrations were below this limit (see Table S4).

3.3. Bioconcentration, toxicokinetics and biotransformation

Concentrations of PHE and its major metabolites (1-OH, 2-OH, 3-OH, 4-OH and 9-OH-PHE) were determined in HepG2, ZF4 and ZFL cells and in the exposure media of each sample at 0h, 24h, 48h and 72h (Table 1). A high bioconcentration capacity of PHE was observed in HepG2 cells because its concentration increased very quickly over time without reach a steady state. In contrast, in ZF4 and ZFL cells the bioconcentration capacity was lower, with quick uptake up to 24h and stabilization up to 72h of exposure. However, the decrease over time of the PHE concentration in the medium was similar for all three cell lines. Metabolite concentration increased over time for HepG2 and ZFL (Fig. 1) but no metabolite concentrations above the limit of detection and quantification were found in experiments with ZF4, probably because this cell line is not of the hepatic type, where xenobiotics are metabolised (Ewa and Danuta, 2017) and does not have CYP450 enzymes (Kang et al., 2010) like the others. In control samples (blank, no cells, and t = 0 h), no metabolite concentrations above the limits of quantification were found.

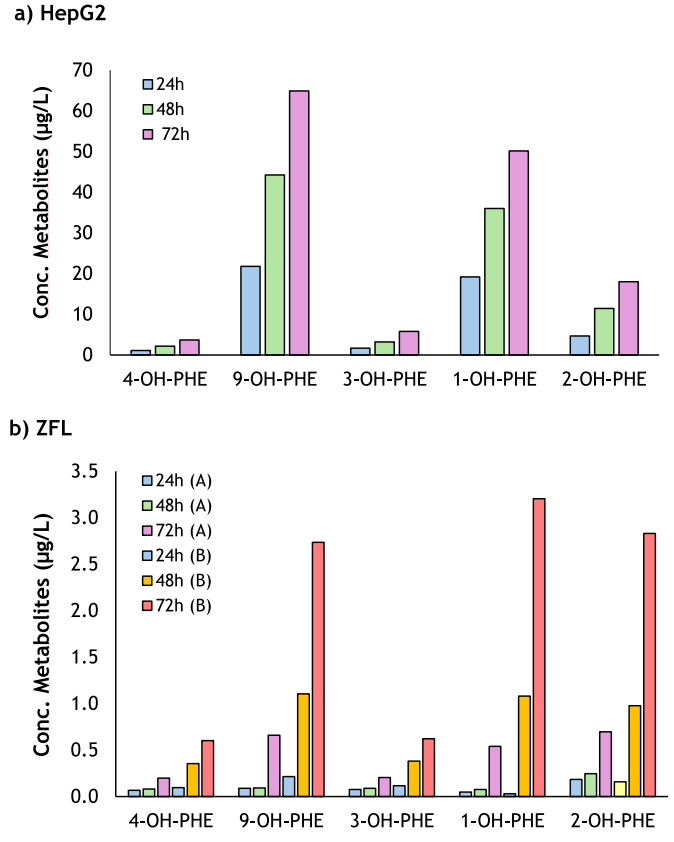

Fig. 1. Transformation of PHE by HepG2 (a) and ZFL (b) over time when exposed to 15 mg L^{-1} and 10 mg L^{-1} (A) and 50 mg L^{-1} (B), respectively.

3.3.1. BCF prediction in in vitro systems with cell lines

As mentioned, BCF was calculated directly using the ratio of concentrations found experimentally in cell lines and growing media (BCF_{exp}, Equation (1)), considering the free dissolved concentration (BCF_{Cfree}, Equation (2)) at each of the times studied (Table 2). Also, for both cases, data was fit using a non-linear regression (Fig. 2) and toxicokinetic values and BCF_k values are calculated for each of the cell lines (Equations (3) and (4)).

For all cases, BCF_{exp} values were much lower than BCF_{Cfree}, as the total concentration measured in the medium is not completely bioavailable, which underestimates the bioaccumulation capacity of the cells. So, for this type of studies with cells, where the analytes can have direct interactions with the components of the growth medium, we consider that it is more correct to use the calculation of the BCFs using the free concentration. When calculating the bioconcentration factors using the first-order toxicokinetic model for HepG2 cells, as concentration found in cells does not reach an steady state value, the values found are different from those previously calculated, showing a BCF_k value greater than BCF_{exp} as this is a projection. In these cases, according to guideline OECD 305 (OECD, 2012), the first-order kinetic fit is a more appropriate estimate for the calculation of BCF. BCF_k values in ZF4 and ZFL cell lines are much closer to BCF_{exp}, as almost achieve a steady state over time, especially in the case of values calculated directly from experimental data. Armitage et al., 2021 (Armitage et al., 2021) provide a review of BCF values for PHE in aquatic environment, including some of the following for vertebrate aquatic animals: Li et al., 2018 (Li et al., 2018), Wang et al., 2018 (Wang et al., 2018) and Xia et al., 2015 (Xia et al., 2015) calculated a BCF of PHE by first-order kinetic fitting in Zebrafish (*Danio rerio*) obtaining values of 913, 584 and 586 L kg^{-1}, respectively. Lo et al., 2016 (Lo et al., 2016) reported a value of 690 L kg^{-1} in Juvenile rainbow trout (Oncorhynchus mykiss), Kobayashi et al., 2013 (Kobayashi et al., 2013) obtained 1040 L kg^{-1} from marine benthic fish, *Pseudopleuronectes yokohamae*, Jonsson et al., 2004 (Jonsson et al., 2004) a value of 1100 L kg^{-1} in *Sheepshead minnow* and Baussant et al., 2001 (Baussant et al., 2001) 963 L kg^{-1} in *Turbot-Scophthalmus maximus*. A summary of these values from the literature together with the values from this study are summarised in Table S7. According to the analysis of variance (ANOVA) performed using Statgraphic 19 (Statgraphics Technologies. Inc, Rockville, MD, USA), the BCF values obtained with HepG2 cells showed significant differences at the 95 % confidence level with respect to those reported in the literature (p = 0.001, Fig. S3a). In contrast, there are no significant differences (p = 0,5533, Fig. S3b) between the data set of experimental values from the literature and the BCF_{Cfree} (72h) and BCF_k (C_{free}) values obtained in this study with ZF4 and ZFL cells. However, BCF_K values considering the toxicokinetics of compounds in an organism are always more suitable for BCF estimation.

In a similar study to this, Balk et al., 2023 (Balk et al., 2023) use the RTL-W1 cell line from rainbow trout liver to estimate bioaccumulation of four different ionic organic compounds, determining experimentally concentrations in cells and culture media, and using same Equation (1) to calculate BCF. Although these authors consider the amount of analytes that adhere to the plastic containers they use, they do not take into account the possible complexation with the growth medium (5% FBS). The results they obtain differ from the QSAR predictions they make using the membrane lipid-water partition coefficient (D_{MLW}). Based on

Table 2
Bioconcentration factor values (BCF_{exp}, BCF_{Cfree} and BCF_k) and toxicokinetic parameters obtained for PHE at exposure concentration of 15 mg L^{-1} in HepG2 and ZF4 and 10 mg L^{-1} (A) and 50 mg L^{-1} (B) in ZFL.

Cell line	Time Exposure	With experimental medium concentration (C_w)					Considering C_{free}				
		BCF_{exp} ($L \cdot kg^{-1}$)	k_1 ($L \cdot \mu g \cdot h^{-1}$)	k_2 ($\mu g \cdot L^{-1}$)	Cw ($\mu g \cdot L^{-1}$)	BCF_k ($L \cdot kg^{-1}$)	BCF_{Cfree} ($L \cdot kg^{-1}$)	k_1 ($L \cdot \mu g \cdot h^{-1}$)	k_2 ($\mu g \cdot L^{-1}$)	C_{free} ($\mu g \cdot L^{-1}$)	BCF_k ($L \cdot kg^{-1}$)
HepG2	24h	37	2.2	0.01	7170	247	2210	127	0.01	122	14919
	48h	70					4040				
	72h	156					8932				
ZF4	24h	9	0.8	0.06	8287	13	520	42	0.06	151	725
	48h	12					652				
	72h	15					639				
ZFL (A)	24h	2	0.3	0.07	5414	4	274	69	0.07	92	986
	48h	3					311				
	72h	4					393				
ZFL (B)	24h	4	2.0	0.09	42216	22	325	117	0.09	718	1300
	48h	6					368				
	72h	7					412				

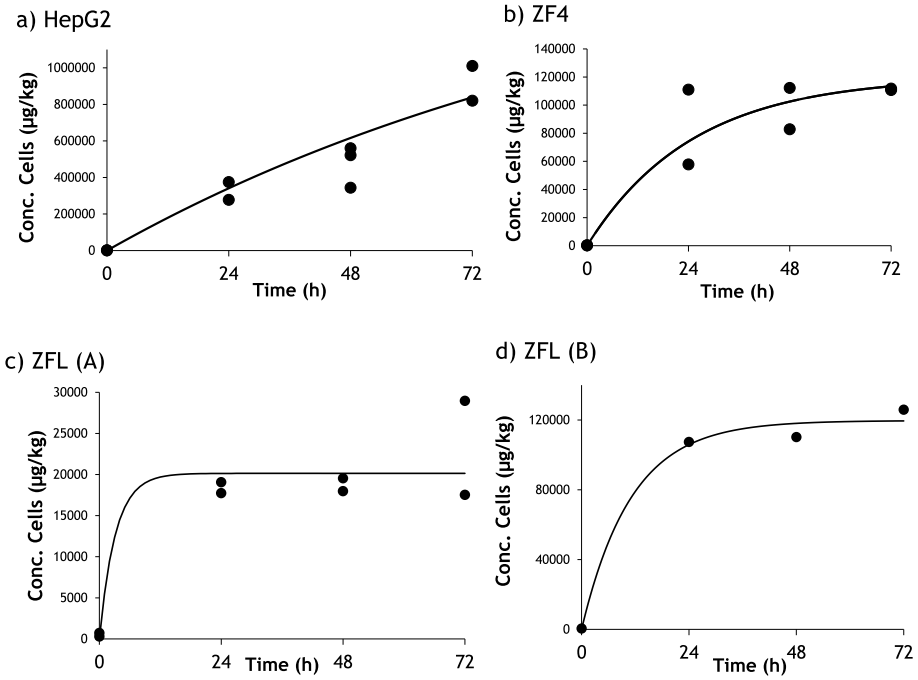

Fig. 2. First-order kinetic fit of the PHE bioconcentration in a) HepG2 (15 mg L^{-1}), b) ZF4 (15 mg L^{-1}), c) ZFL (10 mg L^{-1}, A) and d) ZFL (50 mg L^{-1}, B).

the lipid content in HepG2 cells (3.2% (Fischer et al., 2017)) and fish liver tissues (4% (Balk et al., 2024), bioaccumulation should be similar in the liver cell lines studied. However, the mechanism of absorption, bioaccumulation and biotransformation kinetics must also be considered. The major discrepancy found was the difference in the percentage of uptake that occurred in HepG2 cell lines compared to fish cells (Table S8, Fig. S4). Uptake into liver tissues of apolar-prone xenobiotics such as phenanthrene usually takes place by passive transport (in a chemical concentration gradient from high to low) via simple diffusion between the lipid bilayer or facilitated by membrane transporter proteins, both in human and fish cells (Stott et al., 2015). Because HepG2 are human cancer-like cells, they may be altered, e.g. in these transporter proteins, as well as have a different mechanism of introduction compared to fish cells, which may lead to differences in the uptake of the substances and thus to total bioaccumulation. So, based on these results and because toxicological and bioaccumulation studies are usually carried out in fish models, it was found that the ZF4 and ZFL cell lines with free concentration consideration and the protocol and the analytical determination for cell and medium concentration shown in this study can be a suitable approach for the determination of experimental BCF in a fast, low-cost and non-animal-based method.

3.3.2. *Metabolization constant: depletion and formation approach in IVIVE-BCF model with cells line*

BCF has been estimated with the HepG2, ZF4 and ZFL cells using the IVIVE-BCF model developed by Nichols et al., (2013) (Nichols et al., 2021), where to calculate the metabolization constant two different approaches, first using the rate of substrate depletion in the exposure medium (k_e) (OECD, 2018a) and second, using the method developed in this study based on the rate of formation of the major metabolites (k_f) (Equations (5) and (6)). Both approaches consider the bioavailable concentration (C_{free}) estimated from the experimentally determined concentration in the medium. Table 3 shows the elimination and formation rate calculated from the fits made to the PHE concentration and OH-PHEs concentrations over time (Fig. S5), as well as the parameters calculated afterwards: *In vitro* intrinsic clearance ($CL_{IN\ VITRO,\ INT}$), Hepatic clearance (CL_H), Whole-body metabolism rate (k_{MET}) and BCF_T. For ZF4 because no quantifiable metabolites were found, the formation rate input to the model was zero. According to Black et al., (2021) (Black et al., 2013), a correction was applied to the reaction rate constant (k_e)

Table 3
Input and calculated parameter by IVIVE-BCF model (OECD, 2018c) at exposure concentration of 15 mg L^{-1} in HepG2 and ZF4 and 10 mg L^{-1} (A) and 50 mg L^{-1} (B) in ZFL.

Cell Line	HepG2		ZF4		ZFL (A)		ZFL (B)	
Aproach	Depletion	Formation	Depletion	Formation	Depletion	Formation	Depletion	Formation
Input parameters								
$C_{w,TOT}$ (C_{free}) (mg/L)	0.22	0.22	0.08	0.08	0.1	0.1	0.7	0.7
C_{HEP} (10^6 cells/mL)	0.557	0.557	0.637	0.637	0.557	0.557	0.557	0.557
Reaction Rate (h^{-1})	0.002 ($k_{e,loss}$)	0.001 (k_f)	0.0004 ($k_{e,loss}$)	0 (k_f)	0.004 (k_e)	0.001 (k_f)	0.001 ($k_{e,loss}$)	0.0003 (k_f)
Calculated parameters								
$CL_{IN\ VITRO,\ INT}$ (mL/h/10^6 cells)	0.004	0.0004	0.001	0	0.007	0.002	0.001	0.0005
CL_H (L/d/kg)	0.7	0.3	0.1	0	1.2	0.3	0.2	0.08
k_{MET} (d^{-1})	0.1	0.06	0.02	0	0.2	0.06	0.05	0.02
BCF_{TOT} (L/kg)	1071	1217	1335	1396	898	1231	1253	1344

because the percentage recovery of abiotic losses from volatilisation (% Rec. Vol.) was not within an acceptable range of 80–120% (Table S9). Furthermore, it showed first order kinetics of these losses (Fig. S6) where the reaction rate constant presented a ratio of less than 10 with respect to the depletion rate constant in the samples (Table 3). This correction resulted in a lower metabolization constant and, therefore, a higher BCF. This values obtained with $k_{e,loss}$ were used in the discussion and in the statistical studies. In contrast, the losses of ZFL (experiment A) cells were within this range and therefore did not need to be applied. Because the OECD guidelines use the *in vitro* RT-S9 and RT-HEP systems and trout parameters, the values in this section are treated as hypotheses and preliminary comparative results.

The BCF values obtained with both approaches showed that there were significant differences at the 95% confidence level ($p = 0.003$) with respect experimental *in vivo* values from the literature mentioned on previous section (Table S7). This overestimation may be because the model is based on standardised parameters from trout fish, and zebrafish and human liver have some variation, which would need to be studied. Therefore, the values obtained were closer to the references using more similar aquatic organisms (Fig. S7). However, we consider that we have obtained close values for predicting the bioaccumulation factor. When performing the statistical calculation considering the BCFs obtained individually for each approach, it is found that values obtained using the substrate depletion approach are closer to experimentally calculated with adult fishes (no significant difference, $p = 0.06$, Fig. S7a) compared to using the values of the formation approach ($p = 0.005$, Fig. S7b). This is a consequence of the fact that the reaction constant k_f, calculated with biotransformation data, was found to be lower than k_e, calculated with depletion model, because of the steep drop of substrate concentration versus the low concentration of metabolites formed, resulting in a lower metabolization constant and a higher BCF with the formation approach. These results lead to the conclusion that the use of cell lines can also be useful in the application of the IVIVE-BCF model, improving the cost of experiments and reducing animal experimentation. In addition, it has been shown again that the approach and suppositions set out in the OECD 2018a (OECD, 2018c) have a great potential for BCF assessment, however, as mentioned in this same guideline it has some limitations that need to be further studied to provide more data and improve performance. In this sense, the BCF results and biotransformation kinetics obtained with the methodology developed and the approach of this study can be useful to refine these limitations.

As know, IVIVE-BCF model is defined for the use of primary hepatocytes (RT-HEP) and S9 microsomes (RT-S9) from rainbow trout ad this requires animal experimentation to obtain them and the experiments are limited to 2–4 h of exposure (Fay et al., 2015; Johanning et al., 2012), and, therefore, not suitable for the study of compounds with slow biotransformation kinetics. The use of cell lines provides information on biotransformation kinetics over a longer time up to 72h. In addition, although the immortalised cell lines do not compete as well metabolically as the primary cultures used by IVIVE-BCF (Bell et al., 2018), results obtained in this study shows that the HepG2 and ZFL lines show

Table 4
Resulted recovery (%) in the mass balance at exposure concentration of 15 mg L^{-1} in HepG2 and ZF4 and 10 mg L^{-1} (A) and 50 mg L^{-1} (B) in ZFL.

Time exposure/Cell lines	HepG2	ZF4	ZFL (A)	ZFL (B)
24h	90	87	104	87
48h	82	74	98	72
72h	65	67	82	69

metabolic capacity (Fig. 1 and Fig. S3e,f,g) and that, as the mass balance closes (Table 4), the OH-PHEs studied are the main metabolites and the formation constant represents the major part of the biotransformation.

It is certain that *in vitro* biotransformation data often underpredict actual *in vivo* rates and IVIVE-BCF model with the well-shaken liver model (Nichols et al., 2013) and with the depletion approach gives the highest rates. However, this model is based on the experimental determination of the substrate in the cell medium and it has been shown in this study (section 3.5.1) that cells, and especially liver cells, bioaccumulate and that not all the experimentally determined concentration in the medium was bioavailable, with the result that not all the substrate depletion is biotransformed, some of it remains accumulated. For this reason, it is still necessary to determine the actual concentration inside cells and study the biotransformation kinetics of the compounds to refine the estimation of BCF with this model.

In the IVIVE-BCF model, the nominal concentration (C_{nom}) is used for the BCF calculations (C_{fiss}/C_w) and C_{free} is not considered, assuming that nominal concentration is all bioavailable (Bell et al., 2018). Hennenbeger et al., 2021 (Henneberger et al., 2021) study the difference between $IVIVE_{nom}$ and $IVIVE_{free}$ and report that, although $IVIVE_{nom}$ may still be useful and conservative, $IVIVE_{free}$ should be chosen in preference as it accounts for differences in bioavailability between *in vitro* and *in vivo*. The IVIVE-BCF model performs other calculations where it considers the chemical concentration dissolved in the water ($C_{w,FD}$). However, this concentration is estimated using the concentrations and fractions of particulate and dissolved matter, established by default from models such as Arnot and Gobas, 2003 (Arnot and Gobas, 2003), based on QSAR models for the estimation of BCF in *in vivo* aquatic environments. It is certain that the IVIVE-BCF model has been designed for use in primary hepatocytes or microsomes that do not use FBS for their culture, but it is limited for use with cell lines because the free concentration in the *in vitro* system is highly dependent on the percentage of serum in the culture medium. Therefore, to solve this limitation it is necessary to make a modification as has been done in this study, i.e. to use C_{free} instead of $C_{W,TOT}$ as the concentration in the medium for these calculations. On the other hand, for the extrapolation of the metabolization rate constant (k_{MET}) a correction factor (f_u) is applied that corrects for the difference in free chemical concentration between blood and the *in vitro* system used to measure activity, according to the well-shaken liver model in which it is assumed that there are no diffusion problems (Nichols et al., 2013). However, in an *in vitro* system with cell lines, it has already been shown that this is not the case. In addition,

the results shown in the previous section (section 3.5.1, Table 2), show a great difference between BCF_{free} and BCF_{nom}. This again demonstrates the importance of determining the in-cell concentration in relation to the bioavailable concentration for the cell, rather than using the nominal concentration or the concentration of the cell medium when working in an *in vitro* system with cell lines.

In addition, it has been shown that the combination of the mass balance model for the estimation of the free available concentration in the *in vitro* system and the IVIVE-BCF model can predict BCF using cell lines. Use of immortalised cell lines to complete IVIVE models have been implemented previously by Pree et al., (2016) (Pree and Bruce, 2017) that used HepG2 and ZFL lines as models for the evaluation of PBDE toxicity metrics with IVIVE extrapolation or Bourgeois et al., 2022 (Bourgeois et al., 2022) that combine *in vitro* biotransformation and active transport assays based on RT-HEP and the permanent rainbow trout liver cell line RTL-W1 to predict hepatic clearance.

4. Conclusions

This study had two main objectives: on the one hand, to evaluate whether the HepG2, ZF4 and ZFL cell lines are suitable for BCF and biotransformation kinetics estimation and, on the other hand, to use these cells to improve BCF prediction with the IVIVE model, according to the limitations already mentioned on introduction section (exposure time limitations of RT-HEP and RT-S9, bioaccumulation of very hydrophobic compounds and use of nominal concentration). Both the BCFs directly estimated experimentally *in vitro* and those estimated using the IVIVE model with ZF4 and ZFL cells showed satisfactory concordance with the *in vivo* experimental values found in the literature. But this only occurs when the free concentration was considered. The HepG2 cell line showed an exponential bioaccumulation that does not match with aquatic models normally used without consider their biotransformation processes. However, using the IVIVE model the BCF obtained with HepG2 showed satisfactory concordance with the *in vivo* experimental values found in the literature. Therefore, these results show that the cell lines are suitable for a quick BCF estimation, that it is crucial to consider the free bioavailable concentration for the cells rather than the total concentration in the medium.

On the other hand, this study has shown that when estimating the BCF of hydrophobic compounds, cells may bioaccumulate and therefore part of the substrate concentration would not be metabolised, thus overestimating the metabolization constant with the substrate depletion approximation in the IVIVE-BCF model. The approach and analytical method developed is suitable, rapid, simple, and low-cost for the determination of the parent compound and its metabolites directly inside cells and in the exposure medium to provide information on bioaccumulation and biotransformation kinetics. The use of cell lines, although their metabolic capacity is lower than the *in vitro* systems of primary hepatocytes or microsomes used in the IVIVE-BCF model, allows the study of longer incubations for those compounds with slower kinetics without the need for any animal experimentation. Although these results shown can provide useful information for authors working on the extrapolation of IVIVE models and are promising, further studies with other substances with more hydrophobic properties are needed to generate a large amount of data to compare the advantages of this methodology with other methods that are being proposed as alternatives for the study of bioaccumulation and biotransformation of substances.

CRediT authorship contribution statement

Paloma De Oro-Carretero: Writing – original draft, Visualization, Validation, Supervision, Software, Methodology, Investigation, Formal analysis, Data curation. **Jon Sanz-Landaluze:** Writing – review & editing, Visualization, Validation, Supervision, Software, Resources, Project administration, Methodology, Funding acquisition, Data curation, Conceptualization.

Declaration of competing interest

The authors declare that they have no known competing financial interests or personal relationships that could have appeared to influence the work reported in this paper.

Data availability

Data will be made available on request.

Acknowledgments

The present study was supported by the Spanish Ministry of Science and Innovation [PID 2020 114714 RB 100]. Authors are grateful to Nerea Roher and Marlid Garcia-Ordoñez from Institute of Biotechnology and Biomedicine (Barcelona, Spain) for providing the ZFL cells; to John W. Nichols for providing us with the Spreadsheet of IVIVE-BCF Excel and knowledge about his model; to Sebastian Lungu for providing us with knowledge about the MBM model for the determination of the C_{free} in ZF4 and ZFL. Paloma de Oro thanks the Spanish Ministry of Science and Innovation for her predoctoral contract [PRE2021/097956].

Appendix A. Supplementary data

Supplementary data to this article can be found online at https://doi.org/10.1016/j.chemosphere.2024.143020.

References

Ankley, G.T., Bennett, R.S., Erickson, R.J., Hoff, D.J., Hornung, M.W., Johnson, R.D., Mount, D.R., Nichols, J.W., Russom, C.L., Schmieder, P.K., Serrrano, J.A., Tietge, J. E., Villeneuve, D.L., 2010. Adverse outcome pathways: a conceptual framework to support ecotoxicology research and risk assessment. Environ. Toxicol. Chem. 29, 730–741. https://doi.org/10.1002/etc.34.

Armitage, J.M., Toose, L., Camenzuli, L., Redman, A.D., Parkerton, T.F., Saunders, D., Wheeler, J., Martin, A., Vaiopoulou, E., Arnot, J.A., 2021. Acritical review and weight of evidence approach for assessing the bioaccumulation of phenanthrene in aquatic environments. IEAM 17, 911–925. https://doi.org/10.1002/ieam.4401.

Arnot, J.A., Gobas, F.A.P.C., 2003. A generic QSAR for assessing the bioaccumulation potential of organic chemicals in aquatic food webs. QSAR Comb. Sci. 22, 337–345. https://doi.org/10.1002/qsar.200390023.

Arnot, J.A., Gobas, F.A.P.C., 2006. A review of bioconcentration factor (BCF) and bioaccumulation factor (BAF) assessments for organic chemicals in aquatic organisms. Environ. Rev. 14, 257–297. https://doi.org/10.1139/A06-005.

Balk, F., Hollender, J., Schirmer, K., 2023. Investigating the bioaccumulation potential of anionic organic compounds using a permanent rainbow trout liver cell line. Environ. Inter. 174, 107798 https://doi.org/10.1016/j.envint.2023.107798.

Balk, F., Hüsser, B., Hollender, J., Schirmer, K., 2024. Bioconcentration assessment of three cationic surfactants in permanent fish cell lines. Environ. Sci. Technol. 58, 1452–1461. https://doi.org/10.1021/acs.est.3c05360.

Baussant, T., Sanni, S., Jonsson, G., Skadsheim, A., Børseth, F.G., 2001. Bioaccumulation of polycyclic aromatic compounds: 1. Bioconcentration in two marine species and in semipermeable membrane devices during chronic exposure to dispersed crude oil. Environ. Toxicol. Chem. 20, 1175–1184. https://doi.org/10.1002/etc.5620200606.

Belanger, S.E., Rawlings, J.M., Carr, G.J., 2013. Use of fish embryo toxicity tests for the prediction of acute fish toxicity to chemicals. Environ. Toxicol. Chem. 32, 1768–1783. https://doi.org/10.1002/etc.2244.

Bell, S.M., Chang, X., Wambaugh, J.F., Allen, D.G., Bartels, M., Brouwer, K.L.R., Casey, W.M., Choksi, N., Ferguson, S.S., Fraczkiewicz, G., Jarabek, A.M., Ke, A., Lumen, A., Lynn, S.G., Paini, A., Price, P.S., Ring, C., Simon, T.W., Sipes, N.S., Sprankle, C.S., Strickland, J., Troutman, J., Wetmore, B.A., Kleinstreuer, N.C., 2018. In vitro to in vivo extrapolation for high throughput prioritization and decision making. Toxicol. Vitro 47. https://doi.org/10.1016/j.tiv.2017.11.016.

Birch, H., Kramer, N.I., Mayer, P., 2019. Time-resolved freely dissolved concentrations of semivolatile and hydrophobic test chemicals in in vitro assays - measuring high losses and crossover by headspace solid-phase microextraction. Chem. Res. Toxicol. 32, 1780–1790. https://doi.org/10.1021/acs.chemrestox.9b00133.

Black, S.R., Nichols, J.W., Fay, K.A., Matten, S.R., Lynn, S.G., 2013. Toward improved models for predicting bioconcentration of well-metabolized compounds by rainbow trout using measured rates of in vitro intrinsic clearance. Environ. Toxicol. Chem. 32, 1611–1622. https://doi.org/10.1016/j.tox.2021.152819.

Bols, N.C., Dayeh, V.R., Lee, L.E.J., Schirmer, K., 2005. Use of fish cell lines in the toxicology and ecotoxicology of fish. Piscine cell lines in environmental toxicology. Biochem. Mol. Biol. Fishes 6, 43–84. https://doi.org/10.1016/S1873-0140(05)80005-0.

Bourgeois, Z.M., Comfort, J., Schultz, M., Challis, J.K., Cantin, J., Ji, X., Giesy, J.P., Brinkmann, M., 2022. Hepatic clearance of psychotropic drugs in isolated perfused

fish livers using a combination of two in vitro assays. Environ. Sci. Technol. 56, 15839–15847. https://doi.org/10.1021/acs.est.2c03017.
Brandts, I., Garcia-Ordoñez, M., Tort, L., Teles, M., Roher, N., 2020. Polystyrene nanoplastics accumulate in ZFL cell lysosomes and in zebrafish larvae after acute exposure, inducing a synergistic immune response: in vitro without affecting larval survival in vivo. Environ. Sci.: Nano 7, 2410–2422. https://doi.org/10.1039/d0en00553c.
Castaño, A., Bols, N., Braunbeck, T., Braunbeck, T., Dierickx, P., Halder, M., Isomaa, B., Kawahara, K., Lee, L., Mothersill, C., Pärt, P., Repetto, G., Riego Sintes, J., Rufli, H., Smith, R., Wood, C., Segner, H., 2003. The use of fish cells in ecotoxicology: the report and recommendations of ECVAM workshop 47. ATLA 31, 317–351. https://doi.org/10.1177/026119290303100314.
Cowan-Ellsberry, C.E., McLachlan, M.S., Arnot, J.A., MacLeod, M., McKone, T.E., Wania, F., 2009. Modeling exposure to persistent chemicals in hazard and risk assessment. IEAM 5, 622–679. https://doi.org/10.1897/IEAM_2008-084.1.
De Oro-Carretero, P., Sanz-Landaluze, J., 2023. Bioaccumulation and biotransformation of BDE-47 using zebrafish eleutheroembryos (Danio rerio). Environ. Toxicol. Chem. 42, 835–845. https://doi.org/10.1002/etc.5569.
De Oro-Carretero, P., Sanz-Landaluze J, J., 2023. Miniaturized method for the quantification of persistent organic pollutants and their metabolites in HepG2 cells: assessment of their biotransformation. Anal. Bioanal. Chem. 415, 4813–4825. https://doi.org/10.1007/s00216-023-04781-w.
Di, Dong C., Tsai, M.L., Wang, T.H., Chang, J.H., Chen, C.W., Hung, C.M., 2020. Removal of polycyclic aromatic hydrocarbon (PAH)-contaminated sediments by persulfate oxidation and determination of degradation product cytotoxicity based on HepG2 and ZF4 cell lines. Environ. Sci. Poll. Res. 27, 34596–34605. https://doi.org/10.1007/s11356-019-04421-w.
El-Amrani, S., Pena-Abaurrea, M., Sanz-Landaluze, J., Ramos, L., Guinea, J., Cámara, C., 2012. Bioconcentration of pesticides in Zebrafish eleutheroembryos (Danio rerio). Sci. Total Environ. 425, 184–190. https://doi.org/10.1016/j.scitotenv.2012.02.065.
Ewa, B., Danuta, M.S., 2017. Polycyclic aromatic hydrocarbons and PAH-related DNA adducts. J. Appl. Genet. 58, 321–330. https://doi.org/10.1007/s13353-016-0380-3.
Fay, K.A., Nabb, D.L., Mingoia, R.T., Bischof, I., Nichols, J.W., Segner, H., Johanning, K., Han, X., 2015. Determination of metabolic stability using cryopreserved hepatocytes from rainbow trout (Oncorhynchus mykiss). Curr. Protoc. Toxicol. 65 (4) https://doi.org/10.1002/0471140856.tx0442s65, 42.1-4.42.29.
Fischer, F.C., Henneberger, L., König, M., Bittermann, K., Linden, L., Goss, K., Escher, B. I., 2017. Modeling exposure in the Tox21 in vitro bioassays. Chem. Res. Toxicol. 30, 1197–1208. https://doi.org/10.1021/acs.chemrestox.7b00023.
Fischer, F.C., Cirpka, O.A., Goss, K.U., Henneberger, L., Escher, B.I., 2018. Application of experimental polystyrene partition constants and diffusion coefficients to predict the sorption of neutral organic chemicals to multiwell plates in in vivo and in vitro bioassays. Environ. Sci. Technol. 52, 13511–13522. https://doi.org/10.1021/acs.est.8b04246.
Fu, Q., Fedrizzi, D., Kosfeld, V., Schlechtriem, C., Ganz, V., Derrer, S., Rentsch, D., Hollender, J., 2020. Biotransformation changes bioaccumulation and toxicity of diclofenac in aquatic organisms. Environ. Sci. Technol. 54, 4400–4408. https://doi.org/10.1021/acs.est.9b07127.
Gobas, F.A.P.C., Zhang, X., 1992. Measuring bioconcentration factors and rate constants of chemicals in aquatic organisms under conditions of variable water concentrations and short exposure time. Chemosphere 25, 1961–1971.
Halder, M., Kienzler, A., Whelan, M., 2014. Andrew. EURL ECVAM Strategy to Replace, Reduce and Refine the Use of Fish in Aquatic Toxicity and Bioaccumulation Testing. Worth, and Institute for Health and Consumer Protection. https://data.europa.eu/doi/10.2788/084219.
Hamid, R., Rotshteyn, Y., Rabadi, L., Parikh, R., Bullock, P., 2004. Comparison of alamar blue and MTT assays for high through-put screening. Toxicol. Vitro 703–710. https://doi.org/10.1016/j.tiv.2004.03.012.
Henneberger, L., Mühlenbrink, M., Fischer, F.C., Escher, B.I., 2019a. C18-Coated solid-phase microextraction fibers for the quantification of partitioning of organic acids to proteins, lipids, and cells. Chem. Res. Toxicol. 32, 168–178. https://doi.org/10.1021/acs.chemrestox.8b00249.
Henneberger, L., Mühlenbrink, M., König, M., Schlichting, R., Fischer, F.C., Escher, B.I., 2019b. Quantification of freely dissolved effect concentrations in in vitro cell-based bioassays. Arch. Toxicol. 93, 2295–2305. https://doi.org/10.1007/s00204-019-02498-3.
Henneberger, L., Huchthausen, J., Wojtysiak, N., Escher, B.I., 2021. Quantitative in vitro-to- in vivo extrapolation: nominal versus freely dissolved concentration. Chem. Res. Toxicol. 34, 1175–1182. https://doi.org/10.1021/acs.chemrestox.1c00037.
Johanning, K., Hancock, G., Escher, B., Adekola, A., Bernhard, M.J., Cowan-Ellsberry, C., Domoradzki, J., Dyer, S., Eickhoff, C., Embry, M., Erhardt, S., Fitzsimmons, P., Halder, M., Hill, J., Holden, D., Johnson, R., Rutishauser, S., Segner, H., Schultz, I., Nichols, J., 2012. Assessment of metabolic stability using the rainbow trout (Oncorhynchus mykiss) liver S9 fraction. Curr. Protoc. Toxicol. 1 (14) https://doi.org/10.1002/0471140856.tx1410s53, 10.1-14.10.28.
Jonsson, G., Bechmann, R.K., Bamber, S.D., Baussant, T., 2004. Bioconcentration, biotransformation, and elimination of polycyclic aromatic hydrocarbons in sheepshead minnows (Cyprinodon variegatus) exposed to contaminated seawater. Environ. Toxicol. Chem. 23, 1538–1548. https://doi.org/10.1897/03-173.
Kang, Y., Cheung, K.C., Wong, M.H., 2010. Polycyclic aromatic hydrocarbons (PAHs) in different indoor dusts and their potential cytotoxicity based on two human cell lines. Environ. Int. 36, 542–547. https://doi.org/10.1016/j.envint.2010.04.006.
Knöbel, M., Busser, F.J.M., Rico-Rico, A., Kramer, N.I., Hermens, J.L.M., Hafner, C., Tanneberger, K., Schirmer, K., Scholz, S., 2012. Predicting adult fish acute lethality with the zebrafish embryo: relevance of test duration, endpoints, compound properties, and exposure concentration analysis. Environ. Sci. Technol. 46, 9690–9700. https://doi.org/10.1021/es301729q.
Kobayashi, J., Sakurai, T., Mizukawa, K., Kinoshita, K., Ito, N., Hashimoto, S., Nakajima, D., Kawai, T., Imaizumi, Y., Takada, H., Suzuki, N., 2013. Respiratory uptake kinetics of neutral hydrophobic organic chemicals in a marine benthic fish, Pseudopleuronectes yokohamae. Chemosphere 93, 1479–1486. https://doi.org/10.1016/j.chemosphere.2013.07.031.
Kosfeld, V., Fu, Q., Ebersbach, I., Esser, D., Schauerte, A., Bischof, I., Hollender, J., Schlechtriem, C., 2020. Comparison of alternative methods for bioaccumulation assessment: scope and limitations of in vitro depletion assays with rainbow trout and bioconcentration tests in the freshwater amphipod hyalella azteca. Environ. Toxicol. Chem. 39, 1813–1825. https://doi.org/10.1002/etc.4791.
Kramer, N.I., Krismartina, M., Rico-Rico, A., Blaauboer, B.J., Hermens, J.L.M., 2012. Quantifying processes determining the free concentration of phenanthrene in basal cytotoxicity assays. Chem. Res. Toxicol. 25, 436–445. https://doi.org/10.1021/tx200479k.
Kwon, J.H., Lee, H.J., Escher, B.I., 2020. Bioavailability of hydrophobic organic chemicals on an in vitro metabolic transformation using rat liver S9 fraction. Toxicol. Vitro 66. https://doi.org/10.1016/j.tiv.2020.104835.
Laue, H., Gfeller, H., Jenner, K.J., Nichols, J.W., Kern, S., Natsch, A., 2014. Predicting the bioconcentration of fragrance ingredients by rainbow trout using measured rates of in vitro intrinsic clearance. Environ. Sci. Technol. 48, 9486–9495. https://doi.org/10.1021/es500904h.
Li, Y., Wang, H., Xia, X., Zhai, Y., Lin, H., Wen, W., Wang, Z., 2018. Dissolved organic matter affects both bioconcentration kinetics and steady-state concentrations of polycyclic aromatic hydrocarbons in zebrafish (Danio rerio). Sci. Total Environ. 639, 648–656. https://doi.org/10.1016/j.scitotenv.2018.05.067.
Lo, J.C., Letinski, D.J., Parkerton, T.F., Campbell, D.A., Gobas, F.A.P.C., 2016. In vivo biotransformation rates of organic chemicals in fish: relationship with bioconcentration and biomagnification factors. Environ. Sci. Technol. 50, 13299–13308. https://doi.org/10.1021/acs.est.6b03602.
Lungu-Mitea, S., Vogs, C., Carlsson, G., Montag, M., Frieberg, K., Oskarsson, A., Lundqvist, J., 2021. Modeling bioavailable concentrations in zebrafish cell lines and embryos increases the correlation of toxicity potencies across test systems. Environ. Sci. Technol. 55, 447–457. https://doi.org/10.1021/acs.est.0c04872.
Mackay, D., Fraser, A., 2000. Bioaccumulation of persistent organic chemicals: mechanisms and models. Environ. Poll. 110, 375–391. https://doi.org/10.1016/S0269-7491(00)00162-7.
Nichols, J.W., Schultz, I.R., Fitzsimmons, P.N., 2006. In vitro-in vivo extrapolation of quantitative hepatic biotransformation data for fish. I. A review of methods, and strategies for incorporating intrinsic clearance estimates into chemical kinetic models. Aquatic Toxicol. 78, 74–90. https://doi.org/10.1016/j.aquatox.2006.01.017.
Nichols, J.W., Hoffman, A.D., Ter Laak, T.L., Fitzsimmons, P.N., 2013. Hepatic clearance of 6 polycyclic aromatic hydrocarbons by isolated perfused trout livers: prediction from in vitro clearance by liver S9 fractions. Toxicol. Sci. 136, 359–372. https://doi.org/10.1093/toxsci/kft219.
Nichols, J.W., Huggett, D.B., Arnot, J.A., Fitzsimmons, P.N., Cowan-Ellsberry, C.E., 2021. Evaluation and comparison of in vitro intrinsic clearance rates measured using cryopreserved hepatocytes from humans, rats, and rainbow trout. Toxicology 457, 152819. https://doi.org/10.1002/etc.2219.
Niu, P., Lu, X., Liu, B., Li, Y., Liang, X., Wang, S., Guo, Y., 2020. Bioaccumulation investigation of bisphenol A in HepG2 cells and zebrafishes enabled by cobalt magnetic polystyrene microsphere derived carbon based magnetic solid-phase extraction. Analyst 145, 1433–1444. https://doi.org/10.1039/c9an02324k.
OECD, 2012. Test No. 305: bioaccumulation in fish: aqueous and dietary exposure. OECD Guidel. Test. Chem. 3 https://doi.org/10.1787/9789264185296-en.
OECD, 2013. Test No. 236: fish embryo acute toxicity (FET) test. OECD Guidel. Test. Chem. 2 https://doi.org/10.1787/9789264203709-en.
OECD, 2018a. Test No. 319A: determination of in vitro intrinsic clearance using cryopreserved rainbow trout hepatocytes (RT-HEP). OECD Guidel. Test. Chem. 3 https://doi.org/10.1787/9789264303218-en.
OECD, 2018b. Test No. 319B: determination of in vitro intrinsic clearance using rainbow trout liver S9 sub-cellular fraction (RT-S9). OECD Guidel. Test. Chem. 3 https://doi.org/10.1787/9789264303232-en.
OECD, 2018c. Test No. 280: guidance document on the determination of in vitro intrinsic clearance using cryopreserved hepatocytes (RTHEP) or liver S9 sub-cellular fractions (RT-S9) from rainbow trout and extrapolation to in vivo intrinsic clearance series on testing and assessment. OECD Guidel. Test. Chem. https://one.oecd.org/document/ENV/JM/MONO(2018)12/en/pdf.
OECD, 2021. Test No. 249: fish cell line acute toxicity - the RTgill-W1 cell line assay. OECD Guidel. Test. Chem. 2 https://doi.org/10.1787/c66d5190-en.
Pree, K.L., Bruce, E.D., 2017. Using in vitro to in vivo extrapolation (IVIVE) to develop toxicity metrics for human health risk assessment of polybrominated diphenyl ethers (PBDE). Int. J. Environ. Sci. 74, 42–65. https://doi.org/10.1080/00207233.2016.1226026.
Proença, S., Escher, B.I., Fischer, F.C., Fisher, C., Grégoire, S., Hewitt, N.J., Nicol, B., Paini, A., Kramer, N.I., 2021. Effective exposure of chemicals in in vitro cell systems: a review of chemical distribution models. Toxicol. Vitro 73. https://doi.org/10.1016/j.tiv.2021.105133.
Sanz-Landaluze, J., Pena-Abaurrea, M., Muñoz-Olivas, R., Cámara, C., Ramos, L., 2015. Zebrafish (danio rerio) eleutheroembryo-based procedure for assessing bioaccumulation. Environ. Sci. Technol. 49, 1860–1869. https://doi.org/10.1021/es504685c.
Segner, H., 1998. Fish cell lines as a tool in aquatic toxicology. 1998. EXS 86, 1–38. https://doi.org/10.1007/978-3-0348-8853-0_1.

Segner, H., 2004. Cytotoxicity assays with fish cells as an alternative to the acute lethality test with fish. ATLA 32, 375–382. https://doi.org/10.1177/026119290403200409.

Stott, L.C., Schnell, S., Hogstrand, C., Owen, S.F., Bury, N.R., 2015. A primary fish gill cell culture model to assess pharmaceutical uptake and efflux: evidence for passive and facilitated transport. Aquat. Toxicol. 159, 127–137. https://doi.org/10.1016/j.aquatox.2014.12.007.

Ulrich, N., Endo, S., Brown, T.N., Watanabe, N., Bronner, G., Abraham, M.H., Goss, K.-U., 2017. UFZ-LSER Database v3.2.1 [Internet]. Helmholtz Centre for Environmental Research-UFZ, Leipzig, Germany. Available from: http://www.ufz.de/lserd. (Accessed 5 April 2024).

Wang, H., Li, Y., Xia, X., Xiong, X., 2018. Relationship between metabolic enzyme activities and bioaccumulation kinetics of PAHs in zebrafish (Danio rerio). J. Environ. Sci. 65, 43–52. https://doi.org/10.1016/j.jes.2017.03.037.

Xia, X., Li, H., Yang, Z., Zhang, X., Wang, H., 2015. How does predation affect the bioaccumulation of hydrophobic organic compounds in aquatic organisms? Environ. Sci. Technol. 49, 4911–4920. https://doi.org/10.1021/acs.est.5b00071.

In vitro approach to refine bioconcentration and biotransformation predictions of organic persistent pollutants using cell lines

Supporting information

Modelling free concentration (C_{free}):

The mass balance model (MBM) developed by Fischer et al. 2017 [33] was applied to estimate the protein/lipid bound fractions, depending on the percentage of FBS supplemented and bioavailable concentrations. This model has default parameters set for the HepG2 cell line, however, for ZF4 and ZFL the input data for cell line type and culture medium were left blank and generic parameters were set [12] (Table S1). The binding values for the MBM input of phenanthrene distribution in the relevant BSA and lipid phases were obtained using the UFZ-LSER tool [40] (Table S2). Then, the MBM spreadsheet estimates the fractions of cell (f_{cell}), total medium (f_{medium}), cell membrane (f_{mem}) and the water phase of the medium ($f_{w,medium}$) compartment (Table S3) and applies them to each experimentally determined PHE concentration in the medium to estimate the C_{free} at each exposure time (Table S4).

Table S1. Test system parameters for the experiment with HepG2, ZF4 and ZFL input in Fischer et al. 2017 [33] MBM spreadsheet and system information output from MBM

	HepG2	ZF4	ZFL
Test system parameters			
Medium volume (µL)	10000	10000	10000
Type of base medium	DMEM Glutamax	-	DMEM Glutamax
Fraction of base medium (%)	90	90	90
Type of serum	FBS	FBS	FBS
Fraction of serum (%)	10	10	10
Cell line	HepG2	-	-
Cell number at test start	5571000	6371000	5571000
System information			
Water content (%)	87.4	88.4	88.4
Protein content (%)	9.5	9.3	9.3
Lipid content (%)	3.2	2.3	2.3

Table S2. Chemical parameters input in Fischer et al. 2017 [33]. MBM spreadsheet estimated by LSER Calculation Partition System (pH 7.4, 37 °C) [40].

Compound	log $D_{BSA/w}$ [L/L]	log $D_{lip/w}$ [L/L]
Phenanthrene	3,81	4,67

Table S3. Chemical partitioning estimated by Fischer et al. 2017 [33] MBM spreadsheet.

Cell line	$f_{w,medium}$ (%)	f_{cell} (%)	f_{medium} (%)	f_{mem} (%)
HepG2	1,69	6,04	93,96	4,28
ZF4	1,80	6,54	93,46	4,16
ZFL	1,68	6,12	93,88	3,89

Table S4. Free concentration estimated by Fischer et al. 2017 [33] MBM spreadsheet. The values input and obtained in excel are those expressed in mol/L. The values expressed in µg/L were used for the BCF calculations.

Cell line	Exposure time	$C_{medium\ sample}$ [µg/L]	$C_{medium\ sample}$ [mol/L]	C_{free} [mol/$L_{w,medium}$]	C_{free} [µg/L]
HepG2	0h	13171	7,4 E-05	1,25 E-06	224
	24h	8685	4,9 E-05	8,28 E-07	148
	48h	6921	3,9 E-05	6,60 E-07	118
	72h	6029	3,4 E-05	5,75 E-07	102
ZF4	0h	12269	6,88 E-05	1,25 E-06	85
	24h	8934	5,01 E-05	9,11 E-07	162
	48h	8230	4,62 E-05	8,39 E-07	150
	72h	7698	4,32 E-05	7,85 E-07	140
ZFL	0h	5766	3,24 E-05	5,49 E-07	98
	24h	4089	2,29 E-05	3,90 E-07	69
	48h	3699	2,08 E-05	3,52 E-07	63
	72h	4336	2,43 E-05	4,13 E-07	74
ZFL	0h	42216	2,37 E-04	4,02 E-06	717
	24h	19468	1,09 E-04	1,86 E-06	331
	48h	17609	9,88 E-05	1,68 E-06	299
	72h	18002	1,01 E-04	1,72 E-06	306

Table S5. Limit of detection for PHE and OH-PHE in cells and media samples

LODs (µg·L^{-1})	HepG2		ZF4		ZFL	
Analyte	**Cells**	**Medium**	**Cells**	**Medium**	**Cells**	**Medium**
PHE	1.71	1.12	1.52	2.02	1.03	1.43
4-OH-PHE	2.65	2.15	1.25	1.79	0.38	0.11
9-OH-PHE	2.02	1.87	3.15	4.45	2.40	0.59
3-OH-PHE	2.30	1.59	4.51	11.9	5.26	1.24
1-OH-PHE	1.98	1.11	3.63	4.82	7.22	3.09
2-OH-PHE	2.52	1.67	12.4	11.3	7.11	0.69

Table S6. Limit of quantification for PHE and OH-PHE in cells and media samples

LOQs (µg·L^{-1})	HepG2		ZF4		ZFL	
Analyte	**Cells**	**Medium**	**Cells**	**Medium**	**Cells**	**Medium**
PHE	3.11	2.89	2.86	3.56	2.55	2.87
4-OH-PHE	5.89	4.16	3.25	3.96	0.90	0.28
9-OH-PHE	4.91	3.54	6.91	2.70	6.22	1.22
3-OH-PHE	5.30	4.98	7.61	17.4	2.64	2.62
1-OH-PHE	4.87	3.50	5.61	7.5	3.19	4.10
2-OH-PHE	5.36	4.22	15.7	3.23	3.62	1.04

Table S7. Comparison of BCF values from the literature with the values obtained in this study using different methodologies.

Literature	***in vivo***	*Danio rerio*			*Oncorhynchus mykiss*	*Pseudopleuronectes yokohamae*	*Sheepshead minnow*	*Turbot-Scophthalmus maximus*
	BCF	913	584	586	690	1040	1100	963
This study	***in vitro***	*HepG2*	*ZF4*	*ZFL*	*ZFL*			
	$BCF_{(72h)}$	8932	639	393	412			
	BCF_K	14919	725	986	1300			
	$BCF_{IVIVE\text{-}ke}$	1071	1335	898	1253			
	$BCF_{IVIVE\text{-}kf}$	1217	1396	1231	1344			

Table S8. Percentage losses in cell and cell-free medium samples and percentage uptake of phenanthrene in cells at each exposure time

Cell lines	Time of exposure (h)	Losses in medium with cells (%)*	Losses in medium "no cells" (%)**	% Uptake in cells***
HepG2	24	34	10	24
	48	47	24	24
	72	54	45	9
ZF4	24	27	17	10
	48	33	26	6
	72	37	35	1
ZFL (A)	24	58	42	16
	48	62	44	18
	72	56	45	10
ZFL (B)	24	54	51	3
	48	58	52	5
	72	57	52	5

*Losses in medium with cells (%) $= 100 - \left[\left(\frac{Conc.\ PHE\ in\ medium\ with\ cell\ txh}{Conc.\ PHE\ in\ medium\ 0h}\right) \cdot 100\right]$

**Losses in medium "no cells" (%) $= 100 - \left[\left(\frac{Conc.\ PHE\ in\ medium\ "no\ cells"\ txh}{Conc.\ PHE\ in\ medium\ 0h}\right) \cdot 100\right]$

***Uptake in cells (%) = Losses in medium with cells − Losses in medium "no cells"

Table S9. Recovery of losses from volatilisation (% Rec. Vol) when exposed to 15 mg·L^{-1} in HepG2 and ZF4 experiment and 10 mg·L^{-1} (A) and 50 mg·L^{-1} (B) in ZFL experiment at different exposure times. The percentages were calculated from the ratio of the concentration determined in the medium of the samples without cells ('no cells') from the different exposure times to the initial dilution (time 0h).

% Rec. Vol. / Experiment	HepG2	ZF4	ZFL (A)	ZFL (B)
24h	90	83	97	49
48h	76	74	94	48
72h	59	65	110	48

Figure S1. Recoveries obtained with the different extractants in medium samples of known concentration for a OH-PAH determination.

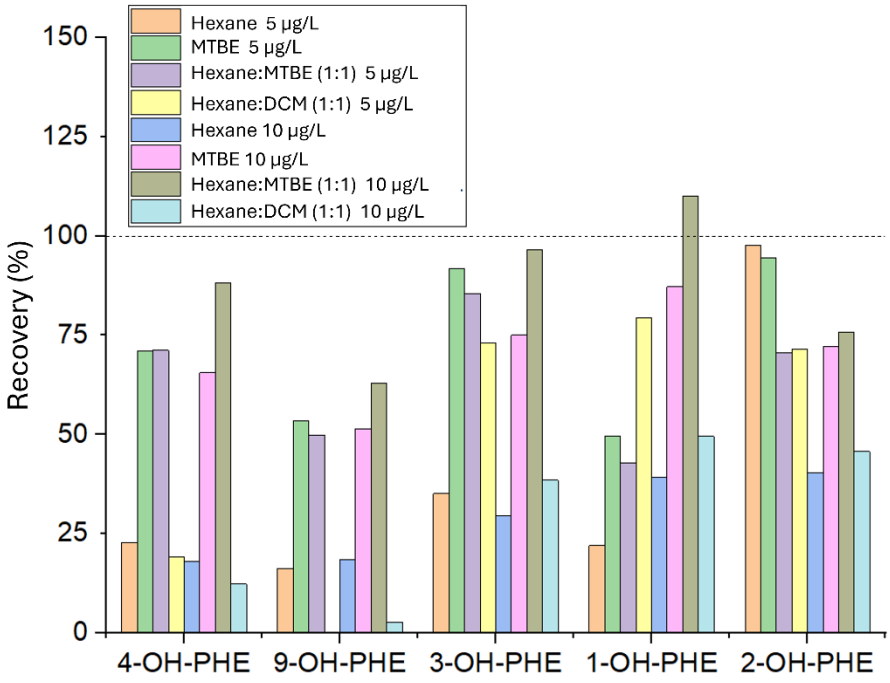

Figure S2. Cell viability of different PHE concentration at 72h of exposure for all types of cell lines.

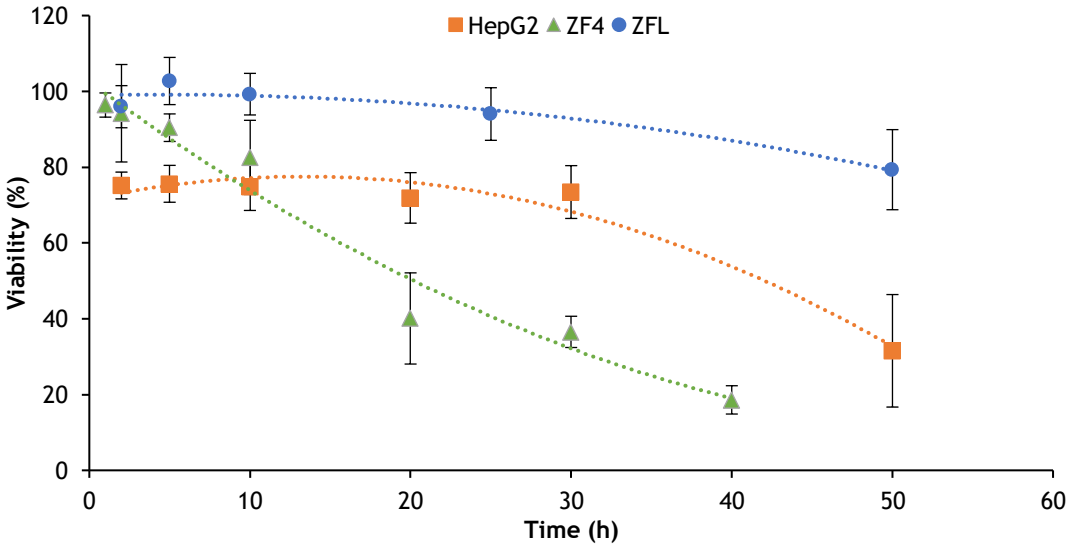

Figure S3. Dispersion of BCFs reported from the literature with BCFs calculated experimentally in this study using the values obtained with (a) ZFL, ZF4 and HepG2 cells or only the values obtained with (b) ZFL and ZF4 cells.

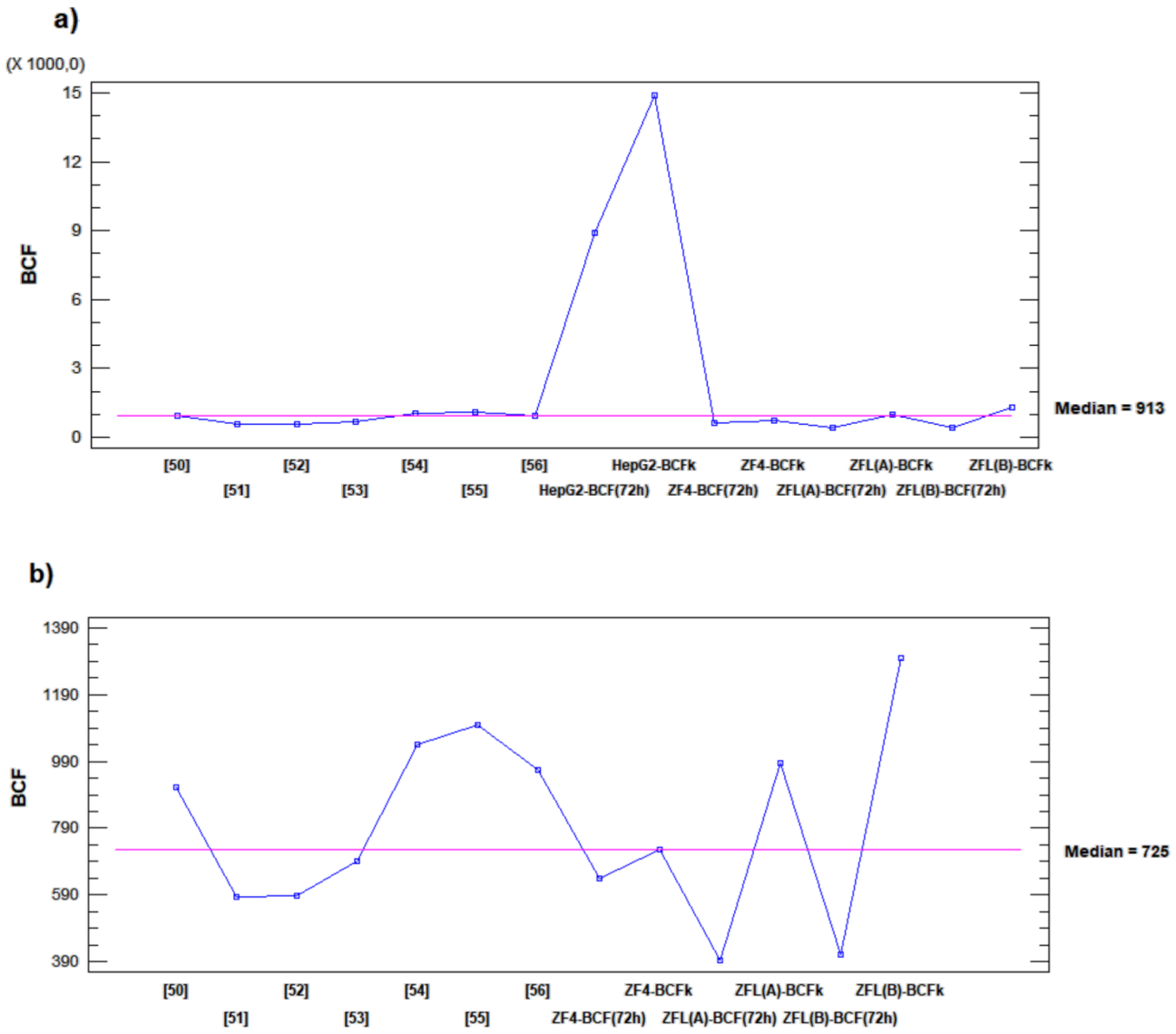

Figure S4. Difference in phenanthrene concentration decline over time in cell-containing medium samples and cell-free medium controls at exposure concentration of 15 mg·L^{-1} in HepG2 (a) and ZF4 (b) and 10 mg·L^{-1} (c) and 50 mg·L^{-1} (d) in ZFL.

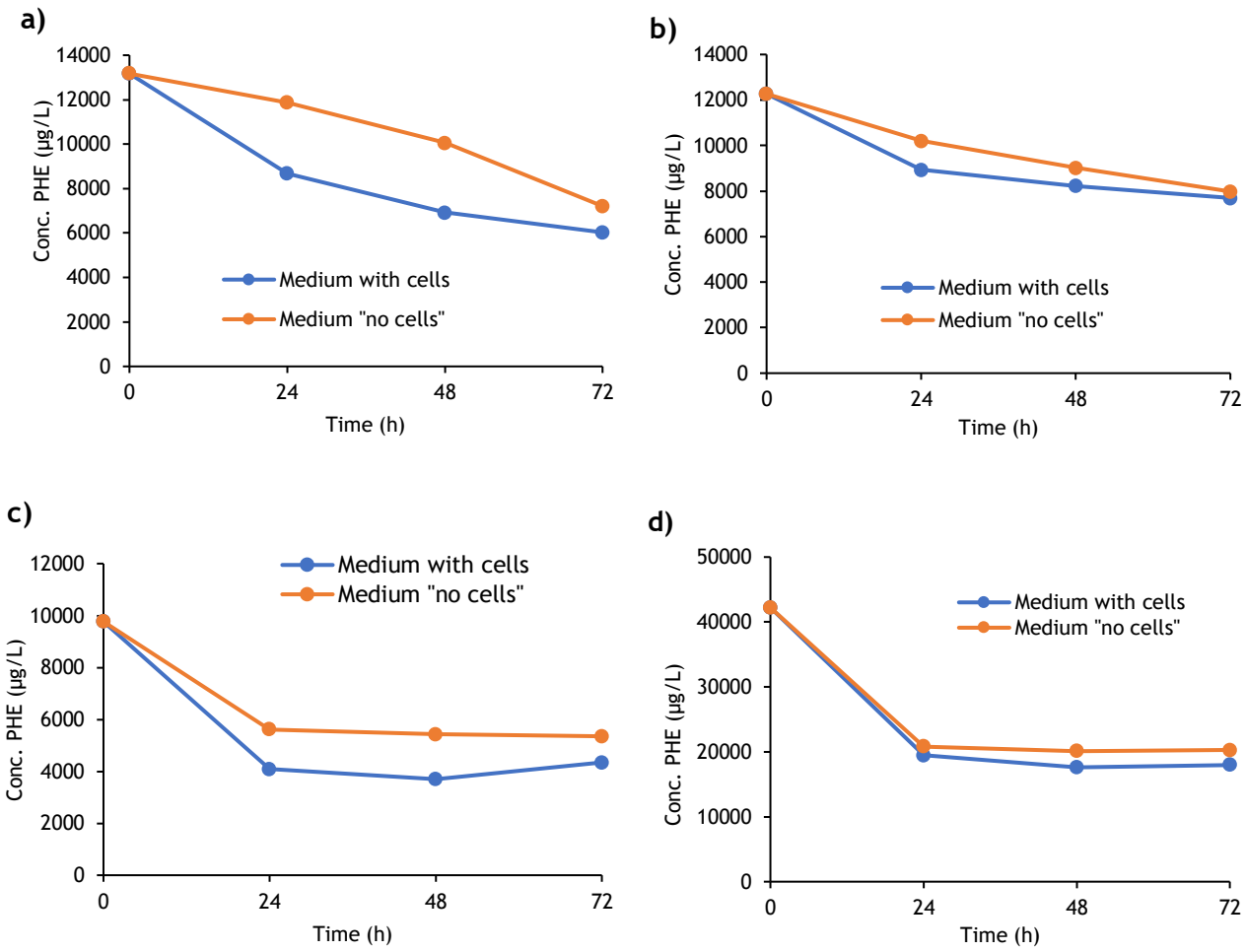

Estimation of intrinsic clearance in vitro for metabolization constant determination and in vivo extrapolation for BCF determination:

The model used is based on the estimation of a metabolization constant (k_{MET}) which is then input into established mass balance models to predict the BCF. For the estimation of this *in vivo* k_{MET}, the *in vitro* intrinsic clearance rate ($CL_{IN\ VITRO,\ INT}$) is estimated and extrapolated to an estimate of hepatic clearance (CL_H).

The estimation of the intrinsic *in vitro* elimination rate was performed using the substrate depletion approach according to OECD 319A [20]. For this purpose, the log10-transformed substrate experimentally concentrations were plotted against time (Figure S5a,b,c,d) and the first-order elimination rate constant (k_e, h^{-1}) was determined as -2.3 × slope of the log-linear decline. According to Black et al. 2021 [44], a correction to the k_e value is applied if the following requirements occur: i) the abiotic losses due to volatilisation observed by calculating the recovery of the negative control samples 'no cells' at each exposure time relative to the initial time are not within an acceptable 80-120% (Table S9), ii) the loss process shows first order kinetics and iii) the ratio of k_e and the volatilisation rate constant (k_{volat}) is less than 10 ($k_e/k_{volat} < 10$). This correction is based on subtracting the volatilisation rate constant (k_{volat}) from the depletion rate constant (k_e). Then, the constant corrected for losses due to volatilisation ($k_{e,loss}$) was determined as -2.3 × slope of the log-linear decline.

In the following, the calculation time based on the BCF-IVIVE model developed by Nichols et al. 2013 [43] and described in the OECD 2018A guideline [22] was used. In the spreadsheet of the model, the values of k_e or $k_{e,loss}$ obtained, the log K_{OW} (PHE = 4.46) and the experimental parameters of the assay were entered: the concentration of cells (C_{HEP}, 10^6 cells/mL) and the total concentration in the medium ($C_{W,TOT}$). For this study, the free concentration estimated (C_{free}) from the total concentration of the medium experimentally determined according to the discussion in the manuscript was introduced in the latter parameter.

On the other hand, in this study, the rate constant was also estimated using the product formation approximation (k_f). This is based on the representation of the experimentally determined metabolite concentration as a function of time (Figure S5e,f,g) and the kinetic fit according to the equations described in the manuscript (Equation 5 and 6). The BCF and all other parameters were estimated with the BCF-IVIVE model in the same way as in the previous case.

Since the OECD guidelines use the *in vitro* RT-S9 and RT-HEP systems and trout parameters, the calculated parameters in this section are treated as hypotheses and preliminary comparative results. The compared parameters were $CL_{IN\ VITRO,\ INT}$, CL_H, k_{MET} and BCF_T (Table 3), because they were those determined with the experimentally obtained values; the rest of the parameters were the same for both models.

Figure S5. Fits performed to determine the reaction rate by substrate depletion method in HepG2 (a), ZF4 (b), ZFL-A (c), ZFL-B (d) and by metabolite formation method in HepG2 (e), ZFL-A (f) y ZFL-B (g). A and B refer to independent experiments performed with ZFL cells at different PHE concentrations (10 mg·L^{-1} and 50 mg·L^{-1}, respectively). HepG2 and ZF4 cells were exposed to 15 mg·L^{-1} PHE.

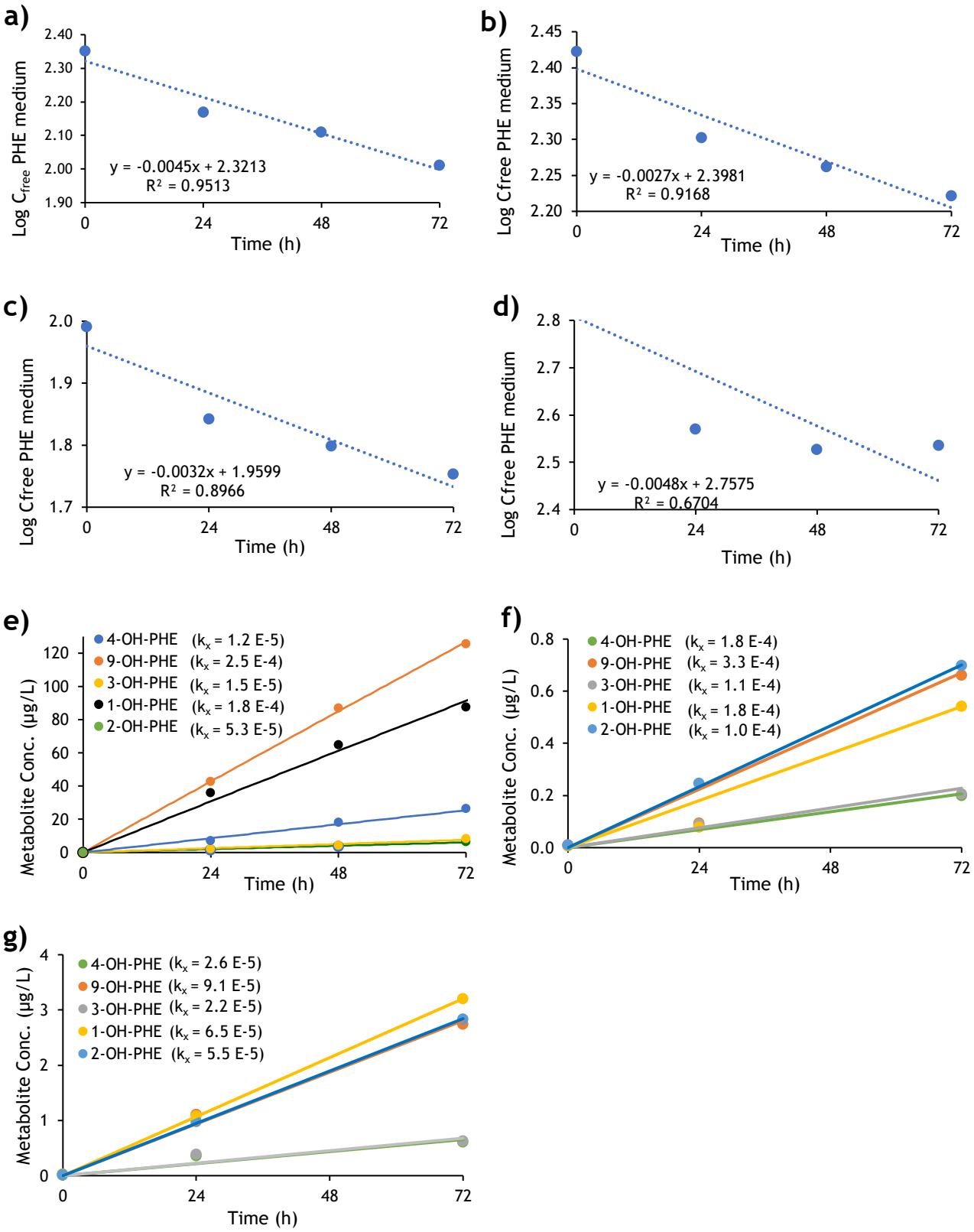

Figure S6. Setting to determine the rate constant of volatilization losses in the a) HepG2, b) ZF4 and c) ZFL (B) cell experiment.

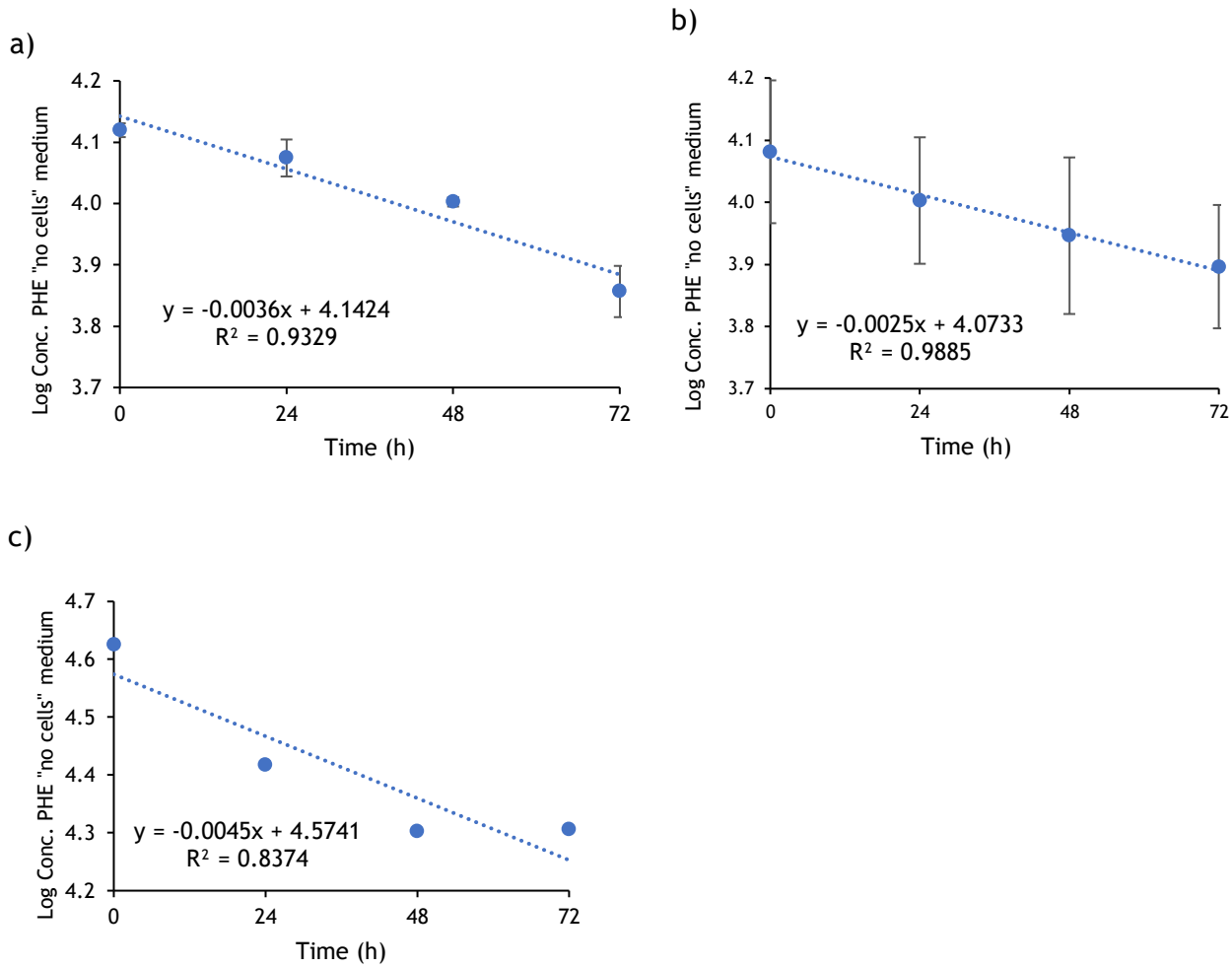

Figure S7. Dispersion of BCFs reported from the literature with BCFs calculated with BCF-IVIVE model using the values obtained with (a) depletion approach and (b) formation approach from HepG2, ZF4 and ZFL experiments.

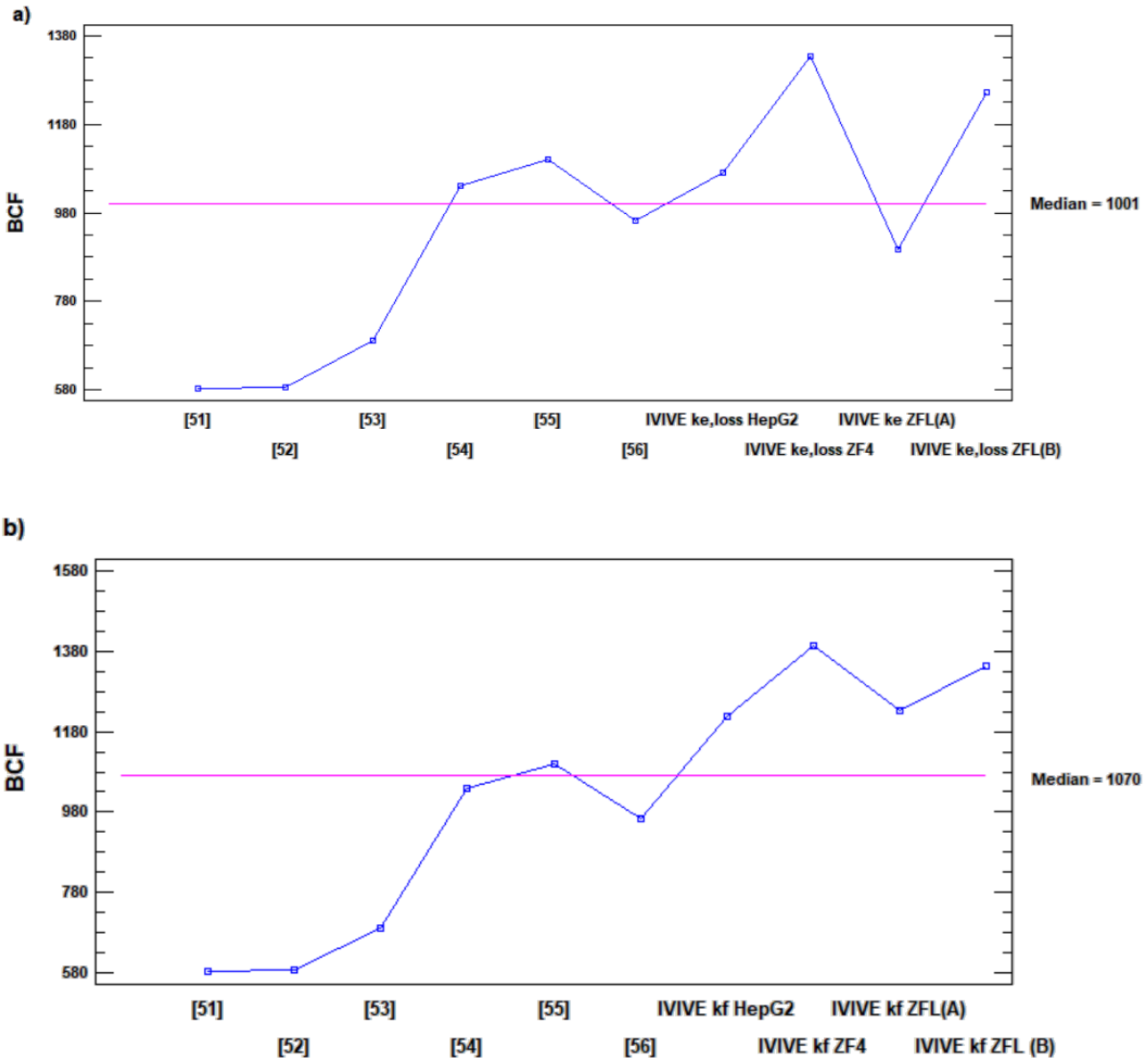

ARTÍCULO 4:

Evaluación de la bioconcentración y biotransformación del BDE-47 *in vitro*: La importancia de las concentraciones biodisponibles e intracelulares.

Assessing bioconcentration and biotransformation of BDE-47 *in vitro*: The relevance of bioavailable and intracellular concentrations.

*Paloma De Oro-Carretero, Jon Sanz-Landaluze**

Journal of Xenobiotics, 15, 93, 2025 (IF: 6.8, Q1)

**Autor de correspondencia.*

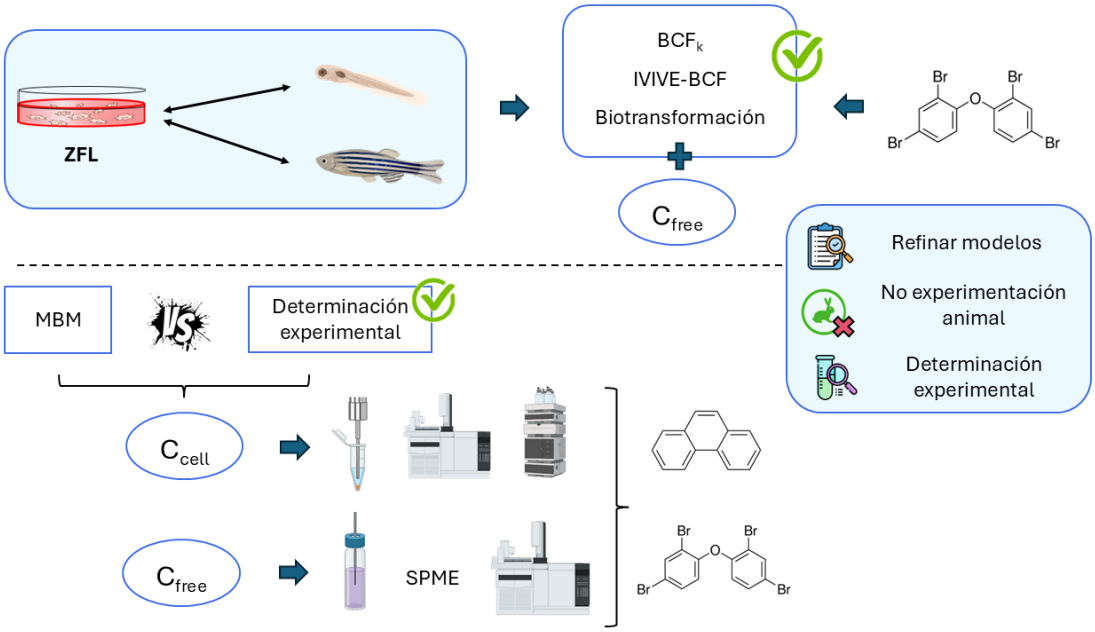

Journal of Xenobiotics

MDPI

Article

Assessing Bioconcentration and Biotransformation of BDE-47 In Vitro: The Relevance of Bioavailable and Intracellular Concentrations

Paloma De Oro-Carretero and Jon Sanz-Landaluze *

Department of Analytical Chemistry, Faculty of Chemical Science, Complutense University of Madrid, Avenida Complutense s/n, 28040 Madrid, Spain; pdeoro@ucm.es

* Correspondence: jsanzlan@ucm.es; Tel.: +34-91-394-4322; Fax: +34-91-394-4329

Abstract: The development of alternative methods that link cellular and predictive toxicity to high-level toxicity is a key focus of current research within the framework of the 3Rs in animal experimentation. In this context, this study aimed to evaluate the previously developed in vitro approach using the zebrafish liver cell line (ZFL) for assessing bioaccumulation and biotransformation of the compound BDE-47, which is more hydrophobic than phenanthrene, and is the compound used in the previous study. For this purpose, experimentally, the internal concentrations in the cells (C_{cell}) and the exposure medium of both BDE-47 and its main metabolites were quantified at different exposure times by GC-MS. Additionally, the free bioavailable concentration (C_{free}) was determined with a solid-phase microextraction (SPME) experiment. With the aim of refine models, C_{cell} and C_{free} were also estimated using a predictive chemical distribution model (MBM). Bioconcentration factors (BCFs) were determined by relating all these values, as well as by toxicokinetic fitting and by in vitro–in vivo extrapolation modelling (IVIVE). The results showed a high concordance with the values obtained in vivo. Moreover, the study highlighted the importance of experimentally determining C_{free} and C_{cell}, as the predicted values can vary depending on the chemical, thereby influencing the BCF outcome. This variation occurs because models do not account for the absorption and biotransformation kinetics of the compounds. The data presented may contribute to refining predictive models.

Keywords: bioaccumulation; biotransformation; in vitro; C_{free}; IVIVE; internal concentration

Academic Editors: Esref Demir and Sam Kacew

Received: 31 March 2025
Revised: 3 June 2025
Accepted: 10 June 2025
Published: 16 June 2025

Citation: De Oro-Carretero, P.; Sanz-Landaluze, J. Assessing Bioconcentration and Biotransformation of BDE-47 In Vitro: The Relevance of Bioavailable and Intracellular Concentrations. *J. Xenobiot.* **2025**, *15*, 93. https://doi.org/10.3390/jox15030093

1. Introduction

Understanding the behavior of chemicals in the environment throughout their life cycle, including bioaccumulation and biotransformation processes, is an essential requirement in ecotoxicological risk assessment and regulatory decision-making [1]. The increasing presence of xenobiotic compounds in the environment, along with the growing demand for 3R (Replacement, Reduction and Refinement) assays, has encouraged the research and design of ethical, fast and economically viable evaluation methodologies [2]. Therefore, emphasis is being placed on the development of alternative fish embryo testing (FET) [3], new approximation methods (NAMs) based on in vitro systems with cell lines [4] and in silico computational modelling and in vitro/in vivo extrapolation models [5].

Within the field of bioaccumulation assessment, Sanz-Landaluze et al. [6] obtained strong correlations of the bioconcentration factor (BCF) using zebrafish (*Danio rerio*) eleutheroembryos and those obtained using adult fish according to the Organization for Economic Co-operation and Development (OECD) guideline 305 [7] for a wide variety of

compounds with different physico-chemical properties. The OECD 2018a guideline [8], referring to the methodology established by Nichols et al. [9], which determines BCF using empirical predictive regression and in vivo extrapolation of in vitro intrinsic clearance (IVIVE), determined according to the OECD 319 guideline [10,11], has shown great potential for BCF prediction. However, it has practical limitations for chemicals metabolized at low rates, due to the use of rainbow trout hepatocyte systems (RT-HEP) and rainbow trout liver subcellular fraction S9 (RT-S9), with assays limited to 4 h. Authors concluded that further studies and different substances are needed to expand the range of applicability of the method. De Oro-Carretero and Sanz-Landaluze evaluated the mentioned IVIVE model with the use of different in vitro systems based on hepatic and/or zebrafish cell lines, allowing assays of up to 72 h, resulting in the use of zebrafish liver cells (ZFL) being a promising approach for the determination of BCF in a quick, cheap and non-experimental way [12]. In addition, the necessity of the determination of the bioavailable concentration (C_{free}) for the cells was demonstrated for a better approximation. This concentration was determined using the mass balance model (MBM) of the different compartments of an in vitro system [13], based on physico-chemical properties of the compounds. It has been shown that for substances with certain physico-chemical properties (more hydrophobic and non-neutral), the modeled C_{free} value may differ from the experimental bioavailable concentration and nominal concentration [14]. Consequently, it is imperative to conduct additional studies on the proposed approach using compounds with varying physicochemical characteristics and reduced metabolization rates.

Polybrominated diphenyl ethers (PBDEs) have been banned for several decades because of their known endocrine toxicity [15]; however, due to their persistent properties [16], the new emerging generation [17], and their metabolites, they continue to be the focus of ecotoxicological study. In this work, the compound 2,2′,4,4′- tetrabromodiphenyl ether (BDE-47) was selected because of its hydrophobic character (log K_{ow} 6.81 [18]), but within the working range of the IVIVE model (log K_{ow} between 3 and 8), and with slower metabolization kinetics, in order to (i) re-evaluate the IVIVE model with the ZFL cell line, (ii) evaluate the determination of C_{free} for BCF approximation with our published in vitro approach, and (iii) evaluate its in vitro biotransformation. The BDE-47 and their main metabolites (BDE-28, hydroxylated and methoxylated compound) concentrations inside the cell (C_{cell}) and in the medium (C_{medium}) were determined using the quick and simple method developed in a previous work [19]. Grasse et al. [20] studied the impact of biotransformation and absorption kinetics on the deviation of MBM model predictions with respect to the internal concentrations of organic compounds in zebrafish embryos for BCF prediction. Therefore, results obtained in these experiments were used to study the deviation of the concentration inside the cells (C_{cell}) obtained by MBM and experimentally for the in vitro determination of BCF. In the same way, the C_{free} values obtained by MBM and those obtained experimentally by a solid-phase microextraction (SPME) experiment [21] were compared. These new results were also compared and discussed together, in this work, with those obtained with the same methodology in the previous study with the compound phenanthrene to provide information on different substances with different behaviors in in vitro systems and in the environment, to help refine the models. Therefore, all references and data found for phenanthrene in this manuscript were either taken from the previous study or calculated from the data reported in this one [12].

2. Materials and Methods

2.1. Reagents and Samples

Solid standard of BDE-47 was purchased from Sigma-Aldrich (Madrid, Spain). Commercial standards of triclosan (TCS) in acetone, and BDE-28 and BDE-99 in methanol were

purchased from Dr. Ehrenstorfer GmbH (Augsburg, Germany); individual standards of 6-MeO-BDE-47, 5-MeO-BDE-47, 3-MeO-BDE-47 in methanol, 5-OH-BDE-47, 3-OH-BDE-47 and 2′-OH-BDE-28 in acetonitrile were supplied by AccuStandard Inc. (New Haven, CT, USA). The derivatization reagent N-tert-butyldimethylsilyl-N-methyltrifuoroacetamide (MTBSTFA) + 1% tert-butyl-methylchlorosilane was supplied by Sigma-Aldrich (Madrid, Spain). High-quality analytical solvents methyl tert-butyl ether (MTBE), dimethyl sulfoxide (DMSO), and hexane were purchased from Scharlab (Barcelona, Spain). Poly (dimethylsiloxane) (PDMS) and Polyacrylate (PA) fibers were supplied by Polymicro Tachnologies, Inc. (Phoenix, AZ, USA).

From Thermo Fisher Scientific (Madrid, Spain), Dulbecco's Modified Eagle Medium (DMEM), Antibiotic/Antimycotic (A/A), TrypLE™ Express, Phosphate Buffered Saline (PBS), Fetal Bovine Serum (FBS), and Trypan Blue 0.4% were obtained. Sigma-Aldrich (Madrid, Spain) supplied bovine insulin, mouse epidermal growth factor (EGF), and 3-(4,5-dimethylthiazol-2-yl)-2,5-diphenyltetrazolium bromide (MTT). The heat-inactivated trout serum was supplied by the Institute of Biotechnology and Biomedicine (Barcelona, Spain). The American Type Culture Collection (ATCC, Manassas, VA, USA) provided the zebrafish liver cell line (ZFL).

ZFL cells were maintained at 28 °C in a humidified atmosphere containing 5% CO_2, using DMEM medium enriched with 10% FBS, 5% antibiotics/antimycotics (A/A), 50 ng/mL EGF, 0.01 mg/mL bovine insulin, and 0.5% heat-inactivated trout serum, following the protocol described by Brandts et al. [22]. The medium was changed every 2 or 3 days and cells passed at 70% confluence.

2.2. Instrument and Apparatus

A Vibra cell VCx130 ultrasound probe from Sonics & Materials Inc., (Newtown, CT, USA) with a 2 mm-diameter titanium microtip and a 130 W high-frequency generator at 20 KHz, Eppendorf 5415R microcentrifuge (Hamburg, Germany), a Genie-2 vortex mixer from Scientific Industries and X50S metal carbide technical nitrogen (Barcelona, Spain) were used for extraction procedures. Incubator-genie from Scientific Industries. CO_2 incubator (MIDI 40), glass and plastic P100 culture plates, 96-well plates and the Multiskan Sky High detector were purchased from Thermo Fisher Scientific (Madrid, Spain).

Instrumental analysis was carried out using an Agilent 7890A Series gas chromatograph, equipped with an HP 7683B autosampler, a microelectron capture detector (μECD), and an HP 5975C VL MSD mass spectrometry detector (Agilent Technologies, Madrid, Spain). Separation was achieved on a ZB-5 capillary column (30 m × 0.25 mm I.D., 0.25 μm film thickness) composed of 95% polydimethylsiloxane.

2.3. Cell Viability Assay

Cell viability was determined by MTT assay. A total of 10,000 cells/well were seeded in 96-well plates under culture conditions for 24 h. Then, the culture medium was replaced by contaminated medium (200 μL) with range of concentrations of BDE-47 (0.2–10 $mg{\cdot}L^{-1}$). Three independent replicates with the same experimental conditions, a control group (cells without pollutant) and a blank group (only cell culture medium) were performed. After 72 h, 20 μL of MTT solution (5 $mg{\cdot}mL^{-1}$) was added to provide a final concentration of 0.5 $mg{\cdot}mL^{-1}$ and incubated for 4 h. Formazan produced in the MTT assay was dissolved using 100 μL DMSO, and absorbance was recorded at 595 nm. The results have been subsequently used for the design of the bioaccumulation and biotransformation experiment.

2.4. Cell Exposure for Bioaccumulation and Biotransformation Evaluation

A total of 2×10^6 ZFL cells were plated in P100 glass dishes and incubated for 24 h under standard culture conditions. Subsequently, the culture medium was replaced with a

contaminated medium, which, according to the cell viability assay, maintained viability above 70% by the end of the exposure period (Section 2.3). Cells were exposed to 1.8 and 2.6 mg·L^{-1} for 24, 48 and 72 h, in two independent experiments. Parallel experiments were conducted under identical conditions to assess losses: one set included cells without contaminated medium, and another consisted of contaminated medium without cells ("no cells"). The obtained pellets were collected from all exposure time, dried under a gentle stream of nitrogen and weighed on a precision analytical balance (±0.00001 g). Finally, the dried cell pellets and their corresponding medium collected at all exposure times, including the starting medium ("t = 0 h"), were stored at −20 °C until analysis.

2.5. Experimental Determination of C_{cell} and C_{medium}

Extraction of BDE-47 and its metabolites was performed simultaneously for each of the samples, cells, and exposure media. Different solvent mixtures were tested as shown in Figure S1. Finally, 500 µL of exposure medium was extracted with 500 µL of hexane: MTBE mixture (1:1) shaken vigorously with a vortex for 30 s. For cells, the pellet obtained (~5 mg) was treated with same solvents but assisted with an ultrasound probe for 1 min at 30% of amplitude and a pulse on/off, with 2 s/5 s for cell samples. The internal standards (IS) BDE-99 and TCS had been previously added. The mixture was centrifuged for 10 min at 10,000 rpm. The organic phase was separated, and the extraction step was repeated. Remaining extracts were evaporated to dryness under a gentle stream of nitrogen and reconstituted in 200 µL isooctane. A total of 80 µL of the volume obtained was derivatized with 20 µL of MTBSTFA at 70 °C for 30 min in the oven and injected into GC-µECD-MS for the OH-BDE quantification. PBDEs and MeO-BDEs were determined by direct injection of the remaining volume of isooctane extracts into the GC-µECD-MS, because PBDEs are not stable after the derivatization process. Due to the difference in concentration in the samples of the metabolites and BDE-47, a double determination was performed and diluted with isooctane for the detection of the latter, so that it was interpolated on the same calibration curve.

The GC–MS-µECD system was used for the separation and determination of BDE-47 and its metabolites. The MS was used for the identification and the µECD for their quantification. Both detectors operate simultaneously, thanks to the use of a flow splitter placed at the end of the chromatographic column. Sample (1 µL) were injected in splitless mode at 280 °C. Helium was used as carrier gas at a constant pressure of 22 psi. Column temperature was programmed to increase from 130 °C (1 min) to 222 °C (1 min) at a rate of 90 °C·min^{-1}, then to 245 °C (1 min) at 1 °C·min^{-1} and finally to 280 °C (8 min) at 45 °C·min^{-1}. The µECD temperature was set at 320 °C and nitrogen was used as makeup gas (30 mL·min^{-1}). The flow ratio of the splitter was 1:1, thanks to the helium input and the restrictor length of each detector, according to the manual supplied by Agilent Technologies [23]. m/z values for the SIM program are collected in Table S1. All limits of detection, quantification and recoveries are shown in Table S2.

2.6. Data Analysis for C_{cell} and C_{free} Prediction with MBM

C_{cell} and C_{free} were determined for the BDE-47 using Fisher et al.'s mass balance model (MBM) [13]. In brief, the test system parameters for the experiment (Table S3) and BDE-47 distribution parameters (Table S4) estimated by the UFZ-LSER Calculation Partition System tool [24] were first entered into the MBM spreadsheet. Although this model includes preset parameters for various cell lines, the input fields for cell-line type and culture medium were left empty for ZFL, and generic parameters were applied instead. Then, data for fractions of cell (f_{cell}), total medium (f_{medium}), cell membrane (f_{mem}) and the water phase of the medium ($f_{w,medium}$) compartment were output (Table S5) and applied to

each experimentally determined BDE-47 C_{medium} to estimate the $C_{free,\ MBM}$ and $C_{cell,\ MBM}$ at each exposure time.

2.7. Experimental Determination of C_{free}

In parallel with the exposure experiment for the evaluation of bioaccumulation and biotransformation described in the previous sections, an experiment was performed to estimate experimentally the free bioavailable concentration ($C_{free,exp}$) in the test medium. For this purpose, an experiment was designed to simulate the test conditions, and C_{free} was determined using solid-phase microextraction (SPME), following the fiber method developed by Henneberger et al. [21].

PDMS-coated glass microfibers (30 µm thick, 13.19 µL/m coating volume) were cut into 1.5 cm pieces and cleaned in methanol for more than 24 h prior to the experiment, with the solvent replaced at least three times. The cleaned and dried fiber was placed in a glass vial with 1 mL of sample exposure medium containing 1.8 and 2.6 mg·L^{-1} BDE-47. Three replicates were prepared for each condition. A portion of the initial sample was stored at −20 °C until analysis. The vials were then sealed and incubated with rotation at 28 °C for 72 h until equilibrium of BDE-47 distribution among the fiber, medium, and binding to the predominant serum protein of the culture (Bovine serum albumin, BSA) was reached [25]. Once at equilibrium, the fibers were extracted from the vials and desorbed with 400 µL isooctane for 24 h with rotation. Finally, the extract was analyzed by GC-MS-µECD, as described in Section 2.5. The concentration of BDE-47 in the initial sample ($C_{med,0h}$) and in the resulting media after equilibration ($C_{med,eq}$) was determined according to the procedure described in Section 2.5, to confirm the actual mass balance.

Since this study evaluates and discusses the behavior of BDE-47 in comparison to observations from a previous study with phenanthrene, as explained in the introduction section, the experimental C_{free} of phenanthrene was also determined, as it had not been measured previously. In this case, the difference in the process was that PA fibers (36 µm thick, 16.71 µL/m coating volume) were used. Samples of 10 and 20 mg·L^{-1} PHE were prepared, and the fibers and samples were incubated for 24–48 h until equilibrium was reached [26,27], and desorbed with hexane for 3 h.

To determine the free concentration, concentration in the SPME fiber (C_{fiber}) was first estimated using Equation (1) from the concentration measured in the desorption extract (C_{des}), the desorption volume (V_{des}) and the coating volume of the fiber (V_{fiber}). This volume was estimated according to the coating volume and the length of the fiber.

$$C_{fiber} = \frac{C_{des} \cdot V_{des}}{V_{fiber}} \quad (1)$$

Next, $C_{free,exp}$ was determined at the time before the SPME fiber was added to the system, according to Equation (2). For this, the concentration measured in the fiber equilibrated with the medium (PDMS-BDE-47-BSA or PA-PHE-BSA), the concentration measured in the initial sample ($C_{med,0h}$), and the partition constant of the equilibrium formed between the fiber and the medium (log $D_{PDMS/medium}$; BDE-47 = 5.84 [25]; log $D_{PA/medium}$; PHE = 6.69 [26]) were used.

$$C_{free} = \frac{C_{med,0h} \cdot V_{sample}}{D_{fiber/medium} \cdot \left(\frac{C_{med,0h} \cdot V_{sample}}{C_{fiber}} - V_{fiber} \right)} \quad (2)$$

2.8. Data Analysis for BCF Determination

2.8.1. BCF Determination by In Vitro Experiment

The first quantitative estimation of BCF was carried out according to the definition of BCF in the official OECD 305 guideline [7]; that is, the ratio between the chemical concentration in the cells (C_{cell}) and the chemical concentration of the surrounding medium (C_{medium}). As explained earlier, C_{cell} can be determined experimentally ($C_{cell,exp}$) or by MBM ($C_{cell,MBM}$). Both these terms can be related to the experimentally determined concentration in the medium (C_{medium}), the free concentration experimentally determined ($C_{free,exp}$) or the free concentration estimated using MBM ($C_{free,MBM}$). The different BCFs obtained from combinations of these values were determined, as shown in Equation (3).

$$BCF_{exp} = \frac{C_{cell,exp}}{C_{medium}};\ BCF_{Cfree} = \frac{C_{cell,exp}}{C_{free}};\ BCF_{MBM} = \frac{C_{cell,MBM}}{C_{free}} \quad (3)$$

The second model to estimate BCF was based on the first-order toxicokinetic model (Equations (4) and (5)), applying mathematical fitting of the experimental concentration values to the theoretical model describing the chemical uptake process [28,29].

$$C_{cell} = \frac{k_1}{k_2} \cdot C_W \left(1 - e^{-k_2 t}\right) \quad (4)$$

$$BCF_k = \frac{C_{cell}}{C_w} = \frac{k_1}{k_2} \quad (5)$$

where C_w is the medium concentration, C_{cell} is the concentration inside cells at any time, t is the exposure time (h), and k_1 ($L \cdot kg^{-1} \cdot h^{-1}$) and k_2 (h^{-1}) are the first-order uptake and elimination rate, respectively. Therefore, the BCF was calculated considering the experimental C_{cell} data ($C_{cell,exp}$) with respect to the C_{medium} ($BCF_{k,Cexp/Cw}$) and with respect to the C_{free} ($BCF_{k,Cexp/Cfree}$), and considering the C_{cell} values obtained with the MBM with respect to C_{medium} ($BCF_{k,CMBM/Cw}$) and with respect to C_{free} ($BCF_{k,CMBM/Cfree}$).

2.8.2. BCF Determination by IVIVE Model

One of the objectives was to assess whether cell lines can be used within the BCF-IVIVE model, relying on intrinsic clearance in vitro, to estimate the biotransformation rate which is subsequently extrapolated to adult fish. This approach is based on the model developed by Nichols et al. [9] and is endorsed by the OECD guideline 319A [10] and OECD 2018a [8]. Briefly, the log10-transformed substrate experimental concentrations in the medium (C_{med}) were plotted against time, and the first-order elimination rate constant (k_e, h^{-1}) was determined as $-2.3 \times$ slope of the log-linear decline. Black et al. [30] indicate that a correction to the elimination rate constant (k_e) should be applied when the following conditions are met: (i) abiotic losses from volatilization, calculated by comparing the recovery of negative control samples ("no cells") at each exposure time to the initial time, fall outside the acceptable range of 80–120%, (ii) the loss process follows first order kinetics, and (iii) the ratio of k_e and the volatilization rate constant (k_{volat}) is below 10 ($k_e/k_{volat} < 10$). Then, the constant corrected for losses due to volatilization ($k_{e,loss}$) was determined as $-2.3 \times$ the difference of the slopes of the sample and the loss control of the log-linear descent. The in vitro constant was then extrapolated to obtain an in vivo metabolization constant (k_{MET}). This was done using experimental cell concentration (C_{HEP}, 10^6 cells/mL) and default parameters derived from rainbow trout. In this study, in addition to estimating BCF with the official model parameters derived from rainbow trout ($BCF_{IVIVE,RT}$), BCF was also estimated with the literature-derived parameters for zebrafish ($BCF_{IVIVE,ZF}$), due to the use of ZFL cells. These exchanged data are shown in Table S6. Finally, the BCF was estimated by the ratio of concentration in the organism to concentration in the medium,

following the standardized model. The concentration in the organism was predicted using the one-compartment model given by Arnot and Gobas [31], which includes the rate constants describing chemical uptake (k_1), loss through the gills (k_2), fecal egestion (k_E), growth rate (k_G) and metabolization rate (k_{MET}). Except for k_{MET}, which is estimated experimentally in vitro, the rest are only dependent on the log K_{OW} of the compound. On the other hand, due to the use of cell lines, the free concentration estimated was introduced instead of the total concentration in the medium ($C_{W,TOT}$).

3. Results and Discussion

3.1. Cell Viability

The dose–response fit is shown in Figure S2. Viability decreased by 30% and 50% with exposure to 0.45 and 2.03 mg·L^{-1} BDE-47, respectively. Yang and Chan also observed similar values of 1.60 and 1.26 mg·L^{-1} LC_{50} (24 h) and LC_{50} (96 h), respectively, using the Alamar Blue viability test for ZFL cells [32]. It is important to consider that these studies employed 10% FBS, which influences the bioavailable concentration to the cells and, consequently, impacts their viability. Therefore, for the calculation of a real value, comparable to studies that do not use such a high composition of supplements in the medium that could interact with BDE-47, the bioavailable concentration should be considered. When applying the percentage of C_{free} obtained in this study (Section 3.2) to the LC_{30} and LC_{50} concentrations obtained, values of 0.55 µg·L^{-1} and 0.12 µg·L^{-1}, respectively, were estimated. Therefore, the MTT assay was performed to estimate the appropriate exposure concentration for bioaccumulation and metabolization experiments, ensuring that cell viability exceeds 70% after 72 h of exposure. Therefore, finally, it was decided to carry out the experiments at 1.8 mg·L^{-1} of BDE-47. Another experiment was performed at a concentration of 2.6 mg·L^{-1} of BDE-47 to find higher concentrations of metabolites.

3.2. Measured Concentrations of BDE-47 in the Culture Medium (Total and Free) and Inside Cells (Experimentally and by MBM)

Concentration of BDE-47 in the exposure media (C_{medium}), in the control medium ($C_{medium,\ no\ cells}$) and inside cells ($C_{cell,exp}$) of each sample at 0 h, 24 h, 48 h and 72 h were determined experimentally, as described in Section 2.5. With the experimental value of C_{medium}, the free concentration ($C_{free,MBM}$) and cell concentration ($C_{cell,MBM}$) were predicted by the mass balance model for each exposure time, as described in Section 2.6. The experimental C_{free} percentage was determined by the SPME fiber experiment, as described in Section 2.7, and applied to the C_{medium} to obtain the experimental C_{free} value ($C_{free,exp}$) for each exposure time. All these results are collected in Figure 1 for the 1.8 mg·L^{-1}. The same trends are found in the 2.6 mg·L^{-1} experiment (Figure S3).

C_{medium} decreased by an average of 79 and 33% over time, from the nominal or initial exposure concentration of the experiment of 1.8 and 2.6 mg·L^{-1}, respectively. This decrease is due to the uptake of BDE-47 into the cells and abiotic losses from the in vitro system. The decrease in $C_{medium,no\ cells}$ observed in the cell-free sample was 29 and 37% with respect to the nominal experimental concentration of 1.8 and 2.6, respectively. Because glass culture plates were used instead of plastic, preventing adhesion losses, and, given the volatile properties of BDE-47 (Henry's law constant (K_H) 1.79 ± 0.21 Pa·m^3·mol^{-1} at 30 °C [33]), the observed losses are likely attributable to evaporation. In a previous study [19], a 14% volatilization loss with an initial exposure of 20 mg·L^{-1} for a HepG2 cell assay at 37 °C was observed (K_H 3.78a ± 0.18 at 30 °C [33]). Therefore, as noted in this work, this loss is dependent on the exposure concentration, so such losses must be quantified and considered for the determination of the metabolization constant with the substrate depletion approach in the IVIVE model (explained in Section 2.8.1), in order not

to overestimate biotransformation and affect the BCF prediction, in accordance with Black et al. [30].

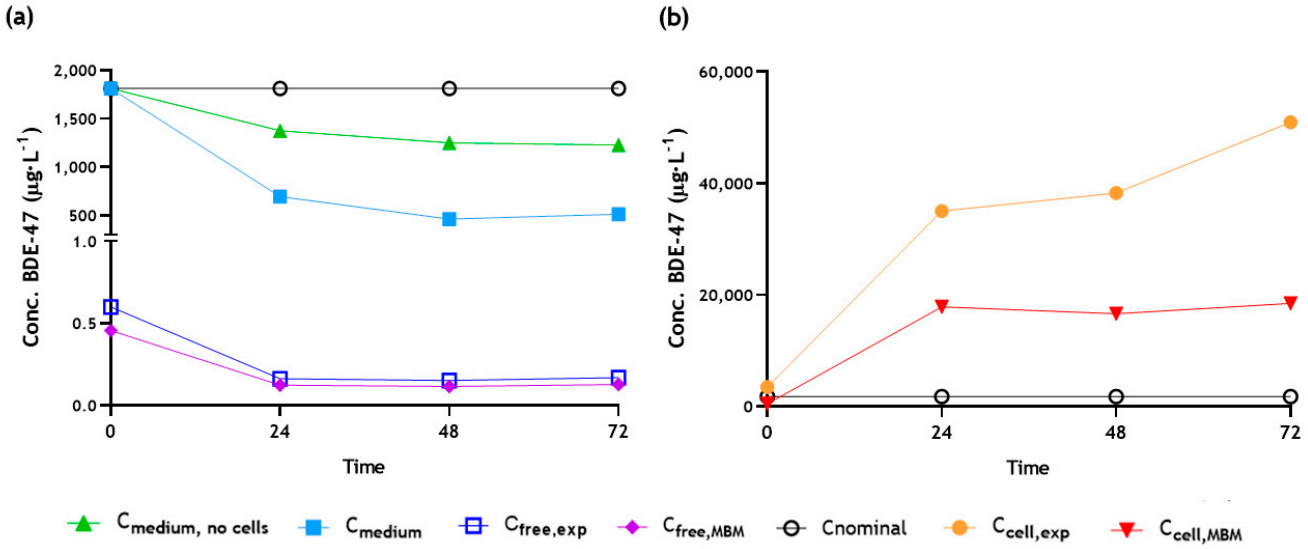

Figure 1. (**a**) Measured values of C_{medium}, $C_{medium,\ no\ cells}$, $C_{free,exp}$ and $C_{free,MBM}$ and (**b**) $C_{cell,exp}$ and $C_{cell,MBM}$ for BDE-47 at different exposure times in the 1.8 mg·L^{-1} experiment ($C_{nominal}$).

Free concentration estimated by MBM ($C_{free,MBM}$) followed the same trend of decreasing with exposure time; however, the values were far below the total concentration present in the medium, with a free concentration of 0.03% of total concentration being observed. Dimitrijevic et al. [34] found stable values of the free concentration over time, but with a decrease from the initial concentration of 30% for the compounds studied with log P_{ow} > 2.59 and up to 50% for the compound tamoxifen (log P_{ow} = 6.84), determined by dialysis in samples of DMEM culture medium supplemented with 10% newborn calf serum and spiked to a final C_{nom} of 5 µmol·L^{-1} with 1% DMSO. Fisher et al. [13] reported that for hydrophobic compounds (log $D_{lipid/water}$ = 7), the free concentration estimated by MBM was up to 4 orders of magnitude lower than the nominal concentration used in their experiments (C_{nom} = 4.86 mg·L^{-1} BDE-47). In a previous study, a free concentration of 1.7% of total concentration for phenanthrene (PHE) assays with ZFL cells was obtained. This difference in behavior between BDE-47 and PHE is due to BDE-47's higher binding constant to the BSA protein of FBS (log DBSA/W = 5.53), compared to PHE (log $D_{BSA/W}$ = 3.81). The BSA protein has three binding domains with two subdomains each [35], and both PAHs and PBDEs bind in the hydrophobic cavities (domains II and III). In the case of PBDEs, the BSA-water partition constant follows a linear trend with respect to the octanol–water partition constant; however, for PAHs this only occurs for those with log K_{ow} < 5 [25], due to binding limitations in the hydrophobic cavities of voluminous PAHs. PBDEs are bulkier but have higher affinity, and other specific binding mechanisms occur, i.e., electrostatic interactions due to the Br of their molecule [36]. This shows that the bioavailable concentration depends not only on the hydrophobicity of the compound, but also on the specific interactions with the serum of the medium and, therefore, it is important to study its behavior in the in vitro system to correctly determine the free concentration.

Regarding the $C_{free,exp}$ determined by SPME experiment, as can be seen in Figures 1a and S3a, the values obtained experimentally did not differ significantly from those obtained by MBM. Table 1 shows the C_{free} values determined, resulting in 0.06% and 0.08% of total concentration in the experiments with 1.8 and 2.6 mg·L^{-1} BDE-47, respectively. The Fisher et al. model [13] is well-defined for various neutral, anionic, cationic and multiprotic organic compounds across different media and cell types. It is not defined for the medium used for

the ZFL cell line. The ZFL cell culture medium, in addition to the 10% FBS considered in the MBM, contains 0.5% rainbow trout serum. The small difference observed in C_{free} calculated from the experiment may be due to the presence of trout serum, which potentially causes a distributional shift in the equilibria present in the in vitro system. As shown in Table S7, trout serum has a higher amount of lipid-to-protein ratio compared to FBS, which may change the interaction dynamics. Given that the trout serum constitutes a small percentage relative to FBS, the interaction is primarily determined by the FBS concentration, resulting in a minimal difference in bioavailable concentration. Huchthausen et al. [14] reported that for substances exhibiting a non-linear binding to the medium components, the modeled C_{free} was underestimated, compared to the experimental one. This difference, although not significant, was observed also for phenanthrene (experimental C_{free} values shown in Table 1), so that bioavailable concentration percentages of 2.4 and 2.9% were obtained experimentally for the 10 and 20 $mg \cdot L^{-1}$ PHE exposures. Even though the MBM estimation yielded close results, experimental determination of C_{free} is strongly encouraged for substances or media types outside the model's defined scope, as demonstrated in this work. Consequently, the BCF results shown in Section 3.3. have been determined using experimental C_{free}.

Table 1. Experimentally estimated bioavailable concentration ($C_{free,exp}$) for BDE-47 and PHE under bioaccumulation and biotransformation experiment conditions.

	C_{nom} ($mg \cdot L^{-1}$)	$C_{free,\ exp}$	% $C_{free,\ exp}$
BDE-47	1.8	(0.4 ± 0.2) $\mu g \cdot L^{-1}$	0.06 ± 0.03
	2.6	(1.14 ± 0.04) $\mu g \cdot L^{-1}$	0.079 ± 0.003
PHE	10	(0.22 ± 0.02) $mg \cdot L^{-1}$	2.4 ± 0.2
	20	(0.52 ± 0.04) $mg \cdot L^{-1}$	2.9 ± 0.2

Due to the bioaccumulative properties of BDE-47 [13,37], C_{cell} values exceeding the initial test concentration were obtained for both experimental and predicted data across all studied time points. Differences between experimental and MBM values were observed. The predicted values show a lower BDE-47 bioaccumulation and the reaching of steady state after 24 h of testing. In contrast, in our previous study on PHE, C_{cell} values estimated with the MBM were significantly higher than those obtained experimentally (the ratio of MBM vs. experimental was above 100%; Table S8). In the same way, Grasse et al. [20] showed that the experimental internal concentrations in zebrafish larvae of 79% of the substances studied (log $D_{lip/w}$: −1.0–6.8) deviated less than 10-fold from the predictions and the rest by up to a factor of 90. These differences can affect the experimental or predicted bioconcentration factor, and consequently, the bioaccumulation assessment of chemicals, as discussed for BDE-47 with ZFL cells in the following section.

3.3. BCF Prediction Using ZFL Cells

3.3.1. BCF Estimation Through In Vitro Assays Using ZFL Cells

BCF results obtained with different approaches explained in Section 2.8.1 are collected in Table 2. First, BCF calculation was based on the ratio between experimentally or MBM-determined cell concentrations and the medium (BCF_{exp} and BCF_{MBM}) or the free dissolved concentration experimentally determined ($BCF_{Cfree,exp}$) (Equation (3)), at each of the times studied. Next, BCF was calculated by fitting the experimental and predicted values using a non-linear regression (Figure S4) and a toxicokinetic model (BCF_k, Equation (5)). The toxicokinetic parameters obtained are reported in Table S9.

Table 2. BCF values ($L \cdot kg^{-1}$) obtained for BDE-47 using in vitro approaches with ZFL cell line.

$C_{nominal}$ BDE-47	1.8 mg·L^{-1}	2.6 mg·L^{-1}
$BCF_{exp,\ 24\ h}$	50	51
$BCF_{exp,\ 48\ h}$	83	55
$BCF_{exp,\ 72\ h}$	100	80
$BCF_{Cfree,exp,\ 24\ h}$	2.2 10^5	1.2 10^5
$BCF_{Cfree,exp,\ 48\ h}$	2.5 10^5	2.1 10^5
$BCF_{Cfree,exp,\ 72\ h}$	3.0 10^5	2.81 10^5
$BCF_{MBM;\ 24\ h,\ 48\ h,\ 72\ h}$	1.4 10^5	1.4 10^5
$BCF_{k\ Ccell\ exp/Cw}$	30	42
$BCF_{k\ Ccell\ MBM/Cw}$	10	23
$BCF_{k\ Ccell\ exp/Cfree,exp}$	74,300	63,435
$BCF_{k\ Ccell\ MBM/Cfree,exp}$	8588	38,558
$BCF_{IVIVE,\ ZF}$	13,885	14,926
$BCF_{IVIVE,\ RT}$	7221	14,184
$BCF_{IVIVE,\ ZF,\ exp}$	22,614	38,948
$BCF_{IVIVE,\ RT,\ exp}$	26,306	48,635

Firstly, the bioconcentration factor (BCF) determined using the experimental total medium concentration (C_{medium}) consistently yielded significantly lower values than when using the free bioavailable concentration, underestimating cellular bioaccumulation capacity (BCF_{exp} vs. $BCF_{Cfree,exp}$). This observation aligns with our previous study on PHE, concluding that, in cell-based assays, where analytes may directly interact with constituents of medium, it is more accurate to calculate BCFs using the free concentration of the analyte. In contrast to results obtained for phenanthrene, $BCF_{k,Cfree}$ and BCF_{Cfree} values resulted in non-matching values. This can be explained because, in the case of BDE-47, steady state was not reached in the ZFL cells during the time of the assay, as it has slower uptake kinetics. In such cases, according to OECD Guideline 305 [7], the first-order kinetic fit provides a more appropriate BCF estimate. Considering $BCF_{k\ Ccell\ exp/Cfree,exp}$ and $BCF_{k\ Ccell\ MBM/Cfree,exp}$ the resulting values were comparable to those obtained in a prior study, where the BCF of BDE-47 using zebrafish eleutheroembryos was determined: $BCF_{48\ h}$ values of 16,392 $L \cdot kg^{-1}$ and 4106 $L \cdot kg^{-1}$ and BCF_k values of 36,363 $L \cdot kg^{-1}$ and 7295 $L \cdot kg^{-1}$ when exposed to 1 $\mu g \cdot L^{-1}$ and 10 $\mu g \cdot L^{-1}$, respectively [38]. A literature review was carried out comparing values obtained in vivo with aquatic organisms and values obtained in silico based on quantitative models of structure–activity relationship (QSAR) models (Table 3). Since there are not many other references in the literature that discuss this topic for BDE47, these values will be used for comparison with the values obtained with the in vitro approach in this study. Briefly, Gustafsson et al. [39] and Vidal-Liñán et al. [40] estimated a BCF of 26,000 $L \cdot kg^{-1}$ and 10,900 $L \cdot kg^{-1}$, respectively, in *Mytilus galloprovincialis* (mussel). With the same degree of magnitude, Mhadhbi et al. [41] reported BCF values of BDE-47 in a young *Psetta maxima* of 24,125, 15,531, and 33,103 $L \cdot kg^{-1}$ at exposure of 1, 0.1, and 0.001 $\mu g \cdot L^{-1}$; Lebrun et al. [42] reported a lower BCF_k in amphipod crustacean *Gammarus pulex*, of close to 5000. The European Chemicals Bureau sets a value of BCF > 5000 in compounds with log K_{ow} between 5 and 8 [41]. Some agencies and authors have developed equations to predict the BCF value in aquatic organisms in relation to the octanol–water partition coefficient [43–47]. These methods are based on the capacity of the substance to be distributed in the lipid fraction, and provide a close approximation of the BCF prediction. Experimentally obtained BCF is preferable because the bioconcentration depends on the physiological responses of each organism, and the absorption and biotransformation kinetics of the compound [48,49].

Table 3. BDE-47 Bioconcentration factor values estimated from the literature and different QSAR models.

Reference	In Vivo Exposure/QSAR Equation	Life Stage	BCF ($L \cdot kg^{-1}$)
[38]	$BCF_{48\,h}$ (1 $\mu g \cdot L^{-1}$)	Zebrafish larvae	16,392
	$BCF_{48\,h}$ (10 $\mu g \cdot L^{-1}$)		4106
	BCF_k (1 $\mu g \cdot L^{-1}$)		36,363
	BCF_k (10 $\mu g \cdot L^{-1}$)		7295
[39]	BCF_k (0.31 $ng \cdot L^{-1}$)	Mytilus galloprovincialis (mussel)	26,000
[40]	BCF_k (8 $\mu g \cdot L^{-1}$)		10,900
[41]	BCF_k (1 $\mu g \cdot L^{-1}$)	young Psetta maxima	24,125
	BCF_k (0.1 $\mu g \cdot L^{-1}$)		15,531
	BCF_k (0.001 $\mu g \cdot L^{-1}$)		33,103
[42]	BCF_k (1 $\mu g \cdot L^{-1}$)	Gammarus pulex	5000
[43]	$\log BCF = -0.20 \cdot \log K_{ow}{}^2 + 2.74 \cdot \log K_{ow} - 4.72$	Aquatic organism	46,200
[44]	$\log BCF = 0.60 \cdot \log K_{ow} - 0.23$	Fish	7180
[45]	$\log BCF = 0.86 \cdot \log K_{ow} - 0.4634$	Zebrafish larvae	247,000
[46]		Fish	13,600
[47]	Total water	Generic lab fish	11,100
	Dissolved water	Generic lab fish	30,800

In the same way, internal concentrations in organisms are often predicted by the mass balance model, assuming passive and non-specific uptake, without modulation of transformation processes, transport and uptake kinetics [50,51]. In this work, it is observed that the estimated $BCF_{k\text{-}CcellMBM/Cfree,exp}$ values were lower than the $BCF_{k\text{-}Ccellexp/Cfree,exp}$ determined with experimental C_{cell}, because this internal value was higher than the one predicted by the Fischer et al. model [13] (Figures 1 and S3). This discrepancy may arise because the model predicts an uptake that reaches steady state at 24 h, but BDE-47, as discussed previously, exhibits slow uptake kinetics in ZFL cells and, based on the experimental values, does not reach stability during the test (Figure S4). In contrast, in our previous study, the estimated C_{cell} values of phenanthrene using the MBM were significantly higher than those obtained experimentally (Table S8), resulting in a higher BCF_{MBM} value (1656 $L \cdot kg^{-1}$) compared to those obtained experimentally with ZFL cells ($BCF_{48\,h}$ = 393 $L \cdot kg^{-1}$ and BCF_k = 986 $L \cdot kg^{-1}$ on exposure to 10 $mg \cdot L^{-1}$ PHE). Unlike BDE-47, phenanthrene reached steady state in ZFL cells during the exposure time (72 h). Although both PAHs and PBDEs undergo biotransformation via cytochrome P450 phase I and II enzymes [52,53], the latter have slower biotransformation kinetics due to their bulkier structure and bromine substituents, which reduce their susceptibility to biotransformation and increase their potential for bioaccumulation. Since phenanthrene is rapidly metabolized and excreted, and these processes are not accounted for in the MBM model, it may result in an over-prediction of the internal concentration in the cell and, consequently, to a higher estimated BCF [20]. Thus, for some substances, the internal concentration estimated by current predictions deviates significantly from the experimental values when the bioaccumulative and biotransformation toxicokinetic of the compound are not considered and, consequently, this could lead to inaccurate assessments of chemical-specific ecotoxicity. Although current models offer rapid screening with a close approximation of substance bioaccumulation, further refinement is required. Incorporating detailed bioaccumulation and biotransformation toxicokinetic studies or supplementing with rapid, simplified assays, such as the in vitro approach presented herein, enhances alignment with experimental observations.

3.3.2. Evaluation of ZFL Cells for BCF Prediction Using the IVIVE Model

BCF was also calculated using the IVIVE-BCF model developed by Nichols et al. [9] with rainbow trout and zebrafish default parameters ($BCF_{IVIVE,RT}$ and $BCF_{IVIVE,ZF}$ Table 2). For this methodology, the fits performed to determine the reaction rate by substrate depletion method and the rate constant of volatilization losses are shown in Figure S5. Following the criteria outlined by Black et al. [30], a correction was applied to the elimination rate constant (k_e) in this study, because the percentage recovery of abiotic volatilization losses (% Rec. Vol.) fell outside the acceptable range of 80–120% (Table S10), the loss process followed first-order kinetics, and the ratio between k_e and the volatilization rate constant (k_{volat}) was less than 10 ($k_e/k_{volat} < 10$). Therefore, Table S11 shows the corrected reaction rate ($k_{e,loss}$) used to determine IVIVE-BCF, as well as the main parameters calculated on the basis of this: in vitro intrinsic clearance ($CL_{IN\ VITRO,\ INT}$), hepatic clearance (CL_H) and whole-body metabolism rate (k_{MET}).

The IVIVE-BCF approach of Nichols et al. [9] is a combination of in vitro and in silico assays, where the absorption (k_1), elimination (k_2), excretion (k_E) and metabolization (k_{MET}) constants are considered. However, while the metabolization constant is derived from in vitro experimental data, the absorption constants and internal organism concentration are estimated solely from the substance's octanol–water partition coefficient, lacking experimental validation. Certainly, the BCF values obtained for BDE-47 using the IVIVE-BCF model (BCF_{IVIVE}, Table 2) strongly match with in vivo values reported in the literature (Table 3), both of those calculated with zebrafish or rainbow trout default parameters. As discussed in Section 3.3.1, predicted intracellular concentrations can deviate significantly from experimental values for certain substances, due to variations in absorption kinetics, which are poorly defined when relying solely on K_{ow}. De Oro-Carretero and Sanz-Landaluze [12] illustrated this phenomenon, wherein the IVIVE-BCF model, utilizing K_{ow}-derived internal concentrations, yielded satisfactory PHE BCF values for ZFL and HepG2 cells. In contrast, the application of experimental cellular internal concentrations within the toxicokinetic model resulted in markedly different BCF values, reflecting the divergent uptake kinetics of the two cell lines. It is shown that, for some substances, it is important to consider the experimental study of the absorption kinetics to obtain a value closer to reality. Therefore, in addition to the BCF_{IVIVE} prediction based on model equations as established by Nichols et al. [8], in this work $BCF_{IVIVE,exp}$ (Table 2) has been calculated in the same way, but using the values of the constants k_1 and k_2 obtained (Table S9) with the experimental values C_{cell} and C_{free}, and adjusting to the units of the model and normalizing with the weight of the fish for extrapolation. Similarly, the values obtained were quite like those obtained in vivo.

With these results, extending our previous in vitro study with phenanthrene, the potential of the IVIVE-BCF model using the ZFL cell line is again demonstrated. This approach enables the evaluation of compounds with slower bioaccumulation and metabolization kinetics, without the need to use hepatocytes and, therefore, animal experimentation. An experimental design and an easy and simple analytical method previously developed [19] have been applied in this study, allowing us to determine the internal concentrations of the cells over time, to estimate the uptake constant experimentally. In this sense, it has been demonstrated that it is possible to incorporate it into the IVIVE-BCF model, as is the case with the determination of the metabolization constant, which, with the combination of extrapolation, can obtain satisfactory results for BCF.

3.4. Biotransformation of BDE-47 in ZFL Cells

This study, along with numerous others on this topic, has demonstrated the importance of studying biotransformation simultaneously with bioaccumulation for accurate BCF

estimation [48,49]. Additional data on the biotransformation of model chemicals in in vitro systems is needed to understand their behavior and for refining predictive models [20].

During exposure of ZFL cells to BDE-47 at 1.6 mg·L^{-1} and 2.8 mg·L^{-1}, concentrations of the metabolites 5-MeO-BDE-47 were detected in the cell samples, and the metabolites 5-OH-BDE-47 and 3-OH-BDE-47 in the medium. The ratios found (the ratio of metabolite concentration to free bioavailable concentration of BDE-47) at each exposure time are shown in Table 4. No concentrations of the mentioned metabolites were detected in the control samples with "no cells" and at the beginning of the experiment ("t = 0 h"), and no concentrations of the metabolites 6-MeO-BDE-47 and 3-MeO-BDE-47 above the limit of quantification were detected in any of the samples. A significant and increasing concentration over time of BDE-28 and 2′-OH-BDE-28 was detected in the cell and medium samples. BDE-28 is a major metabolite resulting from the loss of bromine at the ortho position [54] and, consequently, 2′-OH-BDE-28 is also a metabolite of BDE-47. However, impurities of BDE-28 can be found in commercial BDE-47 standards [55] and, indeed, quantifiable concentrations were found in the 't = 0 h' and 'no cells' samples and, although always below 1% with respect to BDE-47, it cannot be differentiated whether the concentrations found in the samples were due to the biotransformation of BDE-47 or the bioaccumulation of BDE-28 itself, present as impurity. The results for BDE-28 and 2′-OH-BDE-28 were not considered in this study.

Table 4. Biotransformation ratio between metabolites and BDE-47 concentration obtained in this work with ZFL cells and with HepG2 cells and zebrafish larvae obtained in our previous studies.

Model	5-MeO (Cells/Larvae Samples)		3-OH (Medium Samples)		5-OH (Medium Samples)	
$C_{nominal}$ BDE-47	1.6 mg·L^{-1}	2.8 mg·L^{-1}	1.6 mg·L^{-1}	2.8 mg·L^{-1}	1.6 mg·L^{-1}	2.8 mg·L^{-1}
ZFL cells (24 h)	0.11	0.17	0.07	0.08	0.07	0.13
ZFL cells (48 h)	0.12	0.18	0.08	0.08	0.10	0.15
ZFL cells (72 h)	0.15	0.20	0.09	0.15	0.11	0.18
HepG2 cells (48 h)	0.10		0.13		0.2	
Zebrafish embryos (48 h)	0.06–0.13		-		-	

Hydroxylated metabolites (OH-BDEs) were detected in the medium samples, likely due to phase I detoxification reactions involving the introduction of a polar hydroxyl group, facilitating their excretion. Conversely, methoxylated metabolites, derived from the interconversion of OH-BDEs, were found predominantly in the cell samples, presumably because their lower polarity hinders cellular excretion [52]. Similar results were reported when exposing 20 mg·L^{-1} BDE-47 to HepG2 cells [19]. These metabolites can be coupled normally to endogenous compounds in phase II to form other intermediate metabolites. A mass balance (Equations (6) and (7)) has been performed, considering the experimentally determined concentrations of BDE-47 and its metabolites in the cells and the exposure medium at each exposure time (*xh*), as well as the losses due to the volatility of the compound (Equation (8)), and the recovery at the end of the test was estimated (Equation (9)). While acceptable recovery percentages exceeding 70% were achieved (Table 5), the development of a method for the in vitro identification and quantification of intermediate metabolites is crucial for future studies, enabling more comprehensive analysis and subsequent modeling.

$$m_{Total} = mBDE47_{0h} = m_{xh} \quad (6)$$

$$m_{xh} = (mBDE47_{medium})_{xh} + (mBDE47_{cells})_{xh} + (mBDE47_{loss})_{xh} + \left(\sum mMetab._{medium}\right)_{xh} + \left(\sum mMetab._{cells}\right)_{xh} \quad (7)$$

$$mBDE47_{loss\,xh} = \left(mBDE47_{medium\ sample}\right)_{xh} - \left(mBDE47_{medium\ no\ cells}\right)_{xh} \quad (8)$$

$$\text{Recovery}(\%) = \frac{m_{xh}}{mBDE47_{0h}} \cdot 100 \quad (9)$$

Table 5. Recovery (%) obtained in the mass balance at 1.8 mg·L^{-1} and 2.6 mg·L^{-1} of BDE-47 in ZFL.

Time Exposure	Experiment 1.8 mg·L^{-1}	Experiment 2.6 mg·L^{-1}
24 h	77	79
48 h	70	82
72 h	74	97

Using previously obtained data in the exposure of BDE-47 to HepG2 cells and considering the estimated C_{free} percentage, the ratios of the metabolites found were calculated (Table 4), finding ratios very similar for both types of cells from human and fish [19]. All these results, together with those obtained previously with phenanthrene [12], confirms the metabolizing capacity of ZFL cells of compounds with slower kinetics.

In the comparison of in vitro and in vivo values, because in previously reported values with zebrafish eleutheroembryos only the metabolites inside the larvae were determined, not those in the exposure medium, therefore only 5-MeO-BDE-47 is comparable to the results with ZFL cells [38]. The estimated in vivo ratio (Table 4) was of the same order of magnitude as those obtained with the in vitro data. Lungu et al. [51] reported a strong correlation between ZFL cell-line assays, zebrafish embryo assays and in vivo adult zebrafish assays for toxicity effect measurements, but only when linked to modeled bioavailable concentrations. Thus, awaiting further testing with other types of substances, the results obtained show the viability of ZFL cells for biotransformation studies, opening the possibility of being used in IVIVE models for the determination of BCF.

4. Conclusions

This study aimed to re-evaluate our previously developed in vitro approach using a more hydrophobic compound with slower biotransformation kinetics: BDE-47 compared to phenanthrene. Our findings confirm the potential of using zebrafish liver (ZFL) cell lines and the determination of free available concentration (C_{free}) for estimating bioconcentration factors (BCFs) within IVIVE frameworks. The experimental BCF values obtained using this in vitro system showed good agreement with those reported in vivo and from QSAR predictions, supporting its use as a reliable and animal-free alternative.

We also observed that internal concentrations estimated by mass balance models (MBM) may deviate from experimental values, particularly for substances with complex uptake or metabolic kinetics. This highlights the importance of integrating experimental data on absorption, internal concentrations, and metabolization, to improve model accuracy.

Finally, the analytical method and experimental design applied here proved to be rapid, cost-effective, and suitable for integration into IVIVE-BCF modeling. This contributes valuable insights toward refining predictive models and reducing the need for animal testing in environmental risk assessment.

Supplementary Materials: The following supporting information can be downloaded at: https://www.mdpi.com/article/10.3390/jox15030093/s1, Table S1: Mass spectrometer conditions in SIM mode for BDE-47 and their metabolites; Table S2: Limits of detection (LODs), limits of quantification (LOQs) and recoveries for BDE-47 and its metabolites in cells and media samples; Table S3: Test system parameters for the experiment input in MBM spreadsheet and system information output from MBM; Table S4: Chemical parameters input in MBM spreadsheet estimated by UFZ-LSER

Calculation Partition System (pH 7.4, 37 °C); Table S5: Chemical partitioning estimated by MBM spreadsheet; Table S6: Default parameters derived from rainbow trout and zebrafish for IVIVE-BCF estimation model; Table S7: Amount of protein and lipid content in fetal bovine serum (FBS) and rainbow trout serum used to supplement the ZFL cel-l line culture medium; Table S8: Ratio (in %) of the internal concentration estimated by MBM and experimentally for the BDE-47 experiment of this work and the PHE experiment in our previous work, in ZFL cells; Table S9. Toxicokinetic parameters calculated with the cell concentration values obtained experimentally or by MBM and C_{free} obtained experimentally for BDE-47 bioconcentration at 1.8 mg·L^{-1} and 2.6 mg·L^{-1}; Table S10: Recovery of losses from volatilization (% Rec. Vol) when exposed to 1.8 mg·L^{-1} and 2.6 mg·L^{-1} at different exposure times. The percentages were calculated from the ratio of the concentration determined in the medium of the samples without cells ('no cells') from the different exposure times, to the initial dilution (time 0 h); Table S11: Input and calculated parameter by IVIVE-BCF model at 1.8 mg·L^{-1} and 2.6 mg·L^{-1} of BDE-47 using the zebrafish (ZF) and rainbow trout (RT) default parameters (shown in Table S5). The BCF $BCF_{IVIVE,RT}$ and $BCF_{IVIVE,ZF}$ are shown in Table 2; Figure S1: Recoveries obtained with the different extractants in medium samples of known concentration (5 µg·L^{-1}); Figure S2: ZFL cell viability of different BDE-47 concentration at 72 h; Figure S3. (a) Measured values of C_{medium}, $C_{medium,\ no\ cells}$, $C_{free,exp}$ and $C_{free,MBM}$ and (b) $C_{cell,exp}$ and $C_{cell,MBM}$ for BDE-47 at different exposure times in the 2.6 mg·L^{-1} experiment ($C_{nominal}$); Figure S4: First-order kinetic fit of the BDE-47 internal concentration in ZFL cells determined experimentally in the 1.8 (a) and 2.6 mg·L^{-1} (b) experiment; and by MBM in the 1.8 (c) and 2.6 mg·L^{-1} (d) experiment; Figure S5: Fits performed to determine the reaction rate (k_e) by BDE-47 depletion in the 1.8 (a) and 2.6 mg·L^{-1} (b) experiment method and the rate constant of BDE-47 volatilization losses ($k_{e,volat}$) in the 1.8 (c) and 2 mg·L^{-1} (d) experiment; References [8,9,12,13,24,56–58] are cited in the supplementary materials.

Author Contributions: P.D.O.-C.: data curation; formal analysis; investigation; methodology; software; supervision; validation; visualization; roles/writing—original draft. J.S.-L.: conceptualization; data curation; funding acquisition; methodology; project administration; resources; software; supervision; validation; visualization; writing—review and editing. All authors have read and agreed to the published version of the manuscript.

Funding: Support for this study was provided by the Spanish Ministry of Science and Innovation [PID2023-148425NB-I00].

Institutional Review Board Statement: Not applicable.

Informed Consent Statement: Not applicable.

Data Availability Statement: No additional data.

Acknowledgments: The authors gratefully acknowledge Nerea Roher and Marlid Garcia-Ordoñez from the Institute of Biotechnology and Biomedicine (Barcelona, Spain) for supplying the ZFL cells. We also thank John W. Nichols for providing the IVIVE-BCF Excel spreadsheet and for sharing his expertise on the model, as well as Sebastian Lungu for his valuable guidance regarding the MBM model for the determination of the C_{free} in ZFL, and Luise Henneberger for providing us with knowledge on the determination of C_{free} by SPME fibers and for facilitating PA and PDMS fibers. Paloma de Oro thanks the Spanish Ministry of Science and Innovation for her predoctoral contract [PRE2021/097956].

Conflicts of Interest: The authors declare no conflict of interest.

References

1. Bertato, L.; Chirico, N.; Papa, E. Predicting the Bioconcentration Factor in Fish from Molecular Structures. *Toxics* **2022**, *10*, 581. [CrossRef] [PubMed]
2. Hartung, T. Lessons Learned from Alternative Methods and Their Validation for a New Toxicology in the 21st Century. *J. Toxicol. Environ. Health-Part B Crit. Rev.* **2010**, *13*, 277–290. [CrossRef] [PubMed]
3. OECD. Test No. 236: Fish Embryo Acute Toxicity (FET) Test. *Guidel. Test. Chem.* **2013**, 2. Available online: https://www.oecd.org/en/publications/test-no-236-fish-embryo-acute-toxicity-fet-test_9789264203709-en.html (accessed on 19 October 2024).

4. OECD. Test No. 249: Fish Cell Line Acute Toxicity: The RTgill-W1 Cell Line Assay. *Guidel. Test. Chem.* **2021**. Available online: https://www.oecd.org/en/publications/test-no-249-fish-cell-line-acute-toxicity-the-rtgill-w1-cell-line-assay_c66d5190-en.html (accessed on 19 October 2024).
5. Pree, K.L.; Bruce, E.D. Using in Vitro to in Vivo Extrapolation (IVIVE) to Develop Toxicity Metrics for Human Health Risk Assessment of Polybrominated Diphenyl Ethers (PBDE). *Int. J. Environ. Stud.* **2017**, *74*, 42–65. [CrossRef]
6. Sanz-Landaluze, J.; Pena-Abaurrea, M.; Muñoz-Olivas, R.; Cámara, C.; Ramos, L. Zebrafish (*Danio rerio*) Eleutheroembryo-Based Procedure for Assessing Bioaccumulation. *Environ. Sci. Technol.* **2015**, *49*, 1860–1869. [CrossRef]
7. OECD. *Test No. 305: Bioaccumulation in Fish: Aqueous and Dietary Exposure*; OECD Publishing: Paris, France, 2012; Volume 3. [CrossRef]
8. OECD. Test No. 280: Guidance Document on the Determination of in Vitro Intrinsic Clearance Using Cryopreserved Hepatocytes (RT-HEP) or Liver S9 Sub-Cellular Fractions (RT-S9) from Rainbow Trout and Extrapolation to in Vivo Intrinsic Clearance Series on Testing and Assessment. *Guidel. Test. Chem.* **2018**. Available online: https://one.oecd.org/document/ENV/JM/MONO(2018)12/en/pdf (accessed on 19 October 2024).
9. Nichols, J.W.; Huggett, D.B.; Arnot, J.A.; Fitzsimmons, P.N.; Cowan-Ellsberry, C.E. Toward Improved Models for Predicting Bioconcentration of Well-Metabolized Compounds by Rainbow Trout Using Measured Rates of in Vitro Intrinsic Clearance. *Environ. Toxicol. Chem.* **2013**, *32*, 1611–1622. [CrossRef]
10. OECD. Test No. 319A: Determination of in Vitro Intrinsic Clearance Using Cryopreserved Rainbow Trout Hepatocytes (RT-HEP). *Guidel. Test. Chem.* **2018**, *3*. [CrossRef]
11. OECD. Test No. 319B: Determination of in Vitro Intrinsic Clearance Using Rainbow Trout Liver S9 Sub-Cellular Fraction (RT-S9). *Guidel. Test. Chem.* **2018**, *3*. [CrossRef]
12. De Oro-Carretero, P.; Sanz-Landaluze, J. In Vitro Approach to Refine Bioconcentration and Biotransformation Predictions of Organic Persistent Pollutants Using Cell Lines. *Chemosphere* **2024**, *364*, 143020. [CrossRef] [PubMed]
13. Fischer, F.C.; Escher, B.I.; Mühlenbrink, M.; Henneberger, L.; Huchthausen, J.; König, M.; Schlichting, R.; Wiseman, S.; Berggren, E.; Daston, G.; et al. Modeling Exposure in the Tox21 in Vitro Bioassays. *Chem. Res. Toxicol.* **2017**, *30*, 1197–1208. [CrossRef] [PubMed]
14. Huchthausen, J.; Mühlenbrink, M.; König, M.; Escher, B.I.; Henneberger, L. Experimental Exposure Assessment of Ionizable Organic Chemicals in in Vitro Cell-Based Bioassays. *Chem. Res. Toxicol.* **2020**, *33*, 1845–1854. [CrossRef] [PubMed]
15. Butryn, D.M.; Chi, L.H.; Gross, M.S.; McGarrigle, B.; Schecter, A.; Olson, J.R.; Aga, D.S. Retention of Polybrominated Diphenyl Ethers and Hydroxylated Metabolites in Paired Human Serum and Milk in Relation to CYP2B6 Genotype. *J. Hazard. Mater.* **2020**, *386*, 121904. [CrossRef]
16. United Nations Environmental Program. *Stockholm Convention on Persistent Organic Pollutants (POPs), Text and Annexes*; UNEP: Nairobi, Kenya, 2019.
17. Li, M.; Gong, X.; Tan, Q.; Xie, Y.; Tong, Y.; Ma, J.; Wang, D.; Ai, L.; Gong, Z. A Review of Occurrence, Bioaccumulation, and Fate of Novel Brominated Flame Retardants in Aquatic Environments: A Comparison with Legacy Brominated Flame Retardants. *Sci. Total Environ.* **2024**, *939*, 173224. [CrossRef]
18. Pereira, L.C.; de Souza, A.O.; Meireles, G.; Furio Franco-Bernardes, M.; Tasso, M.J.; Bruno, V.; Dorta, D.J.; Palma de Oliveira, D. Comparative Study of Genotoxicity Induced by Six Different PBDEs. *Basic Clin. Pharmacol. Toxicol.* **2016**, *119*, 396–404. [CrossRef]
19. De Oro-Carretero, P.; Sanz-Landaluze, J. Miniaturized Method for the Quantification of Persistent Organic Pollutants and Their Metabolites in HepG2 Cells: Assessment of Their Biotransformation. *Anal. Bioanal. Chem.* **2023**, *415*, 4813–4825. [CrossRef]
20. Grasse, N.; Massei, R.; Seiwert, B.; Scholz, S.; Escher, B.I.; Reemtsma, T.; Fu, Q. Impact of Biotransformation on Internal Concentrations and Specificity Classification of Organic Chemicals in the Zebrafish Embryo (*Danio rerio*). *Environ. Sci. Technol.* **2024**, *58*, 17898–17907. [CrossRef]
21. Henneberger, L.; Mühlenbrink, M.; König, M.; Schlichting, R.; Fischer, F.C.; Escher, B.I. Quantification of Freely Dissolved Effect Concentrations in in Vitro Cell-Based Bioassays. *Arch. Toxicol.* **2019**, *93*, 2295–2305. [CrossRef]
22. Brandts, I.; Garcia-Ordoñez, M.; Tort, L.; Teles, M.; Roher, N. Polystyrene Nanoplastics Accumulate in ZFL Cell Lysosomes and in Zebrafish Larvae after Acute Exposure, Inducing a Synergistic Immune Response: In Vitro without Affecting Larval Survival in Vivo. *Environ. Sci. Nano* **2020**, *7*, 2410–2422. [CrossRef]
23. Agilent Technologies. *Two-Way Splitter Kit with Makeup Gas Installation and Operation Guide*; Agilent G3180B: Santa Clara, CA, USA, 2011.
24. Ulrich, N.; Endo, S.; Brown, T.N.; Watanabe, N.; Bronner, G.; Abraham, M.H.; Goss, K.U. UFZ-LSER Database v3.2.1 [Internet]. Helmholtz Centre for Environmental Research-UFZ. 2017. Available online: https://www.ufz.de/index.php?de=31698&contentonly=1&m=0&lserd_data[mvc]=Public/start (accessed on 19 October 2024).
25. Endo, S.; Mewburn, B.; Escher, B.I. Liposome and Protein-Water Partitioning of Polybrominated Diphenyl Ethers (PBDEs). *Chemosphere* **2013**, *90*, 505–511. [CrossRef] [PubMed]

26. Endo, S.; Goss, K.U. Serum Albumin Binding of Structurally Diverse Neutral Organic Compounds: Data and Models. *Chem. Res. Toxicol.* **2011**, *24*, 2293–2301. [CrossRef] [PubMed]
27. Endo, S.; Droge, S.T.J.; Goss, K.U. Polyparameter Linear Free Energy Models for Polyacrylate Fiber-Water Partition Coefficients to Evaluate the Efficiency of Solid-Phase Microextraction. *Anal. Chem.* **2011**, *83*, 1394–1400. [CrossRef]
28. Gobas, F.A.P.C.; Zhang, X. Measuring Bioconcentration Factors and Rate Constants of Chemicals in Aquatic Organisms Under Conditions of Variable Water Concentrations and Short Exposure Time. *Chemosphere* **1961**, *25*, 1961–1971. [CrossRef]
29. Mackay, D.; Fraser, A. Bioaccumulation of Persistent Organic Chemicals: Mechanisms and Models. **n.d.** [Online]. Available online: www.elsevier.com/locate/envpol (accessed on 19 October 2024).
30. Black, S.R.; Nichols, J.W.; Fay, K.A.; Matten, S.R.; Lynn, S.G. Evaluation and Comparison of in Vitro Intrinsic Clearance Rates Measured Using Cryopreserved Hepatocytes from Humans, Rats, and Rainbow Trout. *Toxicology* **2021**, *457*, 152819. [CrossRef]
31. Arnot Jon, A.; Gobas, F.A.P.C. A Generic QSAR for Assessing the Bioaccumulation Potential of Organic Chemicals in Aquatic Food Webs. *QSAR Comb. Sci.* **2003**, *22*, 337–345. [CrossRef]
32. Yang, J.; Chan, K.M. Evaluation of the Toxic Effects of Brominated Compounds (BDE-47, 99, 209, TBBPA) and Bisphenol A (BPA) Using a Zebrafish Liver Cell Line, ZFL. *Aquat. Toxicol.* **2015**, *159*, 138–147. [CrossRef]
33. Cetin, B.; Odabasi, M. Measurement of Henry's Law Constants of Seven Polybrominated Diphenyl Ether (PBDE) Congeners as a Function of Temperature. *Atmos. Environ.* **2005**, *39*, 5273–5280. [CrossRef]
34. Dimitrijevic, D.; Fabian, E.; Nicol, B.; Funk-Weyer, D.; Landsiedel, R. Toward Realistic Dosimetry in Vitro: Determining Effective Concentrations of Test Substances in Cell Culture and Their Prediction by an in Silico Mass Balance Model. *Chem. Res. Toxicol.* **2022**, *35*, 1962–1973. [CrossRef]
35. Rostamnezhad, F.; Hossein Fatemi, M. Comprehensive Investigation of Binding of Some Polycyclic Aromatic Hydrocarbons with Bovine Serum Albumin: Spectroscopic and Molecular Docking Studies. *Bioorg. Chem.* **2022**, *120*, 105656. [CrossRef]
36. Ma, Q.; Bai, H.; Wang, C.; Xi, G.C.; Zhang, Q.; Meng, X.S.; Chen, Y.X.; Li, J.R.; Ma, H.J.; Guo, L.H. Investigation of Noncovalent Interactions between Hydroxylated Polybrominated Diphenyl Ethers and Bovine Serum Albumin Using Electrospray Ionization-Ion Mobility-Mass Spectrometry. *Int. J. Mass Spectrom.* **2014**, *357*, 34–44. [CrossRef]
37. Klinčić, D.; Dvoršćak, M.; Jagić, K.; Mendaš, G.; Herceg Romanić, S. Levels and Distribution of Polybrominated Diphenyl Ethers in Humans and Environmental Compartments: A Comprehensive Review of the Last Five Years of Research. *Environ. Sci. Pollut. Res.* **2020**, *27*, 5744–5758. [CrossRef]
38. De Oro-Carretero, P.; Sanz-Landaluze, J. Bioaccumulation and Biotransformation of BDE-47 Using Zebrafish Eleutheroembryos (*Danio rerio*). *Environ. Toxicol. Chem.* **2023**, *42*, 835–845. [CrossRef] [PubMed]
39. Gustafsson, K.; Björk, M.; Burreau, S.; Gilek, M. Bioaccumulation kinetics of brominated flame retardants (polybrominated diphenyl ethers) in blue mussels (mytilus edulis). *Environ. Toxicol. Chem.* **1999**, *18*, 1218–1224. [CrossRef]
40. Vidal-Liñán, L.; Bellas, J.; Fumega, J.; Beiras, R. Bioaccumulation of BDE-47 and Effects on Molecular Biomarkers Acetylcholinesterase, Glutathione-S-Transferase and Glutathione Peroxidase in *Mytilus galloprovincialis* Mussels. *Ecotoxicol.* **2015**, *24*, 292–300. [CrossRef]
41. Mhadhbi, L.; Fumega, J.; Beiras, R. Uptake Kinetics, Bioconcentration and Debromination of BDE-47 in Juvenile Marine Fish *Psetta maxima*. *Water Air Soil Pollut.* **2014**, *225*, 2072. [CrossRef]
42. Lebrun, J.D.; Leroy, D.; Giusti, A.; Gourlay-Francé, C.; Thomé, J.P. Bioaccumulation of Polybrominated Diphenyl Ethers (PBDEs) in *Gammarus pulex*: Relative Importance of Different Exposure Routes and Multipathway Modeling. *Aquat. Toxicol.* **2014**, *154*, 107–113. [CrossRef]
43. European Chemicals Agency. Technical Guidance Document on Risk Assessment. Part II. Protection Institute for Health and Consumer. *Eur. Chem. Bur.* **2003**, *337*. Available online: https://hero.epa.gov/hero/index.cfm/reference/details/reference_id/196375 (accessed on 9 June 2025).
44. Arnot Jon, A.; Gobas, F.A.P.C. A Review of Bioconcentration Factor (BCF) and Bioaccumulation Factor (BAF) Assessments for Organic Chemicals in Aquatic Organisms. *Environ. Rev.* **2006**, *14*, 257–297. [CrossRef]
45. Petersen, G.I.; Kristensen, P. Bioaccumulation of Lipophilic Substances in Fish Early Life Stages. *Environ. Toxicol. Chem.* **1998**, *17*, 1385–1395. [CrossRef]
46. U.S. Environmental Protection Agency. Estimation Programs Interface Suite™ for Microsoft® Windows, v 4.1. 2012. Available online: https://hero.epa.gov/hero/index.cfm/reference/details/reference_id/2347246 (accessed on 19 October 2024).
47. ARC Arnot Research and Consulting Inc. EAS-E Suite (Ver.0.972-BETA). 2024. Available online: https://www.plastiverse.org/tools/eas-e-suite (accessed on 19 October 2024).
48. Molina-Fernández, N.; Rainieri, S.; Muñoz-Olivas, R.; De Oro-Carretero, P.; Sanz-Landaluze, J. Development of a Method for Assessing the Accumulation and Metabolization of Antidepressant Drugs in Zebrafish (*Danio rerio*) Eleutheroembryos. *Anal. Bioanal. Chem.* **2021**, *413*, 5169–5179. [CrossRef] [PubMed]
49. Fu, Q.; Fedrizzi, D.; Kosfeld, V.; Schlechtriem, C.; Ganz, V.; Derrer, S.; Rentsch, D.; Hollender, J. Biotransformation Changes Bioaccumulation and Toxicity of Diclofenac in Aquatic Organisms. *Environ. Sci. Technol.* **2020**, *54*, 4400–4408. [CrossRef]

50. Klüver, N.; Vogs, C.; Altenburger, R.; Escher, B.I.; Scholz, S. Development of a General Baseline Toxicity QSAR Model for the Fish Embryo Acute Toxicity Test. *Chemosphere* **2016**, *164*, 164–173. [CrossRef] [PubMed]
51. Lungu-Mitea, S.; Vogs, C.; Carlsson, G.; Montag, M.; Frieberg, K.; Oskarsson, A.; Lundqvist, J. Modeling Bioavailable Concentrations in Zebrafish Cell Lines and Embryos Increases the Correlation of Toxicity Potencies across Test Systems. *Environ. Sci. Technol.* **2021**, *55*, 447–457. [CrossRef] [PubMed]
52. Zheng, X.; Zhu, Y.; Liu, C.; Liu, H.; Giesy, J.P.; Hecker, M.; Lam, M.H.W.; Yu, H. Accumulation and Biotransformation of BDE-47 by Zebrafish Larvae and Teratogenicity and Expression of Genes along the Hypothalamus-Pituitary-Thyroid Axis. *Environ. Sci. Technol.* **2012**, *46*, 12943–12951. [CrossRef]
53. Kang, Y.; Cheung, K.C.; Wong, M.H. Polycyclic Aromatic Hydrocarbons (PAHs) in Different Indoor Dusts and Their Potential Cytotoxicity Based on Two Human Cell Lines. *Environ. Int.* **2010**, *36*, 542–547. [CrossRef]
54. Sun, J.; Liu, J.; Yu, M.; Wang, C.; Sun, Y.; Zhang, A.; Wang, T.; Lei, Z.; Jiang, G. In Vivo Metabolism of 2,2′,4,4′-Tetrabromodiphenyl Ether (BDE-47) in Young Whole Pumpkin Plant. *Environ. Sci. Technol.* **2013**, *47*, 3701–3707. [CrossRef]
55. Wiseman, S.B.; Wan, Y.; Chang, H.; Zhang, X.; Hecker, M.; Jones, P.D.; Giesy, J.P. Polybrominated Diphenyl Ethers and Their Hydroxylated/Methoxylated Analogs: Environmental Sources, Metabolic Relationships, and Relative Toxicities. *Mar. Pollut. Bull.* **2011**, *63*, 179–188. [CrossRef]
56. Castranova, D.; Lawton, A.; Lawrence, C.; Baumann, D.P.; Best, J.; Coscolla, J.; Doherty, A.; Ramos, J.; Hakkesteeg, J.; Wang, C.; et al. The Effect of Stocking Densities on Reproductive Performance in Laboratory Zebrafish (*Danio rerio*). *Zebrafish* **2011**, *8*, 141–146. [CrossRef]
57. Cheng, D.; Shami, G.J.; Morsch, M.; Chung, R.S.; Braet, F. Ultrastructural Mapping of the Zebrafish Gastrointestinal System as a Basis for Experimental Drug Studies. *Biomed. Res. Int.* **2016**, *2016*, 8758460. [CrossRef]
58. Henneberger, L.; Klüver, N.; Mühlenbrink, M.; Escher, B. Trout and Human Plasma Protein Binding of Selected Pharmaceuticals Informs the Fish Plasma Model. *Environ. Toxicol. Chem.* **2020**, *41*, 559–568. [CrossRef] [PubMed]

Assessing bioconcentration and biotransformation of BDE-47 *in vitro*: the relevance of bioavailable and intracellular concentrations

Paloma De Oro-Carretero and Jon Sanz-Landaluze

Department of Analytical Chemistry, Faculty of Chemical Science, Complutense University of Madrid, Avenida Complutense s/n, 28040 Madrid, Spain

Contact emails: pdeoro@ucm.es (P. De Oro-Carretero)*, jsanzlan@ucm.es (J. Sanz-Landaluze)
Phone: +034-91 394 4322; Fax: +034-91 394 4329
*Corresponding author

Supporting information

Table S1. Mass spectrometer conditions in SIM mode for BDE-47 and their metabolites

Analyte	Retention time (min)	m/z	Initial scanning time (min)
BDE-28	11.00	248, 246, 406, 408	8 (solvent delay)
TMDS-TCS	12.92	290, 288, 218	12
BDE-47	17.51	326, 486, 484, 488	15
2'-OH-TBDMS-BDE-28	22.29	423*, 421*, 425, 81	20*
6-MeO-BDE-47	22.38	516, 514*, 518, 420	
3-MeO-BDE-47	24.28	356*, 516, 341, 514	
5-MeO-BDE-47	24.87	516*, 356, 358, 326	
BDE-99	27.33	404, 406, 564, 566	26
5-OH-TBDMS -BDE-47	30.92	502*, 504*, 500, 81	29*
3-OH-TBDMS -BDE-47	35.16	502, 474*, 266, 419	

* A joint window is established, as they elude close retention times, so that the majority m/z of each is monitored (marked in the table). TBDMS-X = tert-butyldimethylsilylated derivative

Table S2. Limits of detection (LODs), limits of quantification (LOQs) and recoveries for BDE-47 and its metabolites in cells and media samples

	LODs (µg·L^{-1})		LOQs (µg·L^{-1})		Recoveries (%)	
Analyte	**Cells**	**Medium**	**Cells**	**Medium**	**Cells**	**Medium**
BDE-47	1.65	2.69	8.63	8.96	80 ± 5	82 ± 9
BDE-28	0.005	0.001	0.016	0.002	100 ± 7	125 ± 9
2'-OH-BDE-28	0.002	0.001	0.006	0.004	75 ± 7	61 ± 9
6-MeO-BDE-47	0.01	0.30	0.02	0.99	67 ± 1	84 ± 9
3-MeO-BDE-47	0.001	0.001	0.005	0.002	81 ± 5	82 ± 9
5-MeO-BDE-47	0.005	0.002	0.017	0.007	90 ± 9	84 ± 7
5-OH-BDE-47	0.002	0.022	0.006	0.074	79 ± 5	114 ± 8
3-OH-BDE-47	0.002	0.001	0.008	0.003	83± 9	95 ± 2

Table S3. Test system parameters for the experiment input in MBM spreadsheet [13] and system information output from MBM

	ZFL
Test system parameters	
Medium volume (µL)	10000
Type of base medium	DMEM Glutamax
Fraction of base medium (%)	90
Type of serum	FBS
Fraction of serum (%)	10
Cell line	-
Cell number at test start	5571000
System information	
Water content (%)	88.4
Protein content (%)	9.3
Lipid content (%)	2.3

Table S4. Chemical parameters input in MBM spreadsheet [13] estimated by UFZ-LSER Calculation Partition System (pH 7.4, 37 °C) [24].

Compound	**log $D_{BSA/water}$ [L/L]**	**log $D_{lipid/water}$ [L/L]**
BDE-47	5.53	6.70

Table S5. Chemical partitioning estimated by MBM spreadsheet [13].

Cell line	$f_{w,medium}$ (%)	f_{cell} (%)	f_{medium} (%)	f_{mem} (%)
ZFL	0.02	7.88	92.12	6.16

Table S6. Default parameters derived from rainbow trout and zebrafish for IVIVE-BCF estimation model (OECD 2018)

	Rainbow Trout	Zebrafish
Modeled body weight (B_{wgM}) (g)	10[a]	0.5[c]
Modeled temperature (T) (°C)	12[b]	28[b]
Fractional liver weight (L_{FBW}) (g liver/g fish)	0.015[a]	0.033[d]
Liver hepatocyte content (L_{HEP}) (10^6 cells/g liver)	510[a]	56.1[e]

[a] [8, 9]
[b] Experiment temperature
[c] [56]
[d] [57]
[e] Estimated

Table S7. Amount of protein and lipid content in fetal bovine serum (FBS) and rainbow trout serum used to supplement the ZFL cel- line culture medium.

Serum	Protein content (g/L)	Lipid content (g/L)	Reference
FBS	71.75	1.57	[13]
Trout Serum	39.69	12.13	[58]

Table S8. Ratio (in %) of the internal concentration estimated by MBM and experimentally for the BDE-47 experiment of this work and the PHE experiment in our previous work [12] in ZFL cells.

Ratio MBM/experimental (%)	**BDE-47 experiment**		**PHE experiment**	
Time exposure / Nominal concentration	1.8 mg·L^{-1}	2.6 mg·L^{-1}	10 mg·L^{-1}	50 mg·L^{-1}
24h	51	73	491	510
48h	44	78	532	449
72h	36	66	421	402

Table S9. Toxicokinetic parameters calculated with the cell concentration values obtained experimentally or by MBM and C_{free} obtained experimentally for BDE-47 bioconcentration at 1.8 mg·L^{-1} and 2.6 mg·L^{-1}

	Experiment 1.8 mg·L^{-1}		**Experiment 2.6 mg·L^{-1}**	
	k_1 (L·µg·h^{-1})	**k_2 (µg·L^{-1})**	**k_1 (L·µg·h^{-1})**	**k_2 (µg·L^{-1})**
$BCF_{K,Cexp/Cw}$	1.20	0.04	2.96	0.17
$BCF_{K,Cexp/Cfree}$	3715	0.04	10784	0.17
$BCF_{K,CMBM/Cw}$	7.838	0.803	2.784	0.121
$BCF_{K,CMBM/Cfree}$	6896	0.803	4627	0.121

Table S10. Recovery of losses from volatilization (% Rec. Vol) when exposed to 1.8 mg·L^{-1} and 2.6 mg·L^{-1} at different exposure times. The percentages were calculated from the ratio of the concentration determined in the medium of the samples without cells ('no cells') from the different exposure times, to the initial dilution (time 0h).

Time exposure / % Rec. Vol.	**Experiment 1.8 mg·L^{-1}**	**Experiment 2.6 mg·L^{-1}**
24h	76	73
48h	69	63
72h	68	52

Table S11. Input and calculated parameter by IVIVE-BCF model [8] at 1.8 mg·L^{-1} and 2.6 mg·L^{-1} of BDE-47 using the zebrafish (ZF) and rainbow trout (RT) default parameters (shown in Table S5). The BCF $BCF_{IVIVE,RT}$ and $BCF_{IVIVE,ZF}$ are shown in Table 2.

Experiment	**1.8 mg·L^{-1}**		**2.6 mg·L^{-1}**	
Default parameters	**ZF**	**RT**	**ZF**	**RT**
Input parameters				
$C_{w,TOT}$ ($C_{free,exp}$) (mg/L)	0.0006		0.0016	
C_{HEP} (10^6 cells/mL)	0.557		0.557	
$k_{e,loss}$ (h^{-1})	0.012		0.002	
Calculated parameters				
Binding correction term (f_U)	0.0495		0.0495	
$CL_{IN\ VITRO,\ INT}$ (mL/h/10^6 cells)	0.0220	0.0220	0.0037	0.0037
CL_H (L/d/kg)	0.0482	0.1972	0.0080	0.0332
k_{MET} (d^{-1})	0.0022	0.0092	0.0004	0.0015
k_1 (L/kg/d)	2091	631	2091	631
k_2 (d^{-1})	0.006	0.002	0.006	0.002

Figure S1. Recoveries obtained with the different extractants in medium samples of known concentration (5 $\mu g \cdot L^{-1}$)

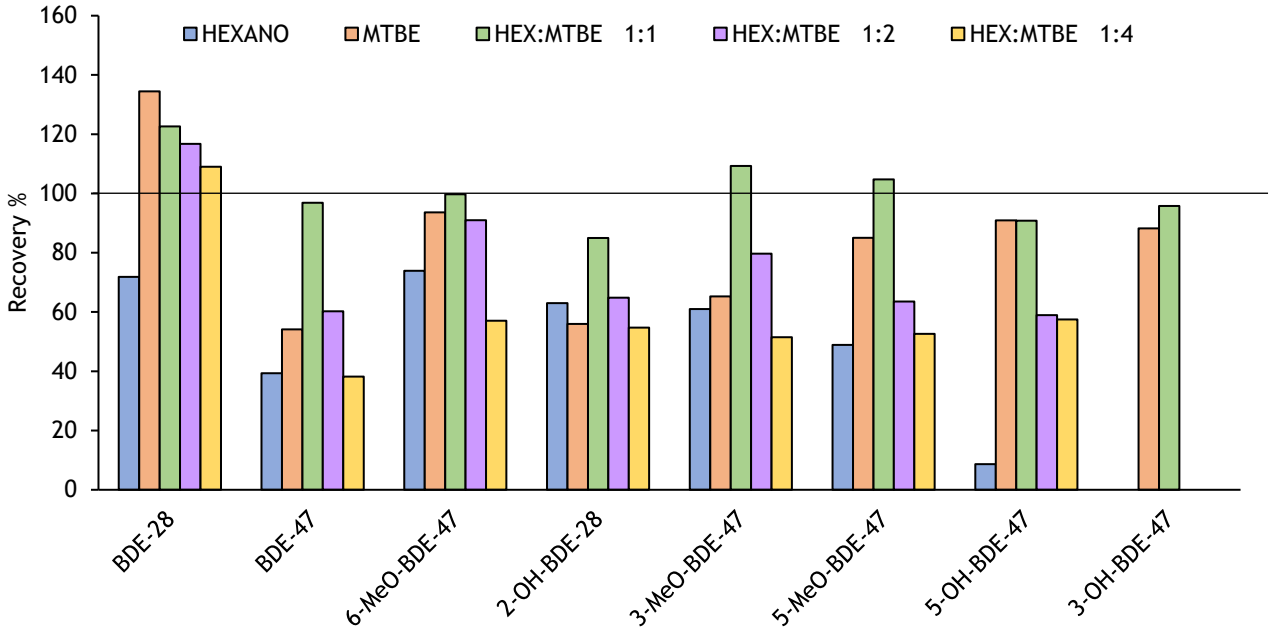

Figure S2. ZFL cell viability of different BDE-47 concentration at 72h

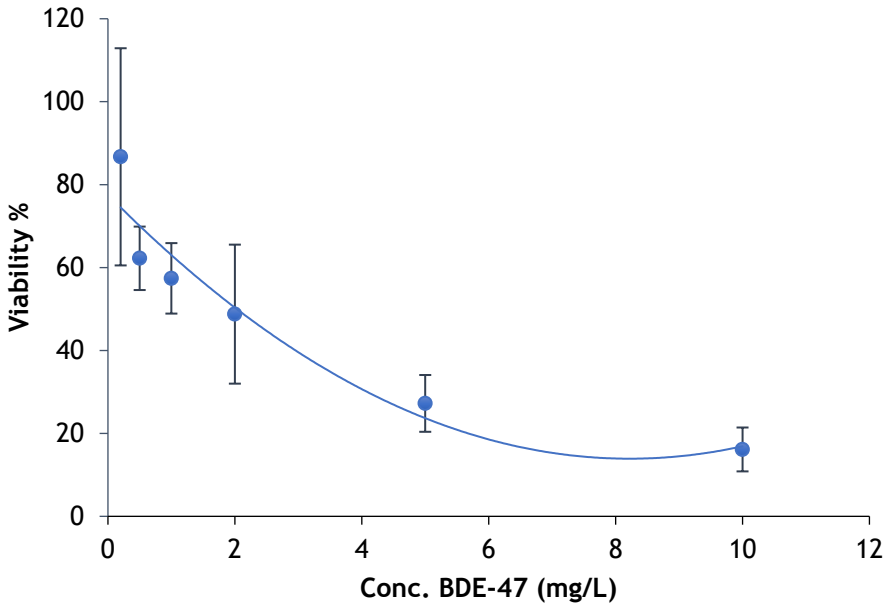

Figure S3. a) Measured values of C_{medium}, $C_{medium,\ no\ cells}$, $C_{free,exp}$ and $C_{free,MBM}$ and b) $C_{cell,exp}$ and $C_{cell,MBM}$ for BDE-47 at different exposure times in the 2.6 mg·L^{-1} experiment ($C_{nominal}$)

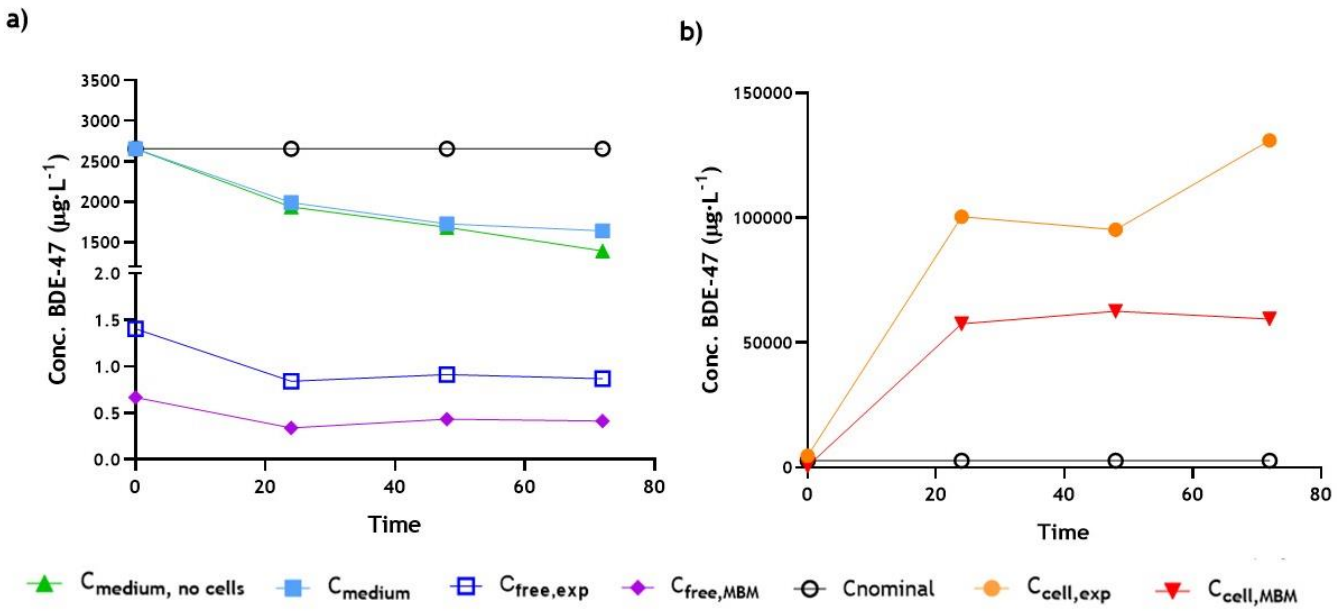

Figure S4. First-order kinetic fit of the BDE-47 internal concentration in ZFL cells determined experimentally in the 1.8 (a) and 2.6 mg·L^{-1} (b) experiment; and by MBM in the 1.8 (c) and 2.6 mg·L^{-1} (d) experiment.

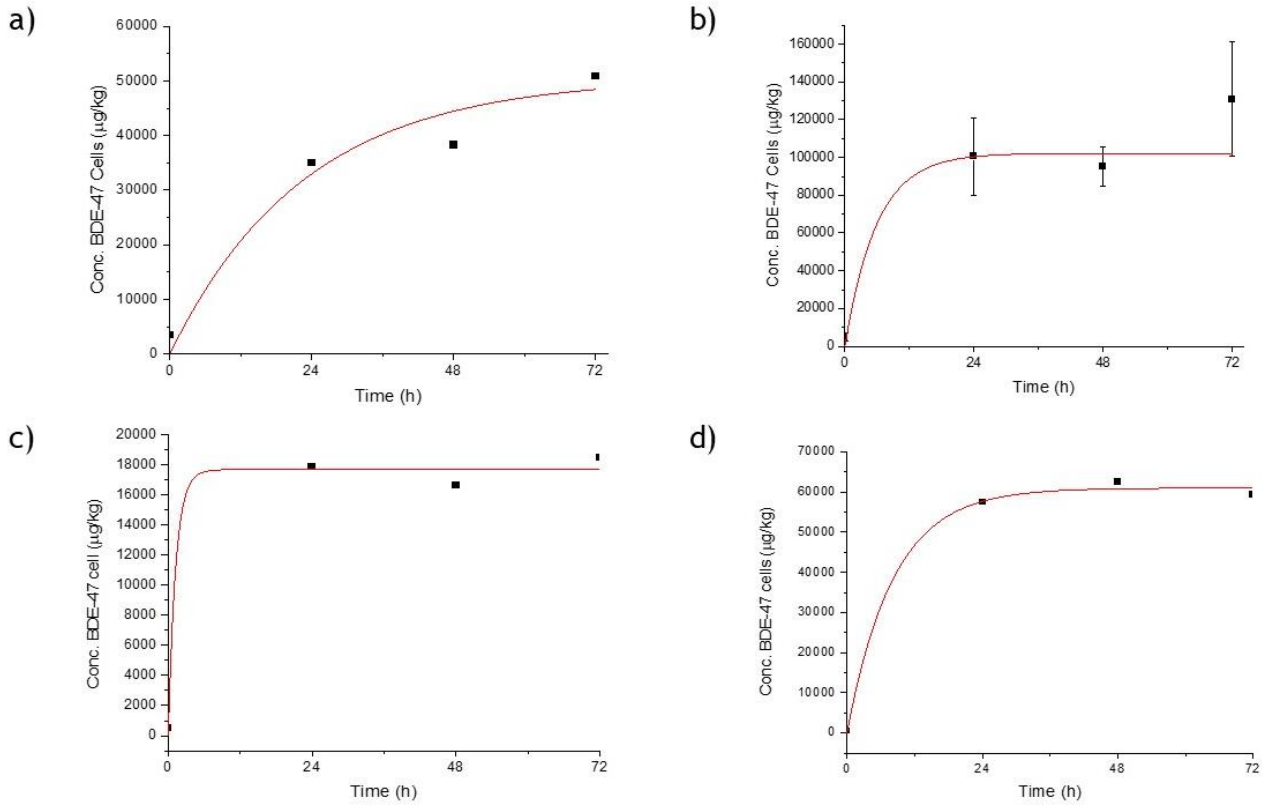

Figure S5. Fits performed to determine the reaction rate (k_e) by BDE-47 depletion in the 1.8 (a) and 2.6 mg·L^{-1} (b) experiment method and the rate constant of BDE-47 volatilization losses ($k_{e,volat}$) in the 1.8 (c) and 2 mg·L^{-1} (d) experiment

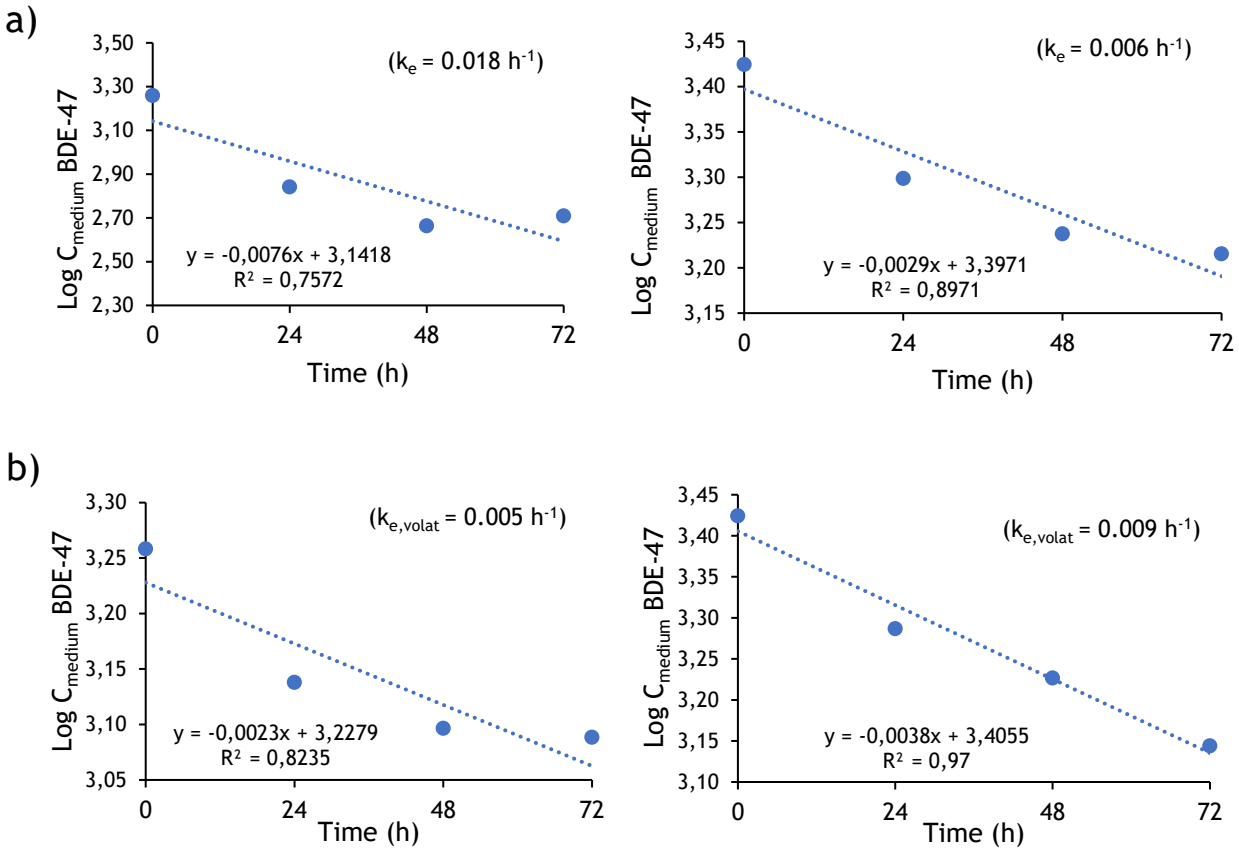

References

[8] OECD. Test No. 280: Guidance Document on the Determination of in Vitro Intrinsic Clearance Using Cryopreserved Hepatocytes (RT HEP) or Liver S9 Sub Cellular Fractions (RT S9) from Rainbow Trout and Extrapolation to in Vivo Intrinsic Clearance Series on Testing and Assessment. Guidel. Test. Chem. 2018. https://one.oecd. org/document/ENV/JM/MONO(2018)12/en/pdf.

[9] Nichols, J. W.; Huggett, D. B.; Arnot, J. A.; Fitzsimmons, P. N.; Cowan Ellsberry, C. E. Toward Improved Models for Predicting Bioconcentration of Well Metabolized Compounds by Rainbow Trout Using Measured Rates of in Vitro Intrinsic Clearance. Environ. Toxicol. Chem. 2013, 32, 7, 1611–1622. https://doi.org/10.1002/etc.2219.

[12] De Oro Carretero, P.; Sanz Landaluze, J. In Vitro Approach to Refine Bioconcentration and Biotransformation Predictions of Organic Persistent Pollutants Using Cell Lines. Chemosphere 2024, 364, 143020. https://doi.org/10.1016/j.chemosphere.2024.143020.

[13] Fischer, F. C.; Escher, B. I.; Mühlenbrink, M.; Henneberger, L.; Huchthausen, J.; König, M.; Schlichting, R.; Wiseman, S.; Berggren, E.; Daston, G.; Hartung, T. Modeling Exposure in the Tox21 in Vitro Bioassays. Chem. Res. Toxicol. 2017, 30, 5, 1197–1208. https://doi.org/10.1021/acs.chemrestox.7b00023.

[24] Ulrich, N.; Endo, S.; Brown, T. N.; Watanabe, N.; Bronner, G.; Abraham, M. H.; Goss, K. U. UFZ-LSER Database v3.2.1 [In-ternet]. Helmholtz Centre for Environmental Research-UFZ. 2017.

[56] Castranova, D.; Lawton, A.; Lawrence, C.; Baumann, D. P.; Best, J.; Coscolla, J.; Doherty, A.; Ramos, J.; Hakkesteeg, J.; Wang, C.; Wilson, C.; Malley, J.; Weinstein, B. M. The Effect of Stocking Densities on Reproductive Performance in Laboratory Zebrafish (Danio rerio). Zebrafish 2011, 8, 3, 141–146. https://doi.org/10.1089/zeb.2011.0688.

[57] Cheng, D.; Shami, G. J.; Morsch, M.; Chung, R. S.; Braet, F. Ultrastructural Mapping of the Zebrafish Gastrointestinal System as a Basis for Experimental Drug Studies. Biomed. Res. Int. 2016, 2016, 8758460. https://doi.org/10.1155/2016/8758460.

[58] Henneberger, L.; Klüver, N.; Mühlenbrink, M.; Escher, B. Trout and Human Plasma Protein Binding of Selected Pharmaceuticals Informs the Fish Plasma Model. Environ. Toxicol. Chem. 2020, 41, 3, 559–568. https://doi.org/10.1002/etc.4934...

2. Aplicación de las metodologías alternativas desarrolladas para la evaluación de la toxicidad, bioacumulación y biotransformación de POPs en presencia de NPLs.

En la actualidad, la evaluación de la toxicidad ambiental se está centrando cada vez más en el **estudio de mezclas** de contaminantes, ya que en los ecosistemas estos no se encuentran de manera aislada, sino que coexisten, pudiendo interaccionar entre ellos y provocando efectos aditivos, antagónicos o sinérgicos en los organismos. Por ello, el estudio de la toxicidad combinada de estos compuestos es fundamental para comprender su impacto real en los organismos y en los ecosistemas.

Como se ha expuesto en la presente Tesis Doctoral, la contaminación por **nanoplásticos** (NPLs) representa una creciente preocupación social debido al incremento de su presencia en el medio ambiente y su potencial para penetrar en los organismos, generando efectos adversos. Además, diversos estudios han evidenciado su capacidad para adsorber sustancias químicas tóxicas del entorno, como los POPs, facilitando así su transferencia a los organismos. No obstante, aún existen discrepancias en relación con los efectos que pueden generar y no se ha dilucidado completamente el mecanismo de acción, tanto de los NPLs como de los POPs, en su contribución global al efecto observado. En este contexto, si bien el **PHE** es un compuesto ampliamente caracterizado a nivel individual, resulta necesario continuar en su estudio, debido a su persistencia, en la comprensión de su comportamiento con otros contaminantes emergentes presentes en el medio ambiente.

En **esta sección**, se examina la toxicidad, bioacumulación y biotransformación de PHE en presencia de nanoplásticos de poliestireno (PS-NPLs) de 44 nm. Se seleccionaron nanoplásticos de poliestireno debido a que es uno de los polímeros más ampliamente utilizados en diversos productos. Además, su densidad intermedia, cercana a la del agua, lo convierte en uno de los más biodisponibles para los organismos acuáticos. Las concentraciones de PS-NPLs que se utilizan no muestran efectos de toxicidad en la exposición individual de acuerdo con estudios previos llevados a cabo en el Instituto de Biotecnología y Biomedicina de la

Universidad Autónoma de Barcelona, con el que se realiza, en colaboración, este estudio. Esto permite evaluar los efectos adicionales que puedan surgir en comparación con los inducidos únicamente por el PHE. Para ello, se aplicaron las metodologías alternativas desarrolladas a lo largo de esta Tesis Doctoral, que incluyen sistemas *in vitro* con líneas celulares de peces de distintos tejidos, hígado (ZFL) e intestinal (RTgutGC) y sistemas *in vivo* con larvas de pez cebra. Este enfoque también permite obtener información más detallada sobre el modo de acción del PHE y los PS-NPLs en relación con la funcionalidad específica de cada órgano y organismo. Las investigaciones de este trabajo se recogen en el último artículo (**Artículo 5**), titulado ***Complex combined effects of polystyrene nanoplastics and phenanthrene in aquatic models (enviado al Journal of Hazardous Materials).***

En primer lugar, se evaluó la **toxicidad** exponiendo células y larvas a distintas concentraciones de PHE, tanto de forma individual como en combinación con dos concentraciones de PS-NPLs, previamente identificadas como no tóxicas. Para la coexposición, se prepararon disoluciones de la mezcla de ambos contaminantes, que fueron incubadas durante más de 24 horas para favorecer una adhesión óptima del PHE a la superficie de los PS-NPLs. En el caso de las células, se evaluó la viabilidad mediante el ensayo MTT y citometría de flujo, utilizando la tinción roja de ácido nucleico BD Via-Probe™. Para las larvas, se determinó el LC_{50} a través de una curva dosis-respuesta. A continuación, se decidió estudiar si diferentes concentraciones de PHE mostraban un efecto en la **internalización de los PS-NPLs** (marcados con Dragon Green). Se realizó un análisis por citometría de flujo para determinar el porcentaje de células con PS-NPLs internalizados, la intensidad de fluorescencia y la obtención de imágenes de células individuales mediante la tecnología de imágenes incorporada en el citómetro. Adicionalmente, se empleó microscopía confocal para confirmar la internalización de los PS-NPLs. En el caso de las larvas, se utilizó una lupa de fluorescencia para su evaluación. Posteriormente, se seleccionaron tres concentraciones de PHE que mostraban diferencias en la internalización de PS-NPLs y, al mismo tiempo, mantenían una viabilidad celular aceptable. Estas concentraciones fueron utilizadas en el experimento de **bioacumulación y biotransformación** de PHE con la presencia

de PS-NPLs. Para ello, se expusieron células y larvas a PHE, tanto de forma individual como en combinación con PS-NPLs, y se cuantificaron las concentraciones de PHE y sus metabolitos (OH-PHEs) mediante la metodología analítica desarrollada. Asimismo, se determinó $\mathbf{C_{free}}$ de PHE en el ensayo *in vitro* utilizando el MBM empleado a lo largo de esta Tesis Doctoral. Finalmente, se calculó el **BCF** para cada una de las condiciones experimentales.

En este estudio se combinó la aplicación de las metodologías alternativas y métodos analíticos desarrollados en los anteriores trabajos junto con la aplicación de otras técnicas bioanalíticas para la evaluación de la toxicidad, bioacumulación y biotransformación de PHE en presencia de PS-NPLs.

ARTÍCULO 5:

Efectos combinados complejos de nanoplásticos de poliestireno y fenantreno en modelos acuáticos.

Complex combined effects of polystyrene nanoplastics and phenanthrene in aquatic models.

*Paloma De Oro-Carretero**‡, *Marlid García-Ordoñez*‡, *Nerea Roher*, *Jon Sanz-Landaluze*

Journal of Hazardous Materials, en revisión, 2025 (IF: 12.2, Q1)

**Autora de correspondencia; ‡ Autoras que han contribuido por igual.*

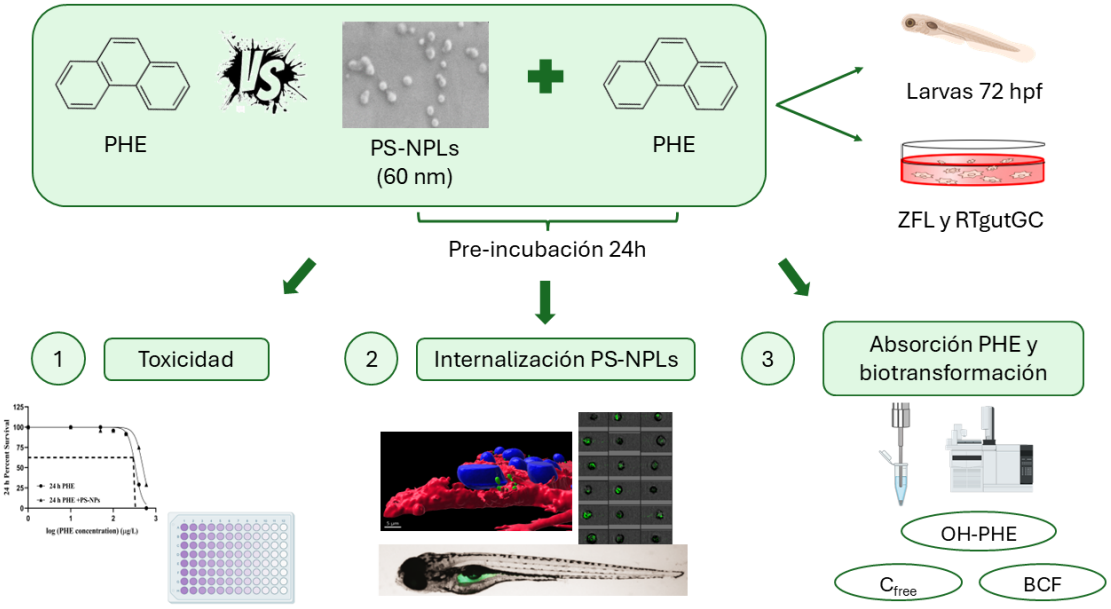

Journal of Hazardous Materials

Complex combined effects of polystyrene nanoplastics and phenanthrene in aquatic models

--Manuscript Draft--

Manuscript Number:	HAZMAT-D-25-03587
Article Type:	Research Paper
Keywords:	Nanoplastics; phenanthrene; zebrafish larvae; cells; effects
Corresponding Author:	Paloma De Oro-Carretero Complutense University of Madrid SPAIN
First Author:	Paloma De Oro-Carretero
Order of Authors:	Paloma De Oro-Carretero
	Marlid Garcia-Ordoñez
	Nerea Roher
	Jon Sanz-Landaluze
Abstract:	Nanoplastic (NPs) pollution is an increasing social concern due to their potential to accumulate in aquatic environments and their ability to penetrate organisms. In addition, they can adsorb toxic chemicals from their surroundings and help to transfer them to organisms. This study evaluated the effects of co-exposure of polystyrene (PS)-NPs and phenanthrene (PHE) on toxicity, accumulation, and metabolization in two fish cell lines (zebrafish liver cells and rainbow trout intestinal cells) and in zebrafish larvae. The uptake of PS-NPs was studied by cytometry and confocal microscopy while PHE uptake and metabolization was determined by extraction and detection of the compound and its major metabolites (hydroxy-phenanthrene, OH-PHEs) by gas chromatography coupled to mass spectrometry. Lower uptake of PS-NPs was observed in intestinal cells and zebrafish larvae in the presence of PHE, but higher uptakes were observed in zebrafish liver cells. Higher concentrations of PHE and its metabolites were detected in the presence of PS-NPs. Interestingly, zebrafish larvae experienced lower toxicity during co-exposure compared to single exposure. These results indicate that the interaction between PS-NPs and PHE presents a synergistic effect with significant complexity, showing cell-type and tissue dependent ecotoxicological effects and suggesting differential pathways of uptake and distribution of these pollutants.

Complex combined effects of polystyrene nanoplastics and phenanthrene in aquatic models

Paloma De Oro-Carretero[1]‡, Marlid Garcia-Ordoñez[2]‡, Nerea Roher[2,3,4] and Jon Sanz-Landaluze[1]

[1]Department of Analytical Chemistry, Faculty of Chemical Science, Universidad Complutense de Madrid, Avenida Complutense s/n, 28040 Madrid, Spain
[2] Institute of Biotechnology and Biomedicine, Universitat Autònoma de Barcelona, 08193 Barcelona, Spain.
[3] Department of Cell Biology, Animal Physiology and Immunology, Universitat Autònoma de Barcelona, 08193 Barcelona, Spain
[4] Bioengineering, Biomaterials and Nanomedicine (CIBER-BBN), Spain

Contact emails: pdeoro@ucm.es (P. De Oro-Carretero)*, marlid.garcia@uab.cat (M. Garcia-Ordoñez), nerea.roher@uab.cat (N. Roher), jsanzlan@ucm.es (J. Sanz-Landaluze)

*Corresponding author
‡ Both authors equally contributed

Graphical Abstract

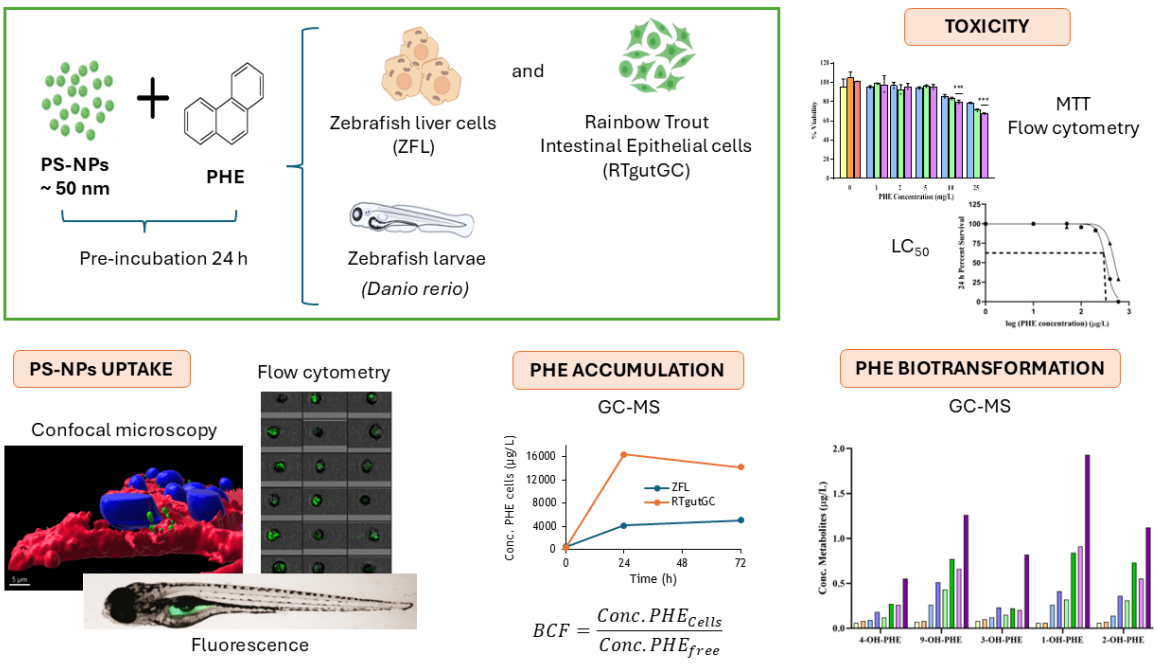

Abstract

Nanoplastic (NPs) pollution is an increasing social concern due to their potential to accumulate in aquatic environments and their ability to penetrate organisms. In addition, they can adsorb toxic chemicals from their surroundings and help to transfer them to organisms. This study evaluated the effects of co-exposure of polystyrene (PS)-NPs and phenanthrene (PHE) on toxicity, accumulation, and metabolization in two fish cell lines (zebrafish liver cells and rainbow trout intestinal cells) and in zebrafish larvae. The uptake of PS-NPs was studied by cytometry and confocal microscopy while PHE uptake and metabolization was determined by extraction and detection of the compound and its major metabolites (hydroxy-phenanthrene, OH-PHEs) by gas chromatography coupled to mass spectrometry. Lower uptake of PS-NPs was observed in intestinal cells and zebrafish larvae in the presence of PHE, but higher uptakes were observed in zebrafish liver cells. Higher concentrations of PHE and its metabolites were detected in the presence of PS-NPs. Interestingly, zebrafish larvae experienced lower toxicity during co-exposure compared to single exposure. These results indicate that the interaction between PS-NPs and PHE presents a synergistic effect with significant complexity, showing cell-type and tissue dependent ecotoxicological effects and suggesting differential pathways of uptake and distribution of these pollutants.

Keywords

Nanoplastics, phenanthrene, co-exposure, zebrafish larvae, cells, effects

Environmental Implications

Nanoplastics have a significant environmental impact, but they rarely exist alone; they interact with other pollutants, which are also highly harmful. Some studies have already shown that nanoplastics act as carriers of toxic compounds, but contradictions remain about their effects and mechanisms of action remain unclear. This work examines co-exposure using different aquatic models to analyze organ- and organism-specific impacts. The goal is to better understand their behavior in the environment and provide information for developing more effective strategies to protect human health, organisms, and ecosystems and its long-term consequences.

Highlights

- Co-exposure to PHE and PS-NPs resulted in lower toxicity compared to individual exposure in zebrafish larvae.
- Higher metabolites concentrations were observed in hepatocytes when PS-NPs were present in the medium
- Cell and tissue type-dependent uptake of PS-NPs upon co-exposure with PHE
- The presence of PS-NPs may induce synergistic or antagonistic effects
- Effects may be influenced by agglomeration state and free PHE availability.
- Co-exposure to PHE and PS-NPs caused both antagonistic and synergistic effects.

1. Introduction

In recent decades, the abusive production [1], use and release of plastics into the environment has become a social, scientific and political problem due to the huge environmental and public health consequences [2]. Plastic residues in both micrometric (diameter less than 5 mm - MPs) and nanometric size (less than 100 nm – NPs; [3], have been found in remote sites such as the Antarctica [4], rural waters and forest landscapes [5], food and beverages [6], as well as inside organisms and aquatic ecosystems [7]. Among all types of plastics, polystyrene (PS) is one of the most widely used polymers in different manufactured products [8] With an intermediate density of 0.96-1.05 g/cm^3, close to that of the water, it is distributed in both surface and bottom waters, making it more bioavailable to aquatic organisms [9, 10].

Concentrations of micro(nano) plastics (MNPs) in aquatic environments are directly correlated with human density and human activity [1]. According to Jambeck *et al.* [11], the largest contribution of plastic into aquatic environments originates from Asian countries (8.82 million metric tons/year), well above European countries (0.31 million metric tonnes/year). The highest concentration of MPs according to the study of Patidar *et al.* [12] in Asia was 372 ± 14.3 items·L^{-1} and 9630 ± 2947 items·kg^{-1} in water and sediments, respectively. In beach sediments from South Africa, 340.7-4757 items·m^{-2} were found [1]. In general, most studies have shown higher densities of MNPs on the seabed in coastal areas, with concentrations reaching up to 7700 items·km^{-2}. This is followed by floating marine litter at over 600 items·km^{-2} and, finally, beaches with a rate of 1 item/m^2 [13].

MNPs may cause adverse effects on organisms and human health [14, 15], because they easily penetrate biological membranes [16] and accumulate inside organisms [17]. However, MNPs are not isolated in the environment and, due to their high surface area/volume ratio and hydrophobicity, they can easily adsorb other pollutants, such as persistent organic pollutants

(POPs) [18], facilitating their transport and internalisation in different living organisms (Trojan horse effect) [19]. Invertebrate models such as Daphnia (*D. magna* and *D. pulex*) and vertebrate models such as zebrafish, are commonly used to study the ecotoxicological effects of MNPs in the aquatic environment [3, 20].

Nanoplastics (NPs) have a much higher specific surface area, having a higher potential to penetrate biological membranes and to transport organic pollutants compared to MPs [21]. In addition, although reliable quantification methods for NPs are still scarce, it is estimated that their concentration could be 10^{14} times higher than that of MPs [22]. Polycyclic aromatic hydrocarbons (PAHs) are ubiquitous in aquatic environments [22], and they are adsorbed onto MNPs by hydrophobic and π–π interactions between the aromatic rings of PHE and polystyrene [23]. The toxicity of PAHs has been extensively studied and includes oxidative stress, endocrine disruption, carcinogenicity and genotoxicity [24, 25]. Phenanthrene (PHE), is one of the most common PAHs found inside marine organisms [26] and is often used as a model for studying uptake and metabolism of small PAHs [27]. The range of PHE concentrations reported by Peng *et al.* [28] in aquatic environments was between 153 $ng \cdot L^{-1}$ and 1460 $\mu g \cdot L^{-1}$. Wu *et al.* [29] reported that PHE exposure concentrations in freshwaters in China range from 45.01 to 379.28 $\mu g \cdot L^{-1}$ and Miura *et al.* [30] found concentrations of 125-375 $pg \cdot m^{-3}$ PHE in the Pacific Ocean. Most studies indicate that pollutant toxicity increases when combined with MNPs, with particular emphasis on pollutant uptake. However, few studies analyse how MNPs, interact with environmental pollutants and affect ecosystems and organisms beyond their general toxicity. This work aims to investigate the interaction between polystyrene nanoplastics (PS-NPs) and PHE, to gain a better understanding of their impact on biological systems, specifically on the uptake and metabolic processes that occur when both substances coexist. In this regard, two *in vitro* models, each representing cells with different biological and functional

backgrounds (i.e. zebrafish liver cells; ZFL, and rainbow trout intestinal cells; RTgutGC), were used. Each one representative of a cell type relevant for absorption (gut cells) and detoxification (liver cells).

In addition, to further understand the interaction and metabolisms of PHE and PS-NP combination *in vivo* we used zebrafish (*Danio rerio*) larvae. The absorption of PS-NPs was studied by fluorescence techniques, whereas PHE uptake and metabolization was determined by extraction and detection of the compound and its major metabolites (hydroxy-phenanthrene, OH-PHEs) by gas chromatography coupled to mass spectrometry.

2. Materials and Methods

2.1. Nanoplastics and chemicals

Fluorescently labelled PS-NPs (42 nm - ref. FSDG001 Dragon Green) and non-labelled PS-NPs (44 nm - ref. PS02002) were purchased from Bang Laboratories (Fisher, IN, USA). PS-NPs were provided as a 1% (w/w) suspension in water with 2 mM NaN_3. The characterization of NPs in different conditions (pure water, PBS, cell culture medium and embryo medium) was performed in a previous study [17]. Individual solid standard of PHE, fluorene (FLU), 1-OH-PHE, 2-OH-PHE, 3-OH-PHE, 4-OH-PHE and 9-OH-PHE were supplied by Sigma Aldrich (Madrid, Spain).

2.2. Preparation of PS-NPs solutions with sorbed PHE (NPs-PHE)

PS-NPs and PHE dilutions were prepared by mixing the corresponding volumes of PS-NPs in PBS and PHE in methanol (MetOH, Scharlab) and then further diluted in culture medium (DMEM for ZFL and L-15 for RTgutGC; see section 2.3) or E3 medium (see section 2.8) for zebrafish larvae, to obtain the final concentrations in the experiments. For flow cytometry and confocal microscopy fluorescent PS-NPs were used. For MTT (3-(4,5-dimethylthiazol-2-yl)-2,5-diphenyltetrazolium bromide, Sigma-Aldrich) viability assays and PHE absorption and

metabolization assays, non-fluorescent PS-NPs were used. All solutions were carried out in sealed glass vials and subsequently incubated for 24 h in the dark at 25 ºC with horizontal rotary shaking (120 rpm).

Concentrations of PS-NPs were selected in a way that did not cause toxicity on individual exposures according to previous studies [17, 31], (i.e. 10, 25 and 50 $mg \cdot L^{-1}$ PS-NPs). On the other hand, PHE concentrations were chosen depending on the final purpose of the assay, always keeping the bioavailable concentration (see supplementary information) below the limit of solubility in aqueous media (0.82 $mg \cdot L^{-1}$; 4.6 μM [32]) and ensuring absorption saturation on the surface of the PS-NPs [21, 33].

2.3. Cell culture

ZFL cells (CRL-2643, American Type Culture Collection, ATCC) were cultured at 28°C, in humidified air atmosphere and 5% CO_2 in Dulbecco's modified Eagle's medium (DMEM; 4.5 $g \cdot L^{-1}$ glucose, supplemented with 10% (v/v) heat-inactivated fetal bovine serum (FBS), 5% (v/v) antibiotic/antimycotic solution, 0.01 $mg \cdot mL^{-1}$ insulin, 50 $ng \cdot mL^{-1}$, EGF and 0.5% (v/v) heat inactivated trout serum; TS), as described in Torrealba *et al.* [34] RTgutGC cells (obtained from Dr. C. Tafalla's laboratory) were cultured at 20°C in Leibovitz's L-15 Medium GlutaMAX™ without CO_2, supplemented with heat-inactivated FBS 10% (v/v) and 1% antibiotic/antimycotic [35]. Subconfluent cultures were detached by adding TrypLE Express (Gibco) for 5 min. All experiments were performed with phenol red-free culture media to avoid any potential phenol red interference [36, 37].

2.4. PHE + PS-NPs cytotoxicity studies in ZFL and RTgutGC cells

The toxicity of PHE in the presence of PS-NPs was assessed using the MTT assay. ZFL and RTgutGC cells were incubated with 2, 5, 10, 25 and 50 $mg \cdot L^{-1}$ and 1, 2, 5, 10, and 25 $mg \cdot L^{-1}$ of PHE, respectively, and in combination with 10 $mg \cdot L^{-1}$ and 50 $mg \cdot L^{-1}$ of PS-NPs (solutions

prepared according to section 2.2). Cells were incubated for 24 and 72 h, then washed with PBS and the MTT (Sigma-Aldrich) was added at 10% of the total volume at a final concentration of 0.5 mg·mL^{-1} and incubated for 30 min. After incubation, the MTT solution was removed, the formazan crystals were dissolved in dimethylsulfoxide (DMSO) and the absorbance quantified at 550 nm on a Victor3 Plate Reader (PerkinElmer). Data were normalized to control readings set at 100%. A one-way ANOVA was performed comparing treatment and control means using Prism software (GraphPad). Three independent assays were carried out using the same conditions.

In addition, cell viability in ZFL cells was tested with BD Via-Probe™ Red Nucleic Acid Stain by flow cytometry. For this, cells were subjected to similar conditions as those in the MTT trial and subsequently detached with TrypLE Express (Gibco) and sedimented by centrifugation at 300×g for 5 minutes. Cell pellets were resuspended in PBS and 0.5 μL of BD Via-Probe™ Red reagent (5-20 nM) was added. A total of 10000 events were recorded by flow cytometry (CytoFLEX Beckman Coulter, Inc.) and data analysed using Flowing Software 2.5.1 (University of Turku, Finland).

2.5. Uptake of PS-NPs in the presence of PHE. Cytometry and confocal microscopy

The uptake of fluorescent PS-NPs at 10 and 50 mg·L^{-1} (non-toxic concentrations) was assessed in ZFL cells under different concentrations of phenanthrene (0, 2, 5, 10, 25 and 50 mg·L^{-1}) during 24 and 72 h. NPs-PHE solutions were prepared according to section 2.2. After treatment, cells were detached with TrypLE Express during 5 min and cells were retrieved by centrifugation at 300 x *g* for 5 min. Pellets were resuspended in PBS for flow cytometry (FACSDiscover S8 Cell Sorter with CellView, BD), and 10,000 events were counted. In addition to the uptake and Mean Fluorescence Intensity (MFI), the imaging technology of the cell sorter was used to analyse some conditions (50 mg·L^{-1} PS-NPs vs 50 mg·L^{-1} PS-NPs + 25

mg·L^{-1} PHE). In the same way, internalization was measured in RTgutGC cells at 25 mg·L^{-1} PS-NPs in combination with 0, 10 and 25 mg·L^{-1} PHE to observe differences in the response of enterocytes after 72 h of exposure. Previous study reported higher internalisation rates in RTgutGC compared to ZFL, thus lower PS-NPs concentrations (i.e. 25 mg·L^{1}) were selected to avoid saturation of the control image [31].

To confirm that the fluorescence observed by cytometry was due to the PS-NPs accumulated inside the ZFL cells and not merely attached to the cell membrane surface, confocal microscopy (Zeiss LSM 700) was performed. ZFL cells were seeded on 35 mm ibidi glass-bottom plates and when 60% confluence was reached, cells were treated with 25 mg·L^{-1} PS-NPs and 25 mg·L^{-1} PS-NPs + 25 mg·L^{-1} PHE for 24 h. Cells were stained with Hoechst (nuclei) and Cell Mask Deep Red (membrane) (Life Technologies). Images were analysed with Imaris v9.3 (Bitplane) and ImageJ (National Institute of Health, USA) software.

2.6. Uptake and metabolization of PHE: Cell and medium extraction and determination by GC-MS.

The exposure and the extraction methodologies were developed in a previous study [38] and used in the current study for ZFL and RTgutGC cell lines. ZFL and RTgutGC cells were treated with 10, 25 and 50 mg·L^{-1} PHE and 10 and 25 mg·L^{-1} PHE, respectively, in combination with 10 and 50 mg·L^{-1} PS-NPs. After 24 and 72 h, the cell media and the cell pellets were collected including initial medium (0 h). For the determination of PHE and its metabolites, the cell pellets were divided into 2 fractions, dried under nitrogen stream and weighted. All samples were stored at -20 ºC until analysis.

For PHE quantification, half of the obtained pellet (~10 mg for ZFL cells and ~5 mg for RTgutGC cells) was extracted with 500 µL of hexane and sonicated with an ultrasound probe (Vibra cell VCx130, 2 mm diameter titanium microtip, 130 W high frequency generator at 20 KHz from Sonics & Materials Inc. USA), for 1 min at 30% amplitude and an on/off:2s/5s pulse.

For medium extraction (500 μL) a liquid-liquid extraction was performed with 500 μL of hexane and vortexed for 1 min. The extraction mixture was centrifuged for 10 min at 13000 x g and the organic extract was measured by gas chromatography (Agilent Technologies Mod. 7890A Series) coupled to mass spectrometry (HP 5975C VL MSD) (GC-MS). Internal standard (fluorene, FLU) was previously added to the extraction step. Samples (1 μL) were injected in splitless mode at 280 ºC with Helium at a constant pressure of 25 psi. The temperature of the column (ZB-5 capillary column 30 m × 0.25 mm I.D., 0.25-μm film thickness) was programmed to increase from 90 ºC (1 min) to 250 ºC (1 min) at a rate of 70 ºC·min^{-1} and then to 270ºC (1 min) at 40 ºC·min^{-1}. The temperature of the ion source and the transfer line of the mass spectrometer was set at 250 and 270 ºC, respectively, and 70 eV for the electron beam. The other half of the pellet obtained and 500 μL of medium was used for OH-PHEs (1-OH, 2-OH, 3-OH, 4-OH and 9-OH-PHE) quantification. The extraction, derivatization, separation and detection methods are described in De Oro and Sanz 2023 [38].

Finally, after quantification of the total PHE concentration in the medium (C_{med}), the bioavailable concentration (C_{free}) was determined using mass balance models (MBM) to relate it to the concentration inside the cells (C_{cell}) and thus to estimate the bioconcentration factor (BCF) at each exposure time (BCF_{24h}, BCF_{72h}). Data analysis for C_{free} and BCF determination is described in the supplementary information as developed in De Oro and Sanz 2024 [39].

2.7. Zebrafish husbandry and breeding

Wild-type zebrafish (*Danio rerio*) were housed in a recirculating aquarium system and maintained at 28°C ± 1°C with a 12-hour light:dark photoperiod. Adult fish were fed twice daily with 2% body weight. Ammonia, nitrite, pH, and nitrate levels were monitored daily. Ammonia was kept below detectable limits, nitrate concentrations did not exceed 100 mg·L^{-1} and the pH was maintained between 6.8 and 7.5 For breeding, one female and three males were

placed in a breeding tank in the late afternoon, and embryos were collected the following morning. Fertilized eggs were collected, extensively washed with water and placed in petri dishes in E3 medium. Unfertilized and dead embryos were separated from viable ones with a plastic pipette (Deltalab). All zebrafish experiments complied with the International Guiding Principles for Research Involving Animals (EU 2010/63) and received prior approval from the Ethics Committee of the Universitat Autònoma de Barcelona (UAB, CEEH number 1582).

2.8. PHE and PHE + PS-NPs toxicity in Zebrafish larvae

Zebrafish larvae were exposed to different nominal concentrations of PHE in the presence or absence of PS-NPs. Control animals were incubated in E3 medium (5 mM NaCl, 0.17 mM KCl, 0.33 mM $CaCl_2$, 0.33mM $MgSO_4$ and 0.1% methylene blue) and the percentage of MetOH used as vehicle. Groups of 24 larvae (n = 48 per condition) were distributed on 96-well plates (Thermo Fisher) with one larvae per well containing 200 µl E3 medium or PS-NPs at 5 $mg \cdot L^{-1}$; alone, or in combination with PHE at concentrations of 1, 10, 50, 100, 200, 400 and 600 $\mu g \cdot L^{-1}$, pre-incubated for 24 h. Mortality data was recorded 24 h post-treatment and analysed with GraphPad software with a logistic dose-response model to fit the data and to estimate the LC_{50} value.

2.9. Uptake of PS-NPs in presence of PHE in Zebrafish Larvae

Groups of four larvae (72 h post fertilization, hpf) per treatment were distributed on 96-well plates (Thermo Fisher) and immersed in 200 µL of E3 medium with PHE (50 $\mu g \cdot L^{-1}$) and PS-NPs (5 $mg \cdot L^{-1}$). Biodistribution in zebrafish larvae was evaluated after 48 h using a fluorescence stereomicroscope (Nikon SMZ800) coupled with a camera (Nikon DS-Fi2). Fluorescence was quantified using ImageJ software 1.53t and expressed as Mean Fluorescence Intensity (MFI) normalized by the larvae area. The experiments were repeated 3 times (n = 12).

2.10. Bioaccumulation of PHE in presence of PS-NPs in Zebrafish Larvae

Groups of 12 and 9 larvae were exposed to 10, 50 and 100 µg·L^{-1} PHE in combination with 5 mg·L^{-1}, respectively, for 24 h. Larvaes of each condition were then washed with fresh medium and stored in the same vial at -20 °C until analysis. The methodology and analytical equipment used for the determination of PHE inside larvae was the same as that used in section 2.6 except for the ultrasound probe (1 min at 40% amplitude and an on/off:1s/s pulse, [40]).

3. Results

3.1. PHE toxicity in the presence of PS-NPs in ZFL and RTgutGC cells

Analysis of viability using the MTT assay revealed that ZFL cells remained viable under all experimental conditions and doses of PS-NPs and PHE (Figure 1), while no significant changes in viability were observed in cells only exposed to PS-NPs (10 mg·L^{-1} and 50 mg·L^{-1}) or MetOH (Figure 1a and b). However, a decrease in viability was observed in ZFL cells to exposed to 50 mg·L^{-1} PHE + PS-NPs for 72 h, with cell viability dropping to 78% and 69% (Figure 1b), although these differences remained below the threshold for significance. Similarly, when we used Vita-Probe staining to assess viability by flow cytometry, no significant differences were observed in ZFL cells exposed to either PHE or PS-NPs. However, ZFL cells exposed to either 25 or 50 mg·L^{-1} PHE + 50 mg·L^{-1} PS-NPs exhibited a significant decrease in viability down to 75% at 24 h and 71% at 72 h (Figure S1).

On the other hand, a more pronounced decrease in RTgutGC cell viability was observed in the MTT assay after 72 h of combined exposure to either 10 or 25 mg·L^{-1} PHE + 50 mg·L^{-1} PS-NPs, with viability significantly dropping to 80% and 71%, respectively (Figure 1c and d). Again, no significant changes in viability were observed in the cells only exposed to PS-NPs (10 mg·L^{-1} and 50 mg·L^{-1}) or MetOH (Figure 1c and d).

3.2. Uptake of PS-NPs in ZFL and RTgutGC cells in the presence of PHE

The uptake of PS-NPs in the presence of different concentrations of PHE in two different cell types was evaluated by flow cytometry. We observed an increase in the percentage of fluorescent cells from 16.0% to 53.5% in ZFL cells exposed to 10 and 50 $mg \cdot L^{-1}$ PS-NPs at 24 h (Figure 2a). When the cells were exposed to PS-NPs + PHE (25 $mg \cdot L^{-1}$), a strong increase in the percentage of fluorescent cells and the total fluorescent signal intensity (MFI) was observed (Figure 2a). Furthermore, as shown in Figure S2, it was observed that the percentage of fluorescent cells increased progressively with rising concentrations of PHE at both 24 h and 72 h after exposure to 50 $mg \cdot L^{-1}$ PS-NPs. However, in the case of 10 $mg \cdot L^{-1}$ PS-NPs, the percentage of fluorescent cells was constant (1-5%) until exposure to 10 $mg \cdot L^{-1}$ PHE, with a subsequent significant increase after exposure to higher concentrations of PHE (25 and 50 $mg \cdot L^{-1}$), reaching percentages of 15% and 75% at 24 h and 79% and 89% at 72 h. Therefore, for the following experiments we decided to test 10, 25, and 50 $mg \cdot L^{-1}$ PHE. Uptake was also confirmed by flow cytometry imaging (Figure 2b) and confocal microscopy (Figure 2c), along with the internalization of PS-NPs in the presence of PHE (Figure 2d). In contrast, as reflected by the values in Figure 2e and confirmed by flow cytometry imaging in Figure 2f, RTgutGC cells show a higher percentage of fluorescent cells (70-80%) than ZFL cells at both 10 and 25 $mg \cdot L^{-1}$ PS-NPs. Moreover, as the concentration of PHE in the medium increased, the MFI decreased (Figure 2e).

3.3. Bioaccumulation and metabolization of PHE in ZFL and RTgutGC cells in presence of PS-NPs

The PHE concentrations inside ZFL and RTgutGC cells (C_{cell}) and in their culture media (C_{med}) at the different exposure scenarios and times (24 h and 72 h) are shown in Table 1. Bioavailable free concentration (C_{free}) was determined from C_{med} by MBM as explained in supporting

information and BCF (C_{cell}/C_{free}) was estimated at each exposure time and condition (Table 1). As for internal PHE uptake, both hepatocytes and enterocytes show a rapid stabilization of PHE concentration, reaching constant values at 24 and 72 h in almost conditions. (Figure S3). In addition, hepatocytes exhibited a higher tendency to internalize and bioaccumulate PHE compared to intestinal cells when exposed solely to PHE. However, the opposite was observed when PHE was combined with PS-NPs, resulting in higher concentrations and BCF values in RTgutGC cells than in ZFL. When examining the cell lines separately, in RTgutGC cells an increase in uptake and bioaccumulation was observed when exposing PHE in combination with PS-NPs compared to PHE alone. In ZFL cells, similar or even lower values of uptake and BCF were observed when PHE was combined with PS-NPs. Figure 3 shows the concentrations of the main PHE metabolites (1-OH, 2-OH, 3-OH, 4-OH and 9-OH-PHE) found in ZFL cells at 10 $mg \cdot L^{-1}$ of PHE, showing that concentration of these metabolites increased over the exposure time. In addition, higher concentrations of PHE metabolites were detected when higher concentrations of PS-NPs were present in the medium. The same trend was observed in the experiments at 25 and 50 $mg \cdot L^{-1}$ PHE (Figure S4). In contrast, no metabolites were detected in RTgutGC cells.

3.4. PHE and PHE + PS-NPs toxicity in zebrafish larvae

We evaluate whether the presence of PS-NPs may modify the toxicity of PHE *in vivo* using zebrafish larvae. Groups of 48 larvae were incubated with PHE at different concentrations in the absence and presence of PS-NPs. From the experimental data, we estimated the LC_{50} of PHE to be 331.8 $\mu g \cdot L^{-1}$ while that of PHE with PS-NPs was 489.9 $\mu g \cdot L^{-1}$ (Figure 4).

3.5. Uptake of PS-NPs by zebrafish larvae in the presence of PHE

Hatched larvae (72 hpf) were incubated with PS-NPs or PS-NPs combined with PHE in E3 medium. After 48 h larvae were anesthetized and imaged using a stereoscopic fluorescent

microscope. Representative images of PS-NPs uptake in the presence or absence of PHE are shown in Figure 5a. The fluorescent PS-NPs accumulate in the digestive tract (Figure 5a) both in the presence or absence of PHE. However, the MFI accumulated in the zebrafish larvae in the presence of PHE was significantly lower (0.0402) (Figure 5b).

3.6. Uptake of PHE in zebrafish Larvae in presence of PS-NPs

Figure 5c shows the PHE concentrations inside the larvae (C_{larvae}) and the BCF ($L \cdot kg^{-1}$) estimated as the ratio of C_{larvae} to the PHE nominal concentration of the different exposure scenarios. The concentrations were normalized according to the number of larvae and the weight of a larvae (0.44 mg, [40]). For all PHE concentrations studied, higher PHE concentrations were observed inside the larvae when exposed in combination with PS-NPs. However, this difference was not statistically significant.

4. Discussion

Many studies have demonstrated the synergistic toxicity of micro- and nanoplastics (MNPs) with organic compounds such as phenanthrene in different organisms [22, 25, 41]. On the other hand, other studies have reported the 'Trojan horse effect' [42] where MNPs act as entry vectors for organic compounds attached to their surface. In this study, we combined discussions of the results on toxicity, absorption and metabolization of PS-NPs and PHE to further explain the observed effects in fish cells lines with different functional backgrounds (liver cells and gut cells) and in living zebrafish larvae.

4.1. Cell and tissue type-dependent effects on PS-NPs and PHE co-exposure

The toxicity results in ZFL and RTgutGC cells indicated an increase in toxicity when PS-NPs and PHE were combined (Figure 1). Katsumiti *et al.* [43] exposed *Mytilus galloprovincialis* hemocytes to 50 nm PS-NPs (10^2–10^{12} particles$\cdot mL^{-1}$) and benzo(a)pyrene (BaP, 250 $\mu g \cdot L^{-1}$) and reported that PAH alone had a higher toxicity (50%) compared to the mixture, but this was

observed at lower PS-NPs concentrations (ranging from 10^{11}-10^{12} particles·mL^{-1}) than in this study. At a concentration of 10^{12} particles·mL^{-1}, the mixture showed slightly higher toxicity (10%) than individual compounds. Wang *et al.* [25] reported a 5-10% increase in the mortality of hematocytes (*Mytilus coruscus)* when exposed to a mixture of NPs (30 µg·L^{-1} and 70 nm) and PHE (5, 50 and 500 µg·L^{-1}) compared to the exposure without NPs. Sun *et al.* [41] found that cell viability of coelomocytes of the earthworm *Eisenia fetida* under combined exposure to higher concentrations of BaP (150 µg·L^{-1}) and PS-NPs (7.5 mg·L^{-1} and 100 nm) was lower than that under single exposure, but not very significant (81% of viability, compared to 82% of only PS-NPs or 85% of BaP). In general, a slight increase (no more than 10%) in the toxicity of mixtures of NPs and PAHs is observed, especially at high concentrations of NPs consistent with the data from our experiments. Notably, the combined effects were either additive or antagonistic, suggesting that MNPs do not universally enhance but occasionally mitigate the toxic effects of PAHs [44].

In this study, the two concentrations of PS-NPs tested showed no toxicity. However, a synergistic effect was observed when PS-NPs and PHE were combined, increasing at higher PS-NPs concentrations. This suggests a 'Trojan horse effect' where PS-NPs facilitate the PHE uptake, leading to higher toxicity. Nevertheless, PHE uptake results (Table 1), indicate that only RTgutGC cells showed higher accumulation of PHE (both in concentration and BCF value) when co-exposed with PS-NPs. When ZFL cells were exposed to PHE in combination with PS-NPs, lower concentrations of PHE and BCF were obtained, although they have a greater tendency than RTgutGC cells to accumulate PHE. Several studies [10, 22, 25], have reported higher PAH accumulation in single exposures compared to co-exposure with MNPs in different organisms. Narayanan *et al.* [22] analysed the zeta potential and hydrodynamic radius of NPs with and without PAHs, finding that PS-NPs adsorption of contaminants increased negative

charges and hydrodynamic size. This suggests that PAH adsorption onto PS-NPs, may reduce PAH concentration in organisms such as microalgae. Another study, using molecular dynamics simulations examined PS-NPs and BaP uptake by dipalmitoylphosphatidylcholine (DPPC) bilayers. The findings showed that PS-NPs adsorb and accumulate BaP in water, facilitating its transport into the bilayer. Additionally, the adsorbed BaP enhanced PS-NP penetration into the DPPC bilayer through hydrophobic interactions [45]. The different functionalities and uptake dynamics of each cell type must be considered. Intestinal cells have a higher PS-NPs uptake capacity than ZFL as observed by flow cytometry and discussed below, however, this was not the case in the presence of PHE in the medium. Therefore, the higher concentration of PHE observed in RTgutGC cells in the presence of PS-NPs, compared to ZFL cells, cannot be attributed to an increased hydrodynamic radius that would prevent ZFL cells from internalizing PS-NPs with adsorbed PHE. Hepatocytes have an increased capacity to metabolise and detoxify xenobiotics and it is well known that aquatic organisms such as fish rapidly biotransform PAHs via cytochrome P450 (CYP1A) [46], playing a crucial role in reducing bioaccumulation [47]. In this study, higher concentrations of the major PHE metabolites were detected when ZFL cells were exposed to PHE in combination with higher concentrations of PS-NPs (Figure 3 and S4), which may explain the lower concentration of PHE found inside the cell. Rehman *et al.* [48] noted alterations in metabolic pathways when zebrafish were exposed to NPs and Li *et al.* [44] reported that co-exposure of MPs and PHE caused changes in metabolic profiles and pathways in zebrafish larvae. Martínez-Alvarez *et al.* [10] observed an increase in cyp1a (CYP450) levels in adult zebrafish when exposed to MPs but this did not occur when exposed in combination with BaP because it was too low concentration for effective bioaccumulation to activate biotransformation. Gene expression studies by Vazirzadeh *et al.* [49] also reported a clear association between the level of MPs and increased expression of liver enzymes such as

glutathione S-transferase (GST) and CYP450, which are responsible for detoxifying pollutants such as PHE.

On the other hand, the focus has always been on the uptake of pollutants due to the presence of MNPs and few studies focus on the opposite effect. In this study, the uptake in ZFL cells increased in both cell number and intensity as there was a higher concentration of PHE in the medium (Figure 2). This may be because free-form PHE caused damage to the cell membrane [50], allowing greater entry of PS-NPs. Another study measured the plasma membrane integrity of mussel hemocytes exposed to 50 nm PS-NPs and BaP and reported a significant descent of viability (membrane integrity) when exposed to the organic contaminant alone in comparison with the mixture with PS-NP [43]. This synergistic effect leads to a higher quantity of PS-NPs and a higher quantity of PHE attached to these PS-NPs, which we could observe in the case of liver cells through the Trojan horse effect. However, the opposite effect was observed for RTgutGC cells, i.e. less PS-NPs in the presence of PHE, although RTgutGC cells have a greater tendency to uptake PS-NPs than ZFL cells. This may be due to the different functionalities and mechanisms of action and absorption of hepatocytes and enterocytes. ZFL cells are hepatocytes expressing specific xenobiotic membrane receptors such as the aryl hydrocarbon receptor (AhR), which plays an important role in the control of PAH metabolism [51], that may lead to a better entry of PS-NPs with PHE attached than in enterocytes. This difference of behavior between different types of cells has been also observed by Wang et al., 2024 [25]. They found that hemocytes, a type of immune cells, exhibited higher sensitivity to pollutant-induced oxidative stress compared to the gills, which exhibit greater resistance to this type of stress. This difference in sensitivity may be attributed to the gills' lower metabolic activity or their reduced uptake of pollutants compared to hemocytes. Moreover, another important aspect is the internalization mechanism according to the cell type and size of the NPs [52, 53].

Ramsperger *et al.* [54] suggested that active endocytosis plays a crucial role for larger plastic particles and that smaller particles are internalized by passive transport into cells. Zhang *et al.* [21] asserted that larger particles can be more easily enveloped by the cell membrane, however, it is a slower and more costly mechanism than passive transport. This difference may be attributed to the results obtained in this study, specifically that the lower internalization of PS-NPs was caused by an increase in size due to the adsorption of PHE on their surface [22].

4.2 Antagonistic and synergistic effects between PHE and PS-NPs in zebrafish larvae

In contrast to cell lines, zebrafish larvae showed decreased viability when PHE was exposed in combination with PS-NPs (Figure 4). Since the concentrations of PS-NPs used in this work are not potentially toxic, the decrease in viability is due to the entry of PHE or to a synergic effect. Using fluorescent based-methodologies, we observed less internalization of PS-NPs in the presence of PHE (Figure 5), possibly due to the increased hydrodynamic size of PS-NPs due to PHE adsorption, as demonstrated by Narayaman *et al.* [22], which could hinder their internalization. This might suggest that less PHE was internalized in larvae due to its adsorption to PS-NPs. However, a higher concentration of PHE was detected inside the larvae when PS-NPs were present in the medium (Figure 5c). Therefore, although the observed increase in concentration is not very significant, and therefore not decisive to show an effect on toxicity, a 'Trojan horse effect' is being observed where the internalizing PS-NPs promote the entry of PHE. [55] showed an additive effect on toxicity when co-exposing 50 nm NPs and phenanthrene in *Daphia magna* and the bioaccumulation of phenanthrene metabolites was significantly increased. Xu *et al.* [56], studied the internalisation of PHE (0.2 $mg \cdot L^{-1}$) and PS-MPs (3 $mg \cdot L^{-1}$) over time in adult zebrafish and observed a synergistic effect, increasing the bioaccumulation of both. The same authors [57] co-exposed PS-NPs (80 nm, 5 $mg \cdot L^{-1}$) and

PHE (0.1 $mg \cdot L^{-1}$) and they also observed a more negative effect on zebrafish embryo morphology and mortality, but only from the time the embryos opened their mouths.

In contrast to previous reports, we observed antagonistic effects on PS-NPs accumulation in the presence of PHE and on toxicity in the presence of PS-NPs, despite a synergistic effect on PHE accumulation. One potential factor influencing these outcomes is the different state of PHE in the two scenarios. Although the total concentration of PHE inside the larvae was higher in the presence of PS-NPs, the free concentration of PHE was lower both in the medium and in the larvae [19]. This free concentration may be the primary cause of the observed toxic effect. Furthermore, free PHE enters faster and easier by passive diffusion [58] compared to the PHE adsorbed by PS-NPs, as observed in fluorescence. Other studies in literature also report antagonistic effects. Trevisan *et al.* [19] suggested that exposure to NPs together with mixed PAHs could activate defence mechanisms that reduce toxicity. Similarly, other studies have reported an antagonistic effect on toxicity [44] and a "cleaning effect" where cleaner or less contaminated MNPs can mitigate the effects of POPs (Koelmans et al., 2013; Zhang & Xu, 2022).

5. Conclusions

The interaction between PS-NPs and PHE is highly complex, with ecotoxicological effects varying across cell and tissue type. Our data show that the combined presence of PS-NPs and PHE induces distinct cellular responses which widely differ across biological systems. These effects include differences in uptake, metabolic activity and toxicity response. The lower uptake of PS-NPs in the presence of PHE in intestinal cells and zebrafish larvae, contrasting with higher uptake in liver cells, suggests a tissue-specific uptake mechanism of these co-pollutants. Moreover, the lower toxicity of PHE in the presence of PS-NPs in zebrafish larvae raises the possibility that PS-NPs may modulate the bioavailability and thus toxicity of organic pollutants.

The high levels of PHE metabolites detected in liver cells further indicate that PS-NPs may alter the xenobiotics metabolism, which could have significant implications for bioaccumulation and long-term toxicity in living organisms.

We hypothesize that NPs can adsorb contaminants, potentially reducing their uptake due to particle agglomeration. This underscores the necessity to consider the combined effects of multiple contaminants in ecological risk assessments, as single contaminant studies may underestimate the hazards posed by complex environmental mixtures. Furthermore, the differential cellular and tissue responses to PS-NPs and PHE exposure highlight the need for targeted research to better understand the mechanisms driving these interactions. Our findings provide an important basis for future investigation aimed at elucidating the long-term ecological consequences of co-pollutant interaction.

Author Contributions

P. De Oro-Carretero and M. García-Ordonez: data curation; formal analysis; investigation; methodology; software; supervision; validation; visualization; writing—original draft. **J. Sanz-Landaluze and N. Roher:** conceptualization; data curation; funding acquisition; methodology; project administration; resources; software; supervision; validation; visualization; writing—review and editing.

Acknowledgments

The present study was supported by the Spanish Ministry of Science and Innovation [PID2023-148425NB-I00]. The authors thank Dr. C. Tafalla's laboratory for providing RTGutGC cells. Paloma de Oro and Marlid Garcia thank the Spanish Ministry of Science and Innovation for their predoctoral contract [PRE2021/097956; PRE2022-103797].

References

[1] M. Kushwaha *et al.*, "Microplastics pollution in the marine environment: A review of sources, impacts and mitigation," Dec. 01, 2024, *Elsevier Ltd*. doi: 10.1016/j.marpolbul.2024.117109.

[2] D. Bidashimwa *et al.*, "Plastic pollution: How can the global health community fight the growing problem?," Jun. 09, 2023, *BMJ Publishing Group*. doi: 10.1136/bmjgh-2023-012140.

[3] M. D. Prokić *et al.*, "Studying microplastics: Lessons from evaluated literature on animal model organisms and experimental approaches," *J Hazard Mater*, vol. 414, Jul. 2021, doi: 10.1016/j.jhazmat.2021.125476.

[4] C. L. Waller *et al.*, "Microplastics in the Antarctic marine system: An emerging area of research," Nov. 15, 2017, *Elsevier B.V.* doi: 10.1016/j.scitotenv.2017.03.283.

[5] D. Materić *et al.*, "Presence of nanoplastics in rural and remote surface waters," *Environmental Research Letters*, vol. 17, no. 5, 2022, doi: 10.1088/1748-9326/ac68f7.

[6] C. Vitali, R. J. B. Peters, H. G. Janssen, and M. W. F. Nielen, "Microplastics and nanoplastics in food, water, and beverages; part I. occurrence," Feb. 01, 2023, *Elsevier B.V.* doi: 10.1016/j.trac.2022.116670.

[7] S. Al-Thawadi, "Microplastics and Nanoplastics in Aquatic Environments: Challenges and Threats to Aquatic Organisms," Jun. 01, 2020, *Springer*. doi: 10.1007/s13369-020-04402-z.

[8] K. Kik, B. Bukowska, and P. Sicińska, "Polystyrene nanoparticles: Sources, occurrence in the environment, distribution in tissues, accumulation and toxicity to various organisms," Jul. 01, 2020, *Elsevier Ltd*. doi: 10.1016/j.envpol.2020.114297.

[9] G. Erni-Cassola, V. Zadjelovic, M. I. Gibson, and J. A. Christie-Oleza, "Distribution of plastic polymer types in the marine environment; A meta-analysis," *J Hazard Mater*, vol. 369, pp. 691–698, May 2019, doi: 10.1016/j.jhazmat.2019.02.067.

[10] I. Martínez-Álvarez, K. Le Menach, M. P. Cajaraville, H. Budzinski, and A. Orbea, "Effects of polystyrene nano- and microplastics and of microplastics with sorbed polycyclic aromatic hydrocarbons in adult zebrafish," *Science of the Total Environment*, vol. 927, Jun. 2024, doi: 10.1016/j.scitotenv.2024.172380.

[11] J. R. Jambeck *et al.*, "Plastic waste inputs from land into the ocean," *Science (1979)*, vol. 347, no. 6223, pp. 768–771, Feb. 2015, doi: 10.1126/science.1260352.

[12] K. Patidar *et al.*, "Assessing the microplastic pandemic: Prevalence, detection, and human health impacts in Asian aquatic environments," *Physics and Chemistry of the Earth*, vol. 137, Feb. 2025, doi: 10.1016/j.pce.2024.103800.

[13] M. Bergmann, L. Gutow, and M. Klages, "Marine Anthropogenic Litter."

[14] C. Shi *et al.*, "Emergence of nanoplastics in the aquatic environment and possible impacts on aquatic organisms," Jan. 01, 2024, *Elsevier B.V.* doi: 10.1016/j.scitotenv.2023.167404.

[15] M. S. L. Yee *et al.*, "Impact of microplastics and nanoplastics on human health," Feb. 01, 2021, *MDPI AG*. doi: 10.3390/nano11020496.

[16] P. A. Stapleton, "Toxicological considerations of nano-sized plastics," *AIMS Environ Sci*, vol. 6, no. 5, pp. 367–378, 2019, doi: 10.3934/environsci.2019.5.367.

[17] I. Brandts, M. Garcia-Ordoñez, L. Tort, M. Teles, and N. Roher, "Polystyrene nanoplastics accumulate in ZFL cell lysosomes and in zebrafish larvae after acute exposure, inducing a synergistic immune response: In vitro without affecting larval

survival in vivo," *Environ Sci Nano*, vol. 7, no. 8, pp. 2410–2422, Aug. 2020, doi: 10.1039/d0en00553c.
[18] Y. Hu *et al.*, "Developmental toxicity and mechanism of polychlorinated biphenyls 126 and nano-polystyrene combined exposure to zebrafish larvae," *Ecotoxicol Environ Saf*, vol. 278, Jun. 2024, doi: 10.1016/j.ecoenv.2024.116419.
[19] R. Trevisan, C. Voy, S. Chen, and R. T. Di Giulio, "Nanoplastics decrease the toxicity of a complex PAH mixture but impair mitochondrial energy production in developing Zebrafish," *Environ Sci Technol*, vol. 53, no. 14, pp. 8405–8415, Jul. 2019, doi: 10.1021/acs.est.9b02003.
[20] J. Bhagat, L. Zang, N. Nishimura, and Y. Shimada, "Zebrafish: An emerging model to study microplastic and nanoplastic toxicity," Aug. 01, 2020, *Elsevier B.V.* doi: 10.1016/j.scitotenv.2020.138707.
[21] Y. Zhang, G. G. Goss, G. G. Goss, and G. G. Goss, "Potentiation of polycyclic aromatic hydrocarbon uptake in zebrafish embryos by nanoplastics," *Environ Sci Nano*, vol. 7, no. 6, pp. 1730–1741, Jun. 2020, doi: 10.1039/d0en00163e.
[22] G. Narayanan, M. Talib, N. Singh, and G. K. Darbha, "Toxic effects of polystyrene nanoplastics and polycyclic aromatic hydrocarbons (chrysene and fluoranthene) on the growth and physiological characteristics of Chlamydomonas reinhardtii," *Aquatic Toxicology*, vol. 268, Mar. 2024, doi: 10.1016/j.aquatox.2024.106838.
[23] L. Liu, R. Fokkink, and A. A. Koelmans, "Sorption of polycyclic aromatic hydrocarbons to polystyrene nanoplastic," *Environ Toxicol Chem*, vol. 35, no. 7, pp. 1650–1655, Jul. 2016, doi: 10.1002/etc.3311.
[24] C. H. Marvin *et al.*, "Considerations for Prioritization of Polycyclic Aromatic Compounds as Environmental Contaminants," Dec. 01, 2020, *American Chemical Society*. doi: 10.1021/acs.est.0c04892.
[25] S. Wang *et al.*, "The combined effects of phenanthrene and micro-/nanoplastics mixtures on the cellular stress responses of the thick-shell mussel Mytilus coruscus," *Environmental Pollution*, vol. 341, Jan. 2024, doi: 10.1016/j.envpol.2023.122999.
[26] B. Liu, L. Gao, L. Ding, L. Lv, and Y. Yu, "Trophodynamics and bioaccumulation of polycyclic aromatic hydrocarbons (PAHs) in marine food web from Laizhou Bay, China," *Mar Pollut Bull*, vol. 194, Sep. 2023, doi: 10.1016/j.marpolbul.2023.115307.
[27] K. Xu *et al.*, "Toxicological effects of nanoplastics and phenanthrene to zebrafish (Danio rerio)," *Gondwana Research*, vol. 108, pp. 127–132, Aug. 2022, doi: 10.1016/j.gr.2021.05.012.
[28] X. Peng, X. Sun, M. Yu, W. Fu, H. Chen, and J. Chen, "Chronic exposure to environmental concentrations of phenanthrene impairs zebrafish reproduction," *Ecotoxicol Environ Saf*, vol. 182, Oct. 2019, doi: 10.1016/j.ecoenv.2019.109376.
[29] J. Wu, Z. Liu, Z. Yan, and X. Yi, "Derivation of water quality criteria of phenanthrene using interspecies correlation estimation models for aquatic life in China," *Environmental Science and Pollution Research*, vol. 22, no. 12, pp. 9457–9463, Jun. 2015, doi: 10.1007/s11356-015-4091-9.
[30] K. Miura *et al.*, "Seasonal and annual changes in PAH concentrations in a remote site in the Pacific Ocean," *Sci Rep*, vol. 9, no. 1, Dec. 2019, doi: 10.1038/s41598-019-47409-9.
[31] I. Brandts *et al.*, "Polystyrene nanoplastics target lysosomes interfering with lipid metabolism through the PPAR system and affecting macrophage functionalization," *Environ Sci Nano*, vol. 10, no. 9, pp. 2245–2258, Jun. 2023, doi: 10.1039/d2en01077a.
[32] N. I. Kramer, M. Krismartina, Á. Rico-Rico, B. J. Blaauboer, and J. L. M. Hermens, "Quantifying processes determining the free concentration of phenanthrene in basal

cytotoxicity assays," *Chem Res Toxicol*, vol. 25, no. 2, pp. 436–445, Feb. 2012, doi: 10.1021/tx200479k.
[33] J. Wang *et al.*, "Size effect of polystyrene microplastics on sorption of phenanthrene and nitrobenzene," *Ecotoxicol Environ Saf*, vol. 173, pp. 331–338, May 2019, doi: 10.1016/j.ecoenv.2019.02.037.
[34] D. Torrealba *et al.*, "Nanostructured recombinant cytokines: A highly stable alternative to short-lived prophylactics," *Biomaterials*, vol. 107, pp. 102–114, Nov. 2016, doi: 10.1016/j.biomaterials.2016.08.043.
[35] A. Kawano *et al.*, "Development of a rainbow trout intestinal epithelial cell line and its response to lipopolysaccharide," *Aquac Nutr*, vol. 17, no. 2, Apr. 2011, doi: 10.1111/j.1365-2095.2010.00757.x.
[36] A. Morgan, D. Babu, B. Reiz, R. Whittal, L. Y. K. Suh, and A. G. Siraki, "Caution for the routine use of phenol red – It is more than just a pH indicator," *Chem Biol Interact*, vol. 310, Sep. 2019, doi: 10.1016/j.cbi.2019.108739.
[37] Nathaphon Kuncharoenwirat, Waranya Chatuphonprasert, and Kanokwan Jarukamjorn, "Effect of phenol red on cell cultures," *IJPS*, vol. 17, pp. 13–23, 2021.
[38] P. De Oro-Carretero and J. Sanz-Landaluze, "Miniaturized method for the quantification of persistent organic pollutants and their metabolites in HepG2 cells: assessment of their biotransformation," *Anal Bioanal Chem*, vol. 415, no. 19, pp. 4813–4825, Aug. 2023, doi: 10.1007/s00216-023-04781-w.
[39] P. De Oro-Carretero and J. Sanz-Landaluze, "In vitro approach to refine bioconcentration and biotransformation predictions of organic persistent pollutants using cell lines," *Chemosphere*, vol. 364, Sep. 2024, doi: 10.1016/j.chemosphere.2024.143020.
[40] P. De Oro-Carretero and J. Sanz-Landaluze, "Bioaccumulation and Biotransformation of BDE-47 Using Zebrafish Eleutheroembryos (Danio rerio)," *Environ Toxicol Chem*, vol. 42, no. 4, pp. 835–845, Apr. 2023, doi: 10.1002/etc.5569.
[41] N. Sun *et al.*, "Compound effect and mechanism of oxidative damage induced by nanoplastics and benzo [a] pyrene," *J Hazard Mater*, vol. 460, Oct. 2023, doi: 10.1016/j.jhazmat.2023.132513.
[42] R. Trevisan, D. Uzochukwu, and R. T. Di Giulio, "PAH Sorption to Nanoplastics and the Trojan Horse Effect as Drivers of Mitochondrial Toxicity and PAH Localization in Zebrafish," *Front Environ Sci*, vol. 8, Jul. 2020, doi: 10.3389/fenvs.2020.00078.
[43] A. Katsumiti, M. P. Losada-Carrillo, M. Barros, and M. P. Cajaraville, "Polystyrene nanoplastics and microplastics can act as Trojan horse carriers of benzo(a)pyrene to mussel hemocytes in vitro," *Sci Rep*, vol. 11, no. 1, Dec. 2021, doi: 10.1038/s41598-021-01938-4.
[44] J. Li, X. Liu, J. Fu, Z. Gong, S. Y. Jiang, and J. P. Chen, "Metabolic profile changes of zebrafish larvae in the single- and co-exposures of microplastics and phenanthrene," *Science of the Total Environment*, vol. 953, Nov. 2024, doi: 10.1016/j.scitotenv.2024.175994.
[45] S. Cheng, Z. Ye, X. Wang, C. Lian, Y. Shang, and H. Liu, "The effects of adsorbed benzo(a)pyrene on dynamic behavior of polystyrene nanoplastics through phospholipid membrane: A molecular simulation study," *Colloids Surf B Biointerfaces*, vol. 224, Apr. 2023, doi: 10.1016/j.colsurfb.2023.113211.
[46] D. R. Livingstone, "The fate of organic xenobiotics in aquatic ecosystems: quantitative and qualitative differences in biotransformation by invertebrates and fish," 1998.

[47] Q. Fu *et al.*, "Biotransformation Changes Bioaccumulation and Toxicity of Diclofenac in Aquatic Organisms," *Environ Sci Technol*, vol. 54, no. 7, pp. 4400–4408, Apr. 2020, doi: 10.1021/acs.est.9b07127.
[48] A. Rehman *et al.*, "Nanoplastic contamination: Impact on zebrafish liver metabolism and implications for aquatic environmental health," *Environ Int*, vol. 187, May 2024, doi: 10.1016/j.envint.2024.108713.
[49] A. Vazirzadeh *et al.*, "Microplastics contamination suppressed immune and health status in cage cultured Barramundi: An investigation on pollution sources, ecotoxicological impacts, and transcription of genes involved in detoxification," *Aquaculture*, vol. 594, Jan. 2025, doi: 10.1016/j.aquaculture.2024.741370.
[50] F. He *et al.*, "Decoding the biological toxicity of phenanthrene on intestinal cells of Eisenia fetida: Effects, toxicity pathways and corresponding mechanisms," *Science of the Total Environment*, vol. 904, Dec. 2023, doi: 10.1016/j.scitotenv.2023.166903.
[51] J. Vondráček and M. Machala, "The Role of Metabolism in Toxicity of Polycyclic Aromatic Hydrocarbons and their Non-genotoxic Modes of Action," *Curr Drug Metab*, vol. 22, no. 8, pp. 584–595, Nov. 2020, doi: 10.2174/1389200221999201125205725.
[52] Z. Hou *et al.*, "Distinct accumulation of nanoplastics in human intestinal organoids," *Science of the Total Environment*, vol. 838, Sep. 2022, doi: 10.1016/j.scitotenv.2022.155811.
[53] S. W. Geum and M. K. Yeo, "Reduction in Toxicity of Polystyrene Nanoplastics Combined with Phenanthrene through Binding of Jellyfish Mucin with Nanoplastics," *Nanomaterials*, vol. 12, no. 9, May 2022, doi: 10.3390/nano12091427.
[54] A. F. R. M. Ramsperger *et al.*, "Environmental exposure enhances the internalization of microplastic particles into cells," 2020.
[55] Y. Ma *et al.*, "Effects of nanoplastics and microplastics on toxicity, bioaccumulation, and environmental fate of phenanthrene in fresh water," *Environmental Pollution*, vol. 219, pp. 166–173, Dec. 2016, doi: 10.1016/j.envpol.2016.10.061.
[56] K. Xu, Y. Zhang, Y. Huang, and J. Wang, "Toxicological effects of microplastics and phenanthrene to zebrafish (Danio rerio)," *Science of the Total Environment*, vol. 757, Feb. 2021, doi: 10.1016/j.scitotenv.2020.143730.
[57] K. Xu *et al.*, "Toxicological effects of nanoplastics and phenanthrene to zebrafish (Danio rerio)," *Gondwana Research*, vol. 108, pp. 127–132, Aug. 2022, doi: 10.1016/j.gr.2021.05.012.
[58] L. C. Stott, S. Schnell, C. Hogstrand, S. F. Owen, and N. R. Bury, "A primary fish gill cell culture model to assess pharmaceutical uptake and efflux: Evidence for passive and facilitated transport," *Aquatic Toxicology*, vol. 159, pp. 127–137, Feb. 2015, doi: 10.1016/j.aquatox.2014.12.007.
[59] M. Zhang and L. Xu, "Transport of micro- and nanoplastics in the environment: Trojan-Horse effect for organic contaminants," 2022, *Taylor and Francis Ltd.* doi: 10.1080/10643389.2020.1845531.
[60] A. A. Koelmans, E. Besseling, A. Wegner, and E. M. Foekema, "Plastic as a carrier of POPs to aquatic organisms: A model analysis," *Environ Sci Technol*, vol. 47, no. 14, pp. 7812–7820, Jul. 2013, doi: 10.1021/es401169n.

Table 1. Medium (C_{med}) and cell (C_{cell}) concentration determined experimentally and free concentration (C_{free}) estimated by MBM

Cell line	ZFL				RTgutGC			
Treatment conditions	**C_{med} ($mg \cdot L^{-1}$)**	**C_{free} ($mg \cdot L^{-1}$)**	**C_{cell} ($mg \cdot kg^{-1}$)**	**BCF ($L \cdot kg^{-1}$)**	**C_{med} ($mg \cdot L^{-1}$)**	**C_{free} ($mg \cdot L^{-1}$)**	**C_{cell} ($mg \cdot kg^{-1}$)**	**BCF ($L \cdot kg^{-1}$)**
10 mg/L PHE (0 h)	11	0.18	-	-	15	0.28	-	-
10 mg/L PHE (24 h)	6	0.09	6	59	9	0.16	2	15
10 mg/L PHE (72 h)	9	0.15	7	49	8	0.15	3	18
10 mg/L PHE + 10 mg/L PS-NPs (0 h)	11	0.19	-	-	14	0.25	-	-
10 mg/L PHE + 10 mg/L PS-NPs (24 h)	7	0.12	4	34	10	0.17	16	82
10 mg/L PHE + 10 mg/L PS-NPs (72 h)	9	0.15	5	33	11	0.20	14	72
10 mg/L PHE + 50 mg/L PS-NPs (0 h)	11	0.19	-	-	13	0.24		
10 mg/L PHE + 50 mg/L PS-NPs (24 h)	8	0.14	5	38	10	0.18	7	37
10 mg/L PHE + 50 mg/L PS-NPs (72 h)	13	0.22	6	26	11	0.20	9	44
25 mg/L PHE (0 h)	25	0.43	-	-	29	0.53	-	-
25 mg/L PHE (24 h)	12	0.20	29	141	13	0.23	6	26
25 mg/L PHE (72 h)	11	0.19	27	146	12	0.22	4	17
25 mg/L PHE + 10 mg/L PS-NPs (0 h)	23	0.38	-	-	24	0.44	-	-
25 mg/L PHE + 10 mg/L PS-NPs (24 h)	17	0.29	32	111	20	0.36	45	126
25 mg/L PHE + 10 mg/L PS-NPs (72 h)	14	0.24	27	113	16	0.30	41	138
25 mg/L PHE + 50 mg/L PS-NPs (0 h)	27	0.46	-	-	28	0.51	-	-
25 mg/L PHE + 50 mg/L PS-NPs (24 h)	16	0.28	37	133	24	0.44	64	145
25 mg/L PHE + 50mg/L PS-NPs (72 h)	14	0.24	24	101	23	0.43	72	169
50 mg/L PHE (0 h)	46	0.78	-	-				
50 mg/L PHE (24 h)	19	0.33	139	423				
50 mg/L PHE (72 h)	18	0.31	118	378				
50 mg/L PHE + 10 mg/L PS-NPs (0 h)	47	0.79	-	-				
50 mg/L PHE + 10 mg/L PS-NPs (24 h)	20	0.34	223	665				
50 mg/L PHE + 10 mg/L PS-NPs (72 h)	18	0.30	162	532				
50 mg/L PHE + 50 mg/L PS-NPs (0 h)	48	0.75	-	-				
50 mg/L PHE + 50 mg/L PS-NPs (24 h)	28	0.47	386	826				
50 mg/L PHE + 50mg/L PS-NPs (72 h)	21	0.36	150	722				

Figure 1. Cell viability of ZFL and RTgutGC cells when exposed to PHE or PHE + PS-NPs (10 mg·L^{-1} and 50 mg·L^{-1}). a) ZFL cells for 24 h, b) ZFL cells for 72 h, c) RTgutGC cells for 24 h and d) RTgutGC cells for 72 h. Significance levels *p < 0.05

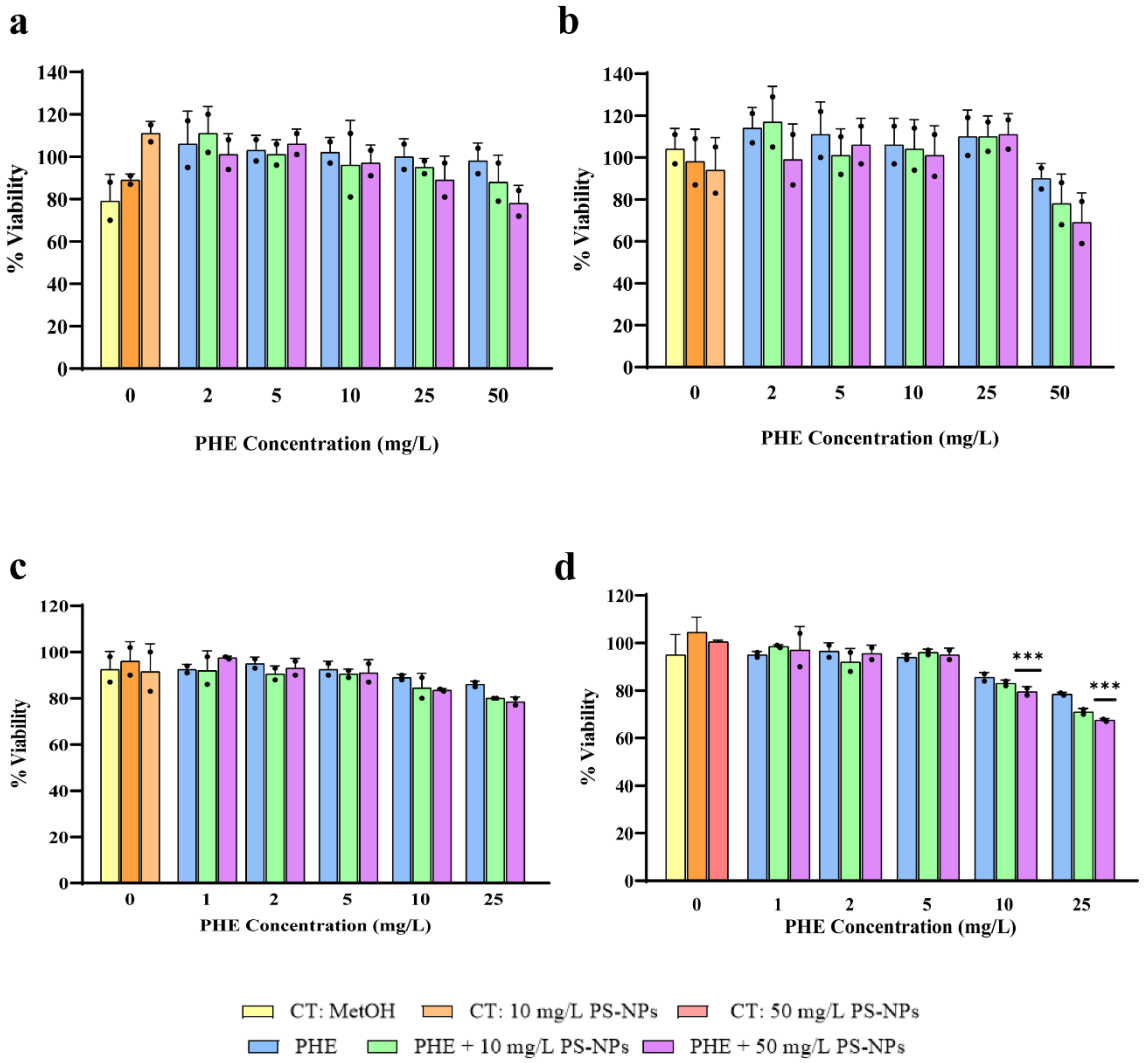

Figure 2. (a, e): Uptake of fluorescently labelled PS-NPs by ZFL or RTgutGC cells. (a) Uptake in ZFL (e) Uptake in RTgutGC cells. (b, f): Individual images of ZFL (b) and RTgutGC (f) cells obtained from single exposure of PS-NPs versus co-exposure with PHE. (c, d): 2D (c) and 3D (d) confocal microscopy images of PS-NPs exposed individually or with PHE. Green fluorescence corresponds to PS-NPs; blue and magenta to Hoechst-stained nuclei (N) and Cell Mask-stained plasma membrane, respectively.

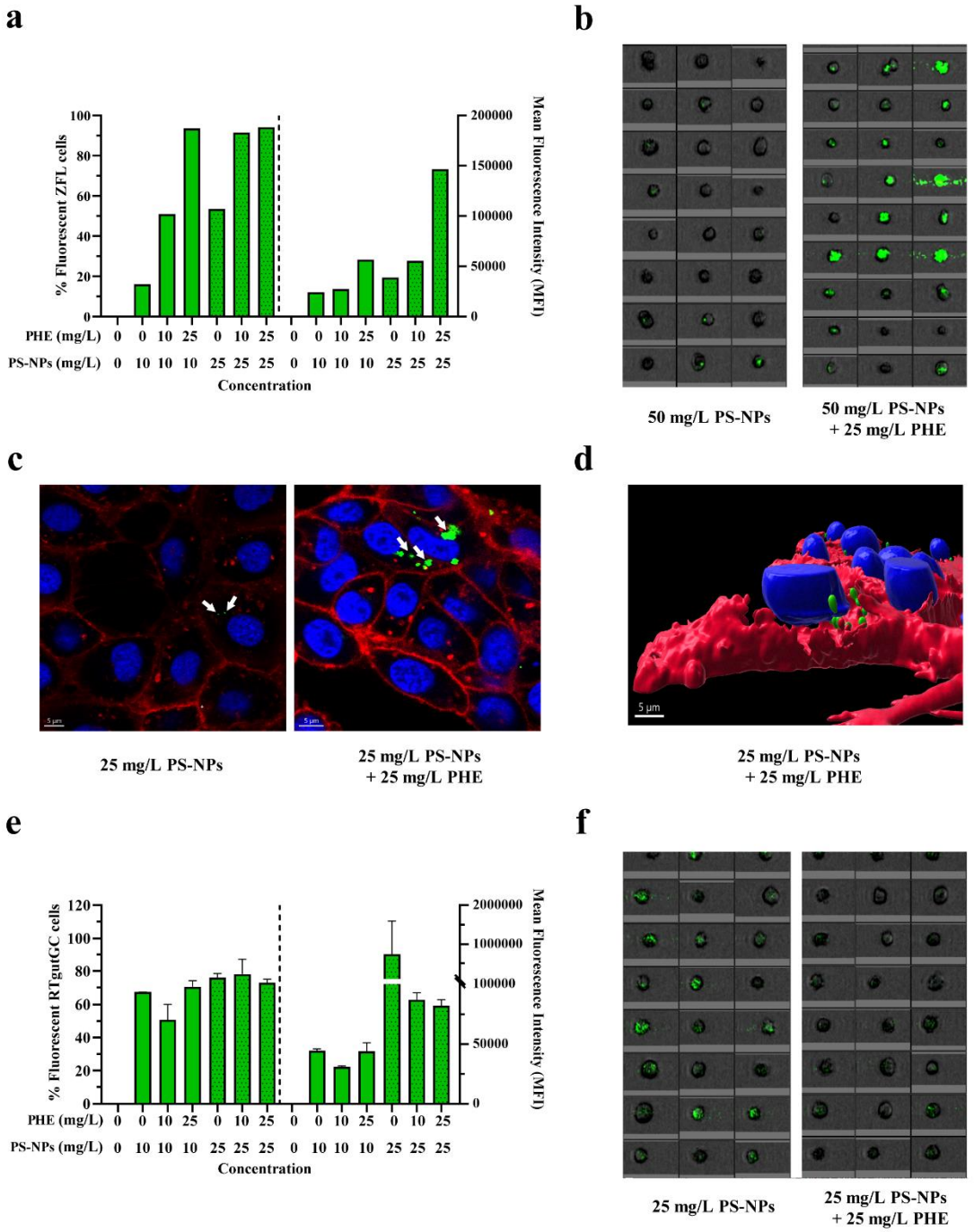

Figure 3. Concentration of PHE metabolites when exposed to nominal 10 mg·L^{-1} PHE with or without 10 mg·L^{-1} or 50 mg·L^{-1} PS-NPs in ZFL cells at 24 h and 72 h

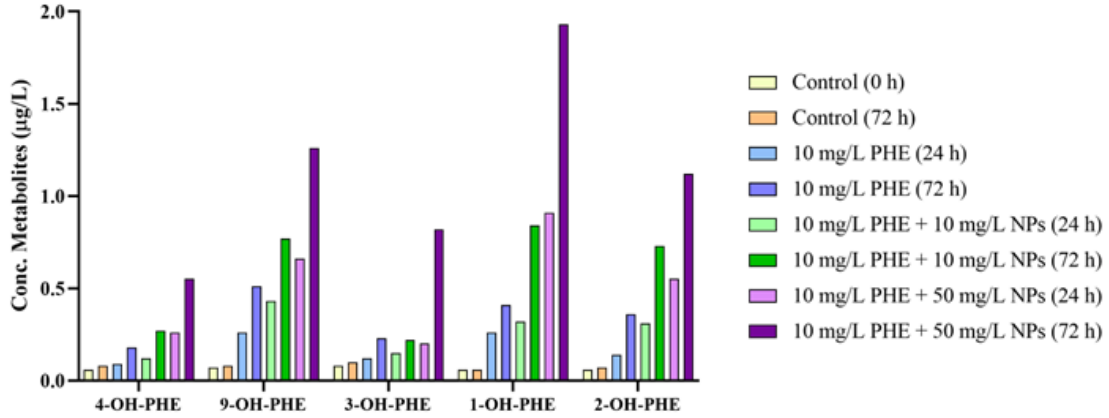

Figure 4. (a) Survival of PHE treated zebrafish larvae or PHE plus PS-NPs (n = 24). (b) Probit analysis of LC_{50} values of 5 mg·L^{-1} PHE and PHE with 5 mg·L^{-1} PS-NPs at nominal concentrations on zebrafish larvae 24 h after exposure.

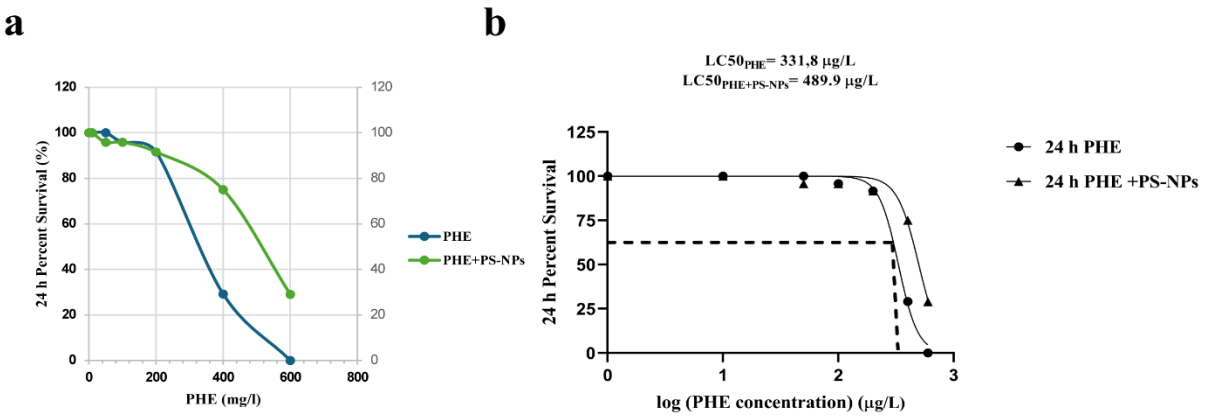

Figure 5. Uptake of PS-NPs in the presence of PHE in zebrafish larvae. (a) Representative images of PS-NPs bioaccumulation. Animals were co-exposed to 5 mg/L of PS-NPs plus PHE for 48 h at 3 dpf. (b) Quantification of the Mean Fluorescence Intensity (MFI) in the zebrafish larvae. Bioaccumulation of PS-NPs was estimated at 5 dpf in the whole larvae. (c) PHE larvae concentration (C_{larvae}) and estimated BCF ($C_{larvae}/C_{exposure}$) 24 h after exposure. Images were analysed with ImageJ and the measured fluorescence was normalized to the larvae area. Statistical differences between treatments were analysed by unpair non-parametric Kolmogorov-Smirnov test Significance levels *p < 0.05. n.d.: not detected.

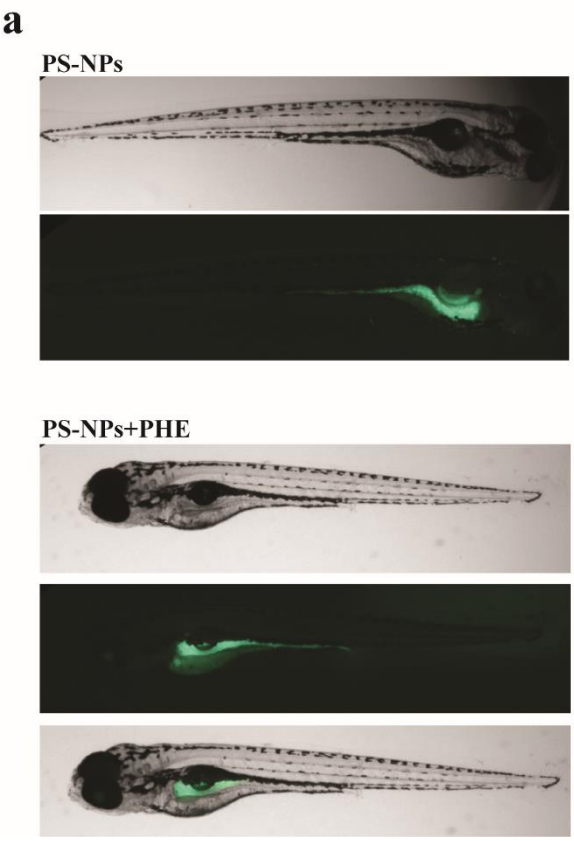

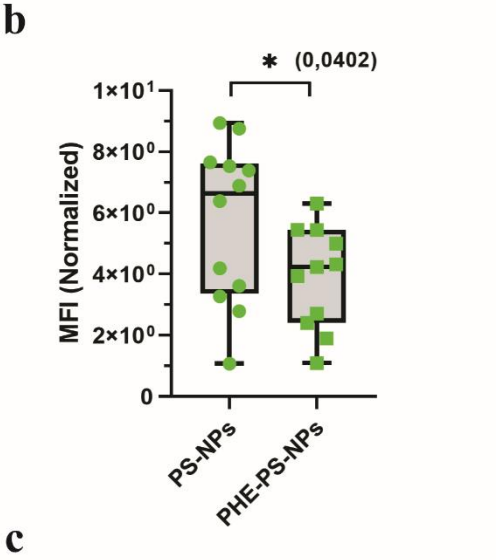

c

Treatment conditions	C_{larvae} (µg·kg^{-1})	BCF (L·kg^{-1})
Control (without PHE and PS-NPs)	n.d.	-
10 µg/L PHE	155	16
50 µg/L PHE	598	12
100 µg/L PHE	3111	31
10 µg/L PHE + 5 mg/L PS-NPs	388	39
50 µg/L PHE + 5 mg/L PS-NPs	698	14
100 µg/L PHE + 5 mg/L PS-NPs	5537	55

Complex combined effects of polystyrene nanoplastics and phenanthrene in aquatic models

Supporting information

Free bioavailable concentration (C_{free}): Importance and data analysis

In vitro cell-based assays are a rapid, simple and cost-effective tool for the evaluation of the effects of chemicals. In these assays, the dose quantification is often used as the nominal concentration (C_{nom}) [1]. However, it is only the freely dissolved concentration (C_{free}) that is bioaccessible for cellular uptake and thus produces effects. This C_{free} can be reduced and differ from C_{nom} because chemicals can be distributed in the *in vitro* test compartments, including the exposure medium with the globular protein bovine serum albumin, the plastic plate and the headspace for some volatile substances [2]. Therefore, the nominal concentrations used in this work were used as an experimental reference, but the effect concentrations had to be determined. There are currently two strategies for estimating C_{free}: advanced analytical experimental methods based on solid-phase microextraction (SPME) [3] and mass balance models (MBM) based on the chemical distribution equilibria in the different compartments of an in vitro system and the physico-chemical properties of the compounds [2].

In this work, the MBM developed by Fisher et al. [1] was used. Briefly, the PHE distribution parameters, obtained with the UFZ-LSER Calculation Partition System tool [4], and the parameters of the test system for the experiment were entered into the MBM spreadsheet to obtain the fractions of the different cellular compartments. These percentages were then applied to each experimentally determined total PHE concentration in the medium (C_{med}) to estimate the C_{free} at each exposure time.

It is true that this model only considers equilibria with an individual compound and does not consider the additional balance that occurs between PHE and polystyrene nanoplastics (PS-NPs). Therefore, for these samples, the concentration will not be as accurate. However, it is a much closer approximation to reality than the nominal concentration and, in addition, it shows a better estimate of the freely dissolved concentration available to be adsorbed on the surface of PS-NPs.

Bioconcentration factor (BCF) determination

In our previous study [5], different methodologies for the estimation of BCF *in vitro* were evaluated. The closest analysis to reality was achieved by considering the absorption kinetics and the bioavailable concentration in the *in vitro* system. However, because the uptake kinetics of phenanthrene in ZFL cells achieved stability over the exposure time, according to OECD 305 [6], the BCF can be approximated by the ratio of the concentration in the organism, i.e. inside the cell (C_{cell}) and the concentration in the medium, in this case, the bioavailable concentration (C_{free}) at each exposure time. Since only two exposure times were studied in this study, which were too short for kinetic study, and the main objective was to compare the accumulation with respect to the presence of PS-NPs in the medium, it was decided to estimate the BCF at each exposure time.

References

[1] F. C. Fischer *et al.*, "Modeling Exposure in the Tox21 in Vitro Bioassays," *Chem Res Toxicol*, vol. 30, no. 5, pp. 1197–1208, May 2017, doi: 10.1021/acs.chemrestox.7b00023.

[2] S. Proença *et al.*, "Effective exposure of chemicals in in vitro cell systems: A review of chemical distribution models," Jun. 01, 2021, *Elsevier Ltd*. doi: 10.1016/j.tiv.2021.105133.

[3] L. Henneberger, M. Mühlenbrink, F. C. Fischer, and B. I. Escher, "C18-Coated Solid-Phase Microextraction Fibers for the Quantification of Partitioning of Organic Acids to Proteins, Lipids, and Cells," *Chem Res Toxicol*, vol. 32, no. 1, pp. 168–178, Jan. 2019, doi: 10.1021/acs.chemrestox.8b00249.

[4] S. ; B. T. N. ; W. N. ; B. G. ; A. M. H. ; G. K.-U. N. E. Ulrich, "UFZ-LSER Database v 3.2 [Internet]," 2017, *Helmholtz Zentrum für Umweltforschung - UFZ, Leipzig, Deutschland*, .

[5] P. De Oro-Carretero and J. Sanz-Landaluze, "In vitro approach to refine bioconcentration and biotransformation predictions of organic persistent pollutants using cell lines," *Chemosphere*, vol. 364, Sep. 2024, doi: 10.1016/j.chemosphere.2024.143020.

[6] OECD 305, "OECD/OCDE 305 OECD GUIDELINES FOR TESTING OF CHEMICALS Bioaccumulation in Fish: Aqueous and Dietary Exposure," 2012.

Figure S1. Cell viability after exposure to different PHE concentrations and in combination with 10 mg·L^{-1} and 50 mg·L^{-1} PS-NPs in a) ZFL cells for 24 h, b) ZFL cells for 72 h measured by BD Via-Probe™ Red Nucleic Acid Stain labelling and flow cytometry. Significance levels *p < 0.05

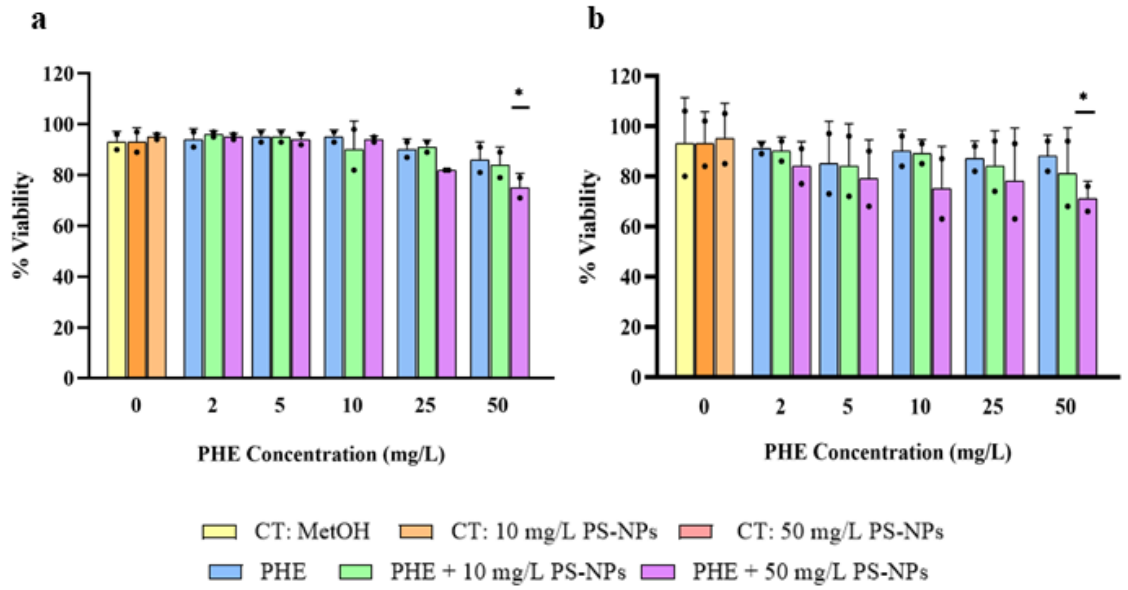

Figure S2. Uptake of fluorescent PS-NPs by ZFL cells after exposure at a) 24 h and b) 72 h. Dose-response: percentage of fluorescent positive cells compared to individual exposure to PS-NPs and in combination with different concentrations of PHE

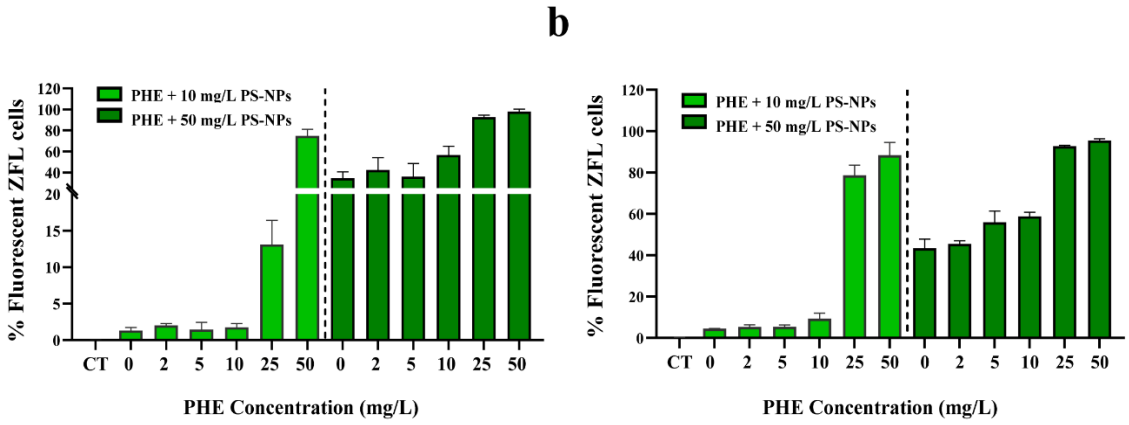

Figure S3. Uptake of PHE by ZFL and RTgutGC cells after exposure to PHE (10, 25 and 50 mg·L^{-1}) and PHE + PS-NPs (10 mg·L^{-1} and 50 mg·L^{-1}) for 24 h and 72 h

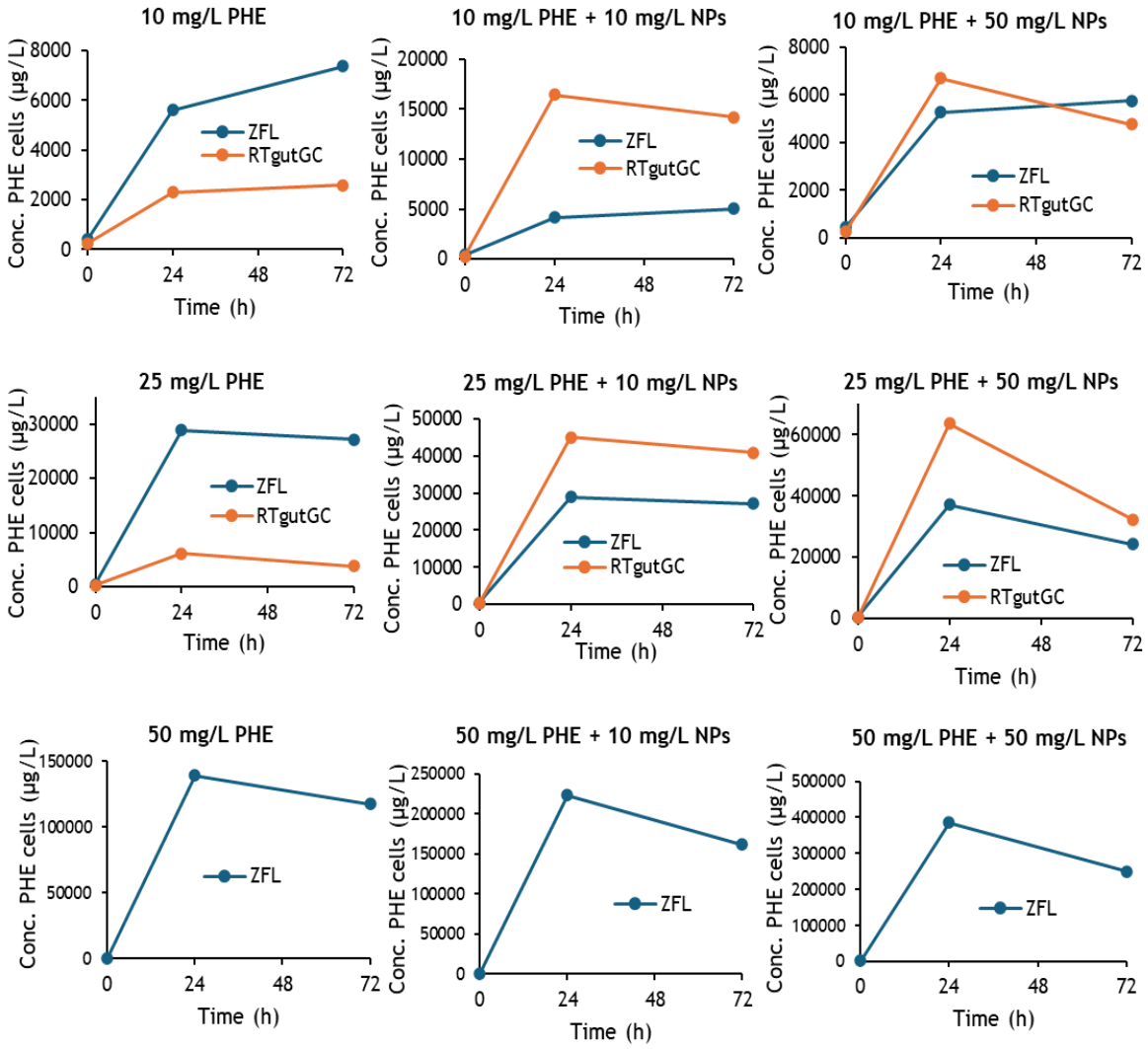

Figure S4. Concentration of PHE metabolites when exposed to 25 mg·L^{-1} (a) and 50mg·L^{-1} (b) PHE individually and in combination with 10 mg·L^{-1} and 50 mg·L^{-1} PS-NPs in ZFL cells at 24h and 72h

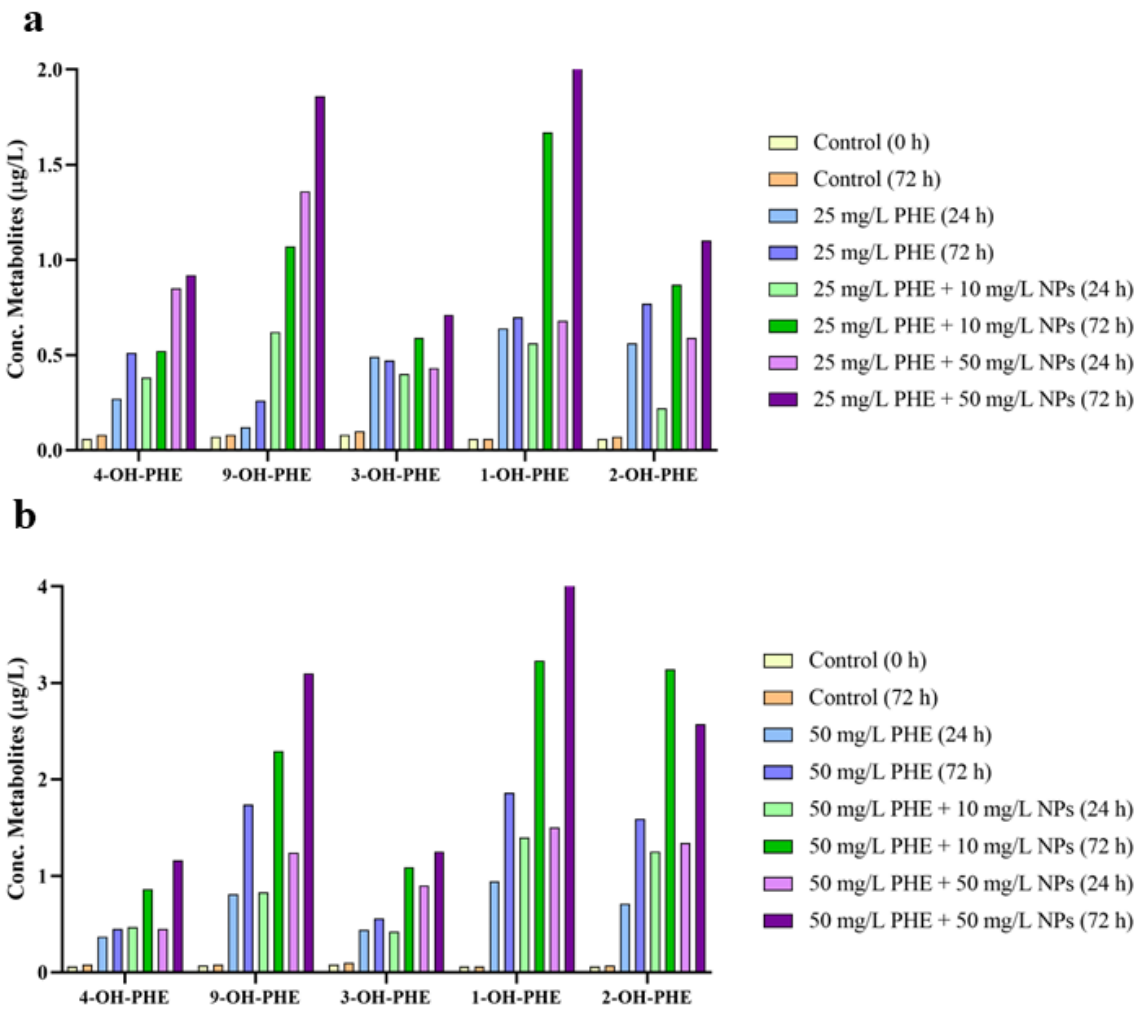

VIII. DISCUSIÓN INTEGRADORA

VIII. DISCUSIÓN INTEGRADORA

En esta sección se realiza una discusión global de los resultados correspondientes a los trabajos expuestos en la *Metodología Experimental* con el fin de ofrecer una perspectiva global de los estudios desarrollados en el marco de esta Tesis Doctoral. El eje central de esta discusión radica en el diseño, evaluación y aplicación de metodologías alternativas para el estudio de la toxicidad, bioacumulación y biotransformación de contaminantes orgánicos persistentes, así como en la optimización de métodos analíticos para alcanzar dicho objetivo. Todo ello desarrollado teniendo en cuenta los actuales enfoques en la experimentación del riesgo químico: **i) la evaluación de la toxicidad conforme al nuevo marco regulador, que exige no solo valorar los efectos de los compuestos, sino también describir su comportamiento y distribución en los organismos y el medio ambiente; y ii) el desarrollo y aplicación de ensayos éticos alineados con el principio de las 3R.** En este contexto, los estudios presentados han tenido como finalidad avanzar en el desarrollo de ensayos que contribuyan a la reducción y el reemplazo de la experimentación animal, al tiempo que proporcionan datos relevantes para el perfeccionamiento de modelos existentes, todo ello mediante enfoques más eficientes y de menor costo. En esta tesis, se plantearon y desarrollaron dos enfoques experimentales: el uso de larvas como modelo *in vivo* y líneas celulares como modelo *in vitro* en la evaluación del cálculo de la bioconcentración y biotransformación de dos compuestos orgánicos considerados como persistentes (PHE y BDE-47). En esta discusión final, se analizan las similitudes, diferencias y la aplicabilidad de ambas metodologías, con el objetivo de evaluar su capacidad para sustituir de manera efectiva a los modelos animales tradicionales. Asimismo, la **aplicación** de las metodologías desarrolladas ha permitido **profundizar en el conocimiento** de los efectos y el comportamiento de estos contaminantes **en presencia** de otros, como los **nanoplásticos**, cuyo reciente impacto en el medio ambiente ha suscitado una gran preocupación social.

Los compuestos PHE y BDE-47 fueron seleccionados como modelos de POPs debido a su dualidad: por un lado, han sido **estudiados mediante modelos tradicionales**, lo que permite evaluar la eficacia de las metodologías alternativas desarrolladas en esta Tesis Doctoral; por otro, su persistencia en el medio

ambiente y la creciente evidencia de su interacción con otros contaminantes emergentes justifican la necesidad de **seguir investigando** su comportamiento y posibles efectos aún no completamente comprendidos.

La **evaluación de la bioacumulación**, según el modelo estandarizado OECD 305, se cuantifica mediante el BCF, el cual se basa en la relación entre la concentración del compuesto dentro del organismo y su concentración en el medio, generalmente determinada a distintos tiempos de exposición para una **determinación toxicocinética**. Por ello, el **diseño experimental de las metodologías alternativas** desarrolladas en esta Tesis Doctoral, tanto con larvas como con líneas celulares, ha sido configurado **en esta dirección para obtener el BCF de forma rigurosa** (**Figura 22**). En el caso de la metodología *in vitro*, debido al uso limitado de 72h para un ensayo continúo con líneas celulares, sumado a su cultivo adherente en la placa y al material disponible, no se realizó fase de depuración. Sin embargo, en todas las metodologías se conservó la necesidad del muestreo a diferentes tiempos de exposición (incluido el tiempo 0) tanto del organismo (larvas o células) como los medios de exposición, las muestras control en paralelo y la concentración del xenobiótico por debajo del LC_{50}.

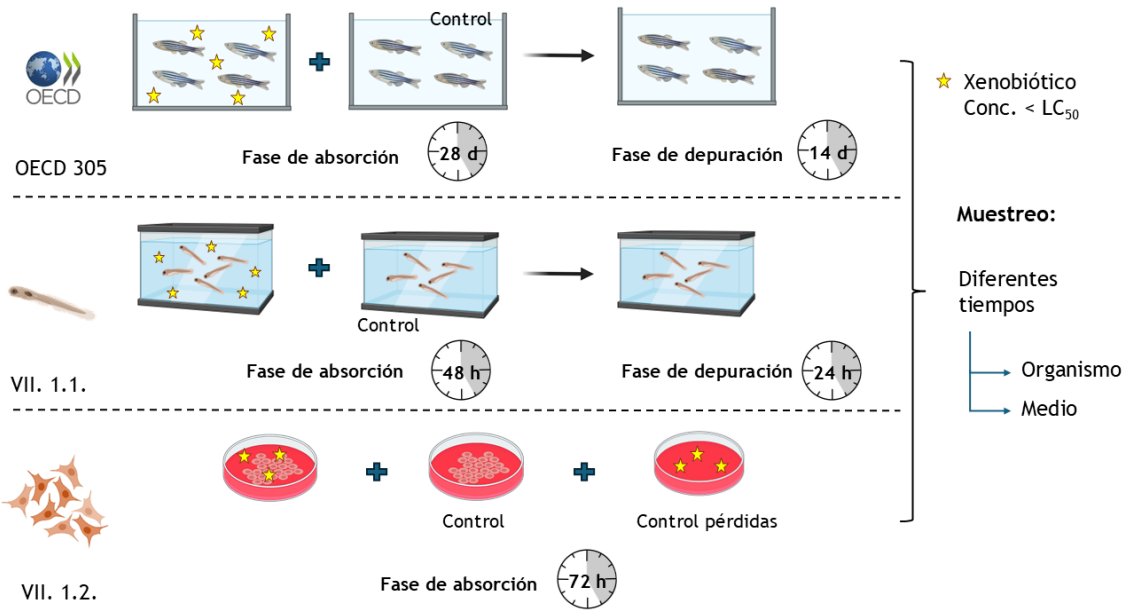

Figura 22. *Diseño experimental en la exposición de las metodologías alternativas propuestas en comparación con la metodología oficial de la OECD.*

En este contexto, resulta imprescindible contar con **métodos analíticos** adecuados para la extracción y determinación de los compuestos tanto en el organismo como en el medio de exposición. Además, dado que uno de los objetivos fundamentales de esta Tesis Doctoral es **estudiar simultáneamente la bioacumulación y la biotransformación**, con el fin de aportar datos sobre la evolución de ambas cinéticas, se requiere un método analítico capaz de detectar de manera simultánea tanto los compuestos parentales como sus principales metabolitos. Para ello, con el fin de evaluar la idoneidad de las metodologías propuestas, se seleccionaron los metabolitos a determinar para cada compuesto, priorizando aquellos que, según la literatura, han sido identificados con mayor frecuencia en organismos: BDE-28, 2'-OH-BDE-28, 6-MeO-BDE-47, 5-MeO-BDE-47, 3-OH-BDE-47 y 5-OH-BDE-47 para el BDE-47; 1-OH-PHE, 2-OH-PHE, 3-OH-PHE, 4-OH-PHE y 9-OH-PHE para el PHE.

Se ha optimizado un **método analítico común para ambas metodologías alternativas** (**Figura 23**), abarcando tanto la determinación de la concentración en larvas (***Artículo 1***) como en líneas celulares (***Artículo 2***), así como en sus respectivos medios de exposición. La extracción se llevó a cabo mediante una técnica de extracción sólido-líquido asistida por ultrasonidos para muestras sólidas y una extracción líquido-líquido para muestras del medio de exposición, empleando un disolvente con afinidad por los compuestos a analizar. En el caso de las larvas se incorporó una etapa adicional de limpieza del extracto, basada en extracción en fase sólida dispersiva, utilizando un adsorbente capaz de eliminar interferencias. Además, debido a la necesidad de detectar compuestos hidroxilados mediante GC, se incorporó un paso previo de derivatización antes de la determinación. El principal **desafío analítico** radicó en el **reducido tamaño de las muestras** (0.44 mg por larva en muestras de 9-15 larvas y 2-5 mg de pellet celular, según la línea celular) y en la necesidad de **extraer simultáneamente compuestos con diferentes propiedades fisicoquímicas,** desde metabolitos hidroxilados polares hasta compuestos apolares. Para superar esta dificultad, se decidió realizar una extracción asistida por una sonda de ultrasonidos junto a la optimización de una mezcla de disolventes de distinta polaridad que ofreciera resultados satisfactorios para todos los compuestos (**Tabla 9**).

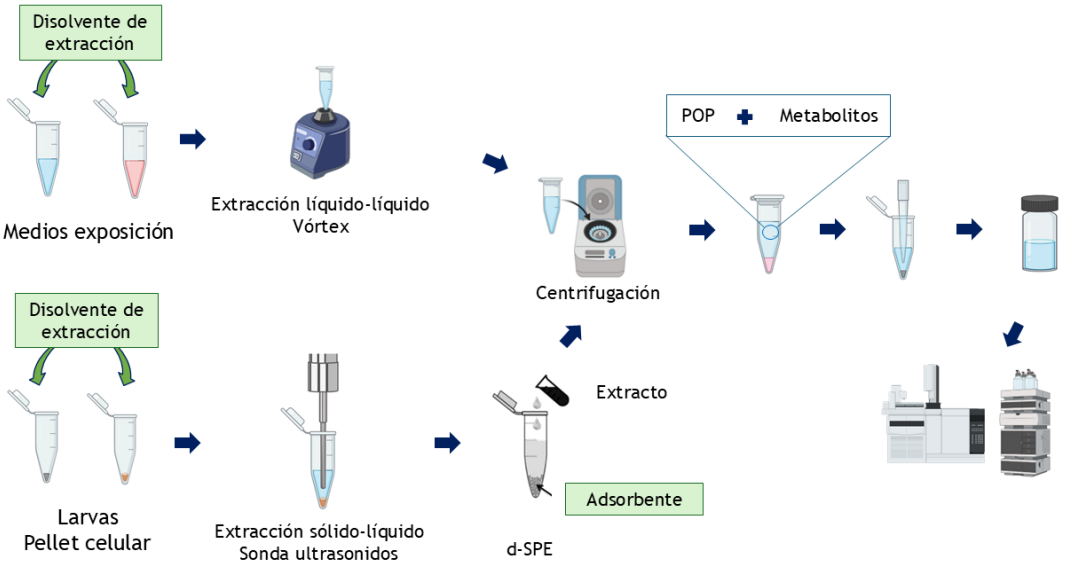

Figura 23. *Método de extracción común para ambas metodologías alternativas.*

Tabla 9*. Disolventes de extracción optimizados para cada extracción.*

Muestra	Compuestos	Disolvente de extracción	Separación y detección
Larvas Medio Larvas	BDE-47 + MeO-BDEs + OH-BDEs	Hexano:MTBE (1:1)	GC-MS-μECD
Larvas Medio Larvas	PHE + OH-PHEs	Hexano	GC-MS
Células: HepG2, ZFL Medio cultivo: HepG2, ZFL	BDE-47 + MeO-BDEs + OH-BDEs	Hexano:MTBE (1:1)	GC-MS-μECD
Células: HepG2, ZFL, ZF4	PHE PHE OH-PHEs	ACN Hexano Hexano:DCM (1:1)	LC-FLD GC-MS GC-MS
Medio cultivo: HepG2, ZF4	PHE PHE OH-PHEs	ACN (+NaCl) Hexano Hexano:DCM (1:1)	LC-FLD GC-MS GC-MS
Medio cultivo: ZFL	PHE PHE OH-PHEs	ACN (+NaCl) Hexano Hexano:MTBE (1:1)	LC-FLD GC-MS GC-MS

La extracción asistida por sonda de ultrasonidos permitió una **extracción miniaturizada**, eficaz para el tratamiento de muestras de pequeño tamaño, sin necesidad de manipulación, debido a la punta de titanio de 2 mm de diámetro compatible con volúmenes de 150 µL a 5 mL. En términos generales, cuando se requirió la **extracción simultánea** de compuestos con diferentes polaridades, el uso de mezclas de disolventes resultó más eficaz que la utilización individual de cada uno, debido al efecto sinérgico entre sus propiedades, creando un entorno de polaridad más equilibrado. Esto amplió el rango de polaridad del sistema extractivo, permitiendo la recuperación simultánea de todas las especies en una sola etapa de extracción y optimizando el proceso. Para el PHE y sus metabolitos OH-PHEs, las mejores recuperaciones se lograron con la mezcla de hexano y DCM, mientras que para el BDE-47 y sus metabolitos MeO-BDEs y OH-BDEs, la combinación más eficiente fue hexano y MTBE. El hexano, altamente apolar, disuelve eficazmente compuestos muy hidrofóbicos como el PHE y el BDE-47. El DCM, por su parte, suele mostrar gran afinidad por los compuestos con anillos aromáticos debido a su interacción con los electrones π y a su capacidad para romper las fuerzas hidrofílicas de los grupos hidroxilados con la fase acuosa. No obstante, el DCM presenta cierta toxicidad y puede generar emulsiones al ser soluble en agua, por lo que se necesitó una centrifugación a elevadas revoluciones por minuto. El BDE-47, con una estructura de anillos aromáticos unidos por un enlace éter y sustituidos por átomos de bromo, no tiene una distribución electrónica tan homogénea como el PHE, reduciendo su solubilidad en DCM. Además, esta estructura lo hace más voluminoso y más apolar en general, lo que hace que el MTBE, más apolar que el DCM, funcione mejor para estos compuestos. La estructura de éter del MTBE le confiere, además, cierta polaridad que le permite disolver eficientemente compuestos de polaridad intermedia. Se encontró una excepción en la extracción de los metabolitos OH-PHEs del medio de exposición de la línea celular ZFL. Esto podría deberse a que el medio de cultivo de dicha línea celular se suplementa con componentes más complejos que tienden a retener los compuestos, por lo que se necesitó una mezcla más apolar para extraerlos eficazmente.

Por otro lado, se evaluaron distintos **adsorbentes en la limpieza** de muestras de larvas para la extracción de BDE-47 y sus metabolitos: PSA y Z-Sep provocaron grandes pérdidas de los compuestos hidroxilados, C18 redujo interferencias lipídicas, pero no eliminó por completo la matriz, mientras que el Florisil permitió recuperaciones equilibradas de PBDEs, MeO-BDEs y OH-BDEs, siendo la mejor opción. Para la extracción de PHE y sus metabolitos, a diferencia con la detección mediante ECD, la selectividad del GC-MS hizo innecesaria la etapa de limpieza

Como resultado, se obtuvo una **metodología miniaturizada adaptable a la determinación de prácticamente cualquier POP neutro**, con la única necesidad de ajustar la composición de disolventes y/o el adsorbente en función de las características específicas de los compuestos analizados. Otra ventaja destacable es la **rapidez y sencillez** del procedimiento, lo que resulta fundamental tanto para el **análisis de cribado** como para su integración en los modelos existentes de predicción del BCF.

Otra de las dificultades enfrentadas fue la **separación cromatográfica** de metabolitos con **estructuras isoméricas**, garantizando al mismo tiempo la **sensibilidad y selectividad** necesarias para su identificación y cuantificación en las bajas concentraciones presentes en las muestras. Este objetivo se alcanzó mediante la optimización de la rampa de temperaturas, en combinación con el uso de detectores de alta sensibilidad específicos para los compuestos analizados, como el FLD para PHE y el ECD para BDE-47. La detección y cuantificación de los metabolitos se llevó a cabo mediante MS, garantizando así una identificación inequívoca. Asimismo, en el caso particular del BDE-47 y sus metabolitos, se utilizó y optimizó un **divisor de flujo** al final de la columna cromatográfica, lo que permitió la **utilización simultánea de ambos detectores**, asegurando la determinación de metabolitos al nivel de trazas, aprovechando las ventajas de cada detector. Los métodos analíticos desarrollados fueron evaluados mediante su aplicación en ensayos de bioacumulación y biotransformación, y la obtención de resultados satisfactorios, como se detalla más adelante, validó su efectividad y capacidad.

La metodología basada en el uso de **eleuteroembriones** (72 hpf) ha sido previamente evaluada dentro del grupo de investigación para una amplia variedad de sustancias químicas con el propósito de determinar el BCF, obteniendo valores comparables a los obtenidos en ensayos con organismos adultos. En este contexto, y considerando la necesidad actual de estudiar de manera simultánea la bioacumulación y la biotransformación, el primer estudio realizado (**Artículo 1**) tuvo como objetivo verificar la eficacia de esta metodología para la evaluación conjunta de ambos procesos. Para ello, se expusieron las larvas, se muestrearon a diferentes tiempos de exposición y se determinaron las concentraciones del BDE-47 y sus metabolitos en el interior de las larvas y medios de exposición, de acuerdo con el diseño experimental y método analítico desarrollado, descritos en la *Sección 1.1* de la *Metodología Experimental* y esquematizados en la **Figura 22** y **23**, respectivamente.

En primer lugar, los perfiles cinéticos de acumulación reflejaron una rápida pero sostenida absorción del BDE-47 durante la fase de exposición, sin alcanzarse el estado estacionario al finalizar esta, a las 48 horas. A partir de las concentraciones determinadas, se calculó el BCF mediante la ratio de estas al final de la etapa de absorción y mediante el modelo toxicocinético, descrito en la *Sección 2.1* de la Introducción. Como consecuencia, los valores calculados de BCF a 48 h y el BCF toxicocinético (BCF_k) no fueron totalmente coincidentes. Según lo estipulado en la guía OECD 305, BCF_k constituye una estimación más precisa de la realidad y fue el valor empleado para el análisis y la discusión. De este modo, se obtuvo un BCF_k de 7294 ± 899 y 36363 ± 5702 $L \cdot kg^{-1}$ en las exposiciones a 10 y 1 $\mu g \cdot L^{-1}$, respectivamente. **Estos valores experimentales mostraron una concordancia satisfactoria con los resultados reportados en la literatura para otros organismos acuáticos y los predichos por los modelos QSAR.** Cabe destacar en esta discusión el hecho de que se obtuvo un valor de BCF_k más elevado en la exposición a una concentración menor. Desde un punto de vista matemático, esto se debe a que la constante de absorción cinética fue superior en la exposición a 1 $\mu g \cdot L^{-1}$ (430 vs. 124 $L \cdot \mu g \cdot h^{-1}$), sumado a una ligera disminución en la constante de desorción (0.01 vs. 0.02 $\mu g \cdot L^{-1}$) en comparación con la exposición a 10 $\mu g \cdot L^{-1}$. Teóricamente, la acumulación de un compuesto depende únicamente de la difusión

y del almacenamiento en lípidos; sin embargo, los valores de BCF presentan una relación con la concentración, probablemente debido a la activación de otros mecanismos fisiológicos durante la internalización de los compuestos[184]. Asimismo, es fundamental determinar la concentración real de los compuestos en el agua durante el experimento, ya que la mayoría de los estudios de bioconcentración calculan el BCF a partir de concentraciones nominales[112]. **Por este motivo, un BCF obtenido experimentalmente es preferible a los métodos QSAR que, aunque han mejorado, aún no modelizan de manera precisa algunos procesos, como la biotransformación.**

En este estudio, se identificaron y cuantificaron los metabolitos BDE-28, 2'-OH-BDE-28 y 5-MeO-BDE-47, tanto en el experimento a mayor concentración, medido únicamente a las 48 h, como en el experimento simultáneo de bioacumulación con exposiciones a 1 y 10 $\mu g \cdot L^{-1}$. Esto permitió observar la evolución de la concentración de los metabolitos a lo largo del tiempo y obtener datos sobre las ratios de biotransformación en relación con la acumulación de BDE-47. Estudios previos, como el realizado por Liu *et al.*[185], evaluaron la biotransformación del BDE-47 en embriones de pez cebra (4 hpf), finalizando el experimento a las 120 hpf (larva) sin detectar la presencia de metabolitos. En la metodología propuesta en esta Tesis Doctoral, la exposición se inició a las 72 hpf, momento en el que la expresión de CYP1A y, como consecuencia, la capacidad metabólica aumenta drásticamente. **Estos resultados ponen de manifiesto la capacidad de los eleuteroembriones a partir de las 72 hpf para biotransformar compuestos, lo que abre la posibilidad de estudiar de manera simultánea la bioacumulación y la biotransformación sin necesidad de recurrir a la experimentación animal o, en su defecto, reduciéndola en gran medida en comparación con la guía actual validada.**

---

112 **Zheng** *et al.* Accumulation and biotransformation Contamination and Toxicology. **2012Liu** *et al.* Bioaccumulation, biotransformation, and toxicity of BDE-47, 6-OH-BDE-47, and 6-MeO-BDE-47 in early life-stages of zebrafish (danio rerio). *Enviro Sci Technol.* **2015**.

184 **McGeer** *et al.* Inverse relationship between bioconcentration factor and exposure concentration for metals: Implications for hazard assessment of metals in the aquatic environment. *Environ Toxicol Chem*. **2003**.

185 **Liu** *et al.* Bioaccumulation, biotransformation, and toxicity of BDE-47, 6-OH-BDE-47, and 6-MeO-BDE-47 in early life-stages of zebrafish (danio rerio). *Enviro Sci Technol.* **2015**.

La siguiente metodología alternativa desarrollada en esta Tesis Doctoral, basada en el uso de **líneas celulares,** se planteó con el objetivo de reemplazar completamente la experimentación animal, así como, refinar los modelos existentes. La guía validada actual OECD 280 para obtener el BCF, se basa en la utilización de hepatocitos o fracciones hepáticas subcelulares S9 de trucha arcoíris, recién aislados de un pez adulto. Por consiguiente, aunque en menor medida en comparación con la guía OECD 305, sigue siendo necesaria cierta experimentación animal. Asimismo, entre las limitaciones descritas en la propia guía, se destaca que los sistemas *in vitro* utilizados presentan una vida útil de 2 a 4 horas, en contraste con las 72 horas que ofrecen las líneas celulares, lo que posibilita la evaluación de compuestos con cinéticas de biotransformación más lentas. A este factor se suman otras ventajas como la rapidez en la obtención de resultados, el menor costo, las condiciones experimentales controladas y una mayor reproducibilidad, posicionando a las líneas celulares como una alternativa prometedora. No obstante, la principal limitación radica en que, al tratarse de sistemas inmortalizados, han perdido parte de su función especializada, lo que impide obtener resultados tan precisos como los que se obtendrían en cultivos primarios. Sin embargo, su aplicación resulta útil en análisis de cribado.

En este contexto, el primer paso fue evaluar la capacidad de biotransformación de las líneas celulares seleccionadas (HepG2, ZFL y ZF4). En el **Artículo 2** se demostró la capacidad de biotransformación de las células HepG2, observándose la presencia de metabolitos a las 48 horas de exposición a PHE y BDE-47. En el caso del PHE, se detectaron todos los OH-PHEs estudiados, con mayores tasas de biotransformación en el medio de exposición que en las células, lo cual se atribuye a la polaridad de estos compuestos y a la función detoxificadora de las células hepáticas. De manera similar, en el experimento con BDE-47 se identificaron los metabolitos 5-OH y 3-OH en el medio de exposición. Sin embargo, el compuesto 5-MeO-BDE-47 y otros metabolitos no identificados se detectaron exclusivamente en el interior celular, probablemente debido a la mayor dificultad de las células hepáticas para detoxificar compuestos apolares. Cabe destacar que en las muestras control se identificó una impureza de BDE-28 en el patrón comercial de BDE-47, ocasionalmente también reportada en otros estudios de la literatura, por lo que su

detección no se consideró en el análisis, debido a la imposibilidad de diferencia la propia bioacumulación del BDE-28 con la concentración debida a la biotransformación del BDE-47. En el **Artículo 3**, para el compuesto PHE, y en el **Artículo 4**, para el compuesto BDE-47, se confirmó la capacidad de biotransformación de la línea celular ZFL, manifestada por el incremento en la concentración de los metabolitos a lo largo del tiempo. En ambos casos, se identificaron los mismos metabolitos que en las células HepG2. Adicionalmente, en el **Artículo 4 se llevó a cabo una comparación de las ratios de metabolización obtenidos (considerando C_{free}) entre ambas líneas celulares y, en el caso del BDE-47, también con respecto a las ratios obtenidas en el Artículo 1, empleando larvas de pez cebra, observándose valores considerablemente concordantes**. Asimismo, se efectuó un balance de masa en cada experimento, obteniéndose recuperaciones superiores al 70%, lo que sugiere que, aunque sería interesante identificar posibles metabolitos intermedios, los compuestos determinados corresponden a los metabolitos mayoritarios. **Estos resultados respaldan el uso de las líneas celulares HepG2 y ZFL para el estudio de la biotransformación.** En cambio, en la línea celular ZF4 no se detectó ningún metabolito, probablemente debido a su limitada capacidad de biotransformación al no presentar funcionalidad hepática.

Una vez evaluada la capacidad de biotransformación, se procedió a analizar la validez del uso de líneas celulares en el modelo IVIVE-BCF descrito en la guía OECD 280. Las investigaciones correspondientes se llevaron a cabo para el compuesto PHE en el **Artículo 3** y para el BDE-47 en el **Artículo 4**. El **modelo IVIVE-BCF** se basa en el enfoque de agotamiento del sustrato para la determinación de la constante de metabolización, donde se evalúa la disminución de la concentración en el medio de exposición a lo largo del tiempo, asumiéndose que dicha cinética corresponde directamente a la cinética de biotransformación. Aplicando el modelo conforme a lo establecido en la guía (explicado en la *Sección. 5.*4 de la Introducción)**,** con las adaptaciones necesarias para considerar las pérdidas por volatilización y la utilización de C_{free} en lugar de la concentración total en el medio, debido a la naturaleza de las líneas celulares en contraposición a los hepatocitos del modelo original, **se obtuvieron valores de BCF para todas las líneas**

celulares (HepG2, ZF4 y ZFL) sin diferencias significativas en comparación con los reportados en la literatura para organismos adultos. Estos hallazgos evidencian que las líneas celulares pueden constituir una alternativa válida para la estimación del BCF mediante el modelo IVIVE-BCF.

No obstante, la **suposición del modelo** de que la depleción del sustrato se debe exclusivamente a la biotransformación podría **sobreestimar la tasa real** de este proceso, ya que las células utilizadas pueden, a su vez, bioacumular el compuesto sin que este sea necesariamente biotransformado, lo cual no se contempla en la estimación. En este contexto, se aprovechó el diseño experimental y el método analítico desarrollados en esta Tesis Doctoral para **evaluar la capacidad de bioacumulación de las células**. Con este fin, se determinaron las concentraciones tanto en las células como en el medio a distintos tiempos de exposición. A partir de estos datos, y con la ayuda del MBM, se calculó C_{free} y, mediante la relación entre estas concentraciones y la aplicación del modelo toxicocinético, se estimaron los valores de BCF y BCF_k, respectivamente, utilizando cada línea celular.

En el **Articulo 3**, se muestran las cinéticas de absorción de las células HepG2, ZFL y ZF4 en la exposición con el compuesto PHE. Se observó que las células HepG2 no alcanzaron el estado estacionario y que los valores de BCF obtenidos fueron significativamente superiores a los reportados en estudios *in vivo* en la literatura. En contraste, las líneas celulares ZFL y ZF4 alcanzaron la estabilidad a lo largo del ensayo, obteniendo BCF más comparables a los valores *in vivo*, cuando se consideró C_{free} en vez de la concentración total del medio. Estos resultados sirvieron para destacar cuatro aspectos clave: i) **las células pueden bioacumular,** lo que impide suponer que la depleción del sustrato en el medio es debida únicamente la biotransformación en las células; por lo que es fundamental conocer la tasa real de metabolización y la concentración en el interior celular; ii) **considerando C_{free}, las líneas celulares pueden servir para una estimación rápida de cribado**; iii) **la importancia de la evaluación experimental** ya que mediante el modelo IVIVE-BCF se obtuvieron valores satisfactorios en comparación con valores *in vivo* con las 3 líneas celulares, sin embargo, el modelo toxicocinético experimental descartó la línea celular HepG2. En el modelo IVIVE-BCF, la concentración en el interior de la célula es estimada mediante un modelo

matemático de absorción a partir de la constante de octanol-agua del compuesto. Si se tiene en cuenta el porcentaje de lípidos de las líneas celulares hepáticas evaluadas, esto es 3.2% en las células HepG2[182]y 4 % en los tejidos de hígado de peces[186], la bioacumulación debería ser similar, lo que no se observó en los resultados experimentales, evidenciando una mayor internalización del compuesto en las células HepG2. Esto podría atribuirse al carácter canceroso de las células HepG2, que podría inducir alteraciones en sus mecanismos de incorporación de compuestos en comparación con las células inmortalizadas no cancerosas de peces; y iv) considerando estos resultados, **la línea celular ZFL se concluye como la más adecuada para estudios simultáneos de bioacumulación y biotransformación**.

En este contexto, y en relación con el aspecto (i), en el **Artículo 3** se optó por estimar una **constante de metabolización basada en la cinética de formación** de los metabolitos mayoritarios, con el propósito de aplicarla posteriormente en el modelo IVIVE-BCF o, en su defecto, aportar datos de biotransformación que contribuyan a la mejora de los modelos existentes. Para ello, se aprovechó el método analítico desarrollado, capaz de determinar la concentración de los metabolitos en el interior celular en función del tiempo de exposición. La constante de formación calculada a partir de los datos de biotransformación del PHE resultó inferior a la obtenida con el modelo de agotamiento, debido a la marcada disminución de la concentración del sustrato en comparación con la baja concentración de metabolitos formados. Esto derivó en una menor constante de metabolización y, en consecuencia, en un mayor BCF. Dicha sobreestimación generó diferencias significativas ($p = 0.01$) con un nivel de confianza del 95 % respecto a los valores de BCF in vivo reportados en la literatura. No obstante, la similitud entre los valores de BCF obtenidos con ambos enfoques fue elevada: 1253 y 1344 $L \cdot kg^{-1}$ mediante los métodos de agotamiento de sustrato y de formación de metabolitos, respectivamente, con una concentración de exposición de 0.7 $mg \cdot L^{-1}$ (C_{free}) en la línea celular ZFL. En consecuencia, al considerar el conjunto de datos, no se observaron diferencias significativas ($p = 0.003$).

[182] **Fischer** *et al.* Modeling exposure in the Tox21 in vitro bioassays. *Chem. Res. Toxicol*. **2017**.
[186] **Balk** *et al.* Bioconcentration assessment of three cationic surfactants in permanent fish cell lines. *Environ. Sci. Technol*. **2024**.

Una de las posibles causas identificadas posteriormente para dicha discrepancia fue el uso de **parámetros** de trucha arcoíris en la **extrapolación**, conforme a la guía estandarizada, debido a la utilización de hepatocitos de esta especie. Sin embargo, tanto el pez cebra como el hígado humano presentan ciertas diferencias fisiológicas y bioquímicas. Por ello, tras confirmar que la línea celular ZFL era la más idónea, como se ha expuesto en los aspectos clave (iii) y (iv), en el **Artículo 4** se evaluó la sustitución de los valores predeterminados de la trucha arcoíris por los correspondientes al pez cebra. Entre los cambios más relevantes se incluyeron: la reducción del peso modelado del pez de 10 a 0.5 g, el aumento de la temperatura de 12 a 28 °C, la fracción lipídica del hígado en relación con el peso total (de 15 % a 33 %), y la disminución del contenido celular hepático de $510 \cdot 10^6$ a $56 \cdot 10^6$ células/g de hígado. Ambas extrapolaciones arrojaron resultados satisfactorios de BCF para el BDE-47, con valores comparables a los reportados *in vivo* y bastante similares entre sí: 14926 y 14184 $L \cdot kg^{-1}$ al emplear los parámetros de trucha arcoíris y pez cebra, respectivamente, con una concentración de exposición de 0.21 $\mu g \cdot L^{-1}$ (C_{free}).

Dado que los valores de BCF obtenidos tras modificar la constante de metabolización y los parámetros de extrapolación son similares a los calculados mediante el modelo IVIVE sin aplicar estos cambios, siguiendo la guía estandarizada, y a la estimación directa basada en el modelo toxicocinético con las concentraciones experimentales en la célula (BCF_k), se puede deducir que la precisión de la estimación depende principalmente de la concentración intracelular y de la concentración en el medio (o, en este caso, de la concentración biodisponible). Por lo tanto, la extrapolación y la constante de metabolización funcionan como parámetros de ajuste cuantitativo sin modificar de manera significativa la conclusión sobre el potencial bioacumulativo del compuesto. En este sentido, y en concordancia con el aspecto clave (iii) expuesto, en el **Artículo 4** se llevó a cabo una **comparación entre las concentraciones intracelulares y biodisponibles obtenidas experimentalmente y aquellas calculadas mediante el modelo de balance de masa**.

El **porcentaje de C_{free}** determinado experimentalmente mediante el ensayo SPME fue del 0.07 % y 2.5 % para el BDE-47 y el PHE, respectivamente, en

comparación con el 0.03 % y 1.7 % estimado mediante el modelo MBM. Cabe destacar que el modelo de Fisher *et al.*[182] está ampliamente definido para diversos compuestos orgánicos, medios y tipos celulares; sin embargo, no contempla las condiciones específicas del medio empleado en la línea celular ZFL. La **ligera discrepancia** observada se debe a que el modelo no considera la presencia de suero de trucha en el medio de cultivo, lo que altera la distribución de los equilibrios en el sistema *in vitro*. En consecuencia, en este caso, se considera **más apropiada la determinación experimental**.

En relación con las **concentraciones intracelulares**, se observó una **discrepancia significativa** entre las determinaciones experimentales y las estimaciones del modelo MBM. En el caso del BDE-47, el modelo subestimó la concentración (ratio MBM/experimental = 59 ± 18 %), mientras que, para el PHE, se observó una sobreestimación (ratio MBM/experimental = 468 ± 52 %). Esta diferencia puede atribuirse a la cinética de biotransformación más acelerada del PHE, un aspecto que no es considerado en el modelo y que puede conducir a una sobrepredicción de la concentración intracelular y, en consecuencia, a una estimación inflada del BCF. Asimismo, el modelo MBM no contempla las diferencias en la cinética de absorción ni en los mecanismos de transporte de cada compuesto. En consecuencia, **para ciertos contaminantes, las predicciones basadas en el coeficiente de partición octanol-agua (K_{ow}) pueden diferir significativamente de los valores experimentales, lo que podría derivar en interpretaciones erróneas sobre su toxicidad específica**. En este contexto, en el **Artículo 4** se llevó a cabo la estimación del BCF mediante el modelo IVIVE-BCF, incorporando las constantes de absorción (k_1) y depuración (k_2) obtenidas a partir del modelo toxicocinético basado en las concentraciones intracelulares experimentales en función del tiempo de exposición, en lugar de utilizar aquellas predichas a partir de K_{ow}. Es importante señalar que dichas constantes experimentales fueron ajustadas a las unidades correspondientes y extrapoladas siguiendo el procedimiento establecido en el modelo. Como resultado, se obtuvieron valores de BCF aproximadamente tres veces superiores a los estimados mediante el modelo MBM

[182] **Fischer** *et al.* Modeling exposure in the Tox21 in vitro bioassays. *Chem. Res. Toxicol*. **2017**.

(ratio $IVIVE_{MBM}/IVIVE_{experimental}$ = 38 %), en línea con la diferencia observada en las concentraciones intracelulares.

Considerando las observaciones, experimentos, discusiones y conclusiones desarrolladas secuencialmente (resumidas en la **Figura 24**) durante la evaluación de esta metodología con líneas celulares, se puede concluir que los modelos predictivos actuales constituyen una herramienta valiosa para estimar de manera rápida y aproximada la bioacumulación de sustancias en organismos *in vivo*. No obstante, el presente trabajo pone de manifiesto varios aspectos fundamentales: (i) la **necesidad de realizar determinaciones experimentales** que reflejen con mayor precisión el comportamiento medioambiental y biológico de las sustancias químicas; (ii) la importancia de **seguir perfeccionando los modelos predictivos** mediante la incorporación de estudios adicionales sobre la cinética de absorción, las concentraciones intracelulares y las tasas de metabolización de los compuestos; y (iii) la relevancia de determinar y **considerar la concentración biodisponible**, especialmente en estudios con líneas celulares. En este contexto, el **método analítico y el diseño experimental presentados en esta Tesis Doctoral han demostrado ser herramientas eficaces**, proporcionando un procedimiento rápido, eficiente y de bajo costo. Asimismo, se ha comprobado su **viabilidad dentro del modelo IVIVE-BCF**, permitiendo la determinación experimental de la constante de metabolización, la estimación de las cinéticas de absorción mediante la integración de un modelo toxicocinético experimental, la cuantificación de la concentración biodisponible y, en combinación con la extrapolación, la obtención de estimaciones satisfactorias del BCF.

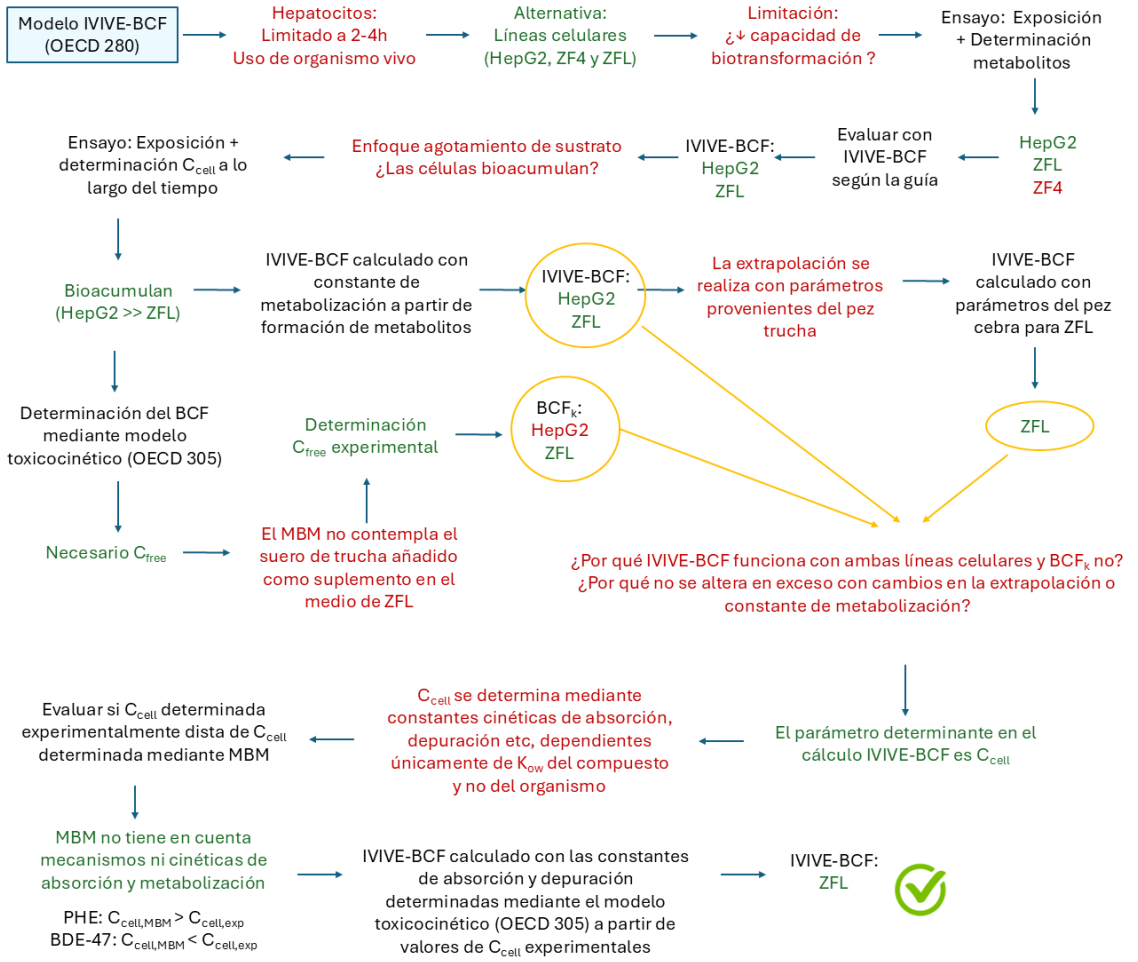

***Figura 24**. Resumen esquematizado de las observaciones, experimentos, discusiones y conclusiones llevadas a cabo de forma secuencial para el desarrollo y evaluación la metodología con líneas celulares.*

Considerando la discusión integradora presentada para ambas metodologías desarrolladas, los resultados obtenidos en la presente Tesis Doctoral son prometedores. Aunque se requieren estudios adicionales con otros tipos de sustancias, **estos hallazgos representan un avance significativo en la implementación de alternativas viables para el reemplazo de la experimentación en animales.** En la **Figura 25** se presenta una comparación entre los valores de BCF reportados en la literatura, determinados mediante ensayos *in vivo* o *in silico* y utilizados a lo largo de las discusiones, y los valores de BCF obtenidos con ambas metodologías desarrolladas en este estudio. De entre todos los valores calculados, se seleccionaron como óptimos aquellos obtenidos mediante la aplicación de criterios adecuados, fundamentados en su comportamiento experimental y matemático, tal como se ha discutido en esta

sección. Es decir, **se consideraron los valores derivados del empleo de la línea celular ZFL, teniendo en cuenta tanto las concentraciones internas en las células como las concentraciones biodisponibles determinadas experimentalmente. Además, se priorizaron los valores obtenidos a partir del modelo toxicocinético ajustado a los datos experimentales, así como aquellos calculados mediante el modelo IVIVE, tanto en su forma estándar, conforme a la normativa vigente, como en una versión modificada. Las modificaciones aplicadas incluyen la incorporación de la constante de metabolización determinada a partir de la cinética de formación de metabolitos, el uso de parámetros de extrapolación específicos para el pez cebra y la introducción de constantes de absorción y depuración ajustadas mediante modelos toxicocinéticos basados en los datos experimentales**. Estas mejoras tienen como objetivo incrementar la precisión en la estimación de la concentración intracelular, permitiendo así una evaluación más robusta y fiable del potencial bioacumulativo de las sustancias estudiadas.

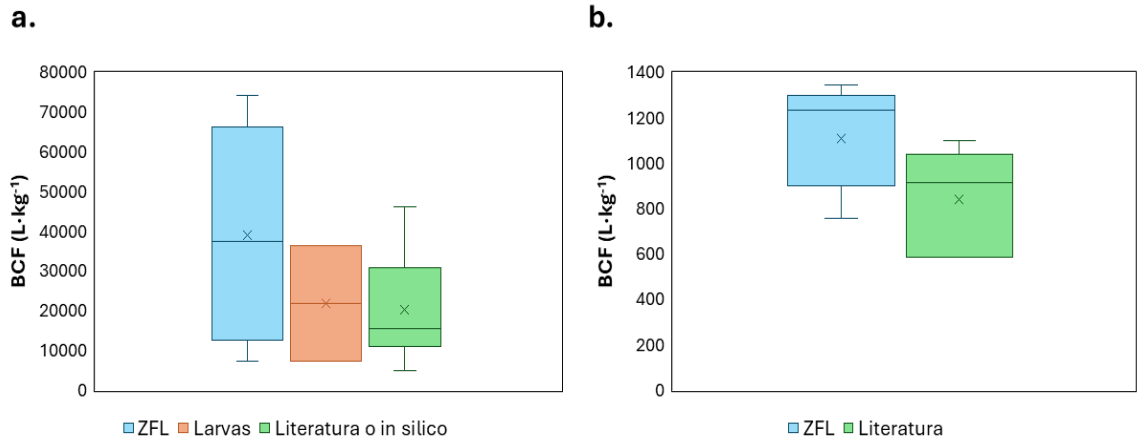

Figura 25. *Comparación de los valores de BCF obtenidos a partir de las metodologías desarrolladas, basadas en la utilización de la línea celular ZFL y larvas de pez cebra, con los BCF reportados en la literatura, determiandos mediante ensayos in vivo o in silico, para el compuesto BDE-47 (a) y PHE (b).*

En esta representación, se observa que **los valores de BCF obtenidos mediante la metodología basada en la línea celular ZFL y en larvas de pez cebra se encuentran dentro del rango de variabilidad de los valores reportados en ensayos con organismos vivos**. Por tanto, ambas metodologías podrían emplearse para evaluar la bioacumulación y biotransformación de contaminantes orgánicos persistentes (POPs) de manera rápida, reproducible y económica, alineándose con el principio de las 3R. No obstante, **ambas presentan ciertas limitaciones en términos de complejidad biológica**. Si bien las líneas celulares permiten obtener información relevante sobre efectos específicos en tejidos de interés, no reflejan la interacción entre órganos. En términos de predictibilidad, las larvas de pez cebra representan un modelo más cercano a la realidad biológica, dado que poseen órganos funcionales y procesos fisiológicos activos, lo que puede ofrecer resultados más comparables a los modelos animales (como se observa en la **Figura 25a**). Sin embargo, su grado de complejidad sigue siendo inferior al de un organismo adulto. Tal como se ha discutido a lo largo de esta Tesis Doctoral, la toxicidad es un fenómeno complejo que involucra diversos procesos de absorción, distribución, metabolismo y excreción, los cuales requieren mayor investigación en larvas y líneas celulares para mejorar la extrapolación de resultados. En este sentido, los métodos analíticos desarrollados proporcionan una herramienta sencilla y robusta para su incorporación en evaluaciones toxicológicas, aportando información valiosa a investigadores dedicados al desarrollo y validación de modelos predictivos. No obstante, **el uso combinado de ambas metodologías puede contribuir significativamente a la comprensión de los mecanismos de acción de las sustancias químicas, así como a la predicción en estudios de cribado de toxicidad, bioacumulación y biotransformación**, reservando los ensayos en organismos vivos solo para aquellos casos en los que sea estrictamente necesario.

Con esta última afirmación se planteó el trabajo final presentado en el **Artículo 5**, en el cual se combinaron ambas metodologías alternativas y se aplicaron los métodos analíticos desarrollados para evaluar la toxicidad del **PHE en presencia de PS-NPLs**, considerando tanto sus efectos como su acumulación y biotransformación. Además de la línea celular ZFL, se empleó la línea celular

RTgutGC, un modelo de tejido intestinal con funcionalidades distintas y relevantes, dado su demostrado potencial para la internalización de NPLs. Asimismo, fue necesario recurrir a técnicas bioanalíticas complementarias, como la citometría de flujo y la microscopía confocal, ambas basadas en fluorescencia, lo que requirió el uso de PS-NPLs marcadas fluorescentemente.

En ambas líneas celulares utilizadas, así como en las larvas de pez cebra, se observó una mayor acumulación del contaminante y, en consecuencia, un incremento en el valor del BCF en los organismos expuestos a PS-NPLs. Además, en las células hepáticas se detectó una mayor cantidad de metabolitos de PHE en presencia de nanoplásticos, lo que confirmó el denominado "efecto caballo de Troya", en el cual los PS-NPLs actúan como vehículos de entrada para los contaminantes adheridos a su superficie, provocando un descenso en la viabilidad celular. Sin embargo, al aumentar la complejidad biológica, es decir, al comparar las larvas de pez cebra con las líneas celulares, se observó una menor toxicidad general en presencia de PS-NPLs. Asimismo, se identificaron efectos opuestos en la captación de PS-NPLs según el tipo de célula, el tejido y el nivel de complejidad biológica durante la exposición conjunta con diferentes concentraciones de PHE. En las células hepáticas se evidenció un efecto sinérgico en la captación de PS-NPLs al aumentar la concentración de PHE, mientras que en las células intestinales y en las larvas de pez cebra se observó un efecto antagónico. Estos resultados subrayan, por un lado, la **importancia de considerar los efectos combinados de múltiples contaminantes en las evaluaciones de riesgo ecotoxicológico**, ya que los estudios centrados en un solo compuesto pueden subestimar los peligros de las mezclas ambientales complejas. Por otro lado, las diferencias en la respuesta celular y tisular a la exposición combinada de PS-NPLs y PHE resaltan la **necesidad de investigaciones más detalladas para comprender los mecanismos que subyacen a estas interacciones**. En este sentido, estos hallazgos proporcionan una base fundamental para futuras investigaciones destinadas a dilucidar los mecanismos de acción y los efectos de la interacción entre contaminantes en distintos niveles biológicos.

Una de las hipótesis consideradas en la discusión del trabajo que podría explicar la diferencia en los efectos observados es la posible aglomeración de partículas o el aumento del radio hidrodinámico de estas debido a la presencia y/o adhesión de PHE en su superficie. Este fenómeno podría dificultar o favorecer la internalización de las partículas, dependiendo de la funcionalidad celular o la complejidad biológica del modelo de estudio. Otra posible explicación para la diferencia en la toxicidad general observada podría ser el distinto estado del PHE, ya sea libre o adherido a la superficie de los PS-NPLs, tanto en el medio de exposición como en el interior celular. Las **investigaciones que continuarán esta Tesis Doctoral** se centrarán en cuantificar experimentalmente el porcentaje de adsorción de PHE en la superficie de los PS-NPLs, así como la concentración libre de PHE en el medio de exposición en presencia de PS-NPLs. Además de las técnicas bioanalíticas cualitativas empleadas para la detección de PS-NPs marcados fluorescentemente, será de gran interés explorar métodos analíticos de cuantificación como sp-ICP-MS, NTA, py-GC-MS y citometría de flujo.

IX. CONCLUSIONES

IX. CONCLUSIONES

A lo largo de la presente Tesis Doctoral se han abordado los objetivos planteados inicialmente. Del análisis de los resultados obtenidos en los diferentes trabajos realizados, se identifican tres conclusiones principales que sintetizan los aportes fundamentales de esta investigación:

- El desarrollo de **metodologías analíticas y diseños experimentales** adecuados ha permitido obtener datos experimentales que pueden integrarse en modelos matemáticos cinéticos y de extrapolación. De esta manera, se logran **resultados más precisos y fiables**, acercándose a una evaluación de la **toxicidad representativa** de un organismo biológico complejo, y se mejora la comprensión de los procesos de interacción de las sustancias químicas con los organismos y el medio ambiente.
- Las líneas celulares hepáticas ZFL (modelo *in vitro*) y las larvas de pez cebra (modelo *in vivo*) han demostrado ser **metodologías alternativas adecuadas** para el estudio de la toxicidad, bioacumulación y biotransformación de contaminantes persistentes como el BDE-47 y el PHE. Ambas metodologías han generado **datos consistentes y comparables a los obtenidos con modelos animales tradicionales y predictivos**, contribuyendo a reducir y reemplazar la experimentación animal, aún presente en la normativa oficial, y a refinar los métodos existentes. Además, se demostró que el uso conjunto de ambos modelos ofrece **información complementaria**, valiosa para estudios de cribado y evaluación de riesgos, gracias a su distinta complejidad biológica.
- Se ha demostrado que la exposición combinada de sustancias como el PHE con nanoplásticos puede modificar la toxicidad, la bioacumulación y la biotransformación de contaminantes, subrayando la necesidad de **considerar efectos combinados en las evaluaciones ecotoxicológicas**. Asimismo, se han establecido bases sólidas para investigaciones futuras en esta área.

A partir de las conclusiones generales, se exponen a continuación las conclusiones específicas extraídas de las mismas:

Métodos analíticos y diseño experimental.

- La extracción asistida por sonda de ultrasonidos permite una preparación de muestra miniaturizada, adecuada para tamaños de muestra pequeños como larvas y células, liberando eficazmente los compuestos internos de forma rápida y sencilla, lo que resulta fundamental para análisis de cribado e integración en modelos predictivos.
- La optimización de mezclas de disolventes facilita la extracción simultánea de compuestos con diferentes propiedades físico-químicas, permitiendo el estudio conjunto de compuestos parentales hidrofóbicos y metabolitos hidroxilados, adaptable a la mayoría de los POPs neutros.
- Los métodos optimizados basados en GC-MS-μECD y LC-FLD permitieron la separación, identificación y cuantificación de los POPs y sus metabolitos isoméricos con sensibilidad y selectividad a nivel de trazas.
- Los protocolos experimentales diseñados siguen los principios de la guía oficial OECD 305, manteniendo elementos clave como el muestreo a tiempos múltiples, el análisis de concentraciones internas y del medio de exposición, el ajuste toxicocinético basado en absorción y desorción, y el control de las concentraciones de exposición.
- El diseño *in vitro* basado en placas de vidrio y controles sin células permite minimizar o considerar las pérdidas por adsorción al plástico y por volatilización o degradación de los compuestos. Además, el uso de placas de gran tamaño facilitó la obtención de suficiente biomasa celular para extracciones reproducibles y cuantificables.

Metodologías alternativas: evaluación de la bioacumulación y biotransformación.

- Las larvas de pez cebra a partir de las 72 hpf demostraron una alta capacidad de metabolización, lo que valida su uso en estudios de biotransformación de contaminantes.
- Las líneas celulares hepáticas inmortalizadas no cancerosas, como ZFL, aunque con menor medida que los cultivos primarios, mostraron una biotransformación suficiente para estudios de cribado toxicológico.

- La determinación de la concentración libre (C_{free}) en sistemas *in vitro* es esencial para evaluar con precisión la biodisponibilidad y, en consecuencia, los procesos toxicológicos. La metodología basada en SPME y el modelo de balance de masas han resultado adecuadas para la incorporación en la determinación del BCF y tasas de metabolización.
- Se ha demostrado que la línea celular ZFL puede sustituir a los hepatocitos en el modelo IVIVE de la guía OECD 280.
- Se ha demostrado que las líneas celulares pueden bioacumular sustancias, lo que influye en la interpretación del enfoque de la depleción de sustrato y subraya la necesidad de medir concentraciones intracelulares tanto de compuestos parental como de metabolitos.
- La modificación de parámetros de extrapolación en el modelo IVIVE, como la sustitución de datos de trucha arcoíris por los de pez cebra, refina la estimación de BCF; sin embargo, la concentración biodisponible y la intracelular son los factores más determinantes.
- La combinación de datos experimentales de absorción y biotransformación mejora las estimaciones de BCF frente a modelos basados únicamente en K_{ow} o balance de masas. Se ha demostrado que puede incorporarse el ajuste toxicocinético de dichos valores en el modelo matemático IVIVE establecido.

Exposición combinada de nanoplásticos de poliestireno.

- La presencia de PS-NPLs incrementó la acumulación de PHE en larvas de pez cebra y líneas celulares, evidenciado en un aumento del valor de BCF.
- En células hepáticas, la exposición combinada a PS-NPLs y PHE generó un aumento de metabolitos detectados, confirmando el efecto "caballo de Troya" en el transporte de contaminantes.
- La exposición conjunta de PS-NPLs y PHE disminuyó la viabilidad celular en líneas hepáticas, indicando un efecto tóxico sinérgico.
- En organismos más complejos, como larvas, la toxicidad general fue menor en presencia de PS-NPLs, lo que sugiere mecanismos de defensa biológicos adicionales.

- Se observaron patrones opuestos de captación de PS-NPLs: un efecto sinérgico en células hepáticas (mayor captación con más PHE) y un efecto antagónico en células intestinales y larvas (menor captación con más PHE).

  Se planteó como hipótesis que la aglomeración de partículas, el aumento del radio hidrodinámico debido a la adsorción de PHE, la diferente funcionalidad celular y la relación de concentración libre y adsorbida en el organismo y en el medio explican los distintos patrones de captación y toxicidad observados.

X. CONCLUSIONS

X. CONCLUSIONS

Throughout this Doctoral Thesis, the initially proposed objectives have been successfully addressed. Based on the analysis of the results obtained in the various studies conducted, three main conclusions have been identified, which synthesize the fundamental contributions of this research:

- The development of **appropriate analytical methodologies and experimental designs** has made it possible to obtain experimental data that can be integrated into kinetic and extrapolation mathematical models. In this way, more **accurate and reliable results** are achieved, approaching a toxicity assessment that is **representative** of a complex biological organism, while also enhancing the understanding of the processes involved in the interaction of chemical substances with organisms and the environment.
- The ZFL hepatic cell lines (*in vitro* model) and zebrafish larvae (*in vivo* model) have proven to be **suitable alternative methodologies** for studying the toxicity, bioaccumulation, and biotransformation of persistent pollutants such as BDE-47 and PHE. Both methodologies have generated **consistent data, comparable to those obtained with traditional and predictive animal models**, contributing to the reduction and replacement of animal experimentation, which is still present in official regulations, and to the refinement of existing methods. Furthermore, it was demonstrated that the combined use of both models provides **complementary information**, valuable for screening studies and risk assessment, due to their differing biological complexity.
- It has been demonstrated that the combined exposure to substances such as PHE with nanoplastics can modify the toxicity, bioaccumulation, and biotransformation of pollutants, emphasizing the **need to consider combined effects in ecotoxicological assessments**. Furthermore, solid foundations have been established for future research in this area.

Based on the general conclusions, the specific conclusions drawn from them are presented below:

Analytical methods and experimental design.

- Ultrasound-assisted extraction allows for miniaturized sample preparation, suitable for small sample sizes such as larvae and cells, effectively releasing internal compounds in a quick and simple manner, which is essential for screening analyses and integration into predictive models.
- The optimization of solvent mixtures facilitates the simultaneous extraction of compounds with different physicochemical properties, allowing for the joint study of hydrophobic parent compounds and hydroxylated metabolites, adaptable to most neutral POPs.
- The optimized methods based on GC-MS-μECD and LC-FLD allowed for the separation, identification, and quantification of POPs and their isomeric metabolites with trace-level sensitivity and selectivity.
- The experimental protocols designed follow the principles of the official OECD 305 guideline, maintaining key elements such as multiple time-point sampling, analysis of internal concentrations and the exposure medium, toxicokinetic adjustment based on absorption and desorption, and control of exposure concentrations.
- The *in vitro* design based on glass plates and cell-free controls allows for the minimization or consideration of losses due to adsorption to plastic and volatilization or degradation of the compounds. Furthermore, the use of large plates facilitated the collection of sufficient cellular biomass for reproducible and quantifiable extractions.

Alternative methodologies: evaluation of bioaccumulation and biotransformation.

- Zebrafish larvae from 72 hpf onward demonstrated a high capacity for metabolism, validating their use in studies of contaminant biotransformation.
- Immortalized non-cancerous hepatic cell lines, such as ZFL, although to a lesser extent than primary cultures, exhibited sufficient biotransformation for toxicological screening studies.

- The determination of free concentration (C_{free}) in *in vitro* systems is essential for accurately assessing bioavailability and, consequently, toxicological processes. The SPME-based methodology and the mass balance model have proven suitable for incorporation in the determination of BCF and metabolism rates.
- It has been demonstrated that the ZFL cell line can replace hepatocytes in the IVIVE model of the OECD 280 guideline.
- It has been demonstrated that cell lines can bioaccumulate substances, which influences the interpretation of the substrate depletion approach and underscores the need to measure intracellular concentrations of both parent compounds and metabolites.
- The modification of extrapolation parameters in the IVIVE model, such as replacing rainbow trout data with zebrafish data, refines the BCF estimation; however, bioavailable and intracellular concentrations are the most determining factors.
- The combination of experimental data on absorption and biotransformation improves BCF estimates compared to models based solely on K_{ow} or mass balance. It has been demonstrated that the toxicokinetic adjustment of these values can be incorporated into the established IVIVE mathematical model.

Combined exposure to polystyrene nanoplastics and PHE.

- The presence of PS-NPLs increased PHE accumulation in zebrafish larvae and cell lines, as evidenced by an increase in the BCF value.
- In hepatic cells, combined exposure to PS-NPLs and PHE resulted in an increase in detected metabolites, confirming the "Trojan horse" effect in contaminant transport.
- The combined exposure to PS-NPLs and PHE decreased cell viability in hepatic cell lines, indicating a synergistic toxic effect.
- In more complex organisms, such as larvae, the overall toxicity was lower in the presence of PS-NPLs, suggesting additional biological defense mechanisms.

- Opposite patterns of PS-NPLs uptake were observed: a synergistic effect in hepatic cells (higher uptake with more PHE) and an antagonistic effect in intestinal cells and larvae (lower uptake with more PHE).

  It was hypothesized that particle agglomeration, the increase in hydrodynamic radius due to PHE adsorption, the different cellular functionality, and the relationship between free and adsorbed concentration in the organism and the medium explain the distinct uptake and toxicity patterns observed.

XI. REFERENCIAS

XI. REFERENCIAS

[1] Silbergeld E.K. Herramientas y enfoques. Toxicología. Capítulo 33. 1998.

[2] Choudhuri S., Patton G.W., Chanderbhan R.F., Mattia A. and Klaassen C.D. From classical toxicology to Tox21: Some critical conceptual and technological advances in the molecular understanding of the toxic response beginning from the last Quarter of the 20th century. Toxicological Sciences 161 (1) 5–22. 2018. DOI: 10.1093/toxsci/kfx186.

[3] Gantenbein U.L. Poison and Its Dose: Paracelsus on Toxicology. Toxicology in the Middle Ages and Renaissance 1–10. 2017. DOI: 10.1016/B978-0-12-809554-6.00001-9.

[4] McCarty L.S., Borgert C.J. and Burgoon L. D. Evaluation of the Inherent Toxicity Concept in Environmental Toxicology and Risk Assessment. Environ Toxicol Chem 39 (12) 2351–2360. 2020. DOI: 10.1002/etc.4881.

[5] Ashauer R. and Escher B.I. Advantages of toxicokinetic and toxicodynamic modelling in aquatic ecotoxicology and risk assessment. J. Environ. Monit. 12, 2056-2061. 2010. DOI: 10.1039/c0em00234h.

[6] REACH No 1907. Regulation (EC) No1907/2006 of the european parliament and of the council. 2006. DOI: 10.04.2014

[7] National Research Council. Toxicity testing in the 21st century: A vision and a strategy. National Academies Press. 2007. DOI: 10.17226/11970.

[8] Escher B.I., Ashauer R., Dyer S., Hermens J.L., Lee J.H., Leslie H.A., Mayer P., Meador J.P., Warne M.S. Crucial role of mechanisms and modes of toxic action for understanding tissue residue toxicity and internal effect concentrations of organic chemicals. Integr Environ Assess Manag 7(1), 28-49. 2011. DOI: 10.1002/ieam.100.

[9] Ankley G.T., Bennett R.S., Erickson R.J., Hoff, D.J. Hornung, M.W., Johnson R.D., Mount D.R., Nichols J.W., Russom C.L., Schmieder P.K., Serrrano J.A., Tietge J.E. and Villeneuve D.L. Adverse outcome pathways: A conceptual framework to support ecotoxicology research and risk assessment. Environmental Toxicology and Chemistry, 29, 730-741. 2010. DOI: 10.1002/etc.34.

[10] Bureš S.M., Cvetnić M., Milološa M.M., Kučić D.G, Markić M., Kušić H., Bolanča T., Rogošić M. and Ukić S. Modeling the toxicity of pollutants mixtures for risk assessment: a review. Environ Chem Lett 19, 1629–1655. 2021. DOI: 10.1007/s10311-020-01107-5.

[11] Arnot J.A. and Gobas F.A.P.C.A review of bioconcentration factor (BCF) and bioaccumulation factor (BAF) assessments for organic chemicals in aquatic organisms. Environmental Reviews. 14 (4) 257-297. 2006. DOI: 10.1139/A06-005.

[12] Mackay D., Celsie A.K.D., Powell D.E., and Parnis J.M. Bioconcentration, bioaccumulation, biomagnification and trophic magnification: A modelling perspective. Environ Sci, 72–85. 2018. DOI: 10.1039/c7em00485k.

[13] Costanza J., Lynch D.G., Boethling R.S., and Arnot J.A. Use of the bioaccumulation factor to screen chemicals for bioaccumulation potential. Environ Toxicol Chem, 31 (10), 2261–2268. 2012, DOI: 10.1002/etc.1944.

[14] Gimeno S., Allan D., Kai P., Remuzat P. and Collard M. Are current regulatory log Kow cut-off values fit-for-purpose as a screening tool for bioaccumulation potential in aquatic organisms? Regulatory Toxicology and Pharmacology 147: 105556. 2024, DOI: 10.1016/j.yrtph.2023.105556.

[15] CE No 1272/2008. Clasificación, etiquetado y envasado de sustancias y mezclas, y por el que se modifican y derogan las Directivas 67/548/CEE y 1999/45/CE y se modifica el Reglamento (CE) no 1907/2006. Diario Oficial de la Unión Europea L 353. 2008.

[16] EPA. Ecological Effects Test Guidelines. Fish BCF. OPPTS 850.1730. 1996.

[17] Guide for Conducting Bioconcentration Tests with Fishes and Saltwater Bivalve Mollusks. ASTM International, West Conshohocken, PA. 2013. DOI: 10.1520/E1022-94R13.

[18] OECD No 305. Bioaccumulation in Fish: Aqueous and Dietary Exposure. 2012.

[19] Gobas F.A.P.C. and Zhang X. Measuring bioconcentration factors and rate constants of chemicals in aquatic organism under conditions of variable water concentrations and short exposure time. Chemosphere 25: 12, 1961-1971. 1992. DOI: 10.1016/0045-6535(92)90035-P.

[20] Mackay D. and Fraser A. Bioaccumulation of persistent organic chemicals: mechanisms and models. Environmental Pollution, 110, 375–391. 2000. DOI: 10.1016/S0269-7491(00)00162-7

[21] Almazroo O.A, Miah M.K., and Venkataramanan R. Drug Metabolism in the Liver. Clinics in Liver Disease 21, 1-20. 2017. DOI: 10.1016/j.cld.2016.08.001.

[22] Ewa B. and Danuta M.Š. Polycyclic aromatic hydrocarbons and PAH-related DNA adducts. J Appl Genetics 58, 321–330. 2017. DOI: 10.1007/s13353-016-0380-3.

[23] Benedetti M.S., Whomsley R., Poggesi I., Cawello W., Mathy F.X., Delporte M.L., Papeleu P. and Watelet J.B. Drug metabolism and pharmacokinetics. Drug Metabolism Reviews 41, 344-390. 2009. DOI: 10.1080/10837450902891295.

[24] Allocati N., Masulli M., Di Ilio C., and Federici L. Glutathione transferases: Substrates, inihibitors and pro-drugs in cancer and neurodegenerative diseases. Oncogenesis 7 (8). 2018. DOI: 10.1038/s41389-017-0025-3.

[25] McCormick J.M., Van Es T., Cooper K. R., White L. A. and Häggblom M. M. Microbially mediated O-methylation of bisphenol a results in metabolites with increased toxicity to the developing Zebrafish (Danio rerio) embryo. Environ Sci Technol 45 (15) 6567–6574. 2011. DOI: 10.1021/es200588w.

[26] Fu Q, Fedrizzi D, Kosfeld V, Schlechtriem C, Ganz V, Derrer S, Rentsch D, and Hollender J. Biotransformation Changes Bioaccumulation and Toxicity of Diclofenac in Aquatic Organisms. Environ Sci Technol 54 (7), 4400–4408. 2020. DOI: 10.1021/acs.est.9b07127.

[27] OECD No 319A. Determination of in vitro intrinsic clearance using cryopreserved rainbow trout hepatocytes (RT-HEP). 2018.

[28] OECD No 319B. Determination of in vitro intrinsic clearance using rainbow trout liver S9 sub-cellular fraction (RT-S9). 2018.

[29] Leonelli S. and Ankeny R.A. What makes a model organism? Endeavour 37(4), 209-12. 2013. DOI: 10.1016/j.endeavour.2013.06.001.

[30] Lima V.A., dos Santos A.B.N., de Morais E.S.G. and Soares A.F. Zebrafish: A Versatile Model Organism for Toxicological Research and Applications. Adv Res 25 (5) 387–396. 2024. DOI: 10.9734/air/2024/v25i51170.

[31] Howe K., Clark M., Torroja C. et al. The zebrafish reference genome sequence and its relationship to the human genome. Nature, 496, 498–503. 2013. DOI: 10.1038/nature12111.

[32] Gemberling M., Bailey T. J., Hyde D. R., and Poss K. D. The zebrafish as a model for complex tissue regeneration. Trends in genetics. 29 (11), 611-20. 2013. DOI: 10.1016/j.tig.2013.07.003.

[33] Mitra A., Mandal S., Banerjee K., Ganguly N., Sasmal P., Banerjee D. and Gupta S. Cardiac Regeneration in Adult Zebrafish: A Review of Signaling and

Metabolic Coordination. Curr Cardiol Rep 27 (15). 2025. DOI: 10.1007/s11886-024-02162-y.

[34] Garcia G.R., Noyes P.D. and Tanguay R.L. Advancements in zebrafish applications for 21st century toxicology. Pharmacology and Therapeutics 161, 11-21. 2016. DOI: 10.1016/j.pharmthera.2016.03.009.

[35] Wang Z., Walker G.W., Muir D.C.G. and Nagatani-Yoshida K. Toward a Global Understanding of Chemical Pollution: A First Comprehensive Analysis of National and Regional Chemical Inventories. Environ Sci Technol 54 (5) 2575–2584. 2020. DOI: 10.1021/acs.est.9b06379.

[36] Muir D.C.G., Getzinger G.J., McBride M., and Ferguson P.L. How Many Chemicals in Commerce Have Been Analyzed in Environmental Media? A 50 Year Bibliometric Analysis. Environ Sci Technol. 57 (25), 9119–9129. 2023. DOI: 10.1021/acs.est.2c09353.

[37] Burden N., Chapman K., Sewell F., and Robinson V. Pioneering. Better Science through the 3Rs: An Introduction to the National Centre for the Replacement, Refinement, and Reduction of Animals in Research (NC3Rs). Journal of the American Association for Laboratory Animal Science. 54(2):198-208. 2015. PMID: 25836967.

[38] OECD No 236. Fish embryo acute toxicity (FET) Test. 2013.

[39] Kimmel C.B., Ballard W.W., Kimmel S.R., Ullmann B., and Schilling T.F. Stages of embryonic development of the zebrafish. Developmental Dynamics 203 (3) 253–310. 1995. DOI: 10.1002/aja.1002030302.

[40] Strähle U., Scholz S., Geisler R., Greiner P., Hollert H., Rastegar S., Schumacher A., Selderslaghs I., Weiss C., Witters H. and Braunbeck T. Zebrafish embryos as an alternative to animal experiments-A commentary on the definition of the onset of protected life stages in animal welfare regulations. Reproductive Toxicology, 33 (2). 128–132. 2012. DOI: 10.1016/j.reprotox.2011.06.121.

[41] DIRECTIVE 2010/63/EU. Protection of animals used for scientific purposes. 2010.

[42] Lungu-Mitea S., Vogs C., Carlsson G., Montag M., Frieberg K., Oskarsson A. and Lundqvist. Modeling Bioavailable Concentrations in Zebrafish Cell Lines and Embryos Increases the Correlation of Toxicity Potencies across Test Systems. Environ Sci Technol 55 (1) 447–457. 2021. DOI: 10.1021/acs.est.0c04872.

[43] Sanz-Landaluze J., Pena-Abaurrea M., Muñoz-Olivas R., Cámara C., and Ramos L. Zebrafish (danio rerio) eleutheroembryo-based procedure for assessing bioaccumulation. Environ Sci Technol 49 (3) 1860–1869. 2015. DOI: 10.1021/es504685c.

[44] Cronin M.T.D., Basiri H., Chrysochoou G., Enoch S.J., Firman J.W., Spînu N., Madden J.C. The predictivity of QSARs for toxicity: Recommendations for improving model performance. Computational Toxicology 33: 100338. 2025. DOI: 10.1016/j.comtox.2024.100338.

[45] Li N. Novel Quantitative Structure–Activity Relationship Tox21 Techniques for Combined Toxicity Prediction. Toxicological Assessment of Combined Chemicals in the Environment. 343–350. 2025. DOI: 10.1002/9781394158355.ch18.

[46] Bittner L., Klüver N., Henneberger L., Mühlenbrink M., Zarfl C., and Escher B.I. Combined Ion-Trapping and Mass Balance Models to Describe the pH-Dependent Uptake and Toxicity of Acidic and Basic Pharmaceuticals in Zebrafish Embryos (Danio rerio). Environ Sci Technol, 53 (13) 7877–7886. 2019. DOI: 10.1021/acs.est.9b02563.

[47] Veltman K., McKone T.E., Huijbregts M.A.J., and Hendriks A.J. Bioaccumulation potential of air contaminants: Combining biological allometry, chemical equilibrium and mass-balances to predict accumulation of air pollutants in various mammals. Toxicol Appl Pharmacol 238 (1) 47–55. 2009. DOI: 10.1016/j.taap.2009.04.012.

[48] ECHA-OECD. OECD QSAR Toolbox (version 4.7). 2012.

[49] EPI Suite. EPA. Estimation Programs Interface SuiteTM for Microsoft® Windows, v 4.11. 2012.

[50] ARC Arnot Research and Consulting Inc. EAS-E Suite. Ver.0.972. 2024.

[51] Arnot J.A., Toose L., Armitage J.M., Embry M., Sangion A., and Hughes L. A weight of evidence approach for bioaccumulation assessmen. Integrated Environmental Assessment and Management 19, 1235–1253. 2023.

[52] Grasse N., Massei R., Seiwert B., Scholz S., Escher B.I., Reemtsma T. and Fu Q. Impact of Biotransformation on Internal Concentrations and Specificity Classification of Organic Chemicals in the Zebrafish Embryo (Danio rerio). Environ Sci Technol 58(40), 17898-17907. 2024. DOI: 10.1021/acs.est.4c04156.

[53] Proença S., Escher B.I., Fischer F.C., Fisher C., Grégoire S., Hewitt N.J., Nicol B., Paini A., Kramer N.I. Effective exposure of chemicals in in vitro cell systems: A review of chemical distribution models. Toxicology in Vitro 73: 105133. 2021. DOI: 10.1016/j.tiv.2021.105133.

[54] Astashkina A., Mann B., and Grainger D. W. A critical evaluation of in vitro cell culture models for high-throughput drug screening and toxicity. Pharmacology and Therapeutics 134, 82-106. 2012. DOI: 10.1016/j.pharmthera.2012.01.001.

[55] Philippeos C., Hughes R.D., Dhawan A., and Mitry R. R. Introduction to cell culture. Methods in Molecular Biology 806, 1–13. 2012. DOI: 10.1007/978-1-61779-367-7_1.

[56] Bols N.C., Dayeh V.R., Lee L.E.J., and Schirmer K. Use of fish cell lines in the toxicology and ecotoxicology of fish. Piscine cell lines in environmental toxicology. Biochemistry and Molecular Biology of Fishes 6, 43-84. 2005. DOI: 10.1016/S1873-0140(05)80005-0.

[57] Haycock J.W. 3D Cell Culture: A Review of Current Approaches and Techniques," in Methods in Molecular Biology, 695, 1-15. 2011. DOI: 10.1007/978-1-60761-984-0_1.

[58] Castaño A., Bols N., Braunbeck T., Dierickx P., Halder M., Isomaa B., Kawahara K., Lee L.E., Mothersill C., Pärt P., Repetto G., Sintes J.R., Rufli H., Smith R., Wood C., Segner H. The Use of Fish Cells in Ecotoxicology. ATLA, 31, 317–351. 2003. DOI: 10.1177/026119290303100314.

[59] Schirmer K. Proposal to improve vertebrate cell cultures to establish them as substitutes for the regulatory testing of chemicals and effluents using fish. Toxicology 224, 163-183. 2006. DOI: 10.1016/j.tox.2006.04.042.

[60] OECD 249. Test Guideline No. 249: Fish Cell Line Acute Toxicity: The RTgill-W1 cell line assay. 2021.

[61] Segner H. Cytotoxicity Assays with Fish Cells as an Alternative to the Acute Lethality Test with Fish. ATLA. 32 (4), 375–382. 2004. DOI: 10.1177/026119290403200409

[62] Stadnicka-Michalak J., Tanneberger K., Schirmer K., and Ashauer R. Measured and modeled toxicokinetics in cultured fish cells and application to in vitro - In vivo toxicity extrapolation. PLoS One 9 (3): e92303. 2014. DOI: 10.1371/journal.pone.0092303.

[63] OECD No. 280. Guidance document on the determination of in vitro intrinsic clearance using cryopreserved hepatocytes (RT-HEP) or liver S9 sub-cellular fractions (RT-S9) from rainbow trout and extrapolation to in vivo intrinsic clearance series on testing and assessment No. 280. 2018.

[64] Laue H., Hostettler L., Badertscher R.P., Jenner K.J., Sanders G., Arnot J.A. and Natsch A. Examining Uncertainty in in Vitro-In Vivo Extrapolation Applied in Fish Bioconcentration Models. Environ Sci Technol, 54 (15) 9483–9494. 2020. DOI: 10.1021/acs.est.0c01492.

[65] Nichols J.W., Huggett D.B., Arnot J.A., Fitzsimmons P.N., and Cowan-Ellsberry C.E. Toward improved models for predicting bioconcentration of well-metabolized compounds by rainbow trout using measured rates of in vitro intrinsic clearance. Environ Toxicol Chem, 32 (7), 1611–1622. 2013. DOI: 10.1002/etc.2219.

[66] Rostamnezhad F. and Fatemi M.H. Comprehensive investigation of binding of some polycyclic aromatic hydrocarbons with bovine serum albumin: Spectroscopic and molecular docking studies. Bioorg Chem 120: 105656. 2022. DOI: 10.1016/j.bioorg.2022.105656.

[67] OECD. Guidance Document on aqueous-phase aquatic toxicity testing of difficult test chemicals No. 23 ENV/JM/MONO(2000)6/REV1," 2019.

[68] Kramer N.I., Krismartina M., Rico-Rico Á., Blaauboer B.J., and Hermens J.L.M. Quantifying processes determining the free concentration of phenanthrene in basal cytotoxicity assays. Chem Res Toxicol 25 (2) 436–445. 2012. DOI: 10.1021/tx200479k.

[69] Huchthausen J., Mühlenbrink M., König M., Escher B.I., and Henneberger L. Experimental Exposure Assessment of Ionizable Organic Chemicals in in Vitro Cell-Based Bioassays. Chem Res Toxicol, 33 (7) 1845–1854. 2020. DOI: 10.1021/acs.chemrestox.0c00067.

[70] Henneberger L., Huchthausen J., Wojtysiak N., and Escher B.I. Quantitative in Vitro-to- In Vivo Extrapolation: Nominal versus Freely Dissolved Concentration. Chem Res Toxicol 34 (4), 1175–1182. 2021. DOI: 10.1021/acs.chemrestox.1c00037.

[71] Birch H., Kramer N.I., and Mayer P. Time-Resolved Freely Dissolved Concentrations of Semivolatile and Hydrophobic Test Chemicals in In Vitro Assays - Measuring High Losses and Crossover by Headspace Solid-Phase Microextraction. Chem Res Toxicol 32 (9) 1780–1790. 2019. DOI: 10.1021/acs.chemrestox.9b00133.

[72] Arnot J.A. and Gobas F.A.P.C. A Generic QSAR for Assessing the Bioaccumulation Potential of Organic Chemicals in Aquatic Food Webs. QSAR Comb Sci 22, 337-345. 2003. DOI: 10.1002/qsar.200390023

[73] Black S.R., Nichols J.W., Fay K.A., Matten S.R., and Lynn S.G. Evaluation and comparison of in vitro intrinsic clearance rates measured using cryopreserved hepatocytes from humans, rats, and rainbow trout. Toxicology 457: 152819. 2021, DOI: 10.1016/j.tox.2021.152819.

[74] Nichols J.W., Hoffman A.D., ter Laak T.L., and Fitzsimmons P.N. Hepatic clearance of 6 polycyclic aromatic hydrocarbons by isolated perfused trout livers: Prediction from In vitro clearance by liver S9 fractions. Toxicological Sciences 136 (2) 359–372. 2013. DOI: 10.1093/toxsci/kft219.

[75] Kosfeld V., Fu Q., Ebersbach I., Esser D., Schauerte A., Bischof I., Hollender J., Schlechtriem C. Comparison of Alternative Methods for Bioaccumulation Assessment: Scope and Limitations of In Vitro Depletion Assays with Rainbow Trout and Bioconcentration Tests in the Freshwater Amphipod Hyalella Azteca. Environ Toxicol Chem 39 (9) 1813–1825. 2020. DOI: 10.1002/etc.4791.

[76] Fay K.A., Nabb D.L., Mingoia R.T., Bischof I., Nichols J.W., Segner H., Johanning K., Han X. Determination of metabolic stability using cryopreserved hepatocytes from rainbow trout (Oncorhynchus mykiss). Curr Protoc Toxicol 65, 4.42.1-4.42.29. 2015. DOI: 10.1002/0471140856.tx0442s65.

[77] Johanning K., Hancock G., Escher B., Adekola A., Bernhard M.J., Cowan-Ellsberry C., Domoradzki J., Dyer S., Eickhoff C., Embry M., Erhardt S., Fitzsimmons P., Halder M., Hill J., Holden D., Johnson R., Rutishauser S., Segner H., Schultz I. and Nichols J. Assessment of metabolic stability using the rainbow trout (Oncorhynchus mykiss) liver S9 fraction. Curr Protoc Toxicol 53, 14.10.1-14.10.28. 2012. DOI: 10.1002/0471140856.tx1410s53.

[78] Balk F., Hollender J., and Schirmer K. Investigating the bioaccumulation potential of anionic organic compounds using a permanent rainbow trout liver cell line. Environ Int 174: 107798. 2023. DOI: 10.1016/j.envint.2023.107798.

[79] Aktar A.B.T., Naseem S., Yasar A., and Naseem Z. Persistent Organic Pollutants (POPs): Sources, types, impacts and their remediation. Environmental and Microbial Biotechnology Environmental Pollution and Remediation. 2021. DOI: 10.1007/978-981-15-5499-5_8.

[80] El-Shahawi M.S., Hamza A., Bashammakh A.S., and Al-Saggaf W.T. An overview on the accumulation, distribution, transformations, toxicity and analytical

methods for the monitoring of persistent organic pollutants. Talanta 80 (5) 1587-1597. 2010. DOI: 10.1016/j.talanta.2009.09.055.

[81] Han D. and Currell M.J. Persistent organic pollutants in China's surface water systems. Sci Total Environ 580 (15), 602-625. 2017. DOI: 10.1016/j.scitotenv.2016.12.007.

[82] Gong P., Xu H., Wang C., Chen Y., Guo L., and Wang X. Persistent organic pollutant cycling in forests. Nature reviews earth and environment 2, 182-197. 2021. DOI: 10.1038/s43017-020-00137-5.

[83] Najam L. and Alam T. Occurrence, Distribution, and Fate of Emerging Persistent Organic Pollutants (POPs) in the Environment. in Emerging Contaminants and Plants, Emerging Contaminants and Associated Treatment Technologie, 135-161. 2023. DOI: 10.1007/978-3-031-22269-6_6

[84] Kumar J.A., Krithiga T., Sathish S., Renita A.A., Prabu D., Lokesh S., Geetha R., Namasivayam S.K.R., Sillanpaa M. Persistent organic pollutants in water resources: Fate, occurrence, characterization and risk analysis. Sci Total Environ 831: 154808. 2022. DOI: 10.1016/j.scitotenv.2022.154808.

[85] Xu W., Wang X., and Cai Z. Analytical chemistry of the persistent organic pollutants identified in the Stockholm Convention: A review. Analytica Chimica Acta 790 (6), 1-13. 2013. DOI: 10.1016/j.aca.2013.04.026.

[86] CE No 1881/2006. REGLAMENTO (CE) No 1881/2006 por el que se fija el contenido máximo de determinados contaminantes en los productos alimenticios. EUR-Lex.

[87] UNEP. UNITED NATIONS SC Stockholm Convention on Persistent Organic Pollutants Preliminary report for the effectiveness evaluation of the Stockholm Convention pursuant to Article 16. 2022.

[88] Reizer E., Viskolcz B., and Fiser B. Formation and growth mechanisms of polycyclic aromatic hydrocarbons: A mini-review. Chemosphere 291(Pt 1): 132793. 2022. DOI: 10.1016/j.chemosphere.2021.132793.

[89] Sverdrup L.E., Nielsen T. and Krogh P.H. Soil ecotoxicity of polycyclic aromatic hydrocarbons in relation to soil sorption, lipophilicity, and water solubility. Environ Sci Technol 36 (11) 2429–2435. 2002, DOI: 10.1021/es010180s.

[90] Dat N.D. and Chang M.B. Review on characteristics of PAHs in atmosphere, anthropogenic sources and control technologies. Sci Total Environ 609 (31), 682-693. 2017. DOI: 10.1016/j.scitotenv.2017.07.204.

[91] Sahu S.K. and Pandit G.G. Estimation of octanol-water partition coefficients for polycylic aromatic hydrocarbons using reverse-phase HPLC. J Liq Chromatogr Relat Technol 26 (1), 135–146. 2003. DOI: 10.1081/JLC-120017158.

[92] Yebra-Pimentel I., Fernández-González R., Martínez-Carballo E., and Simal-Gándara J. A critical review about the health risk assessment of pahs and their metabolites in foods. Critical Reviews in Food Science and Nutrition 55, 1383-1405. 2015. DOI: 10.1080/10408398.2012.697497.

[93] Moorthy B., Chu C., and Carlin D.J. Polycyclic aromatic hydrocarbons: From metabolism to lung cancer. Toxicological Sciences 145, 5-15. 2015. DOI: 10.1093/toxsci/kfv040.

[94] Bleeker E.A.J. and Verbruggen E.M.J. Bioaccumulation of polycyclic aromatic hydrocarbons in aquatic organisms. RIVM report. 2009.

[95] Patel A.B., Shaikh S., Jain K.R., Desai C., and Madamwar D. Polycyclic Aromatic Hydrocarbons: Sources, Toxicity, and Remediation Approaches. Front Microbiol 11: 562813. 2020. DOI: 10.3389/fmicb.2020.562813.

[96] EU 835/2011. Commission Regulation (EC) No 835/2011 amending Regulation No 1881/2006 as regards maximum levels for polycyclic aromatic hydrocarbons in foodstuffs.

[97] Honda M. and Suzuki N. Toxicities of polycyclic aromatic hydrocarbons for aquatic animals. Int J Environ Res Public Health 17 (4) 1363. 2020. DOI: 10.3390/ijerph17041363.

[98] Luo K., Luo X., Cao W., Hochalter J.B., Paiano V., Sipe C.J., Carmella S.G., Murphy S.E., Jensen J., Lam S., Golin A.P., Bergstrom L., Midthun D., Fujioka N., Hatsukami D., Hecht S.S. Cigarette smoking enhances the metabolic activation of the polycyclic aromatic hydrocarbon phenanthrene in humans. Carcinogenesis 42 (4) 570–577. 2021. DOI: 10.1093/carcin/bgaa137.

[99] Krzyszczak A. and Czech B. Occurrence and toxicity of polycyclic aromatic hydrocarbons derivatives in environmental matrices. Sci Total Environ 788, 147738. 2021. DOI: 10.1016/j.scitotenv.2021.147738.

[100] Pietroń W.J. and Małagocki P. Quantification of polybrominated diphenyl ethers (PBDEs) in food. A review. Talanta 167, 411-427. 2017. DOI: 10.1016/j.talanta.2017.02.043.

[101] Wong A., Lei Y.D., Alaee M., and Wania F. Vapor pressures of the polybrominated diphenyl ethers. J Chem Eng Data 46 (2), 239–242. 2001. DOI: 10.1021/je0002181.

[102] Harner T. and Shoeib M. Measurements of octanol-air partition coefficients (KOA) for polybrominated diphenyl ethers (PBDEs): Predicting partitioning in the environment. J Chem Eng Data 47 (2) 228–232. 2002. DOI: 10.1021/je010192t.

[103] Yang C.Y., Wu S.C., Lee C.C., and Shih Y. Translocation of polybrominated diphenyl ethers from field-contaminated soils to an edible plant. J Hazard Mater 351, 215–223. 2018. DOI: 10.1016/j.jhazmat.2018.02.037.

[104] Siddiqi M.A., Laessig R.H., and Reed K. D. Polybrominated Diphenyl Ethers (PBDEs): New Pollutants-Old Diseases. Clin Med Res 1(4), 281-90. 2003. DOI: 10.3121/cmr.1.4.281

[105] Teuten E.L., Xu L., and Reddy C.M. Two abundant bioaccumulated halogenated compounds are natural products. Science 307 (5711), 917–920. 2005. DOI: 10.1126/science.1106882.

[106] de la Torre A., Navarro I., Sanz P., and de los Ángeles M.M. Organophosphate compounds, polybrominated diphenyl ethers and novel brominated flame retardants in European indoor house dust: Use, evidence for replacements and assessment of human exposure. J Hazard Mater 382. 2020. DOI: 10.1016/j.jhazmat.2019.121009.

[107] Ohoro C.R., Adeniji A.O., Okoh A.I. and Okoh O.O. Polybrominated diphenyl ethers in the environmental systems: a review. J Environ Health Sci Engineering 19, 1229-1247. 2021. DOI: 10.1007/s40201-021-00656-3.

[108] Pietron W.J., Malagocki P., and Warenik-Bany M. Feed as a source of polybrominated diphenyl ethers (PBDEs). Environ Res 231(Pt 3): 116257. 2023. DOI: 10.1016/j.envres.2023.116257.

[109] Li F., Xie Q., Li X., Li N., Chi P., Chen J., Wang Z., Hao C. Hormone activity of hydroxylated polybrominated diphenyl ethers on human thyroid receptor-β: In vitro and in silico investigations. Environ Health Perspect 118 (5), 602–606. 2010. DOI: 10.1289/ehp.0901457.

[110] Klinčić D., Dvoršćak M., Jagić K., Mendaš G., and Romanić S.H. Levels and distribution of polybrominated diphenyl ethers in humans and environmental compartments: a comprehensive review of the last five years of research. Environ Sci Pollut Res Int 27(6), 5744-5758. 2020. DOI: 10.1007/s11356-020-07598-7.

[111] Butryn D.M., Chi L.H., Gross M.S., McGarrigle B., Schecter A., Olson J.R., Aga D.S. Retention of polybrominated diphenyl ethers and hydroxylated metabolites in paired human serum and milk in relation to CYP2B6 genotype. J Hazard Mater 386: 121904. 2020. DOI: 10.1016/j.jhazmat.2019.121904.

[112] Zheng X., Zhu Y., Liu C., Liu H., Giesy J.P., Hecker M., Lam M.H., Yu H. Accumulation and biotransformation of BDE-47 by zebrafish larvae and teratogenicity and expression of genes along the hypothalamus-pituitary-thyroid axis. Environ Sci Technol 46 (23) 12943–12951. 2012. DOI: 10.1021/es303289n.

[113] Sun J., Liu J., Yu M., Wang C., Sun Y., Zhang A., Wang T., Lei Z., Jiang G. In vivo metabolism of 2,2′,4,4′-tetrabromodiphenyl ether (BDE-47) in young whole pumpkin plant. Environ Sci Technol 47 (8) 3701–3707. 2013. DOI: 10.1021/es4003263.

[114] Xu X., Wang G., Li Y., and Zhang Y. Biotransformation kinetics and pathways of 2,2′,4,4′-tetrabromodiphenyl ether (BDE-47) and its hydroxylated and methoxylated derivatives (6-OH-BDE-47 and 6-MeO-BDE-47) in earthworms (Eisenia fetida). Sci Total Enviro 855: 158934. 2023. DOI: 10.1016/j.scitotenv.2022.158934.

[115] Usenko C.Y., Hopkins D.C., Trumble S.J. and Bruce E.D. Hydroxylated PBDEs induce developmental arrest in zebrafish. Toxicol Appl Pharmacol 262 (1), 43–51. 2012. DOI: 10.1016/j.taap.2012.04.017.

[116] Choo G., Lee I.S., and. Oh J.E. Species and habitat-dependent accumulation and biomagnification of brominated flame retardants and PBDE metabolites. J Hazard Mater 371, 175–182. 2019. DOI: 10.1016/j.jhazmat.2019.02.106.

[117] Sun H., Li Y., Hao Y., Zhu Y., Yang R., Wang P., Zhang Q., Jiang G. Bioaccumulation and Trophic Transfer of Polybrominated Diphenyl Ethers and Their Hydroxylated and Methoxylated Analogues in Polar Marine Food Webs. Environ Sci Technol 54 (23) 15086–15096. 2020. DOI: 10.1021/acs.est.0c05427.

[118] Cruz R., Cunha S.C., Marques A., and Casal S. Polybrominated diphenyl ethers and metabolites – An analytical review on seafood occurrence. TrAC Trends in Analytical Chemistry 87, 129-144. 2017. DOI: 10.1016/j.trac.2016.12.005.

[119] Benson N.U., Agboola O.D., Fred-Ahmadu O.H., De-la-Torre G.E., Oluwalana A. and Williams A.B. Micro(nano)plastics Prevalence, Food Web Interactions,

and Toxicity Assessment in Aquatic Organisms: A Review. Front Mar Sci 9. 2022. DOI: 10.3389/fmars.2022.851281.

[120] Yu Y., Mo W.Y., and Luukkonen T. Adsorption behaviour and interaction of organic micropollutants with nano and microplastics – A review. Sci Total Environ 797: 149140. 2021. DOI: 10.1016/j.scitotenv.2021.149140.

[121] Hartmann N.B., Hüffer T., Thompson R.C., Hassellöv M., Verschoor A., Daugaard A.E., Rist S., Karlsson T., Brennholt N., Cole M., Herrling M.P., Hess M.C., Ivleva N.P., Lusher A.L., Wagner M. Are We Speaking the Same Language? Recommendations for a Definition and Categorization Framework for Plastic Debris. Environ Sci Technol 53 (3), 1039–1047. 2019. DOI: 10.1021/acs.est.8b05297.

[122] Okoye C.O., Addey C.I., Oderinde O., Okoro J.O., Uwamungu J.Y., Ikechukwu C.K., Okeke E.S., Ejeromedoghene O., Odii E.C. Toxic Chemicals and Persistent Organic Pollutants Associated with Micro-and Nanoplastics Pollution. Chemical Engineering Journal Advances 11: 100310. 2022. DOI: 10.1016/j.ceja.2022.100310.

[123] Trevisan R., Uzochukwu D., and Di Giulio R. T. PAH Sorption to Nanoplastics and the Trojan Horse Effect as Drivers of Mitochondrial Toxicity and PAH Localization in Zebrafish. Front Environ Sci 8. 2020. DOI: 10.3389/fenvs.2020.00078.

[124] Fred-Ahmadu O.H., Bhagwat G., Oluyoye I., Benson N.U., Ayejuyo O.O. and Palanisami T. Interaction of chemical contaminants with microplastics: Principles and perspectives. Sci Total Environ. 706: 135978. 2020. DOI: 10.1016/j.scitotenv.2019.135978.

[125] Atugoda T., Vithanage M., Wijesekara H., Bolan N., Sarmah A.K., Bank M.S, You S, Ok YS. Interactions between microplastics, pharmaceuticals and personal care products: Implications for vector transport. Environ Int. 149: 106367. 2021. DOI: 10.1016/j.envint.2020.106367.

[126] Zuo L.Z., Li H.X., Lin L., Sun Y.X., Diao Z.H., Liu S., Zhang Z.Y., Xu X.R. Sorption and desorption of phenanthrene on biodegradable poly(butylene adipate co-terephtalate) microplastics. Chemosphere 215, 25–32. 2019. DOI: 10.1016/j.chemosphere.2018.09.173.

[127] Hüffer T. and Hofmann T. Sorption of non-polar organic compounds by micro-sized plastic particles in aqueous solution. Environmental Pollution 214, 194–201. 2016. DOI: 10.1016/j.envpol.2016.04.018.

[128] Lee H., Shim W.J., and Kwon J.H. Sorption capacity of plastic debris for hydrophobic organic chemicals. Sci Total Environ 470, 1545–1552. 2014. DOI: 10.1016/j.scitotenv.2013.08.023.

[129] Rochman C.M., Manzano C., Hentschel B.T., Simonich S.L.M., and Hoh E. Polystyrene plastic: A source and sink for polycyclic aromatic hydrocarbons in the marine environment. Environ Sci Technol 47 (24), 13976–13984. 2013. DOI: 10.1021/es403605f.

[130] Zhang Y. and Goss G.G. Potentiation of polycyclic aromatic hydrocarbon uptake in zebrafish embryos by nanoplastics. Environ Sci Nano 7(6), 1730–1741. 2020. DOI: 10.1039/d0en00163e.

[131] Mattsson K., Hansson L.A., and Cedervall T. Nano-plastics in the aquatic environment. Environmental Science: Processes and Impacts 17, 1712-1721. 2015. DOI: 10.1039/c5em00227c.

[132] Lebreton L. and Andrady A. Future scenarios of global plastic waste generation and disposal. Palgrave Commun 5, 6. 2019. DOI: 10.1057/s41599-018-0212-7.

[133] Kushwaha M., Shankar S., Goel D., Singh S., Rahul J., Rachna K., Singh J. Microplastics pollution in the marine environment: A review of sources, impacts and mitigation. Mar Pollut Bull. 209, Part A, 117109. 2024. DOI: 10.1016/j.marpolbul.2024.117109.

[134] Jambeck J.R., Geyer R., Wilcox C., Siegler T.R., Perryman M., Andrady A., Narayan R. and Law K.L. Plastic waste inputs from land into the ocean. Science 347 (6223), 768–771. 2015. DOI: 10.1126/science.1260352.

[135] Patidar K., Alshehri M., Singha W., Alrasheedi M., Younis A.M., Dumka U.C., Ambade B. Assessing the microplastic pandemic: Prevalence, detection, and human health impacts in Asian aquatic environments. Physics and Chemistry of the Earth Parts A/B/C, 137, 103800. 2025. DOI: 10.1016/j.pce.2024.103800.

[136] Waller C.L., Griffiths H.J., Waluda C.M., Thorpe S.E., Loaiza I., Moreno B., Pacherres C.O., Hughes K.A. Microplastics in the Antarctic marine system: An emerging area of research. Sci Total Environ 598, 220-227. 2017. DOI: 10.1016/j.scitotenv.2017.03.283.

[137] Materić D., Peacock M., Dean J., Futter M., Maximov T., Moldan F., Röckmann T. and Holzinger R. Presence of nanoplastics in rural and remote surface waters. Environmental Research Letters 17 (5). 2022. DOI: 10.1088/1748-9326/ac68f7.

[138] Vitali C., Peters R.J.B., Janssen H.G., and Nielen M.W.F. Microplastics and nanoplastics in food, water, and beverages; part I. occurrence. TrAC Trends in Analytical Chemistry 159: 116670. 2023. DOI: 10.1016/j.trac.2022.116670.

[139] Al-Thawadi S. Microplastics and Nanoplastics in Aquatic Environments: Challenges and Threats to Aquatic Organisms. Arab J Sci Eng 45, 4419–4440. 2020. DOI: 10.1007/s13369-020-04402-z.

[140] Kik K., Bukowska B., and Sicińska P. Polystyrene nanoparticles: Sources, occurrence in the environment, distribution in tissues, accumulation and toxicity to various organisms. Environ Pollut. 262, 114297. 2020. DOI: 10.1016/j.envpol.2020.114297.

[141] Erni-Cassola G., Zadjelovic V., Gibson M.I. and Christie-Oleza J.A. Distribution of plastic polymer types in the marine environment; A meta-analysis. J Hazard Mater 369, 691–698. 2019. DOI: 10.1016/j.jhazmat.2019.02.067.

[142] Martínez-Álvarez I., Le Menach K., Cajaraville M.P., Budzinski H. and Orbea A. Effects of polystyrene nano- and microplastics and of microplastics with sorbed polycyclic aromatic hydrocarbons in adult zebrafish. Sci Total Environ 927:172380. 2024. DOI: 10.1016/j.scitotenv.2024.172380.

[143] Shi C., Liu Z., Yu B., Zhang Y., Yang H., Han Y., Wang B., Liu Z., Zhang H. Emergence of nanoplastics in the aquatic environment and possible impacts on aquatic organisms. Sci Total Environ 906, 167404. 2024. DOI: 10.1016/j.scitotenv.2023.167404.

[144] Yee M.S., Hii L.W., Looi C.K., Lim W.M., Wong S.F., Kok Y.Y., Tan B.K., Wong C.Y., Leong C.O. Impact of microplastics and nanoplastics on human health. Nanomaterials 11(2): 496. 2021. DOI: 10.3390/nano11020496.

[145] Stapleton P.A. Toxicological considerations of nano-sized plastics. Environ Sci 6 (5) 367–378. 2019. DOI: 10.3934/environsci.2019.5.367.

[146] Brandts I., Garcia-Ordoñez M., Tort L., Teles M., and Roher N. Polystyrene nanoplastics accumulate in ZFL cell lysosomes and in zebrafish larvae after acute exposure, inducing a synergistic immune response: In vitro without affecting larval survival in vivo. Environ Sci Nano 7 (8) 2410–2422. 2020. DOI: 10.1039/d0en00553c.

[147] Trevisan R., Voy C., Chen S., and Di Giulio R. T. Nanoplastics decrease the toxicity of a complex PAH mixture but impair mitochondrial energy production in developing Zebrafish. Environ Sci Technol 53 (14) 8405–8415. 2019. DOI: 10.1021/acs.est.9b02003.

[148] Hu Y., Nie F., Zhang M., Song Q., Wei W., Lv G., Wei Y., Kang D., Chen Z., Lin H., Chen J. Developmental toxicity and mechanism of polychlorinated biphenyls 126 and nano-polystyrene combined exposure to zebrafish larvae. Ecotoxicol Environ Saf 278: 116419. 2024. DOI: 10.1016/j.ecoenv.2024.116419.

[149] Narayanan G., Talib M., Singh N., and Darbha G.K. Toxic effects of polystyrene nanoplastics and polycyclic aromatic hydrocarbons (chrysene and fluoranthene) on the growth and physiological characteristics of Chlamydomonas reinhardtii. Aquatic Toxicology 268: 106838. 2024. DOI: 10.1016/j.aquatox.2024.106838.

[150] Sun N., Shi H., Li X., Gao C., and Liu R. Combined toxicity of micro/nanoplastics loaded with environmental pollutants to organisms and cells: Role, effects, and mechanism. Environ Int. 171: 107711. 2023. DOI: 10.1016/j.envint.2022.107711.

[151] Wang S., Ma L., Chen L., Sokolova I.M., Huang W., Li D., Hu M., Khan F.U., Shang Y., Wang Y. The combined effects of phenanthrene and micro-/nanoplastics mixtures on the cellular stress responses of the thick-shell mussel Mytilus coruscus. Environmental Pollution 341: 122999. 2024. DOI: 10.1016/j.envpol.2023.122999.

[152] Li J., Liu X., Fu J., Gong Z., Jiang S.Y., and Chen J.P. Metabolic profile changes of zebrafish larvae in the single- and co-exposures of microplastics and phenanthrene. Sci Total Environ 953: 175994. 2024. DOI: 10.1016/j.scitotenv.2024.175994.

[153] Koelmans A.A., Besseling E., Wegner A., and Foekema E.M. Plastic as a carrier of POPs to aquatic organisms: A model analysis. Environ Sci Technol 47 (14) 7812–7820. 2013. DOI: 10.1021/es401169n.

[154] Wang J., Lu S., Bian H., Xu M., Zhu W., Wang H., He C., Sheng L. Effects of individual and combined polystyrene nanoplastics and phenanthrene on the enzymology, physiology, and transcriptome parameters of rice (Oryza sativa L.). Chemosphere 304, 135341. 2022. DOI: 10.1016/j.chemosphere.2022.135341.

[155] Yu Q., Hu X., Yang B., Zhang G., Wang J., and Ling W. Distribution, abundance and risks of microplastics in the environment. Chemosphere 249: 126059. 2020. DOI: 10.1016/j.chemosphere.2020.126059.

[156] Jain A.K., Singh D., Dubey K., Maurya R., Mittal S., and Pandey A.K. Models and Methods for In Vitro Toxicity. In Vitro Toxicology. Chapter 3, 46-65. 2018. DOI: 10.1016/B978-0-12-804667-8.00003-1.

[157] Braunbeck T., Hinton D.E., Streit B., and Segner H. Fish cell lines as a tool in aquatic toxicology. Fish Ecotoxicology 86: 1-38. 1998. DOI: 10.1007/978-3-0348-8853-0_1

[158] Jaroszeski M.J. and Radcfiff G. Fundamentals of Flow Cytometry. Mol Biotechnol 11(1):37-53. 1999. DOI: 10.1007/BF02789175

[159] Adeniji A.O., Okoh O.O., and Okoh A.I. Analytical Methods for Polycyclic Aromatic Hydrocarbons and their Global Trend of Distribution in Water and Sediment: A Review. Recent Insights in Petroleum Science and Engineering. 2018. DOI: 10.5772/intechopen.71163.

[160] Wang X., Lin L., Luan T., Yang L., and Tam N.F.Y. Determination of hydroxylated metabolites of polycyclic aromatic hydrocarbons in sediment samples by combining subcritical water extraction and dispersive liquid-liquid microextraction with derivatization. Anal Chim Acta 753, 57–63. 2012. DOI: 10.1016/j.aca.2012.09.028.

[161] Shelepchikov A.A., Ovcharenko V.V., Kozhushkevich A.I., Brodskii E.S., Komarov A.A., Turbabina K.A. and Kalantaenko A.M. A New Method for Purifying Fat-Containing Extracts in the Determination of Polybrominated Diphenyl Ethers. Journal of Analytical Chemistry 74 (6) 574–583. 2019. DOI: 10.1134/S1061934819040130.

[162] Song S., Yang C., Shao M., Chao J., Zheng N., Wang W., He Y., Li P. Simultaneous determination of polybrominated diphenyl ethers and hydroxylated analogues in human serum using high-performance liquid chromatography-inductively coupled plasma mass spectrometry. J Chromatogr B 1147, 122130. 2020. DOI: 10.1016/j.jchromb.2020.122130.

[163] Motorykin O., Schrlau J., Jia Y., Harper B., Harris S., Harding A., Stone D., Kile M., Sudakin D., Simonich S.L.M. Determination of parent and hydroxy PAHs in personal PM2.5 and urine samples collected during Native American fish smoking activities. Sci Total Environ 505, 694–703. 2015. DOI: 10.1016/j.scitotenv.2014.10.051.

[164] Butryn D.M., Gross M.S., Chi L.H., Schecter A., Olson J.R., and Aga D.S. One-shot' analysis of polybrominated diphenyl ethers and their hydroxylated and methoxylated analogs in human breast milk and serum using gas chromatography-tandem mass spectrometry. Anal Chim Acta 892, 140–147. 2015. DOI: 10.1016/j.aca.2015.08.026.

[165] Yue X., He J., Zhang R., Xu J., Zhou Z., Zhang R., Bi N., Wang Z., Sun C., Wang L., Chen Y., Abliz Z. Biotransformation-based metabolomics profiling method

for determining and quantitating cancer-related metabolites. J Chromatogr A 1580, 80–89. 2018. DOI: 10.1016/j.chroma.2018.10.034.

[166] Johnson-Restrepo B., Olivero-Verbel J., Lu S., Guette-Fernández J., Baldiris-Avila R., O'Byrne-Hoyos I., Aldous K.M., Addink R., Kannan K. Polycyclic aromatic hydrocarbons and their hydroxylated metabolites in fish bile and sediments from coastal waters of Colombia. Environmental Pollution 151 (3), 452–459. 2008. DOI: 10.1016/j.envpol.2007.04.011.

[167] Henneberger L., Mühlenbrink M., König M., Schlichting R., Fischer F.C. and Escher B.I. Quantification of freely dissolved effect concentrations in in vitro cell-based bioassays. Arch Toxicol 93 (8), 2295–2305. 2019. DOI: 10.1007/s00204-019-02498-3.

[168] Endo S., Droge S.T.J. and Goss K.U. Polyparameter linear free energy models for polyacrylate fiber-water partition coefficients to evaluate the efficiency of solid-phase microextraction. Anal Chem 83 (4), 1394–1400. 2011. DOI: 10.1021/ac102868e.

[169] Endo S., Mewburn B., and Escher B.I. Liposome and protein-water partitioning of polybrominated diphenyl ethers (PBDEs). Chemosphere 90 (2), 505–511. 2013. DOI: 10.1016/j.chemosphere.2012.07.069.

[170] Henneberger L., Mühlenbrink M., Fischer F.C., and Escher B.I. C18-Coated Solid-Phase Microextraction Fibers for the Quantification of Partitioning of Organic Acids to Proteins, Lipids, and Cells. Chem Res Toxicol 32 (1), 168–178. 2019. DOI: 10.1021/acs.chemrestox.8b00249.

[171] Flores-Ramírez R., Ortiz-Pérez M.D., Batres-Esquivel L., Castillo C., Ilizaliturri-Hernández C.A., and Díaz-Barriga F. Rapid analysis of persistent organic pollutants by solid phase microextraction in serum samples. Talanta 123, 169–178. 2014. DOI: 10.1016/j.talanta.2014.02.023.

[172] Schmidt K. and Podmore I. Solid Phase Microextraction (SPME) Method Development in Analysis of Volatile Organic Compounds (VOCS) as Potential Biomarkers of Cancer. J Mol Biomark Diagn 06 (06). 2015. DOI: 10.4172/2155-9929.1000253.

[173] Sereshti H., Duman O., Tunç S., Nouri N., and Khorram P. Nanosorbent-based solid phase microextraction techniques for the monitoring of emerging organic contaminants in water and wastewater samples. Microchimica Acta 187(9). 2020. DOI: 10.1007/s00604-020-04527-w/Published.

[174] Huber M.J., Ivleva N.P., Booth A.M., Beer I., Bianchi I., Drexel R., Geiss O., Mehn D., Meier F., Molska A., Parot J., Sørensen L., Vella G., Prina-Mello A.,

Vogel R., Caputo F. Physicochemical characterization and quantification of nanoplastics: applicability, limitations and complementarity of batch and fractionation methods. Anal Bioanal Chem 415 (15) 3007–3031. 2023. DOI: 10.1007/s00216-023-04689-5.

[175] Mahapatra S., Maity J.P., Singha S., Mishra T., Dey G., Samal A.C., Banerjee P., Biswas C., Chattopadhyay S., Patra R.R., Patnaik S., Bhattacharya P. Microplastics and nanoplastics in environment: Sampling, characterization and analytical methods. Groundwater for Sustainable Development 26: 101267. 2024. DOI: 10.1016/j.gsd.2024.101267.

[176] Fu W., Min J., Jiang W., Li Y., and Zhang W. Separation, characterization and identification of microplastics and nanoplastics in the environment. Sci Total Environ 721: 137561. 2020. DOI: 10.1016/j.scitotenv.2020.137561.

[177] Usenko C.Y., Robinson E.M., Usenko S., Brooks B.W., Bruce E.D. PBDE developmental effects on embryonic zebrafish. Environ Toxicol Chem 30(8), 1865. 2011. DOI: 10.1002/etc.570.

[178] Pereira L.C., de Souza A.O., Meireles G., Franco-Bernardes M.F., Tasso M.J., Bruno V., Dorta D.J., de Oliveira D.P. Comparative Study of Genotoxicity Induced by Six Different PBDEs. Pharmacol Toxicol 119(4), 396-404. 2016. DOI: 10.1111/bcpt.12595

[179] CompTox Chemicals Dashboard v2.5.3. EPA. 2024.

[180] Hallare A., Nagel K., Köhler H.R., Triebskorn R. Comparative embryotoxicity and proteotoxicity of three carrier solvents to zebrafish (Danio rerio) embryos. Ecotoxicol Environ Saf. 63(3), 378-88. 2006. DOI: 10.1016/j.ecoenv.2005.07.006.

[181] Fischer F.C., Cirpka O.A., Goss K.U., Henneberger L., Escher B.I. Application of Experimental Polystyrene Partition Constants and Diffusion Coefficients to Predict the Sorption of Neutral Organic Chemicals to Multiwell Plates in in Vivo and in Vitro Bioassays. Environ Sci Technol 52(22),13511-13522. 2018. DOI: 10.1021/acs.est.8b04246.

[182] Fischer F.C., Henneberger L., König M., Bittermann K., Linden L., Goss K.U., Escher B.I. Modeling Exposure in the Tox21 in Vitro Bioassays. Chem Res Toxicol 30(5), 1197-1208. 2017. DOI: 10.1021/acs.chemrestox.7b00023.

[183] Ulrich N., Endo S., Brown T.N., Watanabe N., Bronner G., Abraham M.H., Goss K.U. UFZ-LSER database v 3.2.1 [Internet], Leipzig, Germany, Helmholtz Centre for Environmental Research-UFZ. 2017 [accessed on 05.04.2024]. Available from http://www.ufz.de/lserd.

[184] McGeer J.C., Brix K.V., Skeaff J.M., DeForest D.K., Brigham S.I., Adams W.J., Green A. Inverse relationship between bioconcentration factor and exposure concentration for metals: implications for hazard assessment of metals in the aquatic environment. Environ Toxicol Chem 22(5), 1017-37. 2003. DOI: 10.1002/etc.5620220509.

[185] Liu H., Tang S., Zheng X., Zhu Y., Ma Z., Liu C., Hecker M., Saunders D.M., Giesy J.P., Zhang X., Yu H. Bioaccumulation, biotransformation, and toxicity of BDE-47, 6-OH-BDE-47, and 6-MeO-BDE-47 in early life-stages of zebrafish (Danio rerio). Environ Sci Technol 49(3), 1823-33. 2015. DOI: 10.1021/es503833q.

[186] Balk F., Hüsser B., Hollender J., Schirmer K. Bioconcentration Assessment of Three Cationic Surfactants in Permanent Fish Cell Lines. Environ Sci Technol 58(3), 1452-1461. 2024. DOI: 10.1021/acs.est.3c05360.

XII. GLOSARIO DE TÉRMINOS

XII. GLOSARIO DE TÉRMINOS

ACN	Acetonitrilo *Acetonitrile*
AOPs	Vías de resultados adversos *Adverse Outcome Pathway*
BAF	Factor de bioacumulación *Bioaccumulation Factor*
BCF	Factor de bioconcentración *Bioconcentration Factor*
BDE-47	2,2',4,4'-tetra bromo difenil éter *2,2',4,4'-tetra bromo diphenyl ether*
BSA	Albúmina de Suero Bovino *Bovine Serum Albumin*
$CL_{INVITRO,INT}$	Aclaramiento intrínseco *in vitro* *Intrinsic clearance in vitro*
$CL_{IN\ VIVO,INT}$	Aclaramiento intrínseco *in vivo* *Intrinsic clearance in vivo*
CYP450	Citocromo P450 *Cytochrome P450*
C_{cell}	Concentración en el interior celular *Cell concentration*
C_f	Concentración en el pez *Fish Concentration*
C_{free}	Concentración libre (biodisponible) *Free Concentration (bioavailable)*
C_{nom}	Concentración nominal *Nominal Concentration*
C_w	Concentración en el medio circundante *Water Concentration*
DCM	Diclorometano *Dichloromethane*
DLS	Dispersión Dinámica de Luz

DLS	*Dynamic Light Scattering*
DMSO	Dimetilsulfóxido *Dimethyl sulfoxide*
dpf	Días posteriores a la fertilización *Days post fertilisation*
d-SPE	Extracción en fase sólida dispersiva *Dispersive-Solid phase extraction*
ECD	Detector de Captura Electrónica *Electron Capture Detector*
ECHA	Agencia Europea de Sustancias y Mezclas Químicas *European Chemicals Agency*
EPA	Agencia de protección ambiental *Environmental Protection Agency*
FBS	Suero Bovino Fetal *Fetal Bovine Serum*
FET	Prueba de embriones de peces *Fish Embryo Test*
FLD	Detector de fluorescencia *Fluorescence Detector*
GC	Cromatografía de gases *Gas chromatography*
hpf	Horas posteriores a la fertilización *Hours post fertilisation*
IF	Factor de impacto *Impact factor*
IVIVE	Extrapolación *in vitro-in vivo* *in vitro-in vivo Extrapolation*
k_1	Constante de absorción *Absorption rate*
k_2	Constante de desorción *Desorption rate*
k_E	Tasa de eliminación

k_E	*Elimination rate*
k_f	Tasa de formación *Formation rate*
K_H	Constante de Henry *Henry constant*
k_{MET}	Constante de metabolización *Metabolisation rate*
K_{ow}	Coeficiente de partición octanol-agua *Partition coefficient octanol-water*
LC	Cromatografía de líquidos *Liquid Chromatography*
LC_{50}	Concentración letal 50% *Lethal Concentration 50%*
MBM	Modelos de balance de masas *Mass Balance Model*
MNPLs	Micro(nano)plásticos *Micro(nano)plastics*
MOAs	Modos de acción *Mode of Action*
MS	Espectrometría de masas *Mass Spectrometry*
MTBE	Metil-terc-butil-éter *Methyl-tert-butyl-ether*
MTBSTFA	N-terc-butildimetilsilil-N-metiltrifuoroacetamida *N-tert-butyldimethylsilyl-N-methyltrifuoroacetamide*
MTT	3-(4,5- dimetiltiazol-2-il)-2,5-difeniltetrazolio *3-(4,5- dimethylthiazol-2-yl)-2,5-diphenyltetrazolium*
MeO-BDEs	Metoxi-bromo difenil éter *Methoxy-bromo diphenyl ether*
NAMs	Metodologías de nuevo enfoque *New Approach Methods*
NTA	Análisis de Seguimiento de Nanopartículas

NTA	*Nanoparticle Tracking Analysis*
OECD	Organización para la Cooperación y el Desarrollo Económicos *Organisation for Economic Co-operation and Development*
OH-BDEs	Hidroxi-bromo difenil éter *Hydroxy-bromo diphenyl ether*
OH-PAHs	Hidrocarburos aromáticos policíclicos hidroxilados *Hydroxylated polycyclic aromatic hydrocarbons*
PA	Poliacrilato *Polyacrylate*
PAHs	Hidrocarburos Aromáticos Policíclicos *Polycyclic Aromatic Hydrocarbons*
PBDEs	Éteres de polibromodifenilos *Polybrominated Diphenyl Ethers*
PHE	Fenantreno *Phenanthrene*
POPs	Compuestos orgánicos persistentes *Persistent Organic Pollutants*
PS	Poliestireno *Polystyrene*
Py-GC-MS	Pirólisis-Cromatografía de gases-Espectrometría de masas *Pyrolysis-Gas Chromatography-Mass Spectrometry*
QSAR	Modelos de relación cuantitativa estructura-actividad *Quantitative Structure-Activity Relationship*
REACH	Registro, evaluación, autorización restricción sustancias químicas *Registration, Evaluation, Authorisation restriction of CHemicals*
RT-Hep	Hepatocitos de trucha arcoíris *Rainbow trout-hepatocytes*
RT-S9	Fracción subcelular S9 de trucha arcoíris *Rainbow trout S9 subcellular fraction*
RTgutGC	Línea celular intestinal de trucha arcoíris *Rainbow trout-intestinal cell line*
SEM	Microscopía Electrónica de Barrido

SEM	*Scanning Electron Microscopy*
sp-ICP-MS	Espectrometría masa-Plasma acoplado inductivo-Partícula única *Single Particle-Inductively Coupled Plasma-Mass Spectrometry*
SPME	Microextracción en fase sólida *Solid Phase MicroExtraction*
SS	Estado estacionario *Steady State*
TC	Toxicocinética *Toxicokinetics*
TCS	Triclosán *Triclosan*
TD	Toxicodinámica *Toxicodynamics*
TEM	Microscopía Electrónica de Transmisión *Transmission Electron Microscopy*
ZF4	Línea celular fibroblástica embrionaria de pez cebra *Zebrafish embryonic fibroblast cell line*
ZFL	Línea celular de hígado de pez cebra *Liver Zebrafish cell line*

XIII. ANEXOS

XIII. ANEXOS

ANEXO I: Producción Científica

I.1. Publicaciones científicas incluidas en la Tesis Doctoral.

- Bioaccumulation and biotransformation of BDE-47 using zebrafish eleutheroembryos (*Danio rerio*). P. De Oro-Carretero P. and J. Sanz-Landaluze. *Environ Toxicol Chem* 42(4), 835-845. **2023**. DOI: 10.1002/etc.5569.
- Miniaturized method for the quantification of persistent organic pollutants and their metabolites in HepG2 cells: assessment of their biotransformation P. De Oro-Carretero and J. Sanz-Landaluze. *Anal Bioanal Chem* 415, 4813-4825. **2023**. DOI: 10.1007/s00216-023-04781-w.
- *In vitro* approach to refine bioconcentration and biotransformation predictions of organic persistent pollutants using cell lines. P. De Oro-Carretero and J. Sanz-Landaluze. *Chemosphere* 364, 143020. **2024**. DOI: 10.1016/j.chemosphere.2024.143020.
- Assessing bioconcentration and biotransformation of BDE-47 in vitro: The relevance of bioavailable and intracellular concentrations. P. De Oro-Carretero and J. Sanz-Landaluze. *Journal of Xenobiotics,* 15,93. **2025**. DOI: 10.3390/jox15030093
- Complex combined effects of polystyrene nanoplastics and phenanthrene in aquatic models. P. De Oro-Carretero, M. García-Ordoñez, N. Roher and J. Sanz-Landaluze. *Journal of Hazardous Materials,* en revisión. **2025**.

I.2. Otras publicaciones científicas.

- Consumption of illicit drugs and benzodiazepines in six Spanish cities during different periods of the COVID-19 pandemic. E. Gracia-Lora, A. Pérez-Valenciano, P. De Oro-Carretero, L. Ramírez-García, J. Sanz-Landaluze, M.J Martín-Gutiérrez. *Science Total Enviro* 935, 173356. **2024**. DOI: 10.1016/j.scitotenv.2024.173356.
- Determinación de contaminantes orgánicos persistentes y sus metabolitos mayoritarios en líneas celulares y larvas de pez cebra para estudios de metabolización. P. De Oro-Carretero y J. Sanz-Landaluze. *Actualidad*

Analítica 72, 26-28. **2022**. https://seqa.es/actualidad-analitica-2022/actuanali-spetiembre2022/.

- Development of a method for assessing the accumulation and metabolization of antidepressant drugs in zebrafish (*Danio rerio*) eleutheroembryos. N. Molina-Fernández; S. Rainieri; R. Muñoz-Olivas; P. De Oro-Carretero; J. Sanz-Landaluze. *Anal Bioanal Chem* 413(20), 5169-5179 – **2021**. DOI: 10.1007/s00216-021-03486-2.
- Wastewater-based epidemiology of non-steroidal anti-inflammatory drugs in six cities of Spain: consumption patterns, seasonal trends, and the role of refined correction factors. E. Gracia-Lor, P. De Oro-Carretero, N. Melones-Peña and J. Sanz-Landaluze. *Exposure and Health*, en revisión. **2025**

I.3. Otras publicaciones.

- E. Rodríguez-Rodríguez, I. Mateos-Aparicio, M. Moreno-Guzmán, M. Sánchez-Paniagua López, Irene Ojeda-Fernández, M. Pacheco-Jerez, J. Sanz-Landaluze, E. Espada-Bernabé y P. De Oro-Carretero. Capítulo Libro Actas: APS "APRENDE-T-LOS-RIESGOS"; dando servicio a la comunidad desde la universidad. 3er Congreso Internacional de Educación Crítica e Inclusiva. Hacia una práctica inclusiva y comprometida socialmente. ISBN 978-84-09-64889-4. **2024**.

I.4. Comunicaciones en congresos (relacionados con la Tesis Doctoral).

- P. De Oro Carretero and J. Sanz-Landaluze. *Assessment of the bioaccumulation of organic pollutants using zebrafish liver cells and evaluation of the important in vitro parameters*. **SETAC Europe 35th Annual Meeting - Society of Environmental Toxicology and Chemistry**. Viena, Austria, **2025**. Comunicación oral.
- P. De Oro Carretero. *Bioaccumulation: walking in the 3Rs pathway*. **HEALTHY PLANET Lecture Series**. KUBUS, Helmholtz Centre for Environmental Research (UFZ). Leipzig, Alemania, **2024**. Comunicación oral.
- P. De Oro-Carretero, M. García-Ordoñez, N. Roher and J. Sanz-Landaluze. *Interaction of nanoplastics and phenantrene: evaluation of ecotoxic effects on*

in vivo and in vitro fish models (Danio rerio). **PLASTIC': 3as Jornadas sobre contaminación de plásticos**. Barcelona, España. **2024**. Comunicación oral.

- P. De Oro Carretero and J. Sanz-Landaluze. *Determinación de contaminantes orgánicos en células y su concentración biodisponible como metodología alternativa para predecir la bioacumulación*. **XXIV Reunión de la Sociedad Española de Química Analítica**. Zaragoza, España. **2024**. Comunicación oral.
- P. De Oro-Carretero, M. García-Ordoñez, N. Roher and J. Sanz-Landaluze. *Efecto Caballo de Troya en la Exposición Conjunta de Nanoplásticos y Contaminantes Orgánicos. Evaluación de la Absorción y Toxicidad en Células de Pez Cebra*. **XXIV Reunión de la Sociedad Española de Química Analítica**. Zaragoza, España. **2024**. Comunicación póster.
- P. De Oro Carretero y J. Sanz-Landaluze. *Metodología alternativa in vitro para la evaluación de la bioacumulación de sustancias químicas*. **VIII Jornadas de Promoción de la Investigación Básica para Estudiantes de Ciencias e Ingenierías**. Universidad Rey Juan Carlos, Madrid. **2024**. **1er Premio** a mejor Comunicación Oral.
- V. Pañeda-De la Peña y P. De Oro-Carretero*. Estudios ecotoxicológicos alternativos para un desarrollo sostenible*. II Simposio Universitario de Ciencias para el Desarrollo Sostenible. Universidad Complutense de Madrid, Madrid. **2023**. Comunicación oral.
- P. De Oro Carretero y J. Sanz-Landaluze. *In vitro approach to refine bioconcentration and biotransformation predictions of organic persistant pollutants using cell lines.* **SETAC Europe 33rd Annual Meeting - Society of Environmental Toxicology and Chemistry.** Dublín, Irlanda. **2023**. Comunicación póster**.**
- P. De Oro Carretero. *Metabolitos, ¿prórroga de la toxicidad de los contaminantes?* **6º PhDay Complutense.** Facultad Ciencias Químicas UCM. **2023**. Comunicación oral. **Premio Accésit**.
- P. De Oro Carretero y J. Sanz-Landaluze*. Determinación de contaminantes orgánicos persistentes y sus principales metabolitos en líneas celulares y larvas de pez cebra para estudios de metabolización.* **XXIII Reunión de la**

Sociedad Española de Química Analítica. Oviedo, España. **2022. Premio ABC** al mejor póster.

- P. De Oro Carretero y J. Sanz-Landaluze*. Alternative method to study the bioaccumulation and biotransformation of BDE-47 using zebrafish larvae (Danio rerio).* **1st International Meeting for Young Analytical Chemists (IMYAC).** Cracovia, Polonia. **2021**. Poster flash.
- P. De Oro Carretero y J. Sanz-Landaluze*. Método alternativo para el estudio de la bioacumulación y metabolización del bde-47 usando larvas de pez cebra.* **Simposio Anual Química Avanzada.** Facultad Ciencias Químicas UCM. **2020**. Comunicación oral.

I.5. Otras comunicaciones en congresos.

- J. Huchthausen, J. Braasch, P. De Oro-Carretero, M. König, B.I. Escher. *Critical membrane concentration and baseline toxicity of organic pollutants in a high-throughput rainbow trout gill assay used for environmental hazard assessment.* **SETAC Europe 35th Annual Meeting - Society of Environmental Toxicology and Chemistry**. Viena, Austria, **2025**. Comunicación oral.
- N. Melones-Peña, P. De Oro-Carretero, J. Sanz-Landaluze, E. Gracia-Lor. *Assessing the environmental ecotoxicity of wastewater effluents contaminated with illicit drugs and benzodiazepines: insights from zebrafish liver cell exposure*. **SETAC Europe 35th Annual Meeting - Society of Environmental Toxicology and Chemistry**. Viena, Austria, **2025**. Comunicación póster.

I.5. Proyectos de Investigación.

- *Estrategias (bio)analíticas, ensayos in vitro y análisis de aguas residuales para la evaluación de la presencia, riesgo y nivel exposición de contaminantes medioambientales*. Ministerio de Ciencia e Innovación (MICIN). 125.000€ Yolanda Madrid y Emma Gracia Lor. 01/09/2024-31/08/2027.

- *Impacto del COVID-19 en el patrón de consumo de sustancias adictivas a través de la monitorización de aguas residuales. Evaluación de su toxicidad*

mediante ensayos in vitro. EXP2022/008817, financiado por la Delegación del Gobierno para el Plan Nacional sobre Drogas (Ministerio de Sanidad) correspondiente a fondos del Mecanismo de Recuperación, Transformación y Resiliencia de la Unión Europea- NextGenerationEU. 89.738,15€. Emma Gracia Lor. 1/09/2022- 31/12/2024.

- *Estrategias bioanalíticas para la mejora de la calidad y seguridad de los alimentos: hacia un sistema de alimentación sostenible***.** Ministerio de Ciencia e Innovación (MICIN). PID2020-114714RB-I00. 97.000 €. Yolanda Madrid y Jon Sanz Landaluze. 01/09/2021-31/08/2024.

I.6. Estancias de Investigación.

- Estancia **Internacional** en el Grupo de Investigación *Cell Toxicology del* ***Helmholtz Centre for Environmental Research – UFZ en Leipzig (Alemania)****, del 13 de agosto de 2024 al 13 de noviembre de* ***2024****, bajo la dirección de la doctora Luise Henneberger.* En esta estancia se llevó a cabo la realización de ensayos con la línea celular RTgill como: ensayos de viabilidad celular mediante colorantes fluorescentes y por adquisición de imágenes con un microscopio de alto contenido, determinación del contenido total de proteínas y lípidos de los medios de exposición y las células y la optimización de métodos SPME de alto rendimiento con el dispositivo BioSPME de 96 pines y su posterior medición en HPLC-MS/MS. Con respecto a la presente Tesis Doctoral, se determinó la concentración libremente disuelta de fenantreno en medio de cultivo celular utilizando fibras SPME con recubrimiento de poliacrilato y la simulación del metabolismo del fenantreno utilizando una enzima CYP abiótica.
- Estancia **Nacional** en el Grupo de Investigación *Inmunología Evolutiva del* ***Instituto de Biotecnología y Biomedicina (IBB) – Universitat Autònoma de Barcelona (UAB)****, del* 14 de junio de 2023 hasta el día 27 de julio de **2023** y del 7 de mayo de 2024 hasta el día 14 de junio de **2024***, bajo la dirección de la doctora Nerea Roher.* En esta estancia se llevó a cabo la realización de ensayos de la exposición combinada de nanoplásticos de

poliestireno y fenantreno con las líneas celulares ZFL y RTgutGC y larvas de pez cebra.

- Estancia de **formación** en la ***Unidad de Técnicas Instrumentales, Contaminantes y Espectrometría de Masas*** del ***Laboratorio de Salud Pública del Ayuntamiento de Madrid*** *(Madrid Salud) del 1 de enero de* ***2021*** *hasta el día 31 de julio de* ***2022****, bajo la dirección de Alberto Álamo.* En esta estancia se llevó a cabo el desarrollo de método analíticos para la determinación de melamina en materiales en contacto con alimentos por LC-MS/MS y determinación de contaminantes orgánicos en aguas de consumo y materiales en contacto con alimentos por técnicas de cromatografía-espectrometría de masas.

ANEXO II: Otros méritos

- **Evaluadora Fundación para el Conocimiento madri+d** - para la realización de los procedimientos de evaluación y seguimientos de acuerdo con lo dispuesto en el Real Decreto 822/2021, de 28 de septiembre, por el que se establece la ordenación de las enseñanzas universitarias oficiales y el Real Decreto 640/2021, de 27 de julio, de creación, reconocimiento y autorización de universidades y centros universitarios, y acreditación institucional de centros universitarios. 24/05/**2023**-24/05/**2027**.
- **Presidenta de la sección técnica de estudiantes del Colegio Oficial de Químicos de Madrid y Asociación de Químicos e Ingenieros Químicos de Madrid**. No. 18.324. 2025.
- **Representante del Sector de Resto de Personal Docente en Consejo de Departamento de Química Analítica.** 2023-2027.
- **Comisión organizadora y evaluadora** del **7º PhDay Complutense**. Facultad Ciencias Químicas UCM. **2023**.
- **Censora de revistas científicas** internacionales indexadas en el JCR en el área de conocimiento de Química Analítica, Ciencia del Medio Ambiente y Toxicología.
- **Docente colaboradora y cotutora de Trabajos de Fin de Grado** en el Departamento de Química Analítica de la Facultad de Ciencias Químicas de la Universidad Complutense de Madrid.